ECOLOGY AND BEHAVIOUR OF FREE-RANGING ANIMALS STUDIED BY ADVANCED DATA-LOGGING AND TRACKING TECHNIQUES

EDITED BY: Thomas Wassmer, Dennis Murray, Stan Boutin, Andreas Fahlman and Frants Havmand Jensen

PUBLISHED IN: Frontiers in Ecology and Evolution, Frontiers in Physiology and Frontiers in Marine Science

frontiers Research Topics

Frontiers eBook Copyright Statement

The copyright in the text of individual articles in this eBook is the property of their respective authors or their respective institutions or funders. The copyright in graphics and images within each article may be subject to copyright of other parties. In both cases this is subject to a license granted to Frontiers.

The compilation of articles constituting this eBook is the property of Frontiers.

Each article within this eBook, and the eBook itself, are published under the most recent version of the Creative Commons CC-BY licence. The version current at the date of publication of this eBook is CC-BY 4.0. If the CC-BY licence is updated, the licence granted by Frontiers is automatically updated to the new version.

When exercising any right under the CC-BY licence, Frontiers must be attributed as the original publisher of the article or eBook, as applicable.

Authors have the responsibility of ensuring that any graphics or other materials which are the property of others may be included in the CC-BY licence, but this should be checked before relying on the CC-BY licence to reproduce those materials. Any copyright notices relating to those materials must be complied with.

Copyright and source acknowledgement notices may not be removed and must be displayed in any copy, derivative work or partial copy which includes the elements in question.

All copyright, and all rights therein, are protected by national and international copyright laws. The above represents a summary only. For further information please read Frontiers' Conditions for Website Use and Copyright Statement, and the applicable CC-BY licence.

ISSN 1664-8714
ISBN 978-2-88963-792-8
DOI 10.3389/978-2-88963-792-8

About Frontiers

Frontiers is more than just an open-access publisher of scholarly articles: it is a pioneering approach to the world of academia, radically improving the way scholarly research is managed. The grand vision of Frontiers is a world where all people have an equal opportunity to seek, share and generate knowledge. Frontiers provides immediate and permanent online open access to all its publications, but this alone is not enough to realize our grand goals.

Frontiers Journal Series

The Frontiers Journal Series is a multi-tier and interdisciplinary set of open-access, online journals, promising a paradigm shift from the current review, selection and dissemination processes in academic publishing. All Frontiers journals are driven by researchers for researchers; therefore, they constitute a service to the scholarly community. At the same time, the Frontiers Journal Series operates on a revolutionary invention, the tiered publishing system, initially addressing specific communities of scholars, and gradually climbing up to broader public understanding, thus serving the interests of the lay society, too.

Dedication to Quality

Each Frontiers article is a landmark of the highest quality, thanks to genuinely collaborative interactions between authors and review editors, who include some of the world's best academicians. Research must be certified by peers before entering a stream of knowledge that may eventually reach the public - and shape society; therefore, Frontiers only applies the most rigorous and unbiased reviews.
Frontiers revolutionizes research publishing by freely delivering the most outstanding research, evaluated with no bias from both the academic and social point of view. By applying the most advanced information technologies, Frontiers is catapulting scholarly publishing into a new generation.

What are Frontiers Research Topics?

Frontiers Research Topics are very popular trademarks of the Frontiers Journals Series: they are collections of at least ten articles, all centered on a particular subject. With their unique mix of varied contributions from Original Research to Review Articles, Frontiers Research Topics unify the most influential researchers, the latest key findings and historical advances in a hot research area! Find out more on how to host your own Frontiers Research Topic or contribute to one as an author by contacting the Frontiers Editorial Office: researchtopics@frontiersin.org

ECOLOGY AND BEHAVIOUR OF FREE-RANGING ANIMALS STUDIED BY ADVANCED DATA-LOGGING AND TRACKING TECHNIQUES

Topic Editors:
Thomas Wassmer, Siena Heights University, United States
Dennis Murray, Trent University, Canada
Stan Boutin, University of Alberta, Canada
Andreas Fahlman, Fundación Oceanogràfic de la Comunitat Valenciana, Spain
Frants Havmand Jensen, Woods Hole Oceanographic Institution, United States

Citation: Wassmer, T., Murray, D., Boutin, S., Fahlman, A., Jensen, F. H., eds. (2020). Ecology and Behaviour of Free-Ranging Animals Studied by Advanced Data-Logging and Tracking Techniques. Lausanne: Frontiers Media SA.
doi: 10.3389/978-2-88963-792-8

Table of Contents

05 ***Editorial: Ecology and Behaviour of Free-Ranging Animals Studied by Advanced Data-Logging and Tracking Techniques***
Thomas Wassmer, Frants Havmand Jensen, Andreas Fahlman and Dennis L. Murray

08 ***Biologging Physiological and Ecological Responses to Climatic Variation: New Tools for the Climate Change Era***
Helen E. Chmura, Thomas W. Glass and Cory T. Williams

17 ***Modeling Tissue and Blood Gas Kinetics in Coastal and Offshore Common Bottlenose Dolphins,*** **Tursiops truncatus**
Andreas Fahlman, Frants H. Jensen, Peter L. Tyack and Randall S. Wells

30 ***Strong Interspecific Differences in Foraging Activity Observed Between Honey Bees and Bumble Bees Using Miniaturized Radio Frequency Identification (RFID)***
Danny F. Minahan and Johanne Brunet

40 ***Movement Patterns of African Elephants (*****Loxodonta africana*****) in a Semi-arid Savanna Suggest That They Have Information on the Location of Dispersed Water Sources***
Yussuf A. Wato, Herbert H. T. Prins, Ignas M. A. Heitkönig, Geoffrey M. Wahungu, Shadrack M. Ngene, Steve Njumbi and Frank van Langevelde

48 ***Flight Behavior of Individual Aerial Insectivores Revealed by Novel Altitudinal Dataloggers***
R. Andrew Dreelin, J. Ryan Shipley and David W. Winkler

55 ***Shallow Torpor Expression in Free-Ranging Common Hamsters With and Without Food Supplements***
Carina Siutz, Viktoria Ammann and Eva Millesi

65 ***Movement and Biosonar Behavior During Prey Encounters Indicate That Male Sperm Whales Switch Foraging Strategy With Depth***
Saana Isojunno and Patrick J. O. Miller

80 ***Swimming Energy Economy in Bottlenose Dolphins Under Variable Drag Loading***
Julie M. van der Hoop, Andreas Fahlman, K. Alex Shorter, Joaquin Gabaldon, Julie Rocho-Levine, Victor Petrov and Michael J. Moore

93 ***Recent Advances in Data Logging for Intertidal Ecology***
Richard Judge, Francis Choi and Brian Helmuth

111 ***Fine-Scale Tracking of Ambient Temperature and Movement Reveals Shuttling Behavior of Elephants to Water***
Maria Thaker, Pratik R. Gupte, Herbert H. T. Prins, Rob Slotow and Abi T. Vanak

123 ***Validation of Dive Foraging Indices Using Archived and Transmitted Acceleration Data: The Case of the Weddell Seal***
Karine Heerah, Sam L. Cox, Pierre Blevin, Christophe Guinet and Jean-Benoît Charrassin

138 ***Using Respiratory Sinus Arrhythmia to Estimate Inspired Tidal Volume in the Bottlenose Dolphin (*Tursiops truncatus*)***
Fabien Cauture, Blair Sterba-Boatwright, Julie Rocho-Levine, Craig Harms, Stefan Miedler and Andreas Fahlman

147 ***Diving Behavior and Fine-Scale Kinematics of Free-Ranging Risso's Dolphins Foraging in Shallow and Deep-Water Habitats***
Patricia Arranz, Kelly J. Benoit-Bird, Ari S. Friedlaender, Elliott L. Hazen, Jeremy A. Goldbogen, Alison K. Stimpert, Stacy L. DeRuiter, John Calambokidis, Brandon L. Southall, Andreas Fahlman and Peter L. Tyack

162 ***Behavioral and Physiological Responses of Scandinavian Brown Bears (*Ursus arctos*) to Dog Hunts and Human Encounters***
Luc Le Grand, Neri H. Thorsen, Boris Fuchs, Alina L. Evans, Timothy G. Laske, Jon M. Arnemo, Solve Sæbø and Ole-Gunnar Støen

171 ***Use of Acceleration and Acoustics to Classify Behavior, Generate Time Budgets, and Evaluate Responses to Moonlight in Free-Ranging Snowshoe Hares***
Emily K. Studd, Melanie R. Boudreau, Yasmine N. Majchrzak, Allyson K. Menzies, Michael J. L. Peers, Jacob L. Seguin, Sophia G. Lavergne, Rudy Boonstra, Dennis L. Murray, Stan Boutin and Murray M. Humphries

185 ***Individual Daily and Seasonal Activity Patterns in Fox Squirrels (*Sciurus niger*) Quantified by Temperature-Sensitive Data Loggers***
Thomas Wassmer and Roberto Refinetti

201 ***Overall Dynamic Body Acceleration in Straw-Colored Fruit Bats Increases in Headwinds but Not With Airspeed***
M. Teague O'Mara, Anne K. Scharf, Jakob Fahr, Michael Abedi-Lartey, Martin Wikelski, Dina K. N. Dechmann and Kamran Safi

213 ***An Arduino-Based RFID Platform for Animal Research***
Eli S. Bridge, Jay Wilhelm, Meelyn M. Pandit, Alexander Moreno, Claire M. Curry, Tyler D. Pearson, Darren S. Proppe, Charles Holwerda, John M. Eadie, Tez F. Stair, Ami C. Olson, Bruce E. Lyon, Carrie L. Branch, Angela M. Pitera, Dovid Kozlovsky, Benjamin R. Sonnenberg, Vladimir V. Pravosudov and Jessica E. Ruyle

223 ***Dynamic-Parameter Movement Models Reveal Drivers of Migratory Pace in a Soaring Bird***
Joseph M. Eisaguirre, Marie Auger-Méthé, Christopher P. Barger, Stephen B. Lewis, Travis L. Booms and Greg A. Breed

237 ***Scales of Blue and Fin Whale Feeding Behavior off California, USA, With Implications for Prey Patchiness***
Ladd M. Irvine, Daniel M. Palacios, Barbara A. Lagerquist and Bruce R. Mate

253 ***Matches and Mismatches Between Seabird Distributions Estimated From At-Sea Surveys and Concurrent Individual-Level Tracking***
Matthew J. Carroll, Ewan D. Wakefield, Emily S. Scragg, Ellie Owen, Simon Pinder, Mark Bolton, James J. Waggitt and Peter G. H. Evans

270 ***Behavioral Biomarkers for Animal Health: A Case Study Using Animal-Attached Technology on Loggerhead Turtles***
Alexandra C. Arkwright, Emma Archibald, Andreas Fahlman, Mark D. Holton, Jose Luis Crespo-Picazo, Vicente M. Cabedo, Carlos M. Duarte, Rebecca Scott, Sophie Webb, Richard M. Gunner and Rory P. Wilson

frontiers in Ecology and Evolution

EDITORIAL
published: 28 April 2020
doi: 10.3389/fevo.2020.00113

Editorial: Ecology and Behaviour of Free-Ranging Animals Studied by Advanced Data-Logging and Tracking Techniques

Thomas Wassmer[1], Frants Havmand Jensen[2], Andreas Fahlman[3] and Dennis L. Murray[4]*

[1] Biology Department, Siena Heights University, Adrian, MI, United States, [2] Biology Department, Woods Hole Oceanographic Institution, Woods Hole, MA, United States, [3] Global Diving Research Inc., Ottawa, ON, Canada, [4] Department of Biology, Trent University, Peterborough, ON, Canada

Keywords: data logger, eco physiology, activity pattern, foraging, movement ecology

Editorial on the Research Topic

Ecology and Behaviour of Free-Ranging Animals Studied by Advanced Data-Logging and Tracking Techniques

OPEN ACCESS

Edited and reviewed by:
Elise Huchard, UMR5554 Institut des Sciences de l'Evolution de Montpellier (ISEM), France

****Correspondence:***
Thomas Wassmer
twassmer@sienaheights.edu; tom@wassmer.org

Specialty section:
This article was submitted to Behavioral and Evolutionary Ecology, a section of the journal Frontiers in Ecology and Evolution

Received: *15 March 2020*
Accepted: *07 April 2020*
Published: *28 April 2020*

Citation:
Wassmer T, Jensen FH, Fahlman A and Murray DL (2020) Editorial: Ecology and Behaviour of Free-Ranging Animals Studied by Advanced Data-Logging and Tracking Techniques. Front. Ecol. Evol. 8:113. doi: 10.3389/fevo.2020.00113

INTRODUCTION

Many details of the behavior, life history and eco-physiology of animals, even among intensively-studied species, remain unknown. Direct observation is a laborious process only amenable for accessible and non-cryptic species, whereas traditional radio telemetry does not directly provide information on the diversity and complexity of animal physiology and behavior. Further, both methods are laborious and/or expensive, and may lead to biased data when physiology and/or behaviors are altered by marking or tracking (Boyer-Ontl and Pruetz, 2014; Nowak et al., 2014; Welch et al., 2018; see also Le Grand et al.). Ultimately, these methods provide only a fragmentary overview of animal behavior patterns during periods when individuals can be readily detected and surveyed while leaving activities during other times obscured. However, the ongoing miniaturization, sensor development, and increased affordability of data logging and advanced telemetric devices offers the potential for continuous and intensive data collection, thereby potentially allowing researchers to more rigorously investigate both physiology and behavior of animals that are difficult to study using traditional observational methods. Owing to these new technologies, we are at the cusp of a truly revolutionary opportunity to address important and longstanding knowledge gaps in animal eco-physiology. To that end, the special section entitled Ecology and Behaviour of Free-Ranging Animals Studied by Advanced Data-Logging and Tracking Techniques includes 22 papers that report on and quantify otherwise hidden aspects of the biology of a variety of mammals, birds, and even invertebrates, across diverse environments including land, water, and air. The highlighted studies focus on fields ranging from basic animal behavior and ecology to eco-physiology; several papers adopt an integrative approach, providing a rather comprehensive understanding of individual time budgets and their implications. Ultimately and collectively, these contributions serve as testament to the drastic improvement in the level of ecological inference that can be derived from research studies involving the use of data-logging and tracking devices that are currently available.

ACTIVITY, MOVEMENT, AND ENERGETICS IN THE WATER

Estimating activity and field metabolic rates (FMR) in wild animals, with the accuracy and precision necessary for development of robust bioenergetic models, is an increasingly high priority in ecology. Because FMR can vary with environmental or life history features, measuring variability in behavior or energetics through space or time is often exceedingly challenging. Further, aquatic systems pose especially vexing problems for the deployment of bio-logging tools and measurement of energy expenditure because of water resistance against externally deployed units. A variety of bio-logging tools have become available for such investigations, for example, monitors can help understand heart rate and lung function (Cauture et al.), or establish a correlation between movement and energy use (Arranz et al.) in marine mammals; such investigations can elucidate the physiological limitations associated with living in an aquatic environment. Further, high-resolution multi-sensor tags (e.g. Johnson and Tyack, 2003) can be used to reveal variation in feeding strategies and dive depths (Isojunno and Miller; Irvine et al.), as well as serve to establish broader-scale assessments of regional variability in food availability (Heerah et al.). Multi-sensor data from different populations can be used to model physiological variation across a species' range (Fahlman et al.), and similar approaches may broadly hold promise for understanding how physiology can vary across changing environments. It is important to note that the increasing popularity of bio-logging tags for investigating physiology, behavior and energetics in marine systems should be accompanied by appropriate validation studies assessing potential energetic impacts of tag placement and design. To this end, van der Hoop et al. showed that swimming behavior of bottlenose dolphins was affected by increasing size of tags through increased metabolic cost due to drag, and we highlight the need for similar studies across a range of species, tag types, and environmental conditions before data derived from bio-logging tags be widely used in bioenergetics models. It follows that bio-logging tools can also be used to inform on animal welfare issues by addressing behavioral changes owing to injury or sickness (Arkwright et al.).

ACTIVITY, MOVEMENT, AND ENERGETICS ON THE GROUND

Bio-logging tools are useful for measuring a variety of behaviors in terrestrial systems and are becoming increasingly important as basis for understanding animal responses to stressors or environmental variability. For example, Le Grand et al. used several different logger types to infer the variability in brown bear physiology and behavior relative to several types of anthropogenic disturbance. Temperature sensors are becoming increasingly popular for studying seasonal activity and energetics in terrestrial mammals. For example, Wassmer and Refinetti used temperature data loggers to describe the variability in daily and seasonal activity patterns among individual fox squirrels. Likewise, temperature sensors in hamsters helped reveal whether dietary supplements could induce changes to the intensity of hibernation and associated metabolic rate (Siutz et al.). Along the same lines, temperature sensors attached to GPS transmitters allowed Thaker et al. to infer elephant movement speeds according to ambient temperature. In another study using telemetry in elephants, Wato et al. interpreted the observed directionality in movements to water sources as evidence of animal memory and spatial cognition. Finally, one aspect of bio-logging that is often overlooked concerns the objective classification of behavioral data derived from these devices, and Studd et al. provide a novel template for the robust classification of snowshoe hare behavior derived from accelerometers.

ACTIVITY, MOVEMENT, AND ENERGETICS IN THE AIR

Flying organisms present a unique set of challenges in terms of assessing behavior and energy expenditure, and several developments in this area have helped establish a better understanding of related costs and consequences. O'Mara et al. used GPS loggers and accelerometers to infer the importance of tailwinds on fruit bat energy expenditure, with the important caveat that it remains difficult to infer how simple measures such as overall dynamic body acceleration (ODBA) can be used to assess energetic costs of flight. This is an important point that highlights the need for additional studies relating measurements derived from bio-logging tools to animal behavior or physiology. However, some novel developments hold promise in the interpretation of behavior of aerial organisms, such as those reported by Dreelin et al. that illustrate how altitudinal dataloggers can help understand differences in flight behavior across bird species. Similarly, Eisaguirre et al. applied a sophisticated modeling approach to telemetry data to assess patterns of variation in golden eagle movement and migration. Likewise, telemetry-based tracking of guillemots and razorbills provided novel insight into their distribution and movement patterns compared to traditional boat-based surveys (Carroll et al., 2019). In an interesting methodological investigation, Bridge et al. showed how the deployment of a new open-source RFID data-logging system could be useful for measuring a variety of behavioral responses in several bird species. Finally, an important point regarding the use of bio-logging tools especially for monitoring small aerial organisms concerns the need for miniaturization to avoid deleterious effects of marking on performance. To this end, Minahan and Brunet show how miniaturized loggers can be used to track foraging activity and movements of a variety of bee species.

NAVIGATING A CHANGING ENVIRONMENT

Bio-logging tools can be used to answer basic ecological questions but perhaps their greatest promise relates to establishing important baseline values for behavior and physiology. These baseline values will be critical to understand how animals may respond to future environmental change and can help provide

means for mitigation. Indeed, in their mini review, Chmura et al. highlight the potential use of such technology for detecting, understanding, and forecasting species responses to climate change. Finally, in a general overview Judge et al. reviewed how recent advances in temperature logging reveal thermal stress in a variety of organisms inhabiting the intertidal zone and likely facing dire threats from climate change.

CONCLUSION AND FUTURE CHALLENGES

The variety and novelty of contributions presented in this Research Topic provides an important overview of the many opportunities offered by new technologies in bio-logging. We anticipate that in the next decades existing devices will be refined and further miniaturized, new devices will be developed with added opportunities for understanding animal behavior and physiology, and new tools will become available for analysis of the large amount of data that are collected by these devices. Doubtless, these developments present tremendous opportunities for advancing our understanding of animal performance and responses to environmental change. However, we conclude by offering the important caution that successful application of these devices for addressing basic and applied questions in ecology relies on their proper validation. Indeed, the success of bio-logging tools in providing robust ecological inference depends on the implementation of systematic companion studies that validate their use, as well as additional studies focusing on the proper interpretation of the data that they yield. We consider it as crucial for researchers to resist applying new technologies and analytical tools without the requisite validation studies and system stress tests in controlled settings. How might bio-logging devices affect animal behavior or physiology? What are the best size, shape and attachment methods to minimize impacts? Do all individuals respond similarly to such devices? How well can data from bio-loggers serve as proxies for animal features of interest such as behavior, physiology or energetics? How can we best analyze data derived from a particular type of device? These are important questions that will serve as the foundation for successful application of bio-logging tools in the future, and they can best be answered through close interaction and collaboration between researchers, device manufacturers, and data analysts. Ultimately, we are optimistic that with this proper foundation bio-logging will continue to revolutionize our understanding of animal ecology and how individuals, populations, and species respond to a changing environment.

AUTHOR CONTRIBUTIONS

TW initiated the Research Topic and recruited the other authors as editors, along with Stan Boutin, who is not listed as author on the present paper. TW wrote the first draft of this editorial, with contributions from coauthors. All 5 editors helped develop the Research Topic and contributed to its editorial process.

ACKNOWLEDGMENTS

We wish to thank all authors and reviewers of this Research Topic for their contributions.

REFERENCES

Boyer-Ontl, K. M., and Pruetz, J. D. (2014). Giving the forest eyes: the benefits of using camera traps to study unhabituated chimpanzees (*Pan troglodytes* verus) in Southeastern Senegal. *Int. J. Primatol.* 35, 881–894. doi: 10.1007/s10764-014-9783-3

Carroll, M. J., Wakefield, E. D., Scragg, E. S., Owen, E., Pinder, S., Bolton, M., et al. (2019). Matches and mismatches between seabird distributions estimated from at-sea surveys and concurrent individual-level tracking. *Front. Ecol. Evol.* 7:333. doi: 10.3389/fevo.2019.00333

Johnson, M. P., and Tyack, P. L. (2003). A digital acoustic recording tag for measuring the response of wild marine mammals to sound. *IEEE J. Oceanic Eng.* 28, 3–12. doi: 10.1109/JOE.2002.808212

Nowak, K., le Roux, A., Richards, S. A., Scheijen, C. P. J., and Hill, R. A. (2014). Human observers impact habituated samango monkeys' perceived landscape of fear. *Behav. Ecol.* 25, 1199–1204. doi: 10.1093/beheco/aru110

Welch, R. J., le Roux, A., Petelle, M. B., and Périquet, S. (2018). The influence of environmental and social factors on high- and low-cost vigilance in bat-eared foxes. *Behav. Ecol. Sociobiol.* 72:29. doi: 10.1007/s00265-017-2433-y

Conflict of Interest: The authors declare that the research was conducted in the absence of any commercial or financial relationships that could be construed as a potential conflict of interest.

Copyright © 2020 Wassmer, Jensen, Fahlman and Murray. This is an open-access article distributed under the terms of the Creative Commons Attribution License (CC BY). The use, distribution or reproduction in other forums is permitted, provided the original author(s) and the copyright owner(s) are credited and that the original publication in this journal is cited, in accordance with accepted academic practice. No use, distribution or reproduction is permitted which does not comply with these terms.

frontiers in Ecology and Evolution

MINI REVIEW
published: 03 July 2018
doi: 10.3389/fevo.2018.00092

Biologging Physiological and Ecological Responses to Climatic Variation: New Tools for the Climate Change Era

Helen E. Chmura[1,2], *Thomas W. Glass*[3,4] *and Cory T. Williams*[2,3]*

[1] Department of Neurobiology, Physiology and Behavior, University of California, Davis, Davis, CA, United States, [2] Institute of Arctic Biology, University of Alaska Fairbanks, Fairbanks, AK, United States, [3] Department of Biology and Wildlife, University of Alaska Fairbanks, Fairbanks, AK, United States, [4] Arctic Beringia Program, Wildlife Conservation Society, Fairbanks, AK, United States

In this mini-review, we discuss how biologging technology can be used to detect, understand, and forecast species' responses to climate change. We review studies of phenology, thermal biology, and microhabitat selection as examples to illustrate the utility of a biologging approach in terrestrial and aquatic species. These examples show that biologgers can be used to identify and predict behavioral and physiological responses to climatic variation and directional climate change, as well as to extreme weather events. While there is still considerable debate as to whether phenotypic plasticity is sufficient to facilitate species' responses to climate change or whether responses to short-term climate variability are predictive of climate change response, understanding the scope and nature of plasticity is an important step toward answering these questions. One advantage of the biologging approach is that it can facilitate the measurement of traits at the level of the individual, permitting research that investigates the degree to which physiology and behavior are plastic. As such, combining biologging with metrics of fitness can provide insight into how plasticity might confer population and species resilience to climate change. Increased use of biologgers in experimental manipulations will also yield important insight into how phenotypic flexibility allows some animals to mitigate the negative consequences of climate change. Although biologging studies to date have mostly functioned in measuring phenotypic responses to short-term climate variability, we argue that integrating biologging technology into long-term monitoring programs will be instrumental in documenting and understanding ecological responses to climate change.

Keywords: phenology, microhabitat selection, thermal biology, biologger, climate change

OPEN ACCESS

Edited by:
Thomas Wassmer, Siena Heights University, United States

Reviewed by:
Daniela Campobello, Università degli Studi di Palermo, Italy
Simon Verhulst, University of Groningen, Netherlands
Graeme Clive Hays, Deakin University, Australia

****Correspondence:***
Cory T. Williams
ctwilliams@alaska.edu

Specialty section:
This article was submitted to Behavioral and Evolutionary Ecology, a section of the journal Frontiers in Ecology and Evolution

Received: *19 December 2017*
Accepted: *11 June 2018*
Published: *03 July 2018*

Citation:
Chmura HE, Glass TW and Williams CT (2018) Biologging Physiological and Ecological Responses to Climatic Variation: New Tools for the Climate Change Era. Front. Ecol. Evol. 6:92. doi: 10.3389/fevo.2018.00092

INTRODUCTION

Global climate change is rapidly affecting ecosystems worldwide by altering species' ranges, disrupting trophic interactions, and causing population declines. In addition to causing a rise in global mean temperatures and altering precipitation patterns (IPCC, 2014), anthropogenic climate change is affecting the frequency of climate events (e.g., El Niño and La Niña; Cai et al., 2014, 2015) and is predicted to increase the frequency and severity of extreme events (US Global Change Research Program, 2009; Holland and Bruyère, 2014). Understanding and

predicting how these changes in the abiotic environment will alter ecosystems requires studying biological processes at multiple levels of organization, including within-individual physiological and behavioral adjustments (i.e., plasticity).

Detecting changes in species distribution and abundance with climate change requires long-term sampling. However, short-term observations of individual responses to climatic variation are often used as a proxy to predict consequences of long-term directional climate change. While there is still considerable debate regarding the relative contributions of phenotypic plasticity and evolution in climate change responses, and questions as to whether existing phenotypic plasticity is sufficient to respond to global climate change, understanding the scope of phenotypic plasticity in free-living animals is an important step toward resolving these debates (Merilä and Hendry, 2014). We argue that biologging individual responses to climate variability will likely be informative in developing predictions for climate change response, however it is important to acknowledge that climate change will affect biotic interactions across trophic levels and it is critical to take these possibilities into account when predicting species responses to climate change (Van der Putten et al., 2010). Unfortunately, direct observations of individual responses to climatic variation are often infeasible when individuals have large home ranges or use inaccessible environments. Even when individuals can be observed directly, some responses are cryptic and hard to observe using traditional methods. Although responses to manipulations of the physical or biological environment can be measured in laboratory or in semi-natural settings, these environments cannot reproduce the complexity of natural systems (Van der Putten et al., 2010). Biologging, the use of miniaturized animal-borne devices that log and/or relay data regarding an animal's movements, behavior, physiology and/or environment, offers a solution to these challenges (Rutz and Hays, 2009; **Table 1**). Biologgers can be deployed on free-living animals for extended periods and, when combined with monitoring of abiotic conditions, allow the detection of individual responses to biologically relevant environmental variation. With careful study design, they can also be used to quantify individual, population, and species-level variability in response to short-term climatic variation and long-term climate change. When deployed with experimental manipulations, they can reveal causal mechanisms. As such, they are an important tool in the climate change biologist's toolkit.

In this mini-review, we show what biologging can offer climate change research by featuring case studies of phenology, thermal biology, and microhabitat selection. We focus on how biologging technology has extended our ability to measure the responses of free-ranging subjects to climatic variability, while highlighting the few studies that have documented responses to long-term directional climate change. Finally, we suggest how biologging could be utilized to advance the discipline.

PHENOLOGY

Phenological shifts are widely documented responses to global climate change (Parmesan, 2007; Thackeray et al., 2010) and their potential to disrupt trophic interactions (Visser et al., 1998; Winder and Schindler, 2004; Post and Forchhammer, 2008) has led to concern that phenological mismatch may cause population declines (Both et al., 2010). Biologging can improve understanding of phenological responses to climate change by facilitating detection of cryptic seasonally-recurring life-cycle events (e.g., migration, hibernation, and reproduction) and study of the cues and proximate physiological mechanisms that regulate these transitions.

Novel applications of biologging are expanding as technological advances produce smaller devices with improved sensors, storage, and transmission capabilities. For example, temperature, activity, and/or GPS loggers are used to create precise timelines for implantation and/or parturition in a wide variety of mammals including brown bears *(Ursus arctos)* (**Figure 1A**; **Table 1**), woodland caribou *(Rangifer tarandus caribou),* sea otters *(Enhydra lutris),* and arctic ground squirrels *(Urocitellus parryii)* (Williams et al., 2011; Demars et al., 2013; Esslinger et al., 2014; Friebe et al., 2014; Bieber et al., 2017). GPS and light loggers can detect migration phenology in animals traveling on land, in water, or by air (Yasuda et al., 2010; Bailleul et al., 2012; Van Wijk et al., 2012; Lendrum et al., 2013; Cherry et al., 2016; Weller et al., 2016). In combination, temperature and light loggers can be used to identify dates of hibernation onset and termination in conjunction with immergence and emergence from dens or burrows (**Figure 1B**; Williams et al., 2011, 2017; Friebe et al., 2014). Since miniaturized biologging is a new tool, long-term phenological records collected from biologgers are sparse. However, shifts in timing have been identified in longitudinal studies in larger species (e.g., Bailleul et al., 2012; Hauser et al., 2017). For example, satellite telemetry data collected between 1993 and 2012 indicate that the Chukchi population of beluga whales *(Delphinapterus leucas)* are responding to later sea-ice formation by delaying autumn migration to the Bering Sea, while migration timing for the Beaufort population is not clearly related to freeze-up and remains unchanged (Hauser et al., 2017).

Biologging and environmental data can also be combined to study the environmental cues that regulate phenological timing, allowing the prediction of responses under different climate change scenarios. For example, alignment of GPS collar migration data from polar bears (*Ursus maritimus*) with sea-ice extent data indicates that movement from ice to land is sensitive to local changes in sea-ice cover (Cherry et al., 2016). Similarly, bird migration can be delayed by extreme cold (Briedis et al., 2017) or drought (Tøttrup et al., 2012). These studies highlight the importance of explicitly addressing the role of extreme events in predictive models that assess the impacts of gradual long-term global warming on phenology.

A robust understanding of how environmental cues shape phenology will improve predictions of the extent to which plasticity will facilitate continued phenological adjustment to climate change. For example, biologging of body temperature (T_b) in the arctic ground squirrel has revealed sex differences in phenological flexibility: females extend hibernation in response to late spring snow whereas reproductive males do not (**Figure 1B**; Williams et al., 2017). Biologging has also uncovered migratory plasticity in response to environmental variation on wintering grounds (e.g., Ouwehand and Both, 2017) and along migratory corridors (e.g., Van Wijk et al., 2012). A novel analysis

TABLE 1 | Examples of biologgers frequently used in phenological studies, the research opportunities they provide, and trade-offs to be considered in their deployment.

Sensor type	Examples of use in phenology studies	Opportunities for use	Trade-offs
Satellite-based tracking- Global Positioning Systems (GPS) and Advanced Research and Global Observation Satellite (ARGOS)	Sea-ice affects migratory timing in beluga whales (Bailleul et al., 2012; Hauser et al., 2017) and polar bears (Cherry et al., 2016). Snowpack/snowmelt influence migration in mule deer (Lendrum et al., 2013) and white-fronted geese (Van Wijk et al., 2012).	The impact of climate change has been identified as a key question in movement studies (Hays et al., 2016). Transmitters permit data collection without animal recapture/device recovery. Access to transmitted animal location data allows visitation of clusters to assess/confirm behaviors, such as predation events (Knopff et al., 2009) and pup-rearing (Jacobs and Ausband, 2018), or to collect measurements from ephemeral habitat (e.g., sea ice or snow pack conditions).	GPS has higher accuracy than ARGOS for positioning, but ARGOS and other satellite networks may be used for GPS data recovery and/ or transfer (Tomkiewicz et al., 2010). Transmitters require larger/heavier batteries, which limits deployment on small species. Minimally-invasive external attachment approaches need to be weighed against the potential reduction of negative effects that can be achieved through implantation (Bodey et al., 2018).
Light logger (geolocator)	Delayed arrival can reflect later departure from wintering grounds (pied flycatchers; Ouwehand and Both, 2017) or encountering inclement weather en route (semi-collared flycatcher; Briedis et al., 2017).	Small size allows deployment on a wide variety of species, including songbirds. Light loggers can also be used to measure time above-ground or out-of-nest during daylight hours (Williams et al., 2014).	Data coarser than GPS and recapture is required to download. External attachment required. Negative effects higher for aerial foragers and devices affixed to leg bands (Costantini and Møller, 2013). Drag can be an issue, particularly for wing harness (vs. leg-loop harness; Bowlin et al., 2010).
Temperature logger	Pregnant hoary bats re-enter hibernation during late spring snow storms (Willis et al., 2006). Gestation and parturition detected in hibernating brown bear, particularly when used in combination with accelerometry (Friebe et al., 2014).	Parturition can be identified in a variety of species (Ewbank, 1969; Williams et al., 2011; Esslinger et al., 2014). Core body temperature can be used to identify unsuccessful pregnancies in lab mice (Smarr et al., 2016), though whether this approach is viable in free-living animals is unknown.	Skin and/or subcutaneous temperature will not always reflect core temperature (Rey et al., 2016; Theimer et al., 2017).
Accelerometer	Timing of nocturnal migratory flights documented in songbirds (Bäckman et al., 2017). Influence of seasonal dynamics of resource availability and weather on activity patterns assessed in giant pandas (Zhang et al., 2017).	Dead reckoning theoretically possible when paired with gyroscope and magnetometers. A useful proxy for energy expenditure in terrestrial animals (Halsey et al., 2009) and can measure total and/or activity specific energy expenditures in marine mammals when linked to time activity budgets (Jeanniard-du-Dot et al., 2017).	High frequency (10–25 Hz) logging limits deployment duration due to battery and/or memory limitations such that implantable devices are less feasible; devices with remote download and/or inductive charge not yet available.
Pressure gauges (depth recorder)	Japanese flounder migrate from bay to open sea to provide optimal temperature for eggs (Yasuda et al., 2010). Spawning identified using pop-up satellite tags in halibut (Le Bris et al., 2017).	Frequently used in combination with temperature and salinity sensors to remotely monitor ocean conditions (e.g., Charrassin et al., 2002).	Although understudied, premature tag loss, reduced swimming capacity, and increased predation can be issues for pop-up satellite archival tags (Jepsen et al., 2015).
Heart rate	Seasonal changes in heart rate are caused by photoperiod-induced changes of endogenous heat production in graylag geese (Wascher et al., 2018). Spring increase in heart rate is delayed by nutritional restriction in red deer (Turbill et al., 2011).	Frequently used to estimate daily energy expenditure but requires species-level calibration (Elliott, 2016).	Leadless subcutaneous and intraperitoneal options (e.g., Chaise et al., 2017). Non-surgical ruminal units transmit data via UHF link to a repeater system located in a collar unit, where it is stored (Signer et al., 2010).

by Schmaljohann and Both (2017) used avian migratory tracks to estimate changes in arrival timing attributable to plasticity in migratory speed. They found that plasticity in migratory speed alone is unlikely to explain observed changes in arrival and suggested that changes in departure timing from wintering grounds, possibly due to evolution, may be responsible.

THERMAL BIOLOGY

Biologging allows measurement of how thermal biology influences species performance and fitness (and thus range) in an era of climate change, as well as how organisms respond to thermal extremes and natural disasters.

Ectotherms: Connecting Performance and Species' Ranges

Ectotherms are particularly vulnerable to climate change due to the high thermal sensitivity of their metabolism, physiology, and life-history traits (Deutsch et al., 2008; Paaijmans et al., 2013). This sensitivity is reflected in thermal response curves which describe how trait performance is influenced by operative temperature (T_{op}), a measure of the thermal

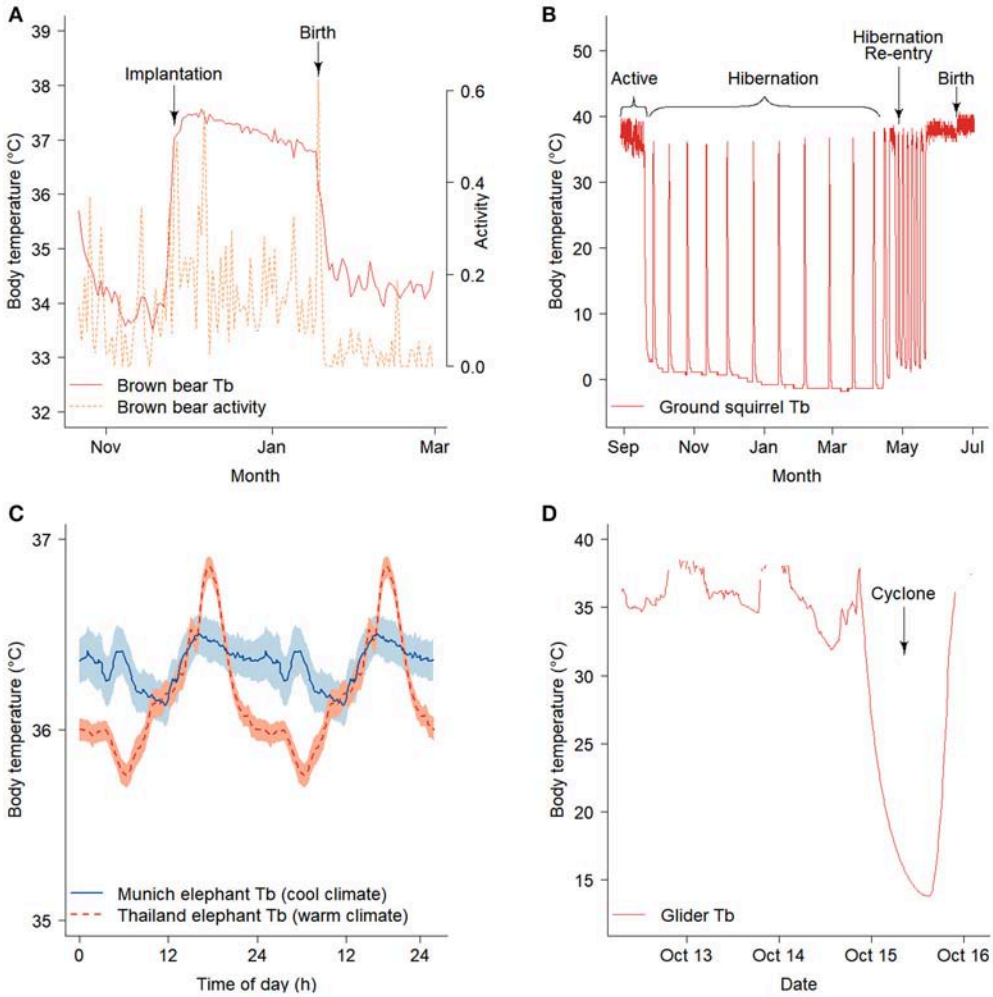

FIGURE 1 | Data collected using biologgers can potentially be used to describe climate-driven changes in the phenology and/or occurrence of reproduction. **(A)** Elevated body temperatures and activity indicate implantation and gestation in female brown bears with an additional a peak in activity characterizing parturition (Friebe et al., 2014). **(B)** Female arctic ground squirrels re-enter hibernation and show unusually late and short bouts of torpor in response to late spring snow storms resulting in delayed parturition (Williams et al., 2017). Biologgers also show the thermal response of animals to extreme events. **(C)** Asian elephants in a warm environment depressed body temperature during the cooler periods of the day to provide a thermal reserve for high temperatures later in the day (shading represents mean +/− s.e.m) (Weissenbock et al., 2012). **(D)** A sugar glider enters torpor while experiencing heavy rains and high winds during a Category 1 cyclone (Nowack et al., 2015). Figures redrawn with permission.

environment that integrates convective and radiative heat transfer on a scale relevant to an animal's microhabitat (Sinclair et al., 2016). Biologging permits the assessment of how environmental changes influence thermal performance, and consequently alter species' distributions. For example, Gannon et al. (2014) used accelerometers to gauge performance in free-living dusky flathead (*Platycephalus fuscus*) and showed that the temperature-dependence of performance likely limits the biogeography of this predatory fish. Using the same approach, Payne et al. (2016) demonstrated that warming tolerance is lower in species with more tropical range limits, consistent with captive studies that indicate low-latitude fishes are more sensitive to ocean warming than species that occupy higher-latitudes (Rummer et al., 2014). The shape of performance curves, however, may differ among traits and thus accelerometry alone cannot provide a complete understanding of how warming will influence biogeography. Heart rate predicts the thermal dependence of metabolism better than activity (Clark et al., 2010), suggesting a role for additional sensors in understanding how thermal limits and performance influence range shifts. Additionally, biologgers may play a crucial role in quantifying changes in thermal performance through acclimatization (i.e., physiological flexibility) and/or developmental plasticity, as well as documenting genetic variation in thermal performance (Kingsolver, 2009; Gaitán-Espitia et al., 2014), which are key aspects of population and species resilience to environmental change (Somero, 2010; Seebacher et al., 2015).

Endotherms: Responding to Aridity and Thermal Extremes

Given the indirect relationship between operative temperature and metabolism in endotherms, they are thought to be somewhat buffered from the direct effects of increasing temperatures (Khaliq et al., 2014). Nevertheless, endotherms in hot arid environments may be vulnerable to climate change since increases in temperature or aridity can cause dehydration from evaporative cooling and overwhelm heat dissipation capacity. Indeed, temperature and aridity can have sublethal fitness costs and even cause direct mortality in birds and mammals (Speakman and Krol, 2010; Du Plessis et al., 2012). Biologging facilitates the measurement of the physiological and behavioral responses endotherms use to cope with high temperatures and aridity, as well as the identification of physiological limits that may shape responses to climate change.

Endotherms that maintain relatively constant T_b (i.e., "homeotherms") can cope with hot arid conditions by deviating from homeothermy. Captive studies indicate that small birds reduce water loss under hot conditions by becoming hyperthermic, reducing the differential between T_b and T_{op} (reviewed in Tieleman and Williams, 1999). Although it has long been hypothesized that desert birds should facilitate passive heat loss and conserve water loss by maintaining a higher T_b set-point (Withers and Williams, 1990), a compilation of laboratory data from 28 species failed to find a difference in the thermal responses of desert and non-desert species (Tieleman and Williams, 1999). However, a recent field-based biologging study by Smit et al. (2013) found that even within a species, desert-dwelling birds have higher T_b set-points than individuals from a population in a wetter, semi-desert region. This highlights the utility of the biologging approach, as the physiology of animals in laboratory conditions may not be representative of physiology in nature.

Biologging studies reveal that large mammals also exhibit hyperthermia in response to high temperatures and aridity. However, unlike small mammals, large mammals benefit from a lower daily minimum T_b as their larger size provides them with high thermal inertia, which creates a thermal reserve for heat storage (reviewed in Hetem et al., 2016). Later in the day, animals allow T_b to rise, reducing water loss by decreasing the differential between T_b and T_{op}. This pattern is particularly extreme in oryx (*Oryx leucoryx*), which alter T_b by more than 4°C across the day in summer but only 1.5°C in winter (Ostrowski et al., 2003; Hetem et al., 2010), although it is also evident in Asian elephants (*Elephas maximus*; **Figure 1C** Weissenbock et al., 2012). In addition to changes in core T_b, some endotherms selectively cool regions of the brain (Midtgård, 1983; Mitchell et al., 2002; Fuller et al., 2016). Although initially demonstrated under laboratory conditions and interpreted as an adaptation to reduce the negative effects of heat stress, technological advancements that allowed blood and brain temperatures to be measured in free-living ungulates demonstrated that selective brain cooling reduces evaporative water loss, rather than preventing hyperthermia (Jessen et al., 1994; Mitchell et al., 1997; Fuller et al., 2007). In sum, biologging T_b in free-living endotherms has already provided insight into the physiological mechanisms that may allow some species to cope with increased temperatures associated with climate change. For most species, however, the physiological limits to warming are not well described and more work is needed to link utilization of heterothermy to fitness consequences in free-living populations.

Endotherms: Responding to Natural Disasters

Climate change is increasing mean temperature, as well climatic variation, leading to more frequent extreme temperature and precipitation events and natural disasters (Easterling et al., 2000; Alexander et al., 2006; Mitchell et al., 2006). Biologging has revealed that heterothermic endotherms (i.e., those that use daily torpor and/or hibernation; Ruf and Geiser, 2015) can depress their metabolism to buffer themselves from unpredictable energetic bottlenecks and/or natural disasters (Nowack et al., 2017). For example, small mammals can substantially reduce their energy consumption following late spring snowstorms, cyclones, or wildfire by entering torpor (**Figure 1D**; Willis et al., 2006; Nowack et al., 2015, 2016; Stawski et al., 2015). Thus, biologging indicates that facultative torpor and/or hibernation may buffer some endotherms from extreme events, analogous to how facultative migrations are used in other species (Streby et al., 2015).

MICROHABITAT SELECTION

Microclimates can provide animals with a wider range of environmental temperatures than are available on a macroclimatic scale (Scheffers et al., 2014) and utilization of microhabitats through behavioral thermoregulation may provide a means for some species to cope with climate change. Biologging allows direct measurement of an animal's experienced environment which can be compared with remotely sensed data of available habitat to investigate how microclimates influence species' ranges. For example, biologged T_b and ambient temperature (T_a) coupled with spatial telemetry data have revealed that habitat use at northern range limits is thermally constrained for a variety of ectotherms including wood turtles (*Glyptemys insculpta*; Dubois et al., 2009), loggerhead turtles (*Caretta caretta*; Schofield et al., 2009), and black rat snakes (*Elaphe obsoleta obsolete*; Blouin-Demers and Weatherhead, 2002). Such studies have the potential to reveal how microhabitat availability and selection influence species' ranges under climate change. To date however, long-term biologging studies that span wide latitudinal gradients are lacking, limiting our understanding of the factors influencing range shifts under climate change.

Ectotherms and endotherms may cope with climate change through the exploitation of spatiotemporal variation in temperature within existing home-ranges. Recent biologging studies reveal that ectotherms can partition daily and seasonal activities across thermally variable microhabitats to alter metabolic rate (e.g., Dubois et al., 2009; Harrison et al., 2016). For example, blacktip reef sharks (*Carcharhinus melanopterus*)

are warmest, but least active, during the day as they move into warm water to increase rates of digestion; they peak in activity while cooling in evenings, since they forage when they have a sensory advantage under low light conditions and a thermal advantage over prey with lower thermal inertia (Papastamatiou et al., 2015). Similarly, biologging in terrestrial birds and small mammals indicates they utilize thermal refugia during periods of high heat and partition demanding activities, such as foraging, to cooler times of day when risk of dehydration is lower (e.g., Martin et al., 2015; Levy et al., 2016). Microhabitat partitioning across the day may be important as climate change is having different effects on daytime and nighttime temperatures (Easterling et al., 1997).

Microhabitat partitioning can also occur on seasonal time-scales. For example, biologgers revealed that female loggerhead turtles seek out warm water areas to accelerate egg development (Fossette et al., 2012). During winter, collar-mounted temperature loggers have been used to investigate the use of nests and burrows as refugia from cold temperatures and harsh winds in red squirrels *(Tamiasciurus hudsonicus*; Studd et al., 2016) and opossums *(Didelphis virginiana*; Kanda et al., 2005). In female polar bears, biologgers were used to both identify incidences of reproductive denning and characterize the microhabitats and substrates preferred by bears for denning, the availability of which may be altered by climate change and human development (Olson et al., 2017). The continued miniaturization of biologgers will open new avenues of research. For example, while nest cavity microclimate variation is known to be an important determinant of nestling growth and survival (Catry et al., 2011; Campobello et al., 2017), biologging may prove useful in understanding how micro-climate influences adult physiology and incubation/provisioning behaviors or nestling post-fledging behavior/survival (e.g., Nord and Nilsson, 2011).

A NOTE OF CAUTION

Despite the power and potential of biologging for monitoring responses to climatic variability/change, serious consideration must be given to its potential to alter the physiological and/or behavioral parameters being measured, or negatively affect the survival and reproductive output of the tagged individual (White et al., 2013; Bodey et al., 2018). Careful consideration must be given to the size, mass, shape, buoyancy, and attachment method of the device, balancing the ecological insight that is provided with the potential deleterious effects (Wilson et al., 2015). Further, researchers need to weigh the benefits of using minimally-invasive external attachment approaches with the potential reduction in negative effects that can be achieved through implantation (Bodey et al., 2018).

CONCLUSION AND FUTURE DIRECTIONS

Biologging is broadly useful for investigating individual, population, and species responses to global climate change, including changes in the frequency of extreme climatic events. Although by no means an exhaustive review, the studies of phenology, thermal biology, and microhabitat selection that we discuss illustrate how biologging approaches can be used to uncover both physiological and behavioral responses to climate change. In cases where longitudinal data are not yet available, biologging studies have already made important contributions to the field by linking environmental variation to alterations in physiology and behavior, which facilitates predictions of climate change response. We caution, however, that predictions may fail if they are based solely on the direct effects of climate variability on individual species, as fitness is strongly influenced by interactions between species (Gilman et al., 2010).

We propose that biologging can contribute further to the field by addressing knowledge gaps and providing new methodological approaches. Research opportunities include (1) connecting biologged behavioral and physiological responses to fitness outcomes, (2) quantifying variation in behavioral and physiological responses across individuals, populations, and species for use in predictive models of plastic and evolutionary responses to climate change, and (3) increasing the use of biologgers in field-based experiments to determine the physiological mechanisms that underlie observed responses to climate variation. With the increasing miniaturization of biologgers, deployment in an ever-growing breadth of taxa, and maturation of longitudinal biologging datasets, we predict that biologging will continue to influence the study of global climate change.

AUTHOR CONTRIBUTIONS

All authors contributed to the review through development of ideas, drafting of initial text, and providing feedback for revisions. HC coordinated revisions amongst authors and prepared figures and CW initiated the project.

ACKNOWLEDGMENTS

CW acknowledges funding from the National Science Foundation grant (IOS-1558056). HC acknowledges salary support from the UC Davis Animal Behavior Graduate Group and an Institutional Development Award (IDeA) from the National Institute of General Medical Sciences of the National Institutes of Health under grant number P20GM103395. The content is solely the responsibility of the authors and does not necessarily reflect the official views of the NIH or NSF.

REFERENCES

Alexander, L. V., Zhang, X., Peterson, T. C., Caesar, J., Gleason, B., Tank, A., et al. (2006). Global observed changes in daily climate extremes of temperature and precipitation. *J. Geophys. Res. Atmosph.* 111:22. doi: 10.1029/2005JD006290

Bäckman, J., Andersson, A., Alerstam, T., Pedersen, L., Sjöberg, S., Thorup, K., et al. (2017). Activity and migratory flights of individual free-flying songbirds throughout the annual cycle: method and first case study. *J. Avian. Biol.* 48, 309–319. doi: 10.1111/jav.01068

Bailleul, F., Lesage, V., Power, M., Doidge, D. W., and Hammill, M. O. (2012). Migration phenology of beluga whales in a changing Arctic. *Clim. Res.* 53, 169–178. doi: 10.3354/cr01104

Bieber, C., Cornils, J. S., Hoelzl, F., Giroud, S., and Ruf, T. (2017). The costs of locomotor activity? Maximum body temperatures and the use of torpor during the active season in edible dormice. *J. Comp. Physiol. B* 187, 803–814. doi: 10.1007/s00360-017-1080-y

Blouin-Demers, G., and Weatherhead, P. J. (2002). Habitat-specific behavioural thermoregulation by black rat snakes (Elaphe obsoleta obsoleta). *Oikos* 97, 59–68. doi: 10.1034/j.1600-0706.2002.970106.x

Bodey, T. W., Cleasby, I. R., Bell, F., Parr, N., Schultz, A., Votier, S. C., et al. (2018). A phylogenetically controlled meta-analysis of biologging device effects on birds: Deleterious effects and a call for more standardized reporting of study data. *Methods Ecol. Evol.* 9, 946–955. doi: 10.1111/2041-210X.12934

Both, C., Van Turnhout, C. A. M., Bijlsma, R. G., Siepel, H., Van Strien, A. J., and Foppen, R. P. B. (2010). Avian population consequences of climate change are most severe for long-distance migrants in seasonal habitats. *Proc. R. Soc. B* 277, 1259–1266. doi: 10.1098/rspb.2009.1525

Bowlin, M. S., Henningsson, P., Muijres, F. T., Vleugels, R. H., Liechti, F., and Hedenström, A. (2010). The effects of geolocator drag and weight on the flight ranges of small migrants. *Methods Ecol. Evol.* 1, 398–402. doi: 10.1111/j.2041-210X.2010.00043.x

Briedis, M., Hahn, S., and Adamik, P. (2017). Cold spell en route delays spring arrival and decreases apparent survival in a long-distance migratory songbird. *BMC Ecol.* 17:8. doi: 10.1186/s12898-017-0121-4

Cai, W., Borlace, S., Lengaigne, M., Van Rensch, P., Collins, M., Vecchi, G., et al. (2014). Increasing frequency of extreme El Niño events due to greenhouse warming. *Nat. Clim. Chang.* 4, 111–116. doi: 10.1038/nclimate2100

Cai, W., Wang, G., Santoso, A., Mcphaden, M. J., Wu, L., et al. (2015). Increased frequency of extreme La Niña events under greenhouse warming. *Nat. Clim. Chang.* 5, 132–137. doi: 10.1038/nclimate2492

Campobello, D., Lindstrom, J., Di Maggio, R., and Sarà, M. (2017). An integrated analysis of micro- and macro-habitat features as a tool to detect weather-driven constraints: a case study with cavity nesters. *PLoS ONE* 12:e0174090. doi: 10.1371/journal.pone.0174090

Catry, I., Franco, A. M. A., and Sutherland, W. J. (2011). Adapting conservation efforts to face climate change: modifying nest-site provisioning for lesser kestrels. *Biol. Cons.* 144: 1111–1119. doi: 10.1016/j.biocon.2010.12.030

Chaise, L. L., Paterson, W., Laske, T. G., Gallon, S. L., McCafferty, D. J., Théry, M., et al. (2017). Implantation of subcutaneous heart rate data loggers in southern elephant seals (*Mirounga leonina*). *Polar Biol.* 40, 2307–2312. doi: 10.1007/s00300-017-2144-x

Charrassin, J. B., Park, Y. H., Maho, Y. L., and Bost, C. A. (2002). Penguins as oceanographers unravel hidden mechanisms of marine productivity. *Ecol. Lett.* 5, 317–319. doi: 10.1046/j.1461-0248.2002.00341.x

Cherry, S. G., Derocher, A. E., and Lunn, N. J. (2016). Habitat-mediated timing of migration in polar bears: an individual perspective. *Ecol. Evol.* 6, 5032–5042. doi: 10.1002/ece3.2233

Clark, T. D., Sandblom, E., Hinch, S. G., Patterson, D. A., Frappell, P. B., and Farrell, A. P. (2010). Simultaneous biologging of heart rate and acceleration, and their relationships with energy expenditure in free-swimming sockeye salmon (Oncorhynchus nerka). *J. Comp. Physiol. B Biochem. Syst. Environ. Physiol.* 180, 673–684. doi: 10.1007/s00360-009-0442-5

Costantini, D., and Møller, A. P. (2013). A meta-analysis of the effects of geolocator application on birds. *Curr. Zool.* 59, 697–706. doi: 10.1093/czoolo/59.6.697

Demars, C. A., Auger-Méth,é, M., Schlägel, U. E., and Boutin, S. (2013). Inferring parturition and neonate survival from movement patterns of female ungulates: a case study using woodland caribou. *Ecol. Evol.* 3, 4149–4160. doi: 10.1002/ece3.785

Deutsch, C. A., Tewksbury, J. J., Huey, R. B., Sheldon, K. S., Ghalambor, C. K., Haak, D. C., et al. (2008). Impacts of climate warming on terrestrial ectotherms across latitude. *Proc. Natl. Acad. Sci. U.S.A.* 105, 6668–6672. doi: 10.1073/pnas.0709472105

Du Plessis, K. L., Martin, R. O., Hockey, P. A. R., Cunningham, S. J., and Ridley, A. R. (2012). The costs of keeping cool in a warming world: implications of high temperatures for foraging, thermoregulation and body condition of an arid-zone bird. *Glob. Change Biol.* 18, 3063–3070. doi: 10.1111/j.1365-2486.2012.02778.x

Dubois, Y., Blouin-Demers, G., Shipley, B., and Thomas, D. (2009). Thermoregulation and habitat selection in wood turtles *Glyptemys insculpta*: chasing the sun slowly. *J. Anim. Ecol.* 78, 1023–1032. doi: 10.1111/j.1365-2656.2009.01555.x

Easterling, D. R., Horton, B., Jones, P. D., Peterson, T. C., Karl, T. R., Parker, D. E., et al. (1997). Maximum and minimum temperature trends for the globe. *Science* 277, 364–367. doi: 10.1126/science.277.5324.364

Easterling, D. R., Meehl, G. A., Parmesan, C., Changnon, S. A., Karl, T. R., and Mearns, L. O. (2000). Climate extremes: observations, modeling, and impacts. *Science* 289, 2068–2074. doi: 10.1126/science.289.5487.2068

Elliott, K. H. (2016). Measurement of flying and diving metabolic rate in wild animals: review and recommendations. *Comp. Biochem. Physiol. A* 202, 63–77. doi: 10.1016/j.cbpa.2016.05.025

Esslinger, G. G., Bodkin, J. L., Breton, A. R., Burns, J. M., and Monson, D. H. (2014). Temporal patterns in the foraging behavior of sea otters in Alaska. *J. Wildlife Manage.* 78, 689–700. doi: 10.1002/jwmg.701

Ewbank, R. (1969). The fall in rectal temperature seen before parturition in sheep. *J. Reprod. Fertil.* 19, 569–571. doi: 10.1530/jrf.0.0190569

Fossette, S., Schofield, G., Lilley, M. K. S., Gleiss, A. C., and Hays, G. C. (2012). Acceleration data reveal the energy management strategy of a marine ectotherm during reproduction. *Func. Ecol.* 26, 324–333. doi: 10.1111/j.1365-2435.2011.01960.x

Friebe, A., Evans, A. L., Arnemo, J. M., Blanc, S., Brunberg, S., Fleissner, G., et al. (2014). Factors affecting date of implantation, parturition, and den entry estimated from activity and body temperature in free-ranging brown bears. *PLoS ONE* 9:e101410. doi: 10.1371/journal.pone.0101410

Fuller, A., Meyer, L. C. R., Mitchell, D., and Maloney, S. K. (2007). Dehydration increases the magnitude of selective brain cooling independently of core temperature in sheep. *Am. J. Physiol. Reg. Integr. Comp. Physio.* 293, R438–R446. doi: 10.1152/ajpregu.00074.2007

Fuller, A., Mitchell, D., Maloney, S. K., and Hetem, R. S. (2016). Towards a mechanistic understanding of the responses of large terrestrial mammals to heat and aridity associated with climate change. *Clim. Change Resp.* 3:10. doi: 10.1186/s40665-016-0024-1

Gaitán-Espitia, J. D., Bacigalupe, L. D., Opitz, T., Lagos, N. A., Timmermann, T., and Lardies, M. A. (2014). Geographic variation in thermal physiological performance of the intertidal crab *Petrolisthes violaceus* along a latitudinal gradient. *J. Exp. Biol.* 217, 4379–4386. doi: 10.1242/jeb.108217

Gannon, R., Taylor, M. D., Suthers, I. M., Gray, C. A., Van Der Meulen, D. E., Smith, J. A., et al. (2014). Thermal limitation of performance and biogeography in a free-ranging ectotherm: insights from accelerometry. *J. Exp. Biol.* 217, 3033–3037. doi: 10.1242/jeb.104455

Gilman, S. E., Urban, M. C., Tewksbury, J., Gilchrist, G. W., and Holt, R. D. (2010). A framework for community interactions under climate change. *TREE* 25, 325–331. doi: 10.1016/j.tree.2010.03.002

Halsey, L. G., Shepard, E. L. C., Quintana, F., Laich, A. G., Green, J. A., and Wilson, R. P. (2009). The relationship between oxygen consumption and body acceleration in a range of species. *Comp. Biochem. Physiol. A* 152, 197–202. doi: 10.1016/j.cbpa.2008.09.021

Harrison, P. M., Gutowsky, L. F., Martins, E. G., Patterson, D. A., Cooke, S. J., and Power, M. (2016). Temporal plasticity in thermal-habitat selection of burbot *Lota lota* a diel-migrating winter-specialist. *J. Fish Biol.* 88, 2111–2129. doi: 10.1111/jfb.12990

Hauser, D. D. W., Laidre, K. L., Stafford, K. M., Stern, H. L., Suydam, R. S., and Richard, P. R. (2017). Decadal shifts in autumn migration timing by Pacific Arctic beluga whales are related to delayed annual sea ice formation. *Glob. Change Biol.* 23, 2206–2217. doi: 10.1111/gcb.13564

Hays, G. C., Ferreira, L. C., Sequeira, A. M. M., Meekan, M. G., Duarte, C. M., Bailey, H., et al. (2016). Key questions in marine megafauna movement ecology. *TREE* 31, 463–475. doi: 10.1016/j.tree.2016.02.015

Hetem, R. S., Maloney, S. K., Fuller, A., and Mitchell, D. (2016). Heterothermy in large mammals: inevitable or implanted? *Biol. Rev.* 91, 187–205. doi: 10.1111/brv.12166

Hetem, R. S., Strauss, W. M., Fick, L. G., Maloney, S. K., Meyer, L. C., Shobrak, M., et al. (2010). Variation in the daily rhythm of body temperature of free-living Arabian oryx (*Oryx leucoryx*): does water limitation drive heterothermy? *J. Comp. Physiol. B Biochem. Syst. Environ. Physiol.* 180, 1111–1119. doi: 10.1007/s00360-010-0480-z

Holland, G., and Bruyère, C. L. (2014). Recent intense hurricane response to global climate change. *Clim. Dynam.* 42, 617–627. doi: 10.1007/s00382-013-1713-0

IPCC (2014). Climate Change 2014: "Synthesis Report," *Contribution of Working Groups, I, II and III to the Fifth Assessment Report of the Intergovernmental Panel on Climate Change,* eds R. K. Pachauri and L. A. Meyer (Geneva: Core Writing Team; IPCC), 151.

Jacobs, C. E., and Ausband, D. E. (2018). Pup-rearing habitat use in a harvested carnivore. *J. Wildl. Manage.* 82, 802–809. doi: 10.1002/jwmg.21434

Jeanniard-du-Dot, T., Guinet, C., Arnould, J. P., Speakman, J. R., and Trites, A. W. (2017). Accelerometers can measure total and activity-specific energy expenditures in free-ranging marine mammals only if linked to time-activity budgets. *Func. Ecol.* 31, 377–386. doi: 10.1111/1365-2435.12729

Jepsen, N., Thorstad, E. B., Havn, T., and Lucas, M. C. (2015). The use of external electronic tags on fish: an evaluation of tag retention and tagging effects. *Anim. Biotelem.* 3:49. doi: 10.1186/s40317-015-0086-z

Jessen, C., Laburn, H. P., Knight, M. H., Kuhnen, G., Goelst, K., and Mitchell, D. (1994). Blood and brain temperatures of free-ranging black wildebeest in their natural environment. *Am. J. Physiol. Regul. Integr. Comp. Physiol.* 267, R1528–1536. doi: 10.1152/ajpregu.1994.267.6.R1528

Kanda, L. L., Fuller, T. K., and Friedland, K. D. (2005). Temperature sensor evaluation of opossum winter activity. *Wildl. Soc. Bull.* 33, 1425–1431. doi: 10.2193/0091-7648(2005)33[1425:TSEOOW]2.0.CO;2

Khaliq, I., Hof, C., Prinzinger, R., Böhning-Gaese, K., and Pfenninger, M. (2014). Global variation in thermal tolerances and vulnerability of endotherms to climate change. *Proc. Biol. Sci.* 281:20141097. doi: 10.1098/rspb.2014.1097

Kingsolver, J. G. (2009). The well-temperatured biologist. (American Society of Naturalists Presidential Address). *Am. Nat.* 174, 755–768. doi: 10.1086/648310

Knopff, K. H., Knopff, A. A., Warren, M. B., and Boyce, M. S. (2009). Evaluating global positioning system telemetry techniques for estimating cougar predation parameters. *J. Wildl. Manage.* 73, 586–597. doi: 10.2193/2008-294

Le Bris, A., Fisher, J. A., Murphy, H. M., Galbraith, P. S., Castonguay, M., Loher, T., et al. (2017). Migration patterns and putative spawning habitats of Atlantic halibut (*Hippoglossus hippoglossus*) in the Gulf of St. Lawrence revealed by geolocation of pop-up satellite archival tags. *ICES J. Mar. Sci.* 75, 135–147. doi: 10.1093/icesjms/fsx098

Lendrum, P. E., Anderson, C. R., Monteith, K. L., Jenks, J. A., and Bowyer, R. T. (2013). Migrating mule deer: effects of anthropogenically altered landscapes. *PLoS ONE* 8:e64548. doi: 10.1371/journal.pone.0064548

Levy, O., Dayan, T., Porter, W. P., and Kronfeld-Schor, N. (2016). Foraging activity pattern is shaped by water loss rates in a diurnal desert rodent. *Am. Nat.* 188, 205–218. doi: 10.1086/687246

Martin, R. O., Cunningham, S. J., and Hockey, P. A. R. (2015). Elevated temperatures drive fine-scale patterns of habitat use in a savanna bird community. *Ostrich* 86, 127–135. doi: 10.2989/00306525.2015.1029031

Merilä, J., and Hendry, A. P. (2014), Climate change, adaptation, and phenotypic plasticity: the problem and the evidence. *Evol. Appl.* 7, 1–14. doi: 10.1111/eva.12137

Midtgård, U. (1983). Scaling of the brain and the eye cooling system in birds: a morphometric analysis of the Rete ophthalmicum. *J. Exp. Zool.* 225, 197–207. doi: 10.1002/jez.1402250204

Mitchell, D., Maloney, S. K., Jessen, C., Laburn, H. P., Kamerman, P. R., and Mitchell, G. (2002). Adaptive heterothermy and selective brain cooling in arid-zone mammals. *Comp. Biochem. Physiol. B,. Biochem. Mol. Biol.* 131, 571–585. doi: 10.1016/S1096-4959(02)00012-X

Mitchell, D., Maloney, S. K., Laburn, H. P., Knight, M. H., Kuhnen, G., and Jessen, C. (1997). Activity, blood temperature and brain temperature of free-ranging springbok. *J. Comp. Physiol. B,. Biochem. Syst. Environ. Physiol.* 167, 335–343. doi: 10.1007/s003600050082

Mitchell, J. F. B., Lowe, J., Wood, R. A., and Vellinga, M. (2006). Extreme events due to human-induced climate change. *Phil. Trans. R. Soc. A* 364, 2117–2133. doi: 10.1098/rsta.2006.1816

Nord, A., and Nilsson, J. A. (2011). Incubation temperature affects growth and energy metabolism in blue tit nestlings. *Am. Nat.* 178, 639–651. doi: 10.1086/662172

Nowack, J., Cooper, C. E., and Geiser, F. (2016). Cool echidnas survive the fire. *Proc. R. Soc. B* 283:20160382. doi: 10.1098/rspb.2016.0382

Nowack, J., Rojas, A. D., Körtner, G., and Geiser, F. (2015). Snoozing through the storm: torpor use during a natural disaster. *Sci. Rep.* 5:11243. doi: 10.1038/srep11243

Nowack, J., Stawski, C., and Geiser, F. (2017). More functions of torpor and their roles in a changing world. *J. Comp. Physiol. B Biochem. Syst. Environ. Physiol.* 187, 889–897. doi: 10.1007/s00360-017-1100-y

Olson, J. W., Rode, K. D., Eggett, D., Smith, T. S., Wilson, R. R., Durner, G. M., et al. (2017). Collar temperature sensor data reveal long-term patterns in southern Beaufort Sea polar bear den distribution on pack ice and land. *Mar. Ecol. Prog. Ser.* 564, 211–224. doi: 10.3354/meps12000

Ostrowski, S., Williams, J. B., and Ismael, K. (2003). Heterothermy and the water economy of free-living Arabian oryx (*Oryx leucoryx*). *J. Exp. Biol.* 206, 1471–1478. doi: 10.1242/jeb.00275

Ouwehand, J., and Both, C. (2017). African departure rather than migration speed determines variation in spring arrival in pied flycatchers. *J. Anim. Ecol.* 86, 88–97. doi: 10.1111/1365-2656.12599

Paaijmans, K. P., Heinig, R. L., Seliga, R. A., Blanford, J. I., Blanford, S., Murdock, C. C., et al. (2013). Temperature variation makes ectotherms more sensitive to climate change. *Glob. Change Biol.* 19, 2373–2380. doi: 10.1111/gcb.12240

Papastamatiou, Y. P., Watanabe, Y. Y., Bradley, D., Dee, L. E., Weng, K., Lowe, C. G., et al. (2015). Drivers of daily routines in an ectothermic marine predator: hunt warm, rest warmer? *PLoS ONE* 10:e0127807. doi: 10.1371/journal.pone.0127807

Parmesan, C. (2007). Influences of species, latitudes and methodologies on estimates of phenological response to global warming. *Glob. Change Biol.* 13, 1860–1872. doi: 10.1111/j.1365-2486.2007.01404.x

Payne, N. L., Smith, J. A., Van Der Meulen, D. E., Taylor, M. D., Watanabe, Y. Y., Takahashi, A., et al. (2016). Temperature dependence of fish performance in the wild: links with species biogeography and physiological thermal tolerance. *Func. Ecol.* 30, 903–912. doi: 10.1111/1365-2435.12618

Post, E., and Forchhammer, M. C. (2008). Climate change reduces reproductive success of an Arctic herbivore through trophic mismatch. *Phil. Trans. R. Soc. B* 363, 2369–2375. doi: 10.1098/rstb.2007.2207

Rey, B., Fuller, A., Hetem, R. S., Lease, H. M., Mitchell, D., and Meyer, L. C. (2016). Microchip transponder thermometry for monitoring core body temperature of antelope during capture. *J. Thermal. Biol.* 55, 47–53. doi: 10.1016/j.jtherbio.2015.11.010

Ruf, T., and Geiser, F. (2015). Daily torpor and hibernation in birds and mammals. *Biol. Rev.* 90, 891–926. doi: 10.1111/brv.12137

Rummer, J. L., Couturier, C. S., Stecyk, J. A. W., Gardiner, N. M., Kinch, J. P., Nilsson, G. E., et al. (2014). Life on the edge: thermal optima for aerobic scope of equatorial reef fishes are close to current day temperatures. *Glob. Change Biol.* 20, 1055–1066. doi: 10.1111/gcb.12455

Rutz, C., and Hays, G. C. (2009). New frontiers in biologging science. *Biol. Lett.* 5, 289–292. doi: 10.1098/rsbl.2009.0089

Scheffers, B. R., Edwards, D. P., Diesmos, A., Williams, S. E., and Evans, T. A. (2014). Microhabitats reduce animal's exposure to climate extremes. *Glob. Change Bio.* 20, 495–503. doi: 10.1111/gcb.12439

Schmaljohann, H., and Both, C. (2017). The limits of modifying migration speed to adjust to climate change. *Nat. Clim. Chang.* 7, 573–576. doi: 10.1038/nclimate3336

Schofield, G., Bishop, C. M., Katselidis, K. A., Dimopoulos, P., Pantis, J. D., and Hays, G. C. (2009). Microhabitat selection by sea turtles in a dynamic thermal marine environment. *J. Anim. Ecol.* 78, 14–21. doi: 10.1111/j.1365-2656.2008.01454.x

Seebacher, F., White, C. R., and Franklin, C. E. (2015). Physiological plasticity increases resilience of ectothermic animals to climate change. *Nat. Clim. Chang.* 5, 61–66. doi: 10.1038/nclimate2457

Signer, C., Ruf, T., Schober, F., Fluch, G., Paumann, T., and Arnold, W. (2010). A versatile telemetry system for continuous measurement of heart rate, body temperature and locomotor activity in free-ranging ruminants. *Methods Ecol. Evol.* 1, 75–85. doi: 10.1111/j.2041-210X.2009.00010.x

Sinclair, B. J., Marshall, K. E., Sewell, M. A., Levesque, D. L., Willett, C. S., Slotsbo, S., et al. (2016). Can we predict ectotherm responses to climate change using thermal performance curves and body temperatures? *Ecol. Lett.* 19, 1372–1385. doi: 10.1111/ele.12686

Smarr, B. L., Zucker, I., and Kriegsfeld, L. J. (2016). Detection of successful and unsuccessful pregnancies in mice within hours of pairing through frequency

analysis of high temporal resolution core body temperature data. *PLoS ONE* 11:e0160127. doi: 10.1371/journal.pone.0160127

Smit, B., Harding, C. T., Hockey, P. A., and Mckechnie, A. E. (2013). Adaptive thermoregulation during summer in two populations of an arid-zone passerine. *Ecology* 94, 1142–1154. doi: 10.1890/12-1511.1

Somero, G. N. (2010). The physiology of climate change: how potentials for acclimatization and genetic adaptation will determine 'winners' and 'losers'. *J. Exp. Biol.* 213, 912–920. doi: 10.1242/jeb.037473

Speakman, J. R., and Krol, E. (2010). Maximal heat dissipation capacity and hyperthermia risk: neglected key factors in the ecology of endotherms. *J. Anim. Ecol.* 79, 726–746. doi: 10.1111/j.1365-2656.2010.01689.x

Stawski, C., Körtner, G., Nowack, J., and Geiser, F. (2015). The importance of mammalian torpor for survival in a post-fire landscape. *Biol. Lett.* 11:20150134 doi: 10.1098/rsbl.2015.0134

Streby, H. M., Kramer, G. R., Peterson, S. M., Lehman, J. A., Buehler, D. A., and Andersen, D. E. (2015). Tornadic storm avoidance behavior in breeding songbirds. *Cur. Biol.* 25, 98–102. doi: 10.1016/j.cub.2014.10.079

Studd, E. K., Boutin, S., Mcadam, A. G., and Humphries, M. M. (2016). Nest attendance of lactating red squirrels (*Tamiasciurus hudsonicus*): influences of biological and environmental correlates. *J. Mammal.* 97, 806–814. doi: 10.1093/jmammal/gyw010

Thackeray, S. J., Sparks, T. H., Frederiksen, M., Burthe, S., Bacon, P. J., Bell, J. R., et al. (2010). Trophic level asynchrony in rates of phenological change for marine, freshwater and terrestrial environments. *Glob. Change Biol.* 16, 3304–3313. doi: 10.1111/j.1365-2486.2010.02165.x

Theimer, T. C., Williams, C. T., Johnson, S. R., Gilbert, A. T., Bergman, D. L., and Buck, C. L. (2017). Den use and heterothermy during winter in free-living, suburban striped skunks. *J. Mammal.* 98, 867–873. doi: 10.1093/jmammal/gyx009

Tieleman, B. I., and Williams, J. B. (1999). The role of hyperthermia in the water economy of desert birds. *Physiol. Biochem. Zool.* 72, 87–100. doi: 10.1086/316640

Tomkiewicz, S. M., Fuller, M. R., Kie, J. G., and Bates, K. K. (2010). Global positioning system and associated technologies in animal behaviour and ecological research. *Phil. Trans. B* 365 , 2163–2176. doi: 10.1098/rstb.2010.0090

Tøttrup, A. P., Klaassen, R. H. G., Kristensen, M. W., Strandberg, R., Vardanis, Y., Lindstrom, A., et al. (2012). Drought in Africa caused delayed arrival of European songbirds. *Science* 338, 1307–1307. doi: 10.1126/science.1227548

Turbill, C., Ruf, T., Mang, T., and Arnold, W. (2011). Regulation of heart rate and rumen temperature in red deer: effects of season and food intake. *J. Exp. Biol.* 214, 963–970. doi: 10.1242/jeb052282

US Global Change Research Program (2009). *Global Climate Change Impacts in the United States: A State of Knowledge Report*. Cambridge; New York, NY: Cambridge University Press.

Van der Putten, W. H., Macel, M., and Visser, M. E. (2010). Predicting species distribution and abundance responses to climate change: why it is essential to include biotic interactions across trophic levels. *Philos. Trans. R. Soc. B Biol. Sci.* 365, 2025–2034. doi: 10.1098/rstb.2010.0037

Van Wijk, R. E., Kolzsch, A., Kruckenberg, H., Ebbinge, B. S., Muskens, G., and Nolet, B. A. (2012). Individually tracked geese follow peaks of temperature acceleration during spring migration. *Oikos* 121, 655–664. doi: 10.1111/j.1600-0706.2011.20083.x

Visser, M. E., Van Noordwijk, A. J., Tinbergen, J. M., and Lessells, C. M. (1998). Warmer springs lead to mistimed reproduction in great tits (*Parus major*). *Proc. R. Soc. B* 265, 1867–1870. doi: 10.1098/rspb.1998.0514

Wascher, C. A., Kotrschal, K., and Arnold, W. (2018). Free-living greylag geese adjust their heart rates and body core temperatures to season and reproductive context. *Sci. Rep.* 8:2142. doi: 10.1038/s41598-018-20655-z

Weissenbock, N. M., Arnold, W., and Ruf, T. (2012). Taking the heat: thermoregulation in Asian elephants under different climatic conditions. *J. Comp. Physiol. B,. Biochem. Syst. Environ. Physiol.* 182, 311–319. doi: 10.1007/s00360-011-0609-8

Weller, T. J., Castle, K. T., Liechti, F., Hein, C. D., Schirmacher, M. R., and Cryan, P. M. (2016). First direct evidence of long-distance seasonal movements and hibernation in a migratory bat. *Sci. Rep.* 6:34585. doi: 10.1038/srep34585

White, C. R., Cassey, P., Schimpf, N. G., Halsey, L. G., Green, J. A., and Portugal, S.J. (2013). Implantation reduces the negative effects of bio-logging devices on birds. *J. Exp. Biol.* 216, 537–542. doi: 10.1242/jeb.076554

Williams, C. T., Buck, C. L., Sheriff, M. J., Richter, M. M., Krause, J. S., and Barnes, B. M. (2017). Sex-dependent phenological plasticity in an arctic hibernator. *Am. Nat.* 190, 854–859. doi: 10.1086/694320

Williams, C. T., Sheriff, M. J., Schmutz, J. A., Kohl, F., Toien, O., Buck, C. L., et al. (2011). Data logging of body temperatures provides precise information on phenology of reproductive events in a free-living arctic hibernator. *J. Comp. Physiol. B Biochem. Syst. Environ. Physiol.* 181, 1101–1109. doi: 10.1007/s00360-011-0593-z

Williams, C. T., Wilsterman, K., Kelley, A. D., Breton, A. R., Stark, H., Humphries, M. M., et al. (2014). Light loggers reveal weather-driven changes in the daily activity patterns of arboreal and semifossorial rodents. *J. Mammal.* 95, 1230–1239. doi: 10.1644/14-MAMM-A-062

Willis, C. K., Brigham, R. M., and Geiser, F. (2006). Deep, prolonged torpor by pregnant, free-ranging bats. *Naturwissenschaften* 93, 80–83. doi: 10.1007/s00114-005-0063-0

Wilson, A. D., Wikelski, M., Wilson, R. P., and Cooke, S. J. (2015). Utility of biological sensor tags in animal conservation. *Conserv. Biol.* 29, 1065–1075. doi: 10.1111/cobi.12486

Winder, M., and Schindler, D. E. (2004). Climate change uncouples trophic interactions in an aquatic ecosystem. *Ecology* 85, 2100–2106. doi: 10.1890/04-0151

Withers, P. C., and Williams, J. B. (1990). Metabolic and respiratory physiology of an arid-adapted australian bird, the spinifex pigeon. *Condor* 92, 961–969. doi: 10.2307/1368732

Yasuda, T., Kawabe, R., Takahashi, T., Murata, H., Kurita, Y., Nakatsuka, N., et al. (2010). Habitat shifts in relation to the reproduction of Japanese flounder *Paralichthys olivaceus* revealed by a depth-temperature data logger. *J. Exp. Mar. Biol. Ecol.* 385, 50–58. doi: 10.1016/j.jembe.2010.02.001

Zhang, J., Hull, V., Ouyang, Z., He, L., Connor, T., Yang, H., et al. (2017). Modeling activity patterns of wildlife using time-series analysis. *Ecol. Evol.* 7, 2575–2584. doi: 10.1002/ece3.2873

Conflict of Interest Statement: The authors declare that the research was conducted in the absence of any commercial or financial relationships that could be construed as a potential conflict of interest.

Copyright © 2018 Chmura, Glass and Williams. This is an open-access article distributed under the terms of the Creative Commons Attribution License (CC BY). The use, distribution or reproduction in other forums is permitted, provided the original author(s) and the copyright owner(s) are credited and that the original publication in this journal is cited, in accordance with accepted academic practice. No use, distribution or reproduction is permitted which does not comply with these terms.

frontiers in Physiology

ORIGINAL RESEARCH
published: 17 July 2018
doi: 10.3389/fphys.2018.00838

Modeling Tissue and Blood Gas Kinetics in Coastal and Offshore Common Bottlenose Dolphins, *Tursiops truncatus*

Andreas Fahlman[1,2]*, *Frants H. Jensen*[3†], *Peter L. Tyack*[4] *and Randall S. Wells*[5]

[1] Global Diving Research, Ottawa, ON, Canada, [2] Fundación Oceanografic de la Comunidad Valenciana, Valencia, Spain, [3] Aarhus Institute of Advanced Studies, Aarhus University, Aarhus, Denmark, [4] Sea Mammal Research Unit, Scottish Oceans Institute, University of St Andrews, St Andrews, United Kingdom, [5] Chicago Zoological Society's Sarasota Dolphin Research Program, Mote Marine Laboratory, Sarasota, FL, United States

OPEN ACCESS

Edited by:
Jose Pablo Vazquez-Medina,
University of California, Berkeley,
United States

Reviewed by:
Luis Huckstadt,
University of California, Santa Cruz,
United States
Michael Tift,
University of California, San Diego,
United States

***Correspondence:**
Andreas Fahlman
afahlman@whoi.edu

†Frants H. Jensen
orcid.org/0000-0001-8776-3606

Specialty section:
This article was submitted to
Aquatic Physiology,
a section of the journal
Frontiers in Physiology

Received: 16 April 2018
Accepted: 14 June 2018
Published: 17 July 2018

Citation:
Fahlman A, Jensen FH, Tyack PL and Wells RS (2018) Modeling Tissue and Blood Gas Kinetics in Coastal and Offshore Common Bottlenose Dolphins, Tursiops truncatus. Front. Physiol. 9:838. doi: 10.3389/fphys.2018.00838

Bottlenose dolphins (*Tursiops truncatus*) are highly versatile breath-holding predators that have adapted to a wide range of foraging niches from rivers and coastal ecosystems to deep-water oceanic habitats. Considerable research has been done to understand how bottlenose dolphins manage O_2 during diving, but little information exists on other gases or how pressure affects gas exchange. Here we used a dynamic multi-compartment gas exchange model to estimate blood and tissue O_2, CO_2, and N_2 from high-resolution dive records of two different common bottlenose dolphin ecotypes inhabiting shallow (Sarasota Bay) and deep (Bermuda) habitats. The objective was to compare potential physiological strategies used by the two populations to manage shallow and deep diving life styles. We informed the model using species-specific parameters for blood hematocrit, resting metabolic rate, and lung compliance. The model suggested that the known O_2 stores were sufficient for Sarasota Bay dolphins to remain within the calculated aerobic dive limit (cADL), but insufficient for Bermuda dolphins that regularly exceeded their cADL. By adjusting the model to reflect the body composition of deep diving Bermuda dolphins, with elevated muscle mass, muscle myoglobin concentration and blood volume, the cADL increased beyond the longest dive duration, thus reflecting the necessary physiological and morphological changes to maintain their deep-diving life-style. The results indicate that cardiac output had to remain elevated during surface intervals for both ecotypes, and suggests that cardiac output has to remain elevated during shallow dives in-between deep dives to allow sufficient restoration of O_2 stores for Bermuda dolphins. Our integrated modeling approach contradicts predictions from simple models, emphasizing the complex nature of physiological interactions between circulation, lung compression, and gas exchange.

Keywords: diving physiology, modeling and simulations, gas exchange, marine mammals, decompression sickness, blood gases, hypoxia

INTRODUCTION

The physiological adaptations that optimize foraging in marine mammals have long interested researchers. Optimal foraging theory implies that marine mammals should change dive behavior and metabolic pathways, and the fraction of aerobic and anaerobic metabolism based on dive depth and prey availability (Carbone and Houston, 1996; Cornick and Horning, 2003). Considerable work has been dedicated to understanding the aerobic limitations of diving air-breathing vertebrates, as these help with understanding foraging limits and efficiency. Kooyman et al. (1983) described the maximum dive duration until increasing blood lactate levels as the aerobic dive limit (ADL). The calculated ADL (cADL) was later defined as the total O_2 stores divided by the rate of O_2 consumption (Butler and Jones, 1997), and has been estimated in a number of species (Kooyman and Ponganis, 1998; Butler, 2006). However, metabolic rate may change over the course of a dive or foraging bout, and a few studies have subsequently estimated the cADL from measured (respirometry: Castellini et al., 1992; Reed et al., 1994, 2000; Hurley and Costa, 2001; Sparling and Fedak, 2004; Fahlman et al., 2008a, 2013) or estimated diving metabolic rate (doubly labeled water, or a proxy of metabolic rate: Boyd et al., 1995; Froget et al., 2001; Butler et al., 2004; Fahlman et al., 2008b).

Most studies agree that the majority of dive durations are well within the ADL/cADL, as this increases foraging efficiency and reduces lengthy surface intervals required to remove accumulated anaerobic by-products such as lactate (Kooyman et al., 1983). However, some species of otariids that feed on the benthos appear to exceed their cADL regularly, while those that feed in shallower water have shorter dive durations and seldom exceed the cADL (Costa et al., 2001). These differences may indicate true variation in foraging behavior, but may also be suggestive of morphological or physiological differences within or between closely related species that alter cADL (Hückstädt et al., 2016). For example, the muscle mass in previous studies was assumed to be similar to that of the Weddell seal (Costa et al., 2001), and such assumptions are often necessary as available data do not exist for all variables and species. However, variation in underwater swimming behavior (Williams, 2001; Fahlman et al., 2013), or morphological variation in muscle mass and fiber type (Pabst et al., 2016) may significantly alter the metabolic cost of foraging.

Large variations in dive behavior also exist within species. In the common bottlenose dolphin (*Tursiops truncatus*), different ecotypes have evolved to occupy different ecological niches (Mead and Potter, 1995; Hoelzel et al., 1998). Coastal bottlenose dolphins inhabit coastal areas and generally perform short (<60 s), shallow (<10 m) dives (Mate et al., 1995), while offshore bottlenose dolphins inhabit offshore, deep-water habitats and regularly dive below 200 m (Klatsky et al., 2007). Interestingly, neither resting metabolic rate nor lung compliance differed between the two ecotypes (Fahlman et al., 2018a,b), but blood hematocrit was significantly higher in the offshore ecotype (Klatsky et al., 2007; Schwacke et al., 2009; Fahlman et al., 2018a). In addition, the offshore ecotype is generally larger (Klatsky et al., 2007), possibly due to larger muscle mass to help increase the available O_2 stores and diving capacity. In an attempt to better understand the physiological limitations of these two ecotypes, and to explore how variation in morphology and anatomy may alter gas dynamics during diving, we used a previously published gas exchange model (Fahlman et al., 2009; Hooker et al., 2009; Hodanbosi et al., 2016) to estimate blood and tissue gas tensions for O_2 (PO_2), CO_2 (PCO_2), and N_2 (PN_2) from high resolution (1 Hz) dive records from coastal bottlenose dolphins from Sarasota Bay, Florida, and offshore bottlenose dolphins sampled near the island of Bermuda.

MATERIALS AND METHODS

Model

The model described in this paper uses the breath-hold diving gas dynamics model developed by Fahlman et al. (2009) and Fahlman et al. (2006), which has been used to estimate lung, blood, and tissue gas tensions in a number of species (Hooker et al., 2009; Kvadsheim et al., 2012; Hodanbosi et al., 2016). A brief summary of the model is included below, with the specific changes made for the current modeling effort. The model was parameterized for bottlenose dolphins and was based on published values available for this species when possible, and otherwise on published values for beaked whales or phocids (as detailed below).

As in previous work, the body was partitioned into 4 compartments; brain (B), fat (F), muscle (M), and central circulation (CC), and one blood compartment (BL, arterial and mixed venous). In the current study, bone was included in the fat compartment as the bones of deep diving whales are high in fat content (Higgs et al., 2010). The central circulatory compartment included heart, kidney, and liver. The muscle compartment included muscle, skin, connective tissue, and all other tissues (Fahlman et al., 2009). In previous studies, the alimentary tract was placed in the central circulation. However, due to its lower metabolic rate, it was placed in the muscle compartment in the current study. The size of each compartment as well as the myoglobin and hemoglobin concentrations were initially taken from data on coastal dolphins (Mallette et al., 2016). As there is little or no information about the body composition of offshore dolphins, changes were made to the body composition of the offshore ecotype to be more like a beaked whale (Pabst et al., 2016).

Lung Gas Stores and Gas Exchange

Gas exchange occurred between the lungs and blood compartment and between the blood compartment and each other compartment (Fahlman et al., 2006). The O_2, CO_2, and N_2 stores in the lung consisted only of a gas phase and were assumed to be homogenous. We assumed that there was no diffusion resistance at the lung-surface interface when an animal was breathing at the water surface (Farhi, 1967). Thus, arterial blood tension of N_2 (Pa_{N2}), O_2 (Pa_{O2}), and CO_2 (Pa_{CO2}) were assumed to be equal to the alveolar partial pressures. For an animal breathing at the surface, we assumed that alveolar partial pressures of N_2 (PA_{N2}), O_2 (PA_{O2}), and CO_2 (PA_{CO2}) were,

respectively, 0.74 ATA, 0.133 ATA, and 0.065 ATA (Fahlman et al., 2015), with 0.062 ATA being water vapor.

During diving, hydrostatic pressure compresses the respiratory system, which causes a pressure-dependent pulmonary shunt to develop (Fahlman et al., 2009). The parameters that describe the structural properties for the alveolar space and conducting airways (Equations 4 and 5 in Bostrom et al., 2008) were updated based on previously published compliance values for the bottlenose dolphin (**Table 1**, Fahlman et al., 2011, 2015; Moore et al., 2014).

Total lung capacity (TLC) included the volume of the dead space (trachea and bronchi, V_D), and the maximum alveolar volume (V_A), i.e., TLC = $V_D + V_A$. It was assumed that gas exchange only occurred in the alveoli and when the diving alveolar volume (DV_A) was equal to 0, gas exchange stopped. We used the equation initially developed by Kooyman (1973), to estimate TLC ($TLC_{est} = 0.135\ M_b^{0.92}$, where M_b is body mass in kg), and later validated for the dolphin (Fahlman et al., 2011, 2015). Dead space volume was assumed to be 7% of TLC (Kooyman, 1973; Fahlman et al., 2011). The relationship between pulmonary shunt and $DV_A\ V_A^{-1}$ was determined using a power function (Bostrom et al., 2008) for data from the harbor seals (Equation 6A in Fahlman et al., 2009).

All pressures were corrected for water vapor pressure, assuming that the respiratory system was fully saturated at 37°C.

TABLE 1 | Parameters used to describe the structural properties of the respiratory system.

Parameter	Equation	
	Equation 4	Equation 5
a	1.05 ± 0.04 (1.1)	
b	0.90 ± 0.06 (1.2)	
c	2.51 ± 0.19 (1.3)	
Kp		−31.0 ± 23 (−12.8)
n		2.4 ± 1.4 (0.91)

The parameters for Equations (4) and (5) in Bostrom et al. (2008) were revised using previously published compliance data from the bottlenose dolphin (Fahlman et al., 2018b). Old values are in parentheses.

Blood and Tissue Gas Stores

As in previous studies, the blood and tissue stores of N_2, CO_2, and O_2 were determined by the solubility coefficients for each gas, as previously detailed (Fahlman et al., 2006). For O_2 and CO_2, the average concentration of hemoglobin for each population was used to estimate the blood O_2 stores and CO_2 storage capacity (**Table 2**). Tissue gas content was determined as previously detailed (Fahlman et al., 2006, 2009).

Compartment Size, Cardiac Output, and Blood Flow Distribution

For the coastal ecotype sampled in Sarasota Bay, the relative size of each compartment was taken from previous studies in

TABLE 2 | Body compartment composition (% of body mass), estimated compartment metabolic rate (rest), and the value used in the model, cardiac output at rest/diving and at the surface, male adult dolphins.

Tissue	Percent of body mass		References
	Sarasota	Bermuda	
Blood	7.1	19.1	Ridgway and Johnston, 1966
Brain	1.0	0.2	Mallette et al., 2016
Fat	31.1	20.7	
Central circulation	3.73	3	
Muscle	57 (35)	57 (50)	
Metabolic rate for a 200 kg animal (l O_2 min^{-1})			
Brain	0.035	0.011	Yazdi et al., 1999; Yeates and Houser, 2008; Noren et al., 2013; Fahlman et al., 2015, 2018a
Fat	0.039	0.024	
Central circulation	0.321	0.255	
Muscle	0.273	0.245	
$\dot{V}O_{2tot}$ rest	0.67$	0.54$	
$\dot{Q}_{tot}$ rest (l min^{-1})	6.0¶	6.0¶	Miedler et al., 2015
Variables for O_2 storage			
[Hb] (g/100 g)	16	16	Ridgway and Johnston, 1966; Noren et al., 2002; Hall et al., 2007; Schwacke et al., 2009
[Mb] (g Mb/100 g muscle)	3	7.3	Noren et al., 2001; Ponganis, 2011; Pabst et al., 2016
Hct (%)	44	57	Ridgway and Johnston, 1966; Hall et al., 2007; Schwacke et al., 2009
O_2 stores for a 200 kg dolphin (l)			
Lung	2.21	2.21	Kooyman, 1989; Kooyman and Ponganis, 1998; Fahlman et al., 2015, 2017b
Tissue	3.82	10.00	
Blood	2.68	7.50	

For muscle, the value in parenthesis is the actual muscle mass used with myoglobin. Data are for the resting data without the multiplier for exercise. $Values for active animals equal to 2x resting values. ¶Values for active animals equal to 3x resting values (Sarasota dolphins) or 7x resting values (Bermuda dolphins).

coastal bottlenose dolphins (**Table 2**; Ridgway and Johnston, 1966; Mallette et al., 2016). For blood and muscle we used species-specific values for blood hematocrit (Ridgway and Johnston, 1966; Hall et al., 2007; Schwacke et al., 2009; Fahlman et al., 2018b), and myoglobin concentration (Noren et al., 2001; Ponganis, 2011). For the deep-diving offshore dolphins, we initially assumed that the animals were similar to the coastal ecotype from Sarasota Bay. However, these assumptions resulted in a cADL that was too short for all Bermuda dolphins. We therefore adjusted the body composition of the Bermuda dolphins, assuming that their body composition was similar to that of deep diving beaked whales (Pabst et al., 2016), and used the body composition for *Mesoplodon* from our previous studies (**Table 2**; Hooker et al., 2009).

For the current study, we assumed that the cardiac output ($\dot{Q}_{tot}$) at the surface was 3 times higher than the $\dot{Q}_{tot}$ measured in resting bottlenose dolphins (31.5 ml min^{-1} kg^{-1}, Miedler et al., 2015). To account for differences in M_b, mass specific $\dot{Q}_{tot}$ (s$\dot{Q}_{tot}$) was adjusted using Equation (5) in Fahlman et al. (2009). During diving, the $\dot{Q}_{tot}$ was reduced to 1/3 of the value at the surface to account for the dive response, i.e., the diving $\dot{Q}_{tot}$ was the same as that measured in resting animals. Blood flow distributions to each tissue at the surface and during diving were iteratively tested to maximize utilization of O_2 to increase the aerobic dive duration (**Table 2**).

Dive Data Used

We used dive data collected from high resolution digital audio and movement recording tags (DTAG, Johnson and Tyack, 2003) attached to the dorsal side of each dolphin by means of four small suction cups, and programmed to release after <24 h. DTAGs were deployed during 2013–2016 in Sarasota Bay and in

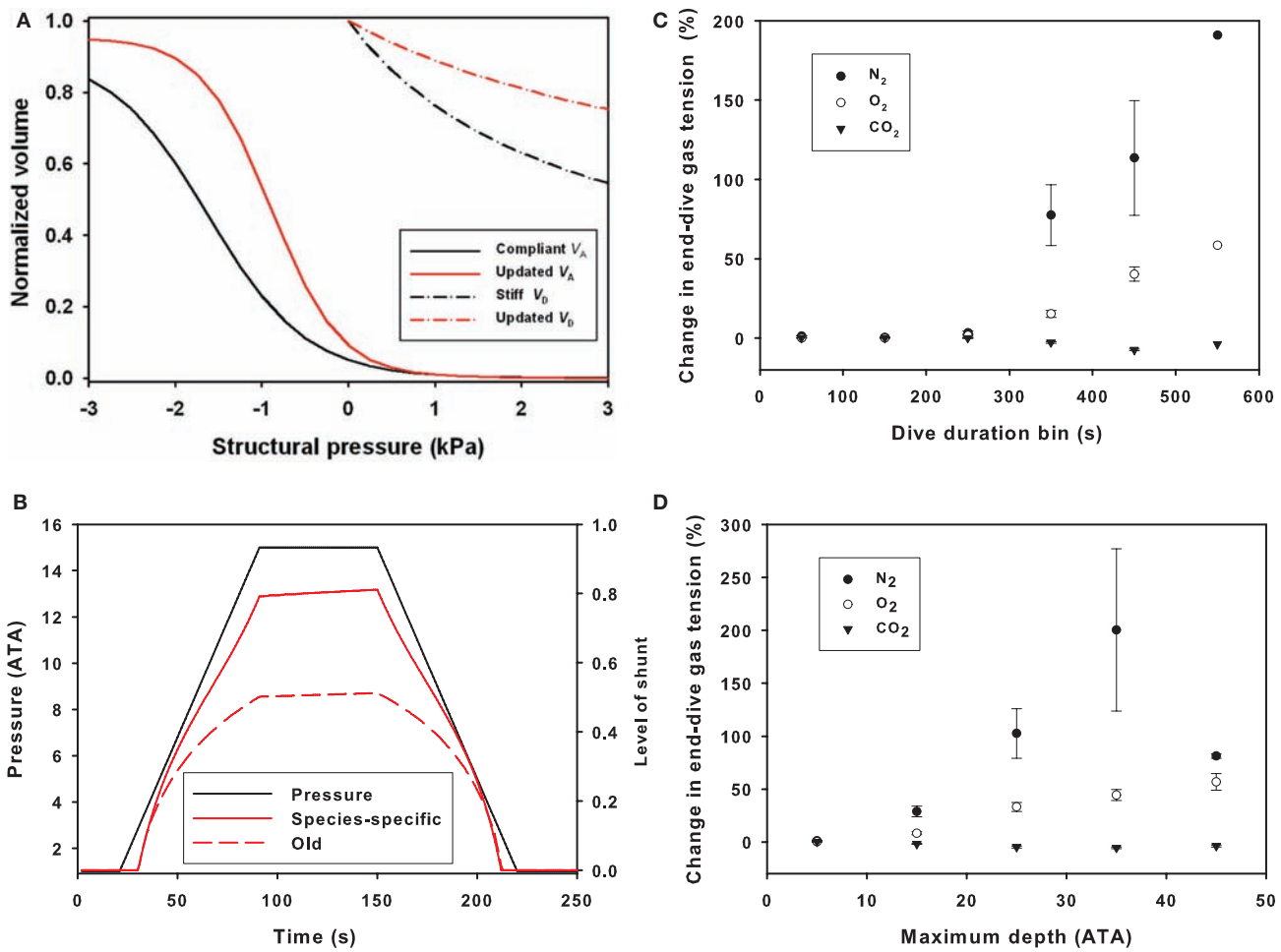

FIGURE 1 | (A) Normalized volume (V_A, alveolar volume; V_D, dead space/tracheal volume) vs. structural pressure for alveolar and dead space compliances based on the estimate from Bostrom et al. (2008), or updated estimates from bottlenose dolphins (Fahlman et al., 2011, 2015). **(B)** Differences in pulmonary shunt with old and updated compliance values for the respiratory system in dolphins during a representative dive to 150 m for an animal with a body composition like the Bermuda dolphin (Fahlman et al., 2009). The average compliant alveoli and medium compliant trachea were used for the base model, and this model was used as a basis of comparison with all other simulations. Changes in end-dive mixed venous N_2, O_2, and CO_2 levels against **(C)** dive duration (sec) or **(D)** maximum dive depth (ATA) when comparing old and revised lung compliance values. The y-axis is the change in percent for [(old-new)/old * 100]. These changes reflect how the structural properties alter the shunt and ventilation-perfusion mismatch (Garcia Párraga et al., 2018).

August of 2016 off the coast of Bermuda, during capture-release operations (e.g., Wells et al., 2004; Klatsky et al., 2007). The dolphins were tagged and data collected under permits issued by NMFS (Scientific Research Permit Number 15543) and the Bermuda Government, Department of Environment and Natural Resources (Research permit number SP160401r).

Data processing was done using the DTAG toolbox (soundtags.st-andrews.ac.uk). Tag depth was sampled at 200 Hz and subsequently down-sampled to 25 Hz during post-processing using a linear phase 10 Hz low-pass FIR filter. Surfacings were used to estimate the zero-pressure offset and to characterize and remove the effect of temperature on estimated depth.

A dive was defined as a submergence deeper than 1.5 m (1.15 ATA) and longer than 10 s. The start and end of each dive was calculated as the first and last point of the dive that exceeded 0.1 m depth, and the surface interval was defined as the time from current dive to previous dive.

RESULTS

Respiratory Compliance

The updated parameters that defined the structural properties (compliance) of the respiratory system resulted in a stiffer upper airway and more compliant alveolar space as compared with the values used in previous studies (**Figure 1A**), which affected the pulmonary shunt (**Figure 1B**). The parameters for respiratory compliance were updated and the model output compared with the results from the previous model (**Figures 1C,D**). The end-dive gas tension increased with both dive duration and maximum dive depth for N_2 and O_2, while for CO_2 there was a slight decrease (**Figures 1C,D**).

Dive Data

There were no significant differences in body mass (M_b, $P > 0.1$, Welch t-value: 1.8, df = 2), body length ($P > 0.9$, t-value: 0.02, df = 5), average number of dives per hour ($P < 0.1$, Welch t-value: 0.3, df = 5), and average surface interval ($P > 0.1$, Welch t-value: 1.3, df = 2, **Table 3**) between ecotypes. There were significant differences in the dive behavior between the two populations, with dive duration ($P < 0.01$, Welch t-value: 4.37, df = 2), maximum dive depth ($P < 0.05$, Welch t-value: 3.95, df = 2), and mean depth per dive ($P < 0.05$, Welch t-value: 3.57, df = 2) being significantly higher in the Bermuda dolphins (**Table 3**, **Figures 2**, **3**). For dives <60 s, the Sarasota dolphins never exceeded a dive depth of 5 m (**Figure 3A**). As the dive duration increased >60 s, so did the maximum depth and also the variation (**Figure 3A**). For the Bermuda dolphins, there was a significant increase in the dive duration as the dive depth increased (**Figure 3B**). Dives <60 s showed little variation and few exceeded 10 m (**Figure 3B**). As the dive duration increased beyond 100 s, the variation in maximum dive depth increased and dives exceeding 100 m became more common (**Figure 3B**). We found no indication that the surface interval increased with dive duration of the previous ($X^2 = 0.27$, df = 1, $P > 0.6$) or next dive $X^2 = 0.05$, df = 1, $P > 0.8$).

TABLE 3 | Descriptive metrics for animals in study.

Animal ID	Place	Sex	M_b	Age	Length (cm)	No. dives	Dives per hour	DD (s)	Maximum dive depth (m)	Mean depth (m)	Surf interval (s)	No. dives > 100 m	No. dives > 200 m
tt13_127b (FB90)	S	F	198	43	259	522	23	35 ± 20 (10–129)	2 ± 0 (1–10)	2 ± 0 (1–8)	124 ± 743 (1–1,4956)	0	0
tt15_131a (FB123)	S	F	166	17	241	1032	50	36 ± 19 (10–128)	2 ± 0 (1–5)	1 ± 0 (1–4)	36 ± 128 (1–2,015)	0	0
tt15_134a (FB199)	S	F	142	13	236	684	39	28 ± 16 (10–110)	2 ± 0 (2–6)	1 ± 0 (1–4.1)	65 ± 165 (1–3,340)	0	0
tt16_128a (FB33)	S	F	195	34	258	214	9	46 ± 25 (10–125)	2 ± 0 (2–6)	1 ± 0 (1–5)	363 ± 2,165 (1–22,572)	0	0
Average			175 ± 26	27 ± 14	248 ± 12	613 ± 341	30 ± 18	36 ± 7*	2 ± 0*	1 ± 0*	147 ± 149		
tt16_243a (Tt0019)	B	M	294	NA	256	491	28.1	65 ± 68 (10–508)	10 ± 21 (1–309)	6 ± 8 (1–247)	62 ± 85(1–706)	6	3
tt16_244a (Tt0021)	B	F	173	NA	238	805	37	63 ± 81 (10–539)	12 ± 37 (2–482)	8 ± 18(01–280)	34 ± 86 (1–1,508)	7	4
tt16_244b (Tt0022)	B	M	282	NA	251	513	30	82 ± 86 (10–487)	20 ± 38 (2–328)	12 ± 17 (1–176)	37 ± 68 (1–1,161)	30	11
Average			250 ± 67		248 ± 9	603 ± 175	32 ± 5	70 ± 10*	14 ± 5*	9 ± 3*	44 ± 15		

*Animal dataset (and ID code), dolphin population (Sarasota-S, Bermuda-B), sex (F-female, M-male), body mass (M_b, kg), straight length, average (± SD) number of dives (No. dives), average dives per hour, average dive duration (sec), average maximum dive depth, average mean depth, and average previous surface interval. *Significant difference between Sarasota and Bermuda animals.*

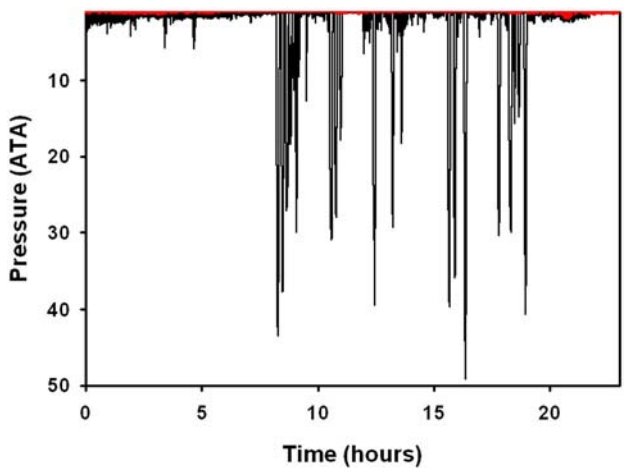

FIGURE 2 | Representative dive data from two bottlenose dolphins in Sarasota Bay, Florida (red line), and Bermuda (black line). Data are plotted on the same axes range to show the differences in diving capacity/behavior. Pressure in ATA where 1 ATA is at the surface and 2 ATA is at 10 m depth.

Cardiac Output and Blood Flow Distribution

For both populations, we assumed that the diving $\dot{Q}_{tot}$ was equal to resting values measured in the bottlenose dolphins (**Table 4**; Miedler et al., 2015). The blood flow distribution for the Sarasota dolphins was able to vary greatly, due to their shorter and shallower dive pattern. For the Bermuda dolphins, deviation from a certain blood flow distribution caused tissues to run out of O_2. The specific variation varied slightly between individual animals, but one distribution pattern that focused perfusion to the central circulation, and minimized flow to the muscle, allowed all dolphins to complete their dives aerobically (**Table 4**).

The blood flow required at the surface to assure that tissues received enough blood to restore O_2 stores at the surface differed between the two ecotypes. For the Sarasota dolphins, the minimum $\dot{Q}_{tot}$ at the surface was 3 times higher than during diving. A surface $\dot{Q}_{tot}$ at least 7 times higher than during diving was required for the Bermuda population to ensure that tissues were saturated with O_2; any lower surface $\dot{Q}_{tot}$ would result in tissue PO_2 continuously decreasing with each dive. In addition, for the Bermuda dolphins, changes in perfusion associated with diving, i.e., the dive response, was set to occur only for dives deeper than 20 m. Consequently, the elevated $\dot{Q}_{tot}$ was required at the surface to help restore blood and tissue O_2 stores.

Blood and Tissue Gas Tensions

In the Sarasota dolphins, there was considerable variation in end-dive blood and tissue PO_2 with dive duration. In **Figure 4**, the muscle is used as a representative tissue to show these variations. In **Figure 4A**, the large variation in muscle PO_2 is shown when the muscle tension is plotted against dive duration. There was a consistent exponential decrease with dive depth (**Figure 4B**). A decrease in the blood and tissue PO_2 was obvious in the Bermuda dolphins for both dive duration (**Figure 4C**) and depth (**Figure 4D**). For the Bermuda dolphins, the decrease in tissue PO_2 varied depending on the level of pulmonary shunt, and the shunt decreased the end dive PO_2 for dives of the same duration or maximum depth (**Figures 4C,D**). The effect of the shunt on end-dive PO_2 was most obvious for the muscle compartment, but was also seen in the other tissues (data not shown).

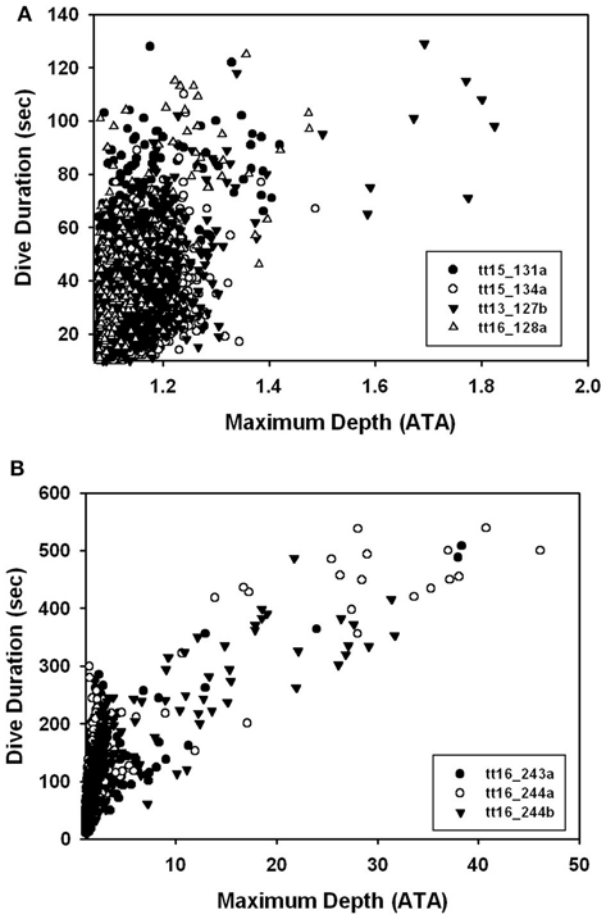

FIGURE 3 | Dive depth vs. dive duration for **(A)** coastal Sarasota and **(B)** offshore Bermuda dolphins.

TABLE 4 | Blood flow distribution (% of total cardiac output), cardiac output ($\dot{Q}_{tot}$), rate of O_2 consumption, for central circulation (CC), muscle (M), brain (B), and fat (F) body compartments for a 200 kg dolphin for animals in Sarasota or Bermuda.

Location	State	Tissue				$\dot{Q}_{tot}$	$\dot{V}O_2$
		CC	M	B	F	$(l \cdot s^{-1})$	$(l\ O_2 \cdot min^{-1})$
Sarasota	Surface	25	65	7	3	0.301	1.34
Sarasota	Dive	70	17	7	6	0.100	1.34
Bermuda	Surface	60	34	4	2	0.704	1.08
Bermuda	Dive	81	9	6	4	0.100	1.08

*The $\dot{Q}_{tot}$ was assumed to be resting during diving and 3 times resting while at the surface for the Sarasota dolphins, but 7 times resting for the Bermuda dolphins. The $\dot{V}O_2$ was assumed to be the same at the surface and while diving and estimated to be 2 × the resting metabolic rate (**Table 1**).*

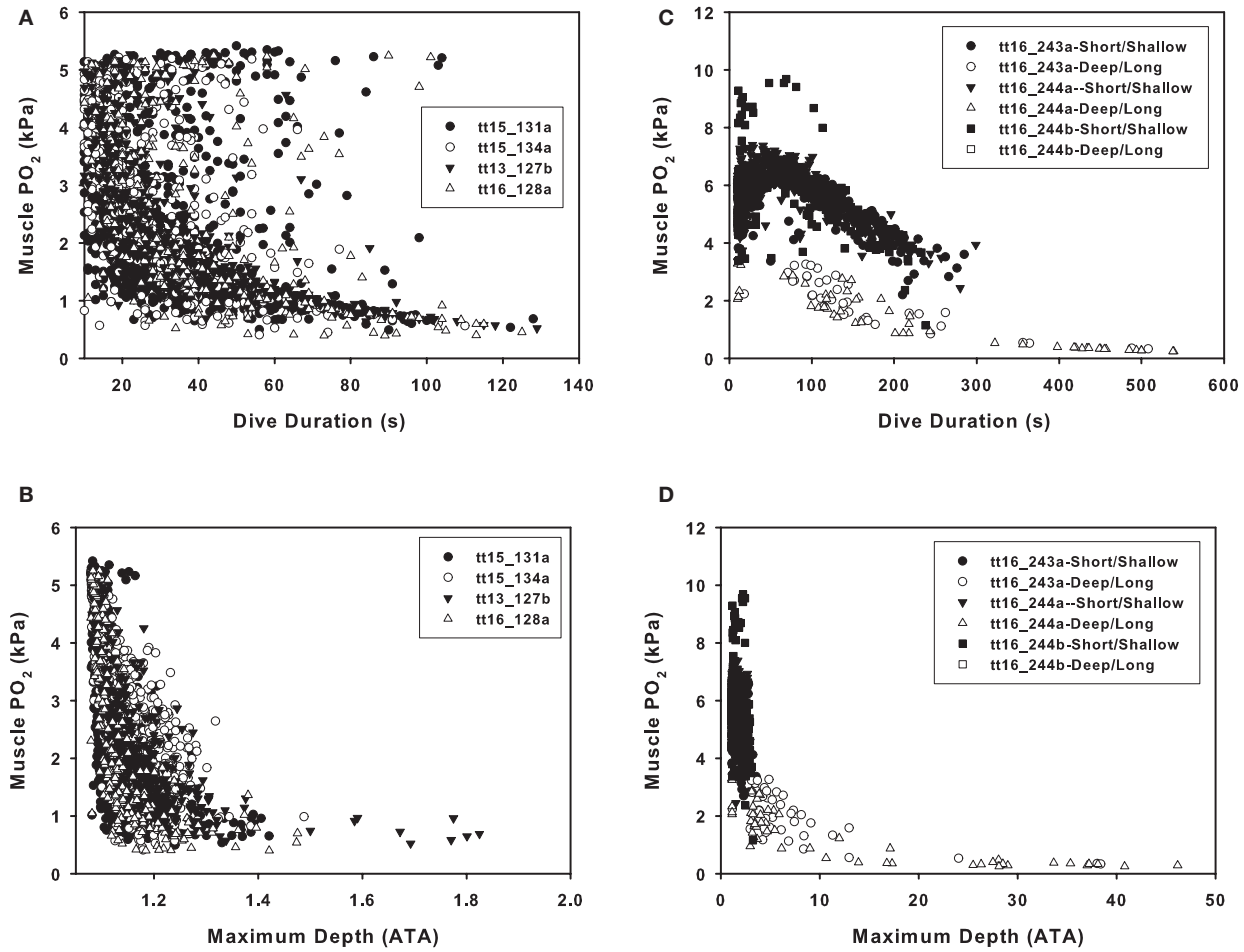

FIGURE 4 | Estimated end-dive muscle PO_2 (kPa) vs. **(A,C)** dive duration or **(B,D)** maximum dive depth (ATA, 1 ATA = 98.07 kPa) in **(A,B)** Sarasota or **(B,D)** Bermuda dolphins.

The estimated blood and tissue PO_2 for a representative dive for dolphins from Sarasota (**Figure 5A**) or Bermuda (**Figure 5B**) showed similar patterns of a decrease in PO_2 during a dive. However, the longer and deeper dive duration resulted in greater changes in blood and tissue PO_2 values in the offshore ecotype. **Figures 5C,D** show the effect of depth on lung volume and pulmonary shunt.

DISCUSSION

In the current study, we modeled tissue and blood PO_2, PCO_2, and PN_2 from fine-scale empirical dive data from bottlenose dolphins of both the coastal and offshore ecotypes to assess potential morphological or physiological adaptations that could help explain the large variation in dive behavior in these divergent populations. The results shows that the structural properties of the respiratory system have a significant effect on pulmonary gas exchange, and these changes are different for gases with different gas solubilities, agreeing with past work suggesting that variation in ventilation and perfusion may be important for managing gases during diving (West, 1962; Farhi and Yokoyama, 1967; Hodanbosi et al., 2016; Garcia Párraga et al., 2018). Furthermore, the results suggest that the deeper and longer dives of the offshore dolphins most likely reflect a greater O_2 storage capacity, potentially combined with foraging of lower energetic cost. Future tagging studies to assess the energetic requirements of the different foraging strategies will be crucial to assess how close to their physiological limits each of these populations are living.

Theoretical work has suggested that the level of gas exchange, $\dot{Q}_{tot}$ and blood flow distribution are important to alter blood and tissue gas levels (Fahlman et al., 2006, 2009). Previously, we suggested that the structural properties of the respiratory system could have a significant effect on the level of gas exchange during breath-hold diving (Bostrom et al., 2008; Fahlman et al., 2009), and how man-made disturbances may alter the risk of gas emboli through changes in the dive profile or physiology (Hooker et al., 2009; Kvadsheim et al., 2012). However, species-specific estimates for the structural properties of the respiratory system were not available and published values from a range of species were used (Bostrom et al., 2008; Fahlman et al., 2009, 2014; Hooker et al.,

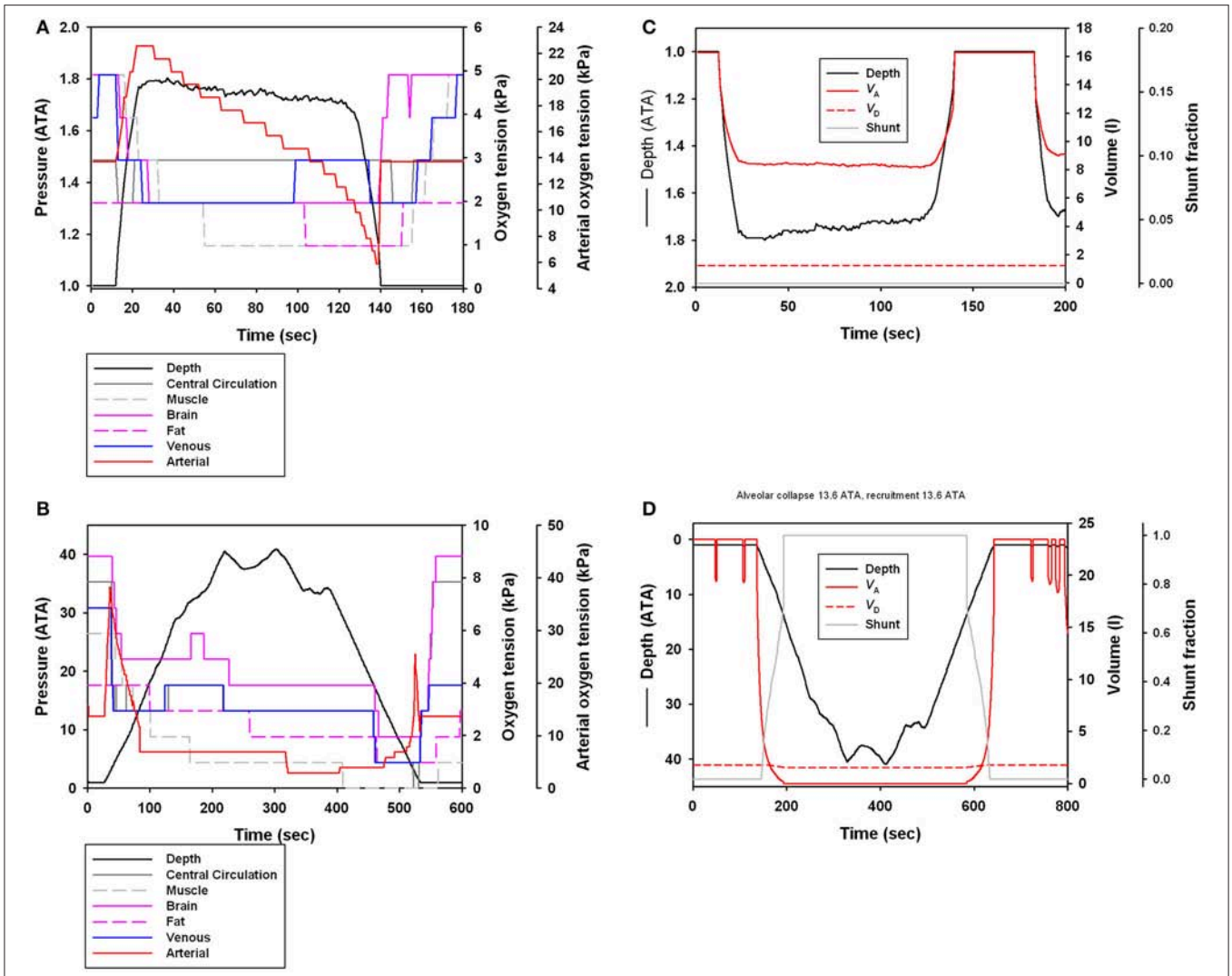

FIGURE 5 | (A,B) Estimated central circulation, muscle, brain, fat, arterial, and venous PO_2 (kPa) or **(C,D)** estimated shunt fraction, alveolar and tracheal volume for a long duration dive (depth in ATA, 1 ATA = 98.07 kPa) in **(A,C)** Sarasota and **(B,D)** Bermuda dolphin.

2009; Kvadsheim et al., 2012), but recent work has suggested that species-specific estimates may significantly alter the model estimates (Hodanbosi et al., 2016). We therefore used recently published data for respiratory compliance (Fahlman et al., 2011, 2015, 2018b), $\dot{Q}_{tot}$ (Miedler et al., 2015), and metabolic rate (Fahlman et al., 2015, 2018a) for coastal and offshore bottlenose dolphin to update the model parameters. These changes altered the compression of the alveolar space, which affects the pressure dependence of the pulmonary shunt (**Figure 1**).

The updated parameters (**Table 1**), with stiffer airways and more compliant alveolar space, increased the level of shunt and reduced gas exchange throughout dives (**Figures 1A,B**). This significantly reduced N_2 exchange during deeper dives as the alveolar space began compressing (**Figures 1C,D**). The updated parameters also affected O_2 exchange, but the effect was less apparent. For CO_2 there was little effect, and for longer and deeper dives, CO_2 exchange was improved. This implies that variation in gas exchange from changes in the alveolar ventilation ($\dot{V}_A$) and $\dot{Q}_{tot}$ relationship ($\dot{V}_A/\dot{Q}_{tot}$) differs for gases with varying gas solubility (West, 1962; Farhi and Yokoyama, 1967). These results agree with theoretical modeling in California sea lions that showed that changes in the structural properties of the respiratory system have a significant effect on the exchange of O_2, CO_2, and N_2 that differs between gas species (Hodanbosi et al., 2016). Together these studies provide additional support for a recent hypothesis suggesting that the lung architecture and varying $\dot{V}_A/\dot{Q}_{tot}$ would enable marine mammals to manipulate which gases are exchanged during diving (Garcia Párraga et al., 2018). While the current model does not include the proposed mechanisms that would alter the $\dot{V}_A/\dot{Q}_{tot}$ relationship, e.g., the effect of heterogeneous pulmonary blood flow and alveolar compression (collateral ventilation), it shows that varying the structural properties, which effectively reduces the $\dot{V}_A/\dot{Q}_{tot}$, the less soluble (N_2) is significantly more

affected as compared with the more soluble gases (O_2 and CO_2) (West, 1962; Farhi and Yokoyama, 1967). Thus, increasing upper airway stiffness and making the alveolar space more compliant causes the compression to occur at shallower depth, as originally hypothesized by Scholander (1940). This increases the level of shunt and reduces diffusion/ventilation, which has the greatest effect on gas with low solubility (West, 1962; Farhi and Yokoyama, 1967). In summary, we propose that the data in the current study agree with the suggestion that varying the $\dot{V}_A/\dot{Q}_{tot}$ ratio may be an efficient way for deep divers to minimize N_2 while still accessing pulmonary O_2 and CO_2 (Garcia Párraga et al., 2018).

The dive behaviors for the two dolphin forms were strikingly different, and demonstrate the large physiological plasticity in cetacean ecotypes. While these differences in dive behavior are undoubtedly related to differences in morphology, physiology and environment, the data presented here provide an interesting comparison of a species' capacity to vary physiological traits. Initially we used the available information for coastal dolphins to model tissue and blood gas dynamics in both populations (**Table 2**). For a 200 kg dolphin, the estimated O_2 stores were 8.7 l (43.6 ml O_2 kg^{-1}), resulting in a calculated aerobic dive limit (cADL) of 6.5 min when assuming a field metabolic rate that is twice that of resting. This cADL is considerably greater than the observed maximum dive durations in the Sarasota dolphins ranging from 2.2 min in the current study (**Table 3**), or up to 4.5 min in previous work (R. Wells, unpublished observation, Wells et al., 2013). The diet of bottlenose dolphins in Sarasota is composed exclusively of fish (>15 different species found in stomach content of 16 stranded animals; Barros and Wells, 1998). Thus, their activity may require a variety of high energy activities from rapid body turns (pinwheel feeding) to tail slaps (fish whacking, kerplunckling) associated with prey capture (Nowacek, 2002), which would increase the daily metabolic rate and reduce the cADL. For a cADL of 2.2–4.5 min, the Sarasota ecotype would have a metabolic scope around 3-6 times their resting metabolic rate (3 times the estimated field metabolic rate in **Table 3**). The metabolic scope is the maximal aerobic metabolic rate divided by the basal metabolic rate and is typically in the range of 3–10; a scope >7 cannot be sustained over long periods (Peterson et al., 1990). Thus, a field metabolic rate that is 6 times higher than the resting value implies that this ecotype would be working at or close to the maximal aerobic capacity for a cADL of 2.2 min. However, another likely explanation is that the coastal dolphins here operate in an environment where they are seldom limited by their dive physiology. The bottlenose dolphins from which dive data were obtained primarily occupy shallow waters in and around Sarasota and Palma Sola bays, with water depths generally <10 m, and often less than a few meters. Thus, our results suggest that they can significantly increase their dive duration if necessary but that they may not need this to exploit prey in their shallow-water habitat.

The Bermuda dolphins, on the other hand, had significantly longer dives than the Sarasota animals. A considerable number of dives exceeded the cADL, even when calculated from twice the resting metabolic rate, and the dolphin ran out of O_2 during long dives. For this reason, we hypothesized that the offshore dolphins must have increased O_2 stores to help increase their dive duration. We are not aware of any published body composition data for offshore delphinids, and to increase the O_2 stores we therefore modeled the body compartments according to the proposed body composition for deep-diving beaked whales, with increased blood and muscle O_2 storage (Peterson et al., 1990) that significantly increased the total O_2 stores (98.6 ml O_2 kg^{-1}), and the cADL (18.2 min, **Table 2**). With a maximal dive duration of 9 min, this provided a considerable scope for the Bermuda dolphins. The O_2 storage capacity of the sperm whale (81 ml O_2 kg^{-1}), hooded seal (90 ml O_2 kg^{-1}), elephant seal (94 ml O_2 kg^{-1}), and Weddell seal (89 ml O2 kg-1, Ponganis, 2015) are lower than our estimated value. The calculations made in the current study are based on assumptions about the blood volume, and muscle mass of these animals, and it is likely that the O_2 storage capacity is lower and the cADL shorter. If we assume that the longest dive represent the upper limit of the cADL, we would need an O_2 storage capacity of approximately 49 ml O_2 kg^{-1}). Thus, we can predict that the O_2 storage capacity is somewhere between these two values for the offshore ecotype.

In addition to a greater O_2 storage capacity, Bermuda dolphins may also have a greater capacity to alter diving metabolic rate. In a previous study, we estimated the field metabolic rate of coastal ecotype bottlenose dolphins to be around 11.7–23.4 ml O_2 min^{-1} kg^{-1}. As there were no differences in the resting metabolic rate of the coastal (Fahlman et al., 2018a) or offshore populations (Fahlman et al., 2018b), this field metabolic rate for offshore dolphins resulted in a cADL of 4.2–8.4 min, which is closer to the maximum dive duration seen for these animals. Studies have indicated that the metabolic cost during longer and deeper dives is similar to or lower than the resting metabolic rate at the surface (Hurley and Costa, 2001; Fahlman et al., 2013), and deeper dives may provide cost savings as the animals may be able to glide during long portions of the dive (Hurley and Costa, 2001; Williams, 2001; Fahlman et al., 2013). Thus, offshore dolphins may also have reduced cost of foraging that increases their cADL. Assessing field metabolic rate from these two populations using validated metabolic proxies, such as activity (acceleration, Fahlman et al., 2008b, 2013), or heart rate (McPhee et al., 2003), could be used to determine how energy is partitioned in this population and resolve some of these questions. In fact, the DTAG data provide such an opportunity and is an objective for future studies.

The dive data from the Bermuda dolphins are suggestive of 2 different types of dives; one shallow (10–70 m, **Figure 3B**) that changes little in depth with duration and another dive type starting at around 100 m depth with a steep increase in dive duration with depth (**Figure 3B**). It is not surprising that deeper dives are generally longer, as the transit to depth is a significant portion of the dive duration. During the deeper dives, the pulmonary shunt alters the blood and tissue gas content, as shown for the end-dive muscle PO_2 in **Figure 4C**. Without access to pulmonary PO_2, the blood O_2 was reduced and more O_2 used from the muscle, pushing down end-dive PO_2. This was not seen in the shallow diving Sarasota dolphins (**Figure 4A**), which never dove to depths where the pulmonary shunt began to alter gas tensions.

The differences in dive behavior had a significant effect on the gas tension in the blood and tissues (**Figure 5**). For both populations there was a continuous decrease in blood gases during the dive but the decrease was more extreme for the Bermuda dolphins (**Figure 5B**), and matching the blood flow to various tissues was more restrictive. This agrees with the suggestion made in previous modeling work that an important aspect of the dive response is to distribute the available perfusion to central tissues like the heart and brain, while blood flow to the muscle should be minimal (Davis and Kanatous, 1999). This allows muscle metabolism to be fueled by endogenous O_2 and assures that the matching of utilization of endogenous and vascular O_2 increases the duration of the dive that is fueled by aerobic metabolism (Davis and Kanatous, 1999).

For both ecotypes, the $\dot{Q}_{tot}$ while diving was assumed equal to the resting value measured in bottlenose dolphins (Miedler et al., 2015). The surface $\dot{Q}_{tot}$ in the Sarasota ecotype was set to 3 times higher than resting, which sufficiently restored O_2 and removed CO_2 from the blood and tissues to avoid continuous changes with repeated dives. In the Bermuda animals, on the other hand, a surface $\dot{Q}_{tot}$ of 3 times resting was not sufficient to restore the O_2 or remove the CO_2 during the longer dives. Initially, $\dot{Q}_{tot}$ was increased to 7 times higher than during diving, but while this improved restoration of blood and tissue O_2 and CO_2 levels, there were still continuous changes with repeated dives. By keeping the $\dot{Q}_{tot}$ elevated for submersions <20 m, however, we were able to sufficiently restore O_2 and remove enough CO_2 to prevent accumulating changes across repeated dives. These results suggest that $\dot{Q}_{tot}$ needs to be maintained during intervening short and shallow dives to allow restoration of normal blood and tissue gas tensions. Staying submerged during this time may help increase the PO_2 and thereby the uptake of O_2. The suggestion that there is little or no cardiovascular modification during shallow dives may be controversial, as most studies have reported changes in heart rate during diving. For example, in the bottlenose dolphin resting at the surface or while submerged the average heart rate were 105 and 40 beats min^{-1}, respectively (Noren et al., 2012). However, the past study provides an estimated surface resting heart rate that is influenced by the respiratory sinus arrhythmia (RSA), which will significantly elevate the resting values. In a more recent paper the surface resting heart rate when accounting for the RSA ranged from 27 to 54 beats min^{-1} (Miedler et al., 2015), thus not very different from the resting diving heart rate reported by Noren et al. (2012). In addition, in the past study it was also reported that the diving heart rate increased with underwater activity by between 40 and 79% (Noren et al., 2012). While our estimated $\dot{Q}_{tot}$ at depths shallower than 20 m may be overestimated, there is experimental evidence that the perfusion is modulated while submerged and future studies could look at how this changes during short and shallow dives.

In the Sarasota dolphins, the dive depth caused a reduction in alveolar volume, but the low pressure did not cause tracheal compression or induce a pulmonary shunt (**Figure 5C**). In the Bermuda dolphins, the arterial PO_2 increased during the descent to a maximum value, and then rapidly declined until the alveoli were reinflated during the ascent at which a second peak was observed (**Figure 5B**). We previously suggested that this pattern of arterial gas tension would support Scholander's hypothesis of pressure-induced hyperoxia as the lungs are compressed, followed by an increasing shunt as the alveoli are compressed until atelectasis (alveolar collapse), in this case at 126 m (**Figure 5D**), when the arterial side reflects the mixed venous (Fahlman et al., 2009; McDonald and Ponganis, 2012). This is supported by empirically measured arterial and venous gas tensions in both seals (Falke et al., 1985) and sea lions (McDonald and Ponganis, 2012). As the dolphin ascends, the alveoli are recruited at a depth of 126 m and gas exchange commences again. At this point, there is a second peak as pulmonary O_2 again saturates the blood (**Figures 5C,D**). The second peak for arterial PO_2 is lower as compared with the peak right before atelectasis, despite equivalent pulmonary PO_2. During the dive, the O_2 in the blood is continuously consumed, causing both the arterial and venous PO_2 to decrease. As the alveoli are recruited at depth, the pulmonary PO_2 increases. The high pulmonary and low venous PO_2 result in an elevated partial pressure gradient that favors diffusion and gas exchange. Thus, pulmonary O_2 diffuses into the pulmonary capillary and helps saturate the arterial blood. In addition, CO_2 is removed from the blood into the lung. Both these processes help prepare the dolphin to minimize the duration of the surface interval as CO_2 is being removed and O_2 being taken up before reaching the surface. Elevated gas exchange at depth also increases N_2 exchange, increasing the tissue and blood tension and the risk for gas emboli. However, the elevated pulmonary pressure as the alveoli open results in an elevated $\dot{V}_A/\dot{Q}_{tot}$ ratio, favoring O_2 and CO_2 exchange, while limiting N_2 exchange (Garcia Párraga et al., 2018). In addition, it has been hypothesized that marine mammals are able to separate the lung into two regions; one region that is ventilated and another atelactic area, with the latter being perfused (Garcia Párraga et al., 2018). This matching of pulmonary blood flow to hypoxic/atelactic regions result in selective gas exchange (Olson et al., 2010; Garcia Párraga et al., 2018), which during normal dives would help reduce the risk for gas emboli, and help prepare the dolphin to restore the O_2 used and removing the CO_2 produced (West, 1962; Farhi and Yokoyama, 1967; Olson et al., 2010). There is also evidence for an arterio-venous shunt that alters the blood gas tensions and could help minimize inert gas uptake during the ascent and help arterialize venous blood (Garcia Párraga et al., 2018).

In a number of marine mammals, there is an anticipatory pre-surfacing tachycardia, which likely increases $\dot{Q}_{tot}$ (Fedak et al., 1988; Thompson and Fedak, 1993; Andrews et al., 1997; Noren et al., 2012; Williams et al., 2017). During natural undisturbed dives, it seems that the change in heart rate begins during the initial stages of the ascent, but a large increase occurs during the later stages of the ascent close to the surface. Close to the surface, the blood and tissue tension would be supersaturated with N_2 and the gas would move from the tissues to the lungs (Fahlman et al., 2009). Elevated $\dot{Q}_{tot}$ at this stage of the dive would result in a decrease in the $\dot{V}_A/\dot{Q}_{tot}$ ratio, which would enhance exchange and removal of N_2. It has been hypothesized that disturbance of normal diving homeostasis, such as exposure to man-made

sound, capture in nets, or any stressful situation may alter the physiology and result in conditions that enhance N_2 uptake and the risk for gas emboli (Fernandez et al., 2005; Hooker et al., 2009; Fahlman et al., 2014; García-Párraga et al., 2014). In turtles, it has been suggested that the stress associated with incidental capture in fishing gear result in a sympathetic response, which opens the arterial pulmonary sphincter, increases pulmonary blood flow, decreases the $\dot{V}_A/\dot{Q}_{tot}$ ratio and increase N_2 uptake and risk of gas emboli (García-Párraga et al., 2014, 2017; Fahlman et al., 2017a). In cetaceans, active management of the pulmonary perfusion has been hypothesized as a mechanism that allow the cetaceans to vary the level of the $\dot{V}_A/\dot{Q}_{tot}$ match in the lung, and develop a shunt even at shallow depths that does not depend on hydrostatic compression (Garcia Párraga et al., 2018). Similar to the turtles, stress in cetaceans may also alter perfusion and the $\dot{V}_A/\dot{Q}_{tot}$ relationship causing increased pulmonary blood flow, increased uptake of N_2 and risk of gas emboli (Fahlman et al., 2006; Hooker et al., 2009). Theoretical modeling has indicated that stress related changes in $\dot{Q}_{tot}$ may increase the risk for gas emboli, and empirical data in the narwhal indicate that the large changes in the diving heart rate occurs deeper under stressful situations (around 170 m) as compared with natural dives (Fahlman et al., 2009, 2014; Hooker et al., 2009; Williams et al., 2017). Thus, this reversal of the diving bradycardia may result in elevated pulmonary blood flow, changes in blood flow distribution within the lung and changes in $\dot{V}_A/\dot{Q}_{tot}$, resulting in elevated N_2 uptake and risk for gas emboli (Garcia Párraga et al., 2018).

In summary, in the current study we show that the dive behavior in deep diving bottlenose dolphins likely requires morphological differences resulting in a greater O_2 storage capacity as compared with the coastal ecotype. It is also possible that the foraging behavior of the offshore population, with longer periods of gliding, results in lower foraging metabolic costs. Our results also indicate the importance of species-specific data when predicting physiological responses of animals. By updating the compliance estimates for the respiratory system, we show additional evidence of how variation in the ventilation/perfusion relationship is able to alter exchange of gases. This result provides additional support for our hypothesis of how marine mammals manage gases during diving and how stress may alter physiology and cause increased N_2 uptake and risk of gas emboli from forming.

DATA AVAILABILITY

The theoretical model and data used in this paper are made freely available at: osf.io/eyxpa.

AUTHOR CONTRIBUTIONS

AF helped collect the dive data, performed the modeling work, data analysis, wrote the first draft of the paper. FHJ collected and extracted the dive data, and helped edit the paper. PT provided the tools to collect the dive data, and helped edit the paper. RW helped collect the dive data and edited the paper.

FUNDING

AF (N00014-17-1-2756), PT (N000141512553) and FHJ (N00014-14-1-0410) were supported by the Office of Naval Research, and FHJ by an AIASCOFUND fellowship from Aarhus Institute of Advanced Studies, Aarhus University, under EU's FP7 program (Agreement No. 609033). PT received funding from the MASTS pooling initiative (The Marine Alliance for Science and Technology for Scotland) and their support is gratefully acknowledged. MASTS is funded by the Scottish Funding Council (grant reference HR09011) and contributing institutions. Funding for the Sarasota Bay and Bermuda fieldwork was provided by Dolphin Quest, Inc., and Office of Naval Research (N00014-14-1-0563).

ACKNOWLEDGMENTS

A special thanks to the many volunteers and staff at Dolphin Quest and the Sarasota Dolphin Research Project who made collection of the dive data possible. A special thanks to Nigel Pollard, the Bermuda Government, the Bermuda Aquarium, Museum and Zoo (BAMZ), and NOAA.

REFERENCES

Andrews, R. D., Jones, D. R., Williams, J. D., Thorson, P. H., Oliver, G. W., Costa, D. P., et al. (1997). Heart rates of northern Elephant seals diving at sea and resting on the beach. *J. Exp. Biol.* 200, 2083–2095.

Barros, N. B., and Wells, R. S. (1998). Prey and feeding patterns of resident bottlenose dolphins (*Tursiops truncatus*) in Sarasota Bay, Florida. *J. Mam.* 79, 1045–1059. doi: 10.2307/1383114

Bostrom, B. L., Fahlman, A., and Jones, D. R. (2008). Tracheal compression delays alveolar collapse during deep diving in marine mammals. *Resp. Physiol. Neurobiol.* 161, 298–305. doi: 10.1016/j.resp.2008.03.003

Boyd, I. L., Woakes, A. J., Butler, P. J., Davis, R. W., and Williams, T. M. (1995). Validation of heart rate and doubly labelled water as measures of metabolic rate during swimming in California sea lions. *Func. Ecol.* 9, 151–160. doi: 10.2307/2390559

Butler, P. J. (2006). Aerobic dive limit. What is it and is it always used appropriately? *Comp. Biochem. Physiol. A.* 145, 1–6. doi: 10.1016/j.cbpa.2006.06.006

Butler, P. J., Green, J. A., Boyd, I. L., and Speakman, J. R. (2004). Measuring metabolic rate in the field: the pros and cons of the doubly labelled water and heart rate methods. *Func. Ecol.* 18, 168–183. doi: 10.1111/j.0269-8463.2004.00821.x

Butler, P. J., and Jones, D. R. (1997). Physiology of diving birds and mammals. *Physiol. Rev.* 77, 837–899. doi: 10.1152/physrev.1997.77.3.837

Carbone, C., and Houston, A. I. (1996). The optimal allocation of time over the dive cycle: an approach based on aerobic and anaerobic respiration. *Anim. Behav.* 51, 1247–1255. doi: 10.1006/anbe.1996.0129

Castellini, M. A., Kooyman, G. L., and Ponganis, P. J. (1992). Metabolic rates of freely diving Weddell seals: correlations with oxygen stores, swim velocity and diving duration. *J. Exp. Biol.* 165, 181–194.

Cornick, L. A., and Horning, M. (2003). A test of hypotheses based on optimal foraging considerations for a diving mammal using a novel experimental approach. *Can. J. Zool.* 81, 1799–1807. doi: 10.1139/z03-179

Costa, D. P., Gales, N. J., and Goebel, M. E. (2001). Aerobic dive limit: how often does it occur in nature? *Comp. Biochem. Physiol. A*. 129, 771–783. doi: 10.1016/S1095-6433(01)00346-4

Davis, R. W., and Kanatous, S. B. (1999). Convective oxygen transport and tissue oxygen consumption in Weddell seals during aerobic dives. *J. Exp. Biol*. 202, 1091–1113.

Fahlman, A., Brodsky, M., Wells, R., McHugh, K., Allen, J., Barleycorn, A., et al. (2018a). Field energetics and lung function in wild bottlenose dolphins, *Tursiops truncatus*, in Sarasota Bay Florida. *Roy. Soc. Open. Sci*. 5:171280. doi: 10.1098/rsos.171280

Fahlman, A., Crespo Picazo, J. L., Sterba-Boatwright, B., Stacy, B. A., and Garcia-Parraga, D. (2017a). Defining risk variables causing gas embolism in loggerhead sea turtles (*Caretta caretta*) caught in trawls and gillnets. *Sci. Rep*. 7:2739. doi: 10.1038/s41598-017-02819-5

Fahlman, A., Hooker, S. K., Olszowka, A., Bostrom, B. L., and Jones, D. R. (2009). Estimating the effect of lung collapse and pulmonary shunt on gas exchange during breath-hold diving: the Scholander and Kooyman legacy Resp. *Physiol. Neurobiol*. 165, 28–39. doi: 10.1016/j.resp.2008.09.013

Fahlman, A., Loring, S. H., Ferrigno, M., Moore, C., Early, G., Niemeyer, M., et al. (2011). Static inflation and deflation pressure-volume curves from excised lungs of marine mammals. *J. Exp. Biol*. 214, 3822–3828. doi: 10.1242/jeb.056366

Fahlman, A., Loring, S. H., Levine, G., Rocho-Levine, J., Austin, T., and Brodsky, M. (2015). Lung mechanics and pulmonary function testing in cetaceans. *J. Exp. Biol*. 218, 2030–2038. doi: 10.1242/jeb.119149

Fahlman, A., Moore, M. J., and Garcia-Parraga, D. (2017b). Respiratory function and mechanics in pinnipeds and cetaceans. *J. Exp. Biol*. 220, 1761–1763. doi: 10.1242/jeb.126870

Fahlman, A., Olszowka, A., Bostrom, B., and Jones, D. R. (2006). Deep diving mammals: dive behavior and circulatory adjustments contribute to bends avoidance. *Respir. Physiol. Neurobiol*. 153, 66–77. doi: 10.1016/j.resp.2005.09.014

Fahlman, A., Svärd, C. D.,Rosen, A. S., Jones, D. R., and Trites, A. W. (2008a). Metabolic costs of foraging and the management of O_2 and CO_2 stores in Steller sea lions. *J. Exp. Biol*. 211, 3573–3580. doi: 10.1242/jeb.023655

Fahlman, A., Svärd, C. D.,Rosen, A. S., Wilson, R. S., and Trites, A. W. (2013). Activity as a proxy to estimate metabolic rate and to partition the metabolic cost of diving vs. breathing in pre- and post-fasted Steller sea lions. *Aquat. Biol*. 18, 175–184. doi: 10.3354/ab00500

Fahlman, A., Tyack, P. L., Miller, P. J., and Kvadsheim, P. H. (2014). How man-made interference might cause gas bubble emboli in deep diving whales. *Front. Physiol.* 5: 13. doi: 10.3389/fphys.2014.00013

Fahlman, A., McHugh, K., Allen, J., Barleycorn, A., Allen, A., Sweeney, J., et al. (2018b). Resting metabolic rate and lung function in wild offshore common bottlenose dolphins, tursiops truncatus, near bermuda. *Front. Physiol.* 9:886. doi: 10.3389/fphys.2018.00886

Fahlman, A., Wilson, R., Svärd, C., D.,Rosen, A. S., and Trites, A. W. (2008b). Activity and diving metabolism correlate in Steller sea lion *Eumetopias jubatus*. *Aquat. Biol*. 2, 75–84. doi: 10.3354/ab00039

Falke, K. J., Hill, R. D., Qvist, J., Schneider, R. C., Guppy, M., Liggins, G. C., et al. (1985). Seal lung collapse during free diving: evidence from arterial nitrogen tensions. *Science* 229, 556–557. doi: 10.1126/science.4023700

Farhi, L. E. (1967). Elimination of inert gas by the lung. *Respir. Physiol*. 3, 1–11. doi: 10.1016/0034-5687(67)90018-7

Farhi, L. E., and Yokoyama, T. (1967). Effects of ventilation-perfusion inequality on elimination of inert gases. *Resp. Physiol*. 3, 12–20. doi: 10.1016/0034-5687(67)90019-9

Fedak, M. A., Pullen, M. R., and Kanwisher, J. (1988). Circulatory responses of seals to periodic breathing: heart rate and breathing during exercise and diving in the laboratory and open sea. *Can. J. Zool*. 66, 53–60. doi: 10.1139/z88-007

Fernandez, A., Edwards, J. F., Rodruiquez, F., Espinosa de los Monteros, A., Herraez, M. P., Castro, P., et al. (2005). "Gas and fat embolic syndrome" involving a mass stranding of beaked whales (Family *Ziphiidae*) exposed to anthropogenic sonar signals. *Vet. Pathol*. 42, 446–457. doi: 10.1354/vp.42-4-446

Froget, G., Butler, P. J., Handrich, Y., and Woakes, A. J. (2001). Heart rate as an indicator of oxygen consumption: influence of body condition in the king penguin. *J. Exp. Biol*. 204, 2133–2144.

García-Párraga, D., Crespo-Picazo, J. L., Bernaldo de Quirós, Y., Cervera, V., Martí-Bonmati, L., Díaz-Delgado, J., et al. (2014). Decompression Sickness ("the bends") in Sea Turtles. *Dis. Aquat. Org*. 111, 191–205. doi: 10.3354/dao02790

Garcia Párraga, D., Moore, M., and Fahlman, A. (2018). Pulmonary ventilation–perfusion mismatch: a novel hypothesis for how diving vertebrates may avoid the bends. *Proc. Roy. Soc. B*. 285:20180482. doi: 10.1098/rspb.2018.0482

García-Párraga, D., Valente, A. L. S., Stacy, B. A., and Wyneken, J. (2017). "Cardiovascular system," in *Sea Turtle Health and Rehabilitation,* eds C. A. Manire, T. M. Norton, B. A. Stacy, C. A. Harms, and C. J. Innis (J. Ross Publishing), 295–320.

Hall, A. J., Wells, R. S., Sweeney, J. C., Townsend, F. I., Balmer, B. C., Hohn, A. A., et al. (2007). Annual, seasonal and individual variation in hematology and clinical blood chemistry profiles in bottlenose dolphins (*Tursiops truncatus*) from Sarasota Bay, Florida. *Comp. Biochem. Physiol. A*. 148, 266–277. doi: 10.1016/j.cbpa.2007.04.017

Higgs, N. D., Little, C. T. S., and Glover, A. G. (2010). Bones as biofuel: a review of whale bone composition with implications for deep-sea biology and palaeoanthropology. *Proc. Roy. Soc. B*. 278, 9–17. doi: 10.1098/rspb.2010.1267

Hodanbosi, M., Sterba-Boatwright, B., and Fahlman, A. (2016). Updating a gas dynamics model using estimates for California sea lions (*Zalophus californianus*). *Resp. Physiol. Neurobiol*. 234, 1–8. doi: 10.1016/j.resp.2016.08.006

Hoelzel, A. R., Potter, C. W., and Best, P. B. (1998). Genetic differentiation between parapatric "nearshore" and "offshore" populations of the bottlenose dolphin. *Proc. Roy. Soc. B*. 265, 1177–1183. doi: 10.1098/rspb.1998.0416

Hooker, S. K., Baird, R. W., and Fahlman, A. (2009). Could beaked whales get the bends? Effect of diving behaviour and physiology on modelled gas exchange for three species: *Ziphius cavirostris, Mesoplodon densirostris* and *Hyperoodon ampullatus*. *Resp. Physiol. Neurobiol*. 167, 235–246. doi: 10.1016/j.resp.2009.04.023

Hückstädt, L. A., Tift, M. S., Riet-Sapriza, F., Franco-Trecu, V., Baylis, A. M. M., Orben, R. A., et al. (2016). Regional variability in diving physiology and behavior in a widely distributed air-breathing marine predator, the South American sea lion *Otaria byronia*. *J. Exp. Biol*. 219, 2320–2330. doi: 10.1242/jeb.138677

Hurley, J. A., and Costa, D. P. (2001). Standard metabolic rate at the surface and during trained submersions in adult California sea lions (*Zalophus californianus*). *J. Exp. Biol*. 204, 3273–3281.

Johnson, M., and Tyack, P. L. (2003). A digital acoustic recording tag for measuring the response of wild marine mammals to sound. *IEEE J. Ocean. Eng.* 28, 3–12. doi: 10.1109/JOE.2002.808212

Klatsky, L. J., Wells, R. S., and Sweeney, J. C. (2007). Offshore bottlenose dolphins (*Tursiops truncatus*): movement and dive behavior near the Bermuda pedestal. *J. Mam*. 88, 59–66. doi: 10.1644/05-MAMM-A-365R1.1

Kooyman, G. L. (1973). Respiratory adaptations in marine mammals. *Am. Zool*. 13, 457–468. doi: 10.1093/icb/13.2.457

Kooyman, G. L. (1989). *Diverse Divers: Physiology and Behavior*. Berlin: Springer-Verlag.

Kooyman, G. L., Castellini, M. A., Davis, R. W., and Maue, R. A. (1983). Aerobic diving limits of immature Weddell seals. *J. Comp. Physiol*. 151, 171–174. doi: 10.1007/BF00689915

Kooyman, G. L., and Ponganis, P. J. (1998). The physiological basis of diving to depth: birds and mammals. *Ann. Rev. Physiol*. 60, 19–32. doi: 10.1146/annurev.physiol.60.1.19

Kvadsheim, P. H., Miller, P. J. O., Tyack, P. L., Sivle, L. L. D., Lam, F.-P. A., and Fahlman, A. (2012). Estimated tissue and blood N_2 levels and risk of *in vivo* bubble formation in deep-, intermediate- and shallow diving toothed whales during exposure to naval sonar. *Front. Physiol*. 3:125. doi: 10.3389/fphys.2012.00125

Mallette, S. D., McLellan, W. A., Scharf, F. S., Koopman, H. N., Barco, S. G., Wells, R. S., et al. (2016). Ontogenetic allometry and body composition of the common bottlenose dolphin (*Tursiops truncatus*) from the U.S. mid-Atlantic. *Mar. Mam. Sci*. 32, 86–121. doi: 10.1111/mms.12253

Mate, B. R., Rossbach, K. A., Nieukirk, S. L., Wells, R. S., Blair Irvine, A., Scott, M. D., et al. (1995). Satellite-monitored movements and dive behavior of a bottlenose dolphins (Tursiops truncatus) in Tampa Bay, Florida. *Mar. Mam. Sci.* 11, 452–463. doi: 10.1111/j.1748-7692.1995.tb00669.x

McDonald, B. I., and Ponganis, P. J. (2012). Lung collapse in the diving sea lion: hold the nitrogen and save the oxygen. *Biol. Lett.* 8, 1047–1049. doi: 10.1098/rsbl.2012.0743

McPhee, J. M., Rosen, D. A. S., Andrews, R. D., and Trites, A. W. (2003). Predicting metabolic rate from heart rate in juvenile Steller sea lions *Eumetopias jubatus*. *J. Exp. Biol.* 206, 1941–1951. doi: 10.1242/jeb.00369

Mead, J. G., and Potter, C. W. (1995). *Recognizing Two Populations off the Bottlenose Dolphin (Tursiops Truncatus) of the Atlantic Coast of North America-Morphologic and Ecologic Considerations*. International Biological Research Institute Reports, 32–44.

Miedler, S., Fahlman, A., Valls Torres, M., Álvaro Álvarez, T., and Garcia-Parraga, D. (2015). Evaluating cardiac physiology through echocardiography in bottlenose dolphins: using stroke volume and cardiac output to estimate systolic left ventricular function during rest and following exercise. *J. Exp. Biol.* 218, 3604–3610. doi: 10.1242/jeb.131532

Moore, C., Moore, M. J., Trumble, S., Niemeyer, M., Lentell, B., McLellan, W., et al. (2014). A comparative analysis of marine mammal tracheas. *J. Exp. Biol.* 217, 1154–1166. doi: 10.1242/jeb.093146

Noren, D. P., Holt, M. M., Dunkin, R. C., and Williams, T. M. (2013). The metabolic cost of communicative sound production in bottlenose dolphins (*Tursiops truncatus*). *J. Exp. Biol.* 216, 1624–1629. doi: 10.1242/jeb.083212

Noren, S. R., Kendall, T., Cuccurullo, V., and Williams, T. M. (2012). The dive response redefined: underwater behavior influences cardiac variability in freely diving dolphins. *J. Exp. Biol.* 215, 2735–2741. doi: 10.1242/jeb.069583

Noren, S. R., Lacave, G., Wells, R. S., and Williams, T. M. (2002). The development of blood oxygen stores in bottlenose dolphins (*Tursiops truncatus*): implications for diving capacity. *J. Zool.* 258, 105–113. doi: 10.1017/S0952836902001243

Noren, S. R., Williams, T. M., Pabst, D. A., McLellan, W. A., and Dearolf, J. L. (2001). The development of diving in marine endotherms: preparing the skeletal muscles of dolphins, penguins, and seals for activity during submergence. *J. Comp. Physiol. B.* 171, 127–134. doi: 10.1007/s003600000161

Nowacek, D. P. (2002). Sequential foraging behaviour of bottlenose dolphins, *Tursiops truncatus*, in Sarasota Bay, FL. *Behaviour* 139, 1125–1145. doi: 10.1163/15685390260437290

Olson, K. R., Whitfield, N. L., Bearden, S. E., St Leger, J., Nilson, E., Gao, Y., et al. (2010). Hypoxic pulmonary vasodilation: a paradigm shift with a hydrogen sulfide mechanism. *Am. J. Physiol. Regul. Integr. Comp. Physiol.* 298, R51–R60. doi: 10.1152/ajpregu.00576.2009

Pabst, D. A., McLellan, W. A., and Rommel, S. A. (2016). How to build a deep diver: the extreme morphology of mesoplodonts. *Int. Comp. Biol.* 56, 1337–1348. doi: 10.1093/icb/icw126

Peterson, C. C., Nagy, K. A., and Diamond, J. (1990). Sustained metabolic scope. *Proc. Natl. Acad. Sci. U.S.A.* 87, 2324–2328. doi: 10.1073/pnas.87.6.2324

Ponganis, P. J. (2011). Diving mammals. *Comp. Physiol.* 1, 517–535. doi: 10.1002/cphy.c091003

Ponganis, P. J. (2015). *Diving Physiology of Marine Mammals and Seabirds*. Cornwall: Cambridge University Press.

Reed, J. Z., Chambers, C., Fedak, M. A., and Butler, P. J. (1994). Gas exchange of captive freely diving grey seals (*Halichoerus grypus*). *J. Exp. Biol.* 191, 1–18.

Reed, J. Z., Chambers, C., Hunter, C. J., Lockyer, C., Kastelein, R., Fedak, M. A., et al. (2000). Gas exchange and heart rate in the harbour porpoise, *Phocoena phocoena*. *J. Comp. Physiol. B.* 170, 1–10. doi: 10.1007/s003600050001

Ridgway, S. H., and Johnston, D. G. (1966). Blood oxygen and ecology of porpoises of three genera. *Science* 151, 456–458. doi: 10.1126/science.151.3709.456

Scholander, P. F. (1940). Experimental investigations on the respiratory function in diving mammals and birds. *Hvalrådets Skrifter* 22, 1–131.

Schwacke, L. H., Hall, A. J., Townsend, F. I., Wells, R. S., Hansen, L. J., Hohn, A. A., et al. (2009). Hematologic and serum biochemical reference intervals for free-ranging common bottlenose dolphins (*Tursiops truncatus*) and variation in the distributions of clinicopathologic values related to geographic sampling site. *Am. J. Vet. Res.* 70, 973–985. doi: 10.2460/ajvr.70.8.973

Sparling, C. E., and Fedak, M. A. (2004). Metabolic rates of captive grey seals during voluntary diving. *J. Exp. Biol.* 207, 1615–1624. doi: 10.1242/jeb.00952

Thompson, D., and Fedak, M. A. (1993). Cardiac responses of grey seals during diving at sea. *J. Exp. Biol.* 174, 139–154.

Wells, R., McHugh, K., Douglas, D., Shippee, S., McCabe, E. B., Barros, N., et al. (2013). Evaluation of potential protective factors against metabolic syndrome in bottlenose dolphins: feeding and activity patterns of dolphins in Sarasota Bay, Florida. *Front. Endo.* 4:139. doi: 10.3389/fendo.2013.00139

Wells, R. S., Rhinehart, H. L., Hansen, L. J., Sweeney, J. C., Townsend, F. I., Stone, R., et al. (2004). Bottlenose dolphins as marine ecosystem sentinels: developing a health monitoring system. *EcoHealth* 1, 246–254. doi: 10.1007/s10393-004-0094-6

West, J. B. (1962). Regional differences in gas exchange in the lung of erect man. *J. Appl. Physiol.* 17, 893–898. doi: 10.1152/jappl.1962.17.6.893

Williams, T. M. (2001). Intermittent swimming by mammals: a strategy for increased energetic efficiency during diving. *Am. Zool.* 41, 166–176. doi: 10.1093/icb/41.2.166

Williams, T. M., Blackwell, S. B., Richter, B., Sinding, M.-H. S., and Heide-Jørgensen, M. P. (2017). Paradoxical escape responses by narwhals (*Monodon monoceros*). Sci*ence* 358, 1328–1331. doi: 10.1126/science.aao2740

Yazdi, P., Kilian, A., and Culik, B. M. (1999). Energy expenditure of swimming bottlenose dolphins (*Tursiops truncatus*). *Mar. Biol.* 134, 601–607. doi: 10.1007/s002270050575

Yeates, L. C., and Houser, D. S. (2008). Thermal tolerance in bottlenose dolphins (*Tursiops truncatus*). *J. Exp. Biol.* 211, 3249–3257. doi: 10.1242/jeb.020610

Conflict of Interest Statement: The authors declare that the research was conducted in the absence of any commercial or financial relationships that could be construed as a potential conflict of interest.

Copyright © 2018 Fahlman, Jensen, Tyack and Wells. This is an open-access article distributed under the terms of the Creative Commons Attribution License (CC BY). The use, distribution or reproduction in other forums is permitted, provided the original author(s) and the copyright owner(s) are credited and that the original publication in this journal is cited, in accordance with accepted academic practice. No use, distribution or reproduction is permitted which does not comply with these terms.

frontiers in Ecology and Evolution

ORIGINAL RESEARCH
published: 05 October 2018
doi: 10.3389/fevo.2018.00156

Strong Interspecific Differences in Foraging Activity Observed Between Honey Bees and Bumble Bees Using Miniaturized Radio Frequency Identification (RFID)

Danny F. Minahan[1]* *and Johanne Brunet*[2,3]

[1] *Department of Integrative Biology, University of Wisconsin, Madison, WI, United States,* [2] *USDA–Agricultural Research Service, Vegetable Crop Research Unit, Department of Entomology, University of Wisconsin, Madison, WI, United States,* [3] *Department of Entomology, University of Wisconsin, Madison, WI, United States*

OPEN ACCESS

Edited by:
Thomas Wassmer, Siena Heights University, United States

Reviewed by:
Monique Gauthier, Université Toulouse III Paul Sabatier, France
Brian R. Johnson, University of California, Davis, United States

***Correspondence:**
Danny F. Minahan
dfminahan@wisc.edu

Specialty section:
This article was submitted to Behavioral and Evolutionary Ecology, a section of the journal Frontiers in Ecology and Evolution

Received: *31 July 2018*
Accepted: *18 September 2018*
Published: *05 October 2018*

Citation:
Minahan DF and Brunet J (2018) Strong Interspecific Differences in Foraging Activity Observed Between Honey Bees and Bumble Bees Using Miniaturized Radio Frequency Identification (RFID). Front. Ecol. Evol. 6:156. doi: 10.3389/fevo.2018.00156

Central place foragers depart from and return to a central location with enough resources for themselves, and in many cases, for the group. Honey bees and bumble bees are eusocial central place foragers. Honey bees have large perennial colonies while bumble bee colonies are annual and considerably smaller. Foraging range, body size, and division of labor also vary between these two bee species. Honey bees use their unique dance language to recruit foragers to the most profitable patches. Bumble bees exploit patches individually and develop trapline foraging patterns. We expect such differences among bee species to engender differences in foraging activity. Moreover, variation in resource availability and in colony needs over the flowering season, can affect bee foraging activity. Finally, spatial variation in resource availability may impact bumble bees to a greater extent than honey bees due to their smaller foraging range. Using miniaturized radio frequency identification (RFID), we tracked the foraging activity of individual bees to and from hives at three sites and over five time periods. Pollen pellets were also collected from bees returning to the hive. We compared the European honey bee, *Apis mellifera*, and the common eastern bumble bee, *Bombus impatiens*. Linear mixed effect models determined the impact of bee species, time of season (period) and site, and their interactions, on multiple foraging metrics calculated from the RFID data and on pollen dry weight. Relative to honey bees, individual bumble bees made more foraging trips each day, resulting in a greater time spent foraging. A greater proportion of RFID tagged bumble bees foraged each day and bumble bees brought heavier pollen sacs to the hive compared to honey bees. Foraging bout duration did not vary between bee species and none of the foraging metrics varied among time periods or among sites. Both bee species brought heavier pollen sacs back to the hive at the beginning and the end of the flowering season. These results are discussed in terms of species differences in foraging strategies, size of individuals and colonies, and temporal variation in colony needs and resource availability.

Keywords: radio-frequency identification, bumble bee, honey bee, foraging activity, pollen pellet, site, time period

INTRODUCTION

Approximately 87% of flowering plants around the globe (Ollerton et al., 2011) and 35% of all crops grown for human consumption (Klein et al., 2007) benefit from animal pollination. Bees are important visitors to both crops and wildflowers, yet many bee species are in decline because of the combined effects of habitat loss, pesticide exposure, and pathogens (Naug, 2009; Cameron et al., 2011; Goulson et al., 2015). Bees are limited by the area of habitat available which is essential for nesting and gathering of floral resources, and the negative impact of habitat loss on bees may be most pronounced in areas where natural habitat is already limited (Winfree et al., 2009). In addition, exposure to neonicotinoid pesticides negatively affects the ability of honey bees to navigate back to their hive following artificial displacement (Fischer et al., 2014) and increases the foraging effort of bumble bees (Stanley et al., 2016). Importantly, these sublethal effects of neonicotinoid pesticide exposure can further exacerbate the negative impacts of pathogens such as Nosema and black queen cell virus on bees (Doublet et al., 2015). Given the numerous challenges facing bees, a better understanding of bee foraging over time and space, and for distinct species would facilitate the development of sound conservation strategies.

Bees are central place foragers, implying that they must depart a nesting site, locate and gather resources, and return with these resources to the hive or nesting area (Charnov, 1976). Honey bees and bumble bees are both generalist eusocial foragers that collect resources from a broad spectrum of plant taxa (Waser et al., 1996). The identity and quality of flowering plant resources can vary through time and space, and, therefore, under optimal foraging theory (Pyke, 1984), the strategies used by central place foragers to gather resources must be amenable to these fluctuations in resource availability (Goulson, 1999). Honey bees will forage at distances generally less than 6 km (Visscher and Seeley, 1982), but only a small fraction may forage within a 0.5 km radius around the hive (Beekman and Ratnieks, 2000), as indicated by waggle dance decoding. In contrast, a foraging range of less than 800 m was identified for several bumble bee species (*Bombus terrestris, B. pratorum, B. pascuorum,* and *B. lapidarius*) using sister-sister pairing with microsatellites (Knight et al., 2005). Wolf and Moritz (2008) obtained comparable results using distance from nest sampling in *B. terrestris*. In addition, the foraging range of bumble bees tends to decrease with increasing resource availability and decreased land fragmentation (Redhead et al., 2016), and high local resource availability can increase queen production (Herrmann et al., 2017). These results suggest possible differences in foraging strategies of honey bees and bumble bees in response to available resources.

Honey bees are perennial with a queen actively laying eggs and the colony capable of surviving multiple years (Seeley, 1978). In contrast, a bumble bee colony is annual, and the founding queen only lives for a single foraging season. New bumble bee queens are produced in the fall, disperse and hibernate through the winter, ultimately building a new hive the following foraging season (Michener, 2000). In addition, while individual bumble bees are larger than honey bees, honey bee colonies are much larger than bumble bee colonies. While a honey bee colony can contain 60,000 workers, a bumble bee colony can have between 50 and 250 workers, depending on the bee species. Moreover, honey bees have a higher level of communication and eusociality with a more structured division of labor relative to bumble bees. A known mode of information transmission for honey bees is the dance language, which communicates the distance, direction, and quality of resources to prospective foragers (Von Frisch, 1967; Seeley et al., 1991). The dance language is thought to allocate foraging workers to the best available patches in the landscape to gather resources (Couvillon and Ratnieks, 2015). While individual honey bees do not all follow dances before foraging, they are more likely to do so if they are novice foragers, have not foraged for a while, or their latest foraging trips were not rewarding (Biesmeijer and Seeley, 2005). Bumble bees, in contrast, do not have a dance language to communicate resource location, but they do actively "run" around the inside of their hive following a return to the hive with resources, possibly to stimulate foraging activity (Dornhaus and Chittka, 2001). In addition, activation of bumble bee foragers occurs following the addition of floral scent into a hive, and this behavior is especially pronounced when the scent is added to honey pots (Molet et al., 2009). Honey bees may therefore locate rewarding resources more efficiently relative than bumble bees.

While bumble bees are known to rely on trapline foraging strategies when visiting flowers, this strategy is not typically used by honey bees (Pasquaretta et al., 2017). Trapline foraging allows individuals to follow learned routes known to be profitable (Thomson et al., 1997; Ohashi et al., 2008). Trapline foraging is considered an optimal strategy, whereby individual bees learn the location of rewarding patches, and repeatedly visit these patches in a predictable route that develops over multiple independent foraging bouts (Lihoreau et al., 2012; Keasar et al., 2013; Woodgate et al., 2017). Trapline foraging increases the overall rewards obtained per plant visit (Williams and Thomson, 1998) and decreases overall search times (Saleh and Chittka, 2007). Pasquaretta et al. (2017) used network analysis to investigate the development of trapline foraging patterns in bumble bees and honey bees and found that bumble bees tend to quickly develop optimal routes at smaller spatial scales, while optimal trapline routes do not develop in honey bees except, possibly, at larger spatial scales.

We expect these differences in life history, body and colony size, division of labor, communication, and foraging strategies to engender differences in foraging activity between these two groups of bees. Foraging activity metrics include foraging bout duration, number of foraging bouts per bee and proportion of foragers gathering resources on a given day. The quicker location of rewards generated with the waggle dance and the trapline foraging of bumble bees may both affect foraging bout duration. The smaller colony size of bumble bees could necessitate a greater proportion of the bumble bee workforce being allocated to foraging relative to honey bees, and at the individual bee level, greater foraging activity per bee. Temporal variation in resource availability over the flowering season could also affect bee foraging. If fewer resources are available early and late in the flowering season, bees may spend more time foraging during these periods relative to the middle of the flowering season to bring sufficient resources to the hive. But colony needs will also affect foraging and are likely to change over the flowering season.

Pollen needs are expected to be greater during brood production while, at least for honey bees, nectar needs may increase later in the season in order to make sufficient honey to survive the winter months. Lastly, variation in resource availability among sites may impact bumble bees to a greater extent than honey bees due to their smaller foraging range (Visscher and Seeley, 1982; Pasquaretta et al., 2017). There are many reasons to expect foraging activity to vary over time, over space and among bee species.

The application of radio frequency identification (RFID) technology has increased enormously over the last 10 years and miniaturization of the tags have permitted its use to determine movement of honey bees and bumble bees to and from their hives (Pahl et al., 2011; Schneider et al., 2012). The use of radio frequency identification (RFID) provides a relatively novel and reliable tool to gather data on individual bees, as each microchip contains a unique identification number. Previous research using RFID demonstrated that honey bees can home in on their hive from 13 km away (Pahl et al., 2011). However, neonicotinoid pesticides can decrease the overall homing success (return rate) of foraging honey bees (Henry et al., 2012) and lower the foraging activity and increase foraging time of honey bee individuals (Schneider et al., 2012). Likewise, bees exposed to Fipronil pesticide via treated feeding sites decreased the number of foraging bouts and increased foraging bout duration (Decourtye et al., 2011). Moreover, RFID data indicated strong diurnal foraging patterns of two bumble bee species at northern latitudes with 24-h daylight sun (Stelzer and Chittka, 2010). RFID technology therefore represents a powerful tool for gathering data on foraging patterns of bees.

In the current study, we used miniaturized radio frequency identification (RFID) techniques to measure and compare the foraging activity of two bee species, the European honey bee, *Apis mellifera*, and the common eastern bumble bee, *Bombus impatiens*. RFID data were collected in 2016 at three separate sites and throughout the flowering season. These data were used to quantify different foraging metrics at the colony, individual bee, and foraging bout levels. In addition, we assessed the weight of pollen pellets bees brought back to the hive following a foraging trip in an attempt to link foraging time to resource acquisition. The impact of bee species, site, time of flowering season, and their interactions on the different foraging metrics and on pollen dry weight were examined using linear mixed effect models. Results are discussed in the context of differences in life history, colony size, and foraging strategies between these two bee species, and with respect to variation in colony needs over time and resource availability over time and space. Identifying spatial, temporal, and species differences in foraging metrics would help land managers improve conservation strategies for pollinator communities.

MATERIALS AND METHODS

Study Area and Bee Species

This study was conducted at the West Madison Agricultural Research Station (WMARS) in Madison, WI. This area is in a suburban-agricultural landscape, with a high proportion of arable experimental crop lands, roadside habitats, and suburban gardens (**Figure 1**). Radio Frequency identification (RFID) data and pollen pellets were collected from three sites in the summer of 2016 (**Figure 1**). Each site was selected based on a qualitative estimate of plant species richness within a 0.5 km radius around the hives and suggested increasing species richness from sites 1, 3, and 2, respectively. One hive of the European honey bee, *A. mellifera,* and one hive of the common eastern bumble bee,

FIGURE 1 | Aerial screenshot of the site locations. One honey bee and one bumble bee hives were located in the middle of each circle depicted as a 0.5 km radius at each location.

B. impatiens were placed at each site and separated by 60 m at site 2, and 100 m at sites 1 and 3. Each honey bee hive consisted of 2- deep frames vertically stacked in a wooden observation hive, with ∼2,000 bees, each of which was housed in a 1.2 m^3 wooden box with an exit tunnel allowing access outside. At the beginning of the experiment the bottom frame of each honey bee hive consisted of approximately half the frame covered in a combination of capped and open brood, while the top frame consisted of at least half a frame of honey. Each hive was queen right. These initial conditions allowed the colony some room to grow, albeit highly limited by the small hive size. Each bumble bee hive (Koppert Biological Systems, Howell, MI, USA) was placed in a small wooden shelter located 0.5 m off the ground and contained ∼75 worker bees at the start of the experiment. Among sites, the hive locations ranged from 700 to 1,500 m apart (sites 1–2: 700 m; sites 1–3 1,500 m; sites 2–3 1,400 m).

Data Collection

Radio Frequency Identification (RFID) data and pollen pellets were collected from the three sites and over five time periods between mid-June and mid-September. Within each period, we collected data for a total of 3 days from each site, moving among sites each day to randomize data collection among sites. Data were collected simultaneously from the honey bee and bumble bee hives at an individual site, using RFID reader pairs specific for honey bees and bumble bees, respectively. This pattern of data collection resulted in 9 data collection days within each period, with each site being visited every 4 to 5 days. Furthermore, the total duration of each period ranged from 10 to 17 days depending on weather (**Table 1**). The RFID data and pollen pellets were typically gathered on non-rainy days when the temperatures ranged between 21 and 35°C.

Radio Frequency Identification

Prior to each of the five data collection periods, a uniquely coded passive RFID tag (mic3–TAG 64-bit RO, iID2000, 13.56 MHz system, 1.0 x 1.6 x 0.5 mm; Microsensys GmbH, Erfurt, Germany) was glued onto the thorax of 70 honey bees and 20 bumble bees at each site as they were observed returning to their hive. We aimed at tagging bees returning with pollen sacs to ensure they were foragers. However, some tagged bees did not have pollen sacs and we assumed they were collecting another resource such as nectar or water. Honey bee foragers rarely return to working inside the hive (reviewed in Johnson, 2010) but tend to remain foragers until their death, or until winter arrives. At each hive, bees traveled through a 1″ diameter tube and through 2 RFID readers spaced 7.5 cm apart. We used one reader pair that was explicitly designed to gather data from honey bees, and another reader pair that was designed for bumble bees (iID2000, 2k6 HEAD; Microsensys GmbH, Erfurt, Germany). Each reader of a pair had a unique identity, and the pair was used to ascertain the direction of travel by bees, i.e., whether a bee was moving in or out of the hive. A foraging bout was indicated when a bee passed through the inner reader, followed by the outer reader, and at least 5 min elapsed until the next encounter with the outer reader, following the method of Gill et al. (2012). The RFID data were collected for 24 h each day and the readers were moved among sites each morning between 8:30 and 10:30 a.m. depending on weather. In general, the readers were moved at 9 a.m. June-August, and then closer to 10 a.m. as the nights became cooler later in August and into September.

TABLE 1 | Range of dates for collection of the Radio Frequency Identification (RFID) data and pollen pellets for each of the five periods over the three sites.

Period	Date range
1	June 14–27
2	July 1–13
3	July 23–August 2
4	August 8–25
5	August 30–September 13

Pollen Collection

To gather pollen, up to twenty individual bumble bees and 40 individual honey bees were caught as they returned to the hive with pollen pellets. These bees did not have RFID tags. Individual bees were collected into 2 dram plastic vials which were placed in a cooler filled with ice packs until a bee was no longer able to move (∼5–10 min for honey bees, 10–20 min for bumble bees). Both pollen pellets were removed from the bee, and each pellet was stored separately in a 1.5 mL microcentrifuge tube. Bees were subsequently released near the hive entrance. Following collection, pollen pellets were kept on ice and, upon return to the laboratory, were placed in a 20°C freezer until ready for drying and weighing. One pollen pellet per bee was dried at 45°C for 24 h and subsequently weighed to the nearest tenth of a milligram.

Statistical Analyses

Radio Frequency Identification

We examined foraging activity metrics, calculated from the RFID data, across multiple levels. At the colony level, the dependent variable was the percentage of tagged bees foraging each day. We did not determine the proportion of the hive that were foragers as we did not want to disturb the hive during the collection of foraging data. At the individual bee level, we computed three dependent variables from the RFID data. For each day, we examined (i) the average duration of a foraging bout per bee (ii) the number of foraging bouts per bee, and (iii) the total duration of foraging per bee (sum of all foraging bout durations per bee). Lastly, at the foraging bout level we used duration of a foraging bout as dependent variable.

We used linear mixed effect models (proc Mixed, SAS v. 9.4) to determine the impact of site, period, bee species and their interactions on the foraging activity metrics. While the fixed effects were similar in all models and included site, period, species and all two-way interactions, the level of replication and the random variables were different across each level of analysis, i.e., colony, individual bee, and foraging bout. For the proportion of tagged bees, the sole colony level foraging activity metric, day was the replicate in the model and the random effect was the three-way interaction, site*period*species (**Table 2**). For analyses examining foraging metrics at the individual bee level,

an individual bee was the replicate and the random factors included the three-way interaction site*period*species together with an additional day (site*period*species) term (**Table 2**). Finally, at the foraging bout level, where a foraging bout itself was the replicate, the random factors included the two three-way interactions present for the individual bee level analyses, together with a bee (site*period*species*day) term (**Table 2**). At the foraging bout level, the duration of a foraging bout was log transformed prior to analysis, while at the individual bee level the foraging bout duration and the number of foraging bouts per bee were log transformed to improve the model residuals.

In all three models the fixed effect explanatory variables were tested against the site*period*species error. In the colony level model, the random effect variable site*period*species was tested against the residual error (**Table 2**). In the individual bee model, the site*period*species random effect was tested against the day (site*period*species) error, while the day (site*period*species) random effect was tested against the model residual error (**Table 2**). Finally, for the model at the foraging bout level, the site*period*species random effect was tested against the day (site*period*species) error, the day (site*period*species) random effect was tested against the bee (site*period*day*bee) error, and the bee (site*period*day*bee) was tested against the model residual error (**Table 2**).

TABLE 2 | The linear mixed effect models used to examine the impact of site, time period, bee species, and their interactions on the different metrics of bee foraging effort, at the colony, individual bee, or foraging bout levels.

Replicate	Fixed effect variables	Random effect variables	Foraging effort
COLONY LEVEL			
Day	Site	Site*Period*Species	% Tagged bees
	Period		
	Species		
	Site*Species		
	Period*Species		
	Site*Period		
INDIVIDUAL BEE LEVEL			
Bee	Site	Site*Period* Species	Average duration of a foraging bout per bee each day
	Period	Day (Site*Period* Species)	
	Species		
	Site*Species		Number of foraging bouts per bee each day
	Period*Species		
	Site*Period		Total foraging bout duration per bee per day
FORAGING BOUT LEVEL			
Foraging bout	Site	Site*Period*Species	Foraging bout Duration
	Period	Day (Site*Period*Species)	
	Species	Bee (Site*Period* Species*Day)	
	Site*Species		
	Period*Species		
	Site*Period		

Pollen Dry Weight

Pollen collection effort is represented by the dry weight of pollen pellets. We used a linear mixed effect model (proc Mixed, SAS v. 9.4) to determine the impact of site, period, bee species, and their interactions on the dry weight of pollen pellets being returned to the hive. The fixed effects in the model included site, period, species and all two-way interactions. A pollen pellet was the unit of replication, and the random factors included the three-way interaction site*period*species together with a day (site*period*species) term (**Table 3**). While the fixed effect explanatory variables were tested against the site*period*species error, the site*period*species random effect was tested against the day (site*period*species) error, and the day (site*period*species) random effect was tested against the model residual error (**Table 3**). Pollen dry weights were square root transformed prior to analyses to improve the residuals of the model.

RESULTS

Radio Frequency Identification

At the colony level, a greater proportion of tagged bumble bees foraged each day (mean ± SE) (0.28 ± 0.03) relative to the proportion of tagged honey bees (0.19 ± 0.02) ($N = 76$ days) (**Table 4**). While we collected RFID data over 9 days at each site, no foraging activity was recorded on some days. This was true for 4 out of 9 days in period 1 for bumble bees and 3 days in period 5. For honey bees, no foraging data were recorded on one day in period 1, 3 days in period 2 and 1 day in periods 3 and 4. Although it varied between bee species, the proportion of tagged bees was not influenced by site or period or by any of the two-way interactions between bee species, site or period (species*site), (species*period), or (site*period) (**Table 4**). In other words, the proportion of bees foraging each day was similar among sites and time of year (period) and the pattern among sites or among periods was similar for the two bee species (**Table 4**). Moreover, the proportion of tagged bees foraging during the different periods was similar among sites (period*site) (**Table 4**).

At the level of the individual bee ($N = 703$ individual bees), none of the factors examined, bee species, site, period, or their

TABLE 3 | Linear mixed effect model used to examine the impact of site, time period, bee species, and their interactions on the weight of individual pollen pellets being returned to the hive by foragers.

Replicate	Fixed effect variables	Random effect variables
Pollen pellet	Site	Site*Period*Species
	Period	Day (Site*Period*Species)
	Species	
	Site*Species	
	Period*Species	
	Site*Period	

TABLE 4 | The impact of site, time period, bee species, and their two-way interactions on different metrics of bee foraging effort at the colony and foraging bout levels.

Fixed effect variable	Colony level			Foraging bout level		
	Proportion tagged bees foraging			Foraging bout duration		
	df	*F*	*P*-value	*df*	*F*	*P*-value
Site	2, 8	0.78	0.491	2, 8	0.25	0.788
Period	4, 8	1.11	0.417	4, 8	2.29	0.148
Species	1, 8	5.37	**0.049**	1, 8	1.16	0.313
Period × Species	4, 8	0.23	0.913	4, 8	0.32	0.854
Site × Species	2, 8	1.10	0.378	2, 8	2.81	0.119
Site × Period	8, 8	0.62	0.746	8, 8	1.47	0.299

*The mixed effect linear models used for analyses at each level of the foraging effort metrics are summarized in **Table 2**. The variables df stands for degrees of freedom, F for the F statistics and P-value is the probability value for the specific factor or interaction in the model. Bold type indicates P < 0.05.*

two-way interactions affected the average duration of a foraging bout (**Table 5**). Foraging bout duration for a bee was similar among sites, among periods, and among bee species (**Table 5**). However, on any given day, the number of foraging trips per bee and the total time a bee spent foraging differed among bee species (**Table 5**). Bumble bees made significantly more foraging trips in a day (5.9 ± 0.4) relative to honey bees (4.6 ± 0.2) and they spent more total time foraging each day (bumble bees: 346.9 min ± 16.2; honey bee: 222.4 min ± 6.6). Site, period and the two-way interactions did not influence either the number of foraging trips per bee or the total time a bee spent foraging each day (**Table 5**). Finally, at the level of a foraging bout ($N = 3{,}502$ foraging bouts), none of the factors or their two-way interactions affected the average duration of a foraging bout (**Table 4**). An average foraging bout lasted 58.5 ± 2.0 min for bumble bees, in contrast to 48.71 ± 0.8 for honey bees. Although it was slightly longer for bumble bees the difference could not be explained by differences between bee species in our model.

Pollen Dry Weight

We obtained the pollen dry weights of 1,598 pollen pellets. There was a statistically significant effect of species and period on the weight of pollen pellets brought back to the hive and a weaker site*species interaction (**Table 6**). Using multiple means comparisons to examine the interaction between site and species, the average pollen pellet weight was always greater for bumble bees than for honey bees (**Figure 2**) and the difference between species was statistically significant at two sites and borderline at the third (Site 1: df = 1, 7; $t = 4.00$; $P = 0.0052$; Site 2: df = 1, 7; $t = 6.56$; $P = 0.0003$; and Site 3: df = 1, 7; $t = 2.34$, $P = 0.052$). We therefore considered the impact of the main factor of species on pollen pellet dry weights. For any foraging bout, bumble bees returned with significantly heavier pollen pellets relative to honey bees (bumble bee: 7.73 mg ± 0.25; honey bee: 3.68 mg ± 0.08) (**Table 6**). Moreover, the weight of pollen pellets brought back to the hive following a foraging bout varied among periods over the flowering season (**Table 6**). Bees returned to the hive with heavier pollen pellets during the first (mean ± SE) (6.81 mg ± 0.24) and last (6.38 mg ± 0.32) periods, relative to the second (4.09 mg ± 0.16), third (3.34 mg ± 0.19), and fourth (3.71 mg ± 0.25) periods (**Figure 3**). The weight of pollen pellets brought back to the hive by individual bees were similar between the first and last periods (**Figure 3**). Such differences among periods were similar for bumble bees and honey bees as indicated by the lack of a statistically significant interaction between period and bee species (**Table 6**).

DISCUSSION

The foraging activity of bumble bees was greater than that of honey bees. Relative to honey bees, an individual bumble bee embarked on more foraging bouts each day. In addition, a greater proportion of bumble bee foragers actually foraged on a given day. However, the duration of a foraging bout did not differ between these two bee species. The average duration of a foraging bout by an individual bee each day lasted 58.5 ± 2.0 min for bumble bees, in contrast to 48.71 ± 0.8 for honey bees. But, because individual bumble bees did more foraging trips in a day, they spent more total time foraging each day.

Foraging bout duration can be affected by the time it takes for bees to reach rewarding resource patches and by the time a bee spends foraging at that resource, collecting either pollen or nectar. The waggle dance can facilitate the location of rewarding resources by honey bees, although not all individual bees observe the dance prior to foraging (Biesmeijer and Seeley, 2005). Moreover, honey bees tend to have a larger foraging range relative to bumble bees (Visscher and Seeley, 1982; Knight et al., 2005). Many foraging models for flower visiting insects assume that the time traveling between patches is negligible relative to the time spend foraging within patches (Goulson, 1999). In contrast to honey bees, bumble bees must learn, and remember profitable locations, and develop trapline foraging patterns among patches (Ohashi et al., 2008), while honey bees do not tend to develop optimal trapline routes (Pasquaretta et al., 2017). Results of the current study suggest that the foraging strategies of both bee species translate into similar foraging bout durations, from the time a bee leaves the hive to the time it returns to the hive. The more individualistic trapline foraging mode of bumble bees seems to permit them to gather resources in the same amount of time as the more direct method of information transmission for resource quality and location communicated by the waggle dance of honey bees (Thomson et al., 1997; Ohashi et al., 2007; Lihoreau et al., 2010; Couvillon et al., 2014; Ratnieks and Shackleton, 2015). Future studies should determine the differences in foraging bout durations between individual honey bees that follow the waggle dance and those that do not to increase our understanding of the impact of honey bee communication on foraging bout duration. Moreover, when comparing bumble bees and honey bees foraging within patches, Brunet (unpublished data) observed similar foraging bout duration within a patch for these two bee species. Future studies should examine in more details the reasons why, despite the various differences in their foraging strategies, foraging bout duration from the time a bee leaves the hive to the time it returns to a hive remains similar between these two bee species.

TABLE 5 | The impact of site, time period, bee species and their two-way interactions on different metrics of bee foraging effort at the individual bee level.

Fixed effect variable	Individual bee level								
	Average foraging bout duration			Total duration of foraging			Number of foraging bouts		
	df	*F*	*P*-value	*df*	*F*	*P*-value	*df*	*F*	*P*-value
Site	2,8	0.13	0.880	2, 8	0.14	0.873	2, 8	0.35	0.714
Period	4,8	1.59	0.266	4, 8	1.08	0.427	4, 8	2.91	0.093
Species	1,8	1.93	0.203	1, 8	13.33	**0.007**	1, 8	9.38	**0.016**
Period × Species	4,8	0.55	0.703	4, 8	0.83	0.541	4, 8	1.73	0.237
Site × Species	2,8	3.13	0.099	2, 8	0.73	0.511	2, 8	0.78	0.491
Site × Period	8,8	1.49	0.293	8, 8	1.51	0.288	8, 8	2.69	0.092

*The mixed effect linear models used for analyses of the foraging effort metrics are summarized in **Table 2**. The variables df stands for degrees of freedom, F for the F statistics and P-value is the probability value for the specific factor or interaction in the model. Bold type indicates P < 0.05.*

TABLE 6 | The impact of site, time period, bee species and their two-way interactions on the average weight of a pollen pellet returned to the hive by foragers.

Fixed effect Variable	*df*	*F*	*P*-value
Site	2, 7	1.97	0.210
Period	4, 7	14.29	**0.002**
Species	1, 7	44.05	**0.0003**
Period × Species	4, 7	1.24	0.376
Site × Species	2, 7	4.88	**0.047**
Site × Period	8, 7	2.46	0.126

*The mixed effect linear model used for the analysis is summarized in **Table 3**. The variables df stands for degrees of freedom, F for the F statistics and P-value is the probability value for the specific factor or interaction in the model. Bold type indicates P < 0.05.*

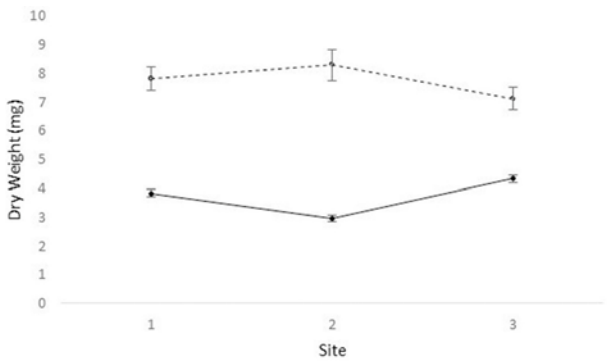

FIGURE 2 | The mean ± dry weight (mg) of individual pollen pellets collected by honey bees (solid line) and bumble bees (dashed line) at sites 1, 2, and 3.

Individual bumble bees spent more time foraging each day and a greater proportion of the foragers were active each day relative to honey bees. Although we did not gather information on the proportion of the colony that were foragers, in order not to disturb the hive during collection of foraging data, the proportion of the foragers that were active each day is a strong descriptor of colony level foraging activity as new foragers were tagged at the start of each time period. The observed interspecific differences were consistent over the flowering season and among sites, as indicated by the lack of significant interactions between bee species and period or site in our mixed model. This pattern supports consistent and stable interspecific differences in the activity levels of honey bees and bumble bees to gather resources. Differences in life history and in colony sizes between these two bee species may help explain observed differences in foraging activity. Bumble bee colonies are annual and small in contrast to the perennial and large honey bee colonies. Given such differences, each bumble bee worker may need to put forth more effort to build up and sustain the colony relative to a honey bee worker. But, if activity level relates to colony size, with an increase in colony size over the season, we would also expect the foraging effort per bee and percent of colony foraging to decrease, which we did not observe. We therefore suspect other factors, besides colony size and life history, help explain observed differences in foraging activities between these two bee species. The more complex division of labor of honey bee colonies could represent such a factor and may facilitate a lower foraging activity per individual and at the colony level. Furthermore, considering the honey bees in this experiment were restricted to a 2-frame observation hive with limited space for the colony to grow, and therefore limiting growth associated changes in colony needs, these results may differ from experiments conducted under more typical circumstances, and further studies should be undertaken on larger hives. Finally, more research is needed to elucidate whether and how differences in life history, colony size, and social structure contribute to interspecific differences in bee foraging activity.

Bumble bees brought heavier pollen pellets back to the hive relative to honey bees, even though both bee species had similar foraging bout durations. Because most bees tend to forage either for pollen or for nectar during a foraging bout (Brunet, unpublished data), this result suggests that bumble bees are more efficient than honey bees at retrieving pollen from the plants they visit. The observed interspecific difference in pollen pellet size may result from honey bees being smaller than bumble bees. Within a bee species, larger pollen, and nectar loads are correlated with increased body size of foragers (Goulson et al., 2002). However, it is unclear how this pattern might translate among bee species. Individual bumble bees made more foraging

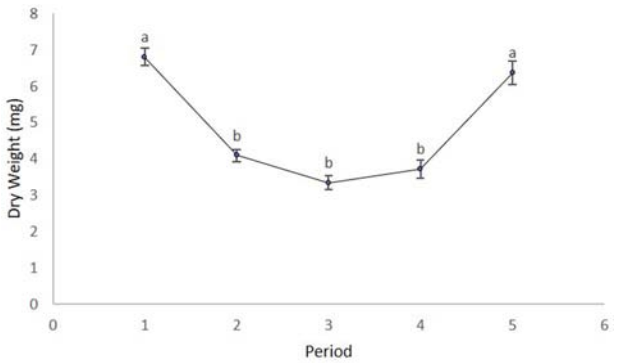

FIGURE 3 | The mean ± dry weight (mg) of individual pollen pellets collected by bees over the five time periods. Time periods with different letters are statistically different from one another as indicated by multiple means tests.

trips in a day and brought back more pollen to the hive each time, relative to honey bees. Moreover, a greater proportion of the bumble bee foragers were active each day relative to honey bees. Such patterns should translate into a greater amount of pollen available per capita for bumble bees relative to honey bees. Bumble bees, due to their larger size, may have greater pollen requirements than honey bees, and indeed bee body size is correlated to the amount of protein received by developing larvae (Roulston and Cane, 2002). Differences in body size among bee species may therefore help explain differences in foraging patterns (Spaethe and Weidenmüller, 2002) that optimize the amount of pollen brought back to the hive to meet a colony's need.

Across all levels, the foraging activity of these two bee species did not vary over the flowering season (period) or among sites. The time a bee spent foraging per bout or per day and the proportion of foragers active each day did not change over the flowering season and did not differ among sites. Moreover, this pattern was true for both bee species. The lack of variation in foraging activity over the season or among sites was surprising. We expected greater foraging activity early and late in the flowering season because of the lower expected resource availability. Moreover, the known differences in foraging ranges between these two bee species suggested among site variation in foraging activity for bumble bees but not for honey bees (Visscher and Seeley, 1982; Pasquaretta et al., 2017). But colony needs may also change over the flowering season. We expect greater pollen needs earlier in the season for both bee species as more brood may be produced relative to later in the season. Later in the season, we expect greater nectar needs for honey bees as they are building honey reserves for the colony to survive the winter months. Bumble bee colonies, however, are producing new queens and may still have high pollen needs. Interestingly, we gathered some data for bumble bees on the proportion of bees returning to the hive with and without pollen pellets. Although the sample sizes were uneven among periods, the trend suggested that most foragers returned to the hive with pollen pellets during the first (95%) and last (96%) periods, while a greater proportion of the foragers returned with nectar in the three middle periods (47, 15, and 33%, respectively).

We did not gather such data for honey bees although it should be determined in future studies. However, because foraging bout duration did not change over the flowering season, these data suggest no apparent differences in the time a bee spends foraging for pollen vs. nectar. The larger pollen production for bumble bees early and late in the flowering season suggest a greater pollen need, possibly for growing larvae early in the season and queen development in late summer/early fall. Interestingly, colony needs can influence the proportion of foragers collecting pollen or nectar but it did not influence foraging activity in general (time spent foraging and proportion of foragers active each day). Moreover, any variation in resource availability over time and space did not significantly influence foraging activity for these two bee species in the current study.

Both bee species brought more pollen back to the hive per foraging bout at the beginning and end relative to the middle periods of the flowering season, even though the time spent foraging remained constant throughout the flowering season. The temporal differences in the amount of pollen gathered suggest that it took longer to collect resources from flowers in mid-summer relative to early or late summer. Couvillon et al. (2014) proposed that summer is the most challenging season for honey bees because bees foraged at greater distances in mid-summer relative to spring and fall. Danner et al. (2017) found honey bees returned the greatest amount of pollen to the hive early in the season, in April and May. Taken together, these results support the notion that summer may be the most challenging season for bees, at least for eusocial bees. One potential explanation for this pattern is that, although resources may increase in mid-summer, the density of bees also increases and, thus, the level of competition for shared resources.

The use of miniaturized RFID allows for continual tracking of individual bees and provides a real-time view of the activity of foraging bees in both field and laboratory contexts and furthers our ability to test hypotheses of optimal foraging in bees and other invertebrates. Future research using RFID could contrast the foraging activity of these two bee species over different landscapes to determine whether the similarities and differences observed in this study are consistent over variable landscapes. Future research could also further elucidate the role of bee size, colony size, communication strategies, and division of labor on their impact to bee foraging behavior. In addition, relating bee foraging activity more directly to available resources, and to energy intake and expenditure would provide crucial understanding as to the optimal foraging behavior of social bees. Future useful technological developments for the study of bees could include designing miniature RFID tags that can be read from a further distance and to permit their use in solitary bees. In addition, the development of affordable and small-scaled technology that could be used to track bees as they move over the landscape, both among flowers and among plants within patches and among patches would represent a breakthrough in the study of bee foraging and bee movement.

CONCLUSIONS

This study is the first to use RFID technology to contrast the foraging activity of two social bee species in a common

landscape. The use of RFID was crucial to revealing differences and similarities in various foraging activity metrics in these two bee species. It permitted the detection of strong interspecific differences in foraging activity that were maintained among time periods and sites. At the level of individual bees and of the colony, bumble bees exhibited greater foraging activity relative to honey bees. Per capita, bumble bees also brought more pollen back to the hive relative to honey bees suggesting a stronger need for pollen for bumble bees. Interestingly, the foraging activity of these two bee species did not vary over time or among sites. Many of the observed trends highlighted interesting and unexpected patterns that could not have been discovered without the use of RFID technology.

DATA AVAILABILITY

The raw data which support the conclusions of this manuscript will be made available by the authors when requested by any qualified researcher.

AUTHOR CONTRIBUTIONS

DM and JB designed the experiment and methodology. DM collected the data. DM and JB worked on data analyses with the help of a statistician. DM led writing the manuscript and JB contributed critically to the drafts and gave final approval for publication.

ACKNOWLEDGMENTS

We thank Alexandra Kois and Kyle Krellwitz for their contribution to both the field and laboratory components of this research. Furthermore, we want to thank Dr. Murray Clayton for his guidance with statistical analyses. This work was supported by funds from the Garden Club of America – Centennial Pollinator Fellowship (2016) to DM and by a Biotechnology Risk Assessment Grant Program competitive grant no. 2013-33522-20999 from the USDA National Institute of Food and Agriculture and by funds from the USDA-ARS to JB.

REFERENCES

Beekman, M., and Ratnieks, F. L. W. (2000). Long-range foraging by the honey-bee, *Apis mellifera L. Funct. Ecol.* 14, 490–496. doi: 10.1046/j.1365-2435.2000.00443.x

Biesmeijer, J. C., and Seeley, T. D. (2005). The use of waggle dance information by honey bees throughout their foraging careers. *Behav. Ecol. Sociobiol.* 59, 133–142. doi: 10.1007/s00265-005-0019-6

Cameron, S. A., Lozier, J. D., Strange, J. P., Koch, J. B., Cordes, N., Solter, L. F., et al. (2011). Patterns of widespread decline in North American bumble bees. *Proc. Natl. Acad. Sci. U.S.A.* 108, 662–667. doi: 10.1073/pnas.1014743108

Charnov, E. L. (1976). Optimal foraging, the marginal value theorem. *Theor. Popul. Biol.* 9, 129–136. doi: 10.1016/0040-5809(76)90040-X

Couvillon, M. J., and Ratnieks, F. L. W. (2015). Environmental consultancy: dancing bee bioindicators to evaluate landscape "health." *Front. Ecol. Evol.* 3:44. doi: 10.3389/fevo.2015.00044

Couvillon, M. J., Schürch, R., and Ratnieks, F. L. W. (2014). Waggle dance distances as integrative indicators of seasonal foraging challenges. *PLoS ONE* 9:93495. doi: 10.1371/journal.pone.0093495

Danner, N., Keller, A., Härtel, S., and Steffan-Dewenter, I. (2017). Honey bee foraging ecology: season but not landscape diversity shapes the amount and diversity of collected pollen. *PLoS ONE* 12:e0183716. doi: 10.1371/journal.pone.0183716

Decourtye, A., Devillers, J., Aupinel, P., Brun, F., Bagnis, C., Fourrier, J., et al. (2011). Honeybee tracking with microchips: a new methodology to measure the effects of pesticides. *Ecotoxicology* 20, 429–437. doi: 10.1007/s10646-011-0594-4

Dornhaus, A., and Chittka, L. (2001). Food alert in bumblebees (*Bombus terestris*): possible mechanisms and evolutionary implications. *Behav. Ecol. Sociobiol.* 50, 570–576. doi: 10.1007/s002650100395

Doublet, V., Labarussias, M., de Miranda, J. R., Moritz, R. F., and Paxton, R. J. (2015). Bees under stress: sublethal doses of a neonicotinoid pesticide and pathogens interact to elevate honey bee mortality across the life cycle. *Environ. Microbiol.* 17, 969–983. doi: 10.1111/1462-2920.12426

Fischer, J., Müller, T., Spatz, A. K., Greggers, U., Grünewald, B., and Menzel, R. (2014). Neonicotinoids interfere with specific components of navigation in honeybees. *PLoS ONE* 9:91364. doi: 10.1371/journal.pone.0091364

Gill, R. J., Ramos-Rodriguez, O., and Raine, N. E. (2012). Combined pesticide exposure severely affects individual-and colony-level traits in bees. *Nature* 491, 105–108. doi: 10.1038/nature11585

Goulson, D. (1999). Foraging strategies of insects for gathering nectar and pollen, and implications for plant ecology and evolution. *Perspect. Plant Ecol. Evol. Syst.* 2, 185–209. doi: 10.1078/1433-8319-00070

Goulson, D., Nicholls, E., Botías, C., and Rotheray, E. L. (2015). Bee declines driven by combined stress from parasites, pesticides, and lack of flowers. *Science* 347:1255957. doi: 10.1126/science.1255957

Goulson, D., Peat, J., Stout, J. C., Tucker, J., Darvill, B., Derwent, L. C., et al. (2002). Can alloethism in workers of the bumblebee, *Bombus terrestris*, be explained in terms of foraging efficiency? *Anim. Behav.* 64, 123–130. doi: 10.1006/anbe.2002.3041

Henry, M., Béguin, M., Requier, F., Rollin, O., Odoux, J. F., Aupinel, P., et al. (2012). A common pesticide decreases foraging success and survival in honey bees. *Science* 336, 348–350. doi: 10.1126/science.1215039

Herrmann, J. D., Haddad, N. M., and Levey, D. J. (2017). Testing the relative importance of local resources and landscape connectivity on Bombus impatiens (Hymenoptera, Apidae) colonies. *Apidologie* 48, 545–555. doi: 10.1007/s13592-017-0499-1

Johnson, B. R. (2010). Division of labor in honeybees: form, function, and proximate mechanisms. *Behav. Ecol. Sociobiol.* 64, 305–316. doi: 10.1007/s00265-009-0874-7

Keasar, T., Motro, U., and Shmida, A. (2013). Temporal reward variability promotes sampling of a new flower type by bumblebees. *YANBE* 86, 747–753. doi: 10.1016/j.anbehav.2013.07.010

Klein, A. M., Vaissière, B. E., Cane, J. H., Steffan-Dewenter, I., Cunningham, S. A., Kremen, C., et al. (2007). Importance of pollinators in changing landscapes for world crops. *Proc. R. Soc. Lond. B Biol. Sci.* 274, 303–313. doi: 10.1098/rspb.2006.3721

Knight, M. E., Martin, A. P., Bishop, S., Osborne, J. L., Hale, R. J., Sanderson, R. A., et al. (2005). An interspecific comparison of foraging range and nest density of four bumblebee (*Bombus*) species. *Mol. Ecol.* 14, 1811–1820. doi: 10.1111/j.1365-294X.2005.02540.x

Lihoreau, M., Chittka, L., and Raine, N. E. (2010). Travel optimization by foraging bumblebees through re-adjustments of traplines after discovery of new feeding locations. *Am. Nat.* 176, 744 – 767. doi: 10.1086/657042

Lihoreau, M., Raine, N. E., Reynolds, A. M., Stelzer, R. J., Lim, K. S., Smith, A. D., et al. (2012). Radar tracking and motion-sensitive cameras on flowers reveal the development of pollinator multi-destination routes over large spatial scales. *PLoS Biol.* 10, 19–21. doi: 10.1371/journal.pbio.1001392

Michener, C. D. (2000). *The Bees of the World*. Baltimore, MD: Johns Hopkins University Press.

Molet, M., Chittka, L., and Raine, N. E. (2009). How floral odours are learned inside the bumblebee (*Bombus terrestris*) nest. *Naturwissenschaften* 96, 213–219. doi: 10.1007/s00114-008-0465-x

Naug, D. (2009). Nutritional stress due to habitat loss may explain recent honeybee colony collapses. *Biol. Conserv.* 142, 2369–2372. doi: 10.1016/j.biocon.2009.04.007

Ohashi, K., Leslie, A., and Thomson, J. D. (2008). Trapline foraging by bumble bees: V. Effects of experience and priority on competitive performance. *Behav. Ecol.* 19, 936–948. doi: 10.1093/beheco/arn048

Ohashi, K., Thomson, J. D., and D'Souza, D. (2007). Trapline foraging by bumble bees: IV. Optimization of route geometry in the absence of competition. *Behav. Ecol.* 18, 1–11. doi: 10.1093/beheco/arl053

Ollerton, J., Winfree, R., and Tarrant, S. (2011). How many flowering plants are pollinated by animals? *Oikos* 120, 321–326. doi: 10.1111/j.1600-0706.2010.18644.x

Pahl, M., Zhu, H., Tautz, J., and Zhang, S. (2011). Large scale homing in honeybees. *PLoS ONE* 6:e19669. doi: 10.1371/journal.pone.0019669

Pasquaretta, C., Jeanson, R., Andalo, C., Chittka, L., and Lihoreau, M. (2017). Analysing plant–pollinator interactions with spatial movement networks. *Ecol. Entomol.* 42, 4–17. doi: 10.1111/een.12446

Pyke, G. H. (1984). Optimal foraging theory: a critical review. *Annu. Rev. Ecol. Syst.* 15, 523–575. doi: 10.1146/annurev.es.15.110184.002515

Ratnieks, F. L. W., and Shackleton, K. (2015). Does the waggle dance help honey bees to forage at greater distances than expected for their body size? *Front. Ecol. Evol.* 3:31. doi: 10.3389/fevo.2015.00031

Redhead, J. W., Dreier, S., Bourke, A. F., Heard, M. S., Jordan, W. C., Sumner, S., et al. (2016). Effects of habitat composition and landscape structure on worker foraging distances of five bumble bee species. *Ecol. Appl.* 26, 726–739. doi: 10.1890/15-0546

Roulston, T. H., and Cane, J. H. (2002). The effect of pollen protein concentration on body size in the sweat bee *Lasioglossum zephyrum* (*Hymenoptera: Apiformes*). *Evol. Ecol.* 16, 49–65. doi: 10.1023/A:1016048526475

Saleh, N., and Chittka, L. (2007). Traplining in bumblebees (*Bombus impatiens*): a foraging strategy's ontogeny and the importance of spatial reference memory in short-range foraging. *Oecologia* 151, 719–730. doi: 10.1007/s00442-006-0607-9

Schneider, C. W., Tautz, J., Grünewald, B., and Fuchs, S. (2012). RFID tracking of sublethal effects of two neonicotinoid insecticides on the foraging behavior of *Apis mellifera*. *PLoS ONE* 7:e30023. doi: 10.1371/journal.pone.0030023

Seeley, T. D. (1978). Life history strategy of the honey bee, *Apis mellifera*. *Oecologia* 32, 109–118. doi: 10.1007/BF00344695

Seeley, T. D., Camazine, S., and Sneyd, J. (1991). Collective decision-making in honey bees: how colonies choose among nectar sources. *Behav. Ecol. Sociobiol.* 28, 277–290.

Spaethe, J., and Weidenmüller, A. (2002). Size variation and foraging rate in bumblebees (*Bombus terrestris*). *Insectes Soc.* 49, 142–146. doi: 10.1007/s00040-002-8293-z

Stanley, D. A., Russell, A. L., Morrison, S. J., Rogers, C., and Raine, N. E. (2016). Investigating the impacts of field-realistic exposure to a neonicotinoid pesticide on bumblebee foraging, homing ability and colony growth. *J. Appl. Ecol.* 53, 1440–1449. doi: 10.1111/1365-2664.12689

Stelzer, R. J., and Chittka, L. (2010). Bumblebee foraging rhythms under the midnight sun measured with radiofrequency identification. *BMC Biol.* 8:93. doi: 10.1186/1741-7007-8-93

Thomson, J. D., Slatkin, M., and Thomson, B. A. (1997). Trapline foraging by bumble bees: II. Definition and detection from sequence data. *Behav. Ecol.* 8, 199–210. doi: 10.1093/beheco/8.2.199

Visscher, P., and Seeley, T. D. (1982). Foraging strategy of honeybee colonies in a temperate deciduous forest. *Ecology* 63, 1790–1801. doi: 10.2307/1940121

Von Frisch, K. (1967). *The Dance Language and Orientation of Bees*. Cambridge, MA: Belknap Press of Harvard University Press.

Waser, N. M., Chittka, L., Price, M. V., Williams, N. M., and Ollerton, J. (1996). Generalization in pollination systems, and why it matters. *Ecology* 77, 1043–1060.

Williams, N. M., and Thomson, J. D. (1998). Trapline foraging by bumble bees: III. Temporal patterns of visitation and foraging success at single plants. *Behav. Ecol.* 9, 612–621. doi: 10.1093/beheco/9.6.612

Winfree, R., Aguilar, R., Vázquez, D. P., LeBuhn, G., and Aizen, M. A. (2009). A meta-analysis of bees' responses to anthropogenic disturbance. *Ecology* 90, 2068–2076. doi: 10.1890/08-1245.1

Wolf, S., and Moritz, R. F. (2008). Foraging distance in *Bombus terrestris L.* (*Hymenoptera: Apidae*). *Apidologie* 39, 419–427. doi: 10.1051/apido:2008020

Woodgate, J. L., Makinson, J. C., Lim, K. S., Reynolds, A. M., and Chittka, L. (2017). Continuous radar tracking illustrates the development of multi-destination routes of bumblebees. *Sci. Rep.* 7:17323. doi: 10.1038/s41598-017-17553-1

Conflict of Interest Statement: The authors declare that the research was conducted in the absence of any commercial or financial relationships that could be construed as a potential conflict of interest.

Copyright © 2018 Minahan and Brunet. This is an open-access article distributed under the terms of the Creative Commons Attribution License (CC BY). The use, distribution or reproduction in other forums is permitted, provided the original author(s) and the copyright owner(s) are credited and that the original publication in this journal is cited, in accordance with accepted academic practice. No use, distribution or reproduction is permitted which does not comply with these terms.

frontiers in Ecology and Evolution

ORIGINAL RESEARCH
published: 25 October 2018
doi: 10.3389/fevo.2018.00167

Movement Patterns of African Elephants (*Loxodonta africana*) in a Semi-arid Savanna Suggest That They Have Information on the Location of Dispersed Water Sources

Yussuf A. Wato [1,2†], Herbert H. T. Prins [1], Ignas M. A. Heitkönig [1], Geoffrey M. Wahungu [3], Shadrack M. Ngene [2], Steve Njumbi [4] and Frank van Langevelde [1,5]*

[1] Resource Ecology Group, Wageningen University, Wageningen, Netherlands, [2] Kenya Wildlife Service, Nairobi, Kenya, [3] National Environment Management Authority, Nairobi, Kenya, [4] International Fund for Animal Welfare, East Africa, Nairobi, Kenya, [5] School of Life Sciences, Westville Campus, University of KwaZulu-Natal, Durban, South Africa

OPEN ACCESS

Edited by:
Thomas Wassmer,
Siena Heights University,
United States

Reviewed by:
Sarah-Anne Jeanetta Selier,
South African National Biodiversity Institute, South Africa
Monique De Jager,
Utrecht University, Netherlands

***Correspondence:**
Herbert H. T. Prins
herbert.prins@wur.nl

†Present Address:
Yussuf A. Wato,
World Wide Fund for Nature, Nairobi, Kenya

Specialty section:
This article was submitted to Behavioral and Evolutionary Ecology, a section of the journal Frontiers in Ecology and Evolution

Received: 12 August 2018
Accepted: 03 October 2018
Published: 25 October 2018

Citation:
Wato YA, Prins HHT, Heitkönig IMA, Wahungu GM, Ngene SM, Njumbi S and van Langevelde F (2018) Movement Patterns of African Elephants (Loxodonta africana) in a Semi-arid Savanna Suggest That They Have Information on the Location of Dispersed Water Sources. Front. Ecol. Evol. 6:167. doi: 10.3389/fevo.2018.00167

Water is a scarce resource in semi-arid savannas where over half of the African elephants (*Loxodonta africana*) populations occur and may therefore influence their movement pattern. A random search is expected for an animal with no information on the location of the target resource, else, a direction-oriented walk is expected. We hypothesized that elephants movement patterns show a stronger directional orientation toward water sources in the dry season compared to the wet season. We investigated the movement paths of four male and four female elephants with hourly GPS fixes in Tsavo National Park, Kenya in 2012–2013. Consistent with our predictions, the movement paths of elephants had longer step lengths, longer squared net displacements, and were directed toward water sources in the dry season as compared to the wet season. We argue that African elephants know the location of dispersed water resources, enabling them to survive with scarce resources in dry savannas. These results can be used in conservation and management of wildlife, through for instance, protection of preferred water sources.

Keywords: Tsavo, wildlife, movement, step length, savanna, directionality, conservation

INTRODUCTION

The movement paths of animals represent behavioral and ecological processes, such as navigation, migration, dispersal, and food searching (Benhamou, 2004) and the distribution of the resources (de Jager et al., 2014). For instance, the movement strategies used by an animal when foraging in a landscape with dispersed resources would be different from those of animals foraging in an area with clustered resources (Bartumeus, 2009). It is generally hypothesized that animals increase tortuosity of their movement paths in areas with high resource density (Bartumeus et al., 2005; Hengeveld, 2007; Bartumeus, 2009). Consequently, the squared net displacement of the animal decreases and the time spent in utilizing these resources increases, leading to efficient resource use (Turchin, 1991). On the other hand, straight and less tortuous movement paths with high net displacement are more efficient in landscapes with dispersed resources (Turchin, 1998; De Knegt et al., 2007; Roshier et al., 2008). Therefore, analysis of the movement paths of animals could give an understanding of the relationship between the resource distribution and foraging efficiency.

Previous studies on movement path analyses were mostly carried out on insects, birds, and small mammals (Turchin, 1991; Viswanathan et al., 1996; Atkinson et al., 2002). However, recent advances in radio-telemetry have made it possible to collect vast quantities of movement data in space and time for both large terrestrial and marine mammals (Austin et al., 2004; Boyce et al., 2010; Sims et al., 2012). Although the movement parameters to be measured vary with the objectives of the study (Marsh and Jones, 1988), generally, parameters such as the distance covered between successive relocations, the turn angles, the directionality of the track and the relationship of the track with properties of the environment that the animal passes through, form the basis of movement path analysis (Root and Kareiva, 1984; Marsh and Jones, 1988; Hengeveld, 2007; Dray et al., 2010; de Knegt et al., 2011; Calenge, 2015; Kölzsch et al., 2015). These movement patterns may in turn determine the frequency with which the animal will encounter the object of interest, which may be food, water, mates, or escape from predation (Marsh and Jones, 1988). To increase resource use efficiency, a random search is expected for a forager with no information on the location of the target resource, whereas a more direction-oriented ballistic walk is expected for a forager with information on the target resource (Valeix et al., 2010). Knowledge on how animals move in their environment can give critical insight on animal's behavior that may be used in the effective management and conservation of species under study.

Water is a scarce resource in semi-arid savanna, where over half of the African elephant *(Loxodonta africana)* populations occur, and may therefore influence the movement strategies used by elephants. Elephants are water dependent and they usually have to drink water every two to three days (Stokke and Du Toit, 2002; Redfern et al., 2005; Smit et al., 2007). To survive in dry savannas, it is therefore critical for elephants to be able to efficiently find the sparsely distributed water sources, especially during the dry season. Based on the elephant's water requirements and the scarcity of water during the dry season, we expect that the movement pattern of the elephant will reflect these seasonal contrasts in water distribution. Although it is not in doubt that the distance to water is a primary environmental factor influencing habitat use by elephants (Verlinden and Gavor, 1998; Chamaillé-Jammes et al., 2007; Smit et al., 2007; Hilbers et al., 2015; Wato et al., 2016; Sianga et al., 2017), it remains unclear how the behavioral responses of elephants change as a result of water scarcity (Polansky et al., 2015). Here, we analyse the movement paths of four male and four female elephants to address the hypothesis that elephant movement patterns show a stronger directional orientation toward water sources in the dry season compared to the wet season. We predict that the movement path for male and female elephants are less tortuous, have longer step lengths, longer net displacements and smaller turning angles and will show stronger directionality toward water sources in the dry season than in the wet season. Past reports indicate that elephants remember and re-visit previously visited sites (De Beer and Van Aarde, 2008; Prins and Van Langevelde, 2008; de Knegt et al., 2011; Polansky et al., 2015) and pass on the information of their historical migration routes through generations (McComb et al., 2001; Moss et al., 2011). Thus, longer step lengths and higher directionality of elephant movement paths toward water sources in the dry season is an indication that elephants use information to travel to these water sources.

MATERIALS AND METHODS

Study Area

We conducted this study in the Tsavo Conservation Area in Kenya, a semi-arid ecosystem spanning an area of ∼48,300 km^2, located at 2°-4° S and 37.5°-39.5° E in the southern part of Kenya (Omondi et al., 2008; Ngene et al., 2012). The area is characterized by a bi-modal rainfall with long rains in mid-March to May, short rains in November to December (Tyrrell and Coe, 1974) and a mean annual rainfall of 250–500 mm (Tyrrell and Coe, 1974; Prins and Loth, 1988). The two rainfall seasons are separated by a 5 months long dry season typically ranging from June through October (Tyrrell and Coe, 1974; Leuthold and Leuthold, 1978; Omondi et al., 2008). There are two permanent rivers in Tsavo (Galana river and Tsavo river) and several seasonal rivers, with Voi and Tiva rivers flowing for a short time in the rainy season (Ayeni, 1975). Other sources of water are the numerous natural waterholes which fill up with water during the rainy season. Some of these waterholes can hold water throughout the short dry season (January-March) but all the natural waterholes dry up around July-August during the long dry season (June to October) (Ayeni, 1975; Mukeka, 2010). In addition, there are three wind-pumped boreholes and a few water reservoirs located around tourist facilities and community owned ranches with constant water supply for animals in the peak of the dry months.

Elephants GPS Data

We used radio-telemetry data from GPS-collared elephants in the Tsavo Conservation Area to investigate the differences in elephants movement patterns between the wet and dry season. During the wet season, there is abundant water for wildlife in the Tsavo ecosystem (Omondi et al., 2008; Mukeka, 2010). However, this area has sparsely distributed permanent water sources in the dry season when the only available water sources for wildlife are reduced to two perennial rivers, three boreholes, and a few water pools constantly refilled by the hoteliers and neighboring community ranchers (Ayeni, 1975). Water has been identified as key resource that affects elephants distribution and their spatial habitat use (Chamaillé-Jammes et al., 2007; Harris et al., 2008; Smit and Grant, 2009; Polansky et al., 2015). For instance, in drier environments, elephants take an average interval of 3 days to drink water and the duration of re-visiting water points differ between sexes (Stokke and Du Toit, 2002), with bull elephants drinking every 3–5 days while breeding herds every 2–4 days (Viljoen, 1989; Leggett, 2006). Furthermore, the breeding herds have been reported to forage close to water sources in the dry season compared to the male elephants (Harris et al., 2008; Sianga et al., 2017).

We monitored four female and four male elephants fitted with satellite-linked GPS collars between March 2012 and June 2013 in the Tsavo Conservation Area in Kenya (**Figure 1**). The individuals that were collared were randomly selected from five sectors in the Tsavo Conservation Area to represent elephant

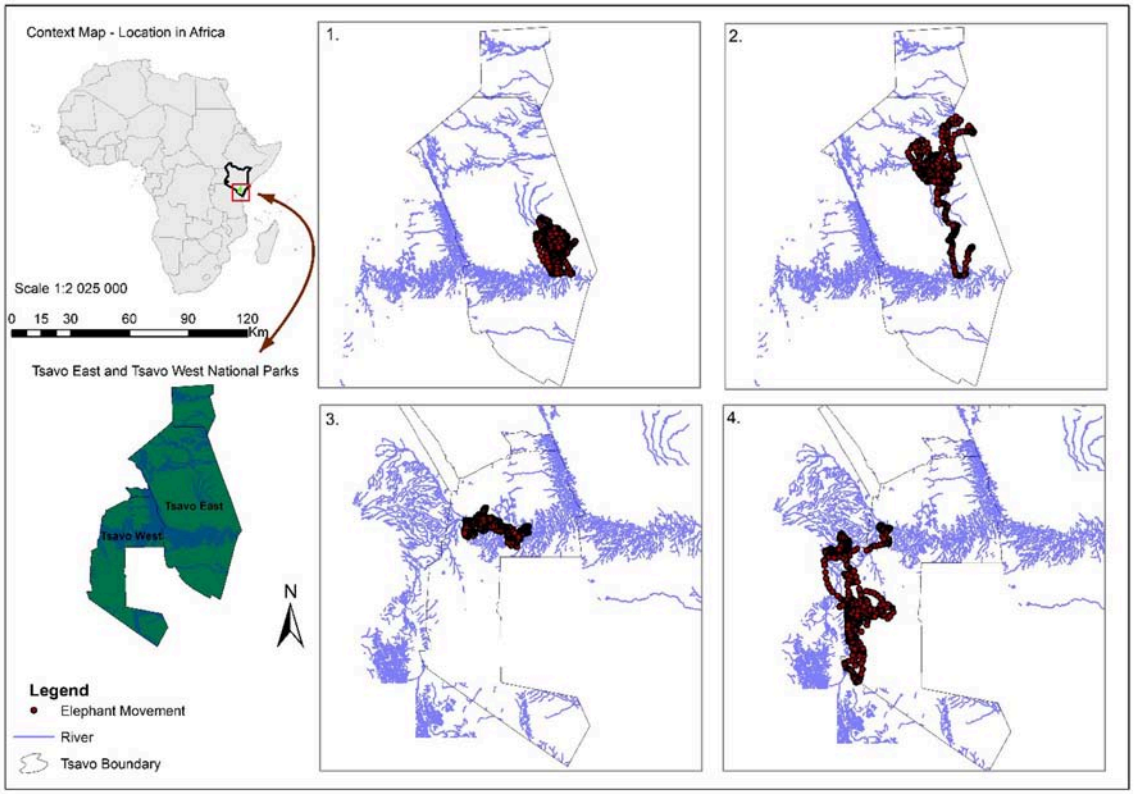

FIGURE 1 | Study areas and the hourly GPS fixes (black dots) for a male elephants in the dry **(1)** and the wet season **(2)**; and for a female elephants in the dry **(3)** and the wet season **(4)**. In both sexes the individuals' movement paths seem to be tightly anchored on a river in the dry season.

movement patterns across the entire park. The procedure for fitting GPS collars are described in Ngene et al. (2012). The GPS collars transmitted hourly fixes and the data were automatically transmitted to a web-linked database at the Tsavo East Research Station in Kenya. The GPS had an error of ∼10 meters for relocation fixes and some hours had missing values caused by obstruction of signals by, for instance, heavy cloud cover or dense tree canopies (Hebblewhite et al., 2007). In our analysis we considered only the successive time steps with GPS fixes.

We analyzed elephant movement patterns for the males and the females in two seasons: the long dry season (June to October 2012) and the long wet season (March to May 2013). These two seasons are distinctly different in the amount of rainfall and would therefore show the relationship between the change in movement pattern related to water availability.

Data Analysis

We calculated the distance covered by each elephant per hour based on the hourly GPS-fixes. We recorded the distance between successive hours to represent a single movement path (i.e., step length) based on the methods described by Root and Kareiva (1984), Marsh and Jones (1988), Turchin (1998), and Hengeveld (2007). We calculated the turn angle as a measure of the change of direction between successive steps with a zero degrees turn corresponding to locomotion on a straight line without change of direction, a negative angle representing a turn to the left and a positive angle representing a turn to the right (Calenge, 2015). We then analyzed the distribution of step lengths, turning angles, and squared net displacement distances (NDD) for both sexes and seasons with AdehabitatLT animal movement analysis package in R (Calenge, 2015). We calculated the parameters of turn angle distributions such as the mean resultant length and the mean direction using CircStats package Version 0.2-4 in R (Lund and Agostinelli, 2015). The mean direction vector represents the mean orientation of the turn angles while the mean resultant length shows the strength of directionality and the concentration of the angles distribution around the mean ($R = 0$ represents a dispersed turn angles distribution and $R = 1$ shows that all angles are equal to the mean direction vector) (Lund and Agostinelli, 2015). We only analyzed the movement paths that were directed toward the nearest water source to focus on the effects of water on movement path. Thus, all the movement paths for the elephants that were further than 15 km from the nearest water sources and those for the individuals returning from drinking water were excluded from the analysis on the assumption that they were foraging and not seeking for water. Since the range of water re-visitation frequency for the Tsavo elephants were 1–4 days for the females and 2–5 days for the males in the dry season, we also excluded all the movement paths of the day following an elephant's visitation to the water sources in the dry season.

The rest of the movement paths were included in the analysis. In order to establish whether the directionality changed with distance from the water source, or whether proximity had no effect, we also stratified our analysis to 5, 10 and 15 km from the water source. We analyzed the effect of the fixed variables; season, sex and distance from the nearest water source, on elephant's movement pattern using linear mixed effects models (LMMs). We used the ID of the elephant as a random effect variable to account for variation due to individual differences. We also checked for the interaction effects between sex and season in our analyses. We performed these analyses using R package lme4 (Bates et al., 2013).

RESULTS

The step lengths per hour for the elephants were significantly longer in the dry season compared to the wet season (**Table 1A**). The step lengths changed with distance from the nearest water point, with the step lengths further from the water (15 km) being significantly shorter than those closer to water points (5 and 10 km) (**Table 1A**). Also, step lengths were longer in the 10 km group than in the 5 km group. Even though both male and female elephants have longer step lengths in the dry season as compared to the wet season, the results showed a significant interaction effect of sex and season (**Figure 2A**). The male elephants have shorter step lengths than the females in the wet (**Table 1A**) and a longer step length in the dry season (**Figure 2A**). Similarly, the squared net displacement for the elephants were significantly longer in the dry season compared to the wet season (**Table 1B**). The squared net displacements were significantly longer further away from water (15 and 10 km) as compared to distance closer to the water (5 km) (**Table 1B**). Furthermore, the squared net displacement was also significantly affected by the interaction between sex and season with squared net displacement for the males being longer than the females in the wet season (**Table 1B**). Both sexes had similarly longer squared net displacements in the dry season (**Figure 2B**). However, the turn angles for both sexes were large in both the wet and the dry season and did not show any significant difference between the seasons.

The mean resultant length of the turning angles for both sexes showed strong directionality in the dry season compared to the wet season (**Figure 3**). The resultant mean length of the turning angles for females were in the same range with males in wet season but much lower than the males in the dry season, although not significantly different (**Figure 3**).

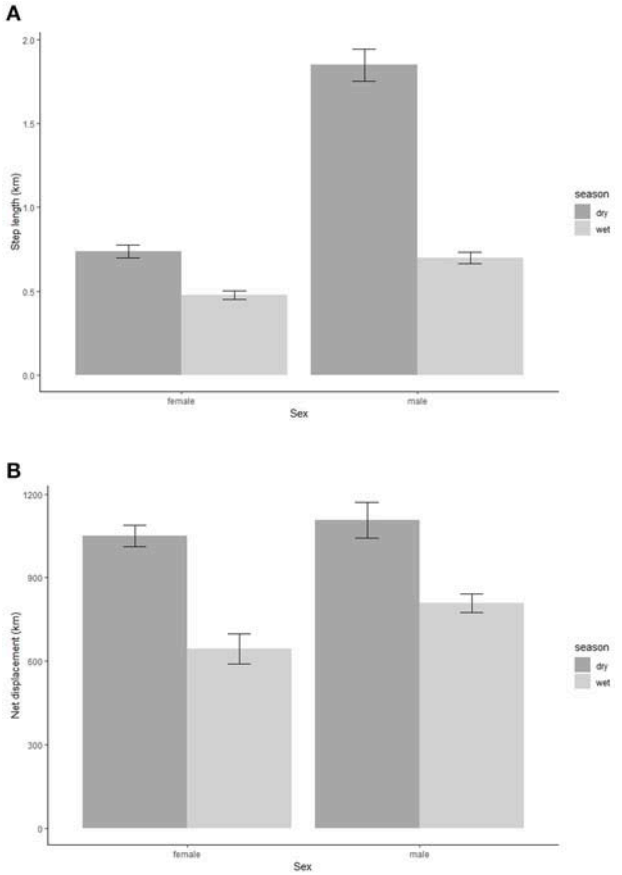

FIGURE 2 | Step length **(A)** and squared net displacement distances **(B)** for the female and the male elephants movement paths in the wet (black bars) and the dry (gray bars) season.

DISCUSSION

The study of animal movement patterns in relation to resource distribution is one of the novel ways to link behavior of individuals to the spatial distribution of resources (Schick et al., 2008; Giuggioli and Bartumeus, 2010). Resource distribution varies in space and time, and can occur in a spectrum ranging from over-dispersed, random, in patches to highly aggregated clusters (Prins and Van Langevelde, 2008; de Knegt et al., 2011). We examined the role of water distribution on the movement pattern of elephants. In this study, we showed how elephant movement patterns change as a result of seasonal variation in water distribution. The results support our predictions that the movement paths of both male and female elephants are less tortuous, resulting in longer step lengths, and have longer squared net displacements in the dry season compared to the wet season. Furthermore, the mean length of the turning angle showed strong directionality toward water sources for both the sexes in the dry season. The movement paths that were removed were for individuals returning from the water source, those that were beyond 15 km from the nearest water source and the paths for all individuals for the day following their return from drinking water during the dry season, which would not contribute to our conclusion.

The Tsavo Conservation Area is an ecosystem undergoing pronounced scarcity of water and in the long dry season, two perennial rivers and three boreholes serve as the primary water source for wildlife. Most of the area is far away from water for much of the year. Most wildlife species, and particularly elephants, require regular water intake (Stokke and Du Toit, 2002; Redfern et al., 2005) and have to travel between the foraging sites and watering points to meet their energy and

TABLE 1 | Results of the LMM models for step length **(A)** and net displacement distances **(B)**.

Variables	β	SE	95% CI		*t*-value	*P*-value
(A) STEP LENGTH						
Intercept	0.7	0.2	0.4	0.1	4.41	0.002*
Dry season	[***]					
Wet season	−0.2	0.1	−0.3	−0.1	−3.76	<0.001***
Female	[***]					
Male	1.2	0.2	0.7	1.6	5.40	<0.001***
Distance−5km	[***]					
Distance−10km	0.1	0.04	0.04	0.2	2.89	<0.004*
Distance−15km	−0.3	0.04	−0.3	−0.2	−6.51	<0.001***
Wet season:male	−1.2	0.1	−1.3	−1.1	−17.45	<0.001***
(B) NET DISPLACEMENT DISTANCE						
Intercept	874	432	28	1720	2.03	ns
Dry season	[***]					
Wet season	−684	33	−750	−619	−20.43	<0.001***
Female	[***]					
Male	208	579	−927	1343	0.36	ns
Distance−5km	[***]					
Distance−10km	310	28	254	365	10.94	<0.001***
Distance−15km	311	29	255	367	10.89	<0.001***
Wet season:male	715	48	622	809	14.98	<0.001***

*Significant codes: 0 "***" >0.001 "*", [***] represents the reference variable. Shown are the fixed effect variables with coefficients (β ± Standard Error), 95% confidence interval (95% CI), t-value and P-value. Main effect coefficients indicate the separate effects of sex, season and distance (km) from the nearest water source on the movement pattern of the male and the female elephants. Interaction coefficients show the combined effect of sex and season on the elephants movement pattern; the dependent variables.*

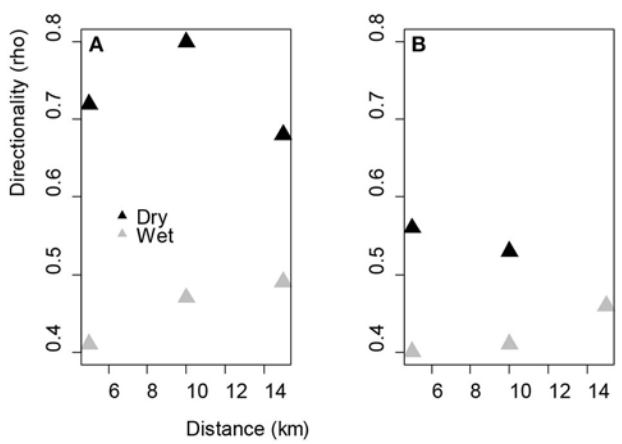

FIGURE 3 | Directionality of the movement patterns at different distances to water sources for **(A)** male elephants in the wet (*Rho* at 5 km = 0.41, 10 km = 0.47, 15 km = 0.49) and dry season (*Rho* at 5 km = 0.72, 10 km = 0.8, 15 km = 0.68) and **(B)** females in the wet (*Rho* at 5 km = 0.40, 10 km = 0.41, 15 km = 0.46) and dry season (*Rho* at 5 km = 0.56, 10 km = 0.53). *Rho* = 0 represents a dispersed turn angles distribution, hence indicates weak directionality, and R = 1 shows that all angles are equal to the mean direction vector, hence indicates strong directionality. Females were not recorded to be at 15 km from the nearest water point in the dry season.

water requirements. For instance, in Kruger National Park, elephants drink water every 2 days during the dry season (Young, 1970), and other studies have shown that the duration of water re-visitation is sex-dependent (Viljoen, 1989; Leggett, 2006). The movement paths of elephants are thus expected to be influenced by the water distribution, and the Tsavo elephants appear to have information about the water locations which supports findings in previous studies (Polansky et al., 2015). Therefore, regular re-visitation of watering points may explain the long step lengths and squared net displacements and the strong directionality toward water sources in the dry season (Chamaillé-Jammes et al., 2013; Polansky et al., 2015). The use of information about the location of the water sources is especially apparent when they show this behavior at long distances from the water sources. A few studies have found a relationship between resource distribution and the movement patterns of other wildlife species (Prins, 1996; Loureiro et al., 2007; Valeix et al., 2010). For instance, in a study of lions in arid savannas, their step lengths and squared net displacements were longer as they headed toward waterholes with high aggregation of prey species (Valeix et al., 2010). Similarly, the study of Eurasian badgers showed that their movement paths were less tortuous as they headed toward their dens and latrine sites (Loureiro et al., 2007).

During the wet season, there is abundant food and water for wildlife in the Tsavo ecosystem (Omondi et al., 2008; Mukeka, 2010). In addition to the perennial rivers that flow throughout the year, most of the natural waterholes across Tsavo ecosystem fill up with water during rainy seasons (Tyrrell and Coe, 1974; Ayeni, 1975). This may explain the short step lengths and squared net displacement distances during the wet season. Some of the natural waterholes have water throughout the rainy season and a few of them extend to the short dry season (January-March) (Ayeni, 1975), hence elephants are not water limited then. Similar movement patterns have been reported for foragers in sites

of abundant resources. For instance, the movement paths of lions hunting close to a waterhole where there were high prey species congregations, had shorter step lengths and squared net displacement distances and their movement paths were more tortuous than when they were further away from a waterhole (Valeix et al., 2010).

Although water is limiting for both sexes in the dry season, female elephants rarely moved further than 10 km from the nearest water source to forage in the dry season while male elephants accessed forage sites beyond 15 km (Sianga et al., 2017). Furthermore, in the dry season, the directionality of movement path for male elephants was much stronger than the female elephants. This is in line with past studies that reported that breeding herds rarely roam far away from drinking water in drier environments (Viljoen, 1989; Leggett, 2006; Young and Van Aarde, 2010). In these mixed herds, the increased costs associated with moving long distances to far foraging sites may be especially stressful for infants and juveniles (Lee and Moss, 1986; Loveridge et al., 2006) and could lead to increased calf mortality (Loveridge et al., 2006; Foley et al., 2008; Young and Van Aarde, 2010). Our results support the hypothesis that elephants initially seek habitats closer to water in the dry season, regardless of the distribution of food (De Beer et al., 2006; Illius, 2006; Chamaillé-Jammes et al., 2007; Evans and Harris, 2008; Wato et al., 2016). However, if there are many water sources, elephants choose those water sources with more vegetation and avoid those that are not associated with suitable vegetation (Harris et al., 2008).

The difference between male and female elephants movement patterns may be also be explained by their social organization (Archie et al., 2011; Moss et al., 2011) and the difference in foraging strategy between the sexes (Lee et al., 2011). The foraging range of male elephants is larger than that of females as they take more risks and disperse to unfamiliar habitats to seek for food and mates (Lee et al., 2011; Skarpe et al., 2014). This foraging behavior may have advantages such as accessing far foraging grounds and water points in dry seasons (Lee et al., 2011; Lindsay, 2011). Moreover, the mixed herd comprises of individuals of different ages and the group's movement is affected by, for instance, calves that may not be able to move fast and far from water sources like the adult elephants (Ngene et al., 2010). The large herds also spread widely while foraging and, probably, while heading to the water sources to drink. Conversely, the bulls move and forage alone or in a bachelor herd without calves to retard their speed (Ngene et al., 2010). Thus, bulls may travel far to forage but also walk in a less spread formation toward the watering point. The difference in foraging strategies among different sexes are common in other sex-dimorphic species like the red deer (Gordon et al., 1989), moose (Miquelle et al., 1992), and many others (Moss et al., 2011). Generally, the differences in foraging strategies in many species appears to be driven by factors such as energy need requirements, reproductive status of an individual, body sizes and the social context, all of which differ between sexes (Miquelle et al., 1992; Lindsay, 2011).

This study shows that water distribution determines the movement paths of elephants. It supports other studies and models that indicated that animals often adjust their movement pattern in relation to critical and scarce resources (Chamaillé-Jammes et al., 2007; Hengeveld, 2007). Our findings reveal that movement paths of African elephants show strong directionality in dry seasons driven by water distribution. We demonstrate that environmental variables can be used to predict general movement patterns of large herbivores and that the findings can be used in conservation and management of wildlife, through for instance, protection of preferred, or critically needed water sources. The method in this study can be replicated to examine directed movement of other species, of which their cognitive abilities are less well-known.

ETHICS STATEMENT

Approval for animal collaring was not required as per the local legislation. Collaring was done for management purposes by the relevant authority (the Kenya Wildlife Service) executed and supervised by the veterinarians of the mentioned authority. Thus, we adhered to all ethical requirements to ensure animal safety.

AUTHOR CONTRIBUTIONS

YW helped in research design, data collection, analysis and writing. HP, FvL, IH, GW, and SMN in research design, data analysis and writing. SN assisted in data collection and editing of the paper.

ACKNOWLEDGMENTS

A special thanks to the Kenya Wildlife Service (KWS), International Fund for Animal Welfare (IFAW), Wageningen University and NUFFIC for the financial and technical support for this project. Our gratitude goes to Tsavo research and park management team for assistance in data collection and field logistics. This is a part of the publicly defended Ph.D. thesis of the first author (see Wato et al., 2016).

REFERENCES

Archie, E. A., Moss, C. J., and Alberts, S. C. (2011). "Friends and relations: kinship and the nature of female elephant social relationships," in *The Amboseli Elephants: A Long-Term Perspective on a Long-Lived Mammal*, eds C. J. Moss and H. Croze (Chicago, IL: University of Chicago Press), 238–245.

Atkinson, R. P. D., Rhodes, C. J., Macdonald, D. W., and Anderson, R. M. (2002). Scale-free dynamics in the movement patterns of jackals. *Oikos* 98, 134–140. doi: 10.1034/j.1600-0706.2002.980114.x

Austin, D., Bowen, W. D., and McMillan Austin, J. I. (2004). Intraspecific variation in movement patterns: modeling individual behaviour in a large marine predator. *Oikos* 105, 15–30. doi: 10.1111/j.0030-1299.1999.12730.x

Ayeni, J. S. O. (1975). Utilization of waterholes in Tsavo National Park (East). *Afr. J. Ecol.* 13, 305–323. doi: 10.1111/j.1365-2028.1975.tb00142.x

Bartumeus, F. (2009). Behavioral intermittence, lévy patterns, and randomness in animal movement. *Oikos* 118, 488–494. doi: 10.1111/j.1600-0706.2009.17313.x

Bartumeus, F., Da Luz, M. G. E., Viswanathan, G. M., and Catalán, J. (2005). Animal search strategies: a quantitative random-walk analysis. *Ecology* 86, 3078–3087. doi: 10.1890/04-1806

Bates, D., Maechler, M., Bolker, B., Walker, S., Christensen, R. H. B., Singmann, H., et al. (2013). *lme4: Linear Mixed-Effects Models Using Eigen and S4*. R package version 10–4. Available online at: https://cran.r-project.org/package=lme4

Benhamou, S. (2004). How to reliably estimate the tortuosity of an animal's path: straightness, sinuosity, or fractal dimension? *J. Theor. Biol*. 229, 209–220. doi: 10.1016/j.jtbi.2004.03.016

Boyce, M. S., Pitt, J., Northrup, J. M., Morehouse, A. T., Knopff, K. H., Cristescu, B., et al. (2010). Temporal autocorrelation functions for movement rates from global positioning system radiotelemetry data. *Philos. Trans. R. Soc. B* 365, 2213–2219. doi: 10.1098/rstb.2010.0080

Calenge, C. (2015). Analysis of *Animal Movements in R: the adehabitatLT Package*. Office national de la chasse et de la faune sauvage.

Chamaillé-Jammes, S., Mtare, G., Makuwe, E., and Fritz, H. (2013). African elephants adjust speed in response to surface-water constraint on foraging during the dry-season. *PLoS ONE* 8:e59164. doi: 10.1371/journal.pone.0059164

Chamaillé-Jammes, S., Valeix, M., and Fritz, H. (2007). Managing heterogeneity in elephant distribution: interactions between elephant population density and surface-water availability. *J. Applied Ecol.* 44, 625–633. doi: 10.1111/j.1365-2664.2007.01300.x

De Beer, Y., Kilian, W., Versfeld, W., and van Aardea, R. J. (2006). Elephants and low rainfall alter woody vegetation in Etosha National Park, Namibia. *J. Arid Environ*. 64, 412–421. doi: 10.1016/j.jaridenv.2005.06.015

De Beer, Y., and Van Aarde, R. J. (2008). Do landscape heterogeneity and water distribution explain aspects of elephant home range in southern Africa's arid savannas? *Journal of Arid Environ*. 72, 2017–2025. doi: 10.1016/j.jaridenv.2008.07.002

de Jager, M., Bartumeus, F., Kölzsch, A., Weissing, F. J., Hengeveld, G. M., Nolet, B. A., et al. (2014). How superdiffusion gets arrested: ecological encounters explain shift from Lévy to Brownian movement. *Proc. R. Soc. B*. 281:20132605. doi: 10.1098/rspb.2013.2605

De Knegt, H. J., Hengeveld, G. M., van Langevelde, F., de Boer, W. F., and Kirkman, K. P. (2007). Patch density determines movement patterns and foraging efficiency of large herbivores. *Behav. Ecol*. 18, 1065–1072. doi: 10.1093/beheco/arm080

de Knegt, H. J., van Langevelde, F., Skidmore, A. K., Delsink, A., Slotow, R., Henley, S., et al. (2011). The spatial scaling of habitat selection by African elephants. *J. Anim. Ecol*. 80, 270–281. doi: 10.1111/j.1365-2656.2010.01764.x

Dray, S., Royer-Carenzi, M., and Calenge, C. (2010). The exploratory analysis of autocorrelation in animal-movement studies. *Ecol. Res*. 25, 673–681. doi: 10.1007/s11284-010-0701-7

Evans, K. E., and Harris, S. (2008). Adolescence in male African elephants, Loxodonta africana, and the importance of sociality. *Anim. Behav*. 76, 779–787. doi: 10.1016/j.anbehav.2008.03.019

Foley, C., Pettorelli, N., and Foley, L. (2008). Severe drought and calf survival in elephants. *Biol. Lett*. 4, 541–544. doi: 10.1098/rsbl.2008.0370

Giuggioli, L., and Bartumeus, F. (2010). Animal movement, search strategies and behavioural ecology: a cross-disciplinary way forward. *J. Anim. Ecol*. 79, 906–909. doi: 10.1111/j.1365-2656.2010.01682.x

Gordon, I. J., Journal, T., and Apr, N. (1989). Vegetation community selection by ungulates on the Isle of Rhum. *J. Appl. Ecol*. 26, 65–79. doi: 10.2307/2403650

Harris, G. M., Russell, G. J., van Aarde, R. I., and Pimm, S. L. (2008). Rules of habitat use by elephants *Loxodonta africana* in southern Africa: insights for regional management. *Oryx* 42, 66–75. doi: 10.1017/S0030605308000483

Hebblewhite, M., Percy, M., and Merrill, E. H. (2007). Are all global positioning system collars created equal? Correcting habitat-induced bias using three brands in the central canadian rockies. *J. Wildl. Manage*. 71, 2026–2033. doi: 10.2193/2006-238

Hengeveld, G. M. (2007). *Moving to Eat: Animal Foraging Movements in a Heterogeneous Environment*. Ph.D. dissertation, Wageningen University, Wageningen, The Netherlands.

Hilbers, J. P., Van Langevelde, F., Prins, H. H., Grant, C. C., Peel, M. J., Coughenour, M. B., et al. (2015). Modeling elephant-mediated cascading effects of water point closure. *Ecol. Appl*. 25, 402–415. doi: 10.1890/14-0322.1.sm

Illius, A.W. (2006). "Linking functional responses and foraging behaviour to population dynamics," in *Large Herbivore Ecology, Ecosystem Dynamics and Conservation*, eds K. Danell, R. Bergström, P. Duncan, and J. Pastor (Cambridge: Cambridge University Press), 71–96.

Kölzsch, A., Alzate, A., Bartumeus, F., de Jager, M., Weerman, E. J., Hengeveld, G. M., et al. (2015). Experimental evidence for inherent Lévy search behaviour in foraging animals. *Proc. R. Soc. B*. 282:20150424. doi: 10.1098/rspb.2015.0424

Lee, P., Lindsay, W. and Moss, C. (2011). "Ecological patterns of variability in demographic rates" in *The Amboseli Elephants,* eds C. J. Moss, H. Croze, and C. L. Phyllis (Chicago, IL: University of Chicago Press), 74–88.

Lee, P. C., and Moss, C. J. (1986). Early maternal investment in male and female African elephant calves. *Behav. Ecol. Sociobiol*. 18, 353–361. doi: 10.1007/BF00299666

Leggett, K. E. A. (2006). Home range and seasonal movement of elephants in the Kunene Region, northwestern Namibia. *African Zool*. 41, 17–36. doi: 10.1080/15627020.2006.11407332

Leuthold, B. M., and Leuthold, W. (1978). Ecology of the giraffe in Tsavo East National Park, Kenya. *Afric. J. Ecol*. 16, 1–20. doi: 10.1111/j.1365-2028.1978.tb00419.x

Lindsay, K. (2011). "Habitat use, diet choice and nutritional status in female and male Amboseli elephants," in *The Amboseli Elephants: A Long-Term Perspective on a Long-Lived Mammal*, eds C. J. Moss, H. Crozem and P. C. Lee (Chicago, IL; London: University of Chicago Press), 51–73.

Loureiro, F., Rosalino, L. M., Macdonald, D. W., and Santos-Reis, M. (2007). Path tortuosity of Eurasian badgers (Meles meles) in a heterogeneous Mediterranean landscape. *Ecol. Res*. 22, 837–844. doi: 10.1007/s11284-006-0325-0

Loveridge, A. J., Hunt, J., Murindagomo, F., and Macdonald, D. (2006). Influence of drought on predation of elephant (Loxodonta africana) calves by lions (Panthera leo) in an African wooded savannah. *J. Zool*. 270, 523–530. doi: 10.1111/j.1469-7998.2006.00181.x

Lund, U., and Agostinelli, C. (2015). *Circstats: Circular Statistics, From "Topics in Circular Statistics"(2001)*. S-plus original by Lund, U. R port by Agostinelli, C. R package version 0.2–4. Available online at: http://CRAN.R-project.org/package=CircStats

Marsh, L. M., and Jones, R. E. (1988). The form and consequences of random walk movement models. *J. Theor. Biol*. 133, 113–131. doi: 10.1016/S0022-5193(88)80028-6

McComb, K., Moss, C., Durant, S. M., Baker, L., and Sayialel, S. (2001). Matriarchs as repositories of social knowledge in African elephants. *Science* 292, 491–494. doi: 10.1126/science.1057895

Miquelle, D. G., Peek, J. M., and Ballenberghe, V. (1992). Sexual segregation in Alaskan moose. *Wildlife Monogr*. 122, 3–57. doi: 10.1017/CBO9781107415324.004

Moss, C. J., Croze, H., and Lee, P. C. (2011). *The Amboseli Elephants: A Long-Term Perspective on a Long-Lived Mammal*. Chicago, IL : Oxford University Press.

Mukeka, J. M. (2010). *Analyzing the Distribution of the African Elephant (Loxodonta africana) in Tsavo, Kenya*. Masters thesis, Miami University.

Ngene, S. M., Njumbi, S., Ngoru, B., Nzisa, M., Bitok, E., Poghon, J., et al. (2012). "Satellite-linked GPS collars deployed on elephants in Tsavo Ecosystem, Kenya," in *Recent Advances in Satellite Research and Development,* eds S. Gardiner, and K. P. Olsen (New York, NY: Nova Publishers).

Ngene, S. M., van Gils, H. A. M. J., van Wieren, S. E., Rasmussen, H., Skidmore, A. K., Prins, H. H. T., et al. (2010). The ranging patterns of elephants in Marsabit protected area, Kenya: the use of satellite-linked GPS collars. *Afric. J. Ecol*. 48, 386–400. doi: 10.1111/j.1365-2028.2009.01125.x

Omondi, P., Bitok, E., Mukeka, J., Mayienda, R., and Litoroh, M. (2008). *Total Aerial Count of Elephants and Other Large Mammal Species of Tsavo–Mkomazi Ecosystem'*. Kenya Wildlife Service Report.

Polansky, L., Kilian, W., and Wittemyer, G.,Polansky, L., Kilian, W., and Wittemyer, G. (2015). Elucidating the significance of spatial memory on movement decisions by African savannah elephants using state–space models. *Proc. R. Soc. B*. 282:20143042. doi: 10.1098/rspb.2014.3042

Prins, H. H. T. (1996). *Ecology and Behaviour of the African Buffalo: Social Inequality and Decision Making*. London: Chapman & Hall.

Prins, H. H. T., and Loth, P. E. (1988). Rainfall patterns as background to plant phenology in northern Tanzania. *J. Biogeogr*. 15, 451–463. doi: 10.2307/2845275

Prins, H. H. T., and Van Langevelde, F. (2008). *Resource Ecology: Spatial and Temporal Dynamics of Foraging*. Berlin: Springer.

Redfern, J. V., Grant, C. C., Gaylard, A., and Getza, W. M. (2005). Surface water availability and the management of herbivore distributions in an African savanna ecosystem. *J. Arid Environ*. 63, 406–424. doi: 10.1016/j.jaridenv.2005.03.016

Root, R. B., and Kareiva, P. M. (1984). (Pieris Rapae): ecological consequences and adaptive significance of markovian movements in a patchy environment. *Ecology* 65, 147–165.

Roshier, D. A., Doerr, V. A., and Doerr, E. D. (2008). Animal movement in dynamic landscapes: Interaction between behavioural strategies and resource distributions. *Oecologia* 156, 465–477. doi: 10.1007/s00442-008-0987-0

Schick, R. S., Loarie, S. R., Colchero, F., Best, B. D., Boustany, A., Conde, D. A., et al. (2008). Understanding movement data and movement processes: current and emerging directions. *Ecol. Lett*. 11, 1338–1350. doi: 10.1111/j.1461-0248.2008.01249.x

Sianga, K., van Telgen, M., Vrooman, J., Fynn, R. W. S., and van Langevelde, F. (2017). Spatial refuges buffer landscapes against homogenization and degradation by large herbivore populations and facilitate vegetation heterogeneity. *Koedoe* 59:a1434. doi: 10.4102/koedoe.v59i2.1434

Sims, D. W., Humphries, N. E., Bradford, R. W., and Bruce, B. D. (2012). Lévy flight and Brownian search patterns of a free-ranging predator reflect different prey field characteristics. *J. Ecol*. 81, 432–442. doi: 10.1111/j.1365-2656.2011.01914.x

Skarpe, C., Du Toit, J. T., and Moe, S. R. (2014). *Elephants and Savanna Woodland Ecosystems: A Study From Chobe National Park, Botswana*. West Sussex, UK: John Wiley & Sons.

Smit, I. P. J., and Grant, C. C. (2009). Managing surface-water in a large semi-arid savanna park: effects on grazer distribution patterns. *J. Nature Conserv*. 17, 61–71. doi: 10.1016/j.jnc.2009.01.001

Smit, I. P. J., Grant, C. C., and Devereux, B. J. (2007). Do artificial waterholes influence the way herbivores use the landscape? Herbivore distribution patterns around rivers and artificial surface water sources in a large African savanna park. *Biol. Conserv*. 136, 85–99. doi: 10.1016/j.biocon.2006.11.009

Stokke, S., and Du Toit, J. T. (2002). Sexual segregation in habitat use by elephants in Chobe National Park, Botswana. *Afric. J. Ecol*. 40, 360–371. doi: 10.1046/j.1365-2028.2002.00395.x

Turchin, P. (1991). Translating foraging movements in heterogeneous environments into the spatial distribution of foragers. *Ecology* 72, 1253–1266. doi: 10.2307/1941099

Turchin, P. (1998). *Quantitative Analysis of Movement: Measuring and Modeling Population Redistribution in Animals and Plants*. Sunderland: Sinauer Associates.

Tyrrell, J., and Coe, M. (1974). The rainfall regime of Tsavo National Park, Kenya and its potential phenological significance. *J. Biogeogr*. 1, 187–192.

Valeix, M., Loveridge, A. J., Davidson, Z., Madzikanda, H., Fritz, H., and Macdonald, D. W. (2010). How key habitat features influence large terrestrial carnivore movements: waterholes and African lions in a semi-arid savanna of north-western Zimbabwe. *Landscape Ecol*. 25, 337–351. doi: 10.1007/s10980-009-9425-x

Verlinden, A., and Gavor, I. K. (1998). Satellite tracking of elephants in northern Botswana. *Afric. J. Ecol*. 36, 105–116. doi: 10.1046/j.1365-2028.1998.00118.x

Viljoen, P. (1989). Habitat selection and preferred food plants of a desert-dwelling elephant population in the northern Namib Desert, South West Africa/Namibia. *Afric. J. Ecol*. 27, 227–240.

Viswanathan, G. M., Afanasyev, V., Buldyrev, S. V., Murphy, E. J., Prince, P. A., and Stanley, H. E. (1996). Lévy flight search patterns of wandering albatrosses. *Nature* 381, 413–441. doi: 10.1038/381413a0

Wato, Y. A., Heitkönig, I. M. A., van Wieren, S. E., Wahungu, G., Prins, H. H. T., and van Langeveldea, F. (2016). Prolonged drought results in starvation of African elephant (*Loxodonta africana*). *Biol. Conserv*. 203, 89–96. doi: 10.1016/j.biocon.2016.09.007

Young, E. (1970). *Water as a Factor in the Ecology of Game in the Kruger National Park*. PhD Thesis. University of Pretoria.

Young, K. D., and Van Aarde, R. J. (2010). Density as an explanatory variable of movements and calf survival in savanna elephants across southern Africa. *J. Anim. Ecol*. 79, 662–673. doi: 10.1111/j.1365-2656.2010.01667.x

Conflict of Interest Statement: The authors declare that the research was conducted in the absence of any commercial or financial relationships that could be construed as a potential conflict of interest.

Copyright © 2018 Wato, Prins, Heitkönig, Wahungu, Ngene, Njumbi and van Langevelde. This is an open-access article distributed under the terms of the Creative Commons Attribution License (CC BY). The use, distribution or reproduction in other forums is permitted, provided the original author(s) and the copyright owner(s) are credited and that the original publication in this journal is cited, in accordance with accepted academic practice. No use, distribution or reproduction is permitted which does not comply with these terms.

frontiers in Ecology and Evolution

ORIGINAL RESEARCH
published: 15 November 2018
doi: 10.3389/fevo.2018.00182

Flight Behavior of Individual Aerial Insectivores Revealed by Novel Altitudinal Dataloggers

R. Andrew Dreelin[1,2]*, *J. Ryan Shipley*[1,2,3] *and David W. Winkler*[1,2,3]

[1] Cornell Lab of Ornithology, Cornell University, Ithaca, NY, United States, [2] Department of Ecology and Evolutionary Biology, Cornell University, Ithaca, NY, United States, [3] Technology for Animal Biology and Environmental Research (TABER), Department of Ecology and Evolutionary Biology, Cornell University, Ithaca, NY, United States

Swallows and martins (Aves: Hirundinidae) are well-studied with respect to their breeding biology, but major aspects of their individual aerial movement behavior and ecology are poorly understood. Atmospheric conditions can strongly influence both the availability and distribution of flying insects that aerial insectivores rely upon. Because aerial insects are often found in distinct clusters within the aerosphere, we wanted to explore whether aerial insectivore flight altitudes were species-specific and if they were associated with atmospheric conditions. We examined these questions with novel tag technology, an altitude datalogger, on breeding populations of Purple Martin (*Progne subis*), Tree Swallow (*Tachycineta bicolor*), and Barn Swallow (*Hirundo rustica*) in upstate New York during the summer of 2016, providing individual-level flight data on a per minute basis. Using mixed models, we investigated differences in flight altitudes between individuals, species, and varying atmospheric conditions. The major findings were that individuals of each species spent significantly different proportions of their time throughout the day in different aerial strata. In addition, higher flying species such as Purple Martins and Tree Swallows responded positively to greater thermal uplift whereas this predictor had no effect on Barn Swallow flight altitudes. Finally, the differing relationships for all species between their flight altitudes and weather variables suggest that each species may use different atmospheric cues for tracking their environment and/or prey. More research spanning greater time scales and a wider range of atmospheric conditions is needed to determine these relationships in finer detail. We encourage broader use of this or similar methodologies to better understand the behavior and ecology of aerial insectivores globally.

Keywords: aerial insectivore, aeroecology, flight, behavior, ecology, swallow, Hirundinidae, datalogger

OPEN ACCESS

Edited by:
Thomas Wassmer, Siena Heights University, United States

Reviewed by:
Adrian C. Gleiss, Murdoch University, Australia
Kathryn Battle, Conservation International, United States

Correspondence:
R. Andrew Dreelin
rad337@cornell.edu

Specialty section:
This article was submitted to Behavioral and Evolutionary Ecology, a section of the journal Frontiers in Ecology and Evolution

Received: *31 July 2018*
Accepted: *23 October 2018*
Published: *15 November 2018*

Citation:
Dreelin RA, Shipley JR and Winkler DW (2018) Flight Behavior of Individual Aerial Insectivores Revealed by Novel Altitudinal Dataloggers. Front. Ecol. Evol. 6:182. doi: 10.3389/fevo.2018.00182

INTRODUCTION

The aerial ecosystem is a dynamic sub-layer of the troposphere closest to Earth's surface. Despite its global presence, the aerial ecosystem, or aerosphere, has received relatively little attention from ecologists until recent decades. In terms of biomass, the aerosphere is primarily comprised of aerial arthropods, often referred to as "aerial plankton," since many of its inhabitants have a limited capacity for powered flight and many use prevailing atmospheric conditions as a mechanism for dispersal (Drake and Farrow, 1989; Russell and Wilson, 1996, 1997; Chapman et al., 2010). The major consumers of this abundant yet ephemeral and patchily distributed resource

are flying vertebrates such as bats and birds, which spend much of their lives in the aerosphere capturing these prey. Although the breeding biology of some avian aerial insectivores is well-known to the point that they are considered model organisms [e.g., Tree Swallows (*Tachycineta bicolor*), (Jones, 2003)], documentation of how they interact with the aerial environment and the drivers of their movement behavior is much more scarce. More information on how these taxa interact with the aerosphere is necessary if we are to have a more comprehensive understanding of how environmental variation and ecological dynamics affect their survival and reproduction.

The emergent discipline of aeroecology seeks to understand the physical characteristics of the aerosphere, the organisms that exist and interact within the aerosphere, and the abiotic and biotic selective pressures exerted by the aerosphere on its inhabitants (Kunz et al., 2008; Chilson et al., 2012). While aeroecology is truly interdisciplinary and has drawn upon a wide range of subjects and technologies to grow and firmly establish itself as a discipline in recent decades, most studies that have been conducted thus far have focused primarily on using coarse-scale radar systems to characterize behavior, usually movements or migrations at the population scale (Kunz et al., 2008; Westbrook, 2008; Kelly et al., 2012; Farnsworth et al., 2016; Horton et al., 2016; Shipley et al., 2017a). Furthermore, technological limitations have constrained organismal-level studies of flight behavior in aerial insectivores to the perspective of human observers from the ground (e.g., Collins, 2000; Manchi and Sankaran, 2010; Shipley et al., 2017a). Thus, connecting an organismal-level framework to large scale phenomena is critical to improve the scientific understanding of the aerial ecosystem and the ecology of its inhabitants.

For instance, although weather conditions crucially impact aerial insectivore ecology, the existing framework of knowledge remains surprisingly simple. Theory dictates that temperature mediates daily abundance of insects in the aerosphere, since warmer temperatures drive their phenology and development (Ratte, 1984) and prompt larger emergences of insects (Taylor, 1963). Most flying insects are found within a few meters off the ground, and their abundance drops off exponentially with altitude (Johnson, 1957; Elkins, 2010). Above these first few meters, factors such as wind speed, direction, and convection can scatter or concentrate aerial plankton, creating ephemeral clumps of insects (Pedgley et al., 1990; Elkins, 2010). By contrast, days characterized by colder temperatures, heavy precipitation, and strong winds can greatly suppress the availability of flying insects and have negative consequences for both adult survival and reproductive success in swallows (Winkler et al., 2013), sometimes resulting in mass mortality events for young nestling swallows (Winkler et al., 2013) and even adults (Elkins, 2010). These conditions can also produce a "lake effect" where aerial insectivores must forage low over the surface of large bodies of water to find prey (Newton, 2007; Elkins, 2010). Beyond this paradigm, however, scientific knowledge of how weather affects the flight behavior of flying vertebrates has remained limited in precision and detail.

Our need for a better understanding of aerial insectivore ecology is even more pressing because aerial insectivores as a guild have experienced significant, broad-scale declines in North America and Europe over the past several decades (Sanderson et al., 2006; Nebel et al., 2010; Oresman et al., 2013; Sauer et al., 2014). Decreasing insect populations and changing insect phenology have been hypothesized to be one of several possible drivers of these declines in insectivorous birds (Hallmann et al., 2017). Thus, beginning to understand how insectivorous birds are moving and foraging in the aerosphere is not only imperative to understanding the ecology of this "hidden ecosystem" and the species within it, but it could also begin to provide insight into some of the possible drivers of these precipitous declines.

Given this need, we set out to gain a comparative, organismal level understanding of the daily flight patterns of several avian aerial insectivores. In upstate New York during the summer of 2016, we deployed data loggers on breeding Tree Swallows (*Tachycineta bicolor*, TRES), Barn Swallows (*Hirundo rustica*, BARS), and Purple Martins (*Progne subis*, PUMA), three species in the same family (Hirundinidae) with well-known breeding biologies, which are also declining in eastern North America. Here we use mixed effect models on flight altitude data to investigate two primary questions: (1) whether basic differences exist between individuals as they move and forage in the aerosphere and whether these differences persist at the level of species and (2) how atmospheric conditions such as temperature, turbulence, dew point, boundary layer, and precipitation rate affect the flight altitude of individual swallows. Because the availability of insects can be concentrated by atmospheric conditions, we predicted that variation in flight altitudes will be greater between species than within species, and that atmospheric conditions influence the flight altitudes of individual of all swallows species similarly.

MATERIALS AND METHODS

We conducted fieldwork from May 22nd to July 20th, 2016, in upstate New York at four locations that support breeding populations of the focal taxa. We sampled Tree Swallows at Unit 1 of the Cornell Experimental Research Ponds in Ithaca (42.505° N, −76.466°W, 335 m) and the Homer C. Thompson Vegetable Research Farm in Freeville (42.518815 N, −76.332651 W, 320 m). We collected data on Purple Martins and Barn Swallows at private residences near Watkins Glen (42.392°N,−76.881°W, 130 m) and Danby (42.288°N, −76.454°W, 395 m), respectively. We collected data on Purple Martins and Barn Swallows at private residences near Watkins Glen (42.392°N,−76.881°W, 130 m) and Danby (42.288°N, −76.454°W, 395 m), respectively. We used specific, known breeding sites for each species to increase the probability of datalogger recapture, but due to the specialized nesting biology of swallows, there was only one study species ***breeding*** at a given site. However, all study species were ***present*** at every site, with the exception of Purple Martins, which were only found at their breeding site. Moreover, behavioral observations at each site confirmed that all species, especially Purple Martins, frequently ventured outside of the immediate airspace of the sampling localities, so any site-specific effects were limited and likely non-significant. The maximum distance

between sites was ∼33 km. Our methods consisted of capturing individual birds and attaching to them data loggers (hereafter referred to as "barologgers") which recorded air temperature and pressure at a frequency of one sample per minute using an onboard low power microprocessor, allowing for near-continuous measurements of flight altitude to the nearest several meters (Shipley et al., 2017b). The barologgers weighed ∼450 mg with epoxy weather-proofing and were attached to the birds using Rappole leg loop harnesses (Rappole and Tipton, 1991) made of 0.5 mm Stretch Magic polymer twine. We recaptured birds between 8 and 13 days after tagging (mean = 8.47 ± 1.73 days). Upon recapture, we removed the barologgers and downloaded their data, deriving flight altitudes using the formula below. We corrected for pressure changes by interpolating to the nearest minute from hourly pressure level readings from the nearest airport weather station (KITH) in Ithaca, NY (42.4908°N, −76.4583°W, 335 m).

$$A = \frac{((\frac{P_0}{P})^{\frac{1}{5.257}} - 1)(T + 273.15)}{0.0065}$$

Where A = barologger altitude (in meters), P_0 = sea level pressure (in pascals), P = barologger pressure (in pascals), and T = barologger temperature (in Kelvin).

For meteorological variables, we acquired data on temperature and dewpoint from KITH, data on turbulence kinetic energy (TKE) from the North American Regional Reanalysis (NARR, Mesinger et al., 2006), and data on boundary layer height and precipitation rate from the Env-DATA Track Annotation Service on Movebank (Dodge et al., 2013). The weather data was interpolated to the minute level to conform with the altitudinal data using bilinear interpolation.

Analysis of Individual Altitude Data

Altitudinal Partitioning

To test for differences in the aerial behavior between the three study species, we partitioned the median altitude per flight bout into six different bins relative to time of day. Starting at 5 a.m. local time, data was divided into dawn, morning, midday, afternoon, evening, and night at 180 min increments. Night was not used for analysis. We analyzed the data using a linear model with log(altitude) as the response variable, and time bin and species as predictors. We also performed pairwise comparisons and independent contrasts using Tukey honest significant differences in a *post-hoc* test.

Atmospheric Effects on Flight Bout Altitude

We also wanted to determine the relationships between flight altitude throughout the day and atmospheric conditions. Because telemetry data tend to demonstrate high degrees of spatial and temporal autocorrelation, we initially checked for autocorrelation calculating the autocorrelation functions for each individual (acf, base R, R Core Team, 2016). Although the characteristics of the autocorrelation relationship can be informative in regard to behavior and movement traits Boyce et al. (2010), we accounted for it in our analyses using two different approaches.

First, we accounted for the temporal autocorrelation using two generalized additive mixed effects models (GAMM) modeled with and without the correlation structure (corAR) fit to the process errors. For each model, the ordinary least squares residuals were used to test for autocorrelation and partial correlation. We compared the naïve model with the corAR model using an information theoretic approach (AICc).

In the second approach, we accounted for temporal autocorrelation by subsetting the data, calculating the median altitude for each flight bout (**Figure 1**). We then analyzed the relationship between median flight bout altitude and the predictor variables using a generalized additive mixed effects model (GAMM) model. We calculated the autocorrelation function for the median flight bout dataset to estimate the remaining temporal autocorrelation.

All generalized additive mixed effects models (GAMMs) were used to compare differences in (log(flight altitudes)) in response to environmental predictor variables. The day of the year, individual identity, and species were included as random effects. Continuous predictor variables were tested for collinearity and those with a Pearson's correlation coefficient (PCC) > 0.5 were excluded from the same model. This resulted in a final predictor set of temperature, thermal uplift, and atmospheric pressure. We analyzed the data with the statistical program R, version 3.3.1 R Core Team (2016).

Animal Ethics and Institutional Approval

All work involving wild animals for this research was approved under protocol 2001-0051 to DW Winkler by the Institutional Animal Care and Use Committee at Cornell University.

RESULTS

Of the 20 barologgers deployed on Tree Swallows, 12 on Barn Swallows, and 7 on Purple Martins, we successfully retrieved 8 from Tree Swallows, 7 from Barn Swallows, and 4 from Purple Martins. On 3 Tree Swallows and 1 Barn Swallow, the barologgers malfunctioned, leaving 5 Tree Swallows and 6 Barn Swallows with usable data. Summary statistics related to logged time recorded, flight altitude, and flight bout durations are summarized in **Table 1**.

Altitudinal Partitioning

In the linear model, both time bin and species were significant as predictors at a $p < 0.05$ level. The results of pairwise comparisons and independent contrasts *post-hoc* test suggested that the greatest differences between species were morning and midday. The complete results are presented in **Figure 2**, **Table 2**.

Atmospheric Effects on Flight Bout Altitude

In the first set of models on entire flight bout data, the naïve, and corAR process model explained 46.5 and 44.1% of the variation in the data. However, visual inspection of the naïve and corAR model coupled with the plot of acf suggested the persistence of temporal autocorrelation. Thus, we decided to only retain the subsampled dataset with the median altitude for each flight bout for analysis. Results of the mixed effects model suggested that all

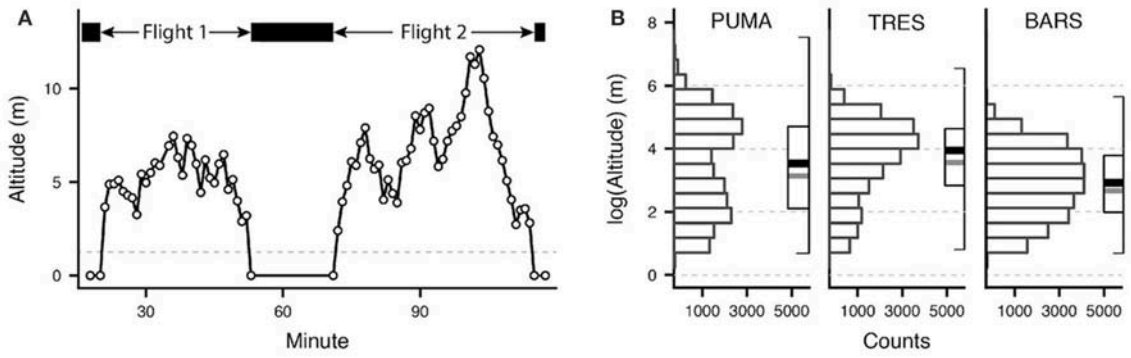

FIGURE 1 | Determination of individual flight bouts and distribution of flight altitudes. In subfigure **(A)**, we considered multiple consecutive data points above an altitude threshold of 2 m (gray dashed line) as an individual flight bout. In the second set of subfigures **(B)**, altitude data from all recorded flight bouts is presented as a histogram and a combined boxplot with the median (thick black line) and the mean (thick gray line). The outer edges of the box represent the IQR.

TABLE 1 | Summary of individual flight bout data.

	Purple Martin (PUMA)	Tree Swallow (TRES)	Barn Swallow (BARS)
Number of individuals (n)	4	5	6
Maximum altitude (m)	1945	661	273
Mean daily maximum altitude (m)	796	276	167
Mean daily altitude (m)	119	69	34
Mean maximum altitude per flight bout (m)	159	73	37

species flight altitudes were affected by time of day, and higher-flying species (PUMA and TRES) were affected by atmospheric conditions such as thermal uplift (**Table 3**, **Figure 3**). In addition, the random effects of both species and day of year were significant as was individual ID. The best model explained 42.6% of the variation in the data and the complete GAMM results are presented in **Table 3**.

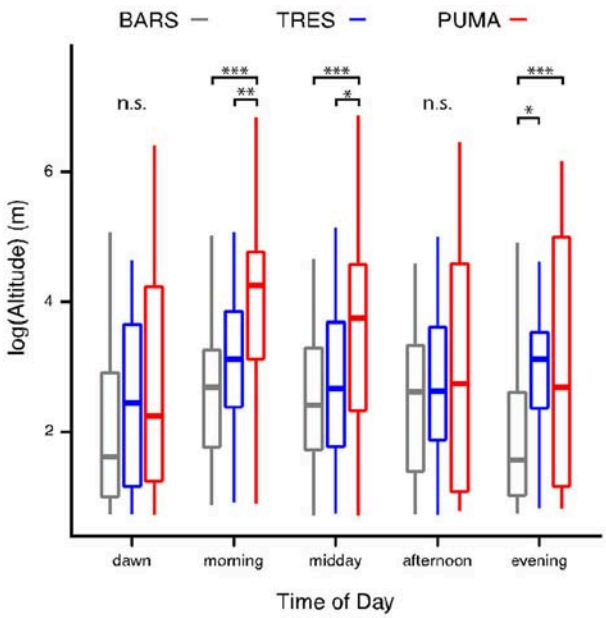

FIGURE 2 | Differences in altitude at different times of day for 3 study species—We compared the median log flight altitude of each flight bout between species using a linear model with pairwise comparison of contrasts using a Tukey HSD test. In 3 out of 5 time bins, there were significant differences between Purple Martins and Barn Swallows. The greatest differences between species occur in morning and midday in this study period. $^{***}p < 0.001$, $^{**}p < 0.01$, $^{*}p < 0.05$, n.s., non-significant.

DISCUSSION

Our results demonstrate that individual Barn Swallows, Tree Swallows, and Purple Martins use significantly different altitude strata in their daily aerial movement and foraging, despite considerable variation and plasticity in their aerial behavior (**Table 2**, **Figure 2**). Independent contrasts suggested that this was most pronounced during late morning and midday, where Purple Martins were consistently the highest species in our study, followed by Tree Swallows and Barn Swallows, respectively. However, these differences were non-existent both at dawn and in the later afternoon. This suggests that there may be a degree of temporally-driven ecological structure in the aerosphere. Since swallows capitalize on ephemeral clusters of insects in the air Elkins (2010), it follows that differences between species should be minimal unless they are consuming different insects that are found at different altitudinal bands. Aerial insectivores feed opportunistically on a wide variety of insect taxa, but previous research has revealed broad differences in diet between Purple Martins, Tree Swallows, and Barn Swallows (Beal, 1918; Brown and Brown, 1999; Winkler et al., 2011; Brown and Tarof, 2013); moreover, Helms et al. (2016) used tag technology similar to this study on Purple Martins to demonstrate from their diets

that insect taxa do in fact have different altitudinal distributions within the aerial environment. Given this, it is intuitive that since aerial insectivores have differentiated diets and since the aerial "plankton" they feed on have distinct altitudinal distributions, then aerial insectivores may partition their foraging into altitudinal bands where they presumably feed on their preferred prey. While more sampling is needed to confirm that these differences truly persist at the species level, this finding represents a novel insight into the ecology of aerial insectivores, and future research should examine dietary differences as a possible explanation for this pattern.

These results also provide novel insight on how prevailing weather conditions can affect the movement behavior of individual avian aerial insectivores. Thermal uplift had a significant, positive effect on median flight bout altitude for the two higher-flying species, Tree Swallows and Purple Martins, but not for Barn Swallows (**Table 3**, **Figure 3**). Foraging strategy may be a explanation for this pattern, since Barn Swallows are smaller and more slender, suited for "coursing" by foraging low over grassy fields and meadows to pick off prey just above the ground; they have even been noted to prefer single, large insects over swarms (Brown and Brown, 1999). Therefore, thermal uplift seems less likely to influence their movement and foraging behavior compared with Tree Swallows and Purple Martins.

TABLE 2 | Results of the Generalized Additive Mixed Model (GAMM) analyzing flight altitude and atmospheric condition predictors.

Predictor	edf	*F*	*p*	sig
s(Temperature): BARS	1.000	3.284	0.070	n.s.
s(Temperature): PUMA	3.542	4.048	0.002	**
s(Temperature): TRES	1.000	0.011	0.915	n.s.
s(Thermal Uplift): BARS	2.735	1.325	0.225	n.s.
s(Thermal Uplift): PUMA	1.717	4.103	0.047	*
s(Thermal Uplift): TRES	2.760	3.853	0.005	**
s(Pressure): BARS	1.000	4.112	0.043	*
s(Pressure): PUMA	1.00	4.149	0.042	*
s(Pressure): TRES	1.00	3.191	0.074	n.s.
s(Minute): BARS	5.813	22.225	<0.001	***
s(Minute): PUMA	6.991	66.783	<0.001	***
s(Minute): TRES	6.385	20.484	<0.001	***
s(Day of Year)	17.518	2.198	<0.001	***
s(Individual)	5.007	0.792	0.035	*
s(Species)	1.894	117.003	<0.001	***
Scale estimate = 0.797				
Adjusted R-squared = 0.426				
Deviance Explained = 44.2%				

****p < 0.001, **p < 0.01, *p < 0.05, n.s., not significant.*

TABLE 3 | *Post-hoc* independent contrasts of time bins.

	Estimate	SE	*t*	*p*
BARS – TRES dawn	−0.33	0.27	−1.23	0.99
BARS – PUMA dawn	−0.65	0.32	−1.98	0.81
TRES – PUMA dawn	0.31	0.32	0.99	0.99
BARS – TRES morning	−0.48	0.18	−2.61	0.36
BARS – PUMA morning	−1.34	0.18	−7.28	**<0.001**
TRES – PUMA morning	0.86	0.21	4.16	**0.003**
BARS – TRES midday	−0.27	0.20	−1.32	0.99
BARS – PUMA midday	−1.11	0.20	−5.30	**<0.001**
TRES – PUMA midday	0.83	0.24	3.37	**0.04**
BARS – TRES afternoon	−0.19	0.21	−0.88	0.99
BARS – PUMA afternoon	−0.44	0.24	1.84	0.88
TRES – PUMA afternoon	0.25	0.26	0.94	0.99
BARS – TRES evening	−0.85	0.23	−3.64	**0.02**
BARS – PUMA evening	−1.15	0.25	−4.55	**<0.001**
TRES – PUMA evening	0.29	0.27	1.07	0.99

Bold values are those that are significant at a p < 0.05.

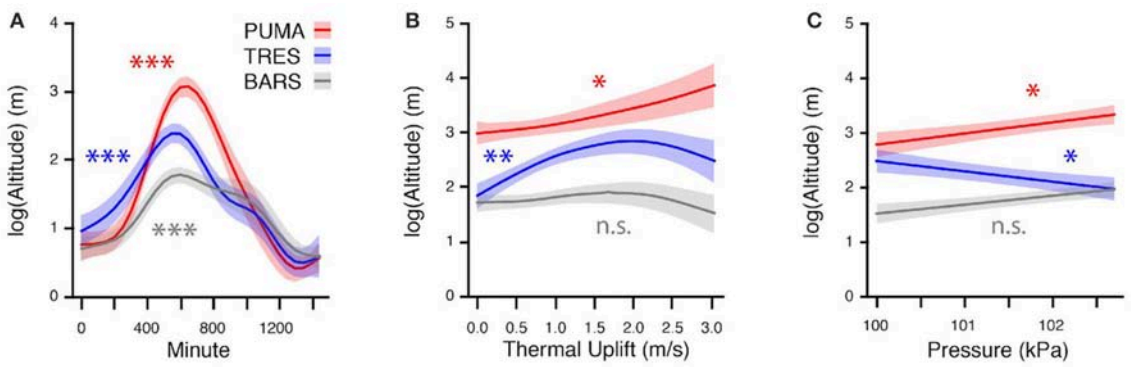

FIGURE 3 | Relationship between predictor variables and flight altitude for three study species. The shaded region represents the standard error for each smooth function estimate. In the first subfigure **(A)**, the relationship between time of day (Minute) and altitude is significant for all three species, with highest altitudes occurring near mid-day. In subfigure **(B)**, Altitude significantly increases with thermal uplift for Purple Martins (PUMA) and Tree Swallows (TRES), but not for Barn Swallows (BARS). In the final subfigure **(C)**, there is no clear relationship between atmospheric pressure and flight bout altitudes, with PUMA and TRES having significant but opposite effects. ***$p < 0.001$, **$p < 0.01$, *$p < 0.05$, n.s., non-significant.

Surprisingly, temperature itself only had a significant, positive effect on the median flight bout altitude of Purple Martins and no other species (**Table 3**, **Figure 3**). This is interesting, since it is thought that temperature mediates daily insect emergence and abundance (Taylor, 1963; Ratte, 1984). However, the relationship between aerial insect abundance and temperature has been shown to be non-linear, where lower temperatures suppress aerial insect activity completely (Winkler et al., 2013). In this study, our samples are restricted to the breeding season, which experiences a considerably smaller range of temperatures than (Winkler et al., 2013). Thus, the relationship between temperature and aerial activity of swallows may be weaker than if we had data across a wider range of temperatures. Finally, the time of day did have a significant effect on median flight altitude for all three species, and the effect on median flight bout altitude was most positive at midday when daily temperatures are highest and insects are likely to be at their greatest height in the aerosphere.

Regardless of any specific predictors, the fact that the relationships between median flight bout altitude and weather variables changed significantly depending on time of day and the date demonstrates that individual swallows are likely to use changing environmental conditions to inform their decisions on when and where to fly and forage. Moreover, the differential response of individuals within each species to the same environmental variables suggests that the study taxa may possess different strategies for foraging in response to weather patterns, although more research is needed to confirm whether these are consistent, species-specific differences.

The varying relationships between flight altitudes and weather variables may be further explained by the ever-changing context of cues and strategies influencing the behavior of individual organisms (Winkler et al., 2014). Future research should address endogenous factors such as age, sex, and body condition that are likely to affect movement behavior. More precise weather data may also be necessary to elucidate the relationships between flight altitude and meteorological variables, as the scale of our weather data was both spatially and temporally coarse. Overall, more research is needed to examine these relationships across more individuals with longer sampling periods and a wider breadth of weather conditions. Additionally, a three-dimensional analysis could greatly help to better understand the relationships between meteorological variables and flight behavior in aerial insectivores.

In using newly developed tools to characterize the aerial behavior of three avian aerial insectivores, we have established a precise, broadly applicable method to better understand the ecology of aerial insectivores globally. This method can contribute further to aeroecology by providing high resolution data on the individual lives of large, flying vertebrates that inhabit the aerosphere. We therefore encourage others interested in the behavioral ecology of aerial insectivores to deploy this or similar technologies on a wider breadth of species across a greater geographic and temporal extent and to conduct careful experiments to better understand the effects of life history, geography, and weather on aerial insectivore behavioral ecology.

DATA AVAILABILITY STATEMENT

The data generated and analyzed to support the conclusions of this study is available upon reasonable request.

AUTHOR CONTRIBUTIONS

All authors conceived and designed the project jointly. JS and DW developed the methodology. RD and JS collected the data. RD and JS formatted and analyzed the data. RD drafted the manuscript. All authors revised the manuscript and approved the version submitted.

FUNDING

This research was in part funded by a NSF research grant to DW (NSF IBDR 1556138) and a research grant to JS from the Cornell Atkinson Center for a Sustainable Future.

ACKNOWLEDGMENTS

We thank the 2016 Ithaca field crew of the Golondrinas de las Americas project, in particular friend and field site manager Teresa Pegan, for their assistance deploying the barologgers. We thank homeowners Dave Crans and Janice Beale for allowing us access to their Purple Martins and Barn Swallows, respectively. Dave Crans is due extra thanks for his assistance in capturing Purple Martins and deploying the barologgers. RD thanks Reid Rumelt for his assistance writing R code and Lynn Johnson at Cornell Statistical Consulting Unit for her advice.

REFERENCES

Beal, F. E. L. (1918). *Food Habits of the Swallows: A Family of Valuable Native Birds (No. 619).* Washington, DC: US Department of Agriculture.

Boyce, M. S., Pitt, J., Northrup, J. M., Morehouse, A. T., Knopff, K. H., Cristescu, B., et al. (2010). Temporal autocorrelation functions for movement rates from global positioning system radiotelemetry data. *Philos. Trans. R. Soc. Lond. B Biol. Sci.* 365, 2213–2219. doi: 10.1098/rstb.2010.0080

Brown, C. R., and Brown, M. B. (1999). "Barn Swallow (*Hirundo rustica*)," in *The Birds of North America,* ed P. G. Rodewald (Ithaca, NY: Cornell Lab of Ornithology). Available online at: https://birdsna.org/Species-Account/bna/species/barswa

Brown, C. R., and Tarof, S. (2013). "Purple Martin (*Progne subis*)," in *The Birds of North America,* ed P. G. Rodewald (Ithaca, NY: Cornell Lab of Ornithology). Available online at: https://birdsna.org/Species-Account/bna/species/purmar

Chapman, J. W., Nesbit, R. L., Burgin, L. E., Reynolds, D. R., Smith, A. D., Middleton, D. R., et al. (2010). Flight orientation behaviors promote optimal migration trajectories in high-flying insects. *Science* 327, 682–685. doi: 10.1126/science.1182990

Chilson, P. B., Frick, W. F., Kelly, J. F., Howard, K. W., Larkin, R. P., Diehl, R. H., et al. (2012). Partly cloudy with a chance of migration: weather, radars, and aeroecology. *Bull. Am. Meteorol. Soc.* 93, 669–686. doi: 10.1175/BAMS-D-11-00099.1

Collins, C. T. (2000). Foraging of glossy and pygmy swiftlets in Palawan, Philippine Islands. *Forktail* 16, 53–55.

Dodge, S., Bohrer, G., Weinzierl, R., Davidson, S. C., Kays, R., Douglas, D., et al. (2013). The environmental-data automated track annotation (Env-DATA) system: linking animal tracks with environmental data. *Mov. Ecol.* 1:3. doi: 10.1186/2051-3933-1-3

Drake, V. A., and Farrow, R. A. (1989). The 'aerial plankton' and atmospheric convergence. *Trends Ecol. Evol.* 4, 381–385.

Farnsworth, A., Van Doren, B. M., Hochachka, W. M., Sheldon, D., Winner, K., Irvine, J., et al. (2016). A characterization of autumn nocturnal migration detected by weather surveillance radars in the northeastern USA. *Ecol. Appl.* 26, 752–770. doi: 10.1890/15-0023

Elkins, N. (2010). *Weather and Bird Behaviour*. London, UK: Bloomsbury Publishing.

Hallmann, C. A., Sorg, M., Jongejans, E., Siepel, H., Hofland, N., Schwan, H., et al. (2017). More than 75 percent decline over 27 years in total flying insect biomass in protected areas. *PLoS ONE* 12:e0185809. doi: 10.1371/journal.pone.0185809

Helms, J. A., Godfrey, A. P., Ames, T., and Bridge, E. S. (2016). Predator foraging altitudes reveal the structure of aerial insect communities. *Sci. Rep.* 6:28670. doi: 10.1038/srep28670

Horton, K. G., Van Doren, B. M., Stepanian, P. M., Farnsworth, A., and Kelly, J. F. (2016). Seasonal differences in landbird migration strategies. *The Auk* 133, 761–769. doi: 10.1642/AUK-16-105.1

Johnson, C. G. (1957). The distribution of insects in the air and the empirical relation of density to height. *J. Anim. Ecol.* 26, 479–494. doi: 10.2307/1760

Jones, J. (2003). Tree Swallows (*Tachycineta bicolor*): a new model organism? *Auk* 120, 591–599. doi: 10.1642/0004-8038(2003)120[0591:TSTBAN]2.0.CO;2

Kelly, J. F., Shipley, J. R., Chilson, P. B., Howard, K. W., Frick, W. F., and Kunz, T. H. (2012). Quantifying animal phenology in the aerosphere at a continental scale using NEXRAD weather radars. *Ecosphere* 3, 1–9. doi: 10.1890/ES11-00257.1

Kunz, T. H., Gauthreaux, S. A., Hristov, N. I., Horn, J. W., Jones, G., Kalko, E. K., et al. (2008). Aeroecology: probing and modeling the aerosphere. *Integr. Comp. Biol.* 48, 1–11. doi: 10.1093/icb/icn037

Manchi, S. S., and Sankaran, R. (2010). Foraging habits and habitat use by Edible-nest and Glossy swiftlets in the Andaman Islands, India. *Wilson J. Ornithol.* 122, 259–272. doi: 10.1676/09-144.1

Mesinger, F., Di Mego, G., Kalnay, E., and Mitchell, K. (2006). North American regional reanalysis. *Bull. Am. Meteorol. Soc.* 87:343. doi: 10.1175/BAMS-87-3-343

Nebel, S., Mills, A., McCracken, J., and Taylor, P. (2010). Declines of aerial insectivores in North America follow a geographic gradient. *Avian Conserv. Ecol.* 5:1. doi: 10.5751/ACE-00391-050201

Newton, I. (2007). Weather related mass mortality events in migrants. *Ibis* 149, 453–467. doi: 10.1111/j.1474-919X.2007.00704.x

Oresman, S., McCracken, J., Bull, M., Winkler, D., Rubega, M., Kearney-McGee, S., et al. (2013). *The Seventh Habitat and the Decline of Our Aerial Insectivores*. Fairfield, CT: Connecticut State of the Birds.

Pedgley, D. E., Scorer, R. S., Purdom, J. F. W., Simpson, J. E., Wickham, P. G., Dickison, R. B. B., et al. (1990). Concentration of flying insects by the wind [and discussion]. *Philos. Trans. R. Soc. Lond. B Biol. Sci.* 328, 631–653. doi: 10.1098/rstb.1990.0133

R Core Team (2016). *R: A Language and Environment for Statistical Computing*. Vienna: R Foundation for Statistical Computing. Available online at: https://www.R-project.org/

Rappole, J. H., and Tipton, A. R. (1991). New harness design for attachment of radio transmitters to small passerines (Nuevo Diseño de Arnés para Atar Transmisores a Passeriformes Pequeños). *J. Field Ornithol.* 62, 335–337.

Ratte, H. T. (1984). "Temperature and insect development," in *Environmental Physiology and Biochemistry of Insects*, ed K. H. Hoffman (Berlin; Heidelberg: Springer), 33–66.

Russell, R. W., and Wilson, J. W. (1997). Radar-observed "fine Lines" in the optically clear boundary layer: reflectivity contributions from aerial plankton and its predators. *Boundary Layer Meteorol.* 82, 235–262.

Russell, R. W., and Wilson, J. W. (1996). Aerial plankton detected by radar. *Nature* 381:200.

Sanderson, F. J., Donald, P. F., Pain, D. J., Burfield, I. J., and Van Bommel, F. P. (2006). Long-term population declines in Afro-Palearctic migrant birds. *Biol. Conserv.* 131, 93–105. doi: 10.1016/j.biocon.2006.02.008

Sauer, J. R., Hines, J. E., Fallon, J. E., Pardieck, K. L., Ziolkowski, D. J. Jr., and Link, W. A. (2014). *The North American Breeding Bird Survey, Results and Analysis 1966 - 2013. Version 01.30.2015* (Laurel, MD: USGS Patuxent Wildlife Research Center).

Shipley, J., Ryan, K. Dreelin, J., Andrew, R., and Winkler, D. W. (2017a). An open-source sensor-logger for recording vertical movement in free-living organisms. *Meth. Ecol. Evol.* 9, 465–471. doi: 10.1111/2041-210X.12893

Shipley, J. R., Kelly, J. F., and Frick, W. F. (2017b). Toward integrating citizen science and radar data for migrant bird conservation. *Remote Sens. Ecol. Conserv.* 4, 127–136. doi: 10.1002/rse2.62

Taylor, L. R. (1963). Analysis of the effect of temperature on insects in flight. *J. Anim. Ecol.* 32, 99–117.

Westbrook, J. K. (2008). Noctuid migration in Texas within the nocturnal aeroecological boundary layer. *Integr. Comp. Biol.* 48, 99–106. doi: 10.1093/icb/icn040

Winkler, D. W., Hallinger, K. K., Ardia, D. R., Robertson, R. J., Stutchbury B. J., and Cohen, R. R. (2011). "Tree Swallow (*Tachycineta bicolor*)," in *The Birds of North America,* ed P. G. Rodewald (Ithaca, NY: Cornell Lab of Ornithology). Available online at: https://birdsna.org/Species-Account/bna/species/treswa

Winkler, D. W., Jørgensen, C., Both, C., Houston, A. I., McNamara, J. M., Levey, D. J., et al. (2014). Cues, strategies, and outcomes: how migrating vertebrates track environmental change. *Mov. Ecol.* 2:10. doi: 10.1186/2051-3933-2-10

Winkler, D. W., Luo, M. K., and Rakhimberdiev, E. (2013). Temperature effects on food supply and chick mortality in tree swallows (*Tachycineta bicolor*). *Oecologia* 173, 129–138. doi: 10.1007/s00442-013-2605-z

Conflict of Interest Statement: The authors declare that the research was conducted in the absence of any commercial or financial relationships that could be construed as a potential conflict of interest.

Copyright © 2018 Dreelin, Shipley and Winkler. This is an open-access article distributed under the terms of the Creative Commons Attribution License (CC BY). The use, distribution or reproduction in other forums is permitted, provided the original author(s) and the copyright owner(s) are credited and that the original publication in this journal is cited, in accordance with accepted academic practice. No use, distribution or reproduction is permitted which does not comply with these terms.

frontiers in Ecology and Evolution

ORIGINAL RESEARCH
published: 16 November 2018
doi: 10.3389/fevo.2018.00190

Shallow Torpor Expression in Free-Ranging Common Hamsters With and Without Food Supplements

Carina Siutz, Viktoria Ammann and Eva Millesi*

Department of Behavioural Biology, University of Vienna, Vienna, Austria

Energy expenditure during winter can be reduced by expressing torpor, which is characterized by decreased metabolic rate and body temperature. In addition to deep, multiday torpor bouts alternating with short arousal episodes during the hibernation period, common hamsters can also enter shallow torpor bouts (STBs), lasting for <24 h at a minimum body temperature between 30 and 20°C. Food supplements provided shortly before winter have been shown to shorten hibernation in males, but did not affect hibernation duration in females. In the presented study, we analyzed the expression of STBs and compared supplemented to unsupplemented common hamsters. Body temperature during winter was recorded using subcutaneously implanted data loggers (iButtons). The results revealed that supplemented males showed more STBs and thus spent more time in shallow torpor than unsupplemented individuals. The duration of STBs, however, was shorter in supplemented males and both mean and minimum body temperature were significantly higher compared to unsupplemented males. In females, shallow torpor expression did not differ between individuals with and without food supplements. STBs were mainly expressed before the onset of the first deep, multiday torpor bout, but the number of STBs was not related to that of deep torpor bouts. These results indicate that in males, shallow torpor combined with feeding on food stores could be the more appropriate overwintering strategy when sufficient external energy reserves are available. Females generally cache more food than males and are therefore assumed to be less affected by the additional food stores. These results underline the flexibility of the species in the use of heterothermy and could enable adequate and rapid responses to changes in food availability.

Keywords: hibernation, shallow torpor, food supplementation, sex differences, common hamster

OPEN ACCESS

Edited by:
Jordi Figuerola,
Estación Biológica de Doñana (EBD), Spain

Reviewed by:
Gerhard Koertner,
University of New England, Australia
Thomas Wassmer,
Siena Heights University, United States

****Correspondence:***
Carina Siutz
carina.siutz@univie.ac.at

Specialty section:
This article was submitted to Behavioral and Evolutionary Ecology, a section of the journal Frontiers in Ecology and Evolution

Received: *30 July 2018*
Accepted: *29 October 2018*
Published: *16 November 2018*

Citation:
Siutz C, Ammann V and Millesi E (2018) Shallow Torpor Expression in Free-Ranging Common Hamsters With and Without Food Supplements. Front. Ecol. Evol. 6:190. doi: 10.3389/fevo.2018.00190

INTRODUCTION

Several bird and mammalian species have the capability to escape unfavorable environmental conditions by saving energy via reducing metabolic rate and body temperature during so-called torpor bouts. Two distinct types of such heterothermy can be distinguished: daily torpor and hibernation. Daily torpor is characterized by torpor bout durations of <24 h, a mean minimum metabolic rate during torpor of about 35% of basal metabolic rate, and minimum body temperatures during torpor usually range between 30 and 20°C. In contrast, hibernators are able to express torpor bouts lasting for several days or weeks, minimum metabolic rate during torpor is reduced to 4–6% of basal metabolic rate, and body temperature usually drops close to ambient

temperature, usually below 10°C (Geiser, 1988, 2004; Heldmaier and Ruf, 1992; Geiser and Ruf, 1995; Buck and Barnes, 2000; Heldmaier et al., 2004; Ruf and Geiser, 2015). In addition, animals expressing daily torpor usually continue foraging and the torpor-arousal cycle is entrained with the light-dark cycle, while hibernators rely on energy reserves (body fat or food stores) and the circadian clock appears to be strongly suppressed (Ruf and Geiser, 2015).

Common hamsters (*Cricetus cricetus*), classified as hibernators, terminate above-ground activity in autumn and remain inside their hibernacula until spring (Weinhold and Kayser, 2006; Siutz et al., 2016). During winter, they rely on food stores (Eibl-Eibesfeldt, 1953; Niethammer, 1982), although recent observations of foraging behavior above-ground during the active season indicate sex differences in energy accumulation strategies: females showed much more food caching activities than males, suggesting larger food stores and hence, a stronger reliance on external energy reserves, while males, which were mainly observed feeding above-ground, appeared to have higher body fat proportions than females, indicating that they rather use internal energy reserves for the winter period (Siutz et al., 2012). Moreover, previous studies demonstrated high individual variations in body temperature patterns during winter. In addition to typical deep torpor bouts, common hamsters are known to regularly express short and shallow torpor (Wollnik and Schmidt, 1995; Wassmer and Wollnik, 1997; Siutz and Millesi, 2017; Siutz et al., 2017), which is characterized by less pronounced drops in body temperature (with minimum values ranging between 30 and 20°C) and a duration shorter than 24 h. Several hibernating mammals express short and shallow torpor, primarily before or after the hibernation period, and although this type of torpor seems to be similar to daily torpor, the physiological mechanisms regulating temperature and metabolic rate resemble those of deep torpor bouts (Wilz and Heldmaier, 2000; Geiser, 2004; Sheriff et al., 2012; Ruf and Geiser, 2015). In common hamsters, however, shallow torpor occurred not only prior to or after, but also during the actual hibernation period, i.e., between deep torpor bouts (Wollnik and Schmidt, 1995; Wassmer and Wollnik, 1997). Finally, hamsters kept under laboratory conditions were found to enter shallow torpor primarily in the morning hours, which was significantly later compared to entry into deep torpor. This daily rhythm of torpor entrance, however, was not found under semi-natural conditions, i.e., without exposure to light-dark cycles (Wassmer and Wollnik, 1997; Wassmer, 1998), indicating that shallow torpor expressed by hamsters is functionally distinct from daily torpor.

In this study, we manipulated food store availability for the winter period in free-ranging common hamsters by providing individuals with additional food shortly before they immerged into their hibernacula. The analysis of hibernation patterns revealed that males with additional food hibernated for shorter periods and, correspondingly, spent less time in deep torpor compared to unsupplemented hamsters, while deep torpor expression was not affected in females (Siutz et al., 2018). The aim of the presented study was to compare patterns of shallow torpor expression between supplemented and unsupplemented hamsters to gain more insight in different overwintering strategies in this species and investigate potential relationships between deep and shallow torpor.

METHODS

Ethical Statement

All procedures were performed in accordance with EU guidelines for the protection of animals used for scientific purposes (Directive 2010/63/EU) and were approved by the ethics committee of the Faculty of Life Sciences, University of Vienna (2015-010), the Austrian Federal Ministry of Education, Science and Research (GZ: BMWFW-66.006/0013-WF/V/3b/2015), and the City of Vienna (MA22-2484/10, MA22-310/11).

Field Techniques

Free-ranging common hamsters, inhabiting urban areas in southern Vienna (Austria), were monitored during their active season (March/April–October/November 2015) by applying capture-mark-recapture techniques. Hamsters were trapped with Tomahawk live traps and released into cone-shaped cotton sacks for investigation allowing animal handling without anesthesia. At first capture, sex and age (adult/juvenile) was determined and, in addition to permanent identification via a subcutaneously implanted transponder (Data Mars), each individual was fur-marked in different, distinguishable patterns for distance recognition. A detailed description of our field methods can be found elsewhere (Franceschini et al., 2007; Franceschini-Zink and Millesi, 2008b; Siutz et al., 2016). All hamsters were monitored until autumn when they terminate above-ground activity and immerge into their hibernaculum (Siutz et al., 2016). This enabled us to define the individual immergence date, which corresponded to the date when an individual was trapped or observed for the last time in autumn and was confirmed by plugged burrows. To detect potential activity during winter, we additionally plugged the burrows with leaves and monitored them at weekly intervals until spring, but we discovered no signs of surface activity. Beginning in March, when hamsters are expected to emerge from their hibernacula (Siutz et al., 2016), we checked the burrows and observed the surrounding area at daily intervals and recaptured active individuals. The individual emergence date was defined as the date when an individual was observed above-ground or trapped for the first time, which coincided with the day when we discovered the removed burrow plug.

Food Supplementation

To provide hamsters with additional food, we placed 500 g sunflower seeds (Dehner Natura, Dehner GmbH, Germany) in front of an individual's hibernaculum and permanently observed the burrow until the hamster had carried all seeds inside, guaranteeing that only the focal individual collected the seeds. We chose sunflower seeds because of their storability and high energetic content (2.45 MJ/100 g, 51.5 g total fat/100 g) (USDA, 2016). Moreover, sunflower seeds are partly available and collected by hamsters, and their nutrient and fatty acid composition is comparable to the natural winter diet of common

hamsters consisting of, e.g., beechnuts, black walnuts, hazelnuts, or acorn at our study site (Roswag et al., 2018). Additionally, sunflower seeds are relatively small and can be quickly cached by hamsters, facilitating the experimental procedure. To ensure that the food was used for the winter period, we supplemented hamsters in late autumn (September/October) shortly before immergence into the hibernaculum.

Common hamsters are strictly protected by the Fauna-Flora-Habitat directives (Appendix IV) and the Bern Convention (Appendix II) and implantation of temperature data loggers (see methods section "hibernation patterns") was permitted for 20 individuals (GZ BMWFW-66.006/0013-WF/V/3b/2015). By monitoring hamsters throughout the active season, we could certainly identify the hibernacula of 18 individuals in autumn. Considering this relatively small sample size and a rather high overwinter mortality rate in this species (on average about 60 %; Franceschini-Zink and Millesi, 2008a), we supplemented all 18 individuals and used hibernation data collected in unsupplemented hamsters in previous years as control (13 females, 13 males). Although this might be a limiting factor of the study, analyses of patterns of deep torpor expression in unsupplemented hamsters, which were already published, revealed no significant effect of year, neither on hibernation performance nor seasonal timing (Siutz et al., 2016). Furthermore, ambient temperatures recorded at our study site during autumn, winter, and spring, as well as, food availability and snow cover showed no inter-year variations and were similar in the season of food supplementation compared to previous years (Siutz et al., 2018). In addition, body mass was similar in males (335.6 ± 13.4 g, $n = 19$) and females (319 ± 16.8 g, $n = 19$) at immergence (Student's t-test: $t = 0.776$, $p = 0.443$) and did not differ between unsupplemented (332.1 ± 13.8 g, $n = 26$) and supplemented individuals (317 ± 16.1 g, $n = 12$; Student's t-test: $t = 0.712$, $p = 0.483$). Finally, the data set included different age classes (adults and subadults), but these were similarly distributed between years, sexes, and groups.

Body Temperature Recording

We recorded individual body temperature during winter at 90-min intervals using temperature data loggers (iButtons, DS1922L-F5#, range: −40 to +85°C, accuracy: ±0.5°C, Maxim Integrated Products International, Dublin, Ireland). Using iButtons to detect changes in body temperature is an approved method and was previously successfully applied in common hamsters (Siutz et al., 2016, 2017; Siutz and Millesi, 2017). Moreover, by using iButtons we could demonstrate that the time a hibernator spent inside its hibernaculum does not necessarily reflect the actual hibernation period (Siutz et al., 2016). The iButtons were coated in a mixture of resin (Elvax ethylene vinyl acetate, DuPont) and paraffin (potted mass: ∼4.5 g) and were gas-sterilized before implantation. Hamsters were trapped at our field site in the morning and immediately transported to a veterinary clinic (∼20 min) where the iButtons were implanted subcutaneously in the neck region (dorsal, between the scapulae) under isoflurane anesthesia. When the animals had recovered from anesthesia, they were returned to the field site (1–2 h after trapping) and released at their burrows, which were blocked in the meantime to prevent other hamsters from entering the burrows. The implantation was done several weeks before autumnal immergence to avoid potential surgery effects on the timing of hibernation. The iButtons were removed in spring using the same technique and was applied to all individuals used in the analyses. We were able to recover iButtons of 12 supplemented individuals (6 females, 6 males).

While regular, deep torpor bouts last for several days and body temperature drops close to ambient temperature (Wollnik and Schmidt, 1995; Wassmer and Wollnik, 1997; Wassmer, 2004; Siutz and Millesi, 2017; Siutz et al., 2017), distinctive shallow torpor bouts (STB) were, according to Wassmer and Wollnik (1997), defined as periods of body temperature between 30 and 20°C and a duration of ≤24 h (**Figure 1**). By combining both minimum body temperature and torpor bout duration, these two types of torpor can be well distinguished as no overlaps were detected (**Figure 2**). Shallow torpor bout duration ranged between 3 and 24 h, although most bouts ranged between 3 and 15 h (only 2 unsupplemented males showed one bout of 16 and 24 h, respectively; **Figure 2**). Previous studies documented another, intermediate type of torpor, which is also characterized by a duration shorter than 24 h, but body temperature drops below 20°C (Wassmer and Wollnik, 1997; Siutz and Millesi, 2017). In the presented study, this torpor type was expressed only in 3 out of 12 supplemented individuals (1 male with 1 bout and 2 females with 1 and 3 bouts, respectively), and in 3 out of 26 unsupplemented individuals (1 male and 2 females with 1 bout each). Due to this low number we excluded this torpor type from analyses. Shallow torpor was expressed by 75% of supplemented (9 out of 12; 5 males, 4 females) and 77 % of unsupplemented individuals (20 out of 26; 11 males, 9 females). Individuals which did not show STBs were evenly distributed among age and sex classes, and their immergence body mass was well within the range of those expressing shallow torpor.

We analyzed the number of STBs, the time spent in shallow torpor (total duration of all torpor bouts; calculated in hours, expressed as days), STB duration (beginning from the sampling interval when body temperature decreased below 30°C until it had reached 30°C again; calculated in hours, expressed as days), minimum body temperature during STB (lowest value of body temperature during a torpor bout), and mean body temperature during STB (beginning from the sampling interval when body temperature decreased below 30°C until it had reached 30°C again). Additionally, we analyzed the temporal (seasonal) pattern of shallow torpor occurrence, i.e., whether STBs were expressed before, during or after the actual hibernation period (defined as the period between the first and last deep torpor bout), but during the period without surface activity (from autumnal immergence to vernal emergence). For that, we compared the number of STBs during the pre-hibernation period (from autumnal immergence until entering the first deep torpor bout), the actual hibernation period (from onset of the first until termination of the last deep torpor bout), and the post-hibernation period (from termination of the last deep torpor bout, until vernal emergence).

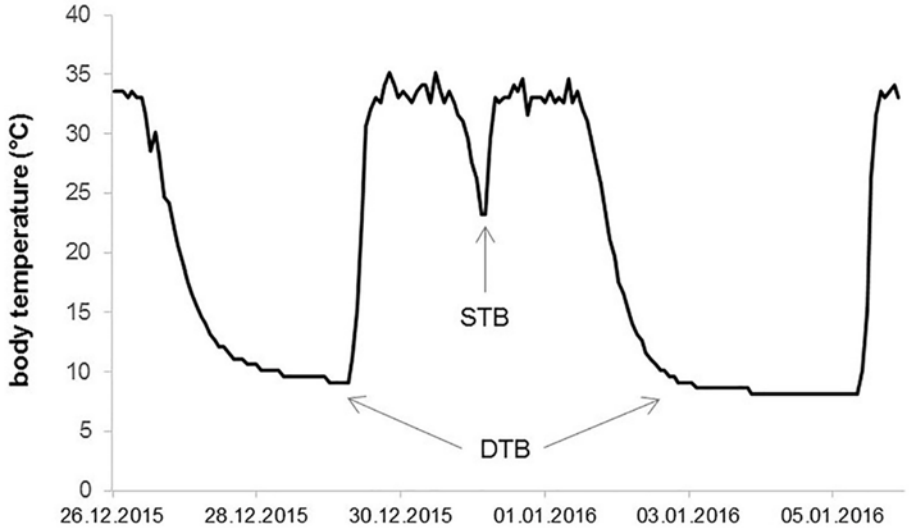

FIGURE 1 | Representative section of a free-ranging common hamster's body temperature pattern demonstrating a shallow torpor bout (STB) between two regular, deep torpor bouts (DTB).

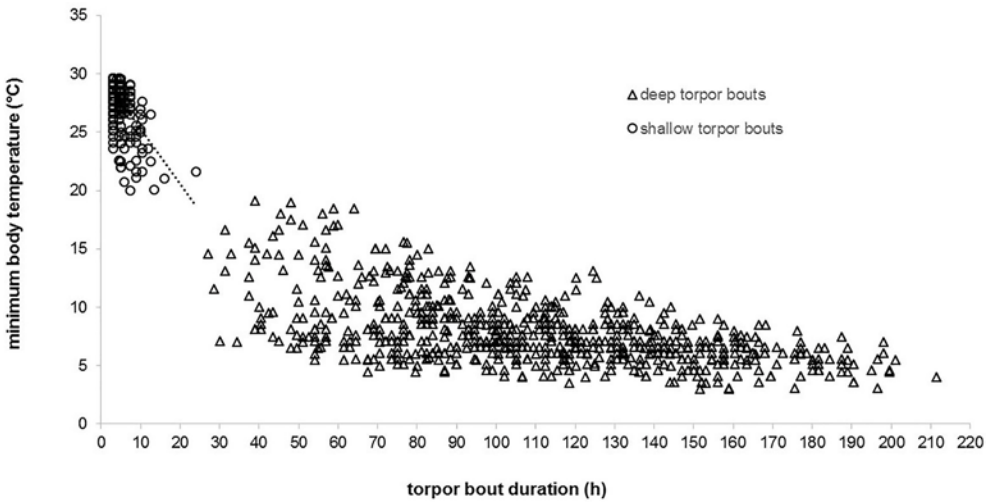

FIGURE 2 | Minimum body temperature and torpor bout duration of every shallow and deep torpor bout expressed by individuals sampled in this study. Shallow torpor bout regression line: $y = -0.4728x + 30.048$, $R^2 = 0.2978$.

Statistics

Statistical analyses were conducted in R (R Core Team, 2015) by using the packages "car" (Fox and Weisberg, 2011) for linear models, "nlme" (Pinheiro et al., 2015) for linear mixed models (LMEs), and "phia" (De Rosario-Martinez, 2015) for *post-hoc* analyses of interaction effects. The parameters number of STBs and time spent in shallow torpor were analyzed by linear models, including the parameters sex, group (supplemented/unsupplemented), and their interaction as predictor variables. In addition, we calculated the same model for these two parameters including individuals without shallow torpor expression. We applied LMEs for the parameters STB duration, minimum body temperature, and mean body temperature and included the parameters sex, group (supplemented/unsupplemented), and their interaction as fixed effects and individual identity as a random effect to correct for repeated measurements. The initial models for all response variables mentioned above included the parameters age (adult/subadult) and immergence body mass as predictor variables, but were removed from the final models as this contributed to AIC (Akaike's information criterion) reduction (**Table S1**). The parameter seasonal occurrence of STBs was analyzed by an LME with the parameters period (pre-hibernation/hibernation/post-hibernation) and group (supplemented/unsupplemented), as well as, their interaction as fixed effects and individual identity as a random effect.

We tested model residuals for normality by Shapiro–Wilk tests and for homoscedasticity using Levene-tests and visually controlled residual and fitted value plots. Statistics were obtained from ANOVA (Type III) tables and all *post-hoc* analyses were Bonferroni-corrected. To analyze relationships between the number of STBs and the duration of the pre-hibernation period, the number of deep torpor bouts, as well as, body mass change over winter, we applied Spearman rank correlations. Significance level was set at $p \leq 0.05$ and results are presented as means ± SE.

RESULTS

Effects of Food Supplementation

We found sex-specific effects of food supplementation on shallow torpor expression (**Table 1**). Supplemented males showed more STBs [$F_{(1,25)} = 11.640$, $p = 0.004$], although of shorter duration ($\chi^2 = 6.004$, $p = 0.029$), and spent more time in shallow torpor than unsupplemented ones [$F_{(1,25)} = 9.236$, $p = 0.011$; **Figure 3**]. Even when including individuals without STBs in the analyses, the number of STBs [$F_{(1,34)} = 7.729$, $p = 0.018$] and time spent in shallow torpor [$F_{(1,34)} = 5.574$, $p = 0.048$] in supplemented males significantly exceeded that of unsupplemented ones. Additionally, minimum and mean body temperature during STBs were higher in supplemented than unsupplemented males (minimum: $\chi^2 = 12.065$, $p = 0.001$; mean: $\chi^2 = 11.770$, $p = 0.001$; **Figure 4**). In contrast to males, shallow torpor expression did not differ between females with and without additional food ($p > 0.412$ in all cases; **Figures 3**, **4**).

TABLE 1 | ANOVA (Type III) table representing effects of sex and group (supplemented/unsupplemented) on shallow torpor expression, as well as, effects of period (before, during, after the actual hibernation period) and group (supplemented/unsupplemented) on shallow torpor occurrence in common hamsters.

Response variable	Predictor variable	DF	*F*-value	*p*-value
Number of STBs	Sex	1	4.825	0.038
	Group	1	0.084	0.775
	Sex × group	1	6.221	0.020
STB duration (h)	Sex	1	2.395	0.134
	Group	1	1.002	0.327
	Sex × group	1	0.799	0.380
Time spent in STB (d)	Sex	1	4.334	0.048
	Group	1	0.617	0.440
	Sex × group	1	6.835	0.015
Minimum T_b during STB (°C)	Sex	1	11.706	0.002
	Group	1	0.110	0.743
	Sex × group	1	4.347	0.048
Mean T_b during STB (°C)	Sex	1	12.095	0.002
	Group	1	0.255	0.618
	Sex × group	1	3.747	0.064
STB occurrence	Period	2	0.358	0.701
	Group	1	0.512	0.481
	Period × group	2	4.406	0.017

STB, shallow torpor bout, T_b, body temperature.

Irrespective of sex, supplemented individuals expressed more STBs during the pre-hibernation period (from autumnal immergence until entering the first deep torpor bout) than unsupplemented ones ($\chi^2 = 11.074$, $p = 0.003$), while no differences between the groups were found during the hibernation (from onset of the first until termination of the last deep torpor bout; $\chi^2 = 0.550$, $p > 0.999$) and post-hibernation period (from termination of the last deep torpor bout, until vernal emergence; $\chi^2 = 0.033$, $p > 0.999$; **Figure 5**). Supplemented hamsters showed more STBs during the pre- than during the post-hibernation period ($\chi^2 = 9.176$, $p = 0.015$; **Figure 5**), while the number of STBs did not differ between the other periods (pre-hibernation vs. hibernation: $\chi^2 = 5.277$, $p = 0.130$; hibernation vs. post-hibernation: $\chi^2 = 0.536$, $p > 0.999$; **Figure 5**). STB occurrence was similar in all three periods in unsupplemented individuals ($p > 0.999$ in all cases; **Figure 5**).

Sex Differences

We found no sex differences among supplemented individuals ($p > 0.184$ in all cases; **Figures 3**, **4**). Among unsupplemented hamsters, the number of STBs [$F_{(1,25)} = 4.825$, $p = 0.075$], STB duration ($\chi^2 = 2.412$, $p = 0.241$), and the time spent in shallow torpor [$F_{(1,25)} = 4.334$, $p = 0.096$] were similar between males and females (**Figure 3**). Unsupplemented females, however, expressed shallow torpor at higher minimum and mean body temperatures than unsupplemented males (minimum: $\chi^2 = 11.788$, $p = 0.001$; mean: $\chi^2 = 12.180$, $p = 0.001$; **Figure 4**).

Relationships Between Shallow and Deep Torpor Expression

In both unsupplemented and supplemented individuals, we found no relationships between the number of STBs and the duration of the pre-hibernation period (unsupplemented: $r_s = 0.161$, $p = 0.498$, $n = 20$; supplemented: $r_s = 0.469$, $p = 0.203$, $n = 9$), the number of deep torpor bouts (unsupplemented: $r_s = -0.320$, $p = 0.170$, $n = 20$; supplemented: $r_s = -0.601$, $p = 0.087$, $n = 9$), or body mass change over winter (unsupplemented: $r_s = -0.074$, $p = 0.778$, $n = 17$; supplemented: $r_s = 0.393$, $p = 0.295$, $n = 9$). Similar results were found in unsupplemented hamsters when including individuals without STB expression (STB number/pre-hibernation duration: $r_s = -0.048$, $p = 0.816$, $n = 26$; STB number/number of deep torpor bouts: $r_s = -0.057$, $p = 0.781$, $n = 26$; STB number/body mass change: $r_s = -0.041$, $p = 0.816$, $n = 21$). Among supplemented hamsters, however, the number of STBs significantly increased with the duration of the pre-hibernation period ($r_s = 0.678$, $p = 0.015$, $n = 12$), while no relationships were found between the number of STBs and the number of deep torpor bouts ($r_s = -0.508$, $p = 0.092$, $n = 12$) and body mass change over winter ($r_s = 0.356$, $p = 0.256$, $n = 12$).

DISCUSSION

Supplemented males showed much more STBs when provided with additional food before winter compared to unsupplemented males while no differences were found among females. Previous analyses of deep torpor expression in the same individuals

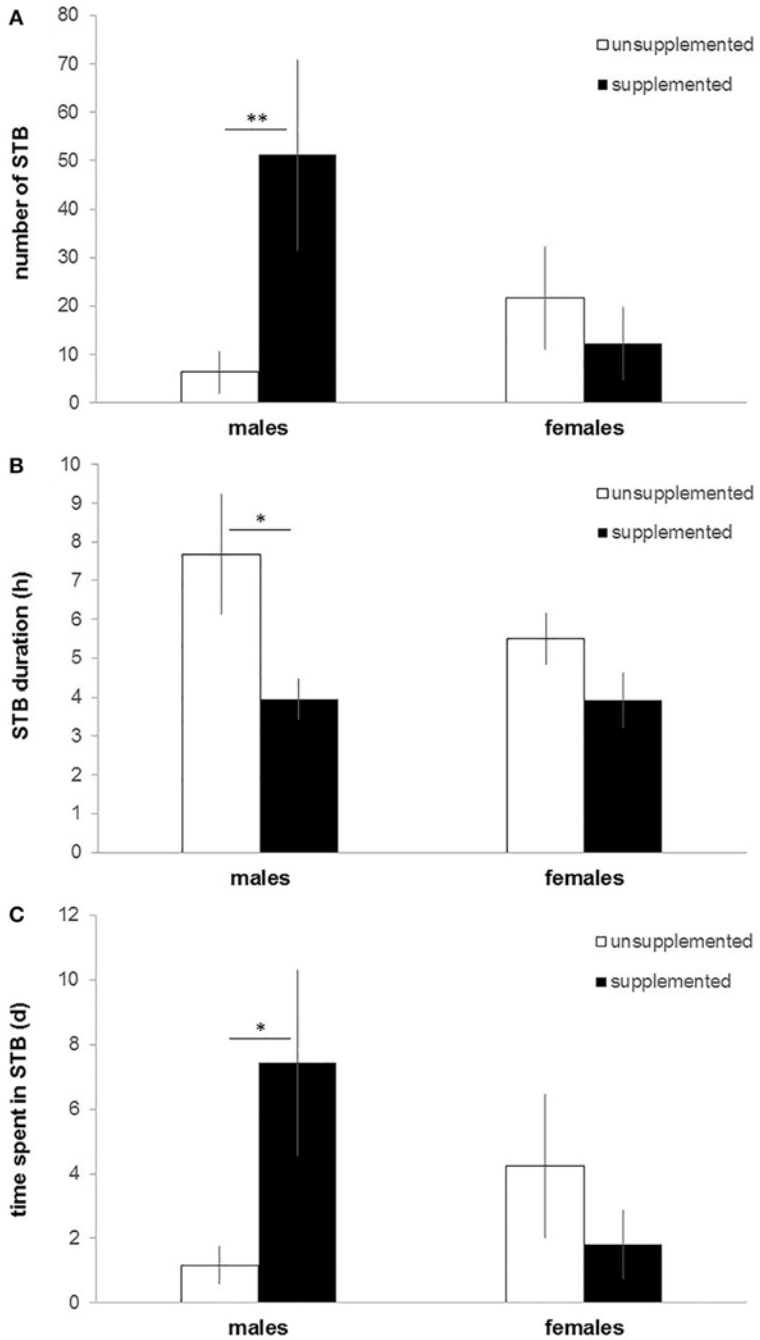

FIGURE 3 | (A) Number of shallow torpor bouts (STB), **(B)** mean duration of STBs, and **(C)** time spent in shallow torpor in supplemented and unsupplemented males and females. $^{*}p \leq 0.05$, $^{**}p \leq 0.01$.

revealed that supplemented males showed a substantially delayed hibernation onset and entered the first deep torpor bout between December 28 and January 30, demonstrating that (depending on the date of immergence) they remained euthermic inside their burrows for 6–13 weeks (Siutz et al., 2018). The results of the presented study showed that this extended euthermic period was frequently interrupted by STBs as this type of torpor was primarily expressed before the individuals entered the first deep torpor bout. Shallow torpor bouts prior to hibernation onset have been documented in some hibernating species and were traditionally thought to be preparatory to deep torpor (Strumwasser, 1958), but more recent studies demonstrated that shallow torpor is not necessary to enter hibernation (e.g., Sheriff et al., 2012) and can be expressed even year-round (Wilz and

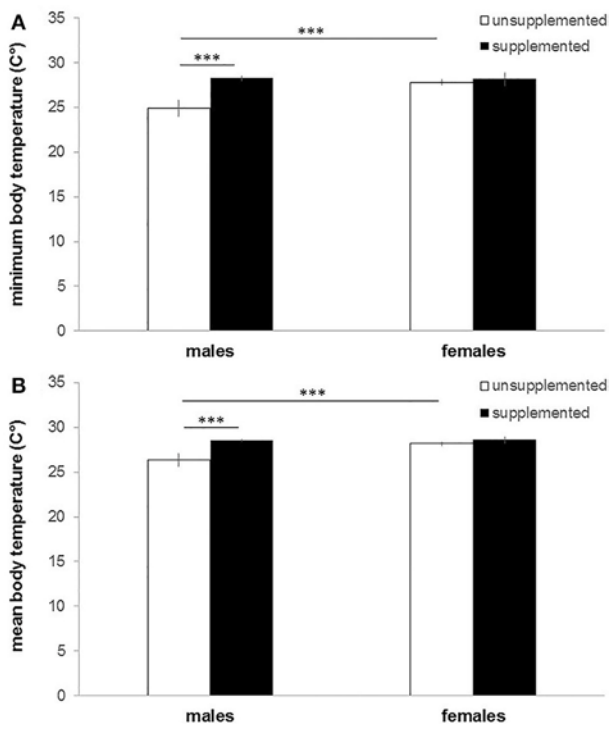

FIGURE 4 | (A) Minimum body temperature and **(B)** mean body temperature during STBs in supplemented and unsupplemented males and females. ***$p \leq 0.001$.

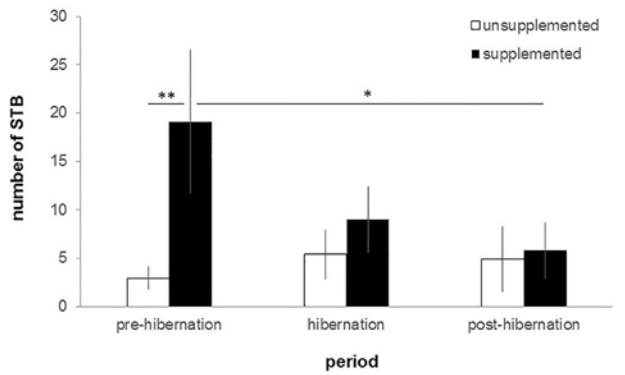

FIGURE 5 | Number of STBs during pre-hibernation (period from immergence into the hibernaculum until hibernation onset, i.e., date of the first deep torpor onset), hibernation (period between onset of the first and termination of the last deep torpor bout), and post-hibernation (period from hibernation end until emergence from the hibernaculum) in supplemented and unsupplemented males and females. *$p \leq 0.05$, **$p \leq 0.01$.

Heldmaier, 2000). Common hamsters, however, seem to differ from other hibernators as particularly the number of STBs but also the associated minimum body temperatures are relatively high. In the presented study, the number of STBs appeared to be positively related to the duration of the pre-hibernation period in supplemented hamsters. One explanation could be that individuals with lower body mass at autumnal immergence required more time to improve body condition before entering hibernation; however, we found no effects of immergence body mass on shallow torpor expression. This indicates that the longer the hamsters delayed hibernation onset, the more STBs are needed to keep the balance between energy expenditure and food availability. We found, however, no relationship between shallow and deep torpor expression. Hence, not only hamsters with a short hibernation period increased the use of shallow torpor, indicating that these are not alternative strategies, which has also been demonstrated under laboratory conditions (Siutz and Millesi, 2017).

The pronounced expression of shallow torpor during the pre-hibernation period in supplemented males rather indicates that the energy expenditure caused by delayed hibernation onset can be, at least partly, compensated. Shallow torpor also represents reduced energy expenditure, albeit not to the same extent as deep torpor bouts with lower metabolic rates reflected by lower body temperatures. It seems, therefore, unlikely that energy savings by shallow torpor even come close to that of hibernation and individuals had to complement this deficit with feeding. In contrast to fat-storing hibernators, which usually show a marked atrophy of the gastrointestinal tract during the hibernation period (Carey, 1990; Hume et al., 2002), food-storing hibernators were found to maintain their intestinal morphology during hibernation and continue to digest when torpid (Humphries et al., 2001; Weitten et al., 2013) and a recent study in common hamsters demonstrated a full maintenance of nutrient assimilation capacities (Weitten et al., 2016). Although individuals were regularly observed feeding during longer euthermic periods between deep torpor bouts under laboratory conditions (Siutz C., personal observation), this could be rather disadvantageous for digestive processes during normal arousals which usually only last for a few hours. The better option, therefore, might be to consume hoarded food mainly during the pre-hibernation period and additionally make use of shallow torpor expression, which would also explain the shorter duration and higher body temperatures of STBs as this might be more beneficial for digestive processes. On the other hand, the higher body temperatures of shallow torpor in supplemented males might simply have resulted from shorter durations of these bouts. It seems, however, unlikely that these findings resulted from inaccurate measurements due to the relatively long sampling interval because only a few individuals showed some very short torpor bouts, but these were evenly distributed between the groups.

Supplemented males emerged from their hibernacula in spring with higher body mass than unsupplemented ones (Siutz et al., 2018). We found no direct relationship between the number of STBs and body mass change over winter, however, we were unable to measure body mass immediately before the onset of hibernation. The use of shallow torpor combined with food intake during the pre-hibernation period most likely resulted in improved body condition compared to autumnal immergence already prior to hibernation onset. Simultaneously, delaying hibernation probably reduced potential costs associated with

torpor as negative effects (e.g., immune suppression, oxidative stress, impaired memory functions) might primarily be related to the low body temperature during deep torpor bouts (Ruf and Geiser, 2015).

With progressing winter and declining ambient temperatures, however, supplemented males hibernated (Siutz et al., 2018) and thus, reduced the number of STBs. During the coldest winter months (January/February; as reflected in minimum body temperatures during deep torpor), expression of deep torpor appeared to be more appropriate because energy savings by shallow torpor might not be sufficient during such periods. This is also supported by previous findings demonstrating that free-ranging hamsters always entered deep torpor during winter (Siutz et al., 2016, 2018), while individuals kept under laboratory or semi-natural conditions frequently showed a combination of shallow and deep torpor or even abandoned deep torpor and exclusively expressed shallow torpor (Wassmer and Wollnik, 1997; Wassmer, 2004). During the post-hibernation period, the extent of shallow torpor expression was similar to the hibernation period and significantly reduced compared to the pre-hibernation period. As hibernating mammals activate their reproductive system and males complete spermatogenesis before vernal emergence (Michener, 1983; Barnes et al., 1986; Barnes, 1996; Millesi et al., 1998), the expression of shallow torpor might constrain these processes.

Among female hamsters, shallow torpor expression did not differ between supplemented and unsupplemented individuals. This is not surprising as they also showed similar timing and duration of hibernation (Siutz et al., 2016). Both supplemented and unsupplemented females remained euthermic inside the hibernacula for several weeks before entering hibernation, although not to the same extent as supplemented males, and hence started to hibernate later than unsupplemented males (Siutz et al., 2016, 2018). One would, therefore, have expected a difference in the use of shallow torpor compared to unsupplemented males, which was only partly supported by our results. Although a marginal trend toward unsupplemented females expressing more STBs than unsupplemented males was observable, the time spent in shallow torpor was similar between the sexes. The reason for this remains unknown as we have no information on the actual quantity and quality of hoarded food in free-ranging hamsters. With our experimental design we aimed at enlarging food stores and ensuring that at least the provided external energy reserves are available (Siutz et al., 2018). The fact, however, that only males intensified shallow torpor in response to food supplements could indicate that mechanisms mediating food intake and/or shallow torpor expression might differ between males and females. Further studies, particularly including measurements of metabolic rate, are required to shed light on these sex-specific patterns of torpor expression.

Finally, the quality of energy reserves has been shown to affect torpor expression. In fat-storing hibernators, high concentrations of polyunsaturated fatty acids (PUFAs), in particular linoleic acid, in diets or white adipose tissue were found to enhance torpor expression (Geiser and Kenagy, 1987; Frank, 1992; Ruf and Arnold, 2008; Giroud et al., 2013; Arnold et al., 2015), while in the food-storing eastern chipmunk (*Tamias striatus*) high dietary PUFAs resulted in torpor reduction (Munro et al., 2005). It seems, however, unlikely that an increased PUFA content *per se* accounted for the results of the presented study. Although sunflower seeds are rich in PUFAs, particularly linoleic acid, the fatty acid composition is similar to the natural diet of common hamsters at our study site. Given that beechnuts and especially black walnuts have a high PUFA (and linoleic acid) content (USDA, 2016), it can be assumed that also unsupplemented hamsters had access to a high-PUFA diet during winter. And again, we provided both males and females with sunflower seeds, but only males increased shallow torpor expression.

In conclusion, our results underline the highly flexible use of heterothermy in common hamsters, especially in males. Such flexibility could be particularly adaptive under unpredictable environmental conditions (Canale and Henry, 2010). It is likely that the frequent use of shallow torpor, in combination with hibernation during the coldest periods, constitutes an optimal strategy for males when food stores, particularly of high energetic value, are available as it allows sufficient food intake facilitating body conditions in the burrow while simultaneously saving energy.

DATA AVAILABILITY

The raw data supporting the conclusions of this manuscript will be made available by the authors, without undue reservation, to any qualified researcher.

AUTHOR CONTRIBUTIONS

CS collected field data, carried out the statistical analyses, and wrote the manuscript. VA collected field data, participated in the analyses, and reviewed drafts of the manuscript. EM conceived and designed the study, acquired funding of the study, and reviewed drafts of the manuscript. All authors read and approved the final manuscript.

FUNDING

This study was funded by the Austrian Science Fund (FWF, Project: 24280-B20).

ACKNOWLEDGMENTS

We would like to thank M. Valent and A. Niebauer for their help in field work.

SUPPLEMENTARY MATERIAL

The Supplementary Material for this article can be found online at: https://www.frontiersin.org/articles/10.3389/fevo.2018.00190/full#supplementary-material

REFERENCES

Arnold, W., Giroud, S., Valencak, T. G., and Ruf, T. (2015). Ecophysiology of omega fatty acids: a lid for every jar. *Physiology* 30, 232–240. doi: 10.1152/physiol.00047.2014

Barnes, B. M. (1996). "Relationships between hibernation and reproduction in male ground squirrels," in *Adaptations to the Cold: 10th International Hibernation Symposium,* eds F. Geiser, A. J. Hulbert, and S. C. Nicol (Armidale, NSW: University of New England Press), 71–80.

Barnes, B. M., Kretzmann, M., Licht, P., and Zucker, I. (1986). The influence of hibernation on testis growth and spermatogenesis in the golden-mantled ground squirrel, *Spermophilus lateralis*. *Biol. Reprod.* 35, 1289–1297. doi: 10.1095/biolreprod35.5.1289

Buck, C. L., and Barnes, B. M. (2000). Effects of ambient temperature on metabolic rate, respiratory quotient, and torpor in an arctic hibernator. *Am. J. Physiol. Regul. Integr. Comp. Physiol.* 279, R255–R262. doi: 10.1152/ajpregu.2000.279.1.R255

Canale, C. I., and Henry, P.-Y. (2010). Adaptive phenotypic plasticity and resilience of vertebrates to increasing climatic unpredictability. *Clim. Res.* 43, 135–147. doi: 10.3354/cr00897

Carey, H. V. (1990). Seasonal changes in mucosal structure and function in ground squirrel intestine. *Am. J. Physiol. Regul. Integr. Comp. Physiol.* 259, R385–R392. doi: 10.1152/ajpregu.1990.259.2.R385

De Rosario-Martinez, H. (2015). *phia: Post-Hoc Interaction Analysis*. R package version 0.2-1. Available online at: https://CRAN.R-project.org/package=phia

Eibl-Eibesfeldt, I. (1953). Zur ethologie des hamsters (*Cricetus cricetus* L.). *Z. Tierpsychol.* 10, 204–254.

Fox, J., and Weisberg, S. (2011). *An R Companion to Applied Regression, 2nd Edn*. Thousand Oaks, CA: Sage. Available online at: http://socserv.socsci.mcmaster.ca/jfox/Books/Companion

Franceschini, C., Siutz, C., Palme, R., and Millesi, E. (2007). Seasonal changes in cortisol and progesterone secretion in Common hamsters. *Gen. Comp. Endocrinol.* 152, 14–21. doi: 10.1016/j.ygcen.2007.02.008

Franceschini-Zink, C., and Millesi, E. (2008a). "Population development and life expectancy in Common hamsters," in *The Common Hamster (Cricetus cricetus): Perspectives on an Endangered Species. Biosystematics and Ecology Series,* eds E. Millesi, H. Winkler, and R. Hengsberger (Vienna: Austrian Academy of Science Press), 45–59.

Franceschini-Zink, C., and Millesi, E. (2008b). Reproductive performance in female common hamsters. *Zoology* 111, 76–83. doi: 10.1016/j.zool.2007.05.001

Frank, C. L. (1992). The influence of dietary fatty acids on hibernation by golden-mantled ground squirrels (*Spermophilus lateralis*). *Physiol. Zool.* 65, 906–920. doi: 10.1086/physzool.65.5.30158549

Geiser, F. (1988). Reduction of metabolism during hibernation and daily torpor in mammals and birds: temperature effect or physiological inhibition? *J. Comp. Physiol. B Biochem. Syst. Environ. Physiol.* 158, 25–37. doi: 10.1007/BF00692726

Geiser, F. (2004). Metabolic rate and body temperature reduction during hibernation and daily torpor. *Annu. Rev. Physiol.* 66, 239–274. doi: 10.1146/annurev.physiol.66.032102.115105

Geiser, F., and Kenagy, G. J. (1987). Polyunsaturated lipid diet lengthens torpor and reduces body temperature in a hibernator. *Am. J. Physiol. Regul. Integr. Comp. Physiol.* 252, R897–R901. doi: 10.1152/ajpregu.1987.252.5.R897

Geiser, F., and Ruf, T. (1995). Hibernation versus daily torpor in mammals and birds: physiological variables and classification of torpor patterns. *Physiol. Zool.* 68, 935–966. doi: 10.1086/physzool.68.6.30163788

Giroud, S., Frare, C., Strijkstra, A., Boerema, A., Arnold, W., and Ruf, T. (2013). Membrane phospholipid fatty acid composition regulates cardiac SERCA activity in a hibernator, the Syrian hamster (*Mesocricetus auratus*). *PLoS ONE* 8:e63111. doi: 10.1371/journal.pone.0063111

Heldmaier, G., Ortmann, S., and Elvert, R. (2004). Natural hypometabolism during hibernation and daily torpor in mammals. *Respir. Physiol. Neurobiol.* 141, 317–329. doi: 10.1016/j.resp.2004.03.014

Heldmaier, G., and Ruf, T. (1992). Body temperature and metabolic rate during natural hypothermia in endotherms. *J. Comp. Physiol. B,. Biochem. Syst. Environ. Physiol.* 162, 696–706. doi: 10.1007/BF00301619

Hume, I., Beiglböck, C., Ruf, T., Frey-Roos, F., Bruns, U., and Arnold, W. (2002). Seasonal changes in morphology and function of the gastrointestinal tract of free-living alpine marmots (*Marmota marmota*). *J. Comp. Physiol. B,. Biochem. Syst. Environ. Physiol.* 172, 197–207. doi: 10.1007/s00360-001-0240-1

Humphries, M. M., Thomas, D. W., and Kramer, D. L. (2001). Torpor and digestion in food-storing hibernators. *Physiol. Biochem. Zool.* 74, 283–292. doi: 10.1086/319659

Michener, G. R. (1983). Spring emergence schedules and vernal behavior of Richardson's ground squirrels: why do males emerge from hibernation before females? *Behav. Ecol. Sociobiol.* 14, 29–38. doi: 10.1007/BF00366653

Millesi, E., Huber, S., Dittami, J., Hoffmann, I., and Daan, S. (1998). Parameters of mating effort and success in male European ground squirrels, *Spermophilus citellus*. *Ethology* 104, 298–313. doi: 10.1111/j.1439-0310.1998.tb00070.x

Munro, D., Thomas, D. W., and Humphries, M. M. (2005). Torpor patterns of hibernating eastern chipmunks *Tamias striatus* vary in response to the size and fatty acid composition of food hoards. *J. Anim. Ecol.* 74, 692–700. doi: 10.1111/j.1365-2656.2005.00968.x

Niethammer, J. (1982). "*Cricetus cricetus* (Linnaeus, 1758) - Hamster (Feldhamster)," in *Handbuch der Säugetiere Europas, Bd. 2/I.,* eds J. Niethammer and F. Krapp (Wiesbaden: Akademische Verlagsgesellschaft Wiesbaden), 7–28.

Pinheiro, J., Bates, D., DebRoy, S., Sarkar, D., and Team, R. C. (2015). *nlme: Linear and Nonlinear Mixed Effects Models*. R package version 3.1-122. Available online at: https://CRAN.R-project.org/package=nlme

R Core Team (2015). *R: A Language and Environment for Statistical Computing*. R Foundation for Statistical Computing, Vienna. Available online at: http://www.R-project.org

Roswag, A., Becker, N. I., Millesi, E., Otto, M. S., Ruoss, S., Sander, M., et al. (2018). Stable isotope analysis as a minimal-invasive method for dietary studies on the highly endangered Common hamster (*Cricetus cricetus*). *Mammalia* 82, 600–606. doi: 10.1515/mammalia-2017-0097

Ruf, T., and Arnold, W. (2008). Effects of polyunsaturated fatty acids on hibernation and torpor: a review and hypothesis. *Am. J. Physiol. Regul. Integr. Comp. Physiol.* 294, R1044–R1052. doi: 10.1152/ajpregu.00688.2007

Ruf, T., and Geiser, F. (2015). Daily torpor and hibernation in birds and mammals. *Biol. Rev.* 90, 891–926. doi: 10.1111/brv.12137

Sheriff, M. J., Williams, C. T., Kenagy, G., Buck, C. L., and Barnes, B. M. (2012). Thermoregulatory changes anticipate hibernation onset by 45 days: data from free-living arctic ground squirrels. *J. Comp. Physiol. B Biochem. Syst. Environ. Physiol.* 182, 841–847. doi: 10.1007/s00360-012-0661-z

Siutz, C., Franceschini, C., and Millesi, E. (2016). Sex and age differences in hibernation patterns of common hamsters: adult females hibernate for shorter periods than males. *J. Comp. Physiol. B Biochem. Syst. Environ. Physiol.* 186, 801–811. doi: 10.1007/s00360-016-0995-z

Siutz, C., and Millesi, E. (2017). Torpor patterns in common hamsters with and without access to food stores. *J. Comp. Physiol. B,. Biochem. Syst. Environ. Physiol.* 187, 881–888. doi: 10.1007/s00360-017-1093-6

Siutz, C., Nemeth, M., Wagner, K.-H., Quint, R., Ruf, T., and Millesi, E. (2017). Effects of food store quality on hibernation performance in common hamsters. *PLoS ONE* 12:e0185913. doi: 10.1371/journal.pone.0185913

Siutz, C., Pluch, M., Ruf, T., and Millesi, E. (2012). "Sex differences in foraging behaviour, body fat, and hibernation patterns of free-ranging Common hamsters," in *Living in a Seasonal World: Thermoregulatory and Metabolic Adaptations,* eds T. Ruf, C. Bieber, W. Arnold, and E. Millesi (Heidelberg: Springer), 155–165. doi: 10.1007/978-3-642-28678-0_14

Siutz, C., Valent, M., Ammann, V., Niebauer, A., and Millesi, E. (2018). Sex-specific effects of food supplementation on hibernation performance and reproductive timing in free-ranging common hamsters. *Sci. Rep.* 8:13082. doi: 10.1038/s41598-018-31520-4

Strumwasser, F. (1958). Factors in the pattern, timing and predictability of hibernation in the squirrel, *Citellus beecheyi*. *Am. J. Physiol.* 196, 8–14. doi: 10.1152/ajplegacy.1958.196.1.8

USDA (2016). *US Department of Agriculture, Agricultural Research Service, Nutrient Data Laboratory*. USDA National Nutrient Database for Standard Reference, Release 28. Version Current: September 2015, slightly revised May 2016.

Wassmer, T. (1998). *Die Zeitliche Organisation des Winterschlafs Beim Europäischen Feldhamster (Cricetus cricetus L.)*. München: Herbert Utz Verlag.

Wassmer, T. (2004). Body temperature and above-ground patterns during hibernation in European hamsters (*Cricetus cricetus* L.). *J. Zool.* 262, 281–288. doi: 10.1017/S0952836903004643

Wassmer, T., and Wollnik, F. (1997). Timing of torpor bouts during hibernation in European hamsters (*Cricetus cricetus* L.). *J. Comp. Physiol. B Biochem. Syst. Environ. Physiol.* 167, 270–279. doi: 10.1007/s003600050074

Weinhold, U., and Kayser, A. (2006). *Der Feldhamster*. Hohenwarsleben: Westarp Wisenschaften.

Weitten, M., Oudart, H., and Habold, C. (2016). Maintenance of a fully functional digestive system during hibernation in the European hamster, a food-storing hibernator. *Comp. Biochem. Physiol. Part A Mol. Integr. Physiol.* 193, 45–51. doi: 10.1016/j.cbpa.2016.01.006

Weitten, M., Robin, J.-P., Oudart, H., Pévet, P., and Habold, C. (2013). Hormonal changes and energy substrate availability during the hibernation cycle of Syrian hamsters. *Horm. Behav.* 64, 611–617. doi: 10.1016/j.yhbeh.2013.08.015

Wilz, M., and Heldmaier, G. (2000). Comparison of hibernation, estivation and daily torpor in the edible dormouse, *Glis glis*. *J. Comp. Physiol. B Biochem. Syst. Environ. Physiol.* 170, 511–521. doi: 10.1007/s003600000129

Wollnik, F., and Schmidt, B. (1995). Seasonal and daily rhythms of body temperature in the European hamster (*Cricetus cricetus*) under semi-natural conditions. *J. Comp. Physiol. B Biochem. Syst. Environ. Physiol.* 165, 171–182. doi: 10.1007/BF00260808

Conflict of Interest Statement: The authors declare that the research was conducted in the absence of any commercial or financial relationships that could be construed as a potential conflict of interest.

Copyright © 2018 Siutz, Ammann and Millesi. This is an open-access article distributed under the terms of the Creative Commons Attribution License (CC BY). The use, distribution or reproduction in other forums is permitted, provided the original author(s) and the copyright owner(s) are credited and that the original publication in this journal is cited, in accordance with accepted academic practice. No use, distribution or reproduction is permitted which does not comply with these terms.

frontiers in Ecology and Evolution

ORIGINAL RESEARCH
published: 28 November 2018
doi: 10.3389/fevo.2018.00200

Movement and Biosonar Behavior During Prey Encounters Indicate That Male Sperm Whales Switch Foraging Strategy With Depth

Saana Isojunno and Patrick J. O. Miller*

Sea Mammal Research Unit, School of Biology, Scottish Oceans Institute, University of St Andrews, St Andrews, United Kingdom

Despite their apex predator role, relatively little is known about the foraging strategies that deep-diving marine mammals employ to target prey resources available at different depths with different costs of access. Using hidden Markov model (HMM) analysis of behavioral time series, we aimed to quantify the potential for multiple foraging strategies during 3,150 terminal echolocation ("buzz") phases of 28 tagged male sperm whales in Northern Norway. Movement metrics included in the HMM reflected the predator's pursuit path (vertical velocity, pitch, and heading variance) and locomotion effort (overall dynamic body acceleration ODBA). We found a highly depth-dependent distribution of four buzz types: "Shallow-sparse" (median 161 m) had the highest inter-buzz intervals, "Mid-active" (372 m) were the longest duration buzzes (median 21 s) and the most active in terms of pitch variance, heading variance and ODBA, while "Deep" and "Deep descent" buzzes (1,130–1,180 m) were the shortest in duration (∼7 s) and least energetic in maneuvers. Regression models for acoustic metrics with both buzz type and depth as explanatory variables revealed that maximum click rate in a buzz had a strong negative linear relationship with ambient pressure (1.2 Hz every 10 atm or 100 m). After accounting for the effects of pressure, buzz click rates were significantly higher during "Mid-active" than other types of buzzes. Within buzzes, apparent click output level (AOL, off-axis level received by the tag, dB re 1 μPa) correlated linearly with $\log_{10}$(inter-click-interval), as expected by acoustic gain control and increasing sensory volume with increasing click rate. These results indicate that while higher acoustic sampling rates were used to track more mobile prey, buzz clicks were produced more sparingly at high ambient pressures where the number of pneumatically produced clicks may be limited before air must be recycled, and where prey seem easier to subdue. The diverse prey base indicated by this study support the feeding requirements of large male sperm whales, and that high feeding rates of more densely distributed and perhaps more predictable resources (e.g., immobile life stages of female *Gonatus fabricii*) likely maintain preference for the deepest foraging habitats (> 1 km) of this generalist predator.

Keywords: buzz, Dtag, hidden Markov model, sound production, pressure effects, prey switching

OPEN ACCESS

Edited by:
Frants Havmand Jensen, Aarhus Institute of Advanced Studies, Denmark

Reviewed by:
Matthew Bowers, Colorado State University, United States
Daniel Paul Costa, University of California, Santa Cruz, United States

****Correspondence:***
Saana Isojunno
si66@st-andrews.ac.uk

Specialty section:
This article was submitted to Behavioral and Evolutionary Ecology, a section of the journal Frontiers in Ecology and Evolution

Received: *31 July 2018*
Accepted: *09 November 2018*
Published: *28 November 2018*

Citation:
Isojunno S and Miller PJO (2018) Movement and Biosonar Behavior During Prey Encounters Indicate That Male Sperm Whales Switch Foraging Strategy With Depth. Front. Ecol. Evol. 6:200. doi: 10.3389/fevo.2018.00200

INTRODUCTION

Deep-diving marine mammals such as sperm whales (*Physeter macrocephalus)* are central-place foragers that need to balance energetic benefits of foraging at depth with the time, energetic, and physiological costs of diving to depth (Houston and Carbone, 1992). Toothed whales use echolocation clicks to search for and capture prey, which can be recorded using animal-attached acoustic recording data loggers (DTAG, Johnson and Tyack, 2003). Similar to bats, the rate and acoustic features of echolocation pulses, or "clicks" in toothed whales, indicate whether the forager is searching for or attempting to capture prey during the terminal "buzz" phase (Johnson et al., 2004; Miller et al., 2004a; Madsen et al., 2013). Thus, acoustic recording of echolocation provides measures of sensory focus and volumes (Wisniewska et al., 2012) in the context of dive behavior and ecology. Characteristics of their ecological niche can be relevant across deep-diving marine mammals that may play key role as top predators in marine food webs (Heithaus et al., 2008) and sentinel species in marine conservation (Sergio et al., 2008). By integrating both movement and acoustic data (Miller et al., 2004a), it is possible to make increasingly detailed inferences about the distribution and maneuverability, and subsequently the energetic value, of targeted prey (Madsen et al., 2005; Johnson et al., 2008; Arranz et al., 2011).

Cephalopods are an important source of biomass in marine food webs, and their availability at depth has been proposed to be one of the major drivers for the evolution of a larger body size and more extreme diving capabilities in a range of squid-eating marine mammals, such as elephant seals, beaked whales, and sperm whales (Clarke, 1996; Klages, 1996; Whitehead et al., 2003; Slater et al., 2010). Cephalopods provide a diverse food source ranging from muscular and protein rich cephalopods to neutrally buoyant ammoniac squids that are lower in energy content (Kawakami, 1980; Clarke, 1996; Santos et al., 1999, 2002). Some species of cephalopod may be relatively easy to catch as they quickly become exhausted after fast swimming (Clarke, 1996) and they may be targeted at more vulnerable stages of vertical migration (e.g., jumbo squid in Gulf of California, Davis et al., 2007) or ontogenetic stage (Simon et al., 2003). As with any generalist predator, marine mammals exploiting such a diverse resource must therefore balance the energetic value with the cost of finding and handling different prey types.

Sperm whales target mesopelagic and bathypelagic prey and can spend >70% of their time foraging (Watwood et al., 2006; Guerra et al., 2017). While cephalopods form the main component of the sperm whale diet, fish can be important regionally, such as in the high-latitude foraging grounds in in New Zealand (Gaskin and Cawthorn, 1967) and North Atlantic (Martin and Clarke, 1986). These high-latitude foraging grounds are frequented by male sperm whales, while female sperm whales remain at lower latitudes (Whitehead, 2003; Teloni et al., 2008). Despite a substantial biomass in the epipelagic zone, male sperm whales also target deeper prey in the high-latitude foraging grounds (Teloni et al., 2008; Fais et al., 2015). Teloni et al. (2008) showed that sperm whales produced more frequent and shorter buzzes during deep (>800 m) dives compared to shallow dives, indicating more sedentary and densely distributed prey at greater depths. Thus, high-latitude sperm whales provide a case study in central-place foraging where the benefit of more accessible prey at shallower depths might weigh against an elevated cost of prey handling compared to food resources available at greater depths—with larger transport costs and recovery times after prolonged diving.

Different prey types imply different challenges to the sensory-motor system during prey capture. Echolocation requires a tight coupling of both sensory and motor systems, and echolocation tactics can vary depending on a behavioral mode (e.g., between searching and pursuit of prey) and with environmental parameters (e.g., clutter and ambient noise conditions) (Schnitzler et al., 2003; Wisniewska et al., 2012; Madsen and Surlykke, 2013). Relatively fast click rates, or inversely, short inter-click-intervals (ICI), coupled with lower source levels during terminal echolocation, or "buzz," appear to be a common feature in all studied odontocetes, and indeed most echolocating bat species, highlighting a key function in acoustic gaze control (Madsen and Surlykke, 2013). Reduced source level and increased sampling rates effectively increase the temporal resolution (data rate) to track likely evasive prey while reducing the complexity of the auditory scene and echo ambiguity (Madsen and Surlykke, 2013). Wisniewska et al. (2012) suggest that during buzzing, porpoises reduce their depth of gaze to a single target while engaging in a more reactive mode of sensory-motor operation, i.e., sensory volume is reduced relative to the motor (or stopping) volume (Wisniewska et al., 2012).

As well as the sensory-motor challenge of different prey types, sperm whale biosonar performance may be challenged by the increased hydrostatic pressure at depth (Madsen P. T. et al., 2002). Sperm whale sound production is thought to be pneumatically driven (Ridgway and Carder, 2001; Huggenberger et al., 2014), and the limited volume of gas available to a breath holding deep diver indicates that gas must be recycled (Madsen P. T. et al., 2002). Several observations of pauses in between bouts of usual clicks (also called "regular clicks" in sperm whales) and following buzzes (e.g., Wahlberg, 2002) suggest that pauses function as air-recycling events. Thus, changes in gas volume or density may influence aspects of echolocation output. The number of usual clicks produced in between recycling events (i.e., usual click train duration) has been shown to decrease with depth, consistent with gas volumes being reduced by hydrostatic pressure (Wahlberg, 2002). However, sperm whale usual click levels and frequency content appear to be relatively unaffected by pressure (Madsen P. T. et al., 2002). Nevertheless, if a certain gas volume is required to produce each click, reduced gas volume under pressure could potentially limit click and buzz production.

We investigated these ecophysiological and biomechanical trade-offs using movement and acoustic data from terminal echolocation buzzes of 28 sperm whales outfitted with data loggers near Lofoten Islands, Norway. We set out to (1) test whether the tagged whales engaged in a generalist strategy, with individuals switching between different movement tactics to capture prey, and if so, (2) test whether the movement tactics varied by depth, indicating diversity in targeted prey between depth layers, and (3) quantify the extent to which acoustic

behavior during prey capture attempts is influenced by depth (hydrostatic pressure) vs. the movement tactics (indicating prey mobility and maneuverability).

To address these objectives, we first used hidden Markov models (HMMs) to classify buzzes according to their inter-buzz-intervals and movement behavior that were *a-priori* expected to be related to characteristics of the targeted prey resources rather than hydrostatic pressure (e.g., buzz duration was therefore excluded from the HMM). We then then tested whether the buzz classification (∼targeted prey) was random with respect to depth in a second analysis step. For the third objective, we modeled echolocation performance during buzzing (maximum click rate and AOL in a buzz) with both hydrostatic pressure and the buzz movement types (∼targeted prey) as explanatory variables. We expected less air to be available for sound production at depth, and thus a reduced number of clicks within a click sequence (i.e., buzz without an air-recycling pause). To test if click rates within buzzes indicate sensory volume, we also tested whether sperm whales simultaneously adjusted click rate and click output levels as expected based upon gain control to target prey at a specific range.

METHODS

Data Collection

DTAG acoustic and movement data were collected aboard 28 tagged sperm whales near Lofoten, Norway in 2005, 2008–2010, and 2016–2017 during the summer months (May–July). The field protocol included (1) tagging the whale from a small rigid-hulled inflatable boat (RHIB) using a cantilevered pole (12–15 m) attached to the bow of the RHIB, (2) re-approaching the tagged whale for photo-identification, (3) visual and VHF tracking of the tagged whale, and (4) recovery of the released tag (after 6–23 h of recording). The 2008–2010 and 2016–2017 deployments were subject to controlled exposure experiments within the 3S (Sea mammals, Sonar, Safety) research project (Miller et al., 2011). Data during all of the experimental exposures, including sound exposures as well as no-sonar control approaches were excluded from this analysis which aimed to focus on baseline behavior. Data were also excluded from the beginning of the tag record until the tag boat no longer re-approached the whale for fluke photographs used in individual identification.

Animal experiments were carried out under permits issued by the Norwegian Animal Research Authority (Permit No. 2004/20607 and S-2007/61201), in compliance with ethical use of animals in experimentation. The research protocol was approved by the University of St Andrews Animal Welfare and Ethics Committee and the Woods Hole Oceanographic Institutional Animal Care and Use Committee. The sound exposure experiments were designed and conducted within the 3S (Sea mammals, Sonar, Safety) research project (Miller et al., 2011).

Depth, pitch and roll data were derived following Johnson and Tyack (2003) and decimated at 5 Hz. Both DTAG version 2 (2005–2010) and version 3 (2016–2017) was used. The hydrophones had a sensitivity between −188 and −190 dB re V/μPa, depending on the tag.

Acoustic Data Processing

DTAG audio recordings were monitored both aurally and visually using spectrograms in Adobe Audition (hereafter termed "auditing"), and the start and end time of regular and buzz click trains were marked. Buzz start time was defined as a change in amplitude and/or spectral content of clicks before a fast run (click rate >5 Hz). Buzz end time was defined as the start of a pause before the next usual click train, exceeding the ICI of the subsequent usual (i.e., regular) clicks, or start of a pause before the next surfacing. In the absence of such a clear pause, the end time of a buzz was identified as the last irregularly spaced buzz clicks (this pattern was also typical of buzzes with a clear pause). For analysis, buzzes were filtered by maximum repetition rate (section Data Filtering below).

Individual clicks within buzzes were detected automatically using a custom-written program in Matlab. To improve signal-to-noise ratio (SNR) for click detection, wave files were first band-pass filtered between 700 Hz and 40 kHz using a 256 point finite-impulse filter. Filtered energy was smoothed (Hanning window 1 ms), and click start and end times were detected based upon thresholds of the median and spread of the smoothed energy.

The received level of buzz clicks arriving on the animal attached recorder (DTAG) was used as a proxy for the relative acoustic output level or "apparent output level" (AOL, Madsen et al., 2005). DTAG attachment location will vary between individual attachments and potentially also within a tag attachment (Johnson et al., 2009) if the tag slides over the animal's body. We did not attempt to compare absolute AOLs across different tag deployments. Instead, we aimed to assess relative changes in AOL within each buzz. This approach assumes that directionality patterns of click transmissions are not correlated with AOL.

In order to measure AOL, a lower order filtering (3rd order Butterworth bandpass between 1 and 40 kHz) of the raw signal was used to reduce effects of flow noise and click rate. Peak-to-peak sound pressure levels (AOL_{pp}) and sound exposure levels (AOL_E) were measured for each click following Madsen (2005). SEL values were accumulated over each 0.5 s time bin ($AOL_{E,0.5s}$) to contrast maximum peak-to-peak levels ($AOL_{max,0.5s}$) with time-integrated sound levels over time.

Data Filtering

Three data structures were defined for analysis: (1) click level data ("click data"), (2) binned time series for 0.5 s bins ("binned data"), and (3) summary statistics for each audited buzz ("buzz data") (**Table 1**). Click data were binned in order to obtain a time-balanced sample for a fine-scale analysis of click rate while buzz data were used to compare and classify buzzes as proxies for prey capture attempts. Maximum click rate for each buzz was obtained from the binned data. Buzzes that did not reach 5 Hz in click rate (Teloni et al., 2008) were not considered to be fast runs, and were excluded from analysis ($N = 7$).

For acoustic analysis, buzzes were filtered to include only the highest quality detections in order to account for variable SNR

TABLE 1 | Measurements and summary statistics.

Data set	Measurement	Description
Click data	AOL_{pp}	Peak-to-peak (apparent output) level (dB rms re 1 μPa) over 3.5 ms window
	AOL_{E90}	Sound exposure (apparent output) level / energy flux density (dB re 1 $\mu Pa^2\ s^{-1}$) over 90% energy window for each click
	ICI (s)	Inter-click-interval; time since previous click detection in seconds
Binned data	Click rate (Hz)	Click detection rate (Hz): number of detected clicks during 0.5 s time bin x2
	Max $AOL_{pp,0.5s}$	Maximum peak-to-peak level (AOL_{pp}) in 0.5 s time bin
	$AOL_{E,0.5s}$	Cumulative sound exposure level of click AOL_{E90} over 0.5 s time bin
	Depth	Mean depth (m) within the 0.5 s time bin
Buzz data	Start time, end time, duration (s)	Audited start time and end time from tag-on time in seconds, time interval between them defines buzz duration
	IBI (min)*	Inter-buzz-interval: the time interval (h) between previous buzz (+any subsequent pause), and the start time of the next buzz
	Pause duration (s)	Time interval between the end of buzz and the start of next buzz or usual click train duration
	Max rate (Hz)	Maximum click rate, at 0.5 s bin resolution
	# max rate peaks	Number of click rate peaks in buzz (from time binned rate data)
	Max $AOL_{pp,buzz}$	Maximum peak-to-peak level (AOL_{pp}) of the buzz
	ODBA*	Root-mean-square (rms) of 2-norm overall dynamic body acceleration
	Vertical velocity*	Mean vertical velocity during the buzz, where vertical velocity was derived from low pass filtered depth time series with a cut-off frequency of 0.2 Hz
	Pitch and heading variance*	Angular variances of the heading and filtered pitch time series over the buzz. The pitch data were filtered using fourth-order butterworth low-pass filter with a deployment-specific cut-off frequency (0.04–0.07 Hz) selected to be <50% of the fundamental fluke stroke frequency
	Depth	Mean depth (m) across 5 Hz depth values during the audited buzz

**Included in the hidden Markov model (HMM) classification of buzz movement types. Sound levels were measured off-axis from the animal-borne tag (DTAG, Johnson et al., 2009), and are therefore referred to as 'apparent output level' (AOL).*

conditions. This more stringent filtering was also necessary to remove occasional false positives of clicks from other non-tagged whales that were included in the automated click detection. Data were first removed within each buzz on a click-by-click basis. Each 0.5 s bin was then deemed to be high quality if no more than 5% of the clicks within it were removed. Similarly, each buzz was accepted if no more than 5% of its clicks and 5% of its time bins were removed.

Clicks were removed as likely false positives when they had clearly different AOL compared to their neighboring clicks. Click AOL_{pp} was first smoothed within each buzz using median filter with a window size of 5. The clicks were then excluded by removing those with raw AOL_{pp} values that were more than 6 dB below or 12 dB above the smoothed median AOL_{pp}. A lower threshold value was used for AOL_{pp} values below the median because they were more likely to originate from other sources than the tagged whale. The thresholds were determined by inspecting the distribution of AOL_{pp} for outliers for each tag. 98% of the AOL_{pp} values that were below the running median AOL_{pp} differed from it by <7 dB, on average across tags (median = 4 dB, range = 1.6–26.6). Clicks with clipped sound levels were also removed. Due to the relatively low AOL of the buzz clicks, clipping was rare (0.1% of all time bins contained any clipping). Clicks and bins with any acoustic clipping were removed from the AOL analysis.

Measurements and summary statistics are listed in **Table 1**. Audit start time and end time defined buzz duration.

Statistical Hypothesis Testing

Three analysis steps were designed to decompose movement classification and echolocation tactics from direct effects of depth (pressure, light) across different prey encounters. First, buzz events were classified using an unsupervised classification algorithm on summary movement variables that were *a priori* expected to be related to prey mobility and maneuverability rather than to the physical effects of depth (e.g., pressure or light conditions). Second, if the existence of multiple buzz movement types was supported, their vertical distribution was tested by modeling depth with the movement classification as a candidate explanatory variable. Third, we tested the importance of the movement classification vs. hydrostatic pressure as explanatory variables for echolocation performance (maximum click rate and AOL in a buzz). Pressure was included either as a linear or inverse-transformed covariate to reflect possible effects of changing air density and volume on pneumatic click production.

Finally, to quantify within-buzz variation in AOL, we modeled both maximum peak-to-peak levels (Max $AOL_{pp,0.5s}$) and time-integrated sound exposure levels ($AOL_{E,0.5s}$) in the time binned data. In order to test whether the AOL metrics were adjusted to sensory volumes and/or potential target range, we compared models with the time-binned click rate and expected transmission loss ($TL = \log_{10}$range) as candidate explanatory variables.

Classification of Movement During Buzzes

Buzzes were classified by fitting multivariate HMMs (Zucchini et al., 2016) to the movement data summarized for each buzz. The buzz summary metrics were modeled as a state-dependent process, and the probability of transition from one latent buzz type to the next was described by a transition probability matrix. The negative log-likelihood of the HMM was minimized using the nlm function in R (package stats). Mixture distributions are multi-modal, and therefore, the minimization is sensitive to the choice of starting values. To check for multiple minima and to ensure the algorithm did not terminate at a local minimum, each model was fitted 50 times with different initial values and the stability of the resulting likelihoods was monitored visually. Initial values for the distributional parameters were calculated from random 10% subsets of the input data, based upon a mean for one-parameter distributions, and both mean and variance for two-parameter distributions (Isojunno et al., 2017).

Movement metrics were selected to be proxies for prey density (inter-buzz-interval IBI), overall prey mobility and subsequent energy expenditure (root mean square of 2-norm overall dynamic acceleration [ODBA], standardized by its median value for each deployment), and prey mobility in three dimensions (vertical velocity, pitch variance, and heading variance) (**Table 1**)—variables that were *a priori* expected to related to prey and not be directly affected by the physical effects of depth (pressure or light conditions). Conversely, duration of the buzz was not included in the classification because duration may be directly limited by the air volume available to the whale at depth (Wahlberg, 2002). Similarly, rolling behavior was not included to avoid any confounding effects of light on body posture. A parametric family of distributions was specified for each metric. IBI was chosen a single-parameter family to allow for long tails in the positive-valued distribution. Vertical speed was specified a Gaussian distribution, and the metrics that were confined between 0 and 1 were specified beta distributions (pitch and heading variance). ODBA, which only takes positive values, was specified a gamma distribution.

Modeling Buzz Depth and Acoustic Metrics

Three models were fitted to the buzz-level data. To test for vertical stratification of the buzz classification (proxy for density and mobility of targeted prey), buzz mean depth was first modeled with the estimated buzz movement type as a factor explanatory variable. The factor covariate therefore captured the mean differences in depth across buzz types. Two acoustic metrics (maximum click rate and maximum AOL_{pp}) were then modeled to test whether they were better explained by hydrostatic pressure (∼depth) and/or the buzz type (∼targeted prey). Maximum values were chosen to reflect the maximum acoustical performance within each buzz. However, to check how the maximum click rate related to the hand-off distance (the distance at which buzz was initiated), the model selection for maximum click rate was repeated with click rate at the first 0.5 s time bin (initial click rate) and the first ICI (inverse-transformed to a rate s^{-1}) as response variables. All acoustic metrics were modeled with ambient pressure (standard atmospheres [atm]) and the buzz classification as explanatory variables.

All three models were fitted within a generalized estimating equation (GEE) where tag identifier was specified as a panel variable to estimate average effects across individuals (function geeglm in r package geepack). Information criteria (QIC) were used to select between models with first-order autoregressive correlation structure or no correlation structure ("independence" working correlation, but still accounting for residual autocorrelation). Empirical ("sandwich") standard error estimates are reported which are robust to the working correlation assumption. Depth as a continuous positive variable was specified a gamma distribution, click rates as a counts over unit time was specified a Poisson (count) distribution, and max AOL_{pp} was modeled as a normal variable.

Log-link was used to allow a log-linear response of the acoustic metrics to hydrostatic pressure. In addition, models with inverse-transformed hydrostatic pressure allowed the estimation of exponential relationships (as expected by Boyle's law). QIC was used to compare models without any covariates (null models) and models with all covariate combinations (one model for depth with buzz as the sole covariate, and five models for each of the two acoustic response variables, with buzz type, hydrostatic pressure and inverse hydrostatic pressure as the candidate covariates). Type III Wald tests were carried out for the full models to test the importance of movement classification in explaining variation in the acoustic metrics, after individual variability and pressure had been accounted for.

Within-Buzz Variation in AOL

Within-buzz binned data were used to investigate variation in AOL as a function of ICI, or inversely, click rate at 0.5 s temporal resolution. A positive correlation was expected under two but not necessarily mutually exclusive scenarios where output click levels are reduced (1) due to gain control at shorter ranges [automated gain control [AGC], Au 1993], indicated by shorter ICI:s, and (2) to optimize sensory volume as acoustic sampling rates are increased. AGC can be achieved by adjustments to source level, hearing sensitivity or both (transmitter vs. receiver-based AGC; Finneran et al., 2013; Supin and Nachtigall, 2013). The transient sonar equation describes the relationship between the transmitted and received levels of sonar (Urick, 1989; Au, 1993). Assuming spherical TL and frequency-dependent absorption α, the equation can be written as:

$$RL = SL - 2 \times 20 \log_{10}(R) - \alpha + TS \quad (1)$$

Where RL and SL are the received and source energy flux density, respectively, R is range and TS is target strength in decibels. Beaked whales (*Mesoplodon*) appear to maintain a relatively constant output on approach to prey (Madsen et al., 2005), while little evidence exists for the presence or lack of AGC in sperm whales. Furthermore, the extent to which sperm whales adjust their click output and rates to their targeted prey during terminal echolocation is not known.

If the ICI of buzz clicks was being adjusted to target range and click output adjusted to concomitant TL, then the sonar equation loss (Equation 1) would predict a logarithmic decrease in buzz click output level. To formalize this expectation, the

expected target range was calculated assuming that ICI equals the two-way travel time (TWTT) of sound between emission and reception of echo (speed of sound assumed a constant 1,490 m/s), plus a processing delay. Processing delay was assumed to be less than the shortest ICI in the fine-filtered data (12 ms). Thus, the expected range was calculated as

$$R = \frac{ICI - 12/1000}{2} * 1490\frac{m}{s} \quad (2)$$

On the other hand, if the whale was adjusting per-click AOL to maintain a stable sensory volume over time, a different relationship of AOL with click rate would be expected. Sound exposure level (SEL, or energy flux density) of transients can be approximated by 10 log to the time integral of the squared pressure over the pulse duration (Madsen, 2005). Because increasing number of clicks increases the total signal duration in a given time interval (higher duty cycle), the per-click AOL should therefore decrease proportionally to $10*\log_{10}$(click rate) in order to maintain a constant SEL.

To statistically test the expected relationships between click rate and AOL, we modeled both Max $AOL_{pp,0.5s}$ and $AOL_{E,0.5s}$ with either click rate (s^{-1}), $\log_{10}$(click rate), or $\log_{10}$(range) as linear covariates. While the time-integrated value of $AOL_{E,0.5s}$ was largely expected to follow the number and AOL_{pp} of individual clicks in a given time bin, by modeling it we could test the expectation of a constant SEL over time under the sensory volume hypothesis. To allow deployment-specific effects on AOL, tag deployment was specified as a factor covariate in every model. Within-buzz autocorrelation in AOL was modeled using 1st order autoregressive correlation structure in a linear mixed model (LMM) with buzz id as a random effect (function lme, package nlme). A LMM was chosen over the GEE approach because the focus of the analysis was within-buzz variation, i.e., variation within the panel variable. AIC was used to compare models. The model was fitted to the fine-filtered binned data, and excluded the last 3 s of each buzz in order to reduce the effect of any clicks produced at the end of the buzz that may no longer reflect prey pursuit.

RESULTS

Data

A total of 3,715 buzzes were audited, of which 3,150 baseline buzzes (from 28 individuals, or 846 min recording time) were included in the analyses ("coarse" data-filtering, **Supplementary Table 1**). Further "fine" data-filtered buzzes (n = 1,891, 490 min) excluded 11 short (<2 s) buzzes, 3 shallow buzzes (average, start or end depth <20 m), almost all ($n = 23/27$) of the buzzes from whale sw08_152a, an unusually noisy tag where flow noise dominated energy from clicks at high repetition rates, and 8/10 buzzes from sw09_141a that was associated with other whales for most of the baseline data period. All the data are provided in the Supplementary Material (**Data Sheets 1–3**, and the **Supplementary Table 2** file).

Classification of Buzz Events Based Upon Movement

AIC decreased for every additional state in the HMM (as is typical for HMMs), but the decrease appeared to level off after 4 states (i.e., "buzz movement types"). The 4-state HMM also produced distinct and biologically interpretable states (**Supplementary Figures 1–5**). We therefore selected the HMM with 4 states for further inference.

The two buzz movement types with the deepest median depths (1,178 and 1,130 m) had the lowest median total ODBA (overall dynamic body acceleration) values (1.5 and 1.6, respectively). Within these two types, the former included more descending vertical speeds (median 1.7 [0.9, 2.3]). The longest median IBI was obtained for the shallowest buzz type (161 m), and the shortest IBI for the second shallowest (372 m) which also had the highest median ODBA (4.1). Based on these results, the four buzz types are hereafter termed as "Shallow-sparse," "Mid-active," "Deep-descent," and "Deep," respectively (**Table 2**).

Depth Distribution of Movement Types

Each buzz movement type had a distinct but a broad depth distribution (**Figures 1**, **2**; see **Supplementary Figures 11–24** for full time series). The buzz type was a significant predictor of depth across individuals in a GEE ($\chi^2 = 62.1$, $p = <0.001$), and the model with buzz type outperformed the null model in terms of the QIC (quasi-information criterion; ΔQIC = 1,276). This result was robust to the exclusion of IBI from the HMM model fit (**Supplementary Figure 6**). Compared to depth, time of day had relatively little effect on the occurrence of buzz types with lower solar elevation slightly increasing the probability of deep-descent buzzes (**Supplementary Figures 7**, **8**). QIC supported "independence" working correlation over an autoregressive structure.

Effects of Pressure and Buzz Movement Type on Acoustic Metrics

The lowest QIC models included both ambient pressure (atm) and buzz type (HMM movement classification) as covariates in both GEEs for maximum click rate and maximum peak-to-peak click level (max AOL_{pp}) across buzzes, and "independence" as working correlation. The same model was selected for maximum click rate and initial click rates representing hand-off distance (first binned click rate and initial inverse-transformed ICI). For the max AOL_{pp}, inverse-transformed pressure was selected over the non-transformed covariate. While Type III Wald tests supported both covariates in the full model for click rate ($p <$ 0.001), there was no support for buzz movement type in the full model for max AOL_{pp} ($p = 0.11$) (**Supplementary Table 2**). These results indicate high variability in max AOL_{pp}, which is not clearly explained by the type of movement behavior during buzz-related prey encounters. Wald tests showed somewhat weaker effects for the initial binned click rate (**Supplementary Table 2**) and initial inverse-transformed ICI (pressure: $\chi^2 = 5.6$, $p = 0.018$; buzz type: $\chi^2 = 13.6$, $p = 0.004$).

Maximum buzz click rate was estimated to decrease by 23% for every 100 atm increase in pressure (90 m), or an average ~1.15 Hz

TABLE 2 | Sample size and summary statistics (median, 95% percentiles) for each buzz type (coarse-filtered data).

	N	Depth (m)	Duration (s)	Pause duration (s)	IBI (min)	ODBA (rms)	Vertical speed (m/s)	Pitch variance (rad^{-100})	Heading variance (rad^{-100})
Shallow-sparse	1,061	160.7	14.1	3.5	3.4	2.8	0.0	4	9.7
		[66, 934.5]	[6.4, 50]	[0, 53.5]	[0.1, 13]	[1.2, 6]	[−1.2, 1.1]	[0.4, 28.6]	[0.4, 79.3]
Mid-active	768	371.5	21.0	0.1	0.3	4.1	0.3	16.2	31.8
		[145.2, 663.1]	[8.5, 79.6]	[0, 24.7]	[0, 2.2]	[2.1, 8.7]	[−0.6, 2.2]	[2.1, 42.3]	[2.4, 84.3]
Deep-descent	275	1177.6	6.8	3.5	0.6	1.5	1.7	1.2	2.2
		[287, 1761.8]	[3.3, 31.4]	[0, 13.7]	[0, 3.9]	[0.7, 3.1]	[0.9, 2.3]	[0.1, 8.9]	[0.1, 44.2]
Deep	1,046	1130.4	7.0	5.2	1.0	1.6	−0.2	1.1	0.8
		[107.4, 1788.5]	[3.9, 19.9]	[0, 19.7]	[0.1, 5.7]	[0.6, 3.7]	[−1.7, 1.1]	[0, 8.6]	[0.1, 7.1]

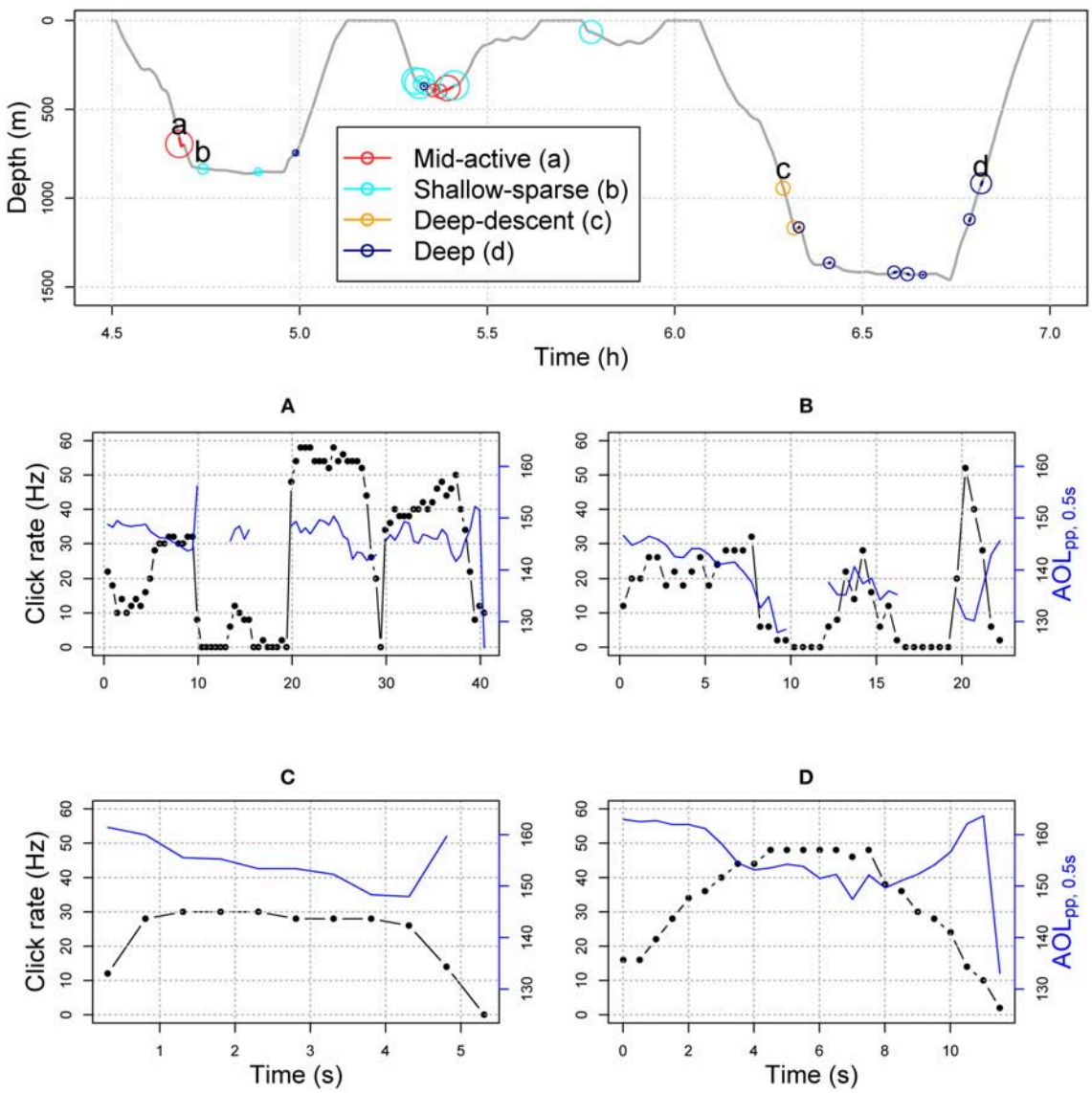

FIGURE 1 | Top panel shows example section of dive profile (sw17_186a) with buzzes color-coded by HMM-classified predator-prey movement type (**Figure 2**). The solid line indicates buzz duration, and greater circle size shows greater ODBA values (overall dynamic body acceleration, **Table 1**). In the middle and bottom panels, connected black circles show time-binned click rate (Hz), and solid blue lines show maximum apparent output level ($AOL_{pp,0.5}$) in each 0.5 s time bin for each example buzz (**A–D**, labeled in the dive profile).

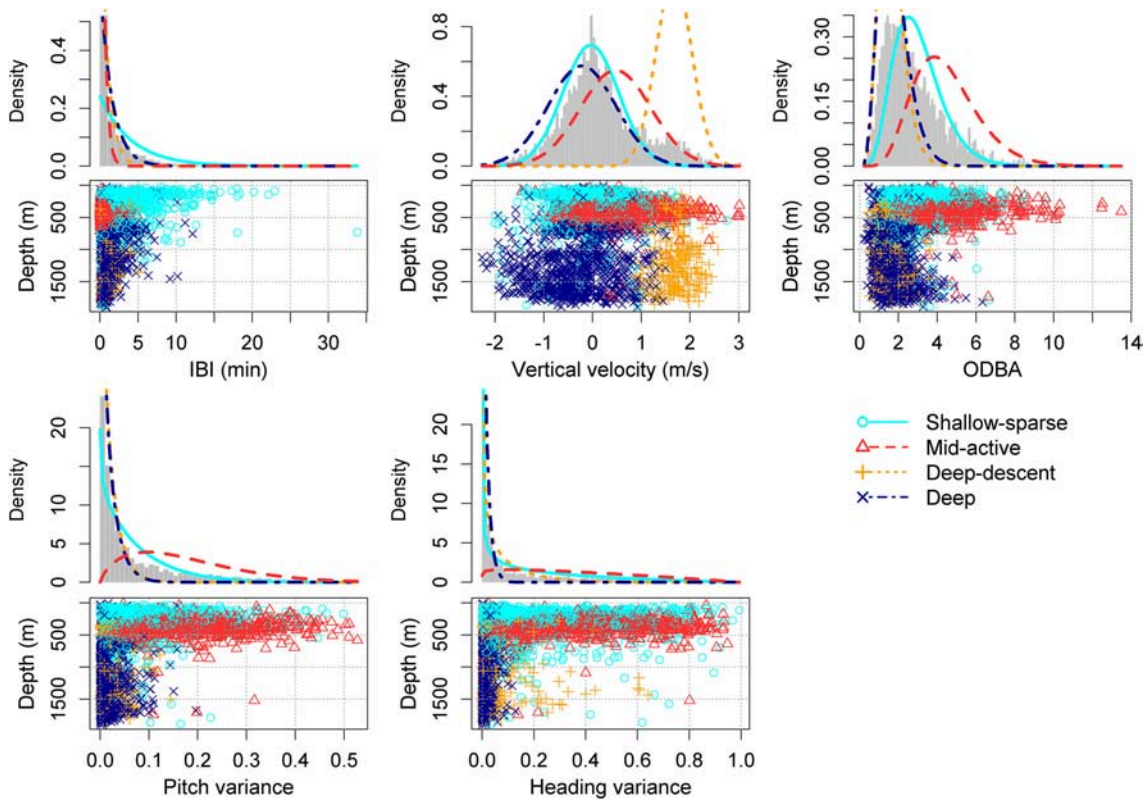

FIGURE 2 | HMM classification of buzz summary variables, chosen to reflect predator-prey movement rather than physical effects of depth (light, or hydrostatic pressure) (**Tables 2**, **3**). Density lines show the estimated state-dependent distributions. ODBA = overall dynamic body acceleration (**Table 1**). Please see **Supplementary Figures 1**–**5** for the equivalent figure with a different number (2–5) of underlying states.

for every 100 m increase in depth (**Figure 3**). A similar but more variable decrease was estimated for initial click rates (17.5 and 22.4% for initial binned rate and first 1/ICI), indicating that click rates were reduced across the entire buzz. For the "Deep" buzz type, which could also be produced at relatively shallow depths (min 81 m), the model estimated the average maximum click rate to decrease from 54.2 Hz [51.2, 57.0] at 100 m depth to 42.8 Hz [41.4, 44.2] at 1,000 m depth. While the maximum click rate was reduced during the two deep buzz types compared to the Shallow-sparse type, there wasn't strong evidence for such an effect on initial click rate. Instead, click rates were elevated by 40% at the start of the Mid-active buzz types compared to the Shallow-sparse buzzes (**Supplementary Table 2**).

Max AOL_{pp} was predicted to decrease exponentially with depth, with the most drastic decrease in level (>1 dB for every 1 atm increase in pressure) estimated when ambient pressure was ≤7 atm (60 m) (**Figure 3**). However, some effect of pressure on max AOL_{pp} may have remained for deeper buzzes as well: fitting the model without the shallow (<100 m) buzzes the effect of inverse pressure was still supported by the Type III Wald tests at 5% significance level ($\chi^2 = 3.95$, $p = <0.047$).

Within-Buzz Variation in AOL

The average ± SD difference between the maximum and minimum value for max $AOL_{pp,0.5s}$ within a buzz was 17.5 dB ± 8.0 (n = 58,079 fine-filtered time bins in 1,891 buzzes) (**Figure 4**). The model selection supported log(click rate) as a linear predictor for the maximum click level ($AOL_{pp,0.5s}$) and log(range) for the cumulative sound exposure level ($AOL_{E,0.5s}$) (**Supplementary Table 3**). The relationship with click rate was negative for $AOL_{pp,0.5s}$ and positive for $AOL_{E,0.5s}$ (**Figures 4E,F**). Thus, the decrease in per-click AOL did not result in a flat response for time-integrated AOL. The multiplier (slope) for $\log_{10}$(Range) was estimated to be 2.8 (SE = 0.06) for $AOL_{pp,0.5s}$ and −3.7 (SE = 0.043) for $AOL_{E,\ 0.5s}$, much lower than expected based on two-way spherical TL (2 × 20 dB, Equation 1). The slope parameter was estimated to be −4.0 (SE = 0.06) for $\log_{10}$(Click rate) in the best model for $AOL_{pp,0.5s}$. The relationship was consistent across the four buzz types (**Supplementary Figure 10**).

DISCUSSION

We aimed to determine whether male sperm whales had different movement patterns during prey encounters, and whether terminal echolocation (buzzing) behavior was related to those movement patterns or pneumatic sound production under hydrostatic pressure at depth. Decomposing the effects of predator movement and depth (pressure) was essential to

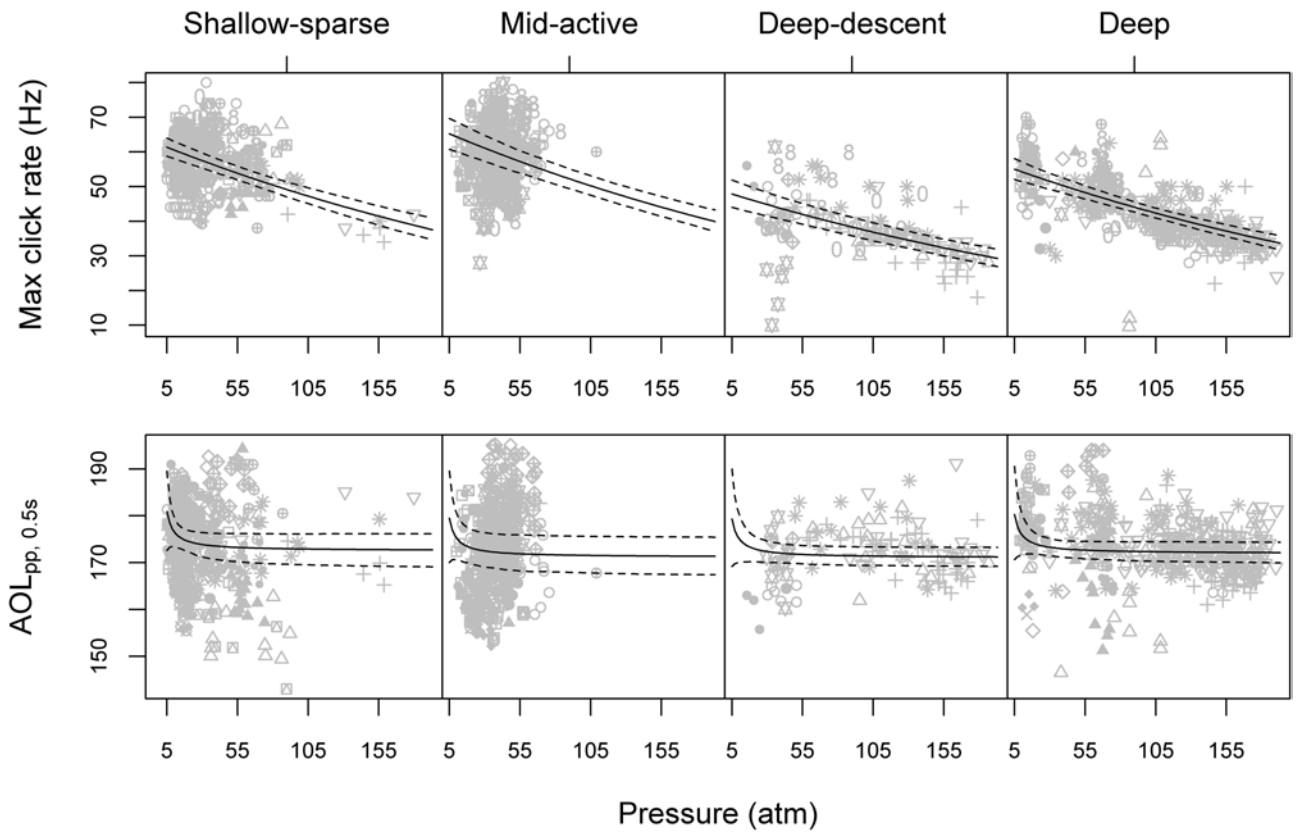

FIGURE 3 | Maximum click rate (top row) and maximum apparent peak-to-peak sound pressure level (AOL_{pp}, bottom row) as a function of average ambient pressure for each buzz, paneled by the HMM classification of predator-prey movement (**Figure 2**). Gray symbols show observed data, with different symbols indicating different tagged animals. Solid and dashed lines show model predictions and 95% parametric bootstrap confidence intervals, based on the full GEE (generalized estimating equation) models for the two acoustic metrics (**Supplementary Table 2**). Please see **Supplementary Figure 9** for the equivalent figure with depth on the x-axis.

evaluate whether sperm whales might target different prey at different depths. There was clear evidence for a linear decrease in buzz click rates (both initial and maximum in the buzz) with depth that could not be explained by buzz movement type alone (**Figure 3**), suggesting a pressure effect on sound production.

Unsupervised classification that included inter-buzz-interval (IBI) and movement summary statistics, but not acoustic metrics or depth itself, resulted in a depth-dependent classification of four buzz types (**Figures 1**, **2**). "Shallow-sparse" and "Mid-active" buzz types had the highest activity levels in terms overall movement (ODBA), while shorter IBI, lower ODBA, and fewer changes in orientation implicated a denser distribution of less mobile prey at depth (median depth >1,100 m) ("Descent-deep" and "Deep" buzz types, **Table 2**). After accounting for effects of pressure, click rates (at the beginning of the buzz especially) were higher during Mid-Active than other types of buzzes (**Table 3**), indicating that higher acoustic sampling rates were used to track prey that required more active capture movements. Our results, spanning across 12 years and 28 individual tag deployments, corroborate previous results from Teloni et al. (2008) that sperm whales engage in at least two different foraging strategies, but also illustrate potential echolocation limitations at depth and multiple movement tactics within a dive (multiple buzz types). Our results also corroborate that sperm whales engage in an active pursuit of prey (Aoki et al., 2012; Fais et al., 2016).

Evidence for Pressure-Driven Effects

Hydrostatic pressure explained a significant amount of variation in buzz click rates (both initial and maximum rates), as well as maximum AOL (peak-to-peak SPL) across buzzes, after accounting for the effect of buzz movement classification (**Supplementary Table 2**). The relationship between maximum click rate and hydrostatic pressure was estimated to be linear, while model selection supported the effect of inverse transformed pressure on maximum AOL (**Figure 3**). Such an exponential relationship would be expected if the maximum AOL was influenced by available volume of air, which is inversely proportional to ambient pressure (Boyle's law). Conversely, the linear relationship between maximum click rate and pressure indicates that air density of compressed gases, rather than their volume may be important for the adjustment of maximum echolocation rate. On the other hand, if a fixed air volume was required to produce each buzz click, an exponential decrease in the total number of clicks produced in each buzz may be expected

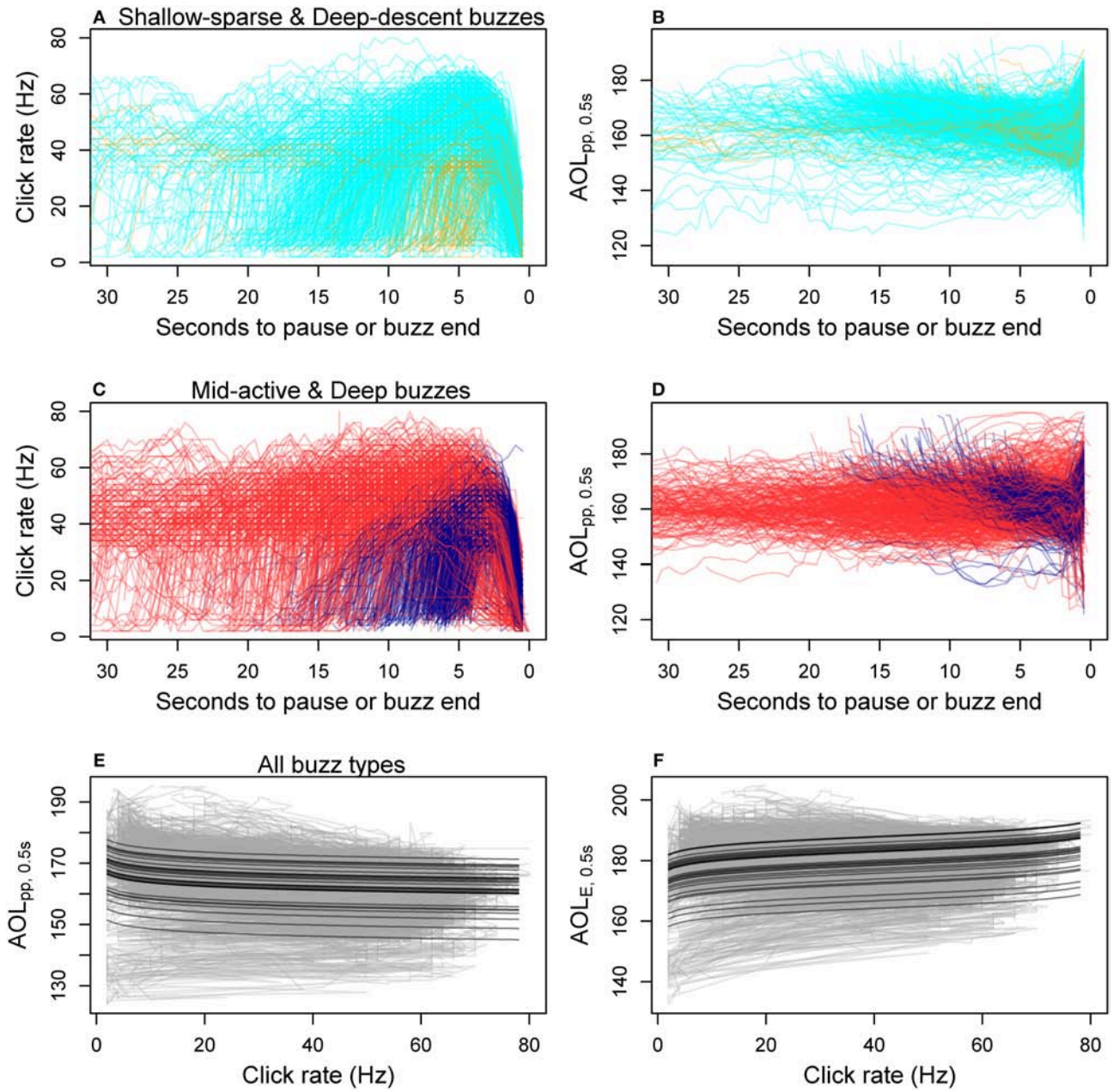

FIGURE 4 | Within-buzz variation in click rate and two apparent output level (AOL) metrics (peak-to-peak and sound exposure level, **Table 1**) measured for each 0.5 s time bin. **(A–D)** show time series data for each fine-filtered buzz ($N = 1891$), color-coded by the HMM classification of predator-prey movement (cyan, Shallow-sparse; orange, Deep-descent; red, Mid-active; dark blue, Deep; **Figure 2**). The bottom two panels show best model fits for the two AOL metrics (**E**: AOL_{pp} ~ log-transformed click rate, **F**: AOL_E ~ log-transformed expected range), with predictions given for each tag deployment as a separate black line. Gray lines show the data time series for each buzz.

as a function of depth. The more variable but significant decrease in the initial click rates as well as data for the total number of clicks support this second prediction (**Figure 5**), although the total number of clicks was not included in the formal analysis due to confounding effects with buzz duration. Furthermore, while the analysis of usual clicks was outside the scope of this work, it is likely that some of the air volume available for a buzz would have been used in the preceding series of usual clicks. Indeed, Wahlberg (2002) showed that the time interval between subsequent pauses as well as the number of usual clicks decreased exponentially at depth (up to 1,500 m).

While we found an exponential decrease in maximum AOL with hydrostatic pressure for buzzes, Madsen P. T. et al. (2002) showed that on-axis output and frequency of sperm whale usual clicks were independent of depth up to 700 m. Multiple factors could explain the discrepancy to the off-axis results

TABLE 3 | Sample size and acoustic characteristics (median, 95% percentiles) of each buzz type (fine-filtered data).

	N	No. of peaks	Click rate (Hz)	Max AOL_{pp}	Max AOL_E
Shallow-sparse	703	3 [1, 15.4]	58 [44, 68]	175.9 [158.6, 188.2]	188.6 [173.9, 195.9]
Mid-active	488	7 [1.2, 29]	60 [44, 74]	172.2 [156.3, 190.2]	186.4 [173.9, 200.5]
Deep-descent	141	2 [1, 15.5]	36 [22.8, 56]	171.4 [160.7, 183.3]	182.2 [174.1, 191.7]
Deep	559	2 [1, 5]	42 [30, 62]	172.4 [160.3, 187.7]	183.3 [172.1, 194]

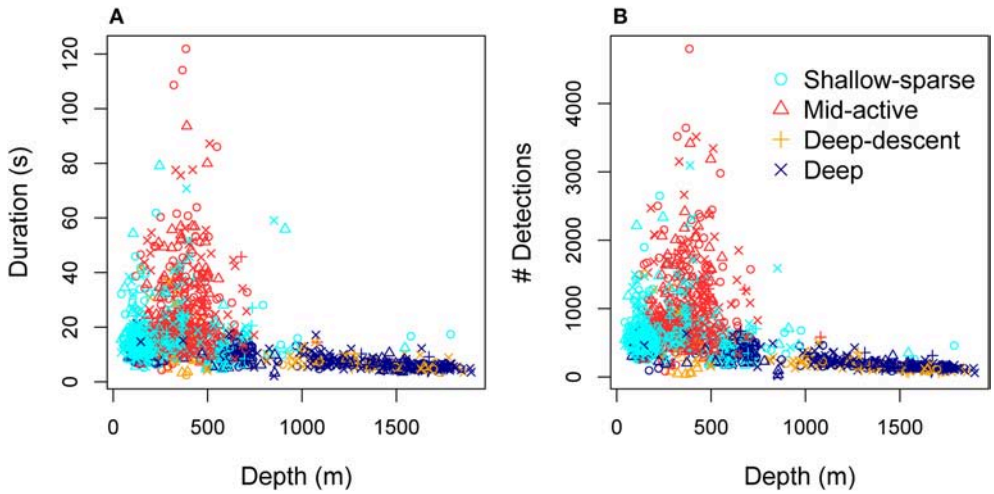

FIGURE 5 | Total duration **(A)** and total number of click detections **(B)** per buzz as a function of depth, color-coded by the HMM classification of predator-prey movement (**Figure 2**, **Tables 2**, **3**).

reported here for buzz clicks, such as narrowing of acoustic beam to retain optimal sonar capacity of on-axis clicks at depth. Sperm whale echolocation clicks are highly directional, and the backward directed beam can be dominated by the initial "p0" pulse produced in the distal air sac (Møhl et al., 2003; Zimmer et al., 2005). Indeed, the sound pressure levels received by the tag may not only represent off-axis levels, but may also be filtered and beamformed by the body of the whale (Johnson et al., 2009). Similarly, Thode and Mellinger (2002) reported a change in the frequency content of usual clicks with depth but the source-receiver aspect was unknown and possibly variable. Therefore, the negative trend in the apparent click levels does not necessarily indicate that on-axis levels were compromised at depth, but could also relate to changes in sound propagation, such as changing of the sound beam as a function of depth. This question could be evaluated by simultaneous acoustic recording at different points of the acoustic beam, e.g., by attaching multiple tags on the same individual or combining animal-borne and remote acoustic recording.

Echolocation Tactics

After accounting for the effects of hydrostatic pressure, we found variation in click rates between the four buzz types. Mid-active buzzes that were the longest in duration and most active buzz type in terms of movement were also associated with increased initial and maximum click rates. Conversely, maximum click rates were the slowest for the two deep, less active, buzz types (**Table 3**). These results are consistent with the need to increase click rate to increase rate of sensory feedback in order to inform predator motor reactions to more mobile prey (Madsen and Surlykke, 2013; Wisniewska et al., 2014). On the other hand, we found no evidence for slower initial ICI associated with longer buzzes that have been suggested to help processing more complex auditory scenes in beaked whales (Johnson et al., 2008).

As expected, within-buzz click rates were correlated with maximum AOL. Maximum peak-to-peak levels ($AOL_{pp,0.5s}$) ranged by 17.5 dB in an average buzz, of which <10 dB was estimated to be due to co-variation with click rate. The per-click reduction in AOL with increasing click rate was not sufficient to completely remove a positive relationship between click rate and sound exposure level ($AOL_{E,0.5s}$) over time. Consistent with the hypothesis that per-click AOL was adjusted to reduce sensory volume, peak levels were best explained by log-transformed click rate. Auditory evoked potential experiments indicate that echolocating odontocetes have the ability to discriminate and track clicks and echoes at high temporal resolution (e.g., 5–20 ms in Risso's dolphins Mooney et al., 2006). Concordantly, in our data, 1% of the buzz clicks had ICI < 15 ms (minimum 12–13 ms). Therefore, if sperm whales tracked individual echoes, their sensory volume per second would increase by a factor of 60 by decreasing ICI from 1 s to 15 ms alone.

While log-transformed target range (calculated based on ICI) outperformed linear click rate as a predictor of $AOL_{pp,0.5s}$,

the slope was estimated to be much lower than what would have been expected for two-way spherical transmission loss (Equation 1). This result indicates that ICI and/or per-click AOL did not fully and/or instantaneously track target range. If ICI corresponded to TWTT, the ranges to targets would have been 40–120 m at the beginning of the buzz (80–92 m for Shallow-sparse, 41–52 m for Mid-active, and 104–123 m for Deep-descent and Deep buzz types) (assuming 0–15 ms processing delay on the median first ICI). These ranges would be relatively long compared to other studied beaked whales, delphinids, and many bats that switch to terminal echolocation ∼1 body length away from their target (Madsen and Surlykke, 2013). Alternatively, sperm whales emit buzz clicks more slowly at the beginning of the buzz, and do not reach their capacity of click-by-click (echo-by-echo) discrimination until the temporal resolution is required. This hypothesis would be consistent with the apparent pneumatic limitations. Low ICIs relative to target range (determined by animal-borne recording of prey echoes) have also been reported at the beginning of the buzz in beaked whales (Madsen et al., 2005) and other toothed whales (DeRuiter et al., 2009; Wisniewska et al., 2014).

Evidence for Different Prey Types

Buzz classification that included IBI and movement, but not depth or acoustic variables, produced a highly depth-dependent distribution (**Figures 1**, **2**). Two buzz types occurred predominantly during deep dives (median >1,100 m): both "Deep" and "Deep-descent" types consisted of short duration (median 7.0 and 6.8 s, respectively) and relatively low movement activity (ODBA) buzzes. The two types differed by vertical velocity, and Deep-descent buzzes were also observed during shallower dives (<500 m, **Figure 2**). "Shallow sparse" and "Mid-active" buzzes were on average more than twice as long in duration and were more active than the deep buzz types. Of all buzz types, Mid-active buzzes were the longest in duration, produced at the shortest intervals and were the most active in terms of movement. These buzzes also included up to 29 peaks in binned click rate, indicating multiple re-approaches (**Table 3**).

These results corroborate previous research showing that that sperm whales engage in an active search-and-pursue strategy (Amano and Yoshioka, 2003; Miller et al., 2004a; Aoki et al., 2012; Fais et al., 2016), but also that the level of activity during prey encounters varied with depth. Increased movement effort indicated that more mobile prey were targeted at shallower depths (<700 m), such as muscular cephalopods or fish. Conversely at deeper depths (∼1,000–1,800 m) sperm whales appeared to either be selecting more prey items or foraging more densely distributed prey that did not require as much movement effort to catch. Furthermore, lower click rates suggest that high acoustic sampling rates were not necessary to detect prey at these depths.

The switch in movement and biosonar tactics during prey capture attempts indicates that sperm whales target prey with different mobility or manoverability, and is consistent with a generalist strategy of male sperm whales that are known to take different species and life stages of cephalopods (Santos et al., 1999; Bjørke, 2001; Simon et al., 2003) as well as fish in their high-latitude foraging grounds (Gaskin and Cawthorn, 1967; Martin and Clarke, 1986). In the Norwegian Sea, sperm whale feeding grounds overlap with the spawning grounds of *Gonatus fabricii* (Bjørke, 2001), which is also the most prevalent prey type in the stomachs of stranded specimens recovered in these waters (Santos et al., 2002; Simon et al., 2003). It has been suggested that sperm whales and pilot whales (*Globicephalas melas*) exploit aggregations of cephalopods that are either dead or are spent after spawning (Clarke, 1996), and that sperm whales may also target egg carrying female *Gonatus fabricii* (Simon et al., 2003). Mature female *Gonatus fabricii* lose their ability to swim and float in the water column as part of ontogenic changes during breeding as their muscle tissue disintegrates and mantle and fins become gelatinous (Bjørke, 2001). Given the high regional and individual variability in sperm whale diet (e.g., Evans and Hindell, 2004), it is possible that a range of more sedentary cephalopods was taken at depth. These could include smaller cephalopods that are generally more bioluminescent, neutrally buoyant, slower swimming and less muscular than larger squids, and therefore likely easier to catch, as well as dead cephalopods that eventually sink to the sea floor (Clarke et al., 1993; Clarke, 1996; Whitehead, 2003).

Based upon the expectation that a predator should optimize energy expenditure for expected returns, the shallow prey types can be expected to contain more energy or other nutritional reward, such as protein contained in more muscular (and hence faster) prey species. Given sperm whales must balance both their energy budget and oxygen stores during diving, foraging on likely lower quality prey at deeper depths is likely to carry other advantages, such as predictable and abundant prey patches (Teloni et al., 2008). Sperm whales can use usual clicks to scan for prey layers hundreds of meters ahead (Madsen P. et al., 2002), and in the beginning of a dive tend to target those layers that were located during previous dives (Fais et al., 2015). Sperm whales could also take advantage of aggregations of terminally spawning cephalopods, and prefer slower, more gelatinous, neutrally buoyant cephalopod species that are easier to capture, despite lower caloric value (Clarke et al., 1993; Clarke, 1996). Interestingly, for sperm whales tagged in a highly productive submarine canyon in New Zealand, the opposite might be the case: benthic buzzes were on average longer (10–30 s) and produced at longer inter-buzz intervals compared to pelagic buzzes, suggesting availability of more calorific and/or agile prey at greater depths (900–1,200 m) (Guerra et al., 2017).

It is possible that sperm whales approached and pursued similar types of prey in different body postures, and hence vertical velocity, depending on whether the individual was transiting or searching within a prey layer. These effects may have over-emphasized the Descent-deep buzz type as a separate movement strategy. Whales could also switch hunting or echolocation strategy for the same prey if their detectability changed with depth. Sea floor might provide both physical shelter and refuge from acoustic detection. It could be informative to assess the role of behavioral state and distance to sea floor in future analyses of prey encounter strategies.

Light conditions influencing the ability of prey to visually detect their predator (or vice-versa) can also be expected to play a role in aquatic foraging. Availability of daylight during the day could allow prey to visually detect their predator earlier, and

thus increase handling time at shallower depths. With the near continuous availability of daylight during the summer months in Norway, our dataset collected was not optimal to address this question. Nevertheless, the probability of a buzz to be of the Descent-deep type decreased with greater solar elevation (**Supplementary Figures 7**, **8**). During the day, the silhouette of aquatic predators may be more visually detectible to their prey, in particular when viewed from below. However, the effect was present in the bathypelagic zone (>1,000 m) where daylight is virtually absent (Warrant and Locket, 2004). Thus, the diurnal effect may be better explained by changes in prey availability due to vertical migration. For negatively buoyant divers, such as sperm whales at deep depths (>300 m, Miller et al., 2004b), these vertical descents may provide a way to increase pursuit speed while minimizing energetic and physiological costs.

Comparative studies have begun to link the maintenance costs and muscular performance of marine mammal predators to the energetic value of their prey (Spitz et al., 2012, 2014). Our results highlight how within-species dietary plasticity might arise from switching foraging strategies between heterogeneously distributed prey, and against ecophysiological and sensory constraints (distance from surface, pressure). In the future, including more sensory traits in the comparative approach (e.g., maximum echolocation rate, output level, hearing group) could further elucidate how toothed whale sensory niches map on to their dietary niche.

DATA AVAILABILITY STATEMENT

The datasets that were analyzed and generated in this manuscript are enclosed with the manuscript as a Supplement, along with a data report.

AUTHOR CONTRIBUTIONS

SI and PM conceived the conceptual approach of the manuscript. SI and PM contributed to the data collection. SI designed and performed the statistical analyses, and drafted the manuscript with feedback from PM.

FUNDING

This work was funded by NL Ministry of Defense, NOR Ministry of Defense, US Office of Naval Research (N00014-08-1-0984, N00014-10-1-0355, N00014-14-1-0390), and FR Ministry of Defense (DGA) (public market n°15860052).

ACKNOWLEDGMENTS

We thank Mark Johnson, Peter Madsen and 3S (Sea mammals, Sonar, Safety project) ship's crew and research team members for efforts on the field data collection and access. We would also like to thank Peter Madsen for his extensive review and constructive feedback on the manuscript. We are also grateful to both reviewers for their insight and helpful suggestions. Visual data were collected using Logger 2000, developed by the International Fund for Animal Welfare (IFAW) to promote benign and non-invasive research. We would also like to thank our sponsors, NL Ministry of Defense, NOR Ministry of Defense, US Office of Naval Research and FR Ministry of Defense (DGA).

SUPPLEMENTARY MATERIAL

The Supplementary Material for this article can be found online at: https://www.frontiersin.org/articles/10.3389/fevo.2018.00200/full#supplementary-material

REFERENCES

Amano, M., and Yoshioka, M. (2003). Sperm whale diving behavior monitored using a suction-cup-attached TDR tag. *Mar. Ecol. Prog. Ser.* 258, 291–295. doi: 10.3354/meps258291

Aoki, K., Amano, M., Mori, K., Kourogi, A., Kubodera, T., and Miyazaki, N. (2012). Active hunting by deep-diving sperm whales: 3D dive profiles and maneuvers during bursts of speed. *Mar. Ecol. Prog. Ser.* 444, 289–301. doi: 10.3354/meps09371

Arranz, P., de Soto, N., A., Madsen, P., T., Brito, A., Bordes, F., and Johnson, M., P. (2011). Following a foraging fish-finder: diel habitat use of Blainville's beaked whales revealed by echolocation. *PLoS ONE* 6:e28353. doi: 10.1371/journal.pone.0028353.

Au, W. (1993). *The Sonar of Dolphins.* New York, NY: Springer Verlag. doi: 10.1007/978-1-4612-4356-4

Bjørke, H. (2001). Predators of the squid *Gonatus fabricii* (Lichtenstein) in the Norwegian Sea. *Fish. Res.* 52, 113–120. doi: 10.1016/S0165-7836(01)00235-1

Clarke, M. R. (1996). Cephalopods as prey III Cetaceans. *Philos. Trans. R. Soc. Lond. Ser. B Biol. Sci.* 351, 1053–1065. doi: 10.1098/rstb.1996.0093

Clarke, M. R., Martins, H. R., and Pascoe, P. (1993). The diet of sperm whales (*Physeter macrocephalus* Linnaeus 1758) off the Azores. *Philos. Trans. R. Soc. Lond. Ser. B Biol. Sci.* 339, 67–82. doi: 10.1098/rstb.1993.0005

Davis, R. W., Jaquet, N., Gendron, D., Markaida, U., Bazzino, G., and Gilly, W. (2007). Diving behavior of sperm whales in relation to behavior of a major prey species, the jumbo squid, in the Gulf of California, Mexico. *Mar. Ecol. Prog. Ser.* 333, 291–302. doi: 10.3354/meps333291

DeRuiter, S. L., Bahr, A., Blanchet, A. M., Hansen, S., F., Kristensen, J. H., and Wahlberg, M. (2009). Acoustic behaviour of echolocating porpoises during prey capture. *J. Exp. Biol.* 212, 3100–3107. doi: 10.1242/jeb.030825

Evans, K., and Hindell, M. A. (2004). The diet of sperm whales (*Physeter macrocephalus*) in southern Australian waters. *ICES J. Mar. Sci.* 61, 1313–1329. doi: 10.1016/j.icesjms.2004.07.026

Fais, A., Johnson, M., Wilson, M., Aguilar Soto, N., and Madsen, P. T. (2016). Sperm whale predator-prey interactions involve chasing and buzzing, but no acoustic stunning. *Sci. Rep.* 6:28562. doi: 10.1038/srep28562

Fais, A., Soto, N. A., Johnson, M. P., Pérez-González, C., and Miller, P. J. O. (2015). Sperm whale echolocation behaviour reveals a directed, prior-based search strategy informed by prey distribution. *Behav. Ecol. Soc.* 69, 663–674. doi: 10.1007/s00265-015-1877-1

Finneran, J. J., Mulsow, J., and Houser, D. S. (2013). Auditory evoked potentials in a bottlenose dolphin during moderate-range echolocation tasks. *J. Acoust. Soc. Am.* 134:4532. doi: 10.1121/1.4826179

Gaskin, D. E., and Cawthorn, M. W. (1967). Diet and feeding habits of the sperm whale (*Physeter Catodon L.*) in the cook strait region of New Zealand. *N. Z. J. Mar. Freshw. Res.* 1, 156–179. doi: 10.1080/00288330.1967.9515201

Guerra, M., Hickmott, L. J., van der Hoop, Rayment, W., Leunissen, E., Slooten, E., et al. (2017). Diverse foraging strategies by a marine top predator: sperm whales exploit pelagic and demersal habitats in the Kaikoura submarine canyon. *Deep-Sea Res. Part I Oceanogr. Res. Papers* 128, 98–108. doi: 10.1016/j.dsr.2017.08.012

Heithaus, M. R., Frid, A., Wirsing, A. J., and Worm, B. (2008). Predicting ecological consequences of marine top predator declines. *Trends Ecol. Evol.* 23, 202–210. doi: 10.1016/j.tree.2008.01.003

Houston, A. I., and Carbone, C. (1992). The optimal allocation of time during the diving cycle. *Behav. Ecol.* 3, 255–265. doi: 10.1093/beheco/3.3.255

Huggenberger, S., André, M., and Oelschläger, H. H. A. (2014). An acoustic valve within the nose of sperm whales physeter macrocephalus. *Mamm. Rev.* 44, 81–87. doi: 10.1111/mam.12017

Isojunno, S., Sadykova, D., DeRuiter, S., Curé, C., Visser, F., Thomas, L., et al. (2017). Individual, ecological, and anthropogenic influences on activity budgets of long-finned pilot whales. *Ecosphere* 8:e02044. doi: 10.1002/ecs2.2044

Johnson, M., Hickmott, L. S., Soto, N. A., and Madsen, P. T. (2008). Echolocation behaviour adapted to prey in foraging Blainville's beaked whale (*Mesoplodon densirostris*). *Proc. R. Soc. Lond. B Biol. Sci.* 275, 133–139. doi: 10.1098/rspb.2007.1190

Johnson, M., Madsen, P. T., Zimmer, W. M., Aguilar de Soto, X. N., and Tyack, P. L. (2004). Beaked whales echolocate on prey. *Proc. Biol. Sci.* 271, 383–386. doi: 10.1098/rsbl.2004.0208

Johnson, M. P., Soto, N. A., and Madsen, P. T. (2009). Studying the behaviour and sensory ecology of marine mammals using acoustic recording tags: a review. *Mar. Ecol. Prog. Ser.* 395, 55–73. doi: 10.3354/meps08255

Johnson, M. P., and Tyack, P. L. (2003). A digital acoustic recording tag for measuring the response of wild marine mammals to sound. *IEEE J. Ocean. Eng.* 28, 3–12. doi: 10.1109/JOE.2002.808212

Kawakami, T. (1980). A review of sperm whale food. *Sci. Rep. Whales Res. Instit.* 32, 199–218.

Klages, N. T. W. (1996). Cephalopods as prey II Seals. *Philos. Trans. R. Soc. Lond. Ser. B Biol. Sci.* 351, 1045–1052 doi: 10.1098/rstb.1996.0092

Madsen, P., Wahlberg, M., and Møhl, B. (2002). Male sperm whale (*Physeter macrocephalus*) acoustics in a high-latitude habitat: implications for echolocation and communication. *Behav. Ecol. Sociobiol.* 53, 31–41. doi: 10.1007/s00265-002-0548-1

Madsen, P. T. (2005). Marine mammals and noise: problems with root mean square sound pressure levels for transients. *J. Acoust. Soc. Am.* 117, 1–6. doi: 10.1121/1.1921508

Madsen, P. T., Aguilar de Soto, N., Arranz, P., and Johnson, M. (2013). Echolocation in Blainville's beaked whales (*Mesoplodon densirostris*). *J. Compar. Physiol. A* 199, 451–469. doi: 10.1007/s00359-013-0824-8

Madsen, P. T., Johnson, M., de Soto, N. A., Zimmer, W. M. X., and Tyack, P. (2005). Biosonar performance of foraging beaked whales (*Mesoplodon densirostris*). *J. Exp. Biol.* 208, 181–194. doi: 10.1242/jeb.01327

Madsen, P. T., Payne, R., Kristiansen, N. U., Wahlberg, M., Kerr, I., and Møhl, B. (2002). Sperm whale sound production studied with ultrasound time/depth-recording tags. *J. Exp. Biol.* 205, 1899–1906. Available online at: http://jeb.biologists.org/content/205/13/1899

Madsen, P. T., and Surlykke, A. (2013). Functional convergence in bat and toothed whale biosonars. *Physiology* 28, 276–283. doi: 10.1152/physiol.00008.2013

Martin, A. R., and Clarke, M. R. (1986). The diet of sperm whales (*Physeter macrocephalus*) captured between Iceland and Greenland. *J. Mar. Biol. Assoc.* 66, 779–790. doi: 10.1017/S0025315400048426

Miller, P., Antunes, R., Alves, A. C., Wensveen, P. J., Kvadsheim, P. H., and Tyack, P. L. (2011). *The 3S Experiments: Studying the Behavioural Effects of Naval Sonar on Killer Whales (Orcinus orca), Sperm Whales (Physeter macrocephalus), and Long-Finned Pilot Whales (Globicephala melas) in Norwegian Waters.* Scottish Oceans Institute Technical Report SOI-2011–I-2010.

Miller, P. J. O., Johnson, M. P., and Tyack, P. L. (2004a). Sperm whale behaviour indicates the use of echolocation click buzzes "creaks" in prey capture. *Proc. R. Soc. Lond. Ser. B* 217, 2239–2247. doi: 10.1098/rspb.2004.2863

Miller, P. J. O., Johnson, M. P., Tyack, P. L., and Terray, E. A. (2004b). Swimming gaits, passive drag and buoyancy of diving sperm whales *Physeter macrocephalus*. *J. Exp. Biol.* 6, 1953–1967. doi: 10.1242/jeb.00993

Møhl, B., Wahlberg, M., Madsen, P. T., Heerfordt, A., and Lund, A. (2003). The monopulsed nature of sperm whale clicks. *J. Acoust. Soc. Am.* 114, 1143–1154. doi: 10.1121/1.1586258

Mooney, T. A., Nachtigall, P. E., and Yuen, M. M. L. (2006). Temporal resolution of the Risso's dolphin, Grampus griseus, auditory system. *J. Compar. Physiol. A* 192, 373–380. doi: 10.1007/s00359-005-0075-4

Ridgway, S. H., and Carder, D. A. (2001). Assessing hearing and sound production in cetaceans not available for behavioral audiograms: experiences with sperm, pygmy sperm, and gray whales. *Aquat. Mammals* 27, 267–276. Available online at: https://aquaticmammalsjournal.org/share/AquaticMammalsIssueArchives/2001/AquaticMammals_27-03/27-03_Ridgway.pdf

Santos, M. B., Pierce, G. J., and Boyle, P. R. (1999). Stomach contents of sperm whales *Physeter macrocephalus* stranded in the North Sea 1990-1996. *Mar. Ecol. Prog. Ser.* 183, 281–294. doi: 10.3354/meps183281

Santos, M. B., Pierce, G. J., García Hartmann, M., Smeenk, C., Addink, M. J., Kuiken, T., et al. (2002). Additional notes on stomach contents of sperm whales *Physeter macrocephalus* stranded in the north-east Atlantic. *J. Mar. Biol. Assoc.* 82, 501–507. doi: 10.1017/S0025315402005787

Schnitzler, H., Moss, C. F., and Denzinger, A. (2003). From spatial orientation to food acquisition in echolocating bats. *Trends Ecol. Evol.* 18, 386–394. doi: 10.1016/S0169-5347(03)00185-X

Sergio, F., Caro, T., Brown, D., Clucas, B., Hunter, J., Ketchum, J., et al. (2008). Top predators as conservation tools: ecological rationale, assumptions, and efficacy. *Ann. Rev. Ecol. Evol. Syst.* 39, 1–19. doi: 10.1146/annurev.ecolsys.39.110707.173545

Simon, M. J., Kristensen, T. K., Tendal, O. S., Kinze, C. C., and Tougaard, S. (2003). *Gonatus fabricii* (*Mollusca*, Theuthida) as an important food source for sperm whales (*Physeter macrocephalus*) in the Northeast Atlantic. *Sarsia North Atlant. Mar. Sci.* 88, 244–246. doi: 10.1080/00364820310001688

Slater, G. J., Price, S. A., Santini, F., and Alfaro, M. E. (2010). Diversity versus disparity and the radiation of modern cetaceans. *Proc. R. Soc. B Biol. Sci.* 277, 3097–3104. doi: 10.1098/rspb.2010.0408

Spitz, J., Ridoux, V., and Brind'Amour A. (2014). Let's go beyond taxonomy in diet description: testing a trait-based approach to prey-predator relationships. *J. Anim. Ecol.* 83, 1137–1148. doi: 10.1111/1365-2656.12218

Spitz, J., Trites, A. W., Becquet, V., Brind'Amour A., Cherel, Y., Galois, R., et al. (2012). Cost of living dictates what whales, dolphins and porpoises eat: the importance of prey quality on predator foraging strategies. *PLoS ONE* 7:e50096. doi: 10.1371/journal.pone.0050096

Supin, A. Y., and Nachtigall, P. E. (2013). Gain control in the sonar of odontocetes. *J. Compar. Physiol. A* 199, 471–478. doi: 10.1007/s00359-012-0773-7

Teloni, V., Mark, J. P., Patrick, M. J. O., and Peter, M. T. (2008). Shallow food for deep divers : dynamic foraging behavior of male sperm whales in a high-latitude habitat. *J. Exp. Mar. Biol. Ecol.* 354, 119–131. doi: 10.1016/j.jembe.2007.10.010

Thode, A., and Mellinger, D. K. (2002). Depth-dependent acoustic features of diving sperm whales (*Physeter macrocephalus*) in the Gulf of Mexico. *J. Acoust. Soc. Am.* 112, 308–321. doi: 10.1121/1.1482077

Urick, R. (1989). Ambient Noise in the Sea. *J. Acoust. Soc. Am.* 86:1626. doi: 10.1121/1.398683

Wahlberg, M. (2002). The acoustic behaviour of diving sperm whales observed with a hydrophone array. *J. Exp. Mar. Biol. Ecol.* 281, 53–62. doi: 10.1016/S0022-0981(02)00411-2

Warrant, E. J., and Locket, N. A. (2004). Vision in the deep sea Vision in the deep sea. *Biol. Rev.* 79, 671–712. doi: 10.1017/S1464793103006420

Watwood, S. L., Miller, P. J. O., Johnson, M., Madsen, P. T., and Tyack, P. L. (2006). Deep-diving foraging behaviour of sperm whales (*Physeter macrocephalus*). *J. Anim. Ecol.* 75, 814–825. doi: 10.1111/j.1365-2656.2006.01101.x

Whitehead, H. (2003). *Sperm Whales: Social Evolution in the Ocean*. Chicago, IL: University of Chicago Press.

Whitehead, H., MacLeod, C. D., and Rodhouse, P. (2003). Differences in the niche breadth among some teuthivorous mesopelagic marine

mammals. *Mar. Mammal Sci.* 19, 400–406. doi: 10.1111/j.1748-7692.2003.tb01118.x

Wisniewska, D. M., Johnson, M., Beedholm, K., Wahlberg, M., and Madsen, P. T. (2012). Acoustic gaze adjustments during active target selection in echolocating porpoises. *J. Exp. Biol.* 215, 4358–4373. doi: 10.1242/jeb.074013

Wisniewska, D. M., Johnson, M., Nachtigall, P. E., and Madsen, P. T. (2014). Buzzing during biosonar-based interception of prey in the delphinids Tursiops truncatus and Pseudorca crassidens. *J. Exp. Biol.* 217, 4279–4282. doi: 10.1242/jeb.113415

Zimmer, W. M. X., Tyack, P. L., Johnson, M. P., and Madsen, P. T. (2005). Three-dimensional beam pattern of regular sperm whale clicks confirms bent-horn hypothesis. *J. Acoust. Soc. Am.* 117, 1473–1485. doi: 10.1121/1.1828501

Zucchini, W., MacDonald, I. L., and Langrock, R. (2016). *Hidden Markov Models for Time Series: An Introduction Using R, 2nd Edn.* Boca Raton, FL: CRC Press, Taylor & Francis Group.

Conflict of Interest Statement: The authors declare that the research was conducted in the absence of any commercial or financial relationships that could be construed as a potential conflict of interest.

Copyright © 2018 Isojunno and Miller. This is an open-access article distributed under the terms of the Creative Commons Attribution License (CC BY). The use, distribution or reproduction in other forums is permitted, provided the original author(s) and the copyright owner(s) are credited and that the original publication in this journal is cited, in accordance with accepted academic practice. No use, distribution or reproduction is permitted which does not comply with these terms.

frontiers in Marine Science

ORIGINAL RESEARCH
published: 11 December 2018
doi: 10.3389/fmars.2018.00465

Swimming Energy Economy in Bottlenose Dolphins Under Variable Drag Loading

Julie M. van der Hoop[1,2], Andreas Fahlman[3], K. Alex Shorter[4], Joaquin Gabaldon[4], Julie Rocho-Levine[5], Victor Petrov[6] and Michael J. Moore[2]*

[1] Department of Zoophysiology, Aarhus University, Aarhus, Denmark, [2] Department of Biology, Woods Hole Oceanographic Institution, Woods Hole, MA, United States, [3] Fundacion Oceanografic, Valencia, Spain, [4] Mechanical Engineering, University of Michigan, Ann Arbor, MI, United States, [5] Dolphin Quest Oahu, Honolulu, HI, United States, [6] Nuclear Engineering and Radiological Sciences, University of Michigan, Ann Arbor, MI, United States

Instrumenting animals with tags contributes additional resistive forces (weight, buoyancy, lift, and drag) that may result in increased energetic costs; however, additional metabolic expense can be moderated by adjusting behavior to maintain power output. We sought to increase hydrodynamic drag for near-surface swimming bottlenose dolphins, to investigate the metabolic effect of instrumentation. In this experiment, we investigate whether (1) metabolic rate increases systematically with hydrodynamic drag loading from tags of different sizes or (2) whether tagged individuals modulate speed, swimming distance, and/or fluking motions under increased drag loading. We detected no significant difference in oxygen consumption rates when four male dolphins performed a repeated swimming task, but measured swimming speeds that were 34% (>1 m s^{-1}) slower in the highest drag condition. To further investigate this observed response, we incrementally decreased and then increased drag in six loading conditions. When drag was reduced, dolphins increased swimming speed (+1.4 m s^{-1}; +45%) and fluking frequency (+0.28 Hz; +16%). As drag was increased, swimming speed (−0.96 m s^{-1}; −23%) and fluking frequency (−14 Hz; 7%) decreased again. Results from computational fluid dynamics simulations indicate that the experimentally observed changes in swimming speed would have maintained the level of external drag forces experienced by the animals. Together, these results indicate that dolphins may adjust swimming speed to modulate the drag force opposing their motion during swimming, adapting their behavior to maintain a level of energy economy during locomotion.

Summary Statement: Biologging and tracking tags add drag to study subjects. When wearing tags of different sizes, dolphins changed their swimming paths, speed, and movements to modulate power output and energy consumption.

Keywords: drag, swimming efficiency, adaptive behavior, tag effect, biomechanics, metabolism

OPEN ACCESS

Edited by:
Cory D. Champagne, National Marine Mammal Foundation, United States

Reviewed by:
Jennifer Maresh, West Chester University, United States
Boris Michael Culik, University of Kiel, Germany
Birgitte I. McDonald, Moss Landing Marine Laboratories, United States

****Correspondence:***
Julie M. van der Hoop
jvanderhoop@whoi.edu

Specialty section:
This article was submitted to Aquatic Physiology, a section of the journal Frontiers in Marine Science

Received: *28 July 2018*
Accepted: *20 November 2018*
Published: *11 December 2018*

Citation:
van der Hoop JM, Fahlman A, Shorter KA, Gabaldon J, Rocho-Levine J, Petrov V and Moore MJ (2018) Swimming Energy Economy in Bottlenose Dolphins Under Variable Drag Loading. Front. Mar. Sci. 5:465. doi: 10.3389/fmars.2018.00465

INTRODUCTION

Tagging studies strive to collect novel data in an environment where observations are difficult; tags can measure animal movement as well as environmental and physiological variables to help interpret animal behavior or performance (Johnson et al., 2009; Crossin et al., 2014; Hussey et al., 2015). Tags do, however, contribute additional weight and bulk, and more relevant in the marine realm, perturb the hydrodynamics of highly streamlined animals. It is important to understand the

impact of these devices not only on the tagged animal's vital rates (e.g., Barron et al., 2010; van der Hoop et al., 2014; Best et al., 2015), but also on their behavior which is often assumed to be representative of the untagged population (Ropert-Coudert and Wilson, 2004; Vandenabeele et al., 2011; Broell et al., 2016).

The physiological and behavioral changes associated with handling, attachment, healing, or sedation that may be involved in the tagging procedure can be difficult to separate, especially for short-term studies (Elliott et al., 2012; Jepsen et al., 2015). During swimming, at a given speed, resistive forces (e.g., drag, weight or buoyancy) created by a tag will require additional work from the animal. Additional thrust must be produced to counter drag or more lift to counter the weight of the tag. Drag forces increase with speed-squared and therefore present a steep trade-off (Bannasch et al., 1994; Jones et al., 2013): animals can maintain speed under higher drag conditions but will need to expend more energy to overcome added drag. Diving vertebrates may have several compensatory mechanisms for this added drag; for example, changes in dive behavior (Webb et al., 1998) that do not result in detectable changes in energy requirements (Fahlman et al., 2008). Additionally, animals may compensate for added drag by reducing their speed to modulate power output (van der Hoop et al., 2014). Experimental protocols manipulating drag on swimmers have been effective in quantifying these trade-offs, effects, and compensation strategies (e.g., Webb, 1971a,b).

In a previous study (van der Hoop et al., 2014), bottlenose dolphins (*Tursiops truncatus*) changed their swimming behavior in response to drag loading from a bio-logging tag (DTAG2; Johnson and Tyack, 2003). Dolphins performing a repeated swimming task slowed down to the point where the tag yielded no increases in drag or power; in doing so, individuals' energy consumption rates were no different. These results suggested that dolphins modify their behavior to adjust metabolic output and energy expenditure when faced with tag-induced drag. Other strategies exist to reduce the metabolic cost of these conditioned swimming tasks, e.g., changing movement paths between markers would enable individuals to reduce their total distance over time (Alexander, 2003; Ohashi et al., 2007). Building on our previous work, this research extends the experimental protocol monitoring swimming speeds and movement patterns to investigate the impact of multiple levels of drag loading to determine whether (1) metabolic rate increases systematically with greater levels of drag loading or (2) whether individuals employ strategies to adjust power output, such as changing speed, swimming distance or kinematics (fine-scale movements recorded on the tags).

MATERIALS AND METHODS

Overview

We trained four male bottlenose dolphins (**Table 1**) with operant conditioning to complete two types of swimming tasks to investigate the effect of drag loading on individuals' metabolic rates, swimming speeds, behaviors and kinematics. All experiments were by voluntary participation without restraint and the dolphin could refuse to participate or withdraw at any point during an experimental trial. Prior to initiating the study, we desensitized animals to the equipment and trained them for novel research-associated behaviors. All trials were conducted in a man-made lagoon (**Figure 1C**) approximately 38 m × 42 m, up to 3.5 m deep, at Dolphin Quest Oahu, Honolulu, HI, United States from 23 September–15 October 2013. Experiments were approved by the Woods Hole Oceanographic Institution Animal Care and Use Committee. A portion of the respirometry and energetics data were previously published elsewhere in a different context (Fahlman et al., 2016).

We defined drag loading as modifying an animal's total hydrodynamic drag by perturbing the fluid flow around the animal. Drag loading was increased on the animals by attaching a suction cup biologging tag and additional urethane elements of equivalent frontal area (*Drag Conditions*, below). The first swimming task (*Metabolic Trials*, below) involved measuring individuals' oxygen consumption before and after a continuous 10 min lap swim under three drag conditions (no tag, tag, tag+8; *Drag Conditions*, below). We did not measure oxygen consumption during the swimming task, but measured recovery rates following exercise as these kinetics can be used as an index for effort and energy stores (*Respirometry*, below; Royce, 1969; Di Prampero et al., 1970; Cohen-Solal et al., 1995). In the second swimming task (*Incremental Loading Trials*, below), two of the animals from the first study swam one lap at a time, as drag was adjusted incrementally through six drag conditions (no tag, tag, tag+2, tag+4, tag+6, tag+8) as swimming path and speed were measured by an aerial camera.

Drag Conditions

The animals performed the swimming tasks with and without the tag loading conditions. Swimming without a drag perturbation

TABLE 1 | Measurements and number and order of experimental metabolic trials.

Dolphin ID	Length (m)	Girth (m)	Body diameter (m)	Mass (kg)	*N* trials completed	Days between trials	Metabolic trial order
6JK5	2.61	1.40	0.45	198	9	2, 1, 2, 1, 4, 2, 4, 6	C, T+8, C, T, T+8, T, C, T, T+8
99L7	2.54	1.21	0.39	167	4	2, 5, 6	C, T, C, T
9FL3	2.73	1.49	0.47	240	9	2, 4, 2, 1, 2, 2, 1, 2	C, T, T+8, C, T+8, T, C, T+8, T
9ON6	2.46	1.28	0.41	171	4	1, 5, 4	T+8, C, T, C

Metabolic trials were performed under control (C, no tag), tag (T, DTAG3), and tag+8 (T+8) conditions. Girth was measured approximately two fingers in front of the dorsal fin after a breath cycle (exhale–inhale). Body diameter was estimated as girth/π.

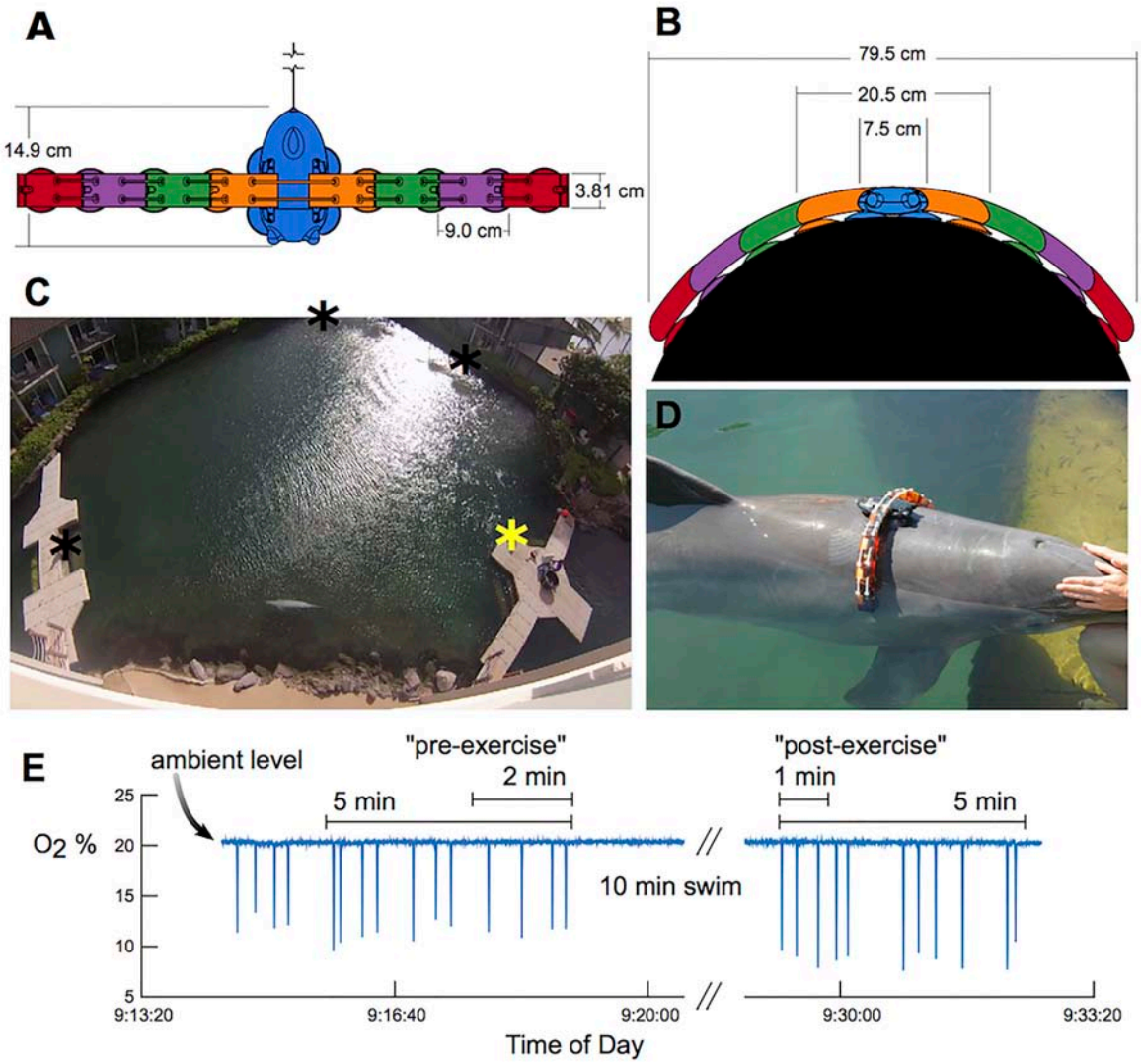

FIGURE 1 | The experimental setup. Top **(A)** and frontal **(B)** views of the DTAG (blue) and additional elements that were attached to increase drag loading. Each element has approximately the same cross-sectional area as the tag alone. **(C)** Dolphins swam between waypoints in the lagoon (stars), and oxygen consumption was measured at the main dock station (yellow star). **(D)** A bottlenose dolphin equipped with the tag+8 configuration: four elements attached on each side of a DTAG (black). **(E)** Example of oxygen concentration (O_2 %) measured with the respirometer over the duration of a metabolic trial, with 2-min "pre-exercise" and 1-min "post-exercise" and 10-min swim periods highlighted. Sudden drops in O_2% reflect inhalations by the dolphin.

was used as the control condition for the experiment. During the tag loading conditions we used a DTAG (version 3; Johnson and Tyack, 2003; Shorter et al., 2013), a suction-cup attached biologging tag approximately 15 cm in length (**Figure 1**), to record fine-scale movement data from the animal. In addition to the 'tag' condition, we also systematically increased the drag loading on the animal by attaching additional urethane elements to either side of the DTAG with zip ties (**Figures 1A,B,D**). Each drag element had approximately the same cross-sectional area as the tag itself. We refer to the resulting increased drag-loading conditions by the number of elements added, e.g., the tag+4 condition includes the tag and an additional four elements and the tag+8 condition includes the tag and an additional eight elements (**Figures 1A,B,D**). For all tag loading conditions, we attached the tag to the back of the animal, between the blowhole and dorsal fin to replicate the location of tags placed on wild animals. Metabolic trials were conducted without the tag (control), and with the tag and tag+8 configurations; Incremental Loading trials included all symmetrical drag loading conditions.

Computational Fluid Dynamics Simulations

In order to estimate the relative drag force between the tag conditions a set of computational fluid dynamics (CFD) simulations using commercial CFD code STAR-CCM+ (Siemens, Munich, Germany) were performed. In these

simulations, the tag geometry was modeled on a semi-cylindrical body in a non-confined channel with fully developed flow. Velocity and turbulence quantities at the flow inlet were obtained by performing simulations for flow in an empty channel assuming periodicity at different velocities 1, 2, 3, and 4 m s^{-1}. The Reynolds number, *Re*, ranged 1.6×10^6–6.6×10^6. Base cell sizes were selected in accordance with previously performed simulations on similar geometries (van der Hoop et al., 2014). The resulting mesh size varied between 20 and 25 million cells depending on the tag geometry. Simulations were performed using the standard k-ε model (Jones and Launder, 1972) in two-layer formulation (Rodi, 1991). While there are limitations associated with the k-ε turbulence model (Lloyd and Espanoles, 2002), this model results in a significant reduction of computational time, and examples in the literature have demonstrated that the k-ε model turbulence mode provides accurate results for geometries and flow conditions comparable to those presented in this work (Sridhar et al., 2010; Kinaci et al., 2015). Further, we were interested in relative differences between the forces created by a range of tag geometries and not absolute estimates of force, a question that lends itself well to an efficient computational approach.

Respirometry

To measure dolphins' respiratory flow and expired oxygen (O_2) and carbon dioxide (CO_2), we used a custom-made Fleisch type pneumotachometer and associated protocols as described in Fahlman et al. (2015). We estimated the O_2 consumption rate ($\dot{V}O_2$, mL O_2 min^{-1}) as previously described in Fahlman et al. (2015, 2016). We summed the total O_2 volume for each breath during the before- and after-exercise periods, and then divided by the duration of those periods to calculate the average $\dot{V}O_2$ before and after exercise. We report $\dot{V}O_2$ as measured (ml O_2 min^{-1}) and as mass-specific ($s\dot{V}O_2$, ml O_2 kg^{-1} min^{-1}) by dividing by the measured body mass of the individuals during the month of the study period (**Table 1**).

We calibrated the gas analyzers (ML206, Harvard Apparatus, sampling at 200 Hz) before and after the experiment using a commercial mixture of 5% O_2, 5% CO_2, and 90% N_2 (blend accuracy 0.10%; Praxair, Inc., Danbury, CT, United States). We used ambient air to check the calibration before and after each experimental trial. We obtained hourly mean air temperature, relative humidity and atmospheric pressure measurements from the National Weather Service database for the times of the trials (National Weather Service, 2015). All gas volumes were converted to standard temperature and pressure for dry air (STPD, Quanjer et al., 1993). Exhaled air was assumed to be saturated at 37°C, and inhaled air volume was corrected for ambient temperature and relative humidity. CO_2 was not removed from the air sample.

We used a specific experimental design to assess the metabolic changes associated with variation in drag, as follows. The dolphin was asked to remain neutrally buoyant at the water surface next to the trainer for at least 5 min immediately prior to exercise while the pneumotachometer was placed over the blow hole allowing the respiratory flow, gas content and metabolic rate to be determined (**Figures 1C,E**). The 'pre-exercise' metabolic rate was determined to be the average $\dot{V}O_2$ over the last 2 min of this period. By this time, the variability in the instantaneous $\dot{V}O_2$ had decreased. After the 10-min swimming task, the dolphin returned immediately to the measurement station, where we continuously measured the respiratory flow and gas composition for a minimum of 5 min. We defined the first 1 min of this period as the 'post-exercise' period over which we calculated the $\dot{V}O_2$. We fitted an exponential function to 30 s averages of measured $\dot{V}O_2$ in the post-exercise period and characterized these kinetics by the recovery half-time ($t_{1/2}$), defined as the time needed for $\dot{V}O_2$ to decrease from its peak value by half (Di Prampero et al., 1970).

Swimming Task 1: Metabolic Trials

To examine the metabolic impacts of increased drag, four dolphins were trained to swim around the lagoon clockwise with one of three drag conditions: control, Tag, or Tag+8. Four trainers, stationed at the same points for each trial (**Figure 1C**), directed the animal as it swam continuously between points for a minimum of 10 min (maximum = 10:33 min:sec). We did not control swimming speed or the total number of laps, but recorded swimming paths to estimate speed (see *Aerial Video*, below). We measured dolphins' metabolic rate before and after this 10-min swimming task (see *Respirometry*, above), but animals breathed freely while swimming. None of the breaths during the swim were measured with the respirometer, but were counted from aerial video to calculate the breathing frequency (breaths min^{-1}). We chose the drag condition for each trial at random for each individual; however, Dolphin 99L7 did not perform any trials with tag+8 due to earlier unsuccessful attempts to complete the task with high drag loading. A trial was terminated if the dolphin was not completing the task as directed, or if the animal chose to stop. Each dolphin performed only one swimming trial per day. All metabolic trials were completed 23 September–15 October 2013 between 8:37 and 11:18, when animals were pre-prandial.

Swimming Task 2: Incremental Drag Loading Trials

To determine the effects of incremental changes in drag loading and unloading on swimming path, speed and kinematics, two bottlenose dolphins swam laps between the same waypoints as above (**Figure 1C**), but in the counter-clockwise direction. After each lap, the animal stopped and drag loading elements were either added or removed. For both animals, the first lap began with the tag+8 loading condition. After each lap, drag elements were removed: tag+8, tag+6, tag+4, tag+2, tag, control. Drag on the animal was then increased in the reverse order, adding two elements after each lap: control, tag, tag+2, tag+4, tag+6, tag+8. A total of 12 laps were completed by each animal. We measured the time it took the animals to complete each lap, and recorded the swimming paths of the dolphins with a camera mounted above the lagoon (see *Aerial Video*, below). The time between laps (for the resistance to be adjusted) was on average 2:19 (*SD*: 2:01, IDs 6JK5) and 2:45 min (*SD*: 2:26, ID 9FL3) with a range of 0:30–8:38 min overall. We did not measure metabolic rate

during this second swimming task. We undertook trials between 12:00 and 15:05 on 14 October (ID 6JK5) and 15 October (ID 9FL3) 2013. Individuals had been fed before the trial, and were reinforced between laps. Approximately, 2 h elapsed between unloading and loading portions of the trial for both individuals.

Aerial Video Data Analysis

We installed a wall-mounted GoPro camera (Hero3 5.0 MegaPixel) to record aerial video footage of the lagoon (**Figure 1C**) during the Metabolic and Incremental Loading trials. Calibration and undistortion of the GoPro video was performed using the OCamCalib Matlab toolbox[1] (Scaramuzza et al., 2006; Rufli et al., 2008). Two separate calibration profiles were generated: one for the 16:9 aspect ratio for videos with frames of 1920 pixels by 1080 pixels, and another for the 4:3 aspect ratio for videos with frames of 1280 pixels by 960 pixels. The video data for all trials were undistorted using its applicable calibration profile and the undistortion tool in the toolbox.

Animal locations in the lagoon during the trials were digitized using Tracker (version 4.87; Brown, 2014) video tracking software. Collected track points were converted from the camera frame to the world frame using projective transforms. These transforms were generated by manually matching image pixel locations with known world coordinates of the lagoon, and computing the transformation matrix using the standard direct linear transformation (DLT) method. As the GoPro was not permanently mounted, each video required a separate transformation from image frame to world frame. Manually tracked points of the dolphins were converted to the world frame using these transformation matrices in homogeneous coordinate transformations. Average lap speed was calculated from the tracked camera data for 12 Metabolic trials (one for each animal × condition).

Tag Data Analysis

Data recorded by the inertial sensors on the DTAG (three-axis accelerometers and magnetometers) were processed with custom fluke-stroke detection algorithms (Johnson, 2015; Shorter et al., 2017). We resolved the amplitude of the body pitch acceleration (radians) and the fluke stroke rate (f, Hz) for all tag and drag loading conditions in Metabolic trials and Incremental Loading trials as in Shorter et al. (2017).

Modeled Drag and Predicted Swimming Speeds

The results from the CFD simulations were used to estimate the relative increase in drag force created by the different tag conditions (**Supplementary Figure S1**). We fitted power functions to the relationship between speed (U; m s^{-1}) and simulated drag (D; N):

$$D = aU^b \tag{1}$$

where a and b are coefficients for the power function derived by least squares (cftool; MATLAB, 2014). The differences in drag forces between the tag and the other loading conditions were then calculated (**Supplementary Figure S1**).

The net drag force (F_d) created by the body of the animal was modeled as:

$$F_d = 0.5\rho U^2 A_w C_d \tag{2}$$

Where, C_d is the drag coefficient (0.01), ρ is the density of the water (1029 kg m^{-3}), U is the relative speed of the animal in the water (1–4 m s^{-1}), and A_w is the wetted surface area of the animal (2.3 m^2) from (Fish, 1993).

Combining Eqs 2 and 3, we calculated the estimated drag forces for dolphins at their observed mean swimming speeds during the experimental conditions. Additionally, we calculated the swimming speed that would result in drag forces comparable to those in the control condition (U_{red}; m s^{-1} has drag forces equal to $D_{control,U\,obs}$; **Supplementary Figure S1**, closed circles), and estimated the forces that would be created if the animals maintained the swimming speed selected during the control condition using Eq. 3.

$$U_{red,condition} = \left(\frac{D_{control\ U=4}}{a}\right)^{(1/b)}. \tag{3}$$

Statistical Analysis

To determine whether metabolic rate differed between individuals or drag conditions, we used two-way ANOVA on three metabolic measures or proxies: post-exercise $\dot{V}O_2$, $\tau_{1/2}$ (min), and breathing frequency during swimming. Our expectation was that all metabolic indices would be higher with increased drag loading. We used two-way ANOVA with *post hoc* Tukey's test to determine whether swimming speed differed significantly between drag loading conditions, while controlling for individual behavior. We used two-way ANOVA to compare the fluke stroke frequency and amplitude between tag and tag+8 conditions during Metabolic trials. Statistical analyses were completed in MATLAB (2014) and R Core Team (2015). Reported values are mean ± SD.

RESULTS

Qualitatively, the CFD simulations illustrate how the tag and the added drag elements increased drag by perturbing the fluid flow around the instrument (**Figure 2**). The tag alone was relatively hydrodynamic with the flow remaining attached to the tag body, but the cup geometry created drag-inducing areas of stagnate recirculating flow. Adding bluff-bodied drag elements greatly affected flow around the tag, resulting in flow separation and large areas of recirculating flow behind the drag elements. As more drag elements were added this effect was magnified, resulting in increased drag and a growing disturbance to the fluid flow.

Metabolic Trials

Four dolphins performed 26 metabolic trials under different drag loading conditions (control, tag, tag+8), the number and order of which we list in **Table 1**. Mean (± SD) air temperature and humidity were 27.3 ± 1.0°C (range 25.0–29.4°C) and 62 ± 5% (48–69%) during the times of the trials. The mean

[1]https://sites.google.com/site/scarabotix/ocamcalib-toolbox

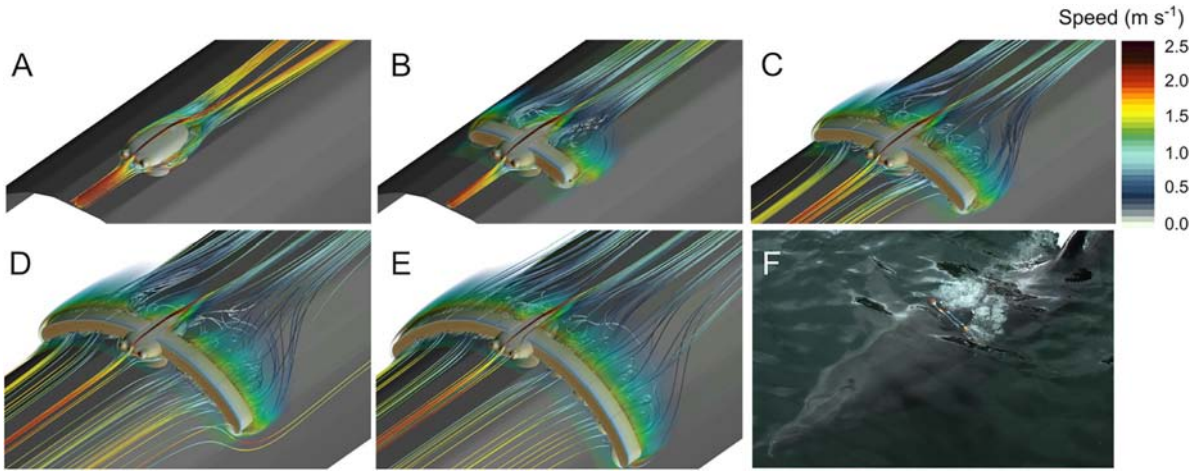

FIGURE 2 | Computational fluid dynamics (CFD) simulation results for the different tag configurations in 2 m s^{-1} flow: **(A)** Tag, **(B)** Tag+2, **(C)** Tag+4, **(D)** Tag+6, and **(E)** Tag+8. These results illustrate how the tag and added drag elements affect the velocity of the flow in the simulation. **(F)** A representative example of how the tag and drag elements modified the flow around the animal during the experiment.

atmospheric pressure was 1016.7 ± 1.1 hPa (1014.8–1018.9 hPa) and mean water temperature in the lagoon was 24.6 ± 0.5°C. Different individuals had significantly different $\dot{V}O_2$ ($F_{3,20}$ = 5.09, $p < 0.0088$) and s$\dot{V}O_2$ ($F_{3,20}$ = 4.31; p = 0.0169) in the first minute after exercise; however, we did not detect a significant effect of drag on either $\dot{V}O_2$ or s$\dot{V}O_2$ (**Figure 3** and **Table 2**).

There was no significant difference in the $\tau_{1/2}$ with drag condition (**Table 2**); $\dot{V}O_2$ returned to half its maximum value after 1.97 ± 1.25 min (e.g., **Figure 4**). $\tau_{1/2}$ was highly variable between individuals ($F_{3,20}$ = 5.41; p = 0.0073). There was no significant effect of drag loading on breathing frequency during the 10-min swimming task (**Table 2** and **Supplementary Figure S2**). Drag condition significantly affected swimming speed (**Figure 5** and **Table 2**); mean swimming speed was no different between control and tag-only conditions (Tukey HSD; p = 0.9182) but, when instrumented with the tag+8, swimming speed was significantly slower compared to in control and tag conditions (by 34 and 33% respectively; Tukey HSD; p = 0.0007 and 0.0009; **Figure 5**). Dolphins swam with significantly lower fluke stroke frequencies at higher drag loading, but no difference in pitch amplitude was detected (**Table 2**).

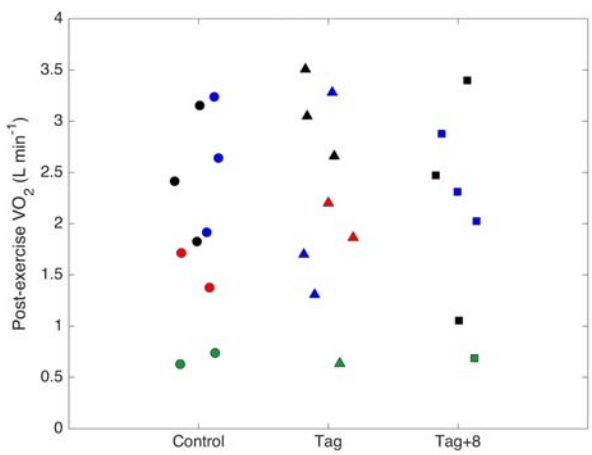

FIGURE 3 | Oxygen consumption rates (VO_2; L min^{-1}) of four bottlenose dolphins (represented by different colors) measured in the first minute after a 10-min swimming trial under control (no tag), tag and tag+8 conditions. Data points represent separate trials.

Incremental Loading Trials

The swimming path of the dolphins during the different loading conditions is presented in **Figure 6**. As drag loading was decreased, the animal's swimming speed and total distance traveled increased. Conversely, as drag loading was increased swimming speed and total distance traveled decreased (**Supplementary Figure S3**). The decreases in swim speed observed compared to the control were similar to predicted values from CFD simulations, if individuals were changing speed to maintain drag forces (**Figure 7**). Compared to the control (no tag), the two dolphins slowed on average 14 ± 4% when wearing just the tag, and slowed 24 ± 7, 27 ± 6, 35 ± 10, and 38 ± 6% with the tag+2, +4, +6, and +8 configurations, respectively (**Figure 7**). CFD simulations predicted a similar pattern but much smaller speed reductions compared to those observed. For example, CFD predicted a 1% speed reduction from the tag only, to 16% speed reduction for the tag+8 (**Figure 7** and **Table 3**). Fluke stroke frequencies increased with swimming speed during Incremental Loading trials (**Figure 8A**). The overall trend was an increase in f as drag was removed from tag+8 to tag; however, individuals differed in the magnitude of responses between conditions (**Figure 8C**). As drag was added again, one individual decreased f while the other remained fairly consistent (**Figure 8C**). Mean fluke stroke amplitude decreased with speed (**Figure 8B**) and as drag was reduced (**Figure 8D**). Amplitudes

TABLE 2 | Mean (± SD) values of mass-specific metabolic rate (sVO_2; ml O_2 kg^{-1} min^{-1}), recovery half time ($\tau_{1/2}$; min), breathing frequency, swimming speed (m s^{-1}), fluke stroke rate (FSR; Hz), and pitch amplitude (radians).

Drag loading condition	sVO_2 (ml O_2 kg^{-1} min^{-1})	$\tau_{1/2}$ (min)	Breath frequency (breaths min^{-1})	Speed (m s^{-1})	FSR (Hz)	Amplitude (rad)
Control	0.0096 (0.0039)	1.45 (1.09)	3.8 (0.9)	3.2 (0.4)	NA	NA
Tag	0.0109 (0.0040)	1.53 (1.05)	3.1 (0.9)	3.2 (0.2)	1.20 (0.06)	0.34 (0.02)
Tag+8	0.0098 (0.0042)	2.08 (1.82)	2.9 (0.5)	2.1 (0.1)	1.04 (0.14)	0.38 (0.10)
$F_{2,20}$	0.20	0.49	2.77	36.8	$F_{1,3}$ = 12.35	$F_{1,3}$ = 0.52
p	0.8193	0.6219	0.0870	0.0004	0.0391	0.5231

F-Statistics and p-values are shown for two-way ANOVA. Note that fluke stroke rate and amplitude are not available for the control (i.e., no tag) condition, as they are measures obtained by the tags themselves.

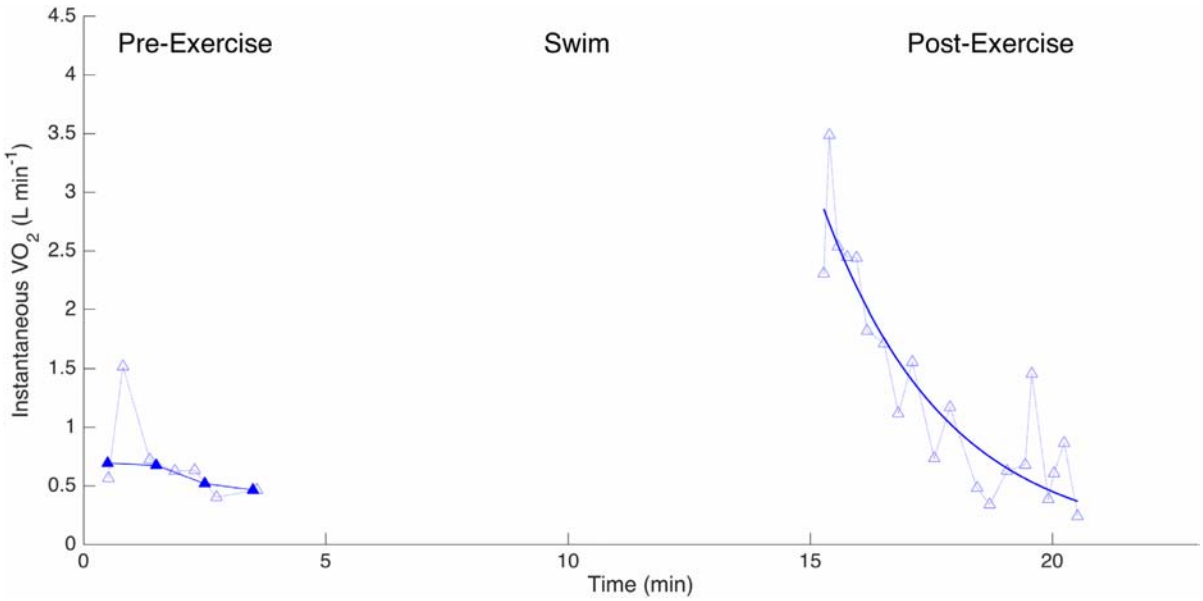

FIGURE 4 | Measurements of instantaneous $\dot{V}O_2$ (oxygen consumption, L min^{-1}) for one dolphin before and after exercise when wearing a biologging tag. Lighter symbols connected with dotted lines reflect individual measurements. Darker symbols with a solid line represent 30-s averages. The solid line post-exercise is the exponential decay curve from which the recovery half-time is calculated.

increased as drag was added again, though the shape of this response varied between individuals (**Figure 8D**).

DISCUSSION

Energy economy plays an important part in behavioral strategies animals employ to locomote (Fish, 1998; Williams et al., 2000); as such, tagged animals may compensate for drag from biologging tags by modifying swimming biomechanics or behavior. In this work, we investigated if and how animals modify their behavior in response to hydrodynamic loading created by tags of increasing size, or if and how they accommodate the increased drag created by the tag.

Despite the significant increase in drag created by the largest tag loading condition, the 10-min exercise period did not lead to a detectable difference in the recovery $\dot{V}O_2$ during the post-exercise period for any of the loading conditions (**Figures 3, 4**). We did not expect a significant effect of the tag-only configuration, given lower drag loading [1.02× total increase, 4 N at 4 m s^{-1} compared to the larger DTAG2 used in van der Hoop et al. (2014); 1.17× total increase; 20 N at 4 m s^{-1}], which also yielded no detectable metabolic effect. But we did expect an increased cost associated with the tag+8 attachment. The simulations predicted that the tag+8 configuration would increase the drag on the dolphins by 77 N at 4 m s^{-1}, a 1.4× total increase, but we detected no consistent or significant metabolic effect during recovery. This could be because the dolphins decreased their swimming speed by 34% and reduced their fluke stroke rates compared to the control condition. This change in speed reduced the estimated drag on the animal by 40% (125 to 74 N; **Figure 5**). The effect of the tag without added drag elements was less dramatic, with no detectable difference in swimming speed between the control and tag conditions (**Figure 5**).

By incrementally changing the tag configuration (Incremental Loading trials), we were able to demonstrate two additional examples where the dolphins modified their behavior in response to small (<20 N) changes in drag. Using a more thorough

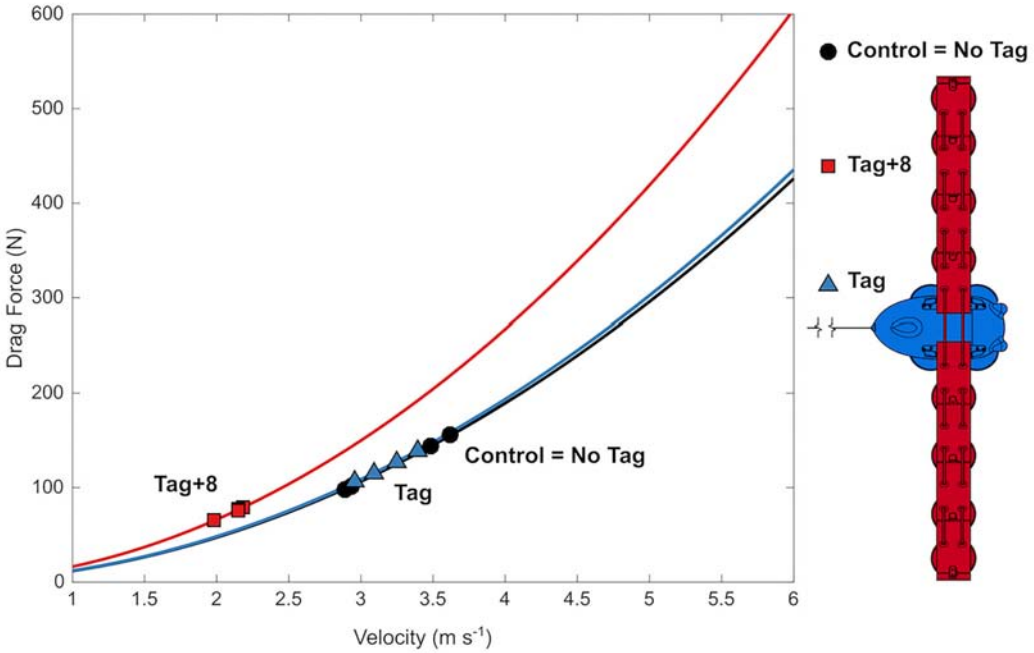

FIGURE 5 | Mean swimming speed decreases with drag loading and estimated total body drag was maintained. Drag forces with velocity (lines) estimated from CFD simulations, and at mean swimming velocities (symbols) observed during 12 Metabolic trials (one for each animal × condition).

combination of data types and analysis methods (camera-tracked speed and position data, along with animal-borne tag data) with a subset of the animals (n = 2) we were able to measure other changes in behavior that occurred in response to the drag loading. When drag was reduced by removing elements (Incremental Loading trials), dolphins changed their fluke stroke rate, swimming speed, and modified their swimming path. As drag was increased again, dolphins reduced fluke stroke rate, slowed down, and decreased total distance traveled (**Figures 6–8** and **Table 3**). We did observe differences in the response to the loading between individuals; for example, one individual showed a large increase in fluke stroke rate between Tag+8 and Tag+4 during unloading (**Figure 8C**) whereas fluke stroke rate was relatively unchanged during re-loading. These differences in response may be related to small changes in amplitude and speed (Fish and Rohr, 1999). We did not detect a difference in fluke stroke amplitude during Metabolic trials, while we did see a decrease in amplitude with speed in the Incremental Loading trials (**Figure 8B**). This may be due to the higher swimming speeds or sample size across a range of drag scenarios; future work to further quantify the timing and interaction between these parameters, and how they change through time and with drag, would address more fundamental questions in swimming biomechanics. Interestingly, when swimming with the added drag during the Incremental Loading trials the animals slowed to speeds that reduced the overall estimated body drag to levels below what the simulations would predict if the animals were just slowing to maintain a constant body drag (**Figure 7**). This reduction in speed is likely not due to animals tiring from the exercise protocol as (1) the recovery time ($\tau_{1/2}$) from Metabolic trials was less than the average time between Incremental Loading trials (i.e., animals likely recovered between laps) and (2) the same changes in swimming speed and kinematics were observed in the shorter Incremental Loading and longer Metabolic trials.

In the Metabolic and Incremental loading trials, individuals reduced their speed more than we expected based on drag forces from CFD models (**Table 3**). CFD modeling predicted a 1–16% reduction in speed across the tag conditions, whereas we observed reductions of 14–38%, significant beyond the tag condition (**Table 2** and **Supplementary Figure S3**). Wearing the tag and additional elements may elicit effects separate from drag (associated with lift forces, handling, the sensation from the suction cups). Improved CFD modeling with full dolphin geometry may also reduce the discrepancy between expected and observed results.

Reduced activity levels have been observed in tagged bottlenose dolphins (Blomqvist and Amundin, 2004) and porpoises (Geertsen et al., 2004), along with significantly lower speeds in instrumented (Lang and Daybell, 1963; Skrovan et al., 1999) or pregnant dolphins (Noren et al., 2011). Other swimmers show similar behavioral changes in response to drag from external tags (Wilson et al., 1986; also reviewed in van der Hoop et al., 2014; Jepsen et al., 2015; Rosen et al., 2017) or other external features (e.g., van der Hoop et al., 2017). The dolphins in this study were able to reduce their speeds as there was no constraint to maintain it. Free-ranging animals face different motivators and constraints; for example, high-speed maneuvers are required to evade predators, pursue prey (Goldbogen

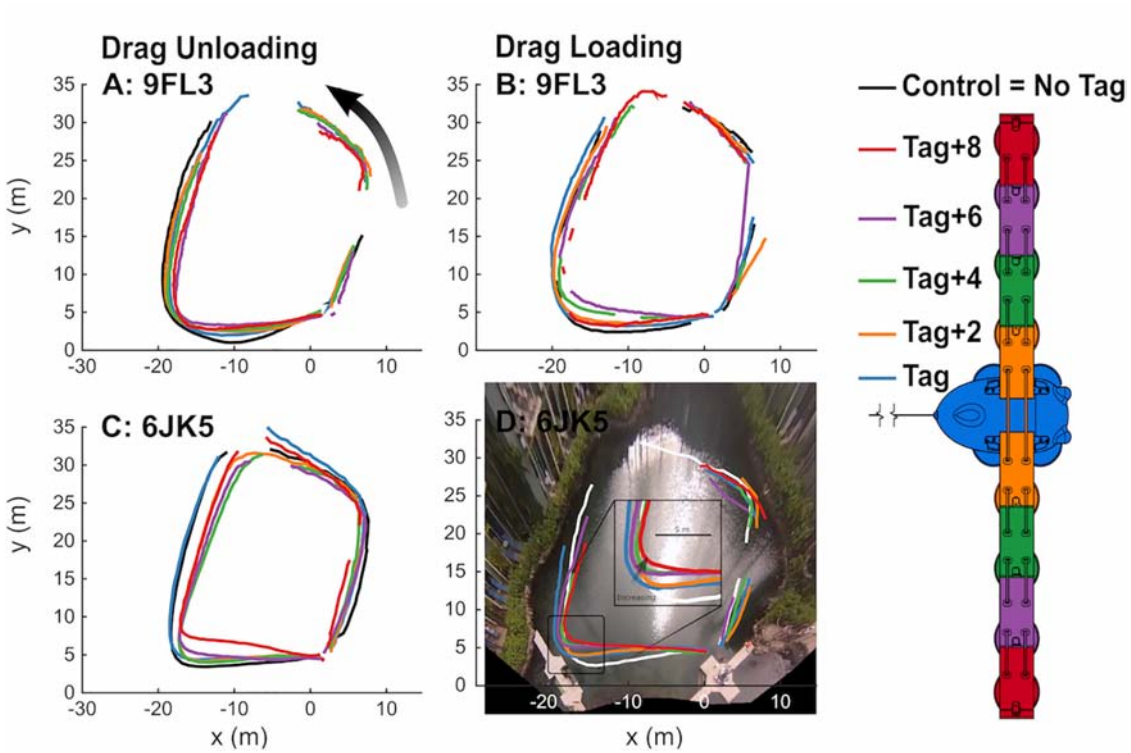

FIGURE 6 | Dolphins progressively changed swimming paths with drag unloading and loading. Paths of swimming dolphins 9FL3 **(A,B)** and 6JK5 **(C,D)** tracked from aerial video footage as they swam counter-clockwise between waypoints. Drag was progressively decreased **(A,C)** and then increased **(B,D)** through drag loading conditions without the tag and up to the tag+8 (right). Gaps in paths reflect time periods when the dolphins were not visible for > 2 time steps, ∼1 s. Note the zoomed inset in **(D)**.

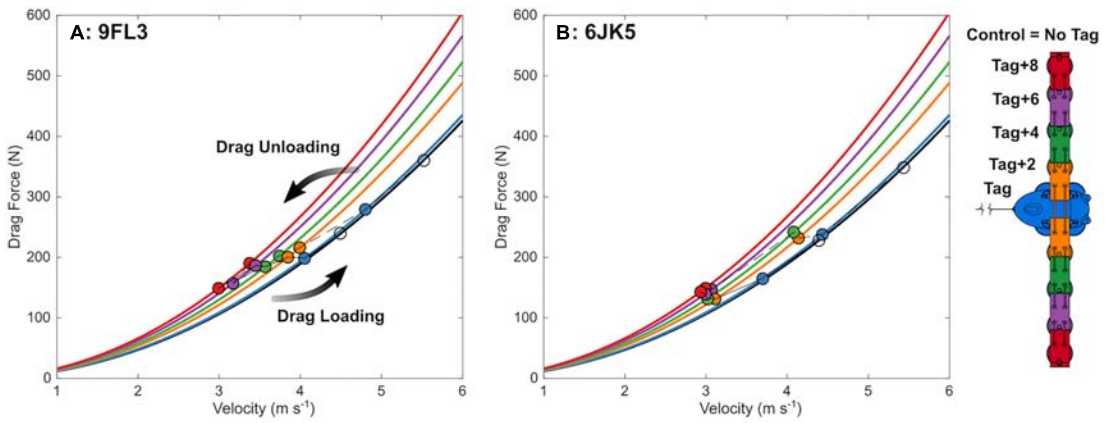

FIGURE 7 | Dolphins changed speed with incremental changes in drag loading, in line with what is expected from simulation models. Observed swimming speed (circles) and expected drag force at that speed (from CFD modeling; lines) in each experimental condition as drag is manipulated on two bottlenose dolphins (**A**: 9FL3 and **B**: 6JK5) by removing (connected by dotted lines) and adding (connected by solid lines) eurethane elements and a biologging tag (schematic right).

et al., 2007; Aguilar Soto et al., 2008) and maintain social cohesiveness (Wursig, 1982). Additional energetic expenses can occur when maintaining speed with higher drag. Fish and eels with external tags show significantly increased metabolic rates when maintaining swimming speeds (reviewed in Jepsen et al., 2015).

It is important to consider how these results in a controlled setting contribute a greater understanding of movement and energy in cetaceans. From an evolutionary standpoint, animals may seek to minimize energetic costs, especially those involved in everyday actions (e.g., routine swimming; Sparrow and Newell, 1998). Movements can be adapted

TABLE 3 | Equations for drag with speed from computational fluid dynamics (CFD) simulations of tags of increasing size and a dolphin without a tag and with tags of increasing size, the absolute (*N*) and percent increase in drag force at 4 m s^{-1}, and the expected absolute (m s^{-1}) and percent reduction in speed required to maintain drag forces when not wearing a tag at 4 m s^{-1}, and the observed speed (m s^{-1}) and change in speed (%) during Incremental Loading trials.

Drag condition	Simulated tags		Simulated tags and dolphin					Observed	
	Equation	Drag force (*N*)	Equation	Drag force (*N*)	Percent increase	Speed (m s^{-1})	Percent reduction	Speed (m s^{-1})	Percent reduction
No tag	–	–	$D = 11.8U^{2.0}$	189	–	4.00	–	5.0 ± 0.7	–
Tag	$D = 0.3U^{1.8}$	4	$D = 12.1U^{2.0}$	193	2	3.95	1	4.2 ± 0.3	14 ± 4
Tag+2	$D = 1.7U^{2.0}$	27	$D = 13.4U^{2.0}$	216	14	3.74	7	3.8 ± 0.2	24 ± 7
Tag+4	$D = 2.5U^{2.1}$	43	$D = 14.4U^{2.0}$	232	23	3.62	10	3.6 ± 0.1	27 ± 6
Tag+6	$D = 3.6U^{2.1}$	62	$D = 15.5U^{2.0}$	251	33	3.48	13	3.2 ± 0.2	35 ± 10
Tag+8	$D = 4.5U^{2.1}$	78	$D = 16.4U^{2.0}$	268	41	3.34	16	3.1 ± 0.2	38 ± 6

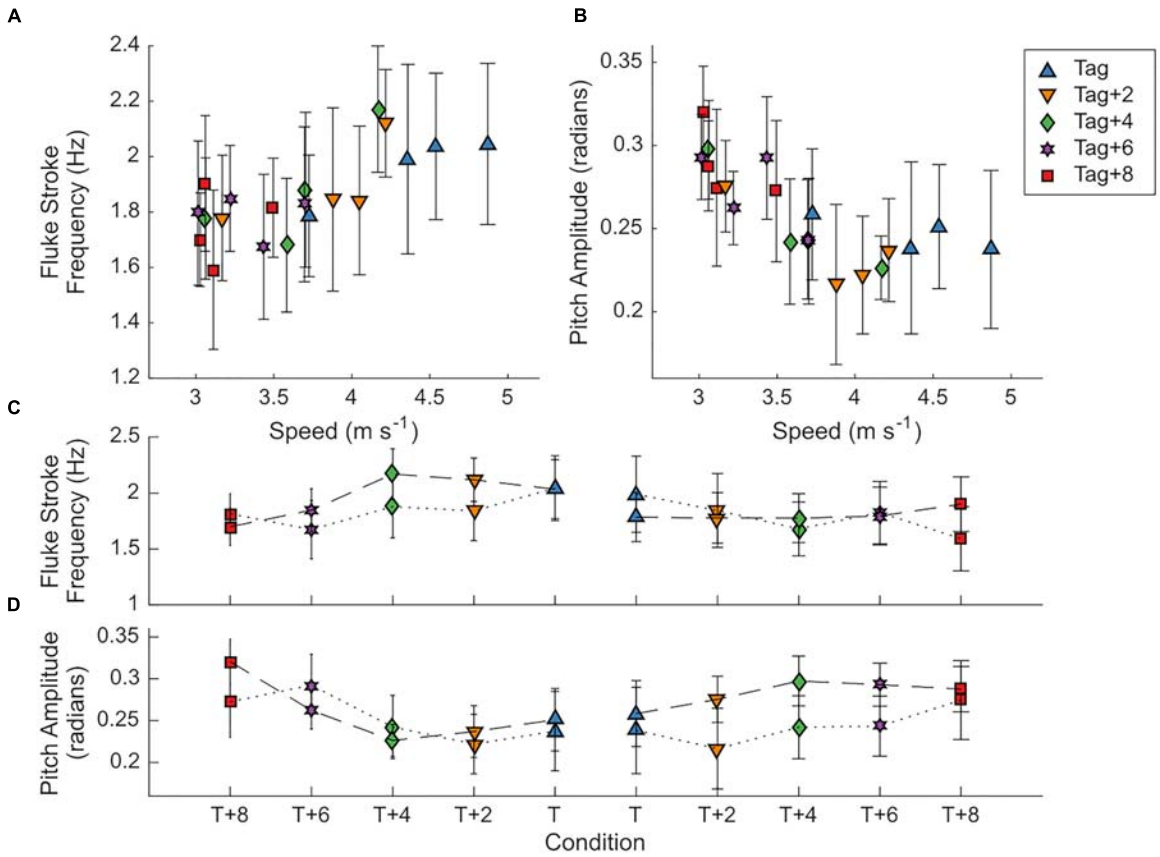

FIGURE 8 | Dolphins changed fine-scale movements with incremental changes in drag loading. **(A,B)** Mean ± SD fluke stroke frequency (Hz) and amplitude (rad) with speed (m s^{-1}) in all drag loading conditions for two individuals. **(C,D)** Mean ± SD fluke stroke frequency (Hz) and amplitude (rad) in two animals (Animal 9FL3 connected by dotted lines; 6JK5 connected by dashed lines) as drag elements and a biologging tag (right) are removed (connected by dotted lines) and then added (connected by solid lines) to manipulate drag loading.

to minimize metabolic energy expenditure with respect to constraints imposed by a task (swim from A to B), the environment (low drag, high drag), and the organism itself (body shape, size). By perceiving a difference in conditions between tasks and adapting behavior to reduce expenditure, the dolphins in this study are *economical* (Sparrow and Newell, 1998; Halsey, 2016). Beyond economy, these results indicate the sensitivity of these dolphins to small changes in their hydrodynamics, which changed their swimming speed (**Figure 7**), fluking (**Figure 8**), and more subtly their swimming paths (**Figure 6**) in response to small changes in drag loading. These results reflect specific responses of dolphins in this controlled setting, which offers the opportunity to combine measurements of individual energetics and biomechanics to

refine our understanding of energetically optimal swimming gaits and help interpret tag data recorded on free-swimming, wild marine mammals.

Implications for Tags on Free-Swimming Animals

Our experimental results indicate that even a relatively small increase from a hydrodynamic tag can result in measurable changes in behavior. The DTAG alone did not strongly or significantly affect the drag load on the bottlenose dolphins tested; as such, we expect it elicits little-to-no effect on animals of similar size and shape. The animal responses to the drag elements illustrate that larger tags, or those that are larger relative to the subject's body size (Portugal et al., 2018), as well as tags that are less hydrodynamically shaped, have the potential to affect measured biomechanics and swimming speed. The DTAG added 4 N at 4 m s^{-1} (increase of 2%) whereas the tag+2 added 27 N (increase of 14%; **Table 3**); these blunt drag elements therefore induce more drag than the original tag, and indicate the importance of shape. These experiments were also conducted with the tag in an optimal location for small cetaceans: between the blowhole and dorsal fin, in the forward-facing orientation. Tags deployed in capture-release programs are typically placed in this preferred position; however, pole-based deployments on cetaceans can result in variable attachment orientation and location. Tags placed on different regions of the body may have considerably different hydrodynamic regimes and will therefore contribute different drag and lift forces and pitching moments: when placed ahead of the point of maximal girth tags can lead to early flow separation and large increases in frontal area (Culik and Wilson, 1991; Healy et al., 2004; Vandenabeele et al., 2014), but those placed too far caudally can result in body destabilization. When oriented sideways or in any direction off-axis, hydrodynamic tags will have a greater frontal area; experimental and simulated drag forces on the similar tag bodies vary by ±10 N depending on orientation (Shorter et al., 2013). Based on these results we recommend that hydrodynamic tag housings continue to be designed and/or refined (Pavlov and Rashad, 2012; Balmer et al., 2013; Shorter et al., 2013; Fiore et al., 2017) as well as adopted (even when this affects the relative size of the tag), and that researchers directly acknowledge the potential tag impacts on their measured data, especially on smaller animals.

CONCLUSION

We sought to quantify the metabolic cost of biologging tags on bottlenose dolphins during a controlled swimming task. A combination of data types (e.g., position, fine-scale movement, speed, and physiological measurements) allowed us to detect and measure alternative or adaptive strategies that tag subjects can use when faced with drag loading. When performing the tasks at their freely-chosen pace, dolphins adjusted their swimming speed and movement patterns, and no change in metabolic cost was detected. Further studies to constrain the task to determine metabolic impact when high-speed behaviors are maintained are required.

DATA AVAILABILITY

All data and code associated with this manuscript have been made available: doi: 10.5281/zenodo.1489118.

AUTHOR CONTRIBUTIONS

JvdH, AF, KS, JR-L, and MM developed concepts and performed fieldwork. JR-L directed animal husbandry and training. JvdH, AF, and JG processed and analyzed data. KS and VP conducted and analyzed simulations. JvdH, AF, KS, VP, JR-L, and MM wrote the manuscript.

FUNDING

Funding for this project was provided by the National Oceanographic Partnership Program (National Science Foundation via the Office of Naval Research N00014-11-1-0113 to MM) and the Office of Naval Research (ONR YIP Award N000141410563 to AF). Dolphin Quest provided in-kind support of animals, crew, and access to resources. JvdH was supported by a Postgraduate Scholarship from the Natural Sciences and Engineering Research Council of Canada.

ACKNOWLEDGMENTS

The authors give special thanks to Dolphin Quest Oahu whose dolphin interactive facility at The Kahala Hotel & Resort served as a critically important controlled research environment for this study. They thank JvdH's thesis committee members for additional comments that improved the manuscript, and D. Zhang and A. Stoldt for assistance with camera and tag data processing.

SUPPLEMENTARY MATERIAL

The Supplementary Material for this article can be found online at: https://www.frontiersin.org/articles/10.3389/fmars.2018.00465/full#supplementary-material

FIGURE S1 | Drag forces on a bottlenose dolphin (black) and a dolphin instrumented with a tag (blue) and tags with additional drag-adding elements as simulated and predicted from computational fluid dynamics (solid lines). Coefficients for the equations for each condition (e.g., $Dtag{+}8 = aU^b$) are listed in **Table 3**. With added drag, dolphins can maintain speed (e.g., 4 m s^{-1}) but experience higher drag forces (open symbols) or can reduce speed (e.g., U_{red},*tag+8*) to maintain the drag force they experience when not wearing a tag (e.g., $D_{control}$, $U = 4$; solid symbols).

FIGURE S2 | Mean breathing frequency of four bottlenose dolphins (each represented by different colors) during a 10-min swimming task when wearing no tag (control; circles), a biologging tag (triangles) and a tag with eight extra drag elements (tag+8; squares).

FIGURE S3 | Total distance traveled (m) versus swimming speed (m s^{-1}) of the two dolphins (Animal 9FL3 open symbols; 6JK5 closed symbols) in the Incremental Loading Trials.

REFERENCES

Aguilar Soto, N., Johnson, M. P., Madsen, P. T., Diaz, F., Dominguez, I., Brito, A., et al. (2008). Cheetahs of the deep sea: deep foraging sprints in short-finned pilot whales off Tenerife (Canary Islands). *J. Anim. Ecol.* 77, 936–947. doi: 10.1111/j.1365-2656.2008.01393.x

Alexander, R. M. N. (2003). *Principles of Animal Locomotion*. Princeton, NJ: Princeton University Press. doi: 10.1515/9781400849512

Balmer, B. C., Wells, R. S., Howle, L. E., Barleycorn, A. A., McLellan, W. A., Ann Pabst, D., et al. (2013). Advances in cetacean telemetry: a review of single-pin transmitter attachment techniques on small cetaceans and development of a new satellite-linked transmitter design. *Mar. Mamm. Sci.* 30, 656–673. doi: 10.1111/mms.12072

Bannasch, R., Wilson, R. P., and Culik, B. M. (1994). Hydrodynamic aspects of design and attachment of a back-mounted device in penguins. *J. Exp. Biol.* 194, 83–96.

Barron, D. G., Brawn, J. D., and Weatherhead, P. J. (2010). Meta-analysis of transmitter effects on avian behaviour and ecology. *Methods Ecol. Evol.* 1, 180–187. doi: 10.1111/j.2041-210X.2010.00013.x

Best, P. B., Mate, B., and Lagerquist, B. (2015). Tag retention, wound healing, and subsequent reproductive history of southern right whales following satellite-tagging. *Mar. Mamm. Sci.* 31, 520–539. doi: 10.1111/mms.12168

Blomqvist, C., and Amundin, M. (2004). An acoustic tag for recording directional pulsed ultrasounds aimed at free-swimming bottlenose dolphins (*Tursiops truncatus*) by conspecifics. *Aquat. Mamm.* 30, 345–356. doi: 10.1578/AM.30.3.2004.345

Broell, F., Burnell, C., and Taggart, C. T. (2016). Measuring abnormal movements in free-swimming fish with accelerometers: implications for quantifying tag and parasite load. *J. Exp. Biol.* 219, 695–705. doi: 10.1242/jeb.133033

Brown, D. (2014). *Tracker Video Analysis and Modeling Tool*. Available at: http://www.cabrillo.edu/∼dbrown/tracker/ accessed 8 November 2014

Cohen-Solal, A., Laperche, T., Morvan, D., Geneves, M., Caviezel, B., and Gourgon, R. (1995). Prolonged kinetics of recovery of oxygen consumption after maximal graded exercise in patients with chronic heart failure. analysis with gas exchange measurements and NMR spectroscopy. *Circulation* 91, 2924–2932. doi: 10.1161/01.CIR.91.12.2924

Crossin, G. T., Cooke, S. J., Goldbogen, J. A., and Phillips, R. A. (2014). Tracking fitness in marine vertebrates: current knowledge and opportunities for future research. *Mar. Ecol. Prog. Ser.* 496, 1–17. doi: 10.3354/meps10691

Culik, B., and Wilson, R. P. (1991). Swimming energetics and performance of instrumented adelie penguins (*Pygoscelis adeliae*). *J. Exp. Biol.* 158, 355–368.

Di Prampero, P. E., Davies, C. T., Cerretelli, P., and Margaria, R. (1970). An analysis of O2 debt contracted in submaximal exercise. *J. Appl. Physiol.* 29, 547–551. doi: 10.1152/jappl.1970.29.5.547

Elliott, K. H., McFarlane-Tranquilla, L., Burke, C. M., Hedd, A., Montevecchi, W. A., and Anderson, W. G. (2012). Year-long deployments of small geolocators increase corticosterone levels in murres. *Mar. Ecol. Prog. Ser.* 466, 1–7. doi: 10.3354/meps09975

Fahlman, A., Hastie, G. D., Rosen, D. A. S., Naito, Y., and Trites, A. W. (2008). Buoyancy does not affect diving metabolism during shallow dives in Steller sea lions *Eumetopias jubatus*. *Aquat. Biol.* 3, 147–154. doi: 10.3354/ab00074

Fahlman, A., Loring, S. H., Levine, G., Rocho-Levine, J., Austin, T., and Brodsky, M. (2015). Lung mechanics and pulmonary function testing in cetaceans. *J. Exp. Biol.* 218, 2030–2038. doi: 10.1242/jeb.119149

Fahlman, A., van der Hoop, J., Moore, M. J., Levine, G., Rocho-Levine, J., and Brodsky, M. (2016). Estimating energetics in cetaceans from respiratory frequency: why we need to understand physiology. *Biol. Open* 5, 436–442. doi: 10.1242/bio.017251

Fiore, G., Anderson, E., Garborg, C. S., Murray, M., Johnson, M., Moore, M. J., et al. (2017). From the track to the ocean: using flow control to improve marine bio-logging tags for cetaceans. *PLoS One* 12:e0170962. doi: 10.1371/journal.pone.0170962

Fish, F. E. (1993). Power output and propulsive efficiency of swimming bottlenose dolphins (*Tursiops truncatus*). *J. Exp. Biol.* 185, 179–193.

Fish, F. E. (1998). Comparative kinematics and hydrodynamics of odontocete cetaceans: morphological and ecological correlates with swimming performance. *J. Exp. Biol.* 201, 2867–2877.

Fish, F. E., and Rohr, J. J. (1999). *Review of Dolphin Hydrodynamics and Swimming Performance*. San Diego, CA: US Navy SPAWAR Systems Center Technical Report 1801. doi: 10.21236/ADA369158

Geertsen, B. M., Teilmann, J., Kastelein, R. A., Vlemmix, H. N. J., and Miller, L. A. (2004). Behaviour and physiological effects of transmitter attachments on a captive harbour porpoise (*Phocoena phocoena*). *J. Cetacean Res. Manag.* 6, 139–146.

Goldbogen, J. A., Pyenson, N. D., and Shadwick, R. E. (2007). Big gulps require high drag for fin whale lunge feeding. *Mar. Ecol. Prog. Ser.* 349, 289–301. doi: 10.1098/rsif.2008.0492

Halsey, L. G. (2016). Terrestrial movement energetics: current knowledge and its application to the optimising animal. *J. Exp. Biol.* 219, 1424–1431. doi: 10.1242/jeb.133256

Healy, M., Chiaradia, A., Kirkwood, R., and Dann, P. (2004). Balance: a neglected factor when attaching external devices to penguins. *Mem. Natl. Inst. Polar Res.* 58, 179–182.

Hussey, N. E., Kessel, S. T., Aarestrup, K., Cooke, S. J., Cowley, P. D., Fisk, A. T., et al. (2015). Aquatic animal telemetry: a panoramic window into the underwater world. *Science* 348:1255642. doi: 10.1126/science.1255642

Jepsen, N., Thorstad, E. B., Havn, T., and Lucas, M. C. (2015). The use of external electronic tags on fish: an evaluation of tag retention and tagging effects. *Anim. Biotelem.* 3:49. doi: 10.1186/s40317-015-0086-z

Johnson, M. (2015). *DTAG Toolbox for MATLAB*. Available at: http://soundtags.st-andrews.ac.uk/dtags/dtag-toolbox/

Johnson, M., Aguilar de Soto, N., and Madsen, P. T. (2009). Studying the behaviour and sensory ecology of marine mammals using acoustic recording tags: a review. *Mar. Ecol. Prog. Ser.* 395, 55–73. doi: 10.3354/meps08255

Johnson, M., and Tyack, P. (2003). A digital acoustic recording tag for measuring the response of wild marine mammals to sound. *IEEE J. Ocean. Eng.* 28, 3–12. doi: 10.1109/JOE.2002.808212

Jones, T. T., Van Houtan, K. S., Bostrom, B. L., Ostafichuk, P., Mikkelsen, J., Tezcan, E., et al. (2013). Calculating the ecological impacts of animal-borne instruments on aquatic organisms. *Methods Ecol. Evol.* 4, 1178–1186. doi: 10.1111/2041-210X.12109

Jones, W. P., and Launder, B. E. (1972). The prediction of laminarization with a two-equation model of turbulence. *Int. J. Heat Mass Transf.* 15, 301–314. doi: 10.1016/0017-9310(72)90076-2

Kinaci, O. K., Sukas, O. F., and Bal, S. (2015). Prediction of wave resistance by a reynolds-averaged navier–stokes equation–based computational fluid dynamics approach. *Proc. Inst. Mech. Eng. Part M* 230, 531–548.

Lang, T. G., and Daybell, D. A. (1963). *Porpoise Performance Tests in a Sea-Water Tank*. Naval Ordnance Test Station Technical Paper 3063. NAVWEPS Report 8060, Ridgecrest, CA: Naval Ordnance Test Station, 32. doi: 10.21236/AD0298742

Lloyd, G., and Espanoles, A. (2002). *Best Practice Guidelines for Marine Applications of Computational Fluid Dynamics*. London: WS Atkins Consultants and Members of the NSC, MARNET-CFD Thernatic Network, 84.

MATLAB (2014). *MATLAB and Statistics Toolbox Release 2014b*. Available at: http://www.mathworks.com/

National Weather Service (2015). *Weather Observations*, Vol. 2013. Honolulu, HI: Honolulu International Airport.

Noren, S. R., Redfern, J. V., and Edwards, E. F. (2011). Pregnancy is a drag: hydrodynamics, kinematics and performance in pre- and post-parturition bottlenose dolphins (*Tursiops truncatus*). *J. Exp. Biol.* 214, 4151–4159. doi: 10.1242/jeb.059121

Ohashi, K., Thomson, J. D., and D'Souza, D. (2007). Trapline foraging by bumble bees: IV. Optimization of route geometry in the absence of competition. *Behav. Ecol.* 18, 1–11. doi: 10.1093/beheco/arl053

Pavlov, V. V., and Rashad, A. M. (2012). A non-invasive dolphin telemetry tag: computer design and numerical flow simulation. *Mar. Mamm. Sci.* 28, E16–E27. doi: 10.1111/j.1748-7692.2011.00476.x

Portugal, S. J., White, C. R., and Börger, L. (2018). Miniaturization of biologgers is not alleviating the 5% rule. *Methods Ecol. Evol.* 9, 1662–1666. doi: 10.1016/j.cbpa.2016.05.025

Quanjer, P. H., Tammeling, G. J., Cotes, J. E., Pedersen, O. F., Peslin, R., and Yernault, J.-C. (1993). Lung volumes and forced ventilatory flows. *Eur. Resp. J.* 6, 5–40. doi: 10.1183/09041950.005s1693

R Core Team (2015). *R: A Language and Environment for Statistical Computing*. Available at: https://www.r-project.org/

Rodi, W. (1991). "Experience with two-layer models combining the k-e model with a one-equation model near the wall," in *Proceedings of the 29th Aerospace Sciences Meeting AIAA 91-0216*, (Reno, NA: AIAA). doi: 10.2514/6.1991-216

Ropert-Coudert, Y., and Wilson, R. P. (2004). Subjectivity in bio-logging science: do logged data mislead? *Mem. Natl. Inst. Polar Res.* 58, 23–33.

Rosen, D. A. S., Gerlinsky, C. G., and Trites, A. W. (2017). Telemetry tags increase the costs of swimming in northern fur seals, *Callorhinus ursinus*. *Mar. Mamm. Sci.* 34, 385–402. doi: 10.1111/mms.12460

Royce, J. (1969). Active and passive recovery from maximal aerobic capacity work. *Int. Z. Angew. Physiol.* 28, 1–8. doi: 10.1007/BF00696033

Rufli, M., Scaramuzza, D., and Siegwart, R. (2008). "Automatic detection of checkerboards on blurred and distorted images," in *Proceedings of the IEEE/RSJ International Conference on Intelligent Robots and Systems (IROS 2008)*, Nice. doi: 10.1109/IROS.2008.4650703

Scaramuzza, D., Martinelli, A., and Siegwart, R. (2006). "A toolbox for easy calibrating omnidirectional cameras," in *Proceedings to IEEE International Conference on Intelligent Robots and Systems (IROS 2006)*, Beijing. doi: 10.1109/IROS.2006.282372

Shorter, K. A., Murray, M. M., Johnson, M., Moore, M. J., and Howle, L. E. (2013). Drag of suction cup tags on swimming animals: modeling and measurement. *Mar. Mamm. Sci.* 30, 726–746. doi: 10.1111/mms.12083

Shorter, K. A., Shao, Y., Ojeda, L., Barton, K., Rocho-Levine, J., van der Hoop, J., et al. (2017). A day in the life of a dolphin: using bio-logging tags for improved animal health and well-being. *Mar. Mamm. Sci.* 33, 785–802. doi: 10.1111/mms.12408

Skrovan, R. C., Williams, T. M., Berry, P. S., Moore, P. W., and Davis, R. W. (1999). The diving physiology of bottlenose dolphins (*Tursiops truncatus*). II. Biomechanics and changes in buoyancy at depth. *J. Exp. Biol.* 202, 2749–2761.

Sparrow, W. A., and Newell, K. M. (1998). Metabolic energy expenditure and the regulation of movement economy. *Psychon. Bull. Rev.* 5, 173–196. doi: 10.3758/BF03212943

Sridhar, D., Bhanuprakash, T. V. K., and Das, H. N. (2010). Frictional resistance calculations on a ship using CFD. *Int. J. Comput. Appl.* 11, 24–31. doi: 10.5120/1577-2109

van der Hoop, J. M., Fahlman, A., Hurst, T., Rocho-Levine, J., Shorter, K. A., Petrov, V., et al. (2014). Bottlenose dolphins modify behavior to reduce metabolic effect of tag attachment. *J. Exp. Biol.* 217, 4229–4236. doi: 10.1242/jeb.108225

van der Hoop, J. M., Nowacek, D. P., Moore, M. J., and Triantafyllou, M. S. (2017). Swimming kinematics and efficiency of entangled North Atlantic right whales. *Endanger. Species Res.* 32, 1–17. doi: 10.3354/esr00781

Vandenabeele, S., Wilson, R., and Grogan, A. (2011). Tags on seabirds: how seriously are instrument-induced behaviours considered? *Anim. Welf.* 20, 559–571.

Vandenabeele, S. P., Grundy, E., Friswell, M. I., Grogan, A., Votier, S. C., and Wilson, R. P. (2014). Excess baggage for birds: inappropriate placement of tags on gannets changes flight patterns. *PLoS One* 9:e92657. doi: 10.1371/journal.pone.0092657

Webb, P. M., Crocker, D. E., Blackwell, S. B., Costa, D. P., and Le Boeuf, B. J. (1998). Effects of buoyancy on the diving behavior of northern elephant seals. *J. Exp. Biol.* 201, 2349–2358.

Webb, P. W. (1971a). The swimming energetics of trout I. Thrust and power output at cruising speeds. *J. Exp. Biol.* 55, 489–520.

Webb, P. W. (1971b). The swimming energetics of trout II. Oxygen consumptin and swimming efficiency. *J. Exp. Biol.* 55, 521–540.

Williams, T. M., Davis, R. W., Fuiman, L. A., Francis, J., Le Boeuf, B. J., Horning, M., et al. (2000). Sink or swim: strategies for cost-efficient diving by marine mammals. *Science* 288, 133–136. doi: 10.1126/science.288.5463.133

Wilson, R. P., Grant, W. S., and Duffy, D. C. (1986). Recording devices on free-ranging marine animals: does measurement affect foraging performance? *Ecology* 67, 1091–1093. doi: 10.2307/1939832

Wursig, B. (1982). Radio tracking dusky porpoises in the South Atlantic. *Mamm. seas* 4, 145–160.

Conflict of Interest Statement: The authors declare that the research was conducted in the absence of any commercial or financial relationships that could be construed as a potential conflict of interest.

Copyright © 2018 van der Hoop, Fahlman, Shorter, Gabaldon, Rocho-Levine, Petrov and Moore. This is an open-access article distributed under the terms of the Creative Commons Attribution License (CC BY). The use, distribution or reproduction in other forums is permitted, provided the original author(s) and the copyright owner(s) are credited and that the original publication in this journal is cited, in accordance with accepted academic practice. No use, distribution or reproduction is permitted which does not comply with these terms.

frontiers in Ecology and Evolution

REVIEW
published: 18 December 2018
doi: 10.3389/fevo.2018.00213

Recent Advances in Data Logging for Intertidal Ecology

*Richard Judge, Francis Choi and Brian Helmuth**

Department of Marine and Environmental Sciences, Marine Science Center, Northeastern University, Nahant, MA, United States

Temperature is among the most ubiquitous determinants of organism growth, survival, and reproduction. Accurate recordings and predictions of how the temperatures of plants and animals vary in time and space are therefore critical to forecasting the likely impacts of global climate change. Intertidal zones have long served as a model ecosystem for examining the role of environmental stress on patterns of species distributions, and are emerging as models for understanding the ecological impacts of climate change. Intertidal environments are among the most physically demanding habitats on the planet, and excursions in body temperature of ectotherms can exceed 25°C over the course of a few hours. It is now well-known that the body temperatures of intertidal organisms can deviate significantly from the temperature of the surrounding air and substrate due to the influence of solar radiation, and that their size, color, morphology, and material properties markedly influence their temperatures. While many intertidal organisms are slow moving or almost entirely sessile, for others, behavior can play a significant role in driving vulnerability to temperature extremes. We explore datalogging methods used in intertidal zones and discuss the advantages and drawbacks of each. We show how measurements made *in situ* reveal patterns of thermal stress that otherwise would be undetectable using more remotely-sensed data. Additionally, we explore the idea that the relevant "grain size" of the physical environment, and thus the spatial scale that must be measured, is a function of (1) the size of the organism relative to local refugia; (2) an organism's ability to sense and to some degree predict near-term environmental conditions; and (3) an animal's movement speed and directionality toward refugia. Similarly, relevant temporal scales depend on the size, behavior, and physiological response of the organism. While miniaturization of dataloggers has significantly improved, several significant limitations still exist, many of which relate to difficulties in recording behavioral responses to changing environmental conditions. We discuss recent innovations in monitoring and modeling intertidal temperatures, and the important role that they have played in bridging ecological and physiological studies of ongoing impacts of climate change.

Keywords: behavior, climate change, biomimetic sensor, intertidal, logging, thermal physiology

OPEN ACCESS

Edited by:
Thomas Wassmer, Siena Heights University, United States

Reviewed by:
Bernardo R. Broitman, Centro de Estudios Avanzados en Zonas Áridas (CEAZA), Chile
Elvira S. Poloczanska, Helmholtz-Gemeinschaft Deutscher Forschungszentren (HZ), Germany

***Correspondence:**
Brian Helmuth
b.helmuth@northeastern.edu

Specialty section:
This article was submitted to Behavioral and Evolutionary Ecology, a section of the journal Frontiers in Ecology and Evolution

Received: *31 July 2018*
Accepted: *28 November 2018*
Published: *18 December 2018*

Citation:
Judge R, Choi F and Helmuth B (2018) Recent Advances in Data Logging for Intertidal Ecology. Front. Ecol. Evol. 6:213. doi: 10.3389/fevo.2018.00213

INTRODUCTION

Temperature is among the most universal determinants of a plant or animal's physiological performance and survival (Somero, 2010; Sinclair et al., 2016). Metabolism, heart rate (in animals with hearts), and enzyme functioning are all strongly temperature-dependent. At whole organism levels, temperature determines rates of growth and reproductive output. For mobile animals, body temperature can drive movement behavior, and thus ability to eat or avoid being eaten by other organisms (e.g., Adolph and Porter, 1993; Kordas et al., 2011). At extreme high or low temperatures, reproductive failure, and/or mortality occur as physiological systems shut down, enzymes cease functioning, or oxygen supply is no longer able to meet metabolic demands (Williams, 1970; Pörtner et al., 2006). Subsequently, temperature has long been recognized as a key driver of the distribution and abundance and hence biodiversity of plants and animals in nature (Hutchins, 1947; Ehrlén and Morris, 2015; Peters et al., 2016). The influence of temperature is especially evident in ectothermic organisms (which comprise the vast majority of species on Earth) that are unable to generate appreciable metabolic heat and thus have body temperatures that change with environmental conditions. While endotherms (birds and mammals) can generate heat through metabolism, they too will die or suffer stress when the maintenance of optimal body temperature becomes too challenging (Porter et al., 2000). Importantly, species display a wide range of responses to body temperature, and a temperature that may be lethal to one species may be optimal for another; while some species can tolerate only very narrow ranges of temperature, others appear to function well over wide ranges (e.g., >20°C; Dell et al., 2014).

Understanding how temperature affects organisms has taken on critical significance in the face of ongoing climate change (Porter et al., 2000; Hobday et al., 2016), as scientists attempt to understand underlying drivers of current observations of mortality events and shifts in distribution, and potentially forecast responses to an even warmer planet (Petchey et al., 2015; Sunday et al., 2015). A key component of this work has been the development of empirical and theoretical approaches that connect what we know about the physiological effects of factors such as temperature, ocean pH, and water availability—often measured under controlled experimental conditions (Somero, 2010; Williams et al., 2011; Gunderson et al., 2016)—with patterns of environmental conditions observed in the field (Denny and Helmuth, 2009). Specifically, numerous physiological studies have measured both the lethal tolerance limits of plants and animals, as well as the non-lethal cumulative effects of exposure to chronic stress (Woodin et al., 2013; Dell et al., 2014; Sinclair et al., 2016). At least in theory, these lab experiments can then be compared against measured environmental conditions (nowcasts and hindcasts) as well as model projections (forecasts) to quantify how patterns of survival, abundance, distribution, reproduction, and growth of key organisms have responded, or likely will respond, to rapid environmental change (Porter et al., 1973).

A major obstacle to such approaches has been a quantitative understanding of the environmental conditions that organisms actually experience in the field (Smale and Wernberg, 2009), and of what spatial and temporal scales we must measure these parameters in order to effectively forecast responses to environmental change (Montalto et al., 2014). The challenge is far more difficult than is often appreciated, especially given the wide availability of environmental data from ground-based weather stations and buoys (e.g., Helmuth, 1998; Kearney et al., 2012), remote sensing platforms (e.g., Geller et al., 2017), and re-analysis databases that present weather data integrated from multiple platforms (e.g., Mesinger et al., 2006; Mislan and Wethey, 2011). Below we briefly explain why such data, while necessary, may at times be insufficient for understanding the effects of climate change on organisms, and then explore various options for recording relevant environmental data at the scale of organisms using logging devices.

We focus on intertidal zones, the regions between the high and low tide lines of the world's coastlines. These habitats have long served as test beds for understanding the causal linkages between organism physiology and local and geographic patterns of distribution (e.g., Doty, 1946; Southward, 1958). Alternately exposed to the aquatic (at high tide) and terrestrial (at low tide) environments, the patterns by which species more or less predictably replace one another moving from the low to high intertidal, i.e., zonation (**Figure 1**), are generally assumed to be determined to a large extent by physiological stress from temperature, desiccation, and time spent feeding (Connell, 1961; Wethey, 1983, 1984; Gilman and Rognstad, 2018). Many of these organisms have been shown experimentally to live close to their stress tolerance limits during low tide (Somero, 2002; Davenport and Davenport, 2005; Harley, 2008). As a result, and because of their enormous ecological importance to coastal environments and easy accessibility to researchers, intertidal zones have contributed significantly to ecological theory (Paine, 1994). Yet, despite their importance, they are also among the environments where we have the least amount of environmental data. Here we use intertidal habitats as a case study, but the concepts that we explore have broad applicability to other environments and organisms including plant communities (e.g., Scherrer and Körner, 2011), terrestrial arthropods (Caillon et al., 2014; Woods et al., 2015), and lichens (Kershaw, 1985).

THE CHALLENGE OF RECORDING INTERTIDAL DATA AT RELEVANT SCALES

Environmental Temperature Data

The role of "temperature" in ecological and physiology studies is ubiquitous. A quick search of the Web of Science with the terms "Temperature" and "Ecolog* or Physiol*" returns almost 700,000 papers published since 1975. Yet the term "temperature" continues to be misused with subsequent carry-on effects for experimental design and interpretation of results. Critically, "temperature" is not a stand-alone variable, but rather a descriptor, and so studies that refer to "the temperature" (e.g., as a descriptor of a site) are about as meaningful as referring to "the color." Most commonly, researchers are referring to air temperature recorded at some fixed elevation

FIGURE 1 | Zonation pattern of mussels and barnacles. The upper intertidal limit to intertidal organisms is generally assumed to be driven by physiological stress and feeding time (Connell, 1961; Wethey, 1983, 1984; Gilman and Rognstad, 2018).

above the substratum, usually by a weather station (T_{air}); Sea Surface Temperature (SST); or, primarily in remote sensing literature, Land Surface Temperature (LST). Such inaccuracies are understandable given how we humans live our daily lives, using reports of near-ground air temperature as an appropriate indicator for how comfortable we are likely to be outside on any given day. Under more extreme conditions, we may also consider indices such as "wind chill" to reflect the influence of wind on heat loss through convection, or a "heat index" to reflect the role that high humidity has in limiting our ability to cool through sweating (Parsons, 2014). But, the assumption that these measurements and indices are physiologically and ecologically relevant to non-human species is often wildly violated. For example, SST can be very different from water temperature just a few meters below the surface (Smale and Wernberg, 2009; Castillo and Lima, 2010; Brewin et al., 2018). In terrestrial alpine environments, temperatures recorded at 2 m above-ground weather stations can be very different than temperatures in and around underlying plant canopies (Scherrer and Körner, 2010). In coastal systems, measurements recorded by offshore buoys (the most common data source) or satellites can differ markedly from those nearshore due to the influence of upwelling and solar heating (Pfister et al., 2007). Kearney (2006) refers to these large-scale measurements (also including those made by weather stations) as "environmental" temperature and explains that they can deviate significantly from those experienced by animals and plants—which drive their physiology and survival.

Many potential problems with the use of environmental data center on the large spatial and temporal scales over which they are, by necessity given the enormous size of the ocean, recorded, and archived. Satellite measurements of SST and LST record averages that integrate temperatures over pixel sizes ranging from 100's to 1,000's of square kilometers. In coastal systems, these pixels can overlap both terrestrial and aquatic measurements and thus can artificially reflect a hybrid of LST and SST. Because of rapid heating due to solar radiation, and cooling effects of internal waves and upwelling, temperatures at even moderate depths can vary by several degrees from SST (Smale and Wernberg, 2009; Castillo and Lima, 2010). Similarly, on land, while surface (substrate) temperature may be an accurate proxy for small organisms that live in close contact with the ground (e.g., Thomas, 1987; Bertness, 1989; Wethey, 2002; Chapperon and Seuront, 2011), LST pixels are typically many orders of magnitude larger than the size of these organisms, and thus are based on spatial averages that when parsed, can reveal extremely high within-pixel heterogeneity (Geller et al., 2017). Air temperature and wind speed change as a function of distance from the ground because of boundary layer effects (Gates, 1980), which is why weather stations typically adhere to standards where the thermometer and anemometer are placed at ∼2 m and 10 m above the ground, respectively (World Meteorological Organization, 2008). Air temperature is thus always, at best, an indirect indicator of substratum temperature. Some animals are nocturnal, making measurements of environmental parameters recorded during the hottest part of the day largely irrelevant (Kearney, 2006). Similarly, in intertidal systems, the timing of low tide determines what part of the day organisms are exposed to the terrestrial, and by contrast, aquatic, environments. Environmental conditions recorded during the hottest part of the day have little relevance to an intertidal organism that is underwater during that period (Helmuth et al., 2002).

For intertidal (and terrestrial) environments, the most important reason why broad-scale weather data are often ineffective as direct proxies for plant and animal temperature is the role of the organism itself in driving heat exchange across its surface through the absorption of heat energy from solar radiation, and the transfer of heat with the surrounding air through wind-driven convection (Porter and Gates, 1969). For example, the color of an animal's skin, shell, or fur significantly affects the amount of solar heat that is either absorbed or reflected (e.g., Mitton, 1977; Erasmus and De Villiers, 1982; Etter, 1988). Likewise, the shape and surface area of an organism drives the rate of convective exchange (Mitchell, 1976). Subsequently, two ectothermic organisms exposed to precisely the same environmental conditions can have body temperatures that radically differ from one another (>10°C; Broitman et al., 2009; Gilman et al., 2015), and can be either substantially hotter (>15°C) or cooler than the temperature of the surrounding air (Helmuth, 1998). Predators and their prey, for example, can experience significant differences in their temperature, and thus in physiological stress, even if they have similar physiological tolerances (Monaco and Helmuth, 2011).

The deviation of animal and plant body temperatures from T_{air}, SST, or LST has enormous implications for how we extrapolate from the lab to the field, and for how we compare physiological stress at different field sites. Recently, physiological ecologists have adopted the use of Thermal Safety Margins (TSM) to quantify the difference between an organism's lethal temperature (usually measured in the lab) and the maximum conditions that it will experience in the field (Sunday et al., 2011). A wide TSM suggests that these organisms may be less susceptible to warming than is an organism already living in

a habitat where it is very close to its lethal limits (Woodin et al., 2013; Dong et al., 2017). In a scenario where body temperature is substantially hotter than air temperature, overall risk will be massively underestimated if physiological limits are compared against air temperature (Marshall et al., 2010). Even the assumption of air temperature as a relative indicator of stressful conditions can be problematic. While some models do predict that the most extreme body temperatures tend to occur on days with high air temperature and maximum solar radiation (Mislan et al., 2014), other comparisons of animal temperature against local air temperature have shown poor relationships, with root mean square errors on the order of 5–9°C (Kish et al., 2016). But, even in instances where air temperature is correlated with body temperature, a mechanism for determining "how hot is too hot" may still be difficult without some means of estimating how much hotter organism temperature is than air temperature under full sun, i.e., the offset (y-intercept) of the correlation (Kish et al., 2016).

An additional distinction, but one that is still frequently misunderstood or at least ignored by many ecologists and physiologists, is the difference between weather and climate (30+ year trends in weather conditions). Specifically, while climate change undeniably affects plants and animals, it does so indirectly through changes in local weather parameters such as air temperature, wind speed, rain, and solar radiation (Stenseth et al., 2002). The role of high frequency (hourly, daily) variability in driving physiological performance and survival remains an active area of research, but recent work shows the important role of time history (Drake et al., 2017; Koussoroplis et al., 2017), as well as that of rare, short-term extreme events (e.g., heat waves; Tsuchiya, 1983; Hobday et al., 2016) that can be masked through temporal averaging (Wethey et al., 2011; Robinet et al., 2013). Spatial variability can also be very high (Herring et al., 2016). Thus, for example, while the recent Paris Agreement made as its goal to limit the increase of the Earth's average global temperature to well below 2°C above pre-industrial levels (UNFCCC, 2015), sites in the Gulf of Maine are already displaying temperature deviations of nearly twice that magnitude over periods lasting several months (Pershing et al., 2015; see also references in chapter 3 on regional temperature trends in the recent IPCC report on 1.5°C Global Warming[1] Hoegh-Guldberg et al., 2018). Subsequently, model projections based on high frequency (hourly) environmental data have been shown to yield very different projections than those based on coarser resolution (6 h: Montalto et al., 2014; monthly mean: Kearney et al., 2012) data inputs.

The end result is that if one wishes to replicate meaningful environmental conditions in a laboratory setting in order to gain insights into the impacts of global climate change, it is not sufficient to simply expose organisms to constant temperatures based on annual means or climatic norms (e.g., based on global or regional increases), as meaningful shorter-term deviations will far exceed these trends. While climatic data such as annual or decadal means made available through datasets such as the World Ocean Atlas are useful when conducting research on the climate system, they are effectively useless in physiological or ecological contexts, as they ignore not only important inter-annual variability but also variation over much shorter time periods which may have highly significant consequences for organisms such as heat waves (for an in-depth discussion of these issues, see Montalto et al., 2014; Denny, 2017).

Several mathematical (heat budget) models are now available to convert weather data (air temperature, wind speed, and solar radiation) into estimates of intertidal organism temperature (Elvin and Gonor, 1979; Bell, 1995; Helmuth, 1998, 1999; Denny and Harley, 2006; Finke et al., 2009; Szathmary et al., 2009; Helmuth et al., 2011; Iacarella and Helmuth, 2011; Sarà et al., 2011; Wethey et al., 2011; Marshall et al., 2015; Mislan and Wethey, 2015; Kish et al., 2016; Dong et al., 2017). These models range in complexity from simple regression-based approaches (Elvin and Gonor, 1979; Kish et al., 2016) to much more sophisticated land-based models (Wethey et al., 2011; Mislan and Wethey, 2015). However, and especially in intertidal ecosystems, their application has still tended to be limited to a few research groups. And, as with all models, their verification requires extensive *in situ* measurements of organism temperature.

Temperature Measurements in the Field

Collectively, these applications underline a critical need for field measurements of temperature at the scale of organisms, and over high temporal frequencies and small spatial scales. Several authors have recently highlighted the use of infrared thermography for recording temperature patterns in the field (**Figure 2**) (Meola and Carlomagno, 2004; Scherrer and Körner, 2010; Chapperon and Seuront, 2011; Lathlean and Seuront, 2014; Van Alstyne and Olson, 2014; Faye et al., 2016a; Lathlean et al., 2017). Thermography produces visible "thermal" images that are converted from infrared energy emitted and reflected on a given surface (Chapperon and Seuront, 2011). This method allows for spatial analysis of a habitat at a small organism's scale including measurements of shell and substratum which can then be used to calculate corresponding tissue temperatures of animals such as gastropods and discern habitat-specific thermoregulatory behavior (Chapperon and Seuront, 2011). There are numerous studies that use this method to examine microhabitats, behavior and physiology in response to thermal stress (e.g., Helmuth, 2002; Bulanon et al., 2009; Montanholi et al., 2010; Woods et al., 2015). Thermal infrared cameras have decreased markedly in price and now are available as part of packages that can be used on drones (Faye et al., 2016b) making their use attractive, especially for obtaining measurements of multiple organisms simultaneously (Scherrer and Körner, 2011). Their primary limitation in intertidal systems is that they typically cannot be left unattended and can only be deployed during low tide. Data measured using thermography are only discrete measurements, limiting temporal analysis to broad frequencies. Moreover, analysis of temperature patterns must be conducted by post-processing of the images obtained. A further complication involves calibration to the surface properties of the organism of interest, specifically the animal or plant's emissivity. This parameter describes the ability of an object to radiate energy in the infrared spectrum and is required in order for the camera

[1]http://ipcc.ch/report/sr15/

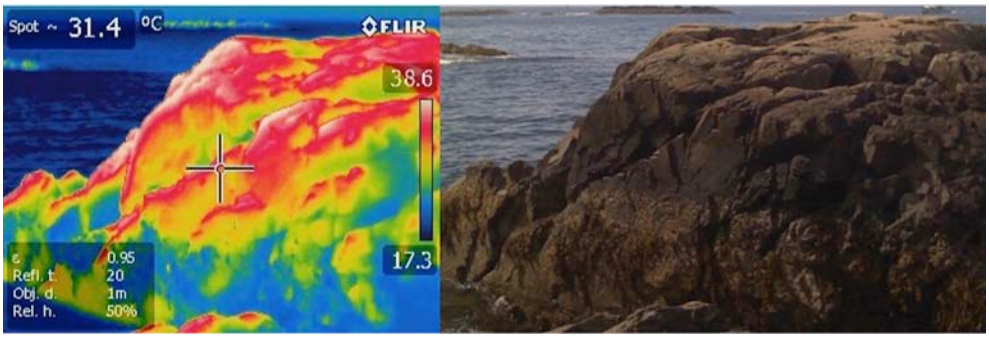

FIGURE 2 | Infrared thermograph of a rocky intertidal site in Nahant, MA USA. Rocky intertidal temperatures range significantly based on complex topography that creates microclimates. These include both areas of high thermal risk and areas of thermal refugia.

to back-calculate temperature. Typically, biological surfaces fall in the range of 0.85–0.95, and so small errors in emissivity will make a difference of only a degree or two. However, some shelled organisms and rock can have much lower values, introducing error unless this is accounted for in image analysis.

An alternative approach that has seen more wide-scale adoption by intertidal researchers is the deployment of small sensors to directly document organism body temperatures in the field. Initially, researchers attempted to follow the lead of terrestrial studies through the use of thermocouples and thermistors connected to a central data logger (Southward, 1958; Lewis, 1963; Hardin, 1968; Vermeij, 1971; Elvin and Gonor, 1979). Early dataloggers include the Portable Chart Recorder (Omega Engineering) used in recording *N. lapillus* body temperatures (Etter, 1988), Stowaway XTR (Onset Computer Corporation) initially used for logging silicone-filled *M. californianus* shells (Helmuth and Hofmann, 2001) and live *P. ochraceus* (Szathmary et al., 2009), Telatemp Datalogger for logging *M. californianus* body temperatures (Fitzhenry et al., 2004), and Campbell CR1000 Datalogger used with *M. californianus* (Fitzhenry et al., 2004), *G. demissa* (Jost and Helmuth, 2007), and *L. irroratus* (Iacarella and Helmuth, 2011). While these devices were valuable for logging multiple body temperatures simultaneously during lab experiments, they often could only be deployed in the field for short periods during low tide. During long-term deployments, flooding, broken cables, and movement of the temperature probe tip made data collection extremely difficult (Helmuth and Hofmann, 2001; but see successful recent application by Gilman et al., 2015).

In the mid to late 1990's, self-contained units with on-board thermistors were introduced commercially by companies such as Dallas/Maxim (iButton), and Onset Computer Corporation (Hobo TidbiT) (**Table 1**). The ready availability of these rugged and relatively inexpensive loggers initiated a new wave of environmental measurements in intertidal systems, and their application continues to this day. But, as often happens with new technology, these instruments were frequently used inappropriately. Specifically, what went largely unrecognized was that just as the shape, color and mass of an organism affect its body temperature, so do those characteristics affect the temperature that a logger will record. When buried in sand or mud (Jost and Helmuth, 2007), or placed in close contact with the surface of a rock (Wethey, 2002; Harley and Helmuth, 2003), these instruments will record temperatures close to that of the substratum because of high rates of thermal conduction. They therefore can serve as effective indicators of body temperature in sessile animals such as barnacles (Wethey, 2002), small snails (Hayford et al., 2015; Marshall et al., 2015) or, on the underside of rocks, crabs (Stillman and Somero, 1996). Such measurements cannot, however be applied to all organisms at a site since all are likely to have very different body temperatures, both due to habitat heterogeneity (microhabitats) as well as a result of their thermal properties, as above. In fact, Denny et al. (2011) showed that variation in mussel temperatures within a single intertidal bench can exceed that observed over several thousand kilometers. Fitzhenry et al. (2004) compared temperature measurements by unmodified TidbiT loggers against body tissue temperature measurements of adjacent mussels in the lab and field and showed that the loggers recorded errors of up to 14°C. Claims of "site level temperature" measurements were therefore shown to be naïve.

A viable alternative which takes advantage of the rugged nature of instruments such as iButtons and TidbiTs is the use of biomimetic instruments (biomimics) designed to mimic the thermal characteristics of the target species of interest (mussels, limpets, barnacles, snails, seastars, etc.; **Table 1**; Helmuth et al., 2002, 2006, 2011; Seabra et al., 2011; Fly et al., 2012; Pincebourde et al., 2012; Monaco et al., 2015; Kish et al., 2016; Kroeker et al., 2016; Drake et al., 2017). These instruments record temperatures that are significantly more accurate (∼1–2°C error) to the body temperatures of animals than are either air temperature or the temperature recorded by unmodified "off the shelf" instruments (Fitzhenry et al., 2004; Lima et al., 2011). Methods for building sensors have usually involved either placing the logger inside of an animal (e.g. mussel, limpet, barnacle, snail) shell and filling the shell with silicone or Scotchcast flame retardant compound both of which adequately approximate the thermal characteristics of tissue (Lima and Wethey, 2009; Denny et al., 2011) (**Figure 3A**) or by embedding them in materials such as epoxy resin (**Figure 3B**; Helmuth and Hofmann, 2001; Lima et al., 2011). A disadvantage of the latter approach is that not

TABLE 1 | Library of intertidal organism biomimics and datalogging technologies.

Biomimic species	Key publications	Datalogger	Components	Memory (measurements)	Battery life	Logger dimensions	Reader/Data transmission
P. ochraceus	Pincebourde et al., 2008 Szathmary et al., 2009 Broitman et al., 2009	Thermochron iButton DS1921G or DS1922L (Maxim Integrated)	Aquazone single-cell foam (Reilly Foam Corp.)	2,048 (DS1921G) or 8,192 (DS1922)	10 years	0.6 × 1.7 cm diameter	DS1402D-DR8 Blue Dot Receptor USB, Serial or Parallel-port 1 Wire adaptor (Maxim Integrated)
S. cariosus	Lima and Wethey, 2009		Real shell, Scotchcast 2130 (3M)				
T. persona	Lima and Wethey, 2009 Lima et al., 2011						
Patella spp.	Lima et al., 2011						
C. tramoserica	Lathlean et al., 2014						
D. orbita							
T. rosea							
Tetraclita spp.	Chan et al., 2016						
C. fornicata	Diederich and Pechenik, 2013						
C. fragilis *S. balanoides*	Wethey, 2002		None				
B. glandula	Harley and Helmuth, 2003 Harley and Lopez, 2003	Thermochron iButton DS1921G or DS1922L (Maxim Integrated)	None	2,048 (DS1921G) or 8,192 (DS1922L)	10 years	0.6 x 1.7cm diameter	DS1402D-DR8 Blue Dot Receptor USB, Serial or Parallel-port 1 Wire adaptor (Maxim Integrated)
S. glomerata	McAfee et al., 2018		Real shell, Scotchcast 2121 (3M)				
G. demissa	Jost and Helmuth, 2007 Helmuth et al., 2016		Real shell, 100% Silicone (GE)				
M. edulis *M. chilensis* *P. canaliculus*	Helmuth et al., 2016						
X. securis	Olabarria et al., 2016						
M. trossulus	Schneider and Helmuth, 2007						
M. californianus	Denny et al., 2011						
C. funebralis	Gleason and Burton, 2016						
M. galloprovincialis	Schneider and Helmuth, 2007 Helmuth et al., 2016 Nicastro et al., 2012 Lathlean et al., 2016a						

(Continued)

TABLE 1 | Continued

Biomimic species	Key publications	Datalogger	Components	Memory (measurements)	Battery life	Logger dimensions	Reader/Data transmission
P. perna	Nicastro et al., 2012 Lathlean et al., 2016a	Hygrochron iButton DS1923 (Maxim Integrated)		8,192	10 years	0.6 x 1.7cm diameter	DS1402D-DR8 Blue Dot Receptor USB, serial or Parallel-port 1 Wire adaptor (Maxim Integrated)
Patella spp. *T. persona* (Desiccation Loggers)	Lima et al., 2011		Real shell, Scotchcast 2130 (3M)				
M. californianus	Helmuth and Hofmann, 2001 Fitzhenry et al., 2004	HOBO TidbiT (Onset)	Premium Marine Resin (Evercoat)	42,000	5 years	3 x 4.1 x 3.7cm	BASE-U-4 USB (Onset)

Seastar
Limpet
Snail

Barnacle
Oyster
Mussel

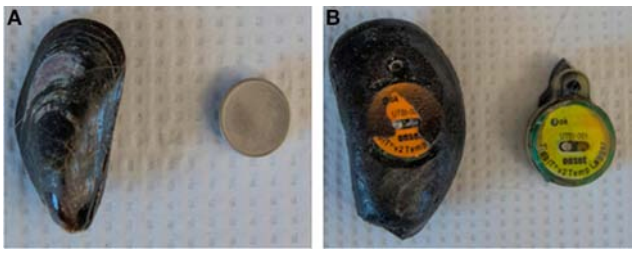

FIGURE 3 | (A) An iButton temperature logger (Maxim Integrated) next to a real *Mytilus edulis* mussel shell. This biomimic is made by filling the shell with silicone and embedding the logger within. **(B)** An unmodified HOBO TidbiT v2 temperature logger (Onset Computer Corporation) next to a biomimic. The biomimic is a custom cast made of Evercoat Premium Marine Resin modeled after a larger (74 mm) mussel (Fitzhenry et al., 2004), more suitable for use approximating body temperatures of the larger *M. californianus* species from the Pacific Ocean.

all sizes or species of animal can be replicated. For example, an organism's "thermal inertia," which defines the amount of energy required to raise its temperature by one degree, can only be matched with non-biological materials such as epoxy over a narrow size range. For mussels, this was shown to occur in the size range of ∼6–8 cm length (Fitzhenry et al., 2004). Biomimics of mussels at sizes smaller or larger than this range requires the use of real shells, which can break in the field after only a few weeks. Nevertheless, "robomussels" and "robolimpets" have now successfully been deployed at sites worldwide, and have provided long-term records of temperatures approximating those of the species of interest (Seabra et al., 2011; Helmuth et al., 2016). Obtaining temperature records of animals too small to contain current data logger designs remains a challenge, and most solutions still require the use of a thermocouple or thermistor (e.g., Gilman et al., 2015). However, emerging technology with smaller batteries (e.g., EnvLogger, WeePit) is poised to open new avenues of exploration for a wider range of animal sizes (**Table 2**).

Long-term records of non-shelled organisms have proven much more elusive, especially for those with a wet surface that cannot be mimicked with epoxy. Loggers constructed of foam have been used to approximate temperatures of intertidal seastars for periods of several months (**Figure 4**; **Table 1**; Fly et al., 2012; Pincebourde et al., 2012; Monaco et al., 2015). But, the lack of a design which effectively mimics water loss (and thus cooling through evaporation) and yet is sufficiently rugged to withstand wave stresses, continues to be a major impediment to understanding the thermal ecology of soft-bodied intertidal organisms.

Despite these challenges, the use of biomimetics in intertidal ecology has yielded major insights that otherwise would likely have gone undetected. First and foremost, these field measurements have shown that in many cases intertidal organisms are living far closer to the limits of their thermal tolerance than would be predicted based on air temperature (e.g., Stillman and Somero, 1996; Helmuth and Hofmann, 2001; Mislan et al., 2014). Second, they have shown that patterns of temperature on local and geographic scales are far more complex

TABLE 2 | New datalogging technologies.

Datalogger	Memory (Measurements)	Battery Life	Dimensions	Data transmission	Pros	Cons
HOBO MX2204 (Onset)	96,000	3–5 years	4.45 × 7.32 × 3.58 cm	Bluetooth low Energy (BLE)	Easy programming and offload, good memory	Cost, Size
WeePit (AlphaMach)	114,000	Not Reported	10 × 11.25 mm	Radio-Frequency Identification (RFID)	Small, very good memory	Needs specific reader to offload data, Cost
EnvLogger (ElectricBlue)	20,000	2 years	7 × 16.5 mm	Near Field Communication (NFC)	Very small, rugged, Easy data offload	Small memory
Wireless Sensor Network—PIDO (Zhou et al., 2018)	NA	NA	NA	Wireless Radio (915 MHz) Node-Node-Sink	No cables, easy data access	Cost, Set-up time

FIGURE 4 | A "roboseastar" biomimic deployed in the intertidal next to live seastars (*Pisaster ochraceus*) and their mussel prey. An iButton temperature logger is embedded within the foam and the unit is affixed to the rock using marine epoxy.

in space and time than previously appreciated. For example, Helmuth et al. (2002, 2006) showed that intertidal mussels along the west coast of North America do not display a geographic gradient in temperatures, but rather conform to a mosaic pattern where sites can be much hotter or colder than predicted based on latitude. These complex patterns have been shown to occur in Europe (Pearson et al., 2009; Seabra et al., 2011) and SE Asia (Dong et al., 2017), although not on the west coast of South America (Finke et al., 2007). Importantly, these observations suggest that climate change may be having significant impacts even well within species' geographic ranges and not just at range boundaries (Place et al., 2008; Pearson et al., 2009; Torossian et al., 2016). Kroeker et al. (2016) expanded on this idea to explore the impacts of multiple stressors acting on mussel populations, and showed mosaic patterns of not just temperature but food availability and ocean pH explained observed geographic patterns in mussel growth. Results from biomimic deployments also have pointed to the likely importance of stepping stones and climate refugia ("rescue sites") in coastal ecosystems, which may enhance the recovery of species following extreme events (Potter et al., 2013; Hannah et al., 2014).

Biomimetic sensors have also opened new avenues for exploring the differential responses of interacting species to environmental stress. Broitman et al. (2009) used biomimics to track the temperatures of predatory seastars and their mussel prey at multiple sites and showed that relative stress levels were significantly affected by differences in the thermal dynamics of the two species. Zardi et al. (2010) found that competition among different lineages of the mussel *Perna perna* were maintained in part by physiological stress that occurred during aerial exposure at low tide.

CURRENT LIMITATIONS AND RECENT ADVANCES IN LOGGER DESIGN

Despite their demonstrated importance in informing ecological theory, intertidal dataloggers still have several limitations. We next examine some of these in detail, along with recent progress being made in overcoming these barriers.

Durability in Wave-Swept Environments

The intertidal environment is unique due to the binary nature of environmental stressors resulting from the tidal cycle. Crashing intertidal waves can produce water velocities exceeding 8 m/s and accelerations of up to 400 m/s^2 (Denny, 1985). Thus, loggers need to resist dislodgement, physical impact and seawater ingress.

Current loggers still face some of these durability limitations, both in their construction and deployment. Two-part marine epoxies are still commonly used to attach intertidal biomimetics to the underlying rock surface. The amount of epoxy must be sufficient to resist removal during storms, yet an excess will affect the thermal characteristics of the logger. While superficially this issue appears trivial, and is not typically considered in terrestrial environments, it represents a major limitation in exposed rocky intertidal systems.

The materials used to construct biomimetic loggers also represent a design limitation, as the thermal conductivity as well as the specific heat capacity will affect their relevance to organisms. The growing availability of plastic and rubber mold-making materials, traditionally used by hobbyists and performing arts professionals, will expand the range of options for future biomimics, particularly for soft-bodied organisms like seastars and macroalgae. One such company called Smooth-On[2] manufactures several user-friendly silicone and urethane-based rubbers, foams and polyester hard epoxies that are traditionally used for sculpting and performing arts. The company has products available in stores on 6 continents and has a global shipping distribution network. These products vary in tear strength resistance, hardness, and conductivity. Those with the highest tear strengths are less likely to break apart due to wave stress, but their other thermal properties must meet the requirements of the organism being considered. In preliminary observations, some of these non-epoxy materials, particularly the ones meant to be vacuum degassed (i.e., the removal of entrapped air bubbles upon pouring), may harden into objects with a textured, semi-permeable surface when poured without vacuum degassing. This technique may facilitate the development of more accurate biomimics that can partially simulate a live organism's ability to retain seawater upon emersion, then release it via evaporation. The materials may be colored to mimic albedo and casted with a UV resistant agent which reduces breakdown in the field due to solar radiation. In addition, some of these materials are food-safe and non-toxic, making them more attractive options for use over traditional materials like polyester epoxy.

Lack of Real-Time Data Capabilities

Scientists have increasingly turned to the acquisition of real-time data from their instruments (Zhou et al., 2018). Utilizing real time data capabilities for sensing in the intertidal environment, however, is extremely challenging due to the tides. While real-time equipped data loggers have been used extensively in terrestrial research (Porter et al., 2005), they are not used commonly in marine research. This is due to the difficulty inherent in transmitting data wirelessly through water. Continuous, real time intertidal sensors are challenging to implement because wireless signals are transmitted very differently in water and air. Real time data transmission also requires considerable battery power, in direct conflict with the need to miniaturize sensors. Zhou et al. (2018) developed an intertidal sensor prototype for real-time data that tackles both the challenges of transmitting in water and battery life (Zhou et al., 2018). Specifically, they created a mesh intertidal wireless sensors network (IT-WSN) whereby sensors communicate and transfer data to each other. Transferring data between sister sensors is a method to strengthen connection. With each logger acting as a stepping stone, data are eventually pushed via a series of nodes to the land-based "base" or "sink" node that is connected to the cloud (**Figure 5**). To enhance battery longevity, a primary limitation to miniaturization, the sensors are designed to log data continuously but transmit data only when sensors are exposed to air at low tide and a strong network link can be made. This is done by incorporating a new complex metric in the sensor (PIDO: Predictive Delay Optimization) which controls for dormancy based on (1) node conditions (dryness of the sensor), (2) link quality (connectivity to sister nodes), and (3) predictability classifier (uploaded tide cycles) to control for dormancy for each sensor. With multiple factors confirming optimal data transmission, real-time PIDO sensors can be deployed for longer periods of time (Zhou et al., 2018).

In other cases, even when data cannot be recorded in real time, methods for facilitating the rapid transfer of data manually can speed data collection. Data from iButton loggers and older, LED-based versions of Onset TidbiT data loggers can only be uploaded to a computer or data shuttle directly using a cabled reader. Data collected by the newest wireless Onset TidbiT Bluetooth loggers (MX2204) are a significant improvement as data can be downloaded via Bluetooth on to a cell phone or other mobile device during low tide. A new Portuguese company, Electric Blue, has developed a small, ruggedized temperature logger (EnvLogger)[3] that can offload data and be programmed using a mobile Android device and has near real-time data capabilities (**Table 2**). This new technology avoids the need to remove the logger from its shell casing or make time-costly modifications to offload data through protruding wires (e.g., Robert and Thompson, 2003; Lima and Wethey, 2009; Lima et al., 2011; Chan et al., 2016). WeePit temperature loggers have not been widely used in intertidal studies, however their large memory and high resolution are useful for long-term deployments. Additionally, it remains unclear whether the logger's data can be transmitted to the PitStop Radio-Frequency Identification (RFID) reader through shell, epoxy, or other biomimic components.

Miniaturization

Rapid advancements in printed circuit board and battery miniaturization have increased the availability of new datalogging technology. Existing sensors and loggers (**Table 1**) are small enough to be used to study many, although not all, intertidal organisms. The size of a self-contained logger is mostly determined by battery size. Some of the first uses of self-contained temperature loggers for intertidal biomimetic applications occurred in 2000-2001 where the first commercially available temperature loggers from Onset were slightly larger in circular diameter than 24 mm, and several cm thick. Some newer models of loggers are significantly smaller.

[2]https://www.smooth-on.com

[3]http://www.electricblue.eu/products/

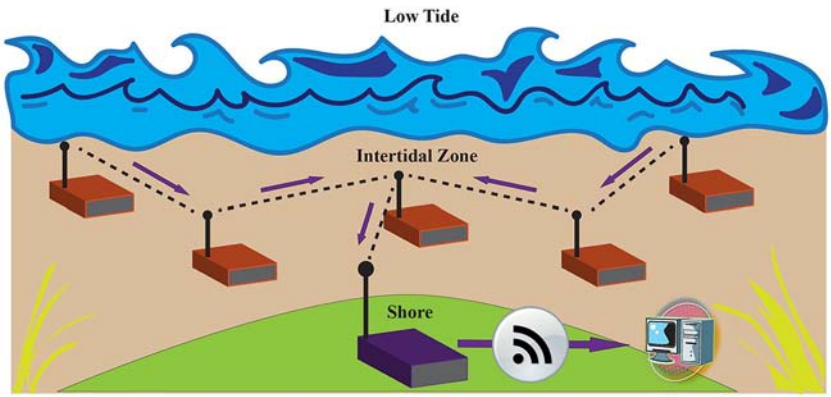

FIGURE 5 | Diagram of a mesh Intertidal Wireless Sensor Network (IT-WSN) that uses PIDO (Predictive Delay Optimization) for more frequent and effective intertidal data transmission as described in Zhou et al. (2018). Environmental data are collected by the sensor nodes (red) where they is then transmitted via links (dashed lines) to other nodes (Freq. = 915 MHz) using the most efficient routing path during low tide. Data are then transmitted to a land-based sink node (purple) before they are offloaded to a computer.

Mimicking Aggregation Effects

Most intertidal bivalves such as mussels and oysters commonly grow in aggregations that range in size from small (<25 cm^2) (Hunt and Scheibling, 2001) to large populations of hundreds of thousands of individuals (Okamura, 1986). Biomimics of shelled molluscs have been shown to record markedly different temperatures when deployed in growth position, in intact beds, as compared to when they are deployed as solitary individuals (Fitzhenry et al., 2004). Generally, loggers such as "robomussels" need to be deployed in intact beds, surrounded by living animals that provide shading (**Figure 6**). This limitation is increasingly important to address due to the extensive die-off of mussels in locations such as the Gulf of Maine (Sorte et al., 2016). The causes of these declines remain uncertain (Sorte et al., 2016), and studies attempting to explore whether the underlying causal factor is related to temperature face the problem that in many locations there are no intact mussel beds in which to deploy sensors. This severely limits our ability to record relevant temperatures in sites where animals have disappeared. An individual that is shaded by conspecifics within a bed can have 40% less surface area exposed to direct sunlight than mussels living as solitary individuals, and the bed as a whole creates a higher thermal inertia (Helmuth, 1998). Therefore, not only does the aggregation buffer any one individual from thermal stress, it also produces a matrix of individuals that can experience significantly different body temperatures based on their spatial position (Denny et al., 2011; Nicastro et al., 2012; Lathlean et al., 2016b). Similarly, oysters that orient their shells vertically to decrease surface area exposed to solar radiation can reduce thermal stress for themselves and smaller invertebrates that live amongst them within an oyster reef (McAfee et al., 2018). As we explore in more detail in a case study below, the development of low-cost open source hardware and software has allowed researchers to begin testing new biomimetic mussel bed devices to provide greater insight into how mussels and other invertebrates that live within beds experience differing environmental conditions, and how these may be mimicked using new sensor designs.

FIGURE 6 | A single robomussel deployed in growth position within a live mussel bed. The presence of surrounding organisms helps improve biomimetic logger accuracy.

Accounting for Behavioral Thermoregulation

One of the biggest challenges facing logging of intertidal temperatures is understanding the role of animal behavior in determining body temperatures (Williams and Morritt, 1995; Williams et al., 2005). Under thermal stress, many organisms are adept at seeking or creating shaded microhabitats such as crevices or the shade of larger organisms (Potter et al., 2013; Scheffers et al., 2013; Sunday et al., 2014) or creating microclimates through aggregation behavior (Nicastro et al., 2012; Olabarria et al., 2016). Others burrow, living in conditions much cooler than those on the surface (Kearney et al., 2010). Leaf-mining insects create microenvironments by burrowing into plant tissue (Pincebourde and Casas, 2006), and crop pests benefit significantly from shade provided by the plants on which they feed (Faye et al., 2017).

Intertidal animals display a wide repertoire of behavioral strategies for thermoregulation. The most common form of behavioral thermoregulation involves pre-emptive movement in to crevices or other shaded microhabitats where heating from

direct solar radiation is minimized, i.e., taking advantage of the immediate thermal landscape (Sears et al., 2016). Like terrestrial organisms, porcelain crabs may compete for cool, shaded areas under large rocks to reduce their body temperatures (Stillman and Somero, 1996). Many snail species are also adept at moving to crevices and other shaded areas to avoid extreme temperatures (Marshall et al., 2010; Cartwright and Williams, 2012; Ng et al., 2017). Monaco et al. (2016) measured potential and realized microhabitats in the more slowly-moving seastar *Pisaster* and found that these animals exhibited a "bet-hedging" strategy that allowed them to avoid extreme conditions, but at the expense of maximized physiological performance.

Slowly-moving or sessile species that are unable to avoid full sun can modify their body temperatures via several mechanisms. Hunt (1997) and Hunt and Scheibling (2002) suggested that individuals of the mussel *Mytilus trossulus* usually moved 1–2 cm in a month-long period, however some may move up to 50 cm over that same stretch. In contrast, Schneider et al. (2005) showed much more rapid movement, but only by small animals. Miller and Dowd (2017) noted that mussels living within a colder tidepool did not reposition themselves as much as those living on hotter bare rock in the high or low intertidal. Gastropods can reorient their shell and remove their foot from the geologic substrate to lower their body temperature (Miller and Denny, 2016).

Intertidal animals also display methods for thermoregulation that do not involve movement to shaded microhabitats. The seastar *Pisaster* has been shown to increase its thermal inertia by taking up cold water into its body during high tides preceding stressful low tide conditions (Pincebourde et al., 2009). The temperatures of intertidal algae likewise remain low as long as sufficient water is present to cool the surface through evaporation, but once significant desiccation occurs, thallus temperatures can skyrocket (Bell, 1995). This combination of desiccation and high temperature has significant effects on photosynthetic rates (Dring and Brown, 1982; Brown, 1987) and is thought to be the main determinant of algal species upper zonation limits in the intertidal zone (Lubchenco, 1980; Brown, 1987). Some species of gastropods can "mushroom" (Williams et al., 2005), cooling their bodies by exposing moist tissue, facilitating the evaporation of water. Yet other species climb atop one another to form chains, minimizing contact with the hot rock surface by all but the bottom-most animal (Ng et al., 2017).

Several studies have suggested the potential importance of shell gaping in bivalves as a means of thermoregulation, although to date results suggest high variability among species. During exposure at low tide, several intertidal bivalve species will remain tightly closed, but during extreme events will open their valves (gape), either to obtain oxygen or, potentially, to cool through evaporation of tissue water. Whether or not this behavior cools animals remains a matter of debate. Excessive levels of cooling through evaporation can lead to desiccation, suggesting significant trade-offs between temperature control and desiccation. Helmuth (1998) presented biophysical models for mussels suggesting that even slight evaporation can lead to notable decreases in body temperature. In contrast, Fitzhenry et al. (2004) forced mussel shells open inside a wind tunnel and compared temperatures to mussels that were forced shut. Their results suggested no significant difference in animal temperature. Miller and Dowd (2017) also found that live *M. californianus* mussels in the intertidal that experienced high body temperatures during low tide (>25°C) generally kept their shells closed more often than cooler mussels meaning this species likely does not utilize cooling through evaporation to control body temperature during hot conditions. Nicastro et al. (2012) showed that individual mussels did not apparently cool as a result of gaping, but suggested that entire beds of mussels, acting in concert, could lead to overall cooling.

Biomimetic sensors, unless attached to or imbedded in a living animal, can thus only provide information on potential body temperatures in the absence of behavioral thermoregulation (Adolph, 1990; Buckley et al., 2013; Díaz et al., 2015). Thus, there is a pressing need to better understand the cues and behavioral "rules" that allow intertidal organisms to proactively move to appropriate microhabitats. Typically this has been accomplished by placing biomimetic sensors in a number of potential microhabitats, and then determining the factors that cause organisms to move among these options, usually in response to trade-offs such as food availability, thermal stress and avoidance of predators (e.g., Monaco et al., 2015). Understanding the relationships between body temperature, shell gaping/orientation behaviors, and desiccation, and to link these trade-offs to physiological and molecular responses (e.g., Williams et al., 2011; Gleason et al., 2017) remains a significant information gap. Examining these factors simultaneously, in both the field and under controlled laboratory settings would provide an understanding of thermal physiological thresholds and how the organisms balance trade-offs. Progress is being made in this arena (**Table 3**). Researchers in the U.K. and the Netherlands have developed a biomonitoring device called the Musselmonitor that measures the amount and timing of mussel shell gaping using hall effect sensors (Allen et al., 2010). This device has been used on the freshwater zebra mussel (*Driessena polymorpha*) and the blue mussel (*Mytilus edulis*). A repeated pattern of shell gaping and closing is a signal of poor water quality. Mussels that spend the vast majority (70–80%) of their time with their shell open indicate good water quality. This device may be used to record early warning indicators of water quality in local areas of saltwater or freshwater, and can even be used to test drinking water quality. Hall effect sensors have also been used with oysters to investigate seasonal shell gaping patterns (Comeau et al., 2012) and gaping in response to the presence of toxic dinoflagellates (Nagai et al., 2006).

A device recently developed by Miller and Dowd (2017) used low cost custom-built printed circuit boards (PCBs) with type K thermocouples, waterproofed hall effect sensors, and an accelerometer/magnetometer to track mussel body temperature, shell gape, and orientation continuously in the field for a period of 21 days. The hall effect sensor, also used in the Musselmonitor, produces a magnetic field across the mussel's

TABLE 3 | Behavioral datalogging methods and technologies for intertidal organisms.

Behavioral variable	Sensors	Ecological variables	Estimated max. field deployment time	Key publications
Locomotion	Radio-Frequency Identification (RFID)	Predation Risk, Thermal Stress, Migration Patterns	4 months	Hayford et al., 2015 Hayford et al., 2018
Shell Gape (bivalves only)	Hall Effect	Water Quality, Thermal Stress (Evap. Cooling), Food Availability	1 month	Nagai et al., 2006 Allen et al., 2010 Miller and Dowd, 2017
Organism Orientation	Magnetometer + Accelerometer	Topography, Thermal Stress	1 month	Miller and Dowd, 2017

two half-shells where the output voltage gradient is proportional to the amount of shell gape. This type of system in the future should be used in controlled laboratory experiments along with other sensors to examine how mussel body temperature, respiration, heart rate, orientation, and shell gape all influence each other and determine the physiological performance of an individual under different conditions. Although these new datalogging capabilities provide researchers with valuable data, they are wired sensors which presents problems for trying to obtain long-term (>1 month) data sets from the field.

We also know surprisingly little about the role of predictability in the environment (temporal autocorrelation) in driving any of these behavioral responses (Helmuth et al., 2006; Dong et al., 2017). Some organisms may be able to behaviorally respond to immediate environmental conditions, for example by quickly moving during low tide to reach shaded microhabitat before critical levels occur. However, many species can only move during high tide, and "hunker in place" at low tide (Ng and Williams, 2006). In order for these organisms to successfully use appropriate microhabitats or to otherwise modify their behavior they must predict, at some level, the likelihood of near-term extreme events based on current conditions. Specifically, environmental conditions need to be temporally autocorrelated, i.e., when extreme conditions on Day 1 presage extreme conditions during the next low tide (Szathmary et al., 2009). However, at the few sites where this idea has been tested (Helmuth et al., 2006; Dong et al., 2017) the most extreme sites are often the least temporally autocorrelated.

FUTURE DEVELOPMENTS IN INTERTIDAL DATALOGGING

The development of newer, more complex biomimetic devices has been enhanced by open-source hardware (microcontroller circuit boards) and software programs such as Arduino and Raspberry Pi. These programs are revolutionizing the way marine scientists can collect oceanic data and have already been used in novel devices such as a microplastics sensor (Edson and Patterson, 2015), a CTD data logger (Lockridge et al., 2016), and a chlorophyll sensor (Leeuw et al., 2013). Novice engineers and programmers can learn to use microcontrollers to build electronic devices (e.g., dataloggers, robots, lights) for customized projects. These microcontrollers can be plugged into a computer via a USB cord and programmed using their corresponding computer applications (e.g., Arduino: Integrated Development Environment). Once programmed, a microcontroller will carry out the user-defined functions within the electrical circuit. First prototypes are typically designed by manually connecting the microcontroller to a solderless breadboard with integrated circuits (usually sensors and actuators) that are connected by jumper wires to form the full circuit. For projects that require smaller, more compact devices, these prototype designs can be documented (i.e., mapped) and submitted for development into custom printed circuit boards (e.g., Miller and Dowd, 2017).

Case Study: Biomimetic Mussel Bed

A project currently underway seeks to develop a biomimetic mussel bed that circumvents some of the issues associated with traditional robomussels. The biomimetic mussel bed consists of 23 mussel-shaped biomimics of sizes ranging from 25 to 60 mm in length—about the size of adolescent-adult *M. edulis* mussels found in muddy embayments and rocky shores on the East Coast of North America. These robomussels are synthesized using a colored UV resistant polyurethane rubber (Econ-80 from Smooth-On) a hard rubber material that closely matches the specific heat of live mussel tissue. The 2-part liquid polyurethane mixture can be poured into a silicone mold of several mussel shaped cavities all of which are fitted with nylon bolts, and two of which are fitted with type K thermocouple sensors. These thermocouples are then connected to an Arduino circuit board encased in a waterproof housing. Each mussel [including the experimental unit(s)] is then secured to an acrylic platform using nylon-insert locknuts, eliminating the need for marine epoxy. It can also be bolted to rock (**Figure 7**) or affixed to muddy bottom using thin rebar.

The Arduino is a microcontroller that can be programmed in the Arduino Integrated Development Environment (IDE) using the C/C++ programming languages. The board can be programmed to collect temperature measurements at any customized interval and stores them on a micro SD card. In

FIGURE 7 | A robomussel bed prototype deployed in the rocky intertidal zone in Nahant, MA USA. The robomussels in this prototype are colored white in order to collect preliminary data on how albedo may affect the accuracy of biomimetic devices.

addition, it uses software interrupts to go into a power-off mode between readings to further conserve power and can extend battery life for over a year (battery life depends on sampling interval). The logger is configured with two thermocouples, allowing for the simultaneous data collection of two different mussels within the bed. However, it uses the One-Wire library so more sensors may be added to the same data line with ease[4].

The project also offers a customized solution for simultaneously logging body temperatures of *Nucella lapillus* gastropod predators foraging on mussels using biomimics. Casts of *Nucella* shells have been constructed to log body temperature of individuals at different positions on the mussel bed. The bed contains screw-in attachment points both on the top and bottom of the bed. Therefore, it is useful for gaining insight into the temperatures experienced by an intertidal predator and its prey based on spatial position. *Nucella* biomimics can be colored which helps account for the effects of albedo of the different color variants found in the wild. Therefore, the logger allows researchers to better understand the role of albedo and spatial position in shaping an organism's thermal experience.

[4]https://github.com/judge-r/Robo-mussel

In situ Movement Tracking

Radio-Frequency Identification (RFID) technology has been used in prior intertidal research for tracking organismal behavior. *Nucella ostrina* gastropods have been shown to advantageously venture into risky areas (i.e., areas closer to thermal maxima) for increased access to food by using the timing of the tide to their advantage (Hayford et al., 2015, 2018). These same investigations found that RFID can be used to replace traditional tagging or marking methods in the intertidal. Their results showed that RFID tagging methods are 10-fold more efficient as a mechanism for relocating specific individuals than were traditional means.

CONCLUSIONS

Significant advances in temperature logging in intertidal systems have provided significant insights in to how this model system will continue to respond to the ongoing threat of climate change. Advances in logger design, both in terms of materials used to construct loggers as well as the size, battery life, and live transmission of data make biomimetics ever more powerful for a wider range of species. A major limitation still lies in understanding the role of thermoregulatory behavior by intertidal animals, both through movement to microhabitats but also through non-movement thermoregulatory behavior. New tools for tracking movement through RFID and for monitoring behaviors such as gaping are opening avenues of research, but they must be coupled with a better understanding of the "grain size" of the environment that the organism perceives. A small crab that is able to scuttle to safety in a crevice when its body temperature exceeds a critical threshold will experience very different temporal and spatial patterns of small-scale refugia than will a large seastar that is limited both by availability of sufficiently large hiding places as well as by movement speed. In contrast, by virtue of a significantly greater thermal inertia, a larger animal may have less need of a hiding place except during extreme events (Monaco et al., 2015). All of these organism-environment interactions are occurring simultaneously at a single site, yet without insights in to the way that they experience their environments and one another our expectations of the impacts of environmental change will likely fail (Broitman et al., 2009; Gilman et al., 2015; Hayford et al., 2015).

The development of data sensing and logging tools that are accurate and most importantly relevant to the species of experimental interest is now more important than ever. This instrumentation must be combined with laboratory and field experiments that holistically evaluate the state of the species from an assemblage-based perspective. Once these approaches are taken, they may potentially be scaled up to regional assessments of species performance and distribution (e.g., Woodin et al., 2013). Advanced biologging techniques will allow for more accurate ecological forecasting that enhances our understanding of what to expect in the future. There are many unique challenges to monitoring intertidal organisms, however the rapid pace of technological improvement is making these challenges easier to overcome, and thus promises new insights from this model system.

AUTHOR CONTRIBUTIONS

All authors contributed equally to the development and writing of the manuscript. RJ led the writing team and created the experimental mussel bed system described in this paper.

ACKNOWLEDGMENTS

This research was supported by NSF grant OCE 1635989 to BH. This is contribution number 385 of the Northeastern University Marine Science Center.

REFERENCES

Adolph, S. C. (1990). Influence of behavioral thermoregulation on microhabitat use by two *Sceloporus* lizards. *Ecology* 71, 315–327. doi: 10.2307/1940271

Adolph, S. C., and Porter, W. P. (1993). Temperature, activity, and lizard life histories. *Am. Nat*. 142, 273–295. doi: 10.1086/285538

Allen, H. J., Waller, W. T., Acevedo, M. F., Morgan, E. L., Dickson, K. L., and Kennedy, J. H. (2010). A minimally invasive technique to monitor valve-movement behavior in bivalves. *Environ. Technol*. 17, 501–507. doi: 10.1080/09593331708616411

Bell, E. C. (1995). Environmental and morphological influences on thallus temperature and desiccation of the intertidal alga *Mastocarpus papillatus* Kützing. *J. Exp. Mar. Biol. Ecol*. 191, 29–55.

Bertness, M. D. (1989). Intraspecific competition and facilitation in a northern acorn barnacle population. *Ecology* 70, 257–268. doi: 10.2307/1938431

Brewin, R. J. W., Smale, D. A., Moore, P. J., Dall'Olmo, G., Miller, P. I., Taylor, B. H., et al. (2018). Evaluating operational AVHRR sea surface temperature data at the coastline using benthic temperature loggers. *Remote Sens*. 10:925. doi: 10.3390/rs10060925

Broitman, B. R., Szathmary, P. L., Mislan, K. A. S., Blanchette, C. A., and Helmuth, B. (2009). Predator–prey interactions under climate change: the importance of habitat vs body temperature. *Oikos* 118, 219–224. doi: 10.1111/j.1600-0706.2008.17075.x

Brown, M. T. (1987). Effects of desiccation on photosynthesis of intertidal algae from a Southern New Zealand shore. *Bot. Mar*. 30, 121–127. doi: 10.1515/botm.1987.30.2.121

Buckley, L. B., Miller, E. F., and Kingsolver, J. G. (2013). Ectotherm thermal stress and specialization across altitude and latitude. *Integr. Comp. Biol*. 53, 571–581. doi: 10.1093/icb/ict026

Bulanon, M., Burks, T. F., and Alchanatis, V. (2009). Image fusion and thermal images for fruitdetection. *Biosyst. Eng*. 103, 12–22. doi: 10.1016/j.biosystemseng.2009.02.009

Caillon, R., Suppo, C., Casas, J., Woods, H. A., and Pincebourde, S. (2014). Warming decreases thermal heterogeneity of leaf surfaces: implications for behavioural thermoregulation by arthropods. *Funct. Ecol*. 28, 1449–1458. doi: 10.1111/1365-2435.12288

Cartwright, S. R., and Williams, G. A. (2012). Seasonal variation in utilization of biogenic microhabitats by littorinid snails on tropical rocky shores. *Mar. Biol*. 159, 2323–2332. doi: 10.1007/s00227-012-2017-3

Castillo, K. D., and Lima, F. P. (2010). Comparison of *in situ* and satellite-derived (MODIS-Aqua/Terra) methods for assessing temperatures on coral reefs. *Limnol. Oceanogr. Methods* 8, 107–117. doi: 10.4319/lom.2010.8.0107

Chan, B. K. K., Lima, F. P., Williams, G. A., Seabra, R., and Wang, H.-Y. (2016). A simplified biomimetic temperature logger for recording intertidal barnacle body temperatures. *Limnol. Oceanogr. Methods* 14, 448–455. doi: 10.1002/lom3.10103

Chapperon, C., and Seuront, L. (2011). Space-time variability in environmental thermal properties and snail thermoregulatory behaviour. *Funct. Ecol*. 25, 1040–1050. doi: 10.1111/j.1365-2435.2011.01859.x

Comeau, L., Mayrand, E., and Mallet, A. (2012). Winter quiescence and spring awakening of the Eastern oyster *Crassostrea virginica* at its northernmost distribution limit. *Mar. Biol*. 159, 2269–2279. doi: 10.1007/s00227-012-2012-8

Connell, J. H. (1961). The influence of interspecific competition and other factors on the distribution of the barnacle *Chthamalus stellatus*. *Ecology* 42, 710–723.

Davenport, J., and Davenport, J. L. (2005). Effects of shore height, wave exposure and geographical distance on thermal niche with of intertidal fauna. *Mar. Ecol. Prog. Ser*. 292, 41–50. doi: 10.2307/24868068

Dell, A. I., Pawar, S., and Savage, V. M. (2014). Temperature dependence of trophic interactions are driven by asymmetry of species responses and foraging strategy. *J. Anim. Ecol*. 84, 70–84. doi: 10.1111/1365-2656.12081

Denny, M. (2017). The fallacy of the average: on the ubiquity, utility and continuing novelty of Jensen's inequality. *J. Exp. Biol*. 220, 139–146. doi: 10.1242/jeb.140368

Denny, M. W. (1985). Wave forces on intertidal organisms: a case study. *Limnol. Oceanogr*. 30, 1171–1187. doi: 10.4319/lo.1985.30.6.1171

Denny, M. W., Dowd, W. W., Bilir, L., and Mach, K. J. (2011). Spreading the risk: small-scale body temperature variation among intertidal organisms and its implications for species persistence. *J. Exp. Mar. Biol. Ecol*. 400, 175–190. doi: 10.1016/j.jembe.2011.02.006

Denny, M. W., and Harley, C. D. G. (2006). Hot limpets: predicting body temperature in a conductance-mediated thermal system. *J. Exp. Biol*. 209, 2409–2419. doi: 10.1242/jeb.02257

Denny, M. W., and Helmuth, B. (2009). Confronting the physiological bottleneck: a challenge from ecomechanics. *Integr. Comp. Biol*. 49, 197–201. doi: 10.1093/icb/icp070

Díaz, F., Denisse, R. A., Salas, A., Galindo-Sanchez, C. E., Gonzalez, M. A., Sanchez, A., et al. (2015). Behavioral thermoregulation and critical thermal limits of giant keyhole limpet *Megathura crenulate* (Sowerby 1825) (Mollusca; Vetigastropoda). *J. Therm. Biol*. 54, 133–138. doi: 10.1016/j.jtherbio.2013.05.007

Diederich, C. M., and Pechenik, J. A. (2013). Thermal tolerance of *Crepidula fornicata* (Gastropoda) life history stages from intertidal and subtidal subpopulations. *Mar. Ecol. Prog. Ser*. 486, 173–187. doi: 10.3354/meps10355

Dong, Y.-W., Li, X.-X., Choi, F. M. P., Williams, G. A., Somero, G. N., and Helmuth, B. (2017). Untangling the roles of microclimate, behaviour and physiological polymorphism in governing vulnerability of intertidal snails to heat stress. *Proc. R. Soc. B* 284:20162367. doi: 10.1098/rspb.2016.2367

Doty, M. S. (1946). Critical tide factors that are correlated with the vertical distribution of marine algae and other organisms along the Pacific coast. *Ecology* 27, 315–328. doi: 10.2307/1933542

Drake, M. J., Miller, N. A., and Todgham, A. E. (2017). The role of stochastic thermal environments in modulating the thermal physiology of an intertidal limpet, *Lottia digitalis*. *J. Exp. Biol*. 220, 3072–3083. doi: 10.1242/jeb.159020

Dring, M. J., and Brown, F. A. (1982). Photosynthesis of intertidal brown algae during and after periods of emersion: a renewed search for physiological causes of zonation. *Mar. Ecol. Prog. Ser*. 8, 301–308. doi: 10.2307/24815108

Edson, E. C., and Patterson, M. R. (2015). "MantaRay: a novel autonomous sampling instrument for *in situ* measurements of environmental microplastic particle concentrations,"in *OCEANS 2015 - MTS/IEEE Washington*. Abstract retrieved from IEEE Xplore (Accession No. 15798895) (Washington, DC).

Ehrlén, J., and Morris, W. F. (2015). Predicting changes in the distribution and abundance of species under environmental change. *Ecol. Lett*. 18, 303–314. doi: 10.1111/ele.12410

Elvin, D. W., and Gonor, J. J. (1979). The thermal regime of an intertidal *Mytilus californianus* Conrad population on the Central Oregon Coast. *J. Exp. Mar. Biol. Ecol*. 39, 265–279.

Erasmus, T., and De Villiers, A. F. (1982). Ore dust pollution and body temperatures of intertidal animals. *Mar. Pollut. Bull*. 13, 30–32.

Etter, R. J. (1988). Physiological stress and color polymorphism in the intertidal snail *Nucella lapillus*. *Evolution* 4, 660–680.

Faye, E., Dangles, O., and Pincebourde, S. (2016a). Distance makes the difference in thermography for ecological studies. *J. Therm. Biol.* 56, 1–9. doi: 10.1016/j.jtherbio.2015.11.011

Faye, E., Rebaudo, F., Cajo, D. Y., Fraunié, S. C., and Dangles, O. (2016b). A toolbox for studying thermal heterogeneity across spatial scales: from unmanned aerial vehicle imagery to landscape metrics. *Methods Ecol. Evol.* 7, 437–446. doi: 10.1111/2041-210X.12488

Faye, E., Rebaudo, F., Carpio, C., Herrera, M., and Dangles, O. (2017). Does heterogeneity in crop canopy microclimates matter for pests? Evidence from aerial high-resolution thermography. *Agric. Ecosyst. Environ.* 246, 124–133. doi: 10.1016/j.agee.2017.05.027

Finke, G. R., Bozinovic, F., and Navarrete, S. A. (2009). A mechanistic model to study the thermal ecology of a southeastern Pacific dominant intertidal mussel and implications for climate change. *Physiol. Biochem. Zool.* 82, 303–313. doi: 10.1086/599321

Finke, G. R., Navarrete, S. A., and Bozinovic, F. (2007). Tidal regimes of temperate coasts and their influences on aerial exposure for intertidal organisms. *Mar. Ecol. Prog. Ser.* 343, 57–62. doi: 10.3354/meps06918

Fitzhenry, T., Halpin, P. M., and Helmuth, B. (2004). Testing the effects of wave exposure, site, and behavior on intertidal mussel body temperatures: applications and limits of temperature logger design. *Mar. Biol.* 145, 339–349. doi: 10.1007/s00227-004-1318-6

Fly, E. K., Monaco, C. J., Pincebourde, S., and Tullis, A. (2012). The influence of intertidal location and temperature on the metabolic cost of emersion in Pisaster ochraceus. *J. Exp. Mar. Biol. Ecol.* 422–423, 20–28. doi: 10.1016/j.jembe.2012.04.007

Gates, D. M. (1980). *Biophysical Ecology*. New York, NY: Springer-Verlag.

Geller, G. N., Halpin, P. N., Helmuth, B., Hestir, E. L., Skidmore, A., Abrams, M. J., et al. (2017). "Remote Sensing for Biodiversity," in *The GEO Handbook on Biodiversity Observation Networks*, eds M. Walters and R. J. Scholes (Cham: Springer), 187–210. doi: 10.1007/978-3-319-27288-7_8

Gilman, S., Hayford, H., Craig, C., and Carrington, E. (2015). Body temperatures of an intertidal barnacle and two whelk predators in relation to shore height, solar aspect, and microhabitat. *Mar. Ecol. Prog. Ser.* 536, 77–88. doi: 10.3354/meps11418

Gilman, S. E., and Rognstad, R. L. (2018). Influence of food supply and shore height on the survival and growth of the barnacle *Balanus glandula* (Darwin). *J. Exp. Mar. Biol. Ecol.* 498, 32–38. doi: 10.1016/j.jembe.2017.10.006

Gleason, L. U., and Burton, R. S. (2016). Regional patterns of thermal stress and constitutive gene expression in the marine snail *Chlorostoma funebralis* in northern and southern California. *Mar. Ecol. Prog. Ser.* 556, 143–159. doi: 10.3354/meps11850

Gleason, L. U., Miller, L. P., Winnikoff, J. R., Somero, G. N., Yancey, P. H., Bratz, D., et al. (2017). Thermal history and gape of individual *Mytilus californianus* correlate with oxidative damage and thermoprotective osmolytes. *J. Exp. Biol.* 220, 4292–4304. doi: 10.1242/jeb.168450

Gunderson, A. R., Armstrong, E. J., and Stillman, J. H. (2016). Multiple stressors in a changing world: the need for an improved perspective on physiological responses to the dynamic marine environment. *Annu. Rev. Mar. Sci.* 8, 357–378. doi: 10.1146/annurev-marine-122414-033953

Hannah, L., Flint, L., Syphard, A. D., Moritz, M. A., Buckley, L. B., and McCullough, I. M. (2014). Fine-grain modeling of species' response to climate change: holdouts, stepping-stones, and microrefugia. *Trends Ecol. Evol.* 29, 390–397. doi: 10.1016/j.tree.2014.04.006

Hardin, D. D. (1968). A comparative study of lethal temperature in limpets *Acmaea digitalis* and *Acmaea scabra*. *Veliger* 11, 78–83.

Harley, C. D. G. (2008). Tidal dynamics, topographic orientation, and temperature-mediated mass mortalities on rocky shores. *Mar. Ecol. Prog. Ser.* 371, 37–46. doi: 10.3354/meps07711

Harley, C. D. G., and Helmuth, B. S. T. (2003). Local and regional scale effects of wave exposure, thermal stress, and absolute vs. effective shore level on patterns of intertidal zonation. *Limnol. Oceanogr.* 48, 1498–1508. doi: 10.4319/lo.2003.48.4.1498

Harley, C. D. G., and Lopez, J. P. (2003). The natural history, thermal physiology, and ecological impacts of intertidal mesopredators, *Oedoparena* spp. (Diptera: Dryomyzidae). *Invertebr. Biol.* 122, 61–73. doi: 10.1111/j.1744-7410.2003.tb00073.x

Hayford, H. A., Gilman, S. E., and Carrington, E. (2015). Foraging behavior minimizes heat exposure in a complex thermal landscape. *Mar. Ecol. Prog. Ser.* 518, 165–175. doi: 10.3354/meps11053

Hayford, H. A., O'Donnell, M., and Carrington, E. (2018). Radio tracking detects thermoregulation at a snail's pace. *J. Exp. Mar. Biol. Ecol.* 499, 17–25. doi: 10.1016/j.jembe.2017.12.005

Helmuth, B. (1999). Thermal biology of rocky intertidal mussels: quantifying body temperatures using climatological data. *Ecology* 80, 15–34.

Helmuth, B. (2002). How do we measure the environment? Linking intertidal thermal physiology and ecology through biophysics. *Integr. Comp. Biol.* 42, 837–845. doi: 10.1093/icb/42.4.837

Helmuth, B., Broitman, B. R., Blanchette, C. A., Gilman, S., Halpin, P., Harley, C. D. G., et al. (2006). Mosaic patterns of thermal stress in the rocky intertidal zone: implications for climate change. *Ecol. Monogr.* 76, 461–479. doi: 10.1890/0012-9615(2006)076[0461:MPOTSI]2.0.CO;2

Helmuth, B., Choi, F., Matzelle, A., Torossian, J. L., Morello, S. L., Mislan, K. A. S., et al. (2016). Long-term, high frequency *in situ* measurements of intertidal mussel bed temperatures using biomimetic sensors. *Sci. Data* 3:160087. doi: 10.1038/sdata.2016.87

Helmuth, B., Harley, C. D. G., Halpin, P. M., O'Donnell, M., Hofmann, G. E., and Blanchette, C. A. (2002). Climate change and latitudinal patterns of intertidal thermal stress. *Science* 298, 1015–1017. doi: 10.1126/science.1076814

Helmuth, B., Yamane, L., Lalwani, S., Matzelle, A., Tockstein, A., and Gao, N. (2011). Hidden signals of climate change in intertidal ecosystems: what (not) to expect when you are expecting. *J. Exp. Mar. Biol. Ecol.* 400, 191–199. doi:10.1016/j.jembe.2011.02.004

Helmuth, B. S., and Hofmann, G. E. (2001). Microhabitats, thermal heterogeneity, and patterns of physiological stress in the rocky intertidal zone. *Biol. Bull.* 201, 374–384. doi: 10.2307/1543615

Helmuth, B. S. T. (1998). Intertidal mussel microclimates: predicting the body temperature of a sessile invertebrate. *Ecol. Monogr.* 68, 51–74.

Herring, S. C., Hoell, A., Hoerling, M. P., Kossin, J. P., Schreck III, C. J. and Stott, P. A. (2016). Explaining extreme events of 2015 from a climate perspective. *Bull. Amer. Meteor. Soc.* 97, S1–S145.

Hobday, A. J., Alexander, L. V., Perkins, S. E., Smale, D. A., Straub, S. C., Oliver, E. C. J., et al. (2016). A hierarchical approach to defining marine heatwaves. *Prog. Oceanogr.* 141, 227–238. doi: 10.1016/j.pocean.2015.12.014

Hoegh-Guldberg, O., Jacob, D., Taylor, M., Bindi, M., Brown, S., Camilloni, I., et al. (2018). "Impacts of 1.5°C global warming on natural and human systems," in *Global Warming of 1.5°C. An IPCC Special Report on the Impacts of Global Warming of 1.5°C Above Pre-industrial Levels and Related Global Greenhouse Gas Emission Pathways, in the Context of Strengthening the Global Response to the Threat of Climate Change, Sustainable Development, and Efforts to Eradicate Poverty*, eds V. Masson-Delmotte, P. Zhai, H. O. Pörtner, D. Roberts, J. Skea, P. R. Shukla, A. Pirani, W. Moufouma-Okia, C. Péan, R. Pidcock, S. Connors, J. B. R. Matthews, Y. Chen, X. Zhou, M. I. Gomis, E. Lonnoy, T. Maycock, M. Tignor, and T. Waterfield. In Press.

Hunt, H. L. (1997). *Structure and Dynamics of Intertidal Mussel (Mytilus trossulus, Mytilus edulis) Assemblages*. PhD Thesis, Dalhousie University, Halifax, NS.

Hunt, H. L., and Scheibling, R. E. (2001). Patch dynamics of mussels on rocky shores: integrating process to understand pattern. *Ecology* 82, 3213–3231. doi: 10.2307/2679845

Hunt, H. L., and Scheibling, R. E. (2002). Movement and wave dislodgement of mussels on a wave-exposed rocky shore. *Veliger* 45, 273–277.

Hutchins, L. W. (1947). The bases for temperature zonation in geographical distribution. *Ecol. Monogr.* 17, 325–335.

Iacarella, J. C., and Helmuth, B. (2011). Experiencing the salt marsh environment through the foot of *Littoraria irrorata*: behavioral responses to thermal and desiccation stresses. *J. Exp. Mar. Biol. Ecol.* 409, 143–153. doi: 10.1016/j.jembe.2011.08.011

Jost, J., and Helmuth, B. (2007). Morphological and ecological determinants of body temperature of *Geukensia demissa*, the Atlantic Ribbed Mussel, and their effects on mussel mortality. *Biol. Bull.* 213, 141–151. doi: 10.2307/25066630

Kearney, M. (2006). Habitat, environment and niche: what are we modelling? *Oikos* 115, 186–191. doi: 10.1111/j.2006.0030-1299.14908.x

Kearney, M., Simpson, S. J., Raubenheimer, D., and Helmuth, B. (2010). Modelling the ecological niche from functional traits. *Philos. Trans. R. Soc. B* 365, 3469–3483. doi: 10.1098/rstb.2010.0034

Kearney, M. R., Matzelle, A., and Helmuth, B. (2012). Biomechanics meets the ecological niche: the importance of temporal data resolution. *J. Exp. Biol.* 215, 922–933. doi: 10.1242/jeb.059634

Kershaw, K. A. (1985). *Physiological Ecology of Lichens*. Cambridge: Cambridge University Press.

Kish, N. E., Helmuth, B., and Wethey, D. S. (2016). Physiologically grounded metrics of model skill: a case study estimating heat stress in intertidal populations. *Conserv. Physiol.* 4:cow038. doi: 10.1093/conphys/cow038

Kordas, R. L., Harley, C. D. G., and O'Connor, M. I. (2011). Community ecology in a warming world: the influence of temperature on interspecific interactions in marine systems. *J. Exp. Mar. Biol. Ecol.* 400, 218–226. doi: 10.1016/j.jembe.2011.02.029

Koussoroplis, A. M., Pincebourde, S., and Wacker, A. (2017). Understanding and predicting physiological performance of organisms in fluctuating and multifactorial environments. *Ecol. Monogr.* 87, 178–197. doi: 10.1002/ecm.1247

Kroeker, K. J., Sanford, E., Rose, J. M., Blanchette, C. A., Chan, F., Chavez, F. P., et al. (2016). Interacting environmental mosaics drive geographic variation in mussel performance and predation vulnerability. *Ecol. Lett.* 19, 771–779. doi: 10.1111/ele.12613

Lathlean, J. A., Ayre, D. J., Coleman, R. A., and Minchinton, T. E. (2014). Using biomimetic loggers to measure interspecific and microhabitat variation in body temperatures of rocky intertidal invertebrates. *Mar. Freshw. Res.* 66, 86–94. doi: 10.1071/MF13287

Lathlean, J. A., and Seuront, L. (2014). Infrared thermography in marine ecology: methods, previous applications, and future challenges. *Mar. Ecol. Prog. Ser.* 514, 263–277. doi: 10.3354/meps10995

Lathlean, J. A., Seuront, L., McQuaid, C. D., Terence, P. T. N., Zardi, G. I., and Nicastro, K. R. (2016a). Cheating the locals: invasive mussels steal and benefit from the cooling effect of indigenous mussels. *PLoS ONE* 11:e0152556. doi: 10.1371/journal.pone.0152556

Lathlean, J. A., Seuront, L., McQuaid, C. D., Terence, P. T. N., Zardi, G. I., and Nicastro, K. R. (2016b). Size and position (sometimes) matter: small-scale patterns of heat stress associated with two co-occurring mussels with different thermoregulatory behaviour. *Mar. Biol.* 163:189. doi: 10.1007/s00227-016-2966-z

Lathlean, J. A., Seuront, L., and Ng, T. P. T. (2017). On the edge: The use of infrared thermography in monitoring responses of intertidal organisms to heat stress. *Ecol. Indic.* 81, 567–577. doi: 10.1016/j.ecolind.2017.04.057

Leeuw, T., Boss, E., and Wright, D. (2013). *In situ* measurements of phytoplankton fluorescence using low cost electronics. *Sensors* 13, 7872–7883. doi: 10.3390/s130607872

Lewis, J. B. (1963). Environmental and tissue temperatures of some tropical intertidal marine animals. *Biol. Bull.* 124, 277–284.

Lima, F., Burnett, N., Helmuth, B., Kish, N., and Aveni-Deforge, K. (2011). "Monitoring the intertidal environment with biomimetic devices," in *Biomimetic Based Applications,* ed A. George (InTech). doi: 10.5772/14153

Lima, F. P., and Wethey, D. S. (2009). Robolimpets: measuring intertidal body temperatures using biomimetic loggers. *Limnol. Oceanogr. Methods* 7, 347–353. doi: 10.4319/lom.2009.7.347

Lockridge, G., Dzwonkowski, B., Nelson, R., and Powers, S. (2016). Development of a low-cost Arduino-based sonde for coastal applications. *Sensors* 16:528. doi: 10.3390/s16040528

Lubchenco, J. (1980). Algal zonation in the New England rocky intertidal community: an experimental analysis. *Ecology* 61, 333–344.

Marshall, D. J., McQuaid, C. D., and Williams, G. A. (2010). Non-climatic thermal adaptation: implications for species' responses to climate warming. *Biol. Lett.* 6, 669–673. doi: 10.1098/rsbl.2010.0233

Marshall, D. J., Rezende, E. L., Baharuddin, N., Choi, F., and Helmuth, B. (2015). Thermal tolerance and climate warming sensitivity in tropical snails. *Ecol. Evol.* 5, 5905–5919. doi: 10.1002/ece3.1785

McAfee, D., Bishop, M. J., Yu, T. N., and Williams, G. A. (2018). Structural traits dictate abiotic stress amelioration by intertidal oysters. *Funct. Ecol.* 27, 249. doi: 10.1111/1365-2435.13210

Meola, C., and Carlomagno, G. M. (2004). Recent advances in the use of infrared thermography. *Meas. Sci. Technol.* 15, 27–58. doi: 10.1088/0957-0233/15/9/R01

Mesinger, F., DiMego, G., Kalnay, E., Mitchell, K., Shafran, P. C., Ebisuzaki, W., et al. (2006). North American regional reanalysis. *Bull. Am. Meteorol. Soc.* 87:3. doi: 10.1175/BAMS-87-3-343

Miller, L. P., and Denny, M. W. (2016). Importance of behavior and morphological traits for controlling body temperature in Littorinid snails. *Biol. Bull.* 220, 209–223. doi: 10.1086/BBLv220n3p209

Miller, L. P., and Dowd, W. W. (2017). Multimodal *in situ* datalogging quantifies inter-individual variation in thermal experience and persistent origin effects on gaping behavior among intertidal mussels (*Mytilus californianus*). *J. Exp. Biol.* 220, 4305–4319. doi: 10.1242/jeb.164020

Mislan, K. A., and Wethey, D. S. (2011). Gridded meteorological data as a resource for mechanistic macroecology in coastal environments. *Ecol. Appl.* 21, 2678–2690. doi: 10.1890/10-2049.1

Mislan, K. A., and Wethey, D. S. (2015). A biophysical basis for patchy mortality during heat waves. *Ecology* 96, 902–907. doi: 10.1890/14-1219.1

Mislan, K. A. S., Helmuth, B., and Wethey, D. S. (2014). Geographical variation in climatic sensitivity of intertidal mussel zonation. *Glob. Ecol. Biogeogr.* 23, 744–756. doi: 10.1111/geb.12160

Mitchell, J. W. (1976). Heat transfer from spheres and other animal forms. *Biophys. J.* 16, 561–569.

Mitton, J. B. (1977). Shell color and pattern variation in *Mytilus edulis* and its adaptive significance. *Chesapeake Sci.* 18, 387–390. doi: 10.2307/1350595

Monaco, C. J., and Helmuth, B. (2011). Tipping points, thresholds and the keystone role of physiology in marine climate change research. *Adv. Mar. Biol.* 60, 123–160. doi: 10.1016/B978-0-12-385529-9.00003-2

Monaco, C. J., Wethey, D. S., Gulledge, S., and Helmuth, B. (2015). Shore-level size gradients and thermal refuge use in the predatory sea star *Pisaster ochraceus*: the role of environmental stressors. *Mar. Ecol. Prog. Ser.* 539, 191–205. doi: 10.3354/meps11475

Monaco, C. J., Wethey, D. S., and Helmuth, B. (2016). Thermal sensitivity and the role of behavior in driving an intertidal predator–prey interaction. *Ecol. Monogr.* 86, 429–447. doi: 10.1002/ecm.1230

Montalto, V., Sarà, G., Ruti, P. M., Dell'Aquila, A., and Helmuth, B. (2014). Testing the effects of temporal data resolution on predictions of the effects of climate change on bivalves. *Ecol. Model.* 278, 1–8. doi: 10.1016/j.ecolmodel.2014.01.019

Montanholi, Y. R., Swanson, K. C., Palme, R., Schenkel, F. S., McBride, B. W., Lu, D., et al. (2010). Assessing feed efficiency in beef steers through feeding behaviour, infrared thermography and glucocorticoids. *Animal* 4, 692–701. doi: 10.1017/S1751731109991522

Nagai, K., Honjo, T., Go, J., Yamashita, H., and Seok Jin, O. (2006). Detecting the shellfish killer *Heterocapsa circularisquama* (Dynophyceae) by measuring bivalve valve activity with a hall element sensor. *Aquaculture* 255, 395–401. doi: 10.1016/j.aquaculture.2005.12.018

Ng, J. S. S., and Williams, G. A. (2006). Intraspecific variation in foraging behaviour: influence of shore height on temporal organization of activity in the chiton *Acanthopleura japonica*. *Mar. Ecol. Prog. Ser.* 321, 183–192. doi: 10.3354/meps321183

Ng, T. P. T., Lau, S. L. Y., Seuront, L., Davies, M. S., Stafford, R., Marshall, D. J., et al. (2017). Linking behaviour and climate change in intertidal ectotherms: insights from littorinid snails. *J. Exp. Mar. Biol. Ecol.* 492, 121–131. doi: 10.1016/j.jembe.2017.01.023

Nicastro, K. R., Zardi, G. I., McQuaid, C. D., Pearson, G. A., and Serrão, E. A. (2012). Love thy neighbour: group properties of gaping behaviour in mussel aggregations. *PLoS ONE* 7:e47382. doi: 10.1371/journal.pone.0047382

Okamura, B. (1986). Group living and the effects of spatial position in aggregations of Mytilus edulis. *Oecologia* 69, 341–347. doi: 10.1007/BF00377054

Olabarria, C., Gestoso, I., Lima, F. P., Vázquez, E., Comeau, L. A., Gomes, F., et al. (2016). Response of two Mytilids to a heatwave: the complex interplay of physiology, behaviour and ecological interactions. *PLoS ONE* 11:e0164330. doi: 10.1371/journal.pone.0164330.3

Paine, R. T. (1994). *Marine Rocky Shores and Community Ecology: An Experimentalist's Perspective*. Oldendorf; Luhe: Ecology Institute.

Parsons, K. (2014). *Human Thermal Environments: The Effects of Hot, Moderate, and Cold Environments on Human Health, Comfort, and Performance*. Boca Raton, FL: CRC Press.

Pearson, G. A., Leston, A. L., and Mota, C. (2009). Frayed at the edges: selective pressure and adaptive response to abiotic stressors are

mismatched in low diversity edge populations. *J. Ecol.* 97, 450–462. doi: 10.1111/j.1365-2745.2009.01481.x

Pershing, A. J., Alexander, M. A., Hernandez, C. M., Kerr, L. A., Le Bris, A., Mills, K. E., et al. (2015). Slow adaptation in the face of rapid warming leads to collapse of the Gulf of Maine cod fishery. *Science* 350:6262, 809–812. doi: 10.1126/science.aac9819

Petchey, O. L., Pontarp, M., Massie, T. M., Kéfi, S., Ozgul, A., Weilenmann, M., et al. (2015). The ecological forecast horizon, and examples of its uses and determinants. *Ecol. Lett.* 18, 597–611. doi: 10.1111/ele.12443

Peters, M. K., Hemp, A., Appelhans, T., Behler, C., Classen, A., Detsch, F., et al. (2016). Predictors of elevational biodiversity gradients change from single taxa to the multi-taxa community level. *Nat. Commun.* 7:13736. doi: 10.1038/ncomms13736

Pfister, C. A., Wootton, J. T., and Neufeld, C. J. (2007). The relative roles of coastal and oceanic processes in determining physical and chemical characteristics of an intensively sampled nearshore system. *Limnol. Oceanogr.* 52, 1767–1775. doi: 10.4319/lo.2007.52.5.1767

Pincebourde, S., and Casas, J. (2006). Leaf miner-induced changes in leaf transmittance cause variations in insect respiration rates. *J. Insect Physiol.* 52, 194–201. doi: 10.1016/j.jinsphys.2005.10.004

Pincebourde, S., Sanford, E., Casas, J., and Helmuth, B. (2012). Temporal coincidence of environmental stress events modulates predation rates. *Ecol. Lett.* 15, 680–688. doi: 10.1111/j.1461-0248.2012.01785.x

Pincebourde, S., Sanford, E., and Helmuth, B. (2008). Interaction between underwater and aerial body temperatures in influencing a top predator feeding rate in the intertidal. *Comp. Biochem. Physiol. Part A Mol. Integr. Physiol.* 150:3. doi: 10.1016/j.cbpa.2008.04.184

Pincebourde, S., Sanford, E., and Helmuth, B. (2009). An intertidal sea star adjusts thermal inertia to avoid extreme body temperatures. *Am. Nat.* 174, 890–897. doi: 10.1086/648065

Place, S. P., O'Donnell, M. J., and Hofmann, G. E. (2008). Gene expression in the intertidal mussel *Mytilus californianus*: physiological response to environmental factors on a biogeographic scale. *Mar. Ecol. Prog. Ser.* 356, 1–14. doi: 10.3354/meps07354

Porter, J., Arzberger, P., Braun, H., Bryant, P., Gage, S., Hansen, T., et al. (2005). Wireless sensor networks for ecology. *BioScience* 55, 561–572. doi: 10.1641/0006-3568(2005)055[0561:WSNFE]2.0.CO;2

Porter, W. P., Budaraju, S., Stewart, W. E., and Ramankutty, N. (2000). Calculating climate effects on birds and mammals: impacts on biodiversity, conservation, population parameters, and global community structure. *Integr. Comp. Biol.* 40, 597–630. doi: 10.1093/icb/40.4.597

Porter, W. P., and Gates, D. M. (1969). Thermodynamic Equilibria of Animals with Environment. *Ecol. Monogr.* 39, 227–244. doi: 10.2307/1948545

Porter, W. P., Mitchell, J. W., Beckman, W. A., and DeWitt, C. B. (1973). Behavioral implications of mechanistic ecology. *Oecologia* 13, 1–54.

Pörtner, H. O., Peck, L. S., and Hirse, T. (2006). Hyperoxia alleviates thermal stress in the Antarctic bivalve, *Laternula elliptica*: evidence for oxygen limited thermal tolerance. *Polar Biol.* 29, 688–693. doi: 10.1007/s00300-005-0106-1

Potter, K. A., Arthur Woods, H., and Pincebourde, S. (2013). Microclimatic challenges in global change biology. *Glob. Change Biol.* 19, 2932–2939. doi: 10.1111/gcb.12257

Robert, K. A., and Thompson, M. B. (2003). Reconstructing Thermochron iButtons to reduce size and weight as a new technique in the study of small animal thermal biology. *Herpetol. Rev.* 34, 130–132.

Robinet, C., Rousselet, J., Pineau, P., Miard, F., and Roques, A. (2013). Are heat waves susceptible to mitigate the expansion of a species progressing with global warming?. *Ecol. Evol.* 3, 2947–2957. doi: 10.1002/ece3.690

Sarà, G., Kearney, M., and Helmuth, B. (2011). Combining heat-transfer and energy budget models to predict thermal stress in Mediterranean intertidal mussels. *Chem. Ecol.* 27, 135–145. doi: 10.1080/02757540.2011.552227

Scheffers, B. R., Edwards, D. P., Diesmos, A., Williams, S. E., and Evans, T. A. (2013). Microhabitats reduce animal's exposure to climate extremes. *Glob. Change Biol.* 20, 495–503. doi: 10.1111/gcb.12439

Scherrer, D., and Körner, C. (2010). Infra-red thermometry of alpine landscapes challenges climatic warming projections. *Glob. Change Biol.* 16, 2602–2613. doi: 10.1111/j.1365-2486.2009.02122.x

Scherrer, D., and Körner, C. (2011). Topographically controlled thermal-habitat differentiation buffers alpine plant diversity against climate warming. *J. Biogeogr.* 38, 406–416. doi: 10.1111/j.1365-2699.2010.02407.x

Schneider, K. R., and Helmuth, B. (2007). Spatial variability in habitat temperature may drive patterns of selection between an invasive and native mussel species. *Mar. Ecol. Prog. Ser.* 339, 157–167. doi: 10.3354/meps339157

Schneider, K. R., Wethey, D. S., Helmuth, B. S. T., and Hilbish, T. J. (2005). Implications of movement behavior on mussel dislodgement: exogenous selection in a *Mytilus* spp. hybrid zone. *Mar. Biol.* 146, 333–343. doi: 10.1007/s00227-004-1446-z

Seabra, R., Wethey, D. S., Santos, A. M., and Lima, F. P. (2011). Side matters: microhabitat influence on intertidal heat stress over a large geographical scale. *J. Exp. Mar. Biol. Ecol.* 400, 200–208. doi: 10.1016/j.jembe.2011.02.010

Sears, M. W., Angilletta, M. J., Schuler, M. S., Borchert, J., Dilliplane, K. F., Stegman, M., et al. (2016). Configuration of the thermal landscape determines thermoregulatory performance of ectotherms. *Proc. Natl. Acad. Sci. U.S.A.* 113, 10595–10600. doi: 10.1073/pnas.1604824113

Sinclair, B. J., Marshall, K. E., Sewell, M. A., Levesque, D. L., Willett, C. S., and Slotsbo, S. (2016). Can we predict ectotherm responses to climate change using thermal performance curves and body temperatures? *Ecol. Lett.* 19, 1372–1385. doi: 10.1111/ele.12686

Smale, D. A., and Wernberg, T. (2009). Satellite-derived SST data as a proxy for water temperature in nearshore benthic ecology. *Mar. Ecol. Prog. Ser.* 387, 27–37. doi: 10.3354/meps08132

Somero, G. N. (2002). Thermal physiology and vertical zonation of intertidal animals: optima, limits, and costs of living. *Integr. Comp. Biol.* 42, 780–789. doi: 10.1093/icb/42.4.780

Somero, G. N. (2010). The physiology of climate change: how potentials for acclimatization and genetic adaptation will determine 'winners' and 'losers'. *J. Exp. Biol.* 213, 912–920. doi: 10.1242/jeb.037473

Sorte, C. J., Davidson, V. E., Franklin, M. C., Benes, K. M., Doellman, M. M., Etter, R. J., et al. (2016). Long-term declines in an intertidal foundation species parallel shifts in community composition. *Glob. Change Biol.* 23, 341–352. doi: 10.1111/gcb.13425

Southward, A. J. (1958). Note on the temperature tolerances of some intertidal animals in relation to environmental temperatures and geographical distribution. *J. Mar. Biol. Assoc. U.K.* 37, 49–66. doi: 10.1017/S0025315400014818

Stenseth, N. C., Mysterud, A., Ottersen, G., Hurrell, J. W., Chan, K. S., and Lima, M. (2002). Ecological effects of climate fluctuations. *Science* 297, 1292–1296. doi: 10.1126/science.1071281

Stillman, J., and Somero, G. (1996). Adaptation to temperature stress and aerial exposure in congeneric species of intertidal porcelain crabs (genus *Petrolisthes*): correlation of physiology, biochemistry and morphology with vertical distribution. *J. Exp. Biol.* 199, 1845–1855.

Sunday, J. M., Bates, A. E., and Dulvy, N. K. (2011). Global analysis of thermal tolerance and latitude in ectotherms. *Proc. R. Soc. Lond. Ser. B* 278, 1823–1830. doi: 10.1098/rspb.2010.1295

Sunday, J. M., Bates, A. E., Kearney, M. R., Colwell, R. K., Dulvy, N. K., Longino, J. T., et al. (2014). Thermal-safety margins and the necessity of thermoregulatory behavior across latitude and elevation. *Proc. Natl. Acad. Sci. U.S.A.* 111, 5610–5615. doi: 10.1073/pnas.1316145111

Sunday, J. M., Pecl, G. T., Frusher, S., Hobday, A. J., Hill, N., Holbrook, N. J., et al. (2015). Species traits and climate velocity explain geographic range shifts in an ocean-warming hotspot. *Ecol. Lett.* 18, 944–953. doi: 10.1111/ele.12474

Szathmary, P. L., Helmuth, B., and Wethey, D. S. (2009). Climate change in the rocky intertidal zone: predicting and measuring the body temperature of a keystone predator. *Mar. Ecol. Prog. Ser.* 374, 43–56. doi: 10.3354/meps07682

Thomas, F. I. M. (1987). *The Hot and Cold of Life on Rocks: Determinants of Body Temperature in the Northern Rock Barnacle, Semibalanus Balanoides*. Master's Thesis, Brown University, Providence, RI.

Torossian, J. L., Kordas, R. L., and Helmuth, B. (2016). Cross-Scale approaches to forecasting biogeographic responses to climate change. *Adv. Ecol. Res.* 55, 371–433. doi: 10.1016/bs.aecr.2016.08.003

Tsuchiya, M. (1983). Mass mortality in a population of the mussel *Mytilus edulis* L. caused by high temperature on rocky shores. *J. Exp. Mar. Biol. Ecol.* 66, 101–111. doi: 10.1016/0022-0981(83)90032-1

UNFCCC (2015). *FCCC/CP/2015/L.9/Rev.1. Adoption of the Paris Agreement.* Paris: UNFCCC, 1–32.

Van Alstyne, K. L., and Olson, T. K. (2014). Estimating variation in surface emissivities of intertidal macroalgae using an infrared thermometer and the effects on temperature measurements. *Mar. Biol.* 161, 1409–1418. doi: 10.1007/s00227-014-2429-3

Vermeij, G. J. (1971). Temperature relationships of some tropical Pacific intertidal gastropods. *Mar. Biol.* 10, 308–314.

Wethey, D. S. (1983). Geographic limits and local zonation: the barnacles *Semibalanus* (*Balanus*) and *Chthamalus* in New England. *Biol. Bull.* 165, 330–341.

Wethey, D. S. (1984). Sun and shade mediate competition in the barnacles *Chthamalus* and *Semibalanus*: a field experiment. *Biol. Bull.* 167, 176–185.

Wethey, D. S. (2002). Biogeography, competition, and microclimate: the barnacle *Chthamalus fragilis* in New England. *Integr. Comp. Biol.* 42, 872–880. doi: 10.1093/icb/42.4.872

Wethey, D. S., Brin, L. D., Helmuth, B., and Mislan, K. A. S. (2011). Predicting intertidal organism temperatures with modified land surface models. *Ecol. Modell.* 222, 3568–3576. doi: 10.1016/j.ecolmodel.2011.08.019

Williams, G. A., De Pirro, M., Cartwright, S., Khangura, K., Ng, W. C., Leung, P. T. Y., et al. (2011). Come rain or shine: the combined effects of physical stresses on physiological and protein-level responses of an intertidal limpet in the monsoonal tropics. *Funct. Ecol.* 25, 101–110. doi: 10.1111/j.1365-2435.2010.01760.x

Williams, G. A., De Pirro, M., Leung, K. M. Y., and Morritt, D. (2005). Physiological responses to heat stress on a tropical shore: the benefits of mushrooming behaviour in the limpet *Cellana grata*. *Mar. Ecol. Prog. Ser.* 292, 213–224. doi: 10.3354/meps292213

Williams, G. A., and Morritt, D. (1995). Habitat partitioning and thermal tolerance in a tropical limpet, *Cellana grata*. *Mar. Ecol. Prog. Ser.* 124, 89–103. doi: 10.3354/meps124089

Williams, R. J. (1970). Freezing tolerance in *Mytilus edulis*. *Comp. Biochem. Physiol.* 35, 145–161.

Woodin, S. A., Hilbish, T. J., Helmuth, B., Jones, S. J., and Wethey, D. S. (2013). Climate change, species distribution models, and physiological performance metrics: predicting when biogeographic models are likely to fail. *Ecol. Evol.* 3, 3334–3346. doi: 10.1002/ece3.680

Woods, H. A., Dillon, M. E., and Pincebourde, S. (2015). The roles of microclimatic diversity and of behavior in mediating the responses of ectotherms to climate change. *J. Therm. Biol.* 54, 86–97. doi: 10.1016/j.jtherbio.2014.10.002

World Meteorological Organization (2008). *Guide to Meteorological Instruments and Methods of Observation, 7th Edn*. WMO Report No. 8, I.2–3.

Zardi, G. I., Nicastro, K. R., McQuaid, C. D., Hancke, L., and Helmuth, B. (2010). The combination of selection and dispersal helps explain genetic structure in intertidal mussels. *Oecologia* 165, 947–958. doi: 10.1007/s00442-010-1788-9

Zhou, X., Ji, X., Wang, B., Cheng, Y., Ma, Z., Choi, F., et al. (2018). Pido: predictive delay optimization for intertidal wireless sensor networks. *Sensors* 18, 1464–1482. doi: 10.3390/s18051464

Conflict of Interest Statement: The authors declare that the research was conducted in the absence of any commercial or financial relationships that could be construed as a potential conflict of interest.

Copyright © 2018 Judge, Choi and Helmuth. This is an open-access article distributed under the terms of the Creative Commons Attribution License (CC BY). The use, distribution or reproduction in other forums is permitted, provided the original author(s) and the copyright owner(s) are credited and that the original publication in this journal is cited, in accordance with accepted academic practice. No use, distribution or reproduction is permitted which does not comply with these terms.

frontiers in Ecology and Evolution

ORIGINAL RESEARCH
published: 25 January 2019
doi: 10.3389/fevo.2019.00004

Fine-Scale Tracking of Ambient Temperature and Movement Reveals Shuttling Behavior of Elephants to Water

Maria Thaker[1,2*†], *Pratik R. Gupte*[1,3,4,5†], *Herbert H. T. Prins*[6], *Rob Slotow*[2,7] *and Abi T. Vanak*[2,3,8]

[1] Centre for Ecological Sciences, Indian Institute of Science, Bangalore, India, [2] School of Life Sciences, University of Kwazulu-Natal, Pietermaritzburg, South Africa, [3] Ashoka Trust for Research in Ecology and the Environment, Bangalore, India, [4] Groningen Institute for Evolutionary Life Sciences, University of Groningen, Groningen, Netherlands, [5] Department of Coastal Systems, Royal Netherlands Institute for Sea Research, Texel, Netherlands, [6] Resource Ecology Group, Wageningen University, Wageningen, Netherlands, [7] Department of Genetics, Evolution and Environment, University College, London, United Kingdom, [8] DBT/Wellcome Trust India Alliance, Hyderabad, India

OPEN ACCESS

Edited by:
Thomas Wassmer,
Siena Heights University,
United States

Reviewed by:
Andrea Fuller,
University of the Witwatersrand,
South Africa
Blandine Françoise Doligez,
Center for the National Scientific
Research (CNRS), France

***Correspondence:**
Maria Thaker
mthaker@iisc.ac.in

† These authors share first authorship

Specialty section:
This article was submitted to
Behavioral and Evolutionary Ecology,
a section of the journal
Frontiers in Ecology and Evolution

Received: 14 August 2018
Accepted: 08 January 2019
Published: 25 January 2019

Citation:
Thaker M, Gupte PR, Prins HHT,
Slotow R and Vanak AT (2019)
Fine-Scale Tracking of Ambient
Temperature and Movement Reveals
Shuttling Behavior of Elephants to
Water. Front. Ecol. Evol. 7:4.
doi: 10.3389/fevo.2019.00004

Movement strategies of animals have been well studied as a function of ecological drivers (e.g., forage selection and avoiding predation) rather than physiological requirements (e.g., thermoregulation). Thermal stress is a major concern for large mammals, especially for savanna elephants *(Loxodonta africana),* which have amongst the greatest challenge for heat dissipation in hot and arid environments. Therefore, elephants must make decisions about where and how fast to move to reduce thermal stress. We tracked 14 herds of elephant in Kruger National Park (KNP), South Africa, for 2 years, using GPS collars with inbuilt temperature sensors to examine the influence of temperature on movement strategies, particularly when accessing water. We first confirmed that collar-mounted temperature loggers captured hourly variation in relative ambient temperatures across the landscape, and, thus, could be used to predict elephant movement strategies at fine spatio-temporal scales. We found that elephants moved slower in more densely wooded areas, but, unexpectedly, moved faster at higher temperatures, especially in the wet season compared to the dry season. Notably, this speed of movement was highest when elephants were approaching and leaving water sources. Visits to water showed a periodic shuttling pattern, with a peak return rate of 10–30 h, wherein elephants were closest to water during the hotter times of the day, and spent longer at water sources in the dry season compared to the wet season. When elephants left water, they showed low fidelity to the same water source, and traveled farther in the dry season than in the wet season. In KNP, where water is easily accessible, and the risk of poaching is low, we found that elephants use short, high-speed bursts of movement to get to water at hotter times of day. This strategy not only provides the benefit of predation risk avoidance, but also allows them to use water to thermoregulate. We demonstrate that ambient temperature is an important predictor of movement and water use across the landscape, with elephants responding facultatively to a "landscape of thermal stress."

Keywords: ***Loxodonta africana*, thermoregulation, GPS telemetry, temperature, water, habitat, shuttle**

INTRODUCTION

Ranging behavior of mammals is influenced by an optimization of multiple ecological drivers, from maximizing resource acquisition and habitat selection (Fortin et al., 2003; Bastille-Rousseau et al., 2018), to minimizing predation risk and competition (Valeix et al., 2009; Thaker et al., 2011; Vanak et al., 2013). We have a strong understanding of movement strategies based on the ecology of animals, but the importance of animal physiology in driving movements is becoming increasingly apparent. For example, the energetics of movement strongly influence how terrestrial carnivores use terrain and other habitat features during hunting (Scantlebury et al., 2014; Williams et al., 2014; Bryce et al., 2017). Similarly, the intensity of locomotion (number of strokes) of Weddell seals *(Leptonychotes weddellii)* directly affects post-dive oxygen consumption (Williams et al., 2004). In ungulates, adaptation to temperature fluctuations influence activity patterns (Hetem et al., 2011; Shrestha et al., 2012) and in savanna elephants (*Loxodonta africana*), chronic stress can restrict the home-ranges of herds and increase use of refugia (Jachowski et al., 2012, 2013; Wato et al., 2016). With advances in animal telemetry allowing for the incorporation of a range of sensors (Kays et al., 2015), and the rapidly developing field of movement ecology (Nathan et al., 2008), we now have an opportunity to understand movement strategies not only as an outcome of balancing ecological drivers, but as a function of physiological requirements and constraints.

One of the strongest drivers of how animals use their environment is ambient temperature (Shrestha et al., 2014; Mitchell et al., 2018). Animals respond to environmental temperature by thermoregulating with physiological adaptations and behavioral strategies (Angilletta, 2009). Most desert dwelling mammals have multiple physiological adaptations to reduce water loss (Cain et al., 2006; Fuller et al., 2014), but they also shift their activity peaks to cooler times of the day or are nocturnal (Walsberg, 2000; Aublet et al., 2009). Occupying habitats or using environmental features that either promote heat loss, such as water sources, or reduce heat gain, such as shade under dense vegetation, constitutes an important class of behavioral responses to heat stress. For example, moose *(Alces alces)* seek refuge from high temperatures in shady coniferous forest in summer (van Beest et al., 2012), and Arabian oryx *(Oryx leucoryx)* select for covered sites during the hottest part of the day (Hetem et al., 2012). Some landscape features, such as water sources, may promote both behavioral and physiological thermoregulation. Replenishment of body water reserves staves off dehydration, and also makes evaporative cooling a viable thermoregulatory strategy (Dunkin et al., 2013). Hence, large herbivores such as Cape buffalo *(Syncerus caffer)* and savanna elephant both wallow as well as drink at water sources to cool down (Prins, 1996; Bennitt et al., 2014; Purdon, 2015).

When water sources are limited, mammals must balance the thermoregulatory benefits against the costs of increased predation and competition (Valeix et al., 2009; Cain et al., 2012; Chamaillé-Jammes et al., 2013; Owen-Smith and Goodall, 2014). Individuals may attempt to avoid such costs by shuttling, i.e., moving frequently between water and safer sites, but this movement increases travel costs and decreases time that could have been spent foraging or resting (Johnson et al., 2002; Cain et al., 2012; Chamaillé-Jammes et al., 2013; Giotto et al., 2015). Water-dependence can introduce periodicity to movement strategies in the short term, and may further result in strong fidelity to known water sources (Giotto et al., 2015). Long term seasonal differences in the distribution and accessibility of water can also influence movement strategies; for example, buffalo in the Okavango delta are closer to permanent water sources in the dry season, when ephemeral sources dry up and water availability across the landscape is reduced (Bennitt et al., 2014). Thus, for mammals living in hot arid and semi-arid areas, temperature is the underlying environmental driver that dictates when and how frequently they access water.

Here we investigate how ambient temperature drives the ranging behavior of the largest land mammal, the savanna elephant. The large size of the elephant makes heat dissipation a greater challenge than heat retention (Wright and Luck, 1984; Williams, 1990). In response, elephants use a range of thermoregulatory strategies, involving both physiological and behavioral mechanisms of losing heat (Buss and Estes, 1971; Wright and Luck, 1984; Myhrvold et al., 2012; Dunkin et al., 2013; Mole et al., 2016). For example, elephants seek shade (Kinahan et al., 2007b), lose heat via the trunk (Williams, 1990), and flap their ears (Hiley, 1975; Wright, 1984; Wright and Luck, 1984), as non-evaporative cooling strategies. At larger spatio-temporal scales, elephants avoid thermal stress by shifting their activity peaks to cooler times of the day, and selecting for thermally stable landscapes with lower variation in daily temperatures (Kinahan et al., 2007a). Elephants are also heavily water dependent, and make periodic visits to water to hydrate, as well as to use evaporative cooling to thermoregulate (Dunkin et al., 2013; Valls-Fox, 2015). Thus, at the landscape scale, environmental temperature and the distribution of accessible water are expected to be important drivers of elephant movement strategies (Purdon and van Aarde, 2017; Wato et al., 2018). Yet, there has been little work to understand the role of thermoregulation on the dynamic landscape-scale movement decisions of elephants (Dunkin et al., 2013). Although other studies have examined the effect of temperature on animal movement, this key environmental predictor is typically derived from global environmental datasets, such as BIOCLIM (Guralnick, 2006), remotely sensed satellite data (Purdon and van Aarde, 2017), or weather station data (Purdon and van Aarde, 2017). Such data, however, are either temporally or spatially mismatched to the scale of animal movement. Here, we use high-resolution position data from GPS telemetry, coupled with instantaneous data from temperature loggers on GPS collars, to track both elephant movement and variation in ambient temperature across the heterogeneous savanna landscape. We first establish that collar temperature is well predicted by ambient temperature, and thus can be used as a fine-scaled measure of variation in the thermal landscape. This approach allows us to test the hypothesis that relative differences in ambient temperature are an important driver of movement strategies of elephants in Kruger National Park, South Africa.

We then closely examine movement behavior in relation to water visits, focusing in particular on the distance traveled and movement rates as elephants approach and leave water sources. With dynamic tracking of the variable thermal landscape and movements at fine spatio-temporal scales, we show how water dependency in wild savanna elephants is dictated by variation in environment temperature.

METHODS

Elephant Tracking Data

The study was conducted in the central and southern part of Kruger National Park (extent: 31.1 °E–32.0 °E, 23.9 °S–25.4 °S) in South Africa, where 14 female African elephants, each from a different herd, were fitted with GPS logger collars (African Wildlife Tracking, **Figure 1**) set to record a location every half

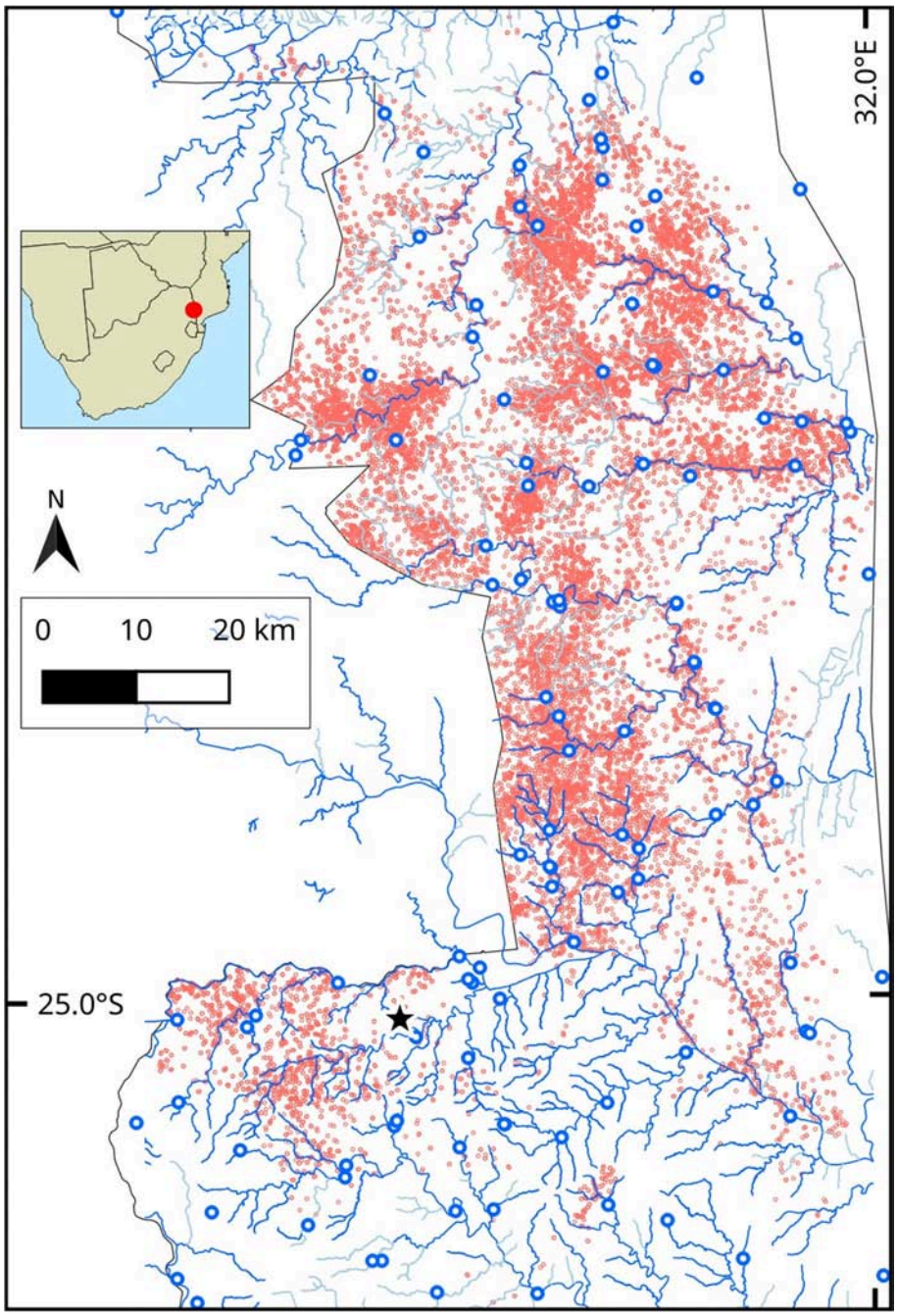

FIGURE 1 | Study area (red circle, inset) in Kruger National Park (KNP), South Africa, showing: Park boundary (gray line), seasonal, and perennial rivers (solid blue lines), open waterholes (blue circles), location of the Skukuza flux tower (star) and positions of 14 elephants over 2 years between August 2007 and 2009 (red points). Only a subset of elephant positions (noon and midnight) are shown for better visibility (red points).

hour. Details of the capture and collaring of these elephants can be found in Birkett et al. (2012). Collars on elephants had inbuilt temperature loggers that were mounted on the GPS chipset, and the entire electronic unit was embedded in dental acrylic. The temperature recorded by the collar-mounted sensor is a combination of ambient, circuit-generated and elephant body temperature (African Wildlife Tracking, *pers. comm.*). For this study, we used location and temperature data from 14 collared elephants over 731 days between August 2007 and August 2009. We classified the data from the study period into the dry and wet seasons based on actual rainfall data during those years (as per Birkett et al., 2012). Each elephant was tracked for an average of 562 days (SD = 175; range = 260–723) over the study period. We obtained 283,737 GPS positions in total from 14 elephants, with roughly equal points in the dry (n = 138,764) and wet seasons (n = 144,973).

Landscape Data

We obtained the following landscape-level data for the study area: (1) percent woody cover, extracted from Bucini et al. (2010), (2) map (line shapefiles) of all waterways logged on OpenStreetMap (n = 939), and (3) locations of active park waterholes (n = 124, South African National Parks). Waterways in the study area included perennial and seasonal rivers ($n_{perennial}$ = 72, $n_{seasonal}$ = 11), streams ($n_{seasonal}$ = 460, $n_{perennial}$ = 363), and one canal. Seasonal rivers and streams were only included in the calculations for the wet season, when we expected them to have water. Waterholes in the study area were of different types and included boreholes (n = 74), concrete dams (n = 8), concrete weir dams (n = 5), earthen dams (n = 30), and pipeline troughs (n = 7). All open waterholes were included in the distance to water calculations in each season. Waterholes were on average 4 km (SD = 3.2 km; range = 0.1–14 km) from each other.

We obtained two measures of ambient temperature at different spatio-temporal scales. At a fine temporal scale, we obtained half-hourly ambient temperature data from the flux tower at Skukuza (24.9°S, 31.5°E from a Rotronic HygroClip2 Temp/RH probe mounted at 16 m height; South African National Parks) over the study period. Ambient temperature data from the Skukuza flux tower (n = 52,608) ranged from 5.6 to 39.3°C in the dry season and 4.2 to 36.9°C in the wet season (seasons defined as per Birkett et al., 2012); daily means ± SD were 21.9 ± 5.4°C and 21.5 ± 5.2°C in the dry and wet seasons, respectively.

At the coarse landscape-scale, we obtained surface reflectance satellite images of the study area taken in the low-gain thermal infrared range (Band 6; wavelength 10.4–12.5 μm; units: Kelvin, converted to degree Celsius) by the Thematic Mapper sensor onboard LANDSAT-5 over the study period (US Geological Service; Schmidt et al., 2013). These remote sensing data were obtained and handled at a resolution of 30 m using Google Earth Engine (Gorelick et al., 2017). As our study area is covered by three separate LANDSAT-5 scenes, we obtained a variable number (minimum = 8) of surface reflectance thermal snapshots at each point from LANDSAT-5 over the study period with <10% cloud cover. We created a spatial composite in Google Earth Engine, and then averaged those at each position; the resulting two-year-mean raster comprised 15,249,291 data points covering the study area. Because LANDSAT-5 crossed the study area between ∼08:30 h and 09:00 h, the data represent only the diurnal thermal landscape (temperature range: 19.4–33.8°C).

Collar Temperature as a Measure of the Thermal Landscape

We tested whether collar temperatures capture variation in the thermal landscape as experienced by elephants at two spatio-temporal scales. At a fine temporal scale, we tested the relationship between collar temperature data with ambient temperature data from the Skukuza flux tower. For this, we collated all elephant positions that were within a 10 km radius of the Skukuza flux tower between 2006 and 2011 (1,706 days;

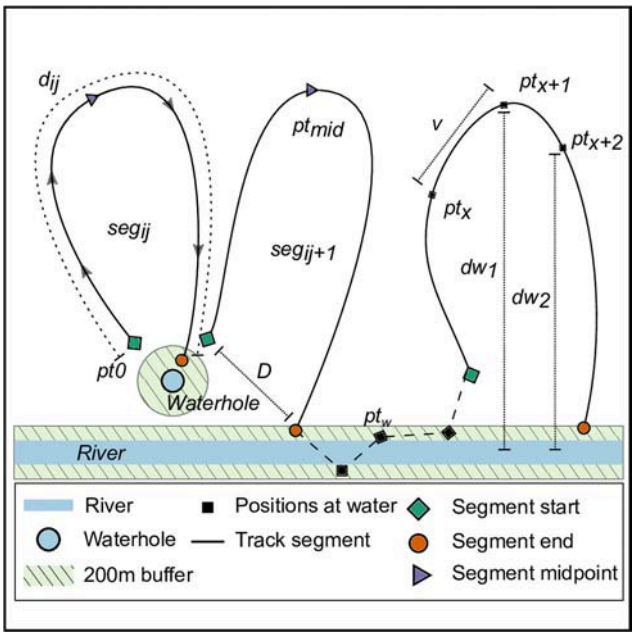

FIGURE 2 | Schematic of elephant track segments between water points. The positions of elephants (black squares, denoted by pt_x) from GPS transmitters on collars within 200 m (green area) of a water source (river: blue rectangle, waterhole: blue circle) were identified as visits to water. For each individual elephant i, we identified track segments j (solid lines, denoted seg_{ij}) as the path joining all positions chronologically between successive departures from and arrivals at water points. Each segment began as the elephant departed the 200 m zone around water (green rhombi, pt_0), and ended at the position where the elephant arrived within a 200 m zone around water (orange circle). Positions at which elephants were continuously within 200 m of a water source (black square, pt_w) are joined by a dashed line, and were not included in the characterization of segments away from water. We calculated the time-difference between each segment's start and end points as the segment time (t_{seg}), and identified the segment's midpoint (purple triangle, pt_{50}) as the elephant position when half the segment time had elapsed ($t_{seg}/2$). We computed the distance traveled between successive positions ($pt_x \rightarrow pt_{x+1}$) in a segment as the steplength (v), and the sum of all v in a segment as the distance traveled along the segment (segment distance, d_{ij}). We calculated the linear distance (segment displacement, D) between each segment's start and end points. Finally, we obtained the linear distance from each elephant position to the nearest water source (dw), the relative change in distance to water at each position ($\Delta dw = dw_2\text{-}dw_1$), and the collar temperature at each position (T_x).

three elephants, $n = 7{,}672$ in dry season, 21,181 in see addition wet season). For each hour of day, we constructed a linear mixed model (LMM) with collar temperature as the response variable, ambient temperature from the flux tower and season as fixed effects, with elephant identity and hour of day as random effects.

We then created Bland-Altman limits of agreement plots (Bland and Altman, 1986), with modifications suitable to repeated measures (Myles and Cui, 2007) to examine deviations of collar temperature from the ambient temperature recorded by the flux tower. The modification consisted of deriving the limits of agreement as the mean ± standard normal deviate [(1.96) * standard deviation attributable to elephant identity] from the LMM above. We took the average of the standard deviation due to elephant identity over each hour to obtain general limits of agreement for a Bland-Altman plot for this data.

At the large spatial scale, we used a linear mixed model to test whether elephant collar temperature was influenced by the following environmental variables: LANDSAT-5 temperature at that location, percent woody cover, and season, with elephant identity as a random effect. We then tested the significance of each fixed effect using a Type II Wald chi-squared test. Since LANDSAT-5 provides data only during the morning, we restricted this analysis to only using collar temperature data between 08:00 h and 10:00 h each day ($n = 35{,}135$).

Elephant Movement in Relation to Temperature, Water, and Habitat Features

To test whether collar temperature was a significant predictor of elephant movement, we used a generalized additive mixed effects model (GAMM) on the speed of movement (km/h). The GAMM also included season as a categorical fixed effect, density of woody vegetation as a continuous fixed effect, and elephant identity as a random effect. We did not include distance to water as a predictor variable in this analysis because that parameter would not distinguish between the movement toward or away from water. We also did not include time of day in the analysis because it is strongly correlated with collar temperature (see **Figure 3A**).

To understand how elephants are distributed relative to water sources we compared actual locations of elephants to 200,000 random points in the landscape in each season using a Kolmogorov-Smirnov test. We then identified GPS positions at which elephants entered and exited a 200 m buffer zone around water sources. We used a 200 m buffer (approximately mean step length for elephant is 195 m in 30 min) to capture visits to water that may have occurred between successive GPS position fixes. We grouped each individual's positions into a set of track segments as follows: Each segment began with the first location when the elephant exited the 200 m buffer around the water source (pt_0, **Figure 2**), and ended when the elephant re-entered a 200 m buffer (at the same or different water source; pt_n, **Figure 2**). We further identified consecutive GPS positions within the 200 m buffer and classified those as residence at water (pt_w, **Figure 2**). The last position of each segment could either be followed by residence at water, or by the first position of the next segment. Positions were not duplicated between segments and residence at water, i.e., a segment end point pt_n was never classified as a residence at water point pt_w.

We calculated the linear distance (hereafter segment displacement) between the start and end positions of a segment (D, **Figure 2**). Next, we computed the actual distance moved along each segment d_{ij} (hereafter, segment distance d) as the sum of the steplengths ($\sum_{x=0}^{x=n} \nu_{xij}$, **Figure 2**), i.e., the cumulative distances between successive points along a segment (pt_{xij} to pt_{x+1ij}). We also calculated the time difference between the start and end positions of a segment as the segment duration. To standardize segments of different durations, we calculated the proportion of the segment completed at each position along the segment, such that the segment start (pt_0 in **Figure 2**) had a value of 0, and the segment end (pt_n) had a value of 1. We characterized the distance to water, collar temperature, and elephant speed at each position in relation to the proportion of the segment traversed.

We then used a segmentation and clustering method that identifies stationary phases in a time series (Picard et al., 2007) to classify positions in each segment based on the change in distance to water at that position in the segment (see dw_1 and dw_2, **Figure 2**). The algorithm clustered segments into three classes of behavioral states: (1) Movement away from water, represented by successive positive values of change in distance to water dw; (2) no change in position relative to a water source, which was expected to be represented by low variance in values of dw; and, (3) movement toward water, which would be represented by successively decreasing distances to water, and, thus, consistent negative values of dw. The minimum length criteria required for determining each behavioral state was 5 GPS positions (2.5 h for data collected at 30 min intervals). We removed segments of over 120 h duration from further consideration as these may represent trips to water sources that are unmapped or ephemeral ($n = 26{,}347$, 9.3% of data away from water). Each of the three behavioral states described above could recur in a segment so long as the minimum length criterion was met, and the total number of state changes was 4 or fewer (five possible phases overall; minimum segment duration required = 25 positions or 12.5 h; maximum allowed duration = 120 h). We identified a total of 2,835 segments, comprising of 137,106 positions (∼ 48% of the raw data) that met the duration criteria required by the stationary-phase based clustering algorithm. From these, we identified points where the behavioral state changed from state 2 (no change relative to water) to state 3 (movement toward water). We used a LMM to determine whether collar temperature and season influenced when elephants begin to move toward water (i.e., "start seeking water," as defined by a state change from 2 to 3), with elephant identity as a random effect.

We used the R statistical environment (R Core Team, 2017) for all analyses, and, specifically, the *lme4*, *mgcv, segclust2d, move,* and *sf* packages to implement LMM, GAMM, stationary phase classification, and general movement and spatial data analyses, respectively (Wood, 2013; Bates et al., 2014; Kranstauber and

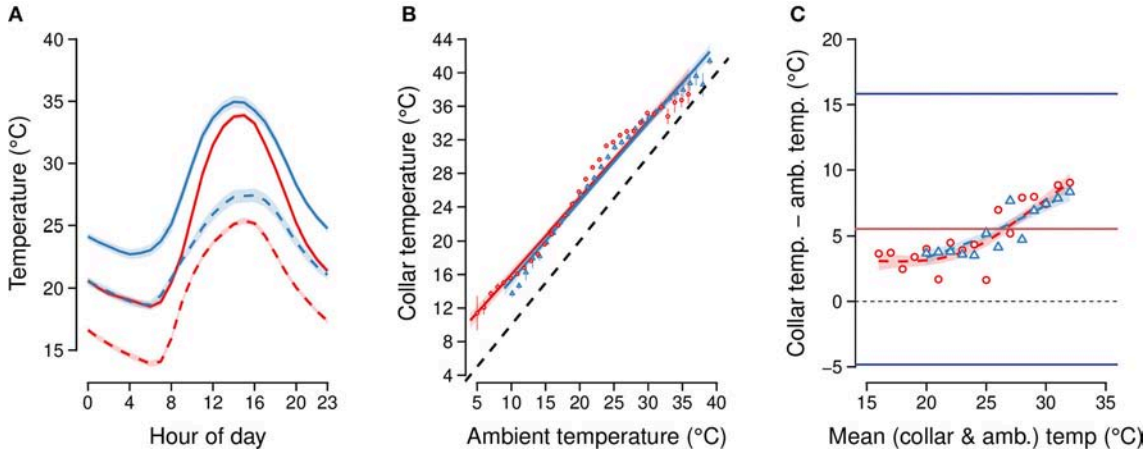

FIGURE 3 | (A) Mean collar temperature (solid lines) and measured ambient temperature from Skukuza flux tower (dashed lines) at each hour of day in each season (dry: red lines, wet: blue lines) over the study period. Ninety-Five percent confidence intervals (CI) about each line are shaded. **(B)** Correlation between mean collar temperature from elephants within 10 km of the Skukuza flux tower (from $n = 3$ elephants) and time-matched ambient temperatures measured by the flux tower in each season (dry: red circles, wet: blue triangles). The dashed line denotes the line of identity where collar temperature equals ambient temperature. Bars represent 95% CI at each point. **(C)** Bland-Altman limits of agreement plot comparing collar temperatures and ambient temperatures from the Skukuza flux tower, accounting for repeated measures of individual elephants and hour of day ($n = 28{,}853$ total comparisons). The bias between the two measures at each mean temperature is marked by symbols colored by season (dry: red circles, wet: blue triangles). The black dashed line marks zero difference between the two measures. The upper and lower limits of agreement are shown as the standard normal deviate (1.96) times the standard deviation due to elephant identity, and are marked by solid blue lines, while the mean difference in measures is marked by the solid red line.

Smolla, 2016; Patin et al., 2018; Pebesma, 2018). **Figure 1** was generated in QGIS 3.2 (QGIS Development Team, 2018), **Figure 2** was generated in Inkscape 0.92.3, and the remaining figures were generated in R.

Ethical Statement

Ethics approval for the capture, handling and collaring of elephants was obtained from the University of KwaZulu-Natal Animal Ethics Committee (Ref: 009/10/Animal). This project was also approved by the South African National Parks (Ref: SLOR660).

RESULTS

General Elephant Movement

Over the two-year study period, collared elephants traveled on average 7.4 (SD = 1.8) and 7.9 (SD = 1.8) km each day in the dry and wet seasons, respectively (LMM estimate = 603.8, t-value = 7.4, Wald II chi-square test $X^2 = 55.3$, $p < 0.01$, with individual elephant variation explaining only 4% of the variance).

Collar Temperatures as a Measure of the Thermal Landscape

Collar temperatures were well predicted by ambient temperatures at both the fine temporal scale and large spatial scale. At the fine temporal scale, collar temperatures from elephant positions ≤10 km away from the Skukuza flux tower were well predicted by hour-matched ambient temperatures from the flux tower (LMM estimate = 0.69; t-value = 121.8; Wald II chi-square test $X^2 = 14{,}837$, $p < 0.01$) and by season (estimate = 0.78; t-value = 15.6; Wald II chi-square test $X^2 = 243.2$, $p < 0.01$; **Figures 3A,B**). Of the random effects, elephant identity explained 6.9% of the variance, while hour of day explained 14.2%; the residual variance was 21.4%.

Elephant identity and hour of day as random effects contributed a standard deviation of 5.3°C which, after multiplication by the standard normal deviate (1.96), was used as the range of agreement between the two temperature measures (**Figure 3C** for Bland-Altman plot). We further found that the mean of the two temperature measures modeled as a thin-plate spline smoothed term was a significant predictor of the difference between the ambient and collar temperatures in each season (GAM, $p < 0.01$, adjusted $R^2 = 0.75$). The GAM fits are increasing curves over the range 15°C–35°C, indicating that the correspondence between collar temperature and flux tower temperature is best at lower temperatures, and decreases at higher temperatures (**Figure 3C**; *cf.* **Figure 3A**).

At the large spatial scale, daytime collar temperatures were also well predicted by the two-year mean LANDSAT-5 temperature (LMM estimate = 0.9, t-value = 4.2; Wald II chi-square test $X^2 = 17.9$, $p < 0.01$) and season (LMM estimate = 0.3, t-value = 6.0; Wald II chi-square test $X^2 = 36.3$, $p < 0.01$). Percent woody cover was also a predictor of collar temperature at this scale (LMM estimate = 0.01, t-value = 2.2; Wald II chi-square test $X^2 = 5.0$, $p = 0.03$).

Overall, we conclude that collar temperature captures variation in environmental temperature at the spatio-temporal scale of interest, and may be used as a reliable indicator of the variation in thermal landscape as experienced by elephants in the study area.

Elephant Movement in Relation to Temperature, Water, and Other Habitat Features

Based on data from all collared elephants over the 2 year study period, we found that collar temperature was a significant predictor of speed (GAMM F = 4,544, $p < 0.01$, **Figure 4A**). Elephants moved faster in the wet season (0.42 ± 0.49 km/h SD) than the dry season (0.39 ± 0.46 km/h SD, GAMM estimate = 15.6, t-value = 17.8, $p < 0.01$). The speed of elephant movement was also lower in denser woodlands (GAMM estimate = −1.6, t-value = −47, $p < 0.01$, **Figure 4B**).

Elephants were distributed closer to water than would be expected by chance (Kolmogorov-Smirnov test; dry season D = 0.09, $p < 0.01$, wet season D = 0.08, $p < 0.01$). Collared elephants were on average 1.5 km (range: 0–8.6 km) and 0.9 km (range: 0–5.9 km) from the nearest water source in the dry and wet seasons, respectively (LMM estimate = −653.8, t-value = -147.9, Wald II chi-square test $X^2 = 21{,}886$, $p < 0.01$). Elephant locations were ≤200 m from a water source 21.6% of the time ($n = 61{,}252$ positions; 19.6% of dry season points; 23.5% of wet season points). From these positions, elephants spent on average 2.6 h (± 2.7 SD) in continuous residence at water in the wet season and 3.5 h (± 4.1 SD) at water in the dry season (LMM estimate = −0.86, t-value = −11.0, Wald II chi-square test $X^2 = 121.4$; $p < 0.01$). Collar temperatures were on average 29.5°C (± 6.4 SD) while elephants were at a water source, with an effect of season (dry season mean = 29.8°C, wet season mean = 29.2°C; LMM estimate = −0.4, t-value = −7.5, Wald II chi-square test $X^2 = 56.8$; $p < 0.01$) and hour of day (LMM estimate = 0.1, t-value = 13.9, Wald II chi-square test $X^2 = 192.4$; $p < 0.01$).

Shuttling behavior to water sources in the dry season typically began at 14:00 (± 5 h SD), when elephants left water, and ended at 11:00 (± 5 h SD) when they returned to water. In the wet season, this segment of movement typically began at 13:00 (± 5 h SD) and ended at 10:00 (± 5 h SD). While moving along these segments, elephants traveled 12 ± 8.5 km over 31 ± 20 h in the dry season, and 10 ± 7 km over 27 ± 7 h in the wet season (all values are mean ± SD; see d_{ij} in **Figure 2**). In 92 % of segments ($n = 2{,}570$ segments), the segment displacement (D, **Figure 2**) was ≥500 m, with a small seasonal difference (mean = 3.8 ± 3.7 km SD in the dry season, 3.6 ± 3.5 km in the wet season; LMM estimate = −273.9, t-value = −2, Wald II chi-square test $X^2 = 4.2$; $p = 0.04$). Segment displacement positively correlated with segment distance traveled in both the dry and wet seasons (t-value = 29.6; Wald II chi-square test $X^2 = 875.2$; $p < 0.001$; **Figure 5**).

Elephants moving along segments traveled at most a distance of 2.6 km (±1.2 SD; range = 0.4–6.9 km) and 1.9 km (± 0.9 SD; range = 0.4–6 km) from the nearest water source in the dry and wet seasons, respectively (dw in **Figures 2**, **6A**; LMM estimate = −0.5, t-value = −88, Wald II chi-square test $X^2 = 7886.2$;

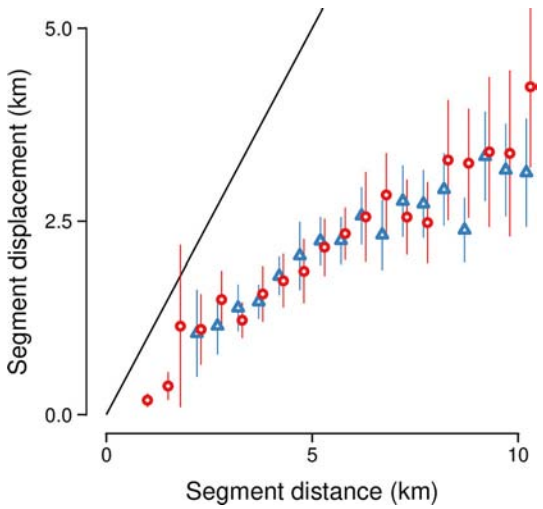

FIGURE 5 | Segment displacement (km) between successive visits to water was positively correlated with the distance traveled along the segment (km). Vertical line ranges show 95% confidence intervals around mean values for the dry season (red circles) and wet season (blue triangles), respectively. The solid black line denotes values where displacement = distance.

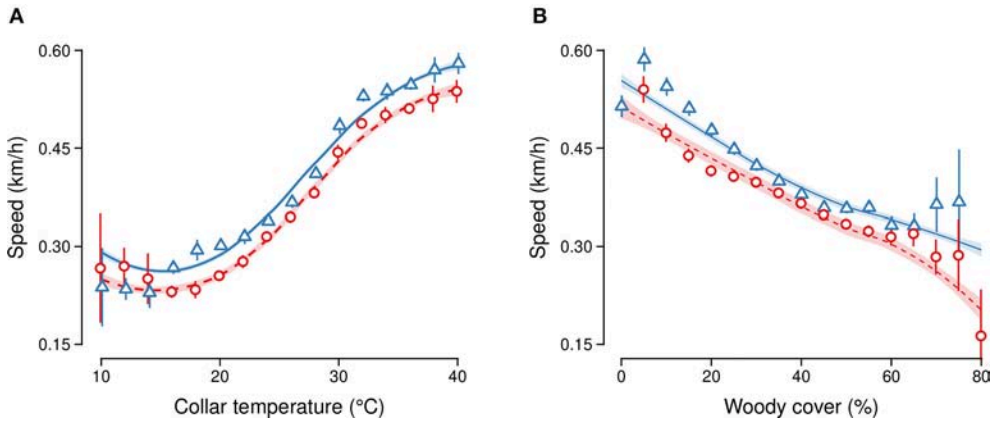

FIGURE 4 | Speed of elephant movement in relation to **(A)** collar temperature (at 2°C intervals) and **(B)** % woody cover (at 5 unit intervals) in the dry (red circles) and wet season (blue triangles). GAMM fit (lines) and 95% confidence intervals (vertical line ranges and shaded areas) are shown for each season separately.

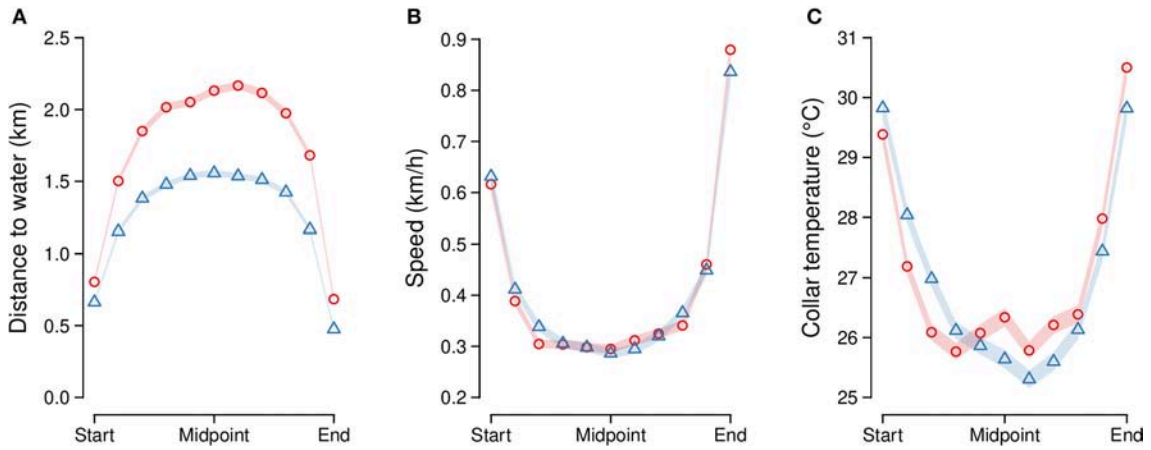

FIGURE 6 | Elephant movement variables along segments between water points at 10% intervals of the segment stage (measured in time): **(A)** distance to the nearest water source (km), **(B)** speed (km/h), and **(C)** collar temperature (°C). Points are separated by season (dry = red circles, wet = blue triangles), and connected by lines. Ninety-five percent confidence intervals around each point are shown (note: CI may be too small to be visible for some points).

$p \leq 0.01$). Elephants moved at an average speed of 0.4 km/h (± 0.2 SD; range = 0.1–1.5 km/h) along segments, with only minor seasonal differences (**Figure 6B**; LMM estimate = 0.01, t-value = 3.8, Wald II chi-square test $X^2 = 14.4$; $p < 0.01$). Notably, however, elephant speed was highest in the initial (mean ± SD = 0.6 ± 0.6 km/h) and final (mean ± SD = 0.8 ± 0.8 km/h) tenth of each segment, and lowest at the segment midpoint (mean ± SD = 0.3 ± 0.4 km/h); this represents a slowing down to 46% of initial speed (approximately half as fast) between the segment start and midpoint, and then a speeding up to 137% (around 1.5 times faster) of initial speed at the segment end (**Figure 6B**; LMM estimate = 0.1, t-value = 52.3, Wald II chi-square test $X^2 = 2738.6$; $p < 0.01$). Collar temperature at the beginning of the segment, as elephants were leaving water, was 29.6°C (± 6.1 SD), dropping to a mean of 26.0°C (SD = 6.22) at segment midpoints, and rising to 30.2°C (± 6.3 SD) at segment endpoints when elephant returned to water (**Figure 6C**; LMM estimate = 1.1, t-value = 21.1, Wald II chi-square test $X^2 = 442.9$; $p < 0.01$). Seasonal differences in collar temperature were detected (LMM estimate = −0.2, t-value = −5.7, Wald II chi-square test $X^2 = 32.1$; $p < 0.01$) but were within the sensitivity of the loggers (1°C).

From the stationary-phase based clustering algorithm analysis, we identified 2,111 state-change points where elephants began to move toward water (n = 1,003 in dry season; 1,108 in wet season). Although elephants began moving toward water at a higher temperature in the dry season than the wet season, this difference was small, with the dry season state change mean only 1°C higher than the wet season mean (dry season mean ± SD = 26 ± 6.4°C, wet season mean = 25 ± 6.1°C; LMM: t-value = −4.1, Wald II $X^2 = 16.7$, $p < 0.01$).

DISCUSSION

Heat dissipation is a major concern for large mammals, especially for mega-herbivores such as the savanna elephant (Wright and Luck, 1984; Williams, 1990; Weissenböck et al., 2012). Here, we show that temperature and water-dependency are strong drivers of the movement of wild free-ranging savanna elephants across large spatio-temporal scales. In KNP, we find that elephants moved faster at higher temperatures. This is a counter-intuitive result, since elephants, like other savanna dwelling herbivores, are expected to reduce metabolic heat generation by resting during the hotter parts of the day (Kinahan et al., 2007a; Leggett, 2010; Mole et al., 2016). If they have to move, they are expected to move slowly, which would generate metabolic heat at a lower rate (Rowe et al., 2013). Importantly, the high rates of movement of elephants in KNP were directed toward a water source, such that they moved fastest when approaching and leaving water, similar to that seen in elephants in Hwange National Park, Zimbabwe (Chamaillé-Jammes et al., 2013). Elephants in KNP were also closest to water at hotter times of the day (similar to Purdon and van Aarde, 2017), contrary to what is seen in other regions of southern Africa (Valeix et al., 2007; Loarie et al., 2009).

In general, elephants in KNP traveled 7–8 km per day, with very low seasonal differences. This is also unexpected, since savanna elephants in the broader southern African region are constrained around water holes during the dry season ("dry season bottleneck": Owen-Smith, 1988; Loarie et al., 2009; Young et al., 2009), and only forage farther afield at the onset of the wet season (Birkett et al., 2012). However, in the southern region of KNP, the density of water holes and surface water is high, and, thus, accessible to elephants throughout the year. We find that speed of movement was marginally faster in the wet season compared to the dry season and matches expectations from earlier studies (Birkett et al., 2012; Chamaillé-Jammes et al., 2013). Although they are moving slightly faster in the wet season, likely because they are grazing more than browsing (Codron et al., 2006), the total distance moved by elephants is similar across seasons. Elephants also moved slower in more densely wooded habitats, irrespective of temperature, likely while foraging or seeking shade (Kinahan et al., 2007a).

The Importance of Accessing Water

The use of various thermoregulatory strategies, such as heat sinks, thermal windows, ear flapping, shade seeking, and dust bathing behavior, are well recognized for elephants (Wright, 1984; Williams, 1990; Kinahan et al., 2007b; Weissenböck et al., 2010; Myhrvold et al., 2012; Dunkin et al., 2013). Perhaps the most important strategy, however, is through evaporative cooling, especially since cutaneous water loss increases with ambient temperature (Dunkin et al., 2013). Thus, heat dissipation through evaporative cooling is more important than water conservation (Dunkin et al., 2013). In hot, water-scarce habitats within the range of savanna elephant, this thermoregulatory mechanism is expected to result in high daily water debt. Therefore, elephants should anchor their movement strategies to water sources (Dunkin et al., 2013). We find that elephants in KNP are rarely more than 1.5 km away from water, and spend ∼22% of the time close to a water source, with longer residence at water during the dry season compared to the wet season. Their movement away from water shows a distinct cyclical pattern in all seasons, with a return to water peaking in frequency at a 10–30 h periodicity (see also Chamaillé-Jammes et al., 2013). During this shuttling, they rarely returned to within 0.5 km of the same water source. Furthermore, the distance that elephants moved between water sources was positively correlated to the total distance moved, indicating that elephants show low fidelity to water sources in KNP, unlike in other southern African countries (Loarie et al., 2009; Valls-Fox, 2015). While shuttling between water visits, elephants moved farther away from water sources and traveled for longer durations in the dry season compared to the wet, although there were marginal differences in the total distance they traveled along the route, or where they returned to. This is again in contrast to that seen in other regions, where elephants tend to move less and have greater site fidelity in the dry season than in the wet season (Loarie et al., 2009).

Water is required for thermoregulatory reasons and for maintaining osmoregulation. However, access to water has costs in terms of higher competition, and predation or poaching risk (Valeix et al., 2008, 2009; Rashidi et al., 2016). In areas with high poaching risk or human activity, elephants use water sources at night to reduce the risk of encountering humans (Von Gerhardt et al., 2014). On the other hand, predation risk at waterholes, especially from lions, typically peaks toward the cooler, night-time hours (Valeix et al., 2010). Therefore, animals looking to reduce predation risk should access water during the day (Valeix et al., 2009). However, animals generally avoid waterholes at the hottest time of the day due to the lack of cover ["sacrifice area": (Brits et al., 2002)] which can induce thermal overloading. Indeed, herbivores across a range of body sizes move less and find shade during the hottest time of day (Walsberg, 2000; Hetem et al., 2007, 2012; Aublet et al., 2009; van Beest et al., 2012). In KNP, where water is easily accessible and the risk of poaching is low, elephants use short, high-speed bursts of movement to get to water at hotter times of the day. This strategy not only provides the benefit of predation risk avoidance, but also allows them to hydrate and immediately cool down. The advantage of never being too far from water is that elephants can benefit from both direct (evaporation) and indirect (reducing water debt from cutaneous evaporative water loss) cooling, since water is the fastest way for large herbivores to lose heat (Dunkin et al., 2013). By shuttling to water in this way, elephants can trade-off a number of ecological and physiological drivers, with physiology in the form of thermoregulation as an important determinant of movement at this spatio-temporal scale.

Using Collar-Mounted Temperature Sensors to Generate a Dynamic Thermal Landscape

The use of collar-mounted temperature sensors allowed us to capture the relative differences in the thermal landscape at the scale of animal movement decisions. Although the temperature recorded from these instruments is always higher than the ambient temperature (especially at higher ambient temperatures) because of the heat generated by the GPS circuitry as well as the animal, we show that the collar-mounted temperature data are still well correlated with ambient temperatures across space and time (as validated from both precise as well as extensive environmental data, even with the variation across seasons, time of day and percent woody cover). We recognize that a more accurate measure of both ambient temperature and heat incidence can be derived from either distributing a large number of temperature sensors in the landscape (Kinahan et al., 2007b) or from animal-mounted black-globe sensors (Hetem et al., 2007), or both (Shrestha et al., 2012, 2014). However, the former is logistically challenging to deploy at the large spatial scales required to capture temperature differences across habitat features. The latter is suitable only for animals that are unlikely to damage the delicate instruments. Our approach here, therefore, uses an instrument that is now easily included in most commercial GPS tracking collars, thereby enabling the examination of movement strategies as a function of relative ambient temperature conditions. We do caution against using such collar mounted sensor data to make inferences about the actual ambient, or the animal's body temperature.

The Need for Water to Thermoregulate has Management Implications

The incorporation of physiological factors into understanding animal ranging and distribution is now being highlighted as essential (Dunkin et al., 2013; Jachowski et al., 2013; Hetem et al., 2014). As large mammals are increasingly restricted to areas smaller than their natural home range (Packer et al., 2013; Di Minin et al., 2016), both the resources they require and the impact that they have on habitats becomes more intensive (Kerley et al., 2008). Thus, more comprehensive management planning, or more intensive management intervention, such as placement of artificial waterholes (cf. Mwakiwa et al., 2013; Hilbers et al., 2015) or food provisioning, can be necessary. Conventionally, managers only consider the ecological basis of such interventions, such as edge effects from boundaries (Laurance, 2000; Vanak et al., 2010) or the piosphere effect (Chamaillé-Jammes et al., 2009). Managers also consider the importance of a "landscape

of fear" (Laundré et al., 2001; Cromsigt et al., 2013), and the potential use of this for achieving spatial heterogeneity in elephant distribution and their impacts on vegetation (SANParks, 2006). Here, we have demonstrated that the importance of facultative responses by elephants, which includes dependence on water, underpins their spatial decisions at the daily scale. Perhaps a physiologically based "landscape of thermal stress" may be a more important determinant of space use for a megaherbivore with low predation risk than the "landscape of fear."

Considering animal movement from a physiological point of view could change the perspective of managers, and, therefore, the basis of their planning and interventions. For example, elephants are known to over-exploit vegetation around water sources (Chamaillé-Jammes et al., 2009), and, thus, managers close artificial water holes to reduce impact. However, water and water-points could be important limiting factors from a physiological rather than ecological perspective. We show that elephants are not site-faithful to water sources in KNP, where currently poaching for elephants is (still) minimal, and, thus, the removal of waterpoints in this reserve could have a greater impact on elephant biology, rather than the intended reduction of elephant-induced impact on vegetation. Reduced access to water may put more thermal stress on elephants, requiring them to walk farther and faster to water, and therefore increase their risk of mortality, especially in times of drought (e.g., Woolley et al., 2008). Such incorporation of both the ecological and physiological bases of animal movement strategies is fundamental to sustainable planning in the longer term, and can guide management interventions.

DATA AVAILABILITY STATEMENT

The datasets analyzed for this study can be found on Movebank http://www.movebank.org/.

AUTHOR CONTRIBUTIONS

MT, ATV, and RS designed the study and collected the primary data. PRG analyzed the data and generated the figures. MT, PRG, and ATV wrote the manuscript with inputs and edits from HHTP and RS.

FUNDING

This work is based on the research supported in part by the National Research Foundation of South Africa (Grant Numbers 103659 to ATV, and Grant FA2006032300024 to RS), Amarula Trust funding to RS, University of Kwazulu-Natal funding to RS, Wageningen University funding to HHTP, Department of Science and Technology of India (FIST) to MT, Department of Biotechnology (DBT-IISC partnership program) to MT.

ACKNOWLEDGMENTS

We thank SANParks for providing weather data from the Skukuza flux tower, and for providing shapefiles of geographic features of Kruger NP. We also thank Markus Hofmeyer and the SANParks veterinary team for the collaring of elephants, and appreciate the critical reviews by AF amd BFD on this manuscript.

REFERENCES

Angilletta, M. J. (2009). *Thermal Adaptation: A Theoretical and Empirical Synthesis.* New York, NY: Oxford University Press Inc. doi: 10.1093/acprof:oso/9780198570875.001.1

Aublet, J. F., Festa-Bianchet, M., Bergero, D., and Bassano, B. (2009). Temperature constraints on foraging behaviour of male Alpine ibex (Capra ibex) in summer. *Oecologia* 159, 237–247. doi: 10.1007/s00442-008-1198-4

Bastille-Rousseau, G., Murray, D. L., Schaefer, J. A., Lewis, M. A., Mahoney, S. P., and Potts, J. R. (2018). Spatial scales of habitat selection decisions: implications for telemetry-based movement modelling. *Ecogr. Cop.* 41, 437–443. doi: 10.1111/ecog.02655

Bates, D., Mächler, M., Bolker, B., and Walker, S. (2014). Fitting linear mixed-effects models using lme4. *J. Stat. Softw.* 67, 1–48. doi: 10.18637/jss.v067.i01

Bennitt, E., Bonyongo, M. C., and Harris, S. (2014). Habitat selection by African buffalo *(Syncerus caffer)* in response to landscape-level fluctuations in water availability on two temporal scales. *PLoS ONE* 9:e101346. doi: 10.1371/journal.pone.0101346

Birkett, P. J., Vanak, A. T., Muggeo, V. M., Ferreira, S. M., and Slotow, R. (2012). Animal perception of seasonal thresholds: changes in elephant movement in relation to rainfall patterns. *PLoS ONE* 7:e38363. doi: 10.1371/journal.pone.0038363

Bland, J. M., and Altman, D. G. (1986). Statistical methods for assessing agreement between two methods of clinical measurement. *The Lancet* 327, 307–310.

Brits, J., Van Rooyen, M. W., and Van Rooyen, N. (2002). Ecological impact of large herbivores on the woody vegetation at selected watering points on the eastern basaltic soils in the Kruger National Park. *Afr. J. Ecol.* 40, 53–60. doi: 10.1046/j.0141-6707.2001.00344.x

Bryce, C. M., Wilmers, C. C., and Williams, T. M. (2017). Energetics and evasion dynamics of large predators and prey: pumas *vs.* hounds. *PeerJ* 5:e3701. doi: 10.7717/peerj.3701

Bucini, G., Hanan, N. P., Boone, R., Smit, I. P. J., Saatchi, S., and Lefsky, M. A. (2010). "Woody fractional cover in Kruger National Park, South Africa: remote-sensing-based maps and ecological insights," in *Ecosystem Function in Savannas Measurement and Modeling at Landscape to Global Scales,* eds M. J. Hill and N. P. Hanan (Boca Raton FL: CRC Press), 219–238.

Buss, I. O., and Estes, J. A. (1971). The functional significance of movements and positions of the pinnae of the African elephant, *Loxodonta africana*. *J. Mammal* 52, 21–27. doi: 10.2307/1378428

Cain, J. W., Krausman, P. R., Rosenstock, S. S., and Turner, J. C. (2006). Mechanisms of thermoregulation and water balance in desert ungulates. *Wildl. Soc. Bull.* 34, 570–581. doi: 10.2193/0091-7648(2006)34[570:MOTAWB]2.0.CO;2

Cain, J. W., Owen-Smith, N., and Macandza, V. A. (2012). The costs of drinking: comparative water dependency of sable antelope and zebra. *J. Zool.* 286, 58–67. doi: 10.1111/j.1469-7998.2011.00848.x

Chamaillé-Jammes, S., Fritz, H., and Madzikanda, H. (2009). Piosphere contribution to landscape heterogeneity: a case study of remote-sensed woody cover in a high elephant density landscape. *Ecogr. Cop.* 32, 871–880. doi: 10.1111/j.1600-0587.2009.05785.x

Chamaillé-Jammes, S., Mtare, G., Makuwe, E., and Fritz, H. (2013). African elephants adjust speed in response to surface-water constraint on foraging during the dry-season. *PLoS ONE* 8:e59164. doi: 10.1371/journal.pone.0059164

Codron, J., Lee-Thorp, J. A., Sponheimer, M., Codron, D., Grant, R. C., and de Ruiter, D. J. (2006). Elephant *(Loxodonta africana)* diets in kruger national park, south africa: spatial and landscape differences. *J. Mammal* 87, 27–34. doi: 10.1644/05-MAMM-A-017R1.1

Cromsigt, J. P. G. M., Kuijper, D. P. J., Adam, M., Beschta, R. L., Churski, M., Eycott, A., et al. (2013). Hunting for fear: innovating management of human–wildlife conflicts. *J. Appl. Ecol.* 50, 544–549. doi: 10.1111/1365-2664.12076

Di Minin, E., Slotow, R., Hunter, L. T., Montesino Pouzols, F., Toivonen, T., Verburg, P. H., et al. (2016). Global priorities for national carnivore conservation under land use change. *Sci. Rep.* 6:23814. doi: 10.1038/srep23814

Dunkin, R. C., Wilson, D., Way, N., Johnson, K., and Williams, T. M. (2013). Climate influences thermal balance and water use in African and Asian elephants: physiology can predict drivers of elephant distribution. *J. Exp. Biol.* 216, 2939–2952. doi: 10.1242/jeb.080218

Fortin, D., Fryxell, J. M., O'Brodovich, L., and Frandsen, D. (2003). Foraging ecology of bison at the landscape and plant community levels: the applicability of energy maximization principles. *Oecologia* 134, 219–227. doi: 10.1007/s00442-002-1112-4

Fuller, A., Hetem, R. S., Maloney, S. K., and Mitchell, D. (2014). Adaptation to heat and water shortage in large, arid-zone mammals. *Physiology* 29, 159–167. doi: 10.1152/physiol.00049.2013

Giotto, N., Gerard, J. F., Ziv, A., Bouskila, A., and Bar-David, S. (2015). Space-use patterns of the asiatic wild ass *(Equus hemionus)*: complementary insights from displacement, recursion movement and habitat selection analyses. *PLoS ONE* 10:e0143279. doi: 10.1371/journal.pone.0143279

Gorelick, N., Hancher, M., Dixon, M., llyushchenko, S., Thau, D., and Moore, R. (2017). Google earth engine: planetary-scale geospatial analysis for everyone. *Remote Sens. Env.* 202, 18–27. doi: 10.1016/j.rse.2017.06.031

Guralnick, R. (2006). The legacy of past climate and landscape change on species' current experienced climate and elevation ranges across latitude: a multispecies study utilizing mammals in western North America. *Glob. Ecol. Biogeogr.* 15, 505–518. doi: 10.1111/j.1466-822X.2006.00231.x

Hetem, R. S., Fuller, A., Maloney, S. K., and Mitchell, D. (2014). Responses of large mammals to climate change. *Temperature* 1, 115–127. doi: 10.4161/temp.29651

Hetem, R. S., Maartin Strauss, W., Heusinkveld, B. G., de Bie S., Prins, H. H. T., and van Wieren, S. E. (2011). Energy advantages of orientation to solar radiation in three African ruminants. *J. Therm. Biol.* 36, 452–460. doi: 10.1016/j.jtherbio.2011.07.012

Hetem, R. S., Maloney, S. K., Fuller, A., Meyer, L. C., and Mitchell, D. (2007). Validation of a biotelemetric technique, using ambulatory miniature black globe thermometers, to quantify thermoregulatory behaviour in ungulates. *J. Exp. Zool. Part Ecol. Genet. Physiol.* 307, 342–356. doi: 10.1002/jez.389

Hetem, R. S., Strauss, W. M., Fick, L. G., Maloney, S. K., Meyer, L. C., Shobrak, M., et al. (2012). Activity re-assignment and microclimate selection of free-living Arabian oryx: responses that could minimise the effects of climate change on homeostasis? *Zoology* 115, 411–416. doi: 10.1016/j.zool.2012.04.005

Hilbers, J. P., Van Langevelde, F., Prins, H. H., Grant, C. C., Peel, M. J., Coughenour, M. B., et al. (2015). Modeling elephant-mediated cascading effects of water point closure. *Ecol. Appl.* 25, 402–415. doi: 10.1890/14-0322.1

Hiley, P. G. (1975). How the elephant keeps its cool. *Nat. Hist.* 84, 34–41.

Jachowski, D. S., Montgomery, R. A., Slotow, R., and Millspaugh, J. J. (2013). Unravelling complex associations between physiological state and movement of African elephants (C Franklin, Ed). *Funct. Ecol.* 27, 1166–1175. doi: 10.1111/1365-2435.12118

Jachowski, D. S., Slotow, R., and Millspaugh, J. J. (2012). Physiological stress and refuge behavior by African elephants. *PLoS ONE* 7:e31818. doi: 10.1371/journal.pone.0031818

Johnson, C. J., Parker, K. L., Heard, D. C., and Gillingham, M. P. (2002). Movement parameters of ungulates and scale-specific responses to the environment. *J. Anim. Ecol.* 71, 225–235. doi: 10.1046/j.1365-2656.2002.00595.x

Kays, R., Crofoot, M. C., Jetz, W., and Wikelski, M. (2015). Terrestrial animal tracking as an eye on life and planet. *Science* 348:aaa2478. doi: 10.1126/science.aaa2478

Kerley, G. I. H., Landman, M., Kruger, L., Owen-Smith, N., Balfour, D., de Boer, W. F., et al. (2008). "Effects of elephants on ecosystems and biodiversity," in *Elephant Manag. A Sci. Assess*, eds R. J. Scholes and K. G. Mennell (Johannesburg, ZA: Wits University Press), 146–205.

Kinahan, A. A., Inge-moller, R., Bateman, P. W., Kotze, A., and Scantlebury, M. (2007a). Body temperature daily rhythm adaptations in African savanna elephants *(Loxodonta africana)*. *Physiol. Behav.* 92, 560–565. doi: 10.1016/j.physbeh.2007.05.001

Kinahan, A. A., Pimm, S. L., and van Aarde, R. J. (2007b). Ambient temperature as a determinant of landscape use in the savanna elephant, Loxodonta africana. *J. Therm. Biol.* 32, 47–58. doi: 10.1016/j.jtherbio.2006.09.002

Kranstauber, B., and Smolla, M. (2016). *Move: Visualizing and Analyzing Animal Track* Data. Available online at: http://CRAN.R-project.org/package=move

Laundré, J. W., Hernández, L., and Altendorf, K. B. (2001). Wolves, elk, and bison: reestablishing the "landscape of fear" in Yellowstone National Park, U.S.A. *Can. J. Zool.* 79, 1401–1409. doi: 10.1139/cjz-79-8-1401

Laurance, W. F. (2000). Do edge effects occur over large spatial scales? *Trends Ecol. Evol.* 15, 134–135. doi: 10.1016/S0169-5347(00)01838-3

Leggett, K. (2010). Daily and hourly movement of male desert-dwelling elephants. *Afr. J. Ecol.* 48, 197–205. doi: 10.1111/j.1365-2028.2009.01101.x

Loarie, S. R., Aarde, R. J. V., and Pimm, S. L. (2009). Fences and artificial water affect African savannah elephant movement patterns. *Biol. Conserv.* 142, 3086–3098. doi: 10.1016/j.biocon.2009.08.008

Mitchell, D., Snelling, E. P., Hetem, R. S., Maloney, S. K., Strauss, W. M., and Fuller, A. (2018). Revisiting concepts of thermal physiology: predicting responses of mammals to climate change. *J. Anim. Ecol.* 87, 956–973. doi: 10.1111/1365-2656.12818

Mole, M. A., Rodrigues DÁraujo, S., van Aarde, R. J., Mitchell, D., and Fuller, A. (2016). Coping with heat: behavioural and physiological responses of savanna elephants in their natural habitat. *Conserv. Physiol.* 4:cow044. doi: 10.1093/conphys/cow044

Mwakiwa, E., de Boer, W. F., Hearne, J. W., Slotow, R., van Langevelde, F., Peel, M., et al. (2013). Optimization of wildlife management in a large game reserve through waterpoints manipulation: a bio-economic analysis. *J. Environ. Manage.* 114, 352–361. doi: 10.1016/j.jenvman.2012.10.029

Myhrvold, C. L., Stone, H. A., and Bou-Zeid, E. (2012). What is the use of elephant hair? *PLoS ONE* 7:e47018. doi: 10.1371/journal.pone.0047018

Myles, P. S., and Cui, J. (2007). Using the Bland–Altman method to measure agreement with repeated measures. *Br. J. Anaesth.* 99, 309–311. doi: 10.1093/bja/aem214

Nathan, R., Getz, W. M., Revilla, E., Holyoak, M., Kadmon, R., Saltz, D., et al. (2008). A movement ecology paradigm for unifying organismal movement research. *Proc. Natl. Acad. Sci. U.S.A.* 105, 19052–19059. doi: 10.1073/pnas.0800375105

Owen-Smith, N. (1988). *Megaherbivores: The Influence of Very Large Body Size on Ecology*. Cambridge: Cambridge University Press. doi: 10.1017/CBO9780511565441

Owen-Smith, N., and Goodall, V. (2014). Coping with savanna seasonality: comparative daily activity patterns of African ungulates as revealed by GPS telemetry. *J. Zool.* 293, 181–191. doi: 10.1111/jzo.12132

Packer, C., Loveridge, A., Canney, S., Caro, T., Garnett, S. T., Pfeifer, M., et al. (2013). Conserving large carnivores: dollars and fence. *Ecol. Lett.* 16, 635–641. doi: 10.1111/ele.12091

Patin, R., Etienne, M.-P., Lebarbier, E., Chamaillé-Jammes, S., and Benhamou, S. (2018). Identifying stationary phases in multivariate time-series for highlighting behavioural modes and home range settlements. *bioRxiv*. doi: 10.1101/444794

Pebesma, E. (2018). Simple Features for R: standardized support for spatial vector data. *R. J.* 10, 439–446. doi: 10.32614/RJ-2018-009

Picard, F., Robin, S., Lebarbier, E., and Daudin, J.-J. (2007). A segmentation/clustering model for the analysis of array CGH data. *Biometrics* 63, 758–766.

Prins, H. H. T. (1996). *Behaviour and Ecology of the African Buffalo: Social Inequality and Decision Making*. London: Chapman and Hall. doi: 10.1007/978-94-009-1527-5

Purdon, A. (2015). *Environmental* Determinants of the Movement Patterns of Elephants *in the Kruger National Park*. University of Pretoria.

Purdon, A., and van Aarde, R. J. (2017). Water provisioning in Kruger National Park alters elephant spatial utilisation patterns. *J. Arid. Env.* 141, 45–51. doi: 10.1016/j.jaridenv.2017.01.014

QGIS Development Team (2018). *QGIS Geographic Information System*. Open Source Geospatial Foundation.

R Core Team (2017). *R: A Language and Environment for Statistical Computing*. Vienna: R Foundation for Statistical Computing.

Rashidi, P., Wang, T., Skidmore, A., Mehdipoor, H., Darvishzadeh, R., Ngene, S., et al. (2016). Elephant poaching risk assessed using spatial and non-spatial

Bayesian models. *Ecol. Model.* 338, 60–68. doi: 10.1016/j.ecolmodel.2016.08.002

Rowe, M. F., Bakken, G. S., Ratliff, J. J., and Langman, V. A. (2013). Heat storage in Asian elephants during submaximal exercise: behavioral regulation of thermoregulatory constraints on activity in endothermic gigantotherms. *J. Exp. Biol.* 216, 1774–1785. doi: 10.1242/jeb.076521

SANParks (2006). *Kruger National Park Elephant Management Plan 2012-2023.*

Scantlebury, D. M., Mills, M. G., Wilson, R. P., Wilson, J. W., Mills, M. E., Durant, S. M., et al. (2014). Flexible energetics of cheetah hunting strategies provide resistance against kleptoparasitism. *Science* 346, 79–81. doi: 10.1126/science.1256424

Schmidt, G., Jenkerson, C. B., Masek, J., Vermote, E., and Gao, F. (2013). *Landsat Ecosystem Disturbance Adaptive Processing System (LEDAPS) Algorithm Description*. Reston, VA: U.S. Geological Survey.

Shrestha, A. K., van Wieren, S. E., van Langevelde, F., Fuller, A., Hetem, R. S., Meyer, L., et al. (2014). Larger antelopes are sensitive to heat stress throughout all seasons but smaller antelopes only during summer in an African semi-arid environment. *Int. J. Biometeorol.* 58, 41–49. doi: 10.1007/s00484-012-0622-y

Shrestha, A. K., van Wieren, S. E., van Langevelde, F., Fuller, A., Hetem, R. S., Meyer, L. C. R., et al. (2012). Body temperature variation of South African antelopes in two climatically contrasting environments. *J. Therm. Biol.* 37, 171–178. doi: 10.1016/j.jtherbio.2011.12.008

Thaker, M., Vanak, A. T., Owen, C. R., Ogden, M. B., Niemann, S. M., and Slotow, R. (2011). Minimizing predation risk in a landscape of multiple predators: effects on the spatial distribution of African ungulates. *Ecology* 92, 398–407. doi: 10.1890/10-0126.1

Valeix, M., Chamaillé-Jammes, S., and Fritz, H. (2007). Interference competition and temporal niche shifts: elephants and herbivore communities at waterholes. *Oecologia* 153, 739–748. doi: 10.1007/s00442-007-0764-5

Valeix, M., Fritz, H., Loveridge, A. J., Davidson, Z., Hunt, J. E., Murindagomo, F., et al. (2009). Does the risk of encountering lions influence African herbivore behaviour at waterholes? *Behav. Ecol. Sociobiol.* 63, 1483–1494. doi: 10.1007/s00265-009-0760-3

Valeix, M., Fritz, H., Matsika, R., Matsvimbo, F., and Madzikanda, H. (2008). The role of water abundance, thermoregulation, perceived predation risk and interference competition in water access by African herbivores. *Afr. J. Ecol.* 46, 402–410. doi: 10.1111/j.1365-2028.2007.00874.x

Valeix, M., Loveridge, A. J., Davidson, Z., Madzikanda, H., Fritz, H., and Macdonald, D. W. (2010). How key habitat features influence large terrestrial carnivore movements: waterholes and African lions in a semi-arid savanna of north-western Zimbabwe. *Landsc. Ecol.* 25, 337–351. doi: 10.1007/s10980-009-9425-x

Valls-Fox, H. (2015). *To drink or not to drink? The Influence of Resource Availability on Elephant Foraging and Habitat Selection in a Semi-Arid Savanna*. University of Montpellier.

van Beest, F. M., Moorter, B., van, and Milner, J. M. (2012). Temperature-mediated habitat use and selection by a heat-sensitive northern ungulate. *Anim. Behav.* 84, 723–735. doi: 10.1016/j.anbehav.2012.06.032

Vanak, A. T., Fortin, D., Thaker, M., Ogden, M., Owen, C., Greatwood, S., et al. (2013). Moving to stay in place: behavioral mechanisms for coexistence of African large carnivores. *Ecology* 94, 2619–2631. doi: 10.1890/13-0217.1

Vanak, A. T., Thaker, M., and Slotow, R. (2010). Do fences create an edge-effect on the movement patterns of a highly mobile mega-herbivore? *Biol. Conserv.* 143, 2631–2637. doi: 10.1016/j.biocon.2010.07.005

Von Gerhardt, K., Van Niekerk, A. V., Kidd, M., Samways, M., and Hanks, J. (2014). The roles of elephant *Loxodonta africana* pathways as a spatial variable in crop-raiding location. *Oryx* 48, 436–444. doi: 10.1017/S003060531200138X

Walsberg, G. E. (2000). Small mammals in hot deserts: some generalizations revisited. *Bioscience* 50, 109–120. doi: 10.1641/0006-3568(2000)050[0109:SMIHDS]2.3.CO;2

Wato, Y. A., Heitkönig, I. M. A., van Wieren, S. E., Wahungu, G. M., Prins, H. T., and van Langevelde, F. (2016). Prolonged drought results in starvation of African elephant *(Loxodonta africana)*. *Biol. Conserv.* 203, 89–96. doi: 10.1016/j.biocon.2016.09.007

Wato, Y. A., Prins, H. H. T., Heitkönig, I. M. A., Wahungu, G. M., Ngene, S. M., Njumbi, S., et al. (2018). Movement patterns of African elephants (*Loxodonta africana*) in a semi-arid savanna suggest that they have information on the location of dispersed water sources. *Front. Ecol. Evol.* 6:167. doi: 10.3389/fevo.2018.00167

Weissenböck, N. M., Arnold, W., and Ruf, T. (2012). Taking the heat: thermoregulation in asian elephants under different climatic conditions. *J. Comp. Physiol. B* 182, 311–319. doi: 10.1007/s00360-011-0609-8

Weissenböck, N. M., Weiss, C. M., Schwammer, H. M., and Kratochvil, H. (2010). Thermal windows on the body surface of African elephants *(Loxodonta africana)* studied by infrared thermography. *J. Therm. Biol.* 35, 182–188. doi: 10.1016/j.jtherbio.2010.03.002

Williams, T. M. (1990). Heat transfer in elephants: thermal partitioning based on skin temperature profiles. *J. Zool.* 222, 235–245. doi: 10.1111/j.1469-7998.1990.tb05674.x

Williams, T. M., Fuiman, L. A., Horning, M., and Davis, R. W. (2004). The cost of foraging by a marine predator, the Weddell seal *Leptonychotes weddellii*: pricing by the stroke. *J. Exp. Biol.* 207, 973–982. doi: 10.1242/jeb.00822

Williams, T. M., Wolfe, L., Davis, T., Kendall, T., Richter, B., Wang, Y., et al. (2014). Instantaneous energetics of puma kills reveal advantage of felid sneak attacks. *Science* 346, 81–85. doi: 10.1126/science.1254885

Wood, S. N. (2013). *Generalized Additive Models: An Introduction With R. Chapman*. Boca Raton, FL: Hall/CRC.

Woolley, L. A., Mackey, R. L., Page, B. R., and Slotow, R. (2008). Modelling the effect of age-specific mortality on elephant Loxodonta africana populations: can natural mortality provide regulation? *Oryx* 42, 49–57. doi: 10.1017/S0030605308000495

Wright, C. P., and Luck, C. P. (1984). Do elephants need to sweat? *South Afr. J. Zool.* 19, 270–274. doi: 10.1080/02541858.1984.11447892

Wright, P. G. (1984). Why do elephants flap their ears? *South Afr. J. Zool.* 19, 266–269. doi: 10.1080/02541858.1984.11447891

Young, K. D., Ferreira, S. M., and Aarde, R. J. V. (2009). Elephant spatial use in wet and dry savannas of southern Africa. *J. Zool.* 278, 189–205. doi: 10.1111/j.1469-7998.2009.00568.x

Conflict of Interest Statement: The authors declare that the research was conducted in the absence of any commercial or financial relationships that could be construed as a potential conflict of interest.

Copyright © 2019 Thaker, Gupte, Prins, Slotow and Vanak. This is an open-access article distributed under the terms of the Creative Commons Attribution License (CC BY). The use, distribution or reproduction in other forums is permitted, provided the original author(s) and the copyright owner(s) are credited and that the original publication in this journal is cited, in accordance with accepted academic practice. No use, distribution or reproduction is permitted which does not comply with these terms.

frontiers in Ecology and Evolution

ORIGINAL RESEARCH
published: 19 February 2019
doi: 10.3389/fevo.2019.00030

Validation of Dive Foraging Indices Using Archived and Transmitted Acceleration Data: The Case of the Weddell Seal

Karine Heerah[1,2], Sam L. Cox[1,3,4], Pierre Blevin[1], Christophe Guinet[1] and Jean-Benoît Charrassin[2]*

[1] Centre d'Etude Biologique de Chizé, UMR 7372 CNRS, Villers-en-Bois, France, [2] UMR 7159 CNRS-IRD-MNHN, LOCEAN-IPSL, Sorbonne Université, Paris, France, [3] Centre National d'Études Spatiales, Toulouse, France, [4] MARBEC (Institut de Recherche pour le Développement), Sète, France

OPEN ACCESS

Edited by:
Andreas Fahlman,
Fundación Oceanográfica, Spain

Reviewed by:
Allyson Hindle,
Massachusetts General Hospital and Harvard Medical School,
United States
Lewis Halsey,
University of Roehampton,
United Kingdom
Tessa van Walsum,
University of Roehampton,
United Kingdom, in collaboration with reviewer LH

***Correspondence:**
Karine Heerah
karine.heerah@hotmail.fr

Specialty section:
This article was submitted to Behavioral and Evolutionary Ecology, a section of the journal Frontiers in Ecology and Evolution

Received: 30 July 2018
Accepted: 28 January 2019
Published: 19 February 2019

Citation:
Heerah K, Cox SL, Blevin P, Guinet C and Charrassin J-B (2019) Validation of Dive Foraging Indices Using Archived and Transmitted Acceleration Data: The Case of the Weddell Seal. Front. Ecol. Evol. 7:30. doi: 10.3389/fevo.2019.00030

Dive data collected from archival and satellite tags can provide valuable information on foraging activity via the characterization of movement patterns (e.g., wiggles, hunting time). However, a lack of validation limits interpretation of what these metrics truly represent in terms of behavior and how predators interact with prey. Head-mounted accelerometers have proven to be effective for detecting prey catch attempt (PrCA) behaviors, and thus can provide a more direct measure of foraging activity. However, device retrieval is typically required to access the high-resolution data they record, restricting use to animals returning to predictable locations. In this study, we present and validate data obtained from newly developed satellite-relay data tags, capable of remotely transmitting summaries of tri-axial accelerometer measurements. We then use these summaries to assess foraging metrics generated from dive data only. Tags were deployed on four female Weddell seals in November 2014 at Dumont d'Urville, and successfully acquired data over ∼2 months. Retrieved archival data for one individual, and transmitted data for four individuals were used to (1) compare and validate abstracted accelerometer transmissions against outputs from established processing procedures, and (2) assess the validity of previously developed dive foraging indices, calculated solely from time-depth measurements. We found transmitted estimates of PrCA behaviors were generally comparable to those obtained from archival processing, although a small but consistent over-estimation was noted. Following this, dive foraging segments were identified either from (1) sinuosity in the trajectories of high-resolution depth archives, or (2) vertical speeds between low resolution transmissions of key depth inflection points along a dive profile. In both cases, more than 93% of the estimated PrCA behaviors (from either abstracted transmissions or archival processing) fell into inferred dive foraging segments (i.e., "hunting" segments), suggesting the two methods provide a reliable indicator of foraging effort. The validation of transmitted acceleration data and

foraging indices derived from time-depth recordings for Weddell seals offers new avenues for the study of foraging activity and dive energetics. This is especially pertinent for species from which tag retrieval is challenging, but also for the post-processing of the numerous low-resolution dive datasets already available.

Keywords: satellite relayed data logger, accelerometers, diving behavior, movement ecology, foraging, sea-ice, biologging

INTRODUCTION

Foraging is a crucial behavior for animals, because obtaining adequate food supply is a basic requirement for all other life-history traits, such as survival, growth and reproduction (Stephens and Krebs, 1986). In marine environments, air-breathing diving predators must find, within the physiological constraints of breath-hold, resources that are heterogeneously distributed in patches across a 3-dimensional dynamic environment (Kooyman and Ponganis, 1998; Benoit-Bird et al., 2013; Goldbogen et al., 2015). In such instances, this selective force is likely very strong. Species may thus adopt foraging strategies and select environmental features associated with the resources needed to maximize reproductive success and survival (i.e., fitness) (MacArthur and Pianka, 1966; Charnov, 1976; Stearns, 1992; Krausman, 1999).

Studying predator-prey interactions is crucial to better understanding the sensory and energetic avenues air-breathing marine predators adopt to maximize resource acquisition in relation to their environment. Despite the importance of measuring foraging activity to this, its quantification in these animals is challenging because they spend most of their time at sea, and often feed on prey aggregated at depth. Consequently, we are only beginning to understand the fine-scale feeding behavior and energy acquisition of many marine predators (Carter et al., 2016). With satellite and archival time-depth recorders, foraging is typically inferred from movement patterns, diving metrics and distinctive dive shapes (Le Boeuf et al., 1988; Wilson et al., 1996; Schreer et al., 2001; Heerah et al., 2017). The fine-scale foraging behaviors of marine predators have also been investigated using esophageal and stomach temperature sensors (Wilson et al., 1995; Charrassin et al., 2001; Horsburgh et al., 2008), Hall sensors (i.e., jaw magnets) and accelerometers (to detect mouth opening events; Wilson et al., 2002; Viviant et al., 2009; Naito et al., 2010) as well as with video cameras (Hooker et al., 2002; Machovsky-Capuska et al., 2011; Naito et al., 2013). Recently, miniaturized head-mounted accelerometers have proven to be effective for detecting prey capture attempts in pinnipeds and penguins, as well as quantifying the energetic expenses associated with diving and foraging (Gleiss et al., 2011; Watanabe and Takahashi, 2013; Ydesen et al., 2014; Volpov et al., 2015; Jeanniard-du-Dot et al., 2016a,b; Jouma'a et al., 2016).

The technological and analytical advances provided by this newer generation of devices (accelerometers and cameras) can yield invaluable information on the strategies marine predators adopt to maximize energy gains in relation to their surrounding environment (Austin et al., 2006; Goldbogen et al., 2011; Guinet et al., 2014; Richard et al., 2016). However, obtaining measured information typically requires device retrieval (Carter et al., 2016). This restricts use to species that return to predictable locations (e.g., central place foragers, such as breeding pinnipeds and seabirds) and limits the validation of more commonly used dive foraging indices. Consequently, studies investigating the fine scale foraging strategies of air breathing marine predators, predator-prey interactions and/or energetic budgets are scarce for individuals/species that spend extended periods at sea and return to inaccessible locations that prevent device retrieval (e.g., sea-ice obligate seal species; e.g., harp *[Pagophilus groenlandicus]*, hooded *[Cystophora cristata]*, leopard *[Hydrurga leptonyx]*, and Weddell *[Leptonychotes weddellii]* seals; (Tynan et al., 2009; Heerah et al., 2017; Vacquie-Garcia et al., 2017).

Satellite Relay Data Loggers (SRDL), can transmit, via satellite (e.g., Argos CLS™ system, http://www.argos-system.org), data collected by archival loggers in near real time (Fedak et al., 2002; Boehme et al., 2009). However, the limited time and bandwidth available for data transmission at the surface, imposed by the animal's diving habits and the Argos CLS™ system, restrict the amount of data that can be sent (messages must be typically <248/256 bits; Fedak et al., 2002; Boehme et al., 2009; CLS, 2016). In the last decade, SRDLs have been widely used for transmitting degraded data on the behavior of marine predators, such as pinnipeds (e.g., dive depth and duration, swimming speed) and ocean data (e.g., temperature and salinity; Block et al., 2011; Fedak, 2013). Recently, a new generation of SRDLs capable of transmitting summarized tri-axial acceleration measurements alongside degraded dive profiles have been developed, and successfully tested on juvenile Southern elephant seals *(Mirounga leonina)* (Cox et al., 2018). These loggers represent an invaluable technological development as they provide novel access to inferences on predator-prey interactions, diving behavior and energetics in near real-time without having to retrieve the devices. This widens the range of species (e.g., non-central foragers) which can be studied along with the foraging, movement ecology questions that can be issued.

Capitalizing on these latest developments, we use this new generation of SRDLs to collect data on foraging activity in a sea-ice obligate species, the Weddell seal, for which device retrieval can be extremely difficult. We validate received transmissions from these devices using archival data uniquely retrieved from one individual, which we process using established high resolution accelerometer processing procedures (Viviant et al., 2009; Gallon et al., 2013; Richard et al., 2014; Vacquié-Garcia et al., 2015b; Cox et al., 2018). Following this, we assess the

validity of previously developed dive foraging indices, calculated solely from time-depth measurements, against the received and validated accelerometer transmissions (Heerah et al., 2014, 2015). Weddell seals spend their entire life cycle around Antarctic sea-ice, spending most of their time resting on or foraging under the sea-ice in areas that are logistically challenging to access. In addition, previous studies have shown they adopt complex diving behaviors, which may complicate the use of commonly used dive metrics to accurately infer foraging activity (Heerah et al., 2014, 2015). Validation of such methods offers new avenues to investigate the diving and foraging behaviors of this and other remote free-ranging marine species and analyse the numerous low-resolution dive datasets already available.

MATERIALS AND METHODS

Tag Deployment and Specifications

Animal Handling

Four adult female Weddell seals (mass: 343 ± 41 kg, length: 242 ± 7 cm, mean ± *SE*, **Table 1**) were captured at Dumont D'Urville (DDU) in East Antarctica (66°40S 140°E) in late November 2014, which is after pup rearing and before molting. Capture and tagging procedures were similar to those described in Heerah et al. (2013) and were approved by the TAAF (French sub-Antarctic and Antarctic territories) ethic committee (authorization # 2014-134, 15/10/2014). Seals were equipped with a new generation of satellite relayed data loggers (SRDLs) known as DSA tags (SCOUT-DSA-296 tag, Wildlife Computer; Cox et al., 2018). These were head mounted on the Weddell seals.

DSA Tags

The DSA tag measures 86*85*29 mm and weighs 192 g (see also Cox et al., 2018). It comprises an Argos transmitter, alongside pressure sensor (recording rate of 1 Hz, resolution of 0.5 m and accuracy of ±1 m + 1% of a reading), tri-axial accelerometer (recording rate of 16 Hz) and wet-dry sensor. Dives were defined as events that lasted at least 60 s with a maximum depth that exceeded 15 m.

Data Outputs From a DSA Tag

Dives were (1) archived, and (2) then processed on-board to create a dive summary, which was later transmitted via the Argos satellite system [**Figures 1**, **2A** (archived dive) and d (transmitted DSA dive)]. These dive summaries were composed of five dive segments. These were defined by identifying the four most characteristic inflection points along a dive profile via a broken stick algorithm (Fedak et al., 2002). For each dive segment, the total time spent performing prey catch attempt (PrCA) behaviors, and the total swimming effort were calculated using an algorithm directly implemented within the DSA tag. DSA algorithms were based on simplified procedures of established techniques (Viviant et al., 2009; e.g., Richard et al., 2014; Vacquié-Garcia et al., 2015a).

For the total time spent in PrCA behaviors, accelerations along the x, y and z axes were used to calculate magnitude in acceleration as $magA_i = \sqrt{x_i^2 + y_i^2 + z_i^2}$. Changes in $magA_i$ over 1 s periods were then calculated by summing the absolute values of the previous 16 successive $magA_i$estimates to give a per second measure of variance, *varS*, as $\sum_{i=2}^{16} \left|\left(magA_i - magA_{i-1}\right)\right|$. A running average across 11 s was then applied to the time series of *varS* to produce *varA*, which represents a per second average variance in acceleration. PrCA behaviors occurred when $varS_i \geq varA_i + thresV$, where *thresV* is a user selectable threshold, here of $5\frac{m}{s}^2$.

For total swimming effort, accelerations from the lateral y-axis were high pass filtered using a second-order IIR Butterworth filter with a 3 dB cut-off set at 0.2 Hz. The absolute total of these accelerations was then taken as the swimming effort.

DSA simplified algorithms and their associated transmitted acceleration outputs (per dive segment summaries of PrCA and swimming effort; hereafter "DSA transmissions") have been assessed and validated for adult and juvenile southern elephant seals (see full details in Cox et al., 2018). We did not have prior information on Weddell seal movements from accelerometers. Thus, where it was necessary to set specific thresholds for the DSA simplified algorithms, the same values as those determined via the analysis of female adult Southern elephant seal accelerometer data were used (see Cox et al., 2018). Female adult Southern elephant seals are comparable in size and weight to Weddell seals (Arnbom et al., 1993; Guinet, 1994; Guinet et al., 2014; Heerah, 2014) and so the transferal of thresholds is appropriate. The tag transmitted each dive summary a maximum of 10 times, with a minimum interval of 15 min between each uplink attempt. Tags were also set to allow for up to 200 total transmission attempts per 24 h to estimate seal locations. PrCA behavior was set to not exceed 100 s per dive segment, although *post-hoc* analyses showed that times spent in PrCA above 60 s per segment were not recorded (i.e., in practice a ceiling of 60 s per segment was applied).

Datasets and Pre-processing Analyses

The two analyses performed in this study were based on two main datasets. First, to assess and validate the DSA simplified algorithms for use on Weddell seals, we used DSA transmissions from one individual (#143468) and coupled these to high-resolution archives that were uniquely retrieved from this seal. It was not possible to retrieve archives from other seals due to the ice obligate behavior of this species. Second, to assess the validity of previously developed dive foraging indices calculated solely from time-depth measurements, these two datasets were used in combination with low-resolution DSA transmissions from a further three seals.

For the first analysis, the high-resolution archives included both detections of PrCA behaviors identified by the DSA simplified algorithms (hereafter "$PrCA_{DSA}$"), and tri-axial acceleration values. From these, high-resolution swimming effort and time spent in PrCA behaviors (hereafter "$PrCA_{archival}$") were calculated using established processing procedures (see Cox et al., 2018 for full details). Briefly, to identify PrCA behaviors, high frequency dynamic accelerations, likely associated with rapid head movements, were isolated from gravitational forces along the three accelerometer axes using a third order high pass digital Butterworth filter of 2.64 Hz (Viviant et al., 2009; Guinet et al., 2014). Along each axis, standard deviations in acceleration were then calculated over a moving window of 1.5 s. K means

TABLE 1 | General information on tag deployment and transmission outputs.

PTT	Mass (kg)	Length (cm)	Deployment	Tag retrieval	Trans. Dur. (day)	N dives	N dives/day	Dive max. depth (m)	Dive dur. (min)	$PrCA_{DSA}$ (sec.)	Swim. Effort ($m{\cdot}s^{-3}$)
143467	238	227	27/11/2014	–	49	667	13 ± 1	120 ± 2	11 ± 0.1	46 ± 1	13 ± 0.1
143468	436	251	27/11/2014	23/01/2015	25	221 DSA 266 archived	9 ± 1	120 ± 5	14 ± 0.5	60 ± 3	12 ± 0.2
143469	339	236	29/11/2014	–	10	55	5 ± 1	82 ± 6	10 ± 1	24 ± 4	11 ± 0.7
143470	358	255	29/11/2014	–	48	469	10 ± 1	129 ± 3	15 ± 0.3	61 ± 1	12 ± 0.1
All	343 ± 41	242 ± 7	–	–	33 ± 9	353 ± 135	9 ± 2	122 ± 1	13 ± 0.1	55 ± 1	13 ± 0.1

Data are given for four adult Weddell seals equipped with DSA tags at Dumont D'Urville (66°40′S 140°E) in November 2014. $PrCA_{DSA}$ corresponds to the estimated number of seconds spent in prey capture attempt behavior by the DSA tag algorithm. Swimming effort (swim effort) is expressed as (total dive swim effort)/(dive duration).

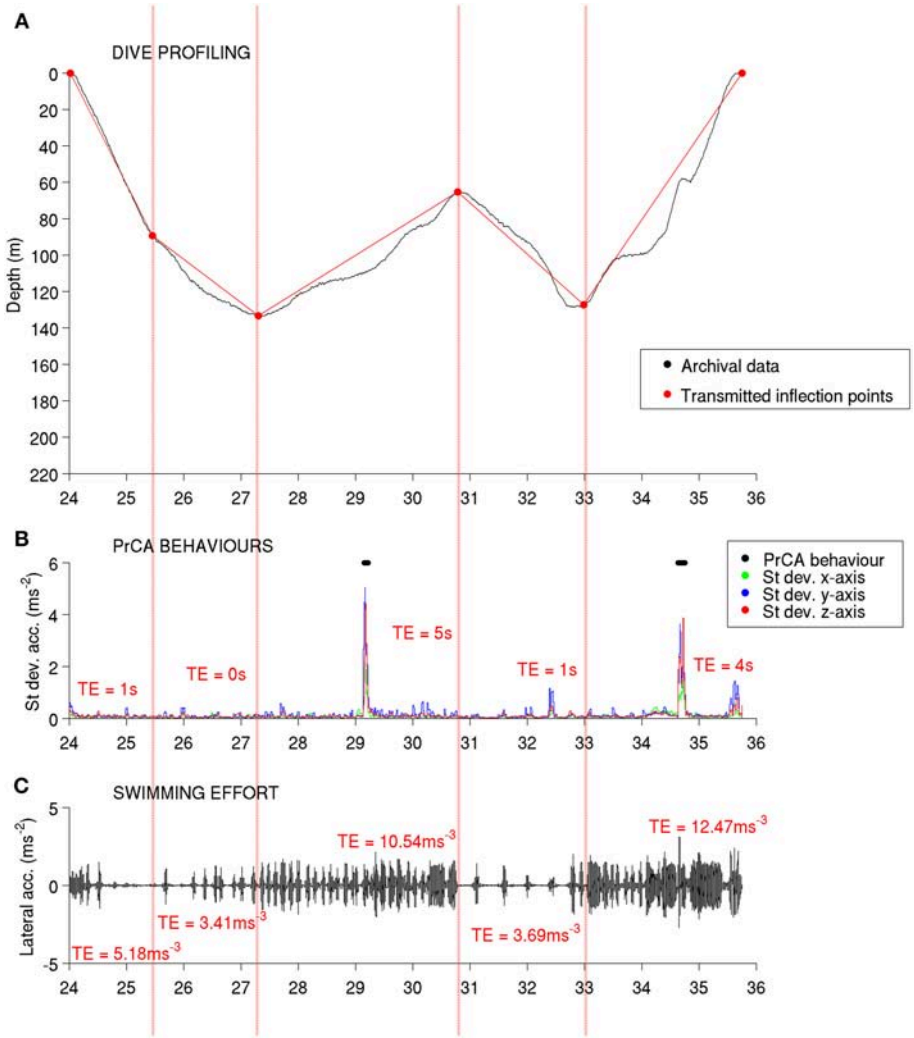

FIGURE 1 | Overview of the high-resolution archives (prior to summarizing) and associated DSA tag data transmissions from one example dive. Red dotted partitions from left to right correspond to each segment [1–5, respectively; identified via an on-board broken-stick algorithm (BS_{DSA})]. From top to bottom: **(A)** depth measurements from high-resolution archives in black and reconstructions from transmitted BS_{DSA} inflection points in red, **(B)** standard deviations in acceleration from high-resolution archives along the three axes (green = *x*, blue = *y* and red = *z*) with identified $PrCA_{archival}$ behaviors marked by black dots, and **(C)** filtered lateral (y) accelerations from high resolution archival data showing stroke amplitudes and rates (used to estimate swimming effort). Red text **(B,C)** corresponds to transmitted estimates (TE) for each segment.

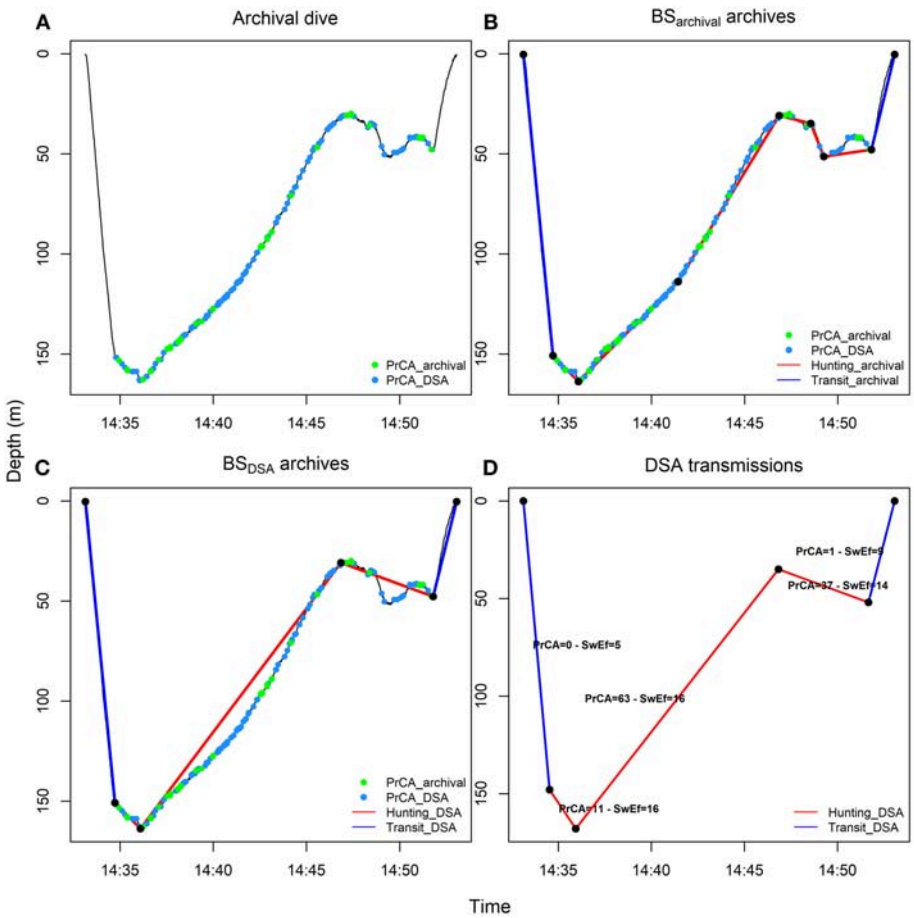

FIGURE 2 | From high-resolution to low-resolution dive profiles. High-resolution archived dives **(A)** were summarized by an optimal number of inflection points ($BS_{archival}$ archives) (**B**, see methods and Heerah et al., 2014) and degraded in SRDL low-resolution dives (BS_{DSA} summarized archives) (**C**, see methods and Heerah et al., 2015). The corresponding dives were also transmitted, along with the associated swimming efforts (Swim effort, expressed in $m{\cdot}s^{-3}$) and time spent in $PrCA_{DSA}$ behaviors per segment **(D)** (see also **Figure 1**). For the later, acceleration records were automatically processed on board the DSA tag before transmission. Red lines represent broken stick segments associated with $hunting_{archival}$ (**B**, sinuous phases of high-resolution dives, $0 <$ vertical sinuosity < 0.9) or $hunting_{DSA}$ (**C,D**, segments associated with reduced vertical velocity of low-resolution dives, vertical velocity $\leq 0.5\ m{\cdot}s^{-1}$) behaviors. Conversely, blue lines represent segments associated with $transit_{archival}$ (**B**, straighter phases of high-resolution dives, $0.9 \leq$ vertical sinuosity ≤ 1) or $transit_{DSA}$ (**C,D**, segments associated with increased vertical velocity of low-resolution dives, vertical velocity $> 0.5\ m{\cdot}s^{-1}$) behaviors. The green and blue dots indicate seconds spent in $PrCA_{archival}$ (estimates from high-resolution archives using well established algorithms) and $PrCA_{DSA}$ (estimates from DSA algorithm before transmission) behaviors, respectively.

clustering was used to group these standard deviations into "low" and "high" states. A PrCA behavior was considered to have occurred within a 1 s period when each of the three axes were in a "high" state at least once along the corresponding section of the 16 Hz resolution time series (**Figure 1** Viviant et al., 2009; Guinet et al., 2014; Vacquié-Garcia et al., 2015a). Swimming efforts were taken by isolating flipper stroke rates and movement intensities. Accelerations along the lateral y-axis were high-pass filtered using a third-order band pass Butterworth filter, centered on the second peak in power intensity as identified from the power spectral density of the signal (between 0.48 and 1 Hz). Swimming effort at a 1 s resolution was then calculated as the absolute sum of peaks (and troughs) of flipper stroke accelerations with absolute amplitudes/intensities of at least 0.3 m/s^2 (Richard et al., 2014).

For comparison to DSA transmissions, the high-resolution estimates of swimming effort and $PrCA_{archival}$ were summarized in two ways, using a broken-stick (BS) algorithm. First, we used the high-resolution archives to generate a SRDL equivalent low-resolution dataset, by constraining the BS algorithm to retain only the four most informative inflection points, similarly to the algorithm implemented on-board the DSA tags [hereafter "BS_{DSA} summarized archives" (Fedak et al., 2002; Heerah et al., 2015; Cox et al., 2018)]. For each segment, the total time spent in PrCA behaviors (in seconds) was taken as the sum of all PrCA behaviors detected in that segment. A per dive segment swimming effort was taken as the sum of all identified swimming effort associated accelerations during that segment divided by the duration of the segment. These BS_{DSA} summarized archives were used for comparisons between the high-resolution archives and

DSA transmissions as well as for calculating and validating a low-resolution foraging index from dive only data ("$hunting_{DSA}$," see below and Heerah et al., 2015). Second, we applied the BS method described in Heerah et al. (2014), to resume each dive into an optimal number of segments (hereafter "$BS_{archival}$ archives"), from which we calculated a high-resolution index of foraging activity using established procedures ("$hunting_{archival}$," see below and Heerah et al., 2014).

Validation of DSA On-Board Processing

To assess and validate the suitability of the DSA algorithms for Weddell seals, we compared DSA transmissions of PrCA behaviors (s) and swimming effort (ms^{-3}), to time matched estimates from the BS_{DSA} summarized archives (Cox et al., 2018). Comparisons were limited to one individual (# 143468, only tag retrieved) and to 70% of archived dives (used transmitted dives = 189,945 segments; archived dives = 270), because of transmission losses (not all archived dives were successfully transmitted; 48 dives) and/or because of errors in transmissions [i.e., repeated times in start/end of dive segments which possibly occur when transmission uplinks are interrupted (Boehme et al., 2009); 1 dive] and time mis-matches (32 transmitted dives did not have archived dives within 10 min of their time-stamp). Similar "errors" have been observed in previous studies using SRDL and DSA transmitted datasets (Labrousse et al., 2015; Heerah et al., 2017; Cox et al., 2018).

Due to potential differences in seal behavior within a dive (e.g., between segments), we assessed how DSA algorithms performed at both the dive and segment scales. For each behavioral variable (time in PrCA behavior and swimming effort), linear regression models were fitted to (1) pooled data encompassing all five segments of a dive (**Supplementary Figure 1**) and (2) data from each segment (i.e., separate regressions for each segment 1–5, **Figure 3**). In all statistical analyses, DSA transmissions were fitted as the response variable and BS_{DSA} summarized archives as the explanatory variable. All models were fitted using standardized data (subtract mean and divide by standard deviation of combined DSA transmissions and summarized high resolution archives to retain 1:1 expectation) and validated using commonly used post-processing techniques of model residuals (Zuur et al., 2009). Intercept, slope and R-squared (R^2) values were used to assess correlations between DSA transmissions and the BS_{DSA} summarized archives. In addition, root mean square errors (RMSE) were calculated between the fitted values of the linear model vs. the BS_{DSA} summarized archives, as well as between the DSA transmissions and BS_{DSA} summarized archives (for both standardized and raw datasets).

Confusion matrices [via the SDMTools package in R (Van der Wal et al., 2014), were used to compare $PrCA_{DSA}$ from $PrCA_{archivalnn}$ and assess when/when not these were in agreement with each other (**Table 2**)]. This analysis was performed at both dive ("*ALL*" in **Table 2**) and segment scales.

Validation of Foraging Activity Inferred From Dive Indices

In previous studies, Heerah et al. (2014, 2015) developed foraging indices that can be calculated for high-resolution (archived) and low-resolution (transmitted) dives from time-depth records solely. Instead of inferring foraging activity by only considering pre-determined parts of a dive (Watanabe et al., 2003; Austin et al., 2006; Kuhn et al., 2009; Le Bras et al., 2016; e.g., bottom phase, Houston and Carbone, 1992), the authors assumed that diving predators would increase the time spent in parts of the water column likely associated with more prey. This would be marked by an increase in vertical sinuosity and a decrease in vertical velocity, characteristic of vertical Area Restricted Search (ARS) behavior as initially hypothesized by Bailleul et al. (2010) and Dragon (2011).

Following the approach fully described in Heerah et al. (2014), high resolution archives were processed with the $BS_{archival}$ method in order to be summarized into an optimal number of segments (**Figures 2A,B**). For the resulting 266 dives (the Gompertz model of the algorithm did not fit for four dives), each dive segment was then associated with a behavioral mode according to its sinuosity. Highly sinuous segments indicated "$hunting_{archival}$" behavior, while more directed segments indicated "$transit_{archival}$" behavior (**Figure 2B**). Vertical sinuosity cannot be calculated for BS_{DSA} summarized archives (5 segments simulated transmitted dives for # 143468) and DSA transmissions. Instead, behavioral mode was defined for each of the five segments according to their vertical velocity (see details in Heerah et al., 2015). "$Hunting_{DSA}$" corresponded to "low-speed" segments and "$transit_{DSA}$" corresponded to "high-speed" segments (**Figures 2C,D**). Successive segments associated with the same behavior were grouped into behavioral bouts/phases. Following this, for each dive we summed the total time spent in $hunting_{archival}$ or $hunting_{DSA}$ mode, resulting in an overall dive foraging effort index.

In order to assess the validity of these foraging indices for Weddell seals and different data resolutions, we calculated the time spent in PrCA behaviors associated with hunting/transit behavioral phases for each of the datasets ($BS_{archival}$ archives, BS_{DSA} summarized archives, DSA transmissions). We fitted linear regression models and calculated R-squared values (as described above) to study (1) the accuracy of hunting time estimation between $BS_{archival}$ archives and equivalent BS_{DSA} summarized archives (**Supplementary Figure 2**); (2) the correlation between the time spent in hunting mode and PrCA behaviors at the bout and dive scale for $BS_{archival}$ and BS_{DSA} summarized archives and DSA transmissions (**Figure 4**; **Table 3**).

RESULTS

DSA Transmissions and Diving Behavior

For the four seals, the DSA tags transmitted data on per segment diving depth, duration, swimming effort and time spent in PrCA behaviors, for time periods of 10–49 days, between November 2014 and January 2015 (**Table 1**; **Figure 2D**). The number of dives transmitted per individual ranged from 55 to 667, resulting in 1,412 total dives, with an average of 9 ± 9 (mean ± *SE*, nSeal = 4, **Table 1**) dives per day.

A DSA tag was retrieved from one individual (# 143468), providing high-resolution archives for 270 dives across 27 days (**Figure 1**). Of these high-resolution dives, 82% were transmitted.

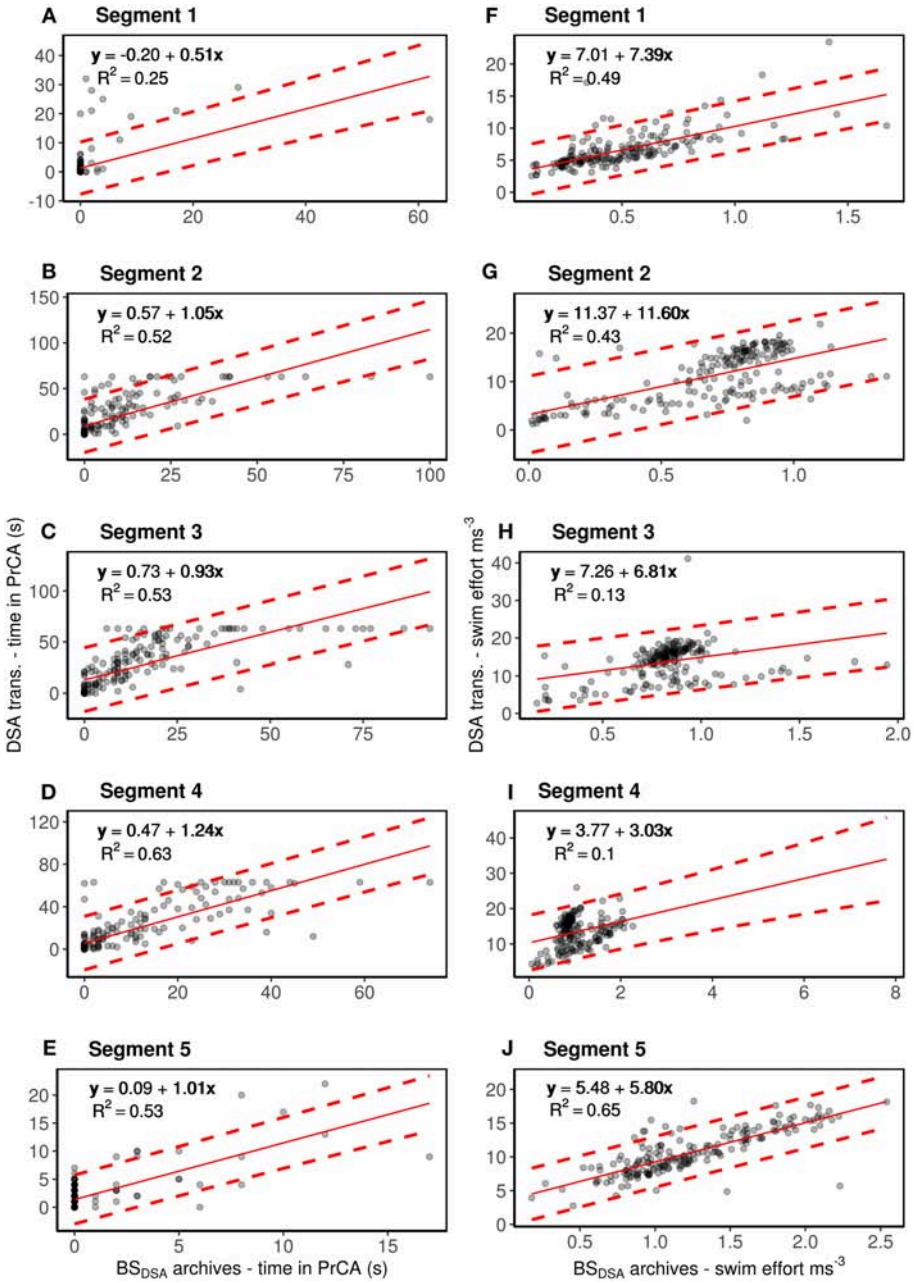

FIGURE 3 | Segment by segment comparisons between DSA transmissions of time spent in PrCA behaviors (column one; **A–E**) and swimming effort (column 2; **F–J**) to estimates from the corresponding BS_{DSA} summarized archives (for one individual #143468). The red line represents the intercept-slope output, with 95% prediction intervals in dashed red. Intercept and slope values close to 0 and 1, respectively reflect stronger correlations/likeness between the two data types than those far from 0 to 1. R^2 values show the amount of variation accounted for by the model. Rows, from top to bottom, correspond to segments one through to five.

84% of dives across the entire dataset (encompassing 4 seals) and 59% of sampling days came from the three seals for which tags were not retrieved (**Table 1**).

Seals dived on average to 122 ± 1 m (max: 344 m) for 13 ± 0.1 min (max: 38 min) and spent 55 ± 1 s in $PrCA_{DSA}$ behaviors (max: 173 s), representing 6 ± 0.4% (max: 21%) of total dive durations (**Table 1**; **Figure 2D**). Relative swimming effort was on average 12.5 ± 0.1 $m \cdot s^{-3}$ (**Table 1**).

Assessment and Validation of DSA Transmissions

Time Spent in PrCA Behaviors

Overall, DSA transmissions of time spent in PrCA behaviors ($PrCA_{DSA}$) were consistently overestimated to those from the BS_{DSA} summarized archives ($PrCA_{archival}$) (n = 189, intercept of 0.40 and slope 1.15 **Supplementary Figure 1**; **Supplementary Table 1**). Nonetheless, R^2 values of 0.61 were

TABLE 2 | Performance metrics from confusion matrices of $PrCA_{DSA}$ (used in DSA transmissions) and $PrCA_{archival}$ (from high-resolution archives) detections.

Performance metric	Description	Seg 1	Seg 2	Seg 3	Seg 4	Seg 5	ALL
True positive rate	True positive/actual positive	0.480	0.568	**0.578**	0.577	0.516	0.571
False positive rate	False positive/actual negative	0.016	0.074	0.085	0.065	**0.012**	0.058
Specificity	True negative/actual negative	0.986	0.926	0.915	0.935	**0.988**	0.942
Precision	True positive/predicted positive	0.163	0.239	0.272	**0.302**	0.216	0.265
Misclassification	(False positive + false negative)/total	0.016	0.088	0.103	0.082	**0.015**	0.071
Accuracy	(True positive + true negative)/total	0.984	0.912	0.897	0.918	**0.985**	0.929
Prevalence	Actual positive/total	0.005	0.039	**0.052**	0.046	0.006	0.035

The best performing dive segment is highlighted in bold. Performance metrics determined using all pooled data are shown under the column "ALL."

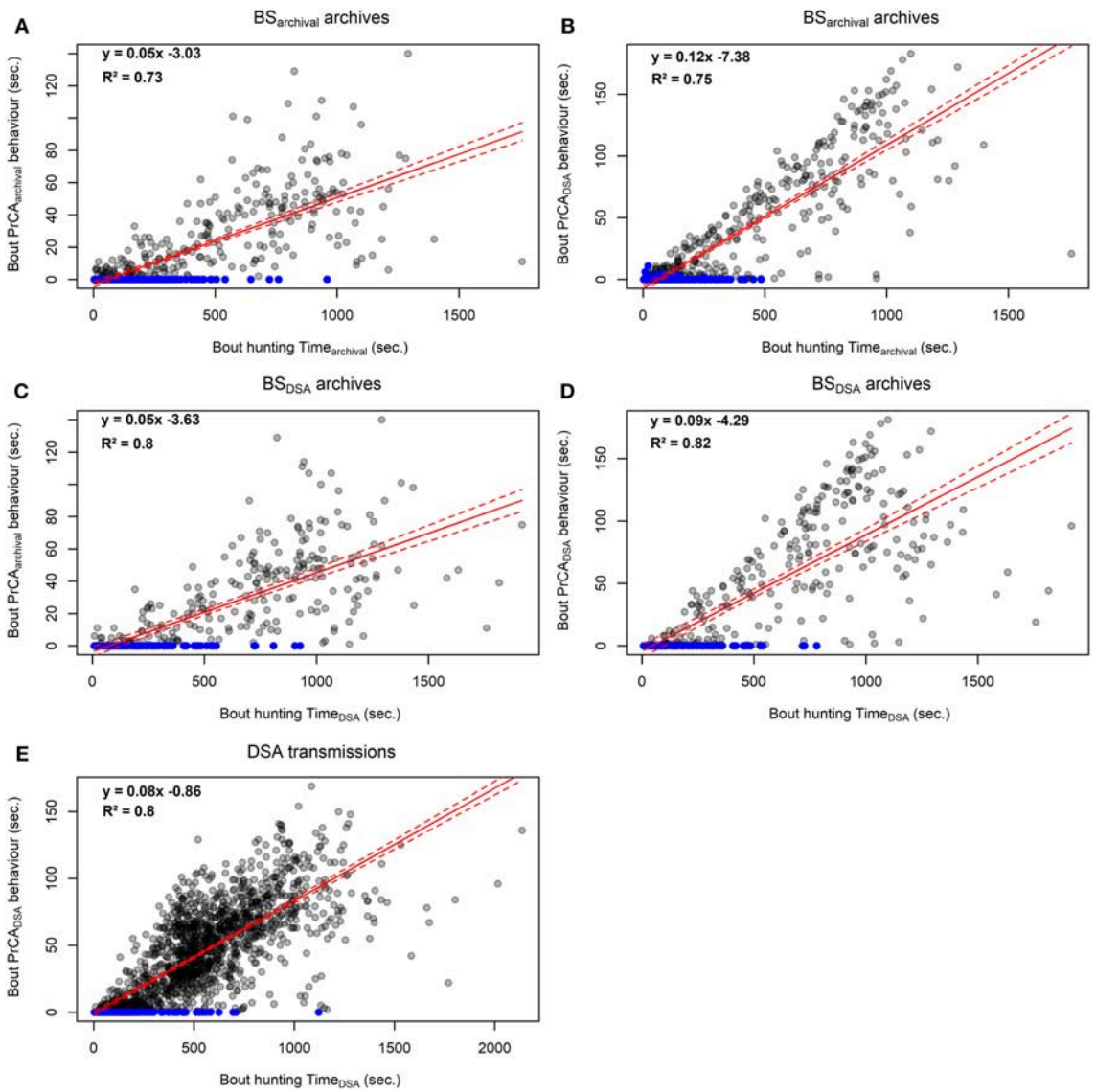

FIGURE 4 | Comparison between foraging bout durations and time spent in PrCA behaviors estimated from high-resolution acceleration archives from established procedures (#143468; **A** and **C**) and simplified DSA algorithms (#143468, **B** and **D**; $n = 4$, **E**). The red line represents the intercept-slope output, with 95% confidence intervals in dashed red. Blue dots indicate hunting bouts during which there was no time spent in PrCA behaviors.

TABLE 3 | Foraging effort outputs from the calculation of high and low-resolution effort indices.

PTT	Data type	Foraging index	Metric used for Foraging index	Hunting Time (min)	$PrCA_{archival}$/Hunting Bout (s)	$PrCA_{archival}$/Transit Bout (s)	$PrCA_{DSA}$/Hunting Bout (s)	$PrCA_{DSA}$/Transit Bout (s)
143468	$BS_{archival}$ archives	Hunting archival	Vertical sinuosity	13 ± 0.4	29 ± 2	1 ± 0.2	62 ± 3	3 ± 0.4
143468	BS_{DSA} archives	Hunting DSA	Vertical velocity	14 ± 0.4	30 ± 2	1 ± 0.1	61 ± 3	1 ± 0.2
143468	DSA			12 ± 0.4			58 ± 2	3 ± 0.2
143467	DSA			8 ± 0.1			42 ± 4	1 ± 0.2
143469	DSA			8 ± 1			23 ± 2	4 ± 0.4
143470	DSA			12 ± 0.2			59 ± 2	1 ± 0.2

*$Hunting_{archival}$ and $hunting_{DSA}$ (see methods and **Figure 2** for description) indicate parts within a high and low-resolution dive, respectively, where a seal intensifies its foraging behavior by increasing its vertical sinuosity ($Hunting_{archival}$) or its vertical velocity ($Hunting_{DSA}$), respectively. Hunting time is the total time spent in hunting behavior per dive. Time spent in $PrCA_{DSA}$ (used for DSA transmissions) and $PrCA_{archival}$ (from high-resolution archives) was calculated for each dive behavioral bout (i.e., successive BS segment with the same behavior).*

satisfactory (**Supplementary Figure 1**; **Supplementary Table 1**). At the segment scale, the DSA algorithms performed best for segments two through to five (**Figure 3**; **Supplementary Table 1**).

Confusion matrix performance metrics generally reflect results from the linear regressions (**Supplementary Figures 1**, **3**; **Table 2**). Overall accuracy and specificity of the algorithm were high (0.93 and 0.94, **Table 2**). Similarly, true positive rates were deemed satisfactory (0.57, **Table 2**). False positive rates and misclassifications were low (0.058 and 0.07, respectively, **Table 2**). At the segment scale, the DSA algorithms performed best for segments two through to four (**Figure 3**; **Supplementary Table 1**).

A ceiling of 60 s in the total time spent in $PrCA_{DSA}$ behaviors during a segment was too low and estimates from the BS_{DSA} summarized archives exceeded this several times (**Figure 3**).

Swimming Effort

Average swimming efforts from the DSA transmissions were also consistently overestimated compared to those from the BS_{DSA} summarized archives ($n = 189$, intercept of 5.93 and slope of 5.82, **Supplementary Figure 1**; **Supplementary Table 1**). Overall, R^2 values were low (0.27, **Supplementary Figure 1**; **Supplementary Table 1**). However, segment by segment comparisons suggest these observations are predominantly driven by the algorithms low performance for segments three and four (R^2 values of 0.13 and 0.10, respectively, **Figure 3**; **Supplementary Table 1**). For segments one, two and five, R^2 values of 0.49, 0.43 and 0.65 were deemed satisfactory (although lesser so for segment two; **Figure 3**; **Supplementary Table 1**).

Validation of Foraging Effort Indices Calculated From Time-Depth Records

Comparison With PrCA Behaviors From Archived Data: From High to Low Resolution

Seal #143468 (retrieved tag, $n = 266$) spent 73 ± 1% (13 ± 0.4 min) and 79 ± 1% (14 ± 0.4 min) of its time spent diving (on average 14 ± 0.4 min) in $hunting_{archival}$ and $hunting_{DSA}$ mode, respectively (**Table 3**). Overall dive $hunting_{archival}$ and $hunting_{DSA}$ times were positively and highly correlated (intercept of 21.7, slope of 1.02 and R^2 of 0.97; **Supplementary Figure 2**).

Overall, hunting phases (either $hunting_{archival}$ and $hunting_{DSA}$) were associated with numerous $PrCA_{DSA}$ (∼ 60 ± 3 s, max: 183 s) and $PrCA_{archival}$ (∼ 30 ± 2 s, max: 140 s) (**Table 3**; **Figure 2**). In addition, 97 and 95% of time spent in $PrCA_{archival}$ and $PrCA_{DSA}$ behaviors, occurred within $hunting_{archival}$ phases of the dives (e.g., **Figure 2B**). Similarly, 98 and 93% of time spent in $PrCA_{archival}$ and $PrCA_{DSA}$ behaviors, respectively, occurred within $Hunting_{DSA}$ phases of the dives (**Figure 2C**). Conversely, transit phases (either $transit_{archival}$ and $transit_{DSA}$) were associated with few PrCA (**Table 3**; **Figure 2**).

At the bout scale, time spent in hunting mode (either $hunting_{archival}$ and $hunting_{DSA}$) correlated well with both the time spent in $PrCA_{archival}$ ($R^2_{Huntingarchival}$ of 0.73, **Figure 4A**; $R^2_{HuntingDSA}$ of 0.8, **Figure 4C**) and $PrCA_{DSA}$ behaviors ($R^2_{Huntingarchival}$ of 0.75, **Figure 4B**; $R^2_{HuntingDSA}$ of 0.68, **Figure 4D**). At the dive scale, the relationship between the time spent in $hunting_{archival}$ mode and PrCA behaviors was slightly weaker ($PrCA_{archival}$: slope of 0.05, intercept of −0.15, R^2 of 0.68, **Supplementary Figure 3A**; $PrCA_{DSA}$: slope of 0.09, intercept of 4.71, R^2 of 0.73, **Supplementary Figure 3B**). The time spent in $hunting_{DSA}$ mode underestimated the time spent in PrCA behaviors, particularly for $PrCA_{DSA}$ ($PrCA_{archival}$: slope of 0.04, intercept of −0.51, R^2 of 0.68, **Supplementary Figure 3C**; $PrCA_{DSA}$: slope of 0.06, intercept of 3.23, R^2 of 0.43, **Supplementary Figure 3D**).

Comparison With PrCA Behaviors From Transmitted Dives

For transmitted DSA dives ($n = 1{,}412$), the time spent in $hunting_{DSA}$ modes represented on average 75 ± 0.4% of corresponding dive durations (10 ± 0.1 min). $Hunting_{DSA}$ phases were associated with 49 ± 1 s (max: 169 s) spent in $PrCA_{DSA}$ behaviors (**Table 3**). Overall, 94% of time spent in $PrCA_{DSA}$ behaviors, occurred within $hunting_{DSA}$ phases of the dives. In contrast, $transit_{DSA}$ phases were associated with 3 ± 0.1 s (37 s) spent in $PrCA_{DSA}$ behaviors.

At the bout scale, time spent in $hunting_{DSA}$ mode correlated well with the time spent in $PrCA_{DSA}$ behaviors (slope of 0.08, intercept of −0.86, R^2 of 0.8, **Figure 4**) while it was weaker at the overall dive scale (slope of 0.05, intercept of 8.82, R^2 of 0.43, **Supplementary Figure 3**).

DISCUSSION

In this study, we present data acquired from a new generation of SRDLs (the DSA tag) that record, process on-board and transmit data from time-depth and tri-axial acceleration records along with Argos locations (see also, Cox et al., 2018). These were successfully deployed on four Weddell seals, allowing novel data to be obtained across a period of 10–49 days. Retrieval of one of these tags, providing high-resolution acceleration records, offered a unique opportunity to assess simultaneously the validity of DSA transmitted outputs and previously developed foraging effort indices for this species. The Weddell seal is a relevant study case on which to apply the procedure because (1) they inhabit unpredictable, dynamic environments where tag retrieval is far from guaranteed (i.e., 25% of tag retrieval in our study), and (2) like other species of pinnipeds, such as the Antarctic fur seal, they have complex diving behaviors that challenge well-established methods to infer foraging activity (Heerah et al., 2014; Viviant et al., 2016). Although some improvements could be made in the DSA algorithm, and analyses comparing high-resolution archives and summarized transmissions were performed on only one individual (but numerous dives, behavioral bouts and segments), we show that both transmitted acceleration and "hunting" foraging indices were reliable in inferring foraging activity and potential prey encounters for Weddell seals. These results offer promising opportunities to post-process the numerous existing SRDL datasets and/or use DSA tags to further understand the energetic budgets involved in the strategies marine predators adopt to maximize resource acquisition in relation to their environment (e.g., Block et al., 2011; Arthur et al., 2016; Richard et al., 2016; Heerah et al., 2017).

Assessment and Validation of DSA Transmissions

PrCA Behaviors

Overall, comparisons of estimates of time spent in PrCA behaviors from DSA transmissions ($PrCA_{DSA}$) to detailed archives ($PrCA_{archival}$) obtained from one Weddell seal were satisfactory, and displayed performance metrics similar to those observed in juvenile southern elephant seals (Cox et al., 2018). However, as in Cox et al. (2018), segment by segment analyses suggested that the DSA algorithm performed better for some segments than others (for an in depth discussion of the possible factors driving this, see Cox et al., 2018). Correlations of time spent in PrCA behaviors were much stronger during segments two through to five than in segment one, as were true positive rates (particularly for segments two through to four). Segments two through to four most likely correspond to the bottom and/or hunting phases of a dive, where individuals concentrate foraging effort and thus perform the majority of PrCA behaviors (Ropert-Coudert et al., 2001; Schreer et al., 2001; Watanabe et al., 2003; Mitani et al., 2004; Heerah et al., 2014; Volpov et al., 2016). Subsequently, it is most important that the algorithm performs adequately during these phases. Whilst positive bias (i.e., over-estimation), false positive rates and RMSE's were slightly increased during these phases relative to segments one and particularly five, this may be attributable to other prey capture behaviors, such as prey chase and handling behaviors, that are picked up by the DSA simplified algorithm and correlate well with true PrCA detections (Cox et al., 2018). Poorer correlations and true detection rates during phases one and, to a lesser extent five (only evident in detection rates) may partially result from a low prevalence of PrCA behaviors while transiting between the surface to/from the water column where they forage, alongside the presence of other behaviors unrelated to PrCA and possibly related to directed swimming motions (Heerah et al., 2014; Viviant et al., 2016).

Despite an overall over-estimation of time spent in $PrCA_{DSA}$ behaviors and some misclassifications compared to time spent in $PrCA_{archival}$ behaviors, the strength of correlations and consistency between segments two to four (the expected foraging parts of the dives), as well as algorithm accuracy, suggest $PrCA_{DSA}$ are reliable enough to quantify foraging effort. However, instead of using time spent in $PrCA_{DSA}$ behaviors as absolute values to quantify dive foraging activity/success, we would recommend using these as a relative index of foraging activity across all dives (e.g., building classes of foraging dives; intense vs. low foraging dives), or to identify parts of the water column where most foraging occurs.

Swimming Effort

Overall, comparisons of DSA transmissions and the detailed archives of swimming effort obtained from one Weddell seal were poor and highly variable. However, segment by segment analyses suggested that this pattern was predominantly driven by particularly low performances for segments three and four. In contrast, comparisons for segments one and five (and a lesser extent two) were good and suggested that the algorithm performed well in these instances. Such a pattern was also observed in juvenile southern elephant seals (Cox et al., 2018). Segments one and five (and sometimes two) correspond to times when individuals tend to perform the directed swimming behaviors associated with the descent and ascent phases of a dive. They also correspond to the dive phases from which swimming effort can be used to infer seal body condition (Biuw, 2003; Richard et al., 2014). Thus, it is most important that algorithms perform well during these segments, as our analyses suggest. Poor algorithm performance during segments three and four, may be due to the presence of more complex movement patterns associated with an increase in foraging related behaviors. For example, active searching alongside prey chasing and handling may increase rolling and horizontal sinuosity movements, which will translate to increased accelerations on the lateral y-axis (used in swimming effort calculations) that are not related to swimming motions (Mitani et al., 2004; Gallon et al., 2013; Viviant et al., 2016; Le Bras et al., 2017).

The results obtained for DSA transmitted swimming efforts make us less confident in using these values for segments two to four (e.g., Jeanniard-du-Dot et al., 2016a,b). Swimming effort during transit phases from/to the surface (segments one and five, and possibly two dependent on dive shape) seem sufficiently reliable and could be used, for instance, in combination with ascent and descent rates, to investigate changes in body condition along

a foraging trip (Beck et al., 2000; Biuw, 2003; Sato et al., 2003; Adachi et al., 2014; Richard et al., 2014). However, swimming efforts from segments three and four (and likely two when it is associated with the 'hunting' phase of a dive) appear much less reliable, making further inference for these parts of the dive difficult.

Inference on Foraging Effort Using Vertical ARS Indices

Overall, for the one individual from which a DSA tag was retrieved, $\text{hunting}_{\text{DSA}}$ time was highly correlated with $\text{hunting}_{\text{archival}}$ time, indicating that low-resolution dive segments of decreased vertical velocity (i.e., "$\text{hunting}_{\text{DSA}}$ mode") are also associated with increased vertical sinuosity (i.e., "$\text{hunting}_{\text{archival}}$ mode"). Moreover, for archived and DSA dives, most time spent in PrCA behaviors (>90%) occurred within hunting phases, during which times spent in PrCA behaviors were around 20 to 30 times higher than those estimated for transit phases. Similarly, at the behavioral bout scale, both indices correlated well with times spent in PrCA behaviors (R^2 between 0.73 and 0.82). At the dive scale, both indices performed similarly in estimating times spent in $\text{PrCA}_{\text{archival}}$ behaviors ($R^2 = 0.68$). However, while $\text{hunting}_{\text{archival}}$ times were well-correlated with times spent in PrCA_{DSA} behaviors ($R^2 = 0.68$), $\text{hunting}_{\text{DSA}}$ times were underestimated and less well-correlated ($R^2 = 0.43$).

An underestimation of times spent in PrCA_{DSA} with $\text{hunting}_{\text{DSA}}$ time may be due to several reasons. First, there is an overall over-estimation of time spent in PrCA_{DSA} compared to $\text{PrCA}_{\text{archival}}$. Second, the relationship between the two variables could be weakened by dives associated with low vertical speed phases which are classified as foraging but not associated with any time spent in PrCA_{DSA} behaviors (3% of dives and 5% of behavioral bouts). This would typically be observed if a seal meanders at depth exploring the water column horizontally to find a prey patch, gliding periods (e.g., drift dives for elephant, gray and fur seals; Beck et al., 2000; Page et al., 2005; Gordine et al., 2015) or a change in orientation (e.g., upside down exploratory dives under the sea-ice to find a breathing hole for Weddell seals and other sea-ice obligate species; Bengtson and Stewart, 1992; Wartzok et al., 1992; Davis et al., 2003). Combined information on prey encounters and 3D diving movements would provide a better understanding of these different scenarios (e.g., Davis et al., 2003; Le Bras et al., 2017). Finally, at the dive scale, as previously shown for other species, considering additional dive metrics, such as depth, duration and ascent/descent rates may increase correlations to estimations of time spent in PrCA behaviors (Viviant et al., 2014; Vacquié-Garcia et al., 2015b; Volpov et al., 2016).

Altogether, these results strengthen the assumption on which "hunting" indices rely, that marine predators would adopt a vertical ARS behavior to increase time spent at favorable parts of the water column (Heerah et al., 2014, 2015; Le Bras et al., 2016; see also MacArthur and Pianka, 1966). The fundamental advantage of this approach over other methods is that it detects foraging activity along the dive profile rather than assuming foraging occurs at putative parts of a dive (Watanabe et al., 2003; Austin et al., 2006; Kuhn et al., 2009; Le Bras et al., 2016, such as bottom time, Houston and Carbone, 1992). Moreover, it relies on sinuosity and velocity thresholds that can be adapted to any species (see Heerah et al., 2014, 2015 for more methodological discussion, scripts and training datasets are also provided). Vertical sinuosity, a feature only captured by high-resolution data and quantified using "wiggles" has been used and associated with successful prey capture in seals, penguins and whales (Simeone and Wilson, 2003; Goldbogen et al., 2006; Bost et al., 2007; Calambokidis et al., 2007; Hanuise et al., 2010; Watanabe and Takahashi, 2013). Associations between hunting times and decreased vertical velocities (which also correspond to increased time spent in a water column layer), were observed and validated for Southern elephant seals (Heerah et al., 2015; Labrousse et al., 2015; Le Bras et al., 2016). Decreased vertical velocity has also been used as a proxy of foraging activity in several other species of diving predators (belugas, Hauser et al., 2015; Antarctic fur seals, Arthur et al., 2016; sea turtles, Chambault et al., 2016; Weddell seals, Heerah et al., 2017), for which only degraded dive transmissions were available. This study provides further validation that the same method can be applied to different species, as well as to both high and low-resolution dive datasets (see Heerah et al., 2014, 2015 for more methodological discussion, scripts and training datasets are also provided). Another advantage is that the hunting indices rely on the sinuosity and velocity of the animal's trajectory which should not be influenced by the logger position on the animal (e.g., back-mounted instead of head-mounted). Typically, Le Bras et al. (2016) showed that PrCA estimated from a head or back mounted accelerometer correlated at 93% (see also Ladds et al., 2016). It also appears that hunting indices can provide a value that correlates well with time spent in PrCA behaviors, despite data being highly degraded for satellite transmission. Nonetheless, to ensure rigorous analyses and ecological conclusions, we would recommend using the hunting indices as proxies of foraging effort, alongside overall prey distribution and availability in the water column, rather than prediction of the exact time spent in PrCAs behaviors (Labrousse et al., 2015; Arthur et al., 2016; Carter et al., 2016; Pascoe et al., 2016; Heerah et al., 2017).

Methodological Sights

In this study, we used outputs from processed high-resolution acceleration data as a baseline reference to validate both DSA transmitted outputs and vertical ARS foraging indices. While acceleration outputs cannot provide direct observation of feeding success, an increasing number of studies have now established links between acceleration peaks and time spent in PrCA behavior or feeding events for pinnipeds as well as numerous diving seabirds (Watanabe and Takahashi, 2013; Ydesen et al., 2014; Volpov et al., 2015). Moreover, acceleration measurements can provide a reliable proxy for energy expenditure (i.e., swimming effort, overall dynamic body acceleration; Gleiss et al., 2011; Skinner et al., 2014; Jeanniard-du-Dot et al., 2016b) and relative measure of body condition (Sato et al., 2003; Richard et al., 2014; Jouma'a et al., 2016). As such, accelerometers have revolutionized our ability to study the behaviors of free-ranging, cryptic species, such as free and far ranging diving animals

(Brown et al., 2013). However, the need to retrieve devices often limits ecological studies to a range of species that return to predictable locations.

Novel SDRLs/DSA tags represent a promising tool to overcome these logistical challenges and extend our knowledge of the foraging activity and energetic budgets of less accessible species (e.g., sea-ice obligate species, juveniles). The algorithm and PrCA detection threshold implemented in the DSA tags here were initially developed for Southern elephant seals, and would probably benefit from further validation at the species level (i.e., simultaneous deployment of video cameras, jaw movement sensors, stomach temperature tags; Viviant et al., 2009; Ydesen et al., 2014; Jorgensen et al., 2015; Volpov et al., 2015). Nonetheless, despite being simplified to meet tag requirements (power limitation and dive by dive functionality), the on-board DSA algorithm relies on well-established acceleration processing techniques, already applied on a wide range of diving species (Viviant et al., 2009; Ydesen et al., 2014; Jorgensen et al., 2015; Volpov et al., 2015). In addition, PrCA detections and swimming effort measurements mostly rely on dynamic combinations of signal processing techniques, clustering analyses and thresholds that evolve with dive records, and thus should be adaptable to a range of species (see Cox et al., 2018 for more details). Cox et al. (2018), suggested several algorithm modifications that could improve the accuracy of $PrCA_{DSA}$ detections and swimming effort measurements, which regarding the similarities observed in outputs for the two species would likely benefit datasets acquired from Weddell seals.

DSA transmissions and hunting indices were validated using high-resolution records from only one individual from which a tag could be retrieved. While ideally further validation should be made on a larger dataset, this provides a realistic insight into the difficulties and logistical challenges faced in studies investigating free-ranging animal behaviors. It also stresses the importance of technological advances, such as the DSA tags presented here, to overcome tag retrieval issues and methodological development. Reliable hunting/foraging indices, to infer functional behaviors even from highly degraded time-depth records, are also important in such developments (Carter et al., 2016). There was an overall consistency, accuracy and correlation strength between acceleration outputs (archived and transmitted) and foraging/hunting indices across Southern elephant seals and Weddell seals, which are two species that display a broad range of different dive types in contrasting environments (Schreer and Testa, 1996; Davis et al., 2003; Dragon et al., 2012; Heerah et al., 2014). The consistency of foraging strategies across species suggests that these developments could be applied to a broad range of diving species (Schreer et al., 2001; Carter et al., 2016). This offers exciting perspectives to expand studies on foraging strategies, and address the under sampling of remote species as well as analyzing pre-existing time-depth records that are prevalent for many species, and have been collected in abundance since the early 1980s (Block et al., 2011; Hussey et al., 2015; Wilmers et al., 2015; Carter et al., 2016).

AUTHOR CONTRIBUTIONS

KH, J-BC, and CG designed the study protocol. KH, J-BC, and PB collected the data. KH and SC performed the analyses and wrote the manuscript. J-BC, CG, and PB significantly contributed to and revised the manuscript.

FUNDING

This study was funded by a CNES-TOSCA project Ecologie des phoques de Weddell et bio-océanographie de la banquise antarctique (PI JBC) and an European Research Council Advanced Grant as part of the program EARLYLIFE under the European Community's Seven Framework (grant agreement FP7/2007–2013/ERC-2012-ADG_20120314; PI Dr. Henri Weimerskirsch).

ACKNOWLEDGMENTS

This study is part of French Polar Institute (Institut Paul Emile Victor, IPEV) research project IPEV #109 (PI H. Weimerskirch). We thank IPEV for logistical support and winterers of the 64th mission in Dumont d'Urville for expert help in the field. More specifically, we warmly thank P. Apelt, A. Thollot, and F. Petit for their investment in the field.

SUPPLEMENTARY MATERIAL

The Supplementary Material for this article can be found online at: https://www.frontiersin.org/articles/10.3389/fevo.2019.00030/full#supplementary-material

REFERENCES

Adachi, T., Maresh, J. L., Robinson, P. W., Peterson, S. H., Costa, D. P., Naito, Y., et al. (2014). The foraging benefits of being fat in a highly migratory marine mammal. *Proc. R. Soc. B Biol. Sci.* 281:20142120. doi: 10.1098/rspb.2014.2120

Arnbom, T., Fedak, M. A., Boyd, I. L., and McConnell, B. J. (1993). Variation in weaning mass of pups in relation to maternal mass, postweaning fast duration, and weaned pup behaviour in southern elephant seals (*Mirounga leonina*) at South Georgia. *Can. J. Zool.* 71, 1772–1781. doi: 10.1139/z93-252

Arthur, B., Hindell, M., Bester, M. N., Oosthuizen, W. C., Wege, M., and Lea, M. (2016). South for the winter? within-dive foraging effort reveals the trade-offs between divergent foraging strategies in a free-ranging predator. *Funct. Ecol.* 30, 1623–1637. doi: 10.1111/1365-2435.12636

Austin, D., Bowen, W. D., McMillan, J. I., and Iverson, S. J. (2006). Linking movement, diving, and habitat to foraging success in a large marine predator. *Ecology* 87, 3095–3108. doi: 10.1890/0012-9658(2006)87[3095:LMDAHT]2.0.CO;2

Bailleul, F., Lesage, V., and Hammill, M. O. (2010). Spherical first passage time: a tool to investigate area-restricted search in three-dimensional movements. *Ecol. Model.* 221, 1665–1673. doi: 10.1016/j.ecolmodel.2010.04.001

Beck, C. A., Bowen, W. D., and Iverson, S. J. (2000). Seasonal changes in buoyancy and diving behaviour of adult grey seals. *J. Exp. Biol.* 203, 2323–2330.

Bengtson, J. L., and Stewart, B. S. (1992). Diving and haulout behavior of crabeater seals in the Weddell Sea, Antarctica, during March 1986. *Polar Biol.* 12, 635–644. doi: 10.1007/BF00236986

Benoit-Bird, K. J., Battaile, B. C., Heppell, S. A., Hoover, B., Irons, D., Jones, N., et al. (2013). Prey patch patterns predict habitat use by top marine predators with diverse foarging strategies. *PLoS ONE* 8:e53348. doi: 10.1371/journal.pone.0053348

Biuw, M. (2003). Blubber and buoyancy: monitoring the body condition of free-ranging seals using simple dive characteristics. *J. Exp. Biol.* 206, 3405–3423. doi: 10.1242/jeb.00583

Block, B. A., Jonsen, I. D., Jorgensen, S. J., Winship, A. J., Shaffer, S. A., Bograd, S. J., et al. (2011). Tracking apex marine predator movements in a dynamic environment. *Nature* 475, 86–90. doi: 10.1038/nature10082

Boehme, L., Lovell, P., Biuw, M., Roquet, F., Nicholson, J., Thorpe, S. E., et al. (2009). Technical note: animal-borne CTD-satellite relay data loggers for real-time oceanographic data collection. *Ocean Sci.* 5, 685–695. doi: 10.5194/os-5-685-2009

Bost, C.-A., Handrich, Y., Butler, P. J., Fahlman, A., Halsey, L. G., Woakes, A. J., et al. (2007). Changes in dive profiles as an indicator of feeding success in king and Adélie penguins. *Deep Sea Res. Part II Top. Stud. Oceanogr.* 54, 248–255. doi: 10.1016/j.dsr2.2006.11.007

Brown, D. D., Kays, R., Wikelski, M., Wilson, R., and Klimley, A. P. (2013). Observing the unwatchable through acceleration logging of animal behavior. *Anim. Biotelemetry* 1:1. doi: 10.1186/2050-3385-1-20

Calambokidis, J., Schorr, G. S., Steiger, G. H., Francis, J., Bakhtiari, M., Marshall, G., et al. (2007). Insights into the underwater diving, feeding, and calling behavior of blue whales from a suction-cup-attached video-imaging tag (CRITTERCAM). *Mar. Technol. Soc. J.* 41, 19–29. doi: 10.4031/002533207787441980

Carter, M. I. D., Bennett, K. A., Embling, C. B., Hosegood, P., and Russell, D. J. F. (2016). Navigating uncertain waters: a critical review of inferring foraging behaviour from location and dive data in pinnipeds. *Mov. Ecol.* 4:25. doi: 10.1186/s40462-016-0090-9

Chambault, P., de Thoisy, B., Heerah, K., Conchon, A., Barrioz, S., Dos Reis, V., et al. (2016). The influence of oceanographic features on the foraging behavior of the olive ridley sea turtle Lepidochelys olivacea along the Guiana coast. *Prog. Oceanogr.* 142, 58–71. doi: 10.1016/j.pocean.2016.01.006

Charnov, E. L. (1976). Optimal foraging, the marginal value theorem. *Theor. Popul. Biol.* 9, 129–136. doi: 10.1016/0040-5809(76)90040-X

Charrassin, J.-B., Kato, A., Handrich, Y., Sato, K., Naito, Y., Ancel, A., et al. (2001). Feeding behaviour of free-ranging penguins determined by oesophageal temperature. *Proc. R. Soc. B Biol. Sci.* 268, 151–157. doi: 10.1098/rspb.2000.1343

CLS (2016). *Argos User's Manual: Worldwide Tracking and Environmental Monitoring by Satellite.* Toulouse: CLS.

Cox, S. L., Orgeret, F., Gesta, M., Rodde, C., Heizer, I., Weimerskirch, H., et al. (2018). Processing of acceleration and dive data on-board satellite relay tags to investigate diving and foraging performance in free-ranging marine predators. *Methods Ecol. Evol.* 9, 64–77. doi: 10.1111/2041-210X.12845

Davis, R. W., Fuiman, L. A., Williams, T. M., Horning, M., and Hagey, W. (2003). Classification of Weddell seal dives based on 3-dimensional movements and video-recorded observations. *Mar. Ecol. Prog. Ser.* 264, 109–122. doi: 10.3354/meps264109

Dragon, A., Bar-Hen, A., Monestiez, P., and Guinet, C. (2012). Horizontal and vertical movements as predictors of foraging success in a marine predator. *Mar. Ecol. Prog. Ser.* 447, 243–257. doi: 10.3354/meps09498

Dragon, A. C. (2011). *Modélisation des Stratégies D'approvisionnement des Eléphants de mer Austraux–Influence de la Variabilité de la Production Primaire et des Conditions Océanographiques Physiques*. Available online at: https://www.locean-ipsl.upmc.fr/AnneCecile.Dragon/manuscript/AC-Dragon_PhD-thesis.pdf

Fedak, M., Lovell, P., McConnell, B., and Hunter, C. (2002). Overcoming the constraints of long range radio telemetry from animals: getting more useful data from smaller packages. *Integr. Comp. Biol.* 42, 3–10. doi: 10.1093/icb/42.1.3

Fedak, M. A. (2013). The impact of animal platforms on polar ocean observation. Fourth *Int. Symp. Bio-Logging Sci.* 88–89, 7–13. doi: 10.1016/j.dsr2.2012.07.007

Gallon, S., Bailleul, F., Charrassin, J. B., Guinet, C., Bost, C. A., Handrich, Y., et al. (2013). Identifying foraging events in deep diving southern elephant seals, *Mirounga leonina*, using acceleration data loggers. *Deep-Sea Res. II* 88–89, 14–22. doi: 10.1016/j.dsr2.2012.09.002

Gleiss, A. C., Wilson, R. P., and Shepard, E. L. C. (2011). Making overall dynamic body acceleration work: on the theory of acceleration as a proxy for energy expenditure. *Methods Ecol. Evol.* 2, 23–33. doi: 10.1111/j.2041-210X.2010.00057.x

Goldbogen, J. A., Calambokidis, J., Oleson, E., Potvin, J., Pyenson, N. D., Schorr, G., et al. (2011). Mechanics, hydrodynamics and energetics of blue whale lunge feeding: efficiency dependence on on krill density. *J. Exp. Biol.* 214, 131–146. doi: 10.1242/jeb.048157

Goldbogen, J. A., Calambokidis, J., Shadwick, R. E., Oleson, E. M., McDonald, M. A., and Hildebrand, J. A. (2006). Kinematics of foraging dives and lunge-feeding in fin whales. *J. Exp. Biol.* 209, 1231–1244. doi: 10.1242/jeb.02135

Goldbogen, J. A., Hazen, E. L., Friedlaender, A. S., Calambokidis, J., DeRuiter, S. L., Stimpert, A. K., et al. (2015). Prey density and distribution drive the three-dimensional foraging strategies of the largest filter feeder. *Funct. Ecol.* 29, 951–961. doi: 10.1111/1365-2435.12395

Gordine, S. A., Fedak, M., and Boehme, L. (2015). Fishing for drifts: detecting buoyancy changes of a top marine predator using a step-wise filtering method. *J. Exp. Biol.* 218, 3816–3824. doi: 10.1242/jeb.118109

Guinet, C. (1994). Poids a la naissance et croissance des éléphants de mer austraux. Quelles informations nous apportent-ils sur le milieu marin? *Recl. Médecine Vét.* 170, 105–110.

Guinet, C., Vacquié-Garcia, J., Picard, B., Bessigneul, G., Lebras, Y., Dragon, A., et al. (2014). Southern elephant seal foraging success in relation to temperature and light conditions: insight into prey distribution. *Mar. Ecol. Prog. Ser.* 499, 285–301. doi: 10.3354/meps10660

Hanuise, N., Bost, C.-A., Huin, W., Auber, A., Halsey, L. G., and Handrich, Y. (2010). Measuring foraging activity in a deep-diving bird: comparing wiggles, oesophageal temperatures and beak-opening angles as proxies of feeding. *J. Exp. Biol.* 213, 3874–3880. doi: 10.1242/jeb.044057

Hauser, D. D., Laidre, K. L., Parker-Stetter, S. L., Horne, J. K., Suydam, R. S., and Richard, P. R. (2015). Regional diving behavior of pacific arctic beluga whales delphinapterus leucas and possible associations with prey. *Mar. Ecol. Prog. Ser.* 541, 245–264. doi: 10.3354/meps11530

Heerah, K. (2014). *Ecologie en mer des phoques de Weddell de l'Antarctique de l'Est en relation avec les param etres physiques de l'environnement–At sea ecology of Weddell seals in East Antarctica in relation with environmental physical parameters*. Available online at: http://eprints.utas.edu.au/22756/ (Accessed June 10, 2017).

Heerah, K., Andrews-Goff, V., Williams, G., Sultan, E., Hindell, M., Patterson, T., et al. (2013). Ecology of weddell seals during winter: influence of environmental parameters on their foraging behaviour. *Deep Sea Res. Part II Top. Stud. Oceanogr.* 88–89, 23–33. doi: 10.1016/j.dsr2.2012.08.025

Heerah, K., Hindell, M., Andrew-Goff, V., Field, I., McMahon, C. R., and Charrassin, J. (2017). Contrasting behavior between two populations of an ice-obligate predator in East Antarctica. *Ecol. Evol.* 7, 606–618. doi: 10.1002/ece3.2652

Heerah, K., Hindell, M., Guinet, C., and Charrassin, J.-B. (2014). A new method to quantify within dive foraging behaviour in marine predators. *PLoS ONE* 9:e99329. doi: 10.1371/journal.pone.0099329

Heerah, K., Hindell, M., Guinet, C., and Charrassin, J.-B. (2015). From high-resolution to low-resolution dive datasets: a new index to quantify the foraging effort of marine predators. *Anim. Biotelemetry* 3:42. doi: 10.1186/s40317-015-0074-3

Hooker, S. K., Boyd, I. L., Jessopp, M., Cox, O., Blackwell, J., Boveng, P. L., et al. (2002). Monitoring the prey-field of marine predators: combining digital imaging with datalogging tags. *Mar. Mammal Sci.* 18, 680–697. doi: 10.1111/j.1748-7692.2002.tb01066.x

Horsburgh, J. M., Morrice, M., Lea, M., and Hindell, M. A. (2008). Determining feeding events and prey encounter rates in a southern elephant seal: a method using swim speed and stomach temperature. *Mar. Mammal Sci.* 24, 207–217. doi: 10.1111/j.1748-7692.2007.00156.x

Houston, A. I., and Carbone, C. (1992). The optimal allocation of time during the diving cycle. *Behav. Ecol.* 3, 255–265. doi: 10.1093/beheco/3.3.255

Hussey, N. E., Kessel, S. T., Aarestrup, K., Cooke, S. J., Cowley, P. D., Fisk, A. T., et al. (2015). Aquatic animal telemetry: a panoramic window into the underwater world. *Science* 348, 1255642–1255642. doi: 10.1126/science.1255642

Jeanniard-du-Dot, T., Guinet, C., Arnould, J. P. Y., Speakman, J. R., and Trites, A. W. (2016a). Accelerometers can measure total and activity-specific energy expenditures in free-ranging marine mammals only if linked to time activity budgets. *Funct. Ecol.* 31, 377–386. doi: 10.1111/1365-2435.12729

Jeanniard-du-Dot, T., Trites, A. W., Arnould, J. P. Y., Speakman, J. R., and Guinet, C. (2016b). Flipper strokes can predict energy expenditure and locomotion costs in free-ranging northern and Antarctic fur seals. *Sci. Rep.* 6:33912. doi: 10.1038/srep33912

Jorgensen, S. J., Gleiss, A. C., Kanive, P. E., Chapple, T. K., Anderson, S. D., Ezcurra, J. M., et al. (2015). In the belly of the beast: resolving stomach tag data to link temperature, acceleration and feeding in white sharks (Carcharodon carcharias). *Anim. Biotelemetry* 3:52. doi: 10.1186/s40317-015-0071-6

Jouma'a, J., Le Bras, Y., Richard, G., Vacquié-Garcia, J., Picard, B., El Ksabi, N., et al. (2016). Adjustment of diving behaviour with prey encounters and body condition in a deep diving predator: the southern elephant seal. *Funct. Ecol.* 30, 636–648. doi: 10.1111/1365-2435.12514

Kooyman, G. L., and Ponganis, P. J. (1998). The physiological basis of diving to depth: birds and mammals. *Annu. Rev. Physiol.* 60, 19–32. doi: 10.1146/annurev.physiol.60.1.19

Krausman, P. R. (1999). Some basic principles of habitat use. *Grazing Behav. Livest. Wildl.* 70, 85–90.

Kuhn, C. E., Crocker, D. E., Tremblay, Y., and Costa, D. P. (2009). Time to eat: measurements of feeding behaviour in a large marine predator, the northern elephant seal Mirounga angustirostris. *J. Anim. Ecol.* 78, 513–523. doi: 10.1111/j.1365-2656.2008.01509.x

Labrousse, S., Vacquié-Garcia, J., Heerah, K., Guinet, C., Sallée, J.-B., Authier, M., et al. (2015). Winter use of sea ice and ocean water mass habitat by southern elephant seals: the length and breadth of the mystery. *Prog. Oceanogr.* 137, 52–68. doi: 10.1016/j.pocean.2015.05.023

Ladds, M. A., Thompson, A. P., Slip, D. J., Hocking, D. P., and Harcourt, R. G. (2016). Seeing it all: evaluating supervised machine learning methods for the classification of diverse otariid behaviours. *PloS ONE* 11:e0166898. doi: 10.1371/journal.pone.0166898

Le Boeuf, B. J., Costa, D. P., Huntley, A. C., and Feldkamp, S. D. (1988). Continuous, deep diving in female northern elephant seals, Mirounga angustirostris. *Can. J. Zool.* 66, 446–458. doi: 10.1139/z88-064

Le Bras, Y., Jouma'a, J., Picard, B., and Guinet, C. (2016). How Elephant Seals (Mirounga leonina) adjust their fine scale horizontal movement and diving behaviour in relation to prey encounter rate. *PLoS ONE* 11:e0167226. doi: 10.1371/journal.pone.0167226

Le Bras, Y., Picard, B., and Guinet, C. (2017). Three-dimensional assessment of hunting strategies in a deep diving predator, southern elephant seal Mirounga leonina. *Mar. Ecol. Prog. Ser.* 573, 255–268. doi: 10.3354/meps12191

MacArthur, R. H., and Pianka, E. R. (1966). On optimal use of a patchy environment. *Am. Nat.* 100, 603–609. doi: 10.1086/282454

Machovsky-Capuska, G. E., Vaughn, R. L., Wursig, B., Katzir, G., and Raubenheimer, D. (2011). Dive strategies and foraging effort in the Australasian gannets *Morus serrator* revealed by underwater videography. *Mar. Ecol. Prog. Ser.* 442, 255–261. doi: 10.3354/meps09458

Mitani, Y., Watanabe, Y., Sato, K., Cameron, M. F., and Naito, Y. (2004). 3D diving behavior of Weddell seals with respect to prey accessibility and abundance. *Mar. Ecol. Prog. Ser.* 281, 275–281. doi: 10.3354/meps281275

Naito, Y., Bornemann, H., Takahashi, A., McIntyre, T., and Plotz, J. (2010). Fine-scale feeding behaviour of Weddell seals revealed by a mandible accelerometer. *Polar Sci.* 4, 309–316. doi: 10.1016/j.polar.2010.05.009

Naito, Y., Costa, D. P., Adachi, T., Robinson, P. W., Fowler, M., and Takahashi, A. (2013). Unravelling the mysteries of a mesopelagic diet: a large apex predator specializes on small prey. *Funct. Ecol.* 27, 710–717. doi: 10.1111/1365-2435.12083

Page, B., McKenzie, J., Hindell, M. A., and Goldsworthy, S. D. (2005). Drift dives by male New Zealand fur seals (Arctocephalus forsteri). *Can. J. Zool.* 83, 293–300. doi: 10.1139/z05-013

Pascoe, P., Lea, M.-A., Mattlin, R. H., McMahon, C. R., Harcourt, R., Thompson, D., et al. (2016). Assessing the utility of two-and three-dimensional behavioural metrics in habitat usage models. *Mar. Ecol. Prog. Ser.* 562, 181–192. doi: 10.3354/meps11947

Richard, G., Cox, S. L., Picard, B., Vacquie-Garcia, J., and Guinet, C. (2016). Southern elephant seals replenish their lipid reserves at different rates according to foraging habitat. *PLoS ONE* 11:e0166747. doi: 10.1371/journal.pone.0166747

Richard, G., Vacquie-Garcia, J., Jouma'a, J., Picard, B., Génin, A., Arnould, J. P. Y., et al. (2014). Variation in body condition during the post-moult foraging trip of southern elephant seals and its consequences on diving behaviour. *J. Exp. Biol.* 217, 2609–2619. doi: 10.1242/jeb.088542

Ropert-Coudert, Y., Kato, A., Baudat, J., Bost, C.-A., Le Maho, Y., and Naito, Y. (2001). Feeding strategies of free-ranging Adélie penguins Pygoscelis adeliae analysed by multiple data recording. *Polar Biol.* 24, 460–466. doi: 10.1007/s003000100234

Sato, K., Mitani, Y., Cameron, M. F., Siniff, D. B., and Naito, Y. (2003). Factors affecting stroking patterns and body angle in diving Weddell seals under natural conditions. *J. Exp. Biol.* 206, 1461–1470. doi: 10.1242/jeb.00265

Schreer, J. F., Kovacs, K. M., and O'Hara Hines, R. J. (2001). Comparative diving patterns of pinnipeds and seabirds. *Ecol. Monogr.* 71, 137–162. doi: 10.1890/0012-9615(2001)071[0137:CDPOPA]2.0.CO;2

Schreer, J. F., and Testa, J. W. (1996). Classification of Weddell Seal diving behavior. *Mar. Mammal Sci.* 12, 227–250. doi: 10.1111/j.1748-7692.1996.tb00573.x

Simeone, A., and Wilson, R. P. (2003). In-depth studies of Magellanic penguin (Spheniscus magellanicus) foraging: can we estimate prey consumption by perturbations in the dive profile? *Mar. Biol.* 143, 825–831. doi: 10.1007/s00227-003-1114-8

Skinner, J. P., Mitani, Y., Burkanov, V. N., and Andrews, R. D. (2014). Proxies of food intake and energy expenditure for estimating the time-energy budgets of lactating northern fur seals *Callorhinus ursinus*. *J. Exp. Mar. Biol. Ecol.* 461, 107–115. doi: 10.1016/j.jembe.2014.08.002

Stearns, S. C. (1992). *The Evolution of life Histories*. Oxford: Oxford University Press.

Stephens, D. W., and Krebs, J. R. (1986). *Foraging theory*. Princeton, NJ: Princeton University Press.

Tynan, C. T., Ainley, D. G., and Stirling, I. (2009). Sea ice: a critical habitat for polar marine mammals and birds. *Sea Ice* 395, 395–424. doi: 10.1002/9781444317145.ch11

Vacquié-Garcia, J., Guinet, C., Dragon, A. C., Viviant, M., Ksabi, N. E., and Bailleul, F. (2015a). Predicting prey capture rates of southern elephant seals from track and dive parameters. *Mar. Ecol. Prog. Ser.* 541, 265–277. doi: 10.3354/meps11511

Vacquié-Garcia, J., Guinet, C., Laurent, C., and Bailleul, F. (2015b). Delineation of the southern elephant seal? s main foraging environments defined by temperature and light conditions. *Deep Sea Res. Part II Top. Stud. Oceanogr.* 113, 145–153. doi: 10.1016/j.dsr2.2014.10.029

Vacquie-Garcia, J., Lydersen, C., Biuw, M., Haug, T., Fedak, M. A., and Kovacs, K. M. (2017). Hooded seal Cystophora cristata foraging areas in the Northeast Atlantic Ocean—Investigated using three complementary methods. *PloS ONE* 12:e0187889. doi: 10.1371/journal.pone.0187889

Van der Wal, J., Falconi, L., Januchowski, S., Shoo, L., and Storlie, C. (2014). *SDMTools*. R package version.

Viviant, M., Jeanniard-du-Dot, T., Monestiez, P., Authier, M., and Guinet, C. (2016). Bottom time does not always predict prey encounter rate in Antarctic fur seals. *Funct. Ecol.* 30, 1834–1844. doi: 10.1111/1365-2435.12675

Viviant, M., Monestiez, P., and Guinet, C. (2014). Can we predict foraging success in a marine predator from dive patterns only? validation with prey capture attempt data. *PLoS ONE* 9:e88503. doi: 10.1371/journal.pone.0088503

Viviant, M., Trites, A. W., Rosen, D. A. S., Monestiez, P., and Guinet, C. (2009). Prey capture attempts can be detected in Steller sea lions and other marine predators using accelerometers. *Polar Biol.* 33, 713–719. doi: 10.1007/s00300-009-0750-y

Volpov, B. L., Hoskins, A. J., Battaile, B. C., Viviant, M., Wheatley, K. E., Marshall, G., et al. (2015). Identification of prey captures in Australian fur seals (*Arctocephalus pusillus dorifeus*) using head-mounted accelerometers:

field validation with animal-born video cameras. *PLoS ONE* 10:e0128789. doi: 10.1371/journal.pone.0128789

Volpov, B. L., Rosen, D. A. S., Hoskins, A. J., Lourie, H. J., Dorville, N., Baylis, A. M. M., et al. (2016). Dive characteristics can predict foraging success in Australian fur seals (Arctocephalus pusillus doriferus) as validated by animal-borne video. *Biol. Open* 5:262–271. doi: 10.1242/bio.016659

Wartzok, D., Elsner, R., Stone, H., Kelly, B. P., and Davis, R. W. (1992). Under-ice movements and the sensory basis of hole finding by ringed and Weddell seals. *Can. J. Zool.* 70, 1712–1722. doi: 10.1139/z92-238

Watanabe, Y., Mitani, Y., Sato, K., Cameron, M. F., and Naito, Y. (2003). Dive depths of Weddell seals in relation to vertical prey distribution as estimated by image data. *Mar. Ecol. Prog. Ser.* 252, 283–288. doi: 10.3354/meps252283

Watanabe, Y. Y., and Takahashi, A. (2013). Linking animal-borne video to accelerometers reveals prey capture variability. *Proc. Natl. Acad. Sci.* 110, 2199–2204. doi: 10.1073/pnas.1216244110

Wilmers, C. C., Nickel, B., Bryce, C. M., Smith, J. A., Wheat, R. E., and Yovovich, V. (2015). The golden age of bio-logging: how animal-borne sensors are advancing the frontiers of ecology. *Ecology* 96, 1741–1753. doi: 10.1890/14-1401.1

Wilson, R., PÜT, K., GrÉMillet, D., Culik, B., Kierspel, M., Regel, J., et al. (1995). Reliability of stomach temperature changes in determining feeding characteristics of seabirds. *J. Exp. Biol.* 198, 1115–1135.

Wilson, R. P., Culik, B. M., Peters, G., and Bannasch, R. (1996). Diving behaviour of gentoo penguins, pygoscelis papua; factors keeping dive profiles in shape. *Mar. Biol.* 126, 153–162. doi: 10.1007/BF00571387

Wilson, R. P., Steinfurth, A., Ropert-Coudert, Y., Kato, A., and Kurita, M. (2002). Lip-reading in remote subjects: an attempt to quantify and separate ingestion, breathing and vocalisation in free-living animals using penguins as a model. *Mar. Biol.* 140, 17–27. doi: 10.1007/s002270100659

Ydesen, K. S., Wisniewska, D. M., Hansen, J. D., Beedholm, K., Johnson, M., and Madsen, P. T. (2014). What a jerk: prey engulfment revealed by high-rate, super-cranial accelerometry on a harbour seal (Phoca vitulina). *J. Exp. Biol.* 217, 2239–2243. doi: 10.1242/jeb.100016

Zuur, A., Ieno, E. N., Walker, N., Saveliev, A. A., and Smith, G. M. (2009). *Mixed Effects Models and Extensions in Ecology with R*. New York, NY: Springer.

Conflict of Interest Statement: The authors declare that the research was conducted in the absence of any commercial or financial relationships that could be construed as a potential conflict of interest.

Copyright © 2019 Heerah, Cox, Blevin, Guinet and Charrassin. This is an open-access article distributed under the terms of the Creative Commons Attribution License (CC BY). The use, distribution or reproduction in other forums is permitted, provided the original author(s) and the copyright owner(s) are credited and that the original publication in this journal is cited, in accordance with accepted academic practice. No use, distribution or reproduction is permitted which does not comply with these terms.

frontiers in Physiology

ORIGINAL RESEARCH
published: 19 February 2019
doi: 10.3389/fphys.2019.00128

Using Respiratory Sinus Arrhythmia to Estimate Inspired Tidal Volume in the Bottlenose Dolphin (*Tursiops truncatus*)

Fabien Cauture[1]*, Blair Sterba-Boatwright[2], Julie Rocho-Levine[3], Craig Harms[4], Stefan Miedler[5] and Andreas Fahlman[1,6]*

[1] Departamento de Investigación, Fundación Oceanogràfic de la Comunidad Valenciana, Valencia, Spain, [2] Department of Mathematics and Statistics, Texas A&M University–Corpus Christi, Corpus Christi, TX, United States, [3] Dolphin Quest, Honolulu, HI, United States, [4] Center for Marine Sciences and Technology, Department of Clinical Sciences, College of Veterinary Medicine, North Carolina State University, Morehead City, NC, United States, [5] Veterinary Cardiology, Alboraya, Spain, [6] Research Group on Biomedical Imaging (GIBI2[30]), Instituto de Investigación Sanitaria La Fe, Valencia, Spain

OPEN ACCESS

Edited by:
John T. Fisher,
Queen's University, Canada

Reviewed by:
Nicolle Jasmin Domnik,
Queen's University, Canada
Filippo Garofalo,
Università della Calabria, Italy
James Duffin,
Thornhill Research Inc., Canada

***Correspondence:**
Fabien Cauture
f.cauture@gmail.com
Andreas Fahlman
afahlman@whoi.edu

Specialty section:
This article was submitted to Aquatic Physiology, a section of the journal Frontiers in Physiology

Received: 16 October 2018
Accepted: 01 February 2019
Published: 19 February 2019

Citation:
Cauture F, Sterba-Boatwright B, Rocho-Levine J, Harms C, Miedler S and Fahlman A (2019) Using Respiratory Sinus Arrhythmia to Estimate Inspired Tidal Volume in the Bottlenose Dolphin (Tursiops truncatus). Front. Physiol. 10:128. doi: 10.3389/fphys.2019.00128

Man-made environmental change may have significant impact on apex predators, like marine mammals. Thus, it is important to assess the physiological boundaries for survival in these species, and assess how climate change may affect foraging efficiency and the limits for survival. In the current study, we investigated whether the respiratory sinus arrhythmia (RSA) could estimate tidal volume (V_T) in resting bottlenose dolphins (*Tursiops truncatus*). For this purpose, we measured respiratory flow and electrocardiogram (ECG) in five adult bottlenose dolphins at rest while breathing voluntarily. Initially, an exponential decay function, using three parameters (baseline heart rate, the change in heart rate following a breath, and an exponential decay constant) was used to describe the temporal change in instantaneous heart rate following a breath. The three descriptors, in addition to body mass, were used to develop a Generalized Additive Model (GAM) to predict the inspired tidal volume (V_{Tinsp}). The GAM allowed us to predict V_{Tinsp} with an average (± SD) overestimate of 3 ± 2%. A jackknife sensitivity analysis, where 4 of the five dolphins were used to fit the GAM and the 5th dolphin used to make predictions resulted in an average overestimate of 2 ± 10%. Future studies should be used to assess whether similar relationships exist in active animals, allowing V_T to be studied in free-ranging animals provided that heart rate can be measured.

Keywords: electrocardiogram, spirometry, marine mammals, diving physiology, cardiorespiratory

INTRODUCTION

Marine mammals forage underwater to obtain food and therefore divide their time at the surface to exchange gasses (O_2 and CO_2) with submersions to different depth and of varying durations. Therefore, a better understanding of the metabolic costs associated with underwater foraging, and proxies to assess energy use would help determine how environmental change may alter survival. By increasing the duration underwater, the opportunity to encounter and obtain food, and thereby the foraging efficiency, should be increased. Man-made environmental change such as over-fishing and global warming could cause changes in prey diversity, availability and location

(Perry et al., 2005), which may have detrimental effects on apex marine predators like dolphins. Changes in prey type, abundance, and distribution could result in increases in both foraging duration and distance in order to obtain enough prey for survival. Overfishing will reduce the probability to encounter food, and movement of prey to deeper depths due to ocean warming will increase the transit time and reduce the available time at the prey patch. Longer foraging bouts, and/or deeper dives may reduce the foraging efficiency and thereby cause challenges to obtain sufficient food for survival (Perry et al., 2005). Thus, understanding the cardiorespiratory traits required by marine mammals to manage life in an extreme environment, the physiological constraints imposed on these animals, and how these limitations may affect physiology and survival are crucial.

When studying animals in the wild, measuring the metabolic cost directly is challenging, and a number of proxies have been proposed and tested. One method is to measure the resting metabolic rate (RMR) by measuring the O_2 consumption rate ($\dot{V}O_2$) during rest (Williams et al., 1993; Yazdi et al., 1999; Kastelein et al., 2000; Yeates and Houser, 2008; Noren et al., 2013; Rechsteiner et al., 2013; Worthy et al., 2013; van der Hoop et al., 2014; Fahlman et al., 2015), and a few studies have determined the diving and foraging metabolic rate of marine mammals during quasi-natural conditions (Kooyman et al., 1973; Sparling and Fedak, 2004; Fahlman et al., 2008, 2013). While RMR may not accurately reflect field metabolic rate (FMR), it provides an index about the minimal metabolic requirements of an individual or population against which FMR can be scaled (Bejarano et al., 2017). One method to scale FMR is to estimate FMR by validated metabolic proxies, such as heart rate (f_H) (Young et al., 2011), activity (Enstipp et al., 2011; Fahlman et al., 2013), or respiratory frequency (f_R) (Fahlman et al., 2016, 2017b; Folkow and Blix, 2017). Combining these methods, the metabolic costs for different populations and activities, such as resting, traveling, and foraging, can be defined. The Fick principle states that:$\dot{V}O_2 = f_R \times V_T \times (\Delta O_2)$, where V_T is tidal volume and ΔO_2 the O_2 extracted from the air inhaled with each breath. By assuming that V_T and ΔO_2 are constant at steady state, it should be possible to estimate $\dot{V}O_2$ from f_R (Folkow and Blix, 1992; Christiansen et al., 2014; Fahlman et al., 2016). While marine mammals are at the surface, f_R can be assessed during focal observations. However, this is not practical during long periods at sea. In addition, studies have shown that both V_T and ΔO_2 change for different activities or during recovery from exercise (Fahlman et al., 2016, 2017b; Folkow and Blix, 2017), so the estimated $\dot{V}O_2$ could be improved by also estimating V_T and ΔO_2. Consequently, methods to assess pattern of breathing (f_R, V_T) would provide significant advances to estimate FMR in marine mammals.

Proxies to estimate FMR from breaths should accurately predict f_R and V_T during continuous recording from free ranging animals (Fahlman et al., 2016; Rojano-Doñate et al., 2018). Such data would allow an assessment of how changes in foraging effort (duration, activity, etc.) alter respiratory function, and estimated FMR. A number of studies have assessed lung function in marine mammals under human care (Olsen et al., 1969; Kerem et al., 1975; Matthews, 1977; Kooyman and Cornell, 1981; Fahlman et al., 2015, 2018a,b, 2019; Fahlman and Madigan, 2016), and at least in the bottlenose dolphin (*Tursiops truncatus*) these data are representative of their wild counterparts, in both shallow and deep diving ecotypes (Fahlman et al., 2018a,b). Such data are important to establish baseline lung function from animals with known health under controlled situations, and provide methods that will allow proxies to be validated that can predict respiratory effort in free ranging animals.

Estimating lung function of wild populations remains difficult. One alternative proxy could be to use the changes in f_H associated with each breath, the Respiratory Sinus Arrhythmia (RSA) (de Burgh Daly, 1986). While RSA is universally present in a number of air-breathing vertebrates such as the toad, horse, dog, seal, and dolphin (Scholander, 1940; Hayano et al., 1996; Cooper et al., 2003; Noren et al., 2004; Harms et al., 2013; Zena et al., 2017; McDonald et al., 2018; Yaw et al., 2018; Piccione et al., 2019), and even in air-breathing fish (Grossman and Taylor, 2007), its physiological significance is debated (Hayano et al., 1996; Yasuma and Hayano, 2004). It has been suggested that RSA improves gas exchange by enhancing the ventilation-perfusion matching and reduces cardiac work (Yasuma and Hayano, 2004; Ben-Tal et al., 2012, 2014). The RSA causes f_H acceleration during inspiration, and deceleration during expiration (Mortola et al., 2015). Thus, continuous recordings of f_H could allow detection of f_R, which when appropriately validated provide ways to estimate field metabolic rate (Fahlman et al., 2016; Rojano-Doñate et al., 2018). Considering recent progress in the development of biologging system that allow continuous recording of the electrocardiogram (ECG) in free-ranging cetaceans (Elmegaard et al., 2016; McDonald et al., 2018), we speculated that RSA may provide a novel method to estimate V_T in bottlenose dolphins. Currently, there is limited availability of commercial data loggers that can measure continuous ECG, and custom built devices range from units with implantable electrodes used in pinnipeds or diving birds (Thompson and Fedak, 1993; Woakes et al., 1995; McDonald and Ponganis, 2014), to those that are attached externally using suction cups (Noren et al., 2004; Elmegaard et al., 2016).

In the current study, we tested the hypothesis that RSA can estimate V_{Tinsp} in resting bottlenose dolphins by recording f_H and respiratory flow while resting at the surface. Our results provide evidence that using the RSA as a proxy allows us to estimate the average V_{Tinsp} of individual dolphins with an average (±SD) overestimation of 2 ± 10% with the data recorded.

MATERIALS AND METHODS

Animals

The study protocols were approved by the Animal Care and Welfare Committee of the Oceanogràfic Foundation (OCE-17-16 and amendment OCE-29-18). Five adult male bottlenose dolphins (*T. truncatus*), housed at Dolphin Quest – Oahu (Honolulu, HI, United States), were used for all the experiments (**Table 1**). All experiments were conducted in January 2018. The dolphins were not restrained and could end the trial at any point. Prior to initiating the study, the dolphins were desensitized to the equipment and trained for novel research-associated

TABLE 1 | Dolphin ID, body mass (M_b), total number of breaths analyzed (N), average (± SD) tidal volume (V_{Tinsp}), and V_{Tinsp} range.

Dolphin ID	M_b (kg)	N	V_{Tinsp} (l)	V_{Tinsp} range (l)
9FL3	235.4	73	3.6 ± 1.0	1.6 – 6.2
01L5	154.6	91	3.2 ± 0.5	2.1 – 4.2
83H1	139.6	53	3.3 ± 0.8	1.8 – 5.6
9ON6	184.1	53	3.9 ± 0.6	2.7 – 5.6
6JK5	206.8	27	4.9 ± 1.2	2.7 – 6.9

behaviors using operant conditioning. Each trial consisted of the animal staying stationary in the water, allowing placement of the equipment. The animals were breathing while continuous measurements were made. Because of familiarity with these procedures, we assumed that the experimental data collected on lung function (respiratory flow) and f_H were representative of a relaxed physiological state.

Data Acquisition

A custom-made Fleisch type pneumotachometer (Mellow Design, Valencia) utilizing a low-resistance laminar flow matrix (Item # Z9A887-2, Merriam Process Technologies, Cleveland, OH, United States) was placed over the blow-hole of the dolphin (Fahlman et al., 2015). Differential pressure across the flow matrix was measured using a differential pressure transducer (ML311 Spirometer Pod, ADInstruments, Colorado Springs, CO, United States), connected to the pneumotachometer with two, 310 cm lengths of 2 mm I.D., firm walled, flexible tubing. The pneumotachometer was calibrated using a 7.0 l calibration syringe (Series 4900, Hans-Rudolph Inc., Shawnee, KS, United States). The signal was integrated and the flow determined assuming a linear response between differential pressure and flow. The linear response of the pneumotachometer was confirmed by calibrating with the 7.0 l syringe immediately before and after each trial, through a series of pump cycles at various flows. The pump cycles allowed the relationship between differential pressure and flows for the expiratory and inspiratory phases to be determined. All gas volumes were converted to standard temperature pressure dry (STPD) (Quanjer et al., 1993). Exhaled air was assumed saturated at 37°C, inhaled air volume was corrected for ambient temperature and relative humidity, and V_T was calculated by integrating the flow as previously detailed (Fahlman et al., 2015).

The electrocardiogram (ECG) was recorded using three gold-plated electrodes mounted inside a silicone suction cup connected to a custom-built data recorder (UUB/1-ECGb, UFI, Morro Bay, CA, United States). The three electrodes were placed on the ventral surface: red on the right side close to the pectoral fin, yellow opposite on the left side, and green on the right side approximately 30 cm more caudally from the red. The suctions cups were filled with conducting gel (Redux Gel, Parker Laboratories) before being placed on the skin. Next, the animal rolled over to ensure the suction cups stayed in place.

The respiratory flow and ECG were recorded at 400 Hz using a data acquisition system (Powerlab 8/35, ADInstruments, Colorado Springs, CO, United States), and displayed on a computer running LabChart (v. 8.1, ADInstruments, Colorado Springs, CO, United States). Initially, the electrodes were adjusted to assure a clear ECG trace. Next, the pneumotachometer was placed over the blow-hole and the animal allowed to breathe spontaneously for up to 10 min.

We used the ECG analysis routine in LabChart to automatically detect the time between R-R peaks using the following settings; typical QRS width = 80 ms, R-waves = 300 ms, pre-P baseline = 120 ms, maximum PR = 240 ms, maximum RT = 400 ms. The detected R peaks were then manually verified and the instantaneous heart rate (if_H) determined from the time between R-R peaks.

Data Processing, Statistical Analysis and Modeling

All data were analyzed using R (version 3.4.3 – © 2017 The R Foundation for Statistical Computing) through RStudio (version 1.1.383 – © 2009–2017 RStudio, Inc.). Initially the temporal changes in if_H were described for each breath. We used a function that fit the exponential decay with time following the beginning of the inspiration for each breath:

$$\mathrm{i}f_H = \text{Base Heart Rate} + e^{-\text{Decay rate}\times\text{Time}} \times \text{Initial change in heart rate} \quad (1)$$

Equation 1 was fit for each breath using the "L-BFGS-B" method of the "optim" function (Byrd et al., 1995), which optimizes parameters between imposed bounds to restrain parameters to physiologically relevant values. Breaths with fewer than seven beats after the inhalation were excluded (44 breaths).

Next the three parameters from Eq. 1 (Base Heart Rate, Decay rate, and initial change in heart rate) for each breath, and body mass (M_b) were fit against inhaled V_T (V_{Tinsp}) using a loess Generalized Additive Model (GAM) (Cleveland, 1979; Hastie and Tibshirani, 1990), with the span fixed at 0.34.

To assess the sensitivity of the model, we generated five different GAMs by excluding all observations from one dolphin each time. The data from the excluded dolphin was then used to predict V_{Tinsp}. The error was computed using the formula:

$$\text{Prediction error} = \frac{(\text{Predicted} - \text{Measured})}{\text{Measured}} \times (-100) \quad (2)$$

where a positive value represents an overestimated prediction.

TABLE 2 | Dolphin ID, average fit parameters for Equation 1 [base heart rate (f_H), decay, initial jump (Δf_H)], and average inspired tidal volume (V_{Tinsp}).

Dolphin ID	Base f_H	Decay	Δf_H	Average V_{Tinsp}
9FL3	34.1	0.0362	37.2	3.6
01L5	37.9	0.0486	46.2	3.2
83H1	39.7	0.0523	46.8	3.3
9ON6	41.2	0.0311	50.5	3.9
6JK5	48.6	0.0280	49.2	4.9
Mean (±SD)	40.3 ± 5.4	0.0393 ± 0.0108	46.0 ± 5.2	3.8 ± 0.7

RESULTS

Data Used for the Analysis

A total of 297 breaths were analyzed following removal of breaths with less than seven heart beats between breaths (**Table 1**). Only spontaneous breaths were used for the analysis, which limited the range of V_T's. In addition, as not all inspired and expired volumes are similar for each breath, we only used the V_{Tinsp} for the analysis.

The average (±SD) V_{Tinsp} was 3.8 ± 0.7 l (range: 1.6–6.9 l, see **Table 1** for individual variation), and the average duration between breaths was 15.3 ± 10.7 s (range: 4–129 s). The average if_H was 74 ± 24 beats min^{-1} (range: 27–293 beats · min^{-1}). The average fit parameters for Equation 1 for each dolphin are reported in **Table 2**.

Predicting V_T From Instantaneous f_H

Figure 1 shows a representative ECG trace, if_H, and respiratory flow in a dolphin over 3 breaths. The average conditions for estimating V_{Tinsp} are reported in **Table 2**, and the GAMs overestimated V_{Tinsp} by an average 3 ± 2% (range of individual average error: 0.3 to 7.4%, **Figure 2**). A sensitivity analysis was performed to assess how the prediction changed with changes in each variable (**Figure 3**). The decay rate and M_b had less influence

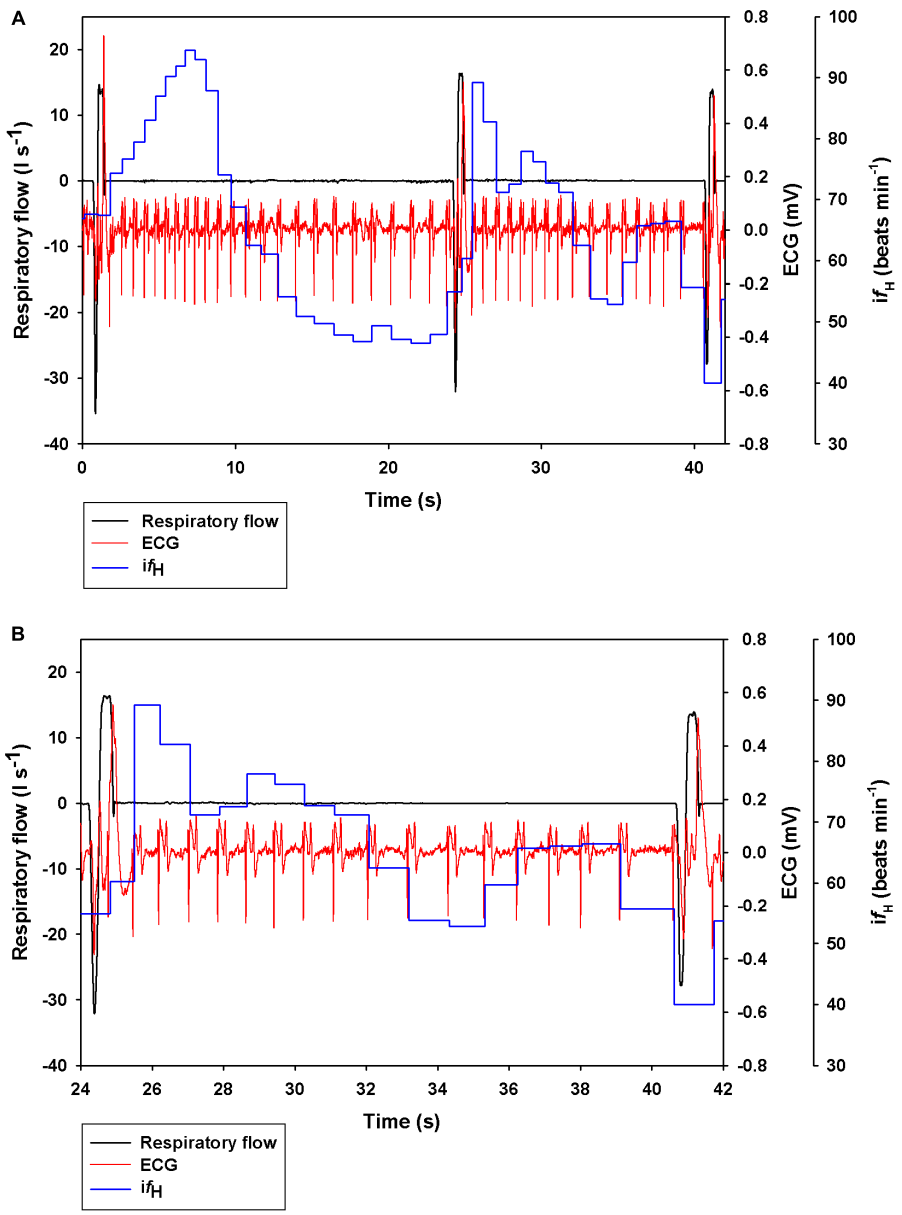

FIGURE 1 | Representative data showing respiratory flow, ECG, and instantaneous heart rate (if_H) in a bottlenose dolphin during **(A)** 3 breaths, or **(B)** zoomed in for the 2nd breath.

on the model output as compared with base f_H and the initial change in f_H.

By removing one dolphin, fitting the GAMs with the four dolphins, and then predicting V_{Tinsp} for the 5th dolphin resulted in an average (±SD) overestimation of 2 ± 10%, (range of individual average error: −10 to 18%, **Figures 4A,B**). The error for individual breaths ranged from 107 to −45%, with 95% confidence limits ranging between 12 to −7% (median: 12 to −10%, **Figure 4B**).

DISCUSSION

The main objective with the current study was to determine if the changes in f_H associated with RSA can be used to predict the V_{Tinsp} in the bottlenose dolphin. For this purpose, we collected continuous ECG and respiratory flow in bottlenose dolphins. A jackknife method to resample the data showed that RSA, in addition to M_b, can be used to predict the average V_{Tinsp} of an individual dolphin to within 2 ± 10% of the measured value, and all individual average prediction errors were less than 20%. This shows that the GAMs should be able to predict the average V_{Tinsp} of individual dolphins using data from another population of bottlenose dolphins. If future studies can verify a similar relationship in active animals, RSA could be a useful proxy to estimate V_{Tinsp} from free-ranging marine mammals as methods to continuously measure f_H are developed.

The average if$_H$ reported in the current study was similar to those reported in previous studies in the bottlenose dolphin (ranging from 60 to 105 beats min^{-1}) (Noren et al., 2004, 2012; Houser et al., 2010), when the f_H is calculated without accounting for the RSA. However, in our past study, using trans-thoracic echocardiography to measure f_H and stroke volume, it was

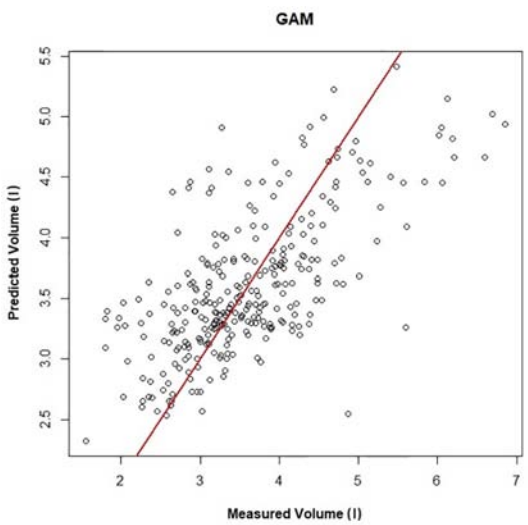

FIGURE 2 | Predicted vs. measured inspired tidal volume (r^2 = 0.45). The GAMs model is used to generate the predicted volume, and measured volume is the inspired tidal volume measured using the pneumotachometer, red line is the line of unity.

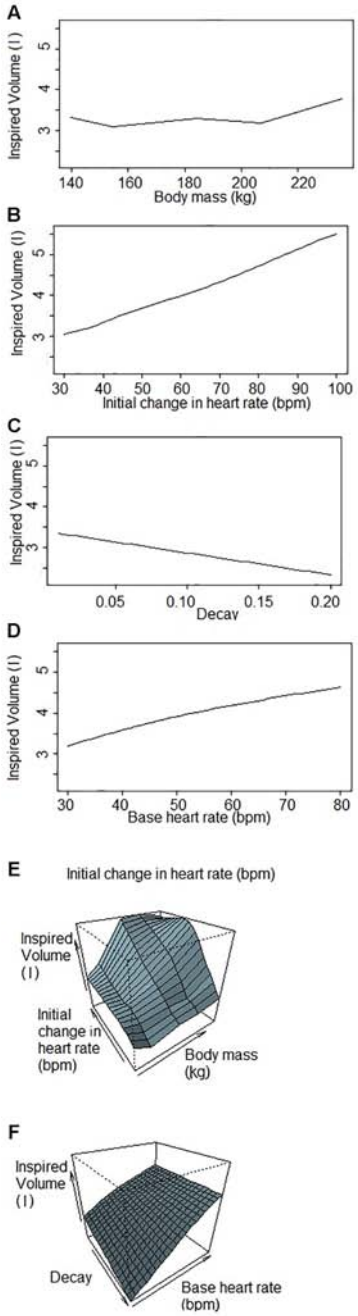

FIGURE 3 | Sensitivity analysis of each variable used to predict inspired tidal volume by the Generalized Additive Model when one (or two) factor(s) changes while others are fixed. Inspired volumes are in liters. **(A)** Inspired volume as a function of body mass. **(B)** Inspired volume as a function of the initial change in heart rate. The initial jump is the parameter of the GAM that explains the most variation in inspired volume of the four parameters. **(C)** Inspired volume as a function of the decay. The decay is the parameter that explains the lowest variation in the GAM. **(D)** Inspired volume as a function of the base heart rate. The base heart rate is the variable that has the second most influence on the inspired volume predicted by the GAM. **(E,F)** Inspired volume as a function of two parameters **(E)** body mass and initial change in heart rate; **(F)** decay and base heart rate. These figures illustrate the covariance of the parameters that have consequences for the predicted inspired volume.

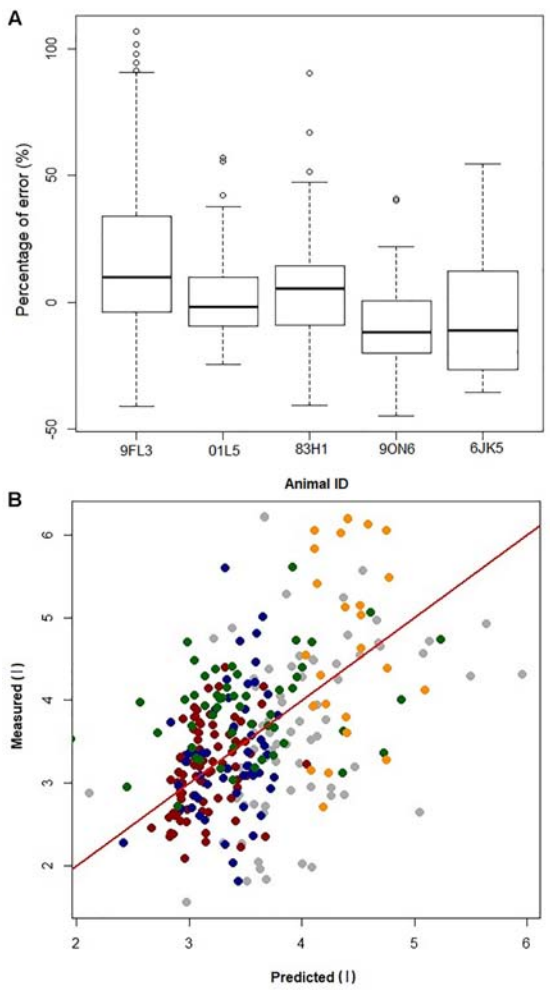

FIGURE 4 | (A) Boxplot of prediction error [error = (predicted–measured)/measured × 100] from jackknife sensitivity analysis, where the data from one dolphin (Animal ID) is removed to generate the GAMs and the resulting GAMs model is used to predict V_{Tinsp} for that dolphin. **(B)** Plot of error in prediction of a single dolphin V_T when building the GAM using data from the other four dolphins. Gray = 9FL3; Red = 01L5; Blue = 83H1; Green = 9ON6; Orange = 6JK5; Red line is identity line.

pointed out that estimating f_H without accounting for the RSA will result in average surface f_H values that are confounded by the f_R (Miedler et al., 2015). This is particularly problematic in marine mammals, with an f_R ranging from 1 to 5 breaths · min^{-1} (Piscitelli et al., 2013; Fahlman et al., 2017a). Consequently, estimating resting f_H without accounting for the RSA will overestimate the resting f_H. As these resting f_H's have been used to assess the magnitude of the cardiovascular changes associated with diving they would erroneously overestimate the magnitude of the dive response (Fahlman et al., unpublished). The average base f_H in the current study (**Table 2**, 40 ± 5 beats min^{-1}) was similar to those reported in our past study in the bottlenose dolphin (f_H = 41 ± 9 beats min^{-1}) (Miedler et al., 2015), where the RSA was accounted for. Consequently, the base f_H reported in the current study is a more appropriate value for the resting f_H in the bottlenose dolphin. If this value is used, it provides an interesting perspective as that value is similar to the diving bradycardia reported in previous studies (Noren et al., 2012). Thus, we propose that future studies should evaluate the resting f_H in voluntary diving animals after correcting for the RSA.

While the current method clearly shows that RSA is useful to estimate V_{Tinsp}, there are a number of limitations with the current method. First of all, due to the limited data set, we aimed to reduce the number of parameters used in the model. To simplify the analysis the current method did not include the duration between breaths. We analyzed each breath separately, which was both time consuming and does not account for the dependence between breaths. However, breathing and f_H are continuous data. Future studies could assess time-series methods to predict V_{Tinsp}, which allows the dependence between breaths to be considered. For Equation 1, there was considerable variation in the fitted values for the base f_H. When accounting for the changes in f_H associated with a breath there is usually minimal variation in the base f_H within one dolphin (Miedler et al., 2015). The large variation could be related to varying duration between breaths, which may alter the base f_H. Thus, for breaths close together the f_H may not have reached the base f_H before the next breath, and may have influenced the f_H variation for the next breath. Based on the current analysis, this method cannot accurately predict the V_{Tinsp} of individual breaths, but was able to provide reliable average estimated V_{Tinsp} for each animal based on the GAMs fitted to the other animals. This is similar to the method using f_H to estimate field metabolic rate, where the there are limitations to estimate the metabolic cost for each dive, but where large data sets are able to estimate the energy requirements for different activities (Fahlman et al., 2004; Halsey et al., 2007; Young et al., 2011). Given the limitations with the current data, we propose that further development of this method may provide an interesting approach to study cardiorespiratory physiology in free-ranging marine mammals.

The V_{Tinsp} in the current study were of limited range (average ± SD = 3.8 ± 0.7 l, range: 1.6–6.9 l). While variation in the V_{Tinsp} during voluntary breaths is difficult to control, animals under managed care can be trained to perform maximal respiratory effort, which allows V_T to vary over a much greater range (Kooyman and Cornell, 1981; Fahlman et al., 2015). For example, maximal respiratory efforts in dolphins in the weight range of the current study would increase the V_T range to around 20 l (Kooyman and Cornell, 1981; Fahlman et al., 2015). It would also be useful to include females and individuals from other age classes to increase the range of variation and allow the model to be used for wild dolphin populations.

In addition, future studies should also assess whether this method is robust enough to study active or free-ranging dolphins. During natural dives f_R and V_T may both be highly variable and irregular, and alterations in the relationship between RSA, vagal tone, f_R, and V_T (de Burgh Daly, 1986; Ben-Tal et al., 2014; Guillén-Mandujano and Carrasco-Sosa, 2014; Mortola et al., 2016) may limit the accuracy of a model developed for dolphins at rest. Thus, changes in activity state, e.g., exercise, rest, travel, diving, may significantly influence autonomic tone and alter the relationship.

Finally, the GAM model does not provide an estimate of uncertainty around the predicted values with new data (data that were not in the dataset used to fit the model), nor does it provide a prediction equation for the non-parametric part of the model. To avoid these drawbacks, additional measurements with a larger range of V_{Tinsp}, f_{R}, and activity states would help define a prediction equation that could be used in free-ranging dolphins. In addition, we propose that this method could be used for other cetaceans and marine mammal species that exhibit significant RSA. If future studies are able to verify that this method is able to estimate f_{R} and V_{Tinsp} in actively swimming or diving dolphins this method may provide a predictive procedure for free-ranging mammals that may significantly enhance our knowledge of how marine mammals partition energy use during diving, and how the environment may limit foraging efficiency.

In summary, we show that that RSA can be used to accurately predict the average V_{Tinsp} of individual resting bottlenose dolphins with an average overestimated error of $2 \pm 10\%$. While a number of factors appear to alter RSA (de Burgh Daly, 1986), the universal existence of RSA in vertebrates, and the suggestions that it is independent of body size (Piccione et al., 2019), could provide a method to study cardiorespiratory physiology in free ranging marine vertebrates, from marine mammals, to birds and reptiles, unraveling important mechanisms to understand the ecophysiology of these species.

DATA AVAILABILITY STATEMENT

The data used in this study are freely available at the following link: osf.io/buwdp.

AUTHOR CONTRIBUTIONS

FC performed the data and statistical analysis and drafted the first draft of the manuscript. BS-B provided statistical advice and edited the manuscript. JR-L supervised all animal training and helped with all research trials. CH helped conceive the study and helped consult with the methods. SM helped with the trials and the analysis. AF conceived the study, designed the experiments, collected the data, provided funding, helped with the data analysis, and helped to draft the manuscript. All authors helped to revise the various drafts and gave final permission to publish the study.

FUNDING

Funding for this project was provided by the Office of Naval Research (ONR YIP Award # N000141410563 and ONR Award # N000141613088). Dolphin Quest provided in kind support of animals, crew, and access to resources.

ACKNOWLEDGMENTS

A special thanks to all the trainers and staff at Dolphin Quest Oahu, who made this study possible, and to Peter Madsen and Julie Van der Hoop who provided helpful advice and comments on early versions of this manuscript. We thank the reviewers who provides constructive criticism, which we believe significantly improved this article.

REFERENCES

Bejarano, A. C., Wells, R. S., and Costa, D. P. (2017). Development of a bioenergetic model for estimating energy requirements and prey biomass consumption of the bottlenose dolphin *Tursiops truncatus*. *Ecol. Model.* 356, 162–172. doi: 10.1016/j.ecolmodel.2017.05.001

Ben-Tal, A., Shamailov, S. S. J., and Paton, F. R. (2012). Evaluating the physiological significance of respiratory sinus arrhythmia: looking beyond ventilation–perfusion efficiency. *J. Physiol.* 590, 1989–2008. doi: 10.1113/jphysiol.2011.222422

Ben-Tal, A., Shamailov, S. S. J., and Paton, F. R. (2014). Central regulation of heart rate and the appearance of respiratory sinus arrhythmia: new insights from mathematical modeling. *Math. Biosci.* 255, 71–82. doi: 10.1016/j.mbs.2014.06.015

Christiansen, F., Rasmussen, M. H., and Lusseau, D. (2014). Inferring energy expenditure from respiration rates in minke whales to measure the effects of whale watching boat interactions. *J. Exp. Mar. Biol. Ecol.* 459, 96–104. doi: 10.1016/j.jembe.2014.05.014

Cleveland, W. S. (1979). Robust locally weighted regression and smoothing scatterplots. *J. Am. Stat. Assoc.* 74, 829–836. doi: 10.1080/01621459.1979.10481038

Cooper, H. E., Parkes, M. J., and Clutton-Brock, T. H. (2003). CO2-dependent components of sinus arrhythmia from the start of breath holding in humans. *Am. J. Physiol. Heart Circ. Physiol.* 285, H841–H848. doi: 10.1152/ajpheart.01101.2002

de Burgh Daly, M. (1986). "Interactions Between Respiration and Circulation," in *Handbook of Physiology-the Respiratory System, Control of Breathing*, Eds N. S. Cherniak and J. G. Widdicombe (Bethesda, MD: American Physiological Society).

Elmegaard, S. L., Johnson, M., Madsen, P. T., and McDonald, B. I. (2016). Cognitive control of heart rate in diving harbor porpoises. *Curr. Biol.* 26, R1167–R1176. doi: 10.1016/j.cub.2016.10.020

Enstipp, M. R., Ciccione, S., Gineste, B., Milbergue, M., Ballorain, K. Y., Ropert-Coudert, Y., et al. (2011). Energy expenditure of freely swimming adult green turtles (*Chelonia mydas*) and its link with body acceleration. *J. Exp. Biol.* 214, 4010–4020. doi: 10.1242/jeb.062943

Fahlman, A., Brodsky, M., Miedler, S., Dennison, S., Ivančić, M., Levine, G. et al. (2019). Ventilation and gas exchange before and after voluntary static surface breath-holds in clinically healthy bottlenose dolphins, *Tursiops truncatus*. *J. Exp. Biol.* (in press). doi: 10.1242/jeb.192211

Fahlman, A., Brodsky, M., Wells, R., McHugh, K., Allen, J., Barleycorn, A., et al. (2018a). Field energetics and lung function in wild bottlenose dolphins, *Tursiops truncatus*, in sarasota bay florida. *Roy. Soc. Open. Sci.* 5:171280. doi: 10.1098/rsos.171280

Fahlman, A., McHugh, K., Allen, J., Barleycorn, A., Allen, A., Sweeney, J., et al. (2018b). Resting metabolic rate and lung function in wild offshore common bottlenose dolphins, *Tursiops truncatus*, near bermuda. *Front. Physiol.* 9:886. doi: 10.3389/fphys.2018.00886

Fahlman, A., Handrich, Y., Woakes, A. J., Bost, C. A., Holder, R., Duchamp, C., et al. (2004). Effect of fasting on the VO2-fh relationship in king penguins, aptenodytes patagonicus. *Am. J. Physiol.* 287, R870–R877.

Fahlman, A., Loring, S. H., Levine, G., Rocho-Levine, J., Austin, T., and Brodsky, M. (2015). Lung mechanics and pulmonary function testing in cetaceans *J. Exp. Biol.* 218, 2030–2038. doi: 10.1242/jeb.119149

Fahlman, A., and Madigan, J. (2016). Respiratory function in voluntary participating patagonia sea lions in sternal recumbency. Front. Physiol. 7:528. doi: 10.3389/fphys.2016.00528

Fahlman, A., Moore, M. J., and Garcia-Parraga, D. (2017a). Respiratory function and mechanics in pinnipeds and cetaceans. *J. Exp. Biol.* 220, 1761–1763. doi: 10.1242/jeb.126870

Fahlman, A., van der Hoop, J., Moore, M. J., Levine, G., Rocho-Levine, J., and Brodsky, M. (2017b). Response to 'On the importance of understanding physiology when estimating energetics in cetaceans'. *Biol. Open* 6, 307–308. doi: 10.1242/bio.023143

Fahlman, A., Svärd, C., Rosen, D. A. S., Jones, D. R., and Trites, A. W. (2008). Metabolic costs of foraging and the management of O2 and CO2 stores in steller sea lions. *J. Exp. Biol.* 211, 3573–3580. doi: 10.1242/jeb.023655

Fahlman, A., Svärd, C., Rosen, D. A. S., Wilson, R. S., and Trites, A. W. (2013). Activity as a proxy to estimate metabolic rate and to partition the metabolic cost of diving vs. breathing in pre- and post-fasted Steller sea lions. *Aquat. Biol.* 18, 175–184. doi: 10.3354/ab00500

Fahlman, A., van der Hoop, J., Moore, M., Levine, G., Rocho-Levine, J., and Brodsky, M. (2016). Estimating energetics in cetaceans from respiratory frequency: why we need to understand physiology. *Biol. Open* 15, 436–442. doi: 10.1242/bio.017251

Folkow, L. P., and Blix, A. S. (1992). Metabolic rates of minke whales (*Balaenoptera acutorostrata*) in cold water. *Acta. Physiol. Scand.* 146, 141–150. doi: 10.1111/j.1748-1716.1992.tb09402.x

Folkow, L. P., and Blix, A. S. (2017). On the importance of understanding physiology when estimating energetics in cetaceans. *Biol. Open* 6, 306–308. doi: 10.1242/bio.023929

Grossman, P., and Taylor, E. W. (2007). Toward understanding respiratory sinus arrhythmia: relations to cardiac vagal tone, evolution and biobehavioral functions. *Biol. Psychol.* 74, 263–285. doi: 10.1016/j.biopsycho.2005.11.014

Guillén-Mandujano, A., and Carrasco-Sosa, S. (2014). Additive effect of simultaneously varying respiratory frequency and tidal volume on respiratory sinus arrhythmia. *Auton. Neurosci.* 186, 69–76. doi: 10.1016/j.autneu.2014.08.003

Halsey, L. G., Fahlman, A., Handrich, Y., Schmidt, A., Woakes, A. J., and Butler, P. J. (2007). How accurately can we estimate energetic costs in a marine top predator, the king penguin? *Zoology* 110, 81–92.

Harms, C. A., Jensen, E. D., Townsend, F. I., Hansen, L. J., Schwacke, L. H., and Rowles, T. K. (2013). Electrocardiograms of bottlenose dolphins (*Tursiops truncatus*) out of water: habituated colelction versus wild postcapture animals. *J. Zoo Wildlife Med.* 44, 972–981. doi: 10.1638/2013-0093.1

Hastie, T., and Tibshirani, R. (1990). Generalized additive models. *Stat. Sci.* 43:335.

Hayano, J., Yasuma, F., Okada, A., Mukai, S., and Fujinami, T. (1996). Respiratory sinus arrhythmia. a phenomenon improving pulmonary gas exchange and circulatory efficiency. *Circulation* 94, 842–847. doi: 10.1161/01.CIR.94.4.842

Houser, D. S., Dankiewicz-Talmadge, L. A., Stockard, T. K., and Ponganis, P. J. (2010). Investigation of the potential for vascular bubble formation in a repetitively diving dolphin. *J. Exp. Biol.* 213, 52–62. doi: 10.1242/jeb.028365

Kastelein, R. A., Mosterd, J., Schooneman, N. M., and Wiepkema, P. R. (2000). Food consumption, growth, body dimensions, and respiration rates of captive false killer whales (*Pseudorca crassidens*). *Aquat. Mam.* 26, 33–44.

Kerem, D. H., Kylstra, J. A., and Saltzman, H. A. (1975). Respiratory flow rates in the sea lion. *Undersea Biomed. Res.* 2, 20–27.

Kooyman, G. L., and Cornell, L. H. (1981). Flow properties of expiration and inspiration in a trained bottle-nosed porpoise. *Physiol. Zool.* 54, 55–61. doi: 10.1086/physzool.54.1.30155804

Kooyman, G. L., Kerem, D. H., Campbell, W. B., and Wright, J. J. (1973). Pulmonary gas exchange in freely diving weddell seals (*Leptonychotes weddelli*). *Resp. Physiol.* 17, 283–290. doi: 10.1016/0034-5687(73)90003-0

Matthews, R. C. (1977). *Pulmonary Mechanics of California Sea Lions, Zalophus Californianus*. San Diego: San Diego State University.

McDonald, B. I., Johnson, M., and Madsen, P. T. (2018). Dive heart rate in harbour porpoises is influenced by exercise and expectations. *J. Exp. Biol.* 221:jeb168740. doi: 10.1242/jeb.168740

McDonald, B. I., and Ponganis, P. J. (2014). Deep-diving sea lions exhibit extreme bradycardia in long duration dives. *J. Exp. Biol.* 217, 1525–1534. doi: 10.1242/jeb.098558

Miedler, S., Fahlman, A., Valls Torres, M., Álvaro Álvarez, T., and Garcia-Parraga, D. (2015). Evaluating cardiac physiology through echocardiography in bottlenose dolphins: using stroke volume and cardiac output to estimate systolic left ventricular function during rest and following exercise. *J. Exp. Biol.* 218, 3604–3610. doi: 10.1242/jeb.131532

Mortola, J. P., Marghescu, D., and Siegrist-Johnstone, R. (2015). Respiratory sinus arrhythmia in young men and women at different chest wall configurations. *Clin. Sci.* 128, 507–516. doi: 10.1042/CS20140543

Mortola, J. P., Marghescu, D., and Siegrist-Johnstone, R. (2016). Thinking about breathing: effects on respiratory sinus arrhythmia. *Resp. Physiol. Neurobiol.* 223, 28–36. doi: 10.1016/j.resp.2015.12.004

Noren, D. P., Holt, M. M., Dunkin, R. C., and Williams, T. M. (2013). The metabolic cost of communicative sound production in bottlenose dolphins (*Tursiops truncatus*). *J. Exp. Biol.* 216, 1624–1629. doi: 10.1242/jeb.083212

Noren, S. R., Cuccurullo, V., and Williams, T. M. (2004). The development of diving bradycardia in bottlenose dolphins (*Tursiops truncatus*). *J. Comp. Physiol. B.* 174, 139–147. doi: 10.1007/s00360-003-0398-9

Noren, S. R., Kendall, T., Cuccurullo, V., and Williams, T. M. (2012). The dive response redefined: underwater behavior influences cardiac variability in freely diving dolphins. *J. Exp. Biol.* 215, 2735–2741. doi: 10.1242/jeb.069583

Olsen, C. R., Hale, F. C., and Elsner, R. (1969). Mechanics of ventilation in the pilot whale. *Resp. Physiol.* 7, 137–149. doi: 10.1016/0034-5687(69)90001-2

Perry, A. L., Low, P. J., Ellis, J. R., and Reynolds, J. D. (2005). Climate change and distribution shifts in marine fishes. *Science* 308, 1912–1915. doi: 10.1126/science.1111322

Piccione, G., Giudice, E., Giannetto, C., and Mortola, J. P. (2019). The magnitude of respiratory sinus arrhythmia of a large mammal (the horse) is like that of humans. *Resp. Physiol. Neurobiol.* 259, 170–172. doi: 10.1016/j.resp.2018.09.006

Piscitelli, M. A., Raverty, S. A., Lillie, M. A., and Shadwick, R. E. (2013). A review of cetacean lung morphology and mechanics. *J. Morphol.* 274, 1425–1440. doi: 10.1002/jmor.20192

Quanjer, P. H., Tammeling, G. J., Cotes, J. E., Pedersen, O. F., Peslin, R., and Yernault, J.-C. (1993). Lung volumes and forced ventilatory flows. *Euro. Resp. J.* 6, 5–40. doi: 10.1183/09041950.005s1693

Rechsteiner, E. U., Rosen, D. A. S., and Trites, A. W. (2013). Energy requirements of pacific white-sided dolphins (*Lagenorhynchus obliquidens*) as predicted by a bioenergetic model. *J. Mam.* 94, 820–832. doi: 10.1371/journal.pone.0105958

Rojano-Doñate, L., McDonald, B. I., Wisniewska, D. M., Johnson, M., Teilmann, J., Wahlberg, M., et al. (2018). High field metabolic rates of wild harbour porpoises. *J. Exp. Biol.* 221:jeb185827. doi: 10.1242/jeb.185827

Scholander, P. F. (1940). *Experimental Investigations on the Respiratory Function in Diving Mammals and Birds*. Oslo: I kommisjon hos Jacob Dybwad.

Sparling, C. E., and Fedak, M. A. (2004). Metabolic rates of captive grey seals during voluntary diving. *J. Exp. Biol.* 207, 1615–1624. doi: 10.1242/jeb.00952

Thompson, D., and Fedak, M. A. (1993). Cardiac responses of grey seals during diving at sea. *J. Exp. Biol.* 174, 139–154.

van der Hoop, J. M., Fahlman, A., Hurst, T., Rocho-Levine, J., Shorter, A. K., Petrov, V., et al. (2014). Bottlenose dolphins modify behavior to reduce metabolic effect of tag attachment. *J. Exp. Biol.* 217, 4229–4236. doi: 10.1242/jeb.108225

Williams, T. M., Friedl, W. A., and Haun, J. E. (1993). The physiology of bottlenose dolphins (*Tursiops truncatus*): heart rate, metabolic rate and plasma lactate concentration during exercise. *J. Exp. Biol.* 179, 31–46.

Woakes, A. J., Butler, P. J., and Bevan, R. M. (1995). Implantable data logging system for heart rate and body temperature: its application to the estimation of field metabolic rates in antarctic predators. *Med. Biol. Eng. Comput.* 33, 145–151. doi: 10.1007/BF02523032

Worthy, G. A. J., Worthy, T. A. M., Yochem, P. K., and Dold, C. (2013). Basal metabolism of an adult male killer whale (*Orcinus orca*). *Mar. Mam. Sci.* 30, 1229–1237. doi: 10.1242/jeb.137513

Yasuma, F., and Hayano, J.-I. (2004). Respiratory sinus arrhythmia. *Chest* 125, 683–690. doi: 10.1378/chest.125.2.683

Yaw, T. J., Kraus, M. S., Ginsburg, A., Clayton, L. A., Hadfield, C. A., and Gelzer, A. R. (2018). Comparison of a smartphone-based electrocardiogram device with standard six-lead electrocardiogram in the Atlantic bottlenose dolphin (*Tursiops truncatus*). *J. Zoo Wildlife Med.* 49, 689–695. doi: 10.1638/2017-0140.1

Yazdi, P., Kilian, A., and Culik, B. M. (1999). Energy expenditure of swimming bottlenose dolphins (*Tursiops truncatus*). *Mar. Biol.* 134, 601–607. doi: 10.1007/s002270050575

Yeates, L. C., and Houser, D. S. (2008). Thermal tolerance in bottlenose dolphins (*Tursiops truncatus*). *J. Exp. Biol.* 211, 3249–3257. doi: 10.1242/jeb.020610

Young, B. L., Rosen, D. A., Hindle, A. G., Haulena, M., and Trites, A. W. (2011). Dive behaviour impacts the ability of heart rate to predict oxygen consumption in steller sea lions (*Eumetopias jubatus*) foraging at depth. *J. Exp. Biol.* 214, 2267–2275. doi: 10.1242/jeb.047340

Zena, L. A., Leite, C. A. C., Longhini, L. S., Dias, D. P. M., da Silva, G. S. F., Hartzler, L. K., et al. (2017). Analysis of the respiratory component of heart rate variability in the cururu toad *Rhinella schneideri*. *Sci. Rep.* 7:16119. doi: 10.1038/s41598-017-16350-0

Conflict of Interest Statement: The authors declare that the research was conducted in the absence of any commercial or financial relationships that could be construed as a potential conflict of interest.

Copyright © 2019 Cauture, Sterba-Boatwright, Rocho-Levine, Harms, Miedler and Fahlman. This is an open-access article distributed under the terms of the Creative Commons Attribution License (CC BY). The use, distribution or reproduction in other forums is permitted, provided the original author(s) and the copyright owner(s) are credited and that the original publication in this journal is cited, in accordance with accepted academic practice. No use, distribution or reproduction is permitted which does not comply with these terms.

frontiers in Ecology and Evolution

ORIGINAL RESEARCH
published: 12 March 2019
doi: 10.3389/fevo.2019.00053

Diving Behavior and Fine-Scale Kinematics of Free-Ranging Risso's Dolphins Foraging in Shallow and Deep-Water Habitats

Patricia Arranz[1,2]*, Kelly J. Benoit-Bird[3], Ari S. Friedlaender[4,5], Elliott L. Hazen[6], Jeremy A. Goldbogen[7], Alison K. Stimpert[8], Stacy L. DeRuiter[9], John Calambokidis[10], Brandon L. Southall[4,5], Andreas Fahlman[11,12] and Peter L. Tyack[1]

[1] Sea Mammal Research Unit, School of Biology, Scottish Oceans Institute, University of St Andrews, St Andrews, United Kingdom, [2] Biodiversity, Marine Ecology and Conservation Group, Department of Animal Biology, University of La Laguna, La Laguna, Spain, [3] Monterey Bay Aquarium Research Institute, Moss Landing, CA, United States, [4] Institute of Marine Sciences, University of California, Santa Cruz, Santa Cruz, CA, United States, [5] Southall Environmental Associates, Aptos, CA, United States, [6] Environmental Research Division, NOAA Southwest Fisheries Science Center, Monterey, CA, United States, [7] Department of Biology, Hopkins Marine Station, Stanford University, Monterey, CA, United States, [8] Vertebrate Ecology Lab, Moss Landing Marine Laboratories, Moss Landing, CA, United States, [9] Department of Mathematics and Statistics, Calvin College, Grand Rapids, MI, United States, [10] Cascadia Research Collective, Olympia, WA, United States, [11] Fundación Oceanogràfic, Valencia, Spain, [12] Woods Hole Oceanographic Institution, Woods Hole, MA, United States

OPEN ACCESS

Edited by:
Thomas Wassmer,
Siena Heights University,
United States

Reviewed by:
Stephen J. Trumble,
Baylor University, United States
Kagari Aoki,
University of Tokyo, Japan

***Correspondence:**
Patricia Arranz
arranz@ull.es

Specialty section:
This article was submitted to Behavioral and Evolutionary Ecology, a section of the journal Frontiers in Ecology and Evolution

Received: 25 July 2018
Accepted: 14 February 2019
Published: 12 March 2019

Citation:
Arranz P, Benoit-Bird KJ, Friedlaender AS, Hazen EL, Goldbogen JA, Stimpert AK, DeRuiter SL, Calambokidis J, Southall BL, Fahlman A and Tyack PL (2019) Diving Behavior and Fine-Scale Kinematics of Free-Ranging Risso's Dolphins Foraging in Shallow and Deep-Water Habitats. Front. Ecol. Evol. 7:53. doi: 10.3389/fevo.2019.00053

Air-breathing marine predators must balance the conflicting demands of oxygen conservation during breath-hold and the cost of diving and locomotion to capture prey. However, it remains poorly understood how predators modulate foraging performance when feeding at different depths and in response to changes in prey distribution and type. Here, we used high-resolution multi-sensor tags attached to Risso's dolphins (*Grampus griseus*) and concurrent prey surveys to quantify their foraging performance over a range of depths and prey types. Dolphins ($N = 33$) foraged in shallow and deep habitats [seabed depths less or more than 560 m, respectively] and within the deep habitat, in vertically stratified prey features occurring at several aggregation levels. Generalized linear mixed-effects models indicated that dive kinematics were driven by foraging depth rather than habitat. Bottom-phase duration and number of buzzes (attempts to capture prey) per dive increased with depth. In deep dives, dolphins were gliding for >50% of descent and adopted higher pitch angles both during descent and ascents, which was likely to reduce energetic cost of longer transits. This lower cost of transit was counteracted by the record of highest vertical swim speeds, rolling maneuvers and stroke rates at depth, together with a 4-fold increase in the inter-buzz interval (IBI), suggesting higher costs of pursuing, and handling prey compared to shallow-water feeding. In spite of the increased capture effort at depth, dolphins managed to keep their estimated overall metabolic rate comparable across dive types. This indicates that adjustments in swimming modes may enable energy balance in deeper dives. If we think of the surface as a central

place where divers return to breathe, our data match predictions that central place foragers should increase the number and likely quality of prey items at greater distances. These dolphins forage efficiently from near-shore benthic communities to depth-stratified scattering layers, enabling them to maximize their fitness.

Keywords: deep diving odontocete, foraging energetics, marine mammal, *Grampus griseus,* activity level, prey value, central place foraging theory

INTRODUCTION

When animals are foraging, their efficiency can be defined as the difference in energy gained from ingesting prey relative to the energy expenditures associated with searching for and capturing prey (Parker et al., 1996). Therefore, to increase efficiency, animals must minimize the cost of prey capture (Williams et al., 2000) and/or increase the energetic benefits from prey (Watanabe and Takahashi, 2013; Watanabe et al., 2014). To minimize locomotor costs, aquatic animals adopt gliding gaits, and slow swimming speeds to decrease drag and the energetic requirements of searching for food (Williams, 2001; Fahlman et al., 2008, 2013; Watanabe et al., 2011). To increase energy intake, they can increase feeding rates by extending the time spent in a prey patch (Doniol-Valcroze et al., 2011; Wilson et al., 2011), or selecting prey patches of higher quality (Orians and Pearson, 1979). Higher quality prey can take the form of larger bodied prey for animals that take prey individually (i.e., particle feeders, hunting predators), greater densities of the same type for multiple-prey loaders (i.e., filter feeders or grazers), or other prey changes that decrease handling time or increase catch per unit effort. Moreover, the cumulative benefit from a foraging bout may increase due to a combination of these processes and mechanisms (Daniel et al., 2008; Doniol-Valcroze et al., 2011; Gibb et al., 2016). However, what remains poorly understood is how predators modulate foraging performance when faced with heterogeneous, dynamic prey-scapes (Friedlaender et al., 2016).

Many animals across taxonomic groups and environments are central place foragers where feeding bouts occur far from a return location (Houston and McNamara, 1985). Air-breathing divers can be described as central place foragers, where the sea surface is the return location that provides a critical source of oxygen replenishment (Kramer, 1988). In this context, divers face the conflicting demands of oxygen conservation during apnea and the energetic costs associated with diving, swimming, and feeding (Davis et al., 2004). Therefore, diving foragers must balance managing oxygen stores while maximizing net energy intake during feeding at depth (Hazen et al., 2015). If the high energetic costs of feeding deplete body oxygen stores, this in turn would reduce aerobic diving capacity and thus impose a potential constraint on foraging performance (Croll et al., 2001; Acevedo-Gutiérrez et al., 2002; Goldbogen et al., 2012).

Central place foraging theory predicts that predators should only swim farther from the central place to encounter increasing numbers or quality of prey (Carbone and Houston, 1996). When the same prey resource is targeted, diminishing energetic returns are expected at increasing distances from the central place, because of increased travel time. Thus, at greater distances animals should feed on higher value prey to optimize foraging efficiency (Schoener, 1969, 1979). It is known that toothed whales (Odontoceti) hunt and capture individual prey across a wide size range (Clarke, 1996; Andersen et al., 2016); however it remains unclear whether odontocetes selectively vary feeding rates when feeding at different depths and/or modulate their locomotor and diving performance in response to changes in prey distribution and availability. To test the above hypothesis, we explore the fine-scale foraging behavior and kinematics of the cephalopod-eating Risso's dolphin using motion-sensing and acoustic recording tag data to quantify the foraging performance of this species in the wild.

MATERIALS AND METHODS

Dolphin Data Collection

Archival tags (Johnson and Tyack, 2003) were attached dorsally to free-ranging Risso's dolphins off Santa Catalina Island, California during field efforts from 2010 through 2016. The tags had a suction-cup system that released at local sunset, or unintentionally due to movement of the dolphins. They were positively buoyant and transmitted a VHF signal when at the surface, allowing tracking, and recovery. Stereo acoustic data were sampled with 16-bit resolution at a sampling rate of 240 kHz, except for tag gg11_216a where 120 kHz was used. Data from the other sensors were sampled at 200 Hz per channel and converted into depth, pitch, roll, and heading of the tagged animal, following methods described in Johnson and Tyack (2003). Pressure and accelerometer data were decimated to 20 and 5 Hz, respectively, before analysis. Analyses were carried out in Matlab 9.1.0 (http://www.mathworks.es/) using the DTAG toolbox (https://www.soundtags.org/dtags/dtag-toolbox/) and custom-made scripts. A subset of 18 tagged dolphins were subject to controlled acoustic playback exposure experiments (CEE) (**Table 1**). Detailed exposure protocols are described in Southall et al. (2012). Dives were classified as "non-CEE," "pre-exposure," "CEE," or "post-exposure," depending on the time overlap with the onset and end of the acoustic stimuli. Generalized additive mixed models (GAMMs) were used to assess the effect of CEE mode and type on two representative metrics of foraging performance. We fitted GAMMs using maximum dive depth and buzz rate as response variables, including CEE categorical data as a factor and individual dolphin as random effect, to identify potential behavioral responses as a function of CEE mode (non-CEE, pre-CEE, during-CEE, and post-CEE) and type (non-CEE, Control, PRN, Simul-MFA, Real MFA). As we were testing a specific hypothesis no model selection was needed. This statistical

approach allowed us to assess whether there was a behavioral response as a consequence of CEE, which was important to determine if the full *Grampus* tag dataset could be pooled across CEE modes and types for further analysis. Foraging models were fitted as a functions of dive metrics and of CEE modes and types, using the mgcv 1.8–15 package (Wood, 2011) in R 3.3.2 "Sincere Pumpkin Patch" (http://www.R-project.org/).

Focal follows of tagged animals were conducted whenever possible, avoiding approaches closer than 25 m. Observations were made from the tag boat with the aid of binoculars and VHF radio tracking equipment. Individuals were identified via photos of their dorsal fin and scar pattern, which facilitated tagging different individuals every time. Location of the tagged animals was recorded with a GPS on board and seabed depth at dolphin sighting locations was extracted using NOAA's NGDC bathymetric charts in ArcMap 9.2 (Environmental Systems Resource Institute, Redlands, CA, USA) with 3-arc second resolution (https://www.ngdc.noaa.gov/mgg/coastal/grddas06/grddas06.htm). Average seabed depth was estimated from all positions gathered during each tag deployment and the maximum depth of the deepest dive recorded among the 33 dolphins. This was 560 m, considering that in the deep-water habitat the seabed must be deeper than the deepest dive recorded. In this way dolphins were broadly classified as foraging in a shallow or deep-water habitat (**Table 1**). Only two of the dolphins (data sets gg14_223a and gg14_253a) were close to the boundary defined by this depth threshold, as they remained above average seabed depths of 450 and 500 m, respectively. Those depths may have allowed deep diving but if so, foraging would likely have occurred close to the seabed, in the benthic boundary layer (Angel and Boxshall, 1990). Given the differences between benthopelagic and pelagic organisms, these dolphins were classified as in a shallow-water habitat. Moreover, data for each dive were analyzed with respect to which habitat the dolphin was in, based on the seabed depth of the closest focal follow position gathered within 15 min of the start or end of a given dive. We acknowledge the low accuracy of these estimates but the seabed depth at the nearest focal follow location was considered a representative measure of the type of foraging habitat used by the animal. Dives without focal follow information within the 15 min time window was not considered for kinematic analyses.

Prey Data Collection

Data on the distribution of prey in the Catalina Basin, off the eastern coast of Santa Catalina Island, California, comprising the deep-water habitat of the dolphins, were obtained from ship and underwater autonomous vehicle (AUV) based hydroacoustic surveys. The ship transects covered seabed depths ranging from 300 to 900 m and the AUV sampled pre-defined depths between 50 and 500 m, depending on the location of prey layers. Both platforms were equipped with Simrad EK60 echo sounders at 38 and 120 kHz. The AUV survey provides a 15 × 10 cm sampling resolution in horizontal and vertical planes, respectively. This allowed individual animals to be observed within scattering features, whereas the ship-based sensors provided a view of entire features. Comprehensive explanation of the sensors and platforms used is provided by Moline et al. (2015) while Benoit-Bird et al. (2017) provide a detailed description of biological sampling and active acoustics methodology. Briefly, acoustic scattering data were processed using Echoview and individual prey detected from the AUV within scattering features were identified as single targets (Sawada et al., 1993), providing measurements of target strength at two frequencies. Frequency differencing was used to facilitate coarse taxonomic classification (i.e., fish, squid, or crustacean) while target strength was used as a proxy of length within each taxonomic class. Calculation of inter-individual spacing of prey in layers was measured using the nearest neighbor distance for each individual target sampled by the AUV, both in the beam and along the track. The dominant composition of layers identified from the active acoustics was determined using a net towed at relatively high speed (1–2.2 m s^{-1}) that captured mobile organisms between 1 and 35 cm body length. This catch matched the composition identified acoustically (Benoit-Bird et al., 2017). Sampling of the deep-water habitat of the dolphins was coincident in space and time with tagging of two of the 33 dolphins (tag id gg13_266b and gg13_267a, **Table 1**). The spatial coverage of the prey mapping and its overlap with the tag data is presented in Figure 2 in Arranz et al. (2018). Another 15 dolphins were tagged in the same general habitat, 6 of them in the same year. Prey fields in the shallow-water habitat were not sampled in this study. Dolphins in shallow-water habitat were mostly tagged in 2013, when increased upwelling productivity conditions may have influenced prey availability, particularly of market squid (*Doryteuthis opalescens*) in coastal waters off the island. Hence the dolphin's foraging opportunities were higher close to shore (Vanderzee et al. pers. comm.). This was supported by visual observations during tagging in 2013, when market squid were observed at the surface and in the mouths of Risso's dolphins. Dives occurring within the shallow-water habitat were classified based on their depth distribution as *Shallow* (<100 m depth) or *Intermediate* (>100 m), for comparison of dive parameters.

Kinematic Analyses

Dives were defined as vertical excursions exceeding 20 m depth. Dives recorded within 15 min of tag-on were excluded from the analysis, to remove data potentially affected by the tagging procedure (the 15 min duration is roughly equivalent to two deep dives or 5 shallow dives by this species). Incomplete dives at the start or end of the record (caused by a delay in triggering the salt water switch or release at depth) were also excluded. Dives performed in the deep-water habitat were classified according to their maximum depth and the prey feature targeted in the bottom phase (*sensu* Arranz et al., 2018). Echolocation clicks and buzzes from the tagged dolphin, respectively, indicative of prey search and capture attempts within dives, were isolated using a supervised click detector together with spectrogram visualizations of acoustic recordings, following the methods described in Arranz et al. (2016). The interpretation that buzzes are associated with prey capture attempts has been confirmed for several echolocating marine mammals, including sperm whales (Miller et al., 2004), beaked whales (Johnson et al., 2004), pilot whales (Aguilar de Soto et al., 2008), porpoises (Deruiter et al.,

TABLE 1 | Risso's dolphins tagged off California from 2010 to 2016.

Tag record ID	Age class	CEE type	Tag on (h:m)	RD (h)	FD/Ttal Dives (Nr)	Pre/CEE/ Post dives (Nr)	Seabed depth (m)/(Nr)	Habitat type
gg10_266a	Unknown	Non-CEE	10:01	0.3	0/ 4	4/0/ 0	773 [312–859]/26	DE
gg10_266b	Unknown	Non-CEE	10:01	1.8	0/ 4	4 /0/ 0	773 [312–859]/26	DE
gg11_266a	Adult	Non-CEE	7:29	0.6	0/ 1	1/0/0	809[646–933]/6	DE
gg11_272a	Adult	Non-CEE	13:25	4.5	0/2	2/0/0	1015 [963–1188]/50	DE
gg13_204a	Adult	Non-CEE	11:35	0.7	1 / 4	4/0/0	164 [31–507]/30	SH
gg13_215a	Adult	Non-CEE	12:38	1.4	0/0	0/0/0	717 [705–729]/2	DE
gg13_230a	Adult	Non-CEE	15:00	1.5	3/11	11/0/0	662 [491–854]/41	DE
gg13_264a	Sub-adult	Non-CEE	10:57	1.0	5/7	7/0/0	111 [83–143]/8	SH
gg13_267a*	Adult	Non-CEE	11:44	6.8	21/24	24/0/0	598 [408–746]/11	DE
gg13_270a	Adult	Non-CEE	09:25	0.7	8/8	8/0/0	295 [75–478]/27	SH
gg13_270b	Sub-adult	Non-CEE	13:58	3.3	0/4	4/0/0	400 [230–478]	SH
gg15_223a+	Adult	Non-CEE	08:28	2.3	16/20	20/0/0	483 [378–584]/35	SH
gg_14_253a+	Sub-adult	Non-CEE	13:07	1.3	5 /7	7/0/0	467 [98–511]/14	SH
gg16_230a	Adult	Non-CEE	12:30	1.25	4/7	7/0/0	337[184–460]/3	SH
gg16_237a	Adult	Non-CEE	09:15	1.75	4/9	9/0/0	531[531–531]/2	DE
gg13_204b	Adult	CTRL	13:35	3.3	1/2	2/0/0	164 [31–507]/30	SH
gg13_212a	Sub-adult	CTRL	16:00	1.1	0/6	5/1/0	242 [90–472]/8	SH
gg13_261a	Adult	CTRL	8:58	4.9	10/13	13/0/0	592 [212–813]/73	DE
gg13_262a	Adult	CTRL	7:25	6.4	19/21	19/0/2	76 [19–173]/62	SH
gg13_262b#	Adult	CTRL	8:26	13.5	28/29	3/0/26	83 [69–856]/77	SH
gg13_262c#	Adult	CTRL	9:57	9.9	5/13	1/0/12	83 [69–856]/77	SH
gg14_254a	Sub-adult	CTRL	08:36	3.3	0/8	8/0/0	127 [9–245]/2	SH
gg11_265a	Unknown	PRN	12:41	6.6	36/53	27/3/23	103 [89–290]/39	SH
gg12_209a	Unknown	PRN	14:13	3.8	0/0	0/0/0	978 [393–1232]/97	DE
gg13_190a	Adult	Real MFA	12:40	5.1	6/10	9/0/1	621 [104–1170]/35	DE
gg13_213a	Adult	Real MFA	16:09	0.3	0/1	1/0/0	575[153–984]/9	DE
gg11_216a	Unknown	Simul MFA	12:18	8.4	33/37	0/5/32	573 [387–634]/54	DE
gg11_264a	Unknown	Simul MFA	10:52	5.3	0/7	4/0/3	569 [450–692]/44	DE
gg11_269a	Unknown	Simul MFA	11:30	9.9	3/11	0/1/10	654 [240–901]/72	DE
gg13_255a	Adult	Simul MFA	14:00	6.5	3/7	4/0/3	345 [231–911]/70	SH
gg13_255b	Adult	Simul MFA	15:18	4.4	0/0	0/0/0	618 [424–1286]/17	DE
gg13_266a	Juvenile	Simul MFA	11:17	3.1	0/5	5/0/0	228 [39–489]/36	SH
gg13_266b*	Adult	Simul MFA	11:23	2.3	12/13	11/2/0	762 [540–788]/41	DE

*Tag record ID: identification of the tag recording from each dolphin. CEE type: Type of control exposure experiment (CEE) - Non-CEE, outside the context of CEEs; CTRL, control; PRN, Pseudo-random noise; Real MFA, Real Medium Frequency Sonar (MFA); Simul MFA, Simulated MFA. Tag on: Local time of tag deployment; RD: record duration, in hours. FD/Ttal dives: Nr of foraging dives and total Nr of dives recorded. Pre/CEE/Post dives: Nr of dives recorded before during and after the CEE transmissions. Seabed depth: mean and range in brackets of the bathymetry at the positions of the tagged dolphin's focal follows with Nr of focal follows. Habitat: Type of habitat where dolphins distributed (see methods for detailed description of habitat classification). *Dolphins with concurrent prey data available. +Dolphins likely foraging benthopelagically. #Dolphins moved offshore during the afternoon.*

2009), and belugas (Ridgway et al., 2014). Foraging dives were defined as including one or more buzzes. For each dive, the mean descent and ascent depth rates and the proportion of descent time spent gliding were computed. Fluke strokes were identified in the recordings as cyclic variations in the pitch with a magnitude >3 degrees and with a period between 0.4 and 5 s, estimated from a nominal fluking period of 1.5 s for Risso's dolphin. The stroke count was verified visually by checking the pitch angle in random sections of the record. Glides were defined as 10 s time intervals with no stroking. Descent, bottom and ascent phases in dives were defined following a 70% rule, as in Arranz et al. (2016). The descent phase of each dive was considered the period from when the dolphin left the surface to the first time the depth exceeded 70% of the maximum dive depth. The ascent phase started at the last time the depth exceeded 70% of maximum dive depth and ended when the dolphin reached the surface. The bottom phase was defined as the period from the first to the last time the depth exceeded 70% of the maximum dive depth. The inter-buzz interval (IBI) was estimated as the time elapsed since the end of a buzz and the start of the next one. The vertical swim speed was computed as the rate of change in depth (as in Aguilar de Soto et al., 2008).

Energetic Analyses

As a proxy for the activity level of the dolphins we computed the overall dynamic body acceleration (ODBA, Wilson et al., 2006)

as the norm of the high-pass filtered acceleration resulting from the movement of the animal and recorded by the tag sensors (ODBA tool from the soundtags toolbox). Cut-on frequency required for ODBA estimation was set to 0.35 Hz (about half of the normal stroking rate for these dolphins). Previous studies have shown that ODBA is a reasonable proxy for metabolic rate in marine mammals (Fahlman et al., 2013) although other studies report difficulty in observing such a relationship (Halsey et al., 2011; Halsey, 2017). An exploratory analysis of this relationship in Risso's dolphins is presented here, assuming that for each individual dolphin, the lowest ODBA recorded on each dive ($ODBA_{min}$) corresponded to the $\dot{V}O_{2min}$, or estimated resting metabolic rate (RMR) and the highest ODBA for each dive ($ODBA_{max}$) corresponded to its $\dot{V}O_{2max}$ or estimated maximum metabolic rate.

For comparative purposes, we modeled $\dot{V}O_{2min}$ in three ways (**Table S1** in Data Sheet S1): (1) using the measured $\dot{V}O_{2min}$ from the smaller bottlenose dolphin (*Tursiops truncatus)* (Equation 3.2 in Fahlman et al., 2018) and scaled allometrically for the larger Risso's dolphin, (2) assuming an average mass-specific $\dot{V}O_{2min}$ of 3.9 ml O_2 kg min^{-1} (Figure 3B in Fahlman et al., 2018) and multiplying by the estimated body mass (M_b), or (3) using Kleiber's equation (Equation 1) for terrestrial mammals and the estimated M_b of the tagged dolphin (Kleiber, 1947). The M_b of tagged Risso's dolphins was approximated from individual age class (**Table 1**), implying a mass of 500 kg for adults and 300 kg for sub-adults and juveniles (Jefferson et al., 2008).

$$\dot{V}O_{2min} = 0.00993 * M_b^{0.75} \quad (1)$$

$\dot{V}O_{2max}$ was modeled in two different ways (**Table S1** in Data Sheet S1): scaling up $\dot{V}O_{2min}$ (1) by 5 times or Metabolic Equivalents of Task (MET's, Savage et al., 2007), a level of exercise that one would expect animals to undertake routinely; or (2) by the Hoppeler equation (Equation 2) (Weibel and Hoppeler, 2005).

$$\dot{V}O_{2max} = 0.118 * M_b^{0.87} \quad (2)$$

A regression equation was built using estimated $\dot{V}O_{2min}$, a $\dot{V}O_{2max}$ for each dolphin, in one of the ways described above, estimated $ODBA_{min}$ and $ODBA_{max}$ for a given dive. We acknowledge reasonable concerns about generating a regression equation from

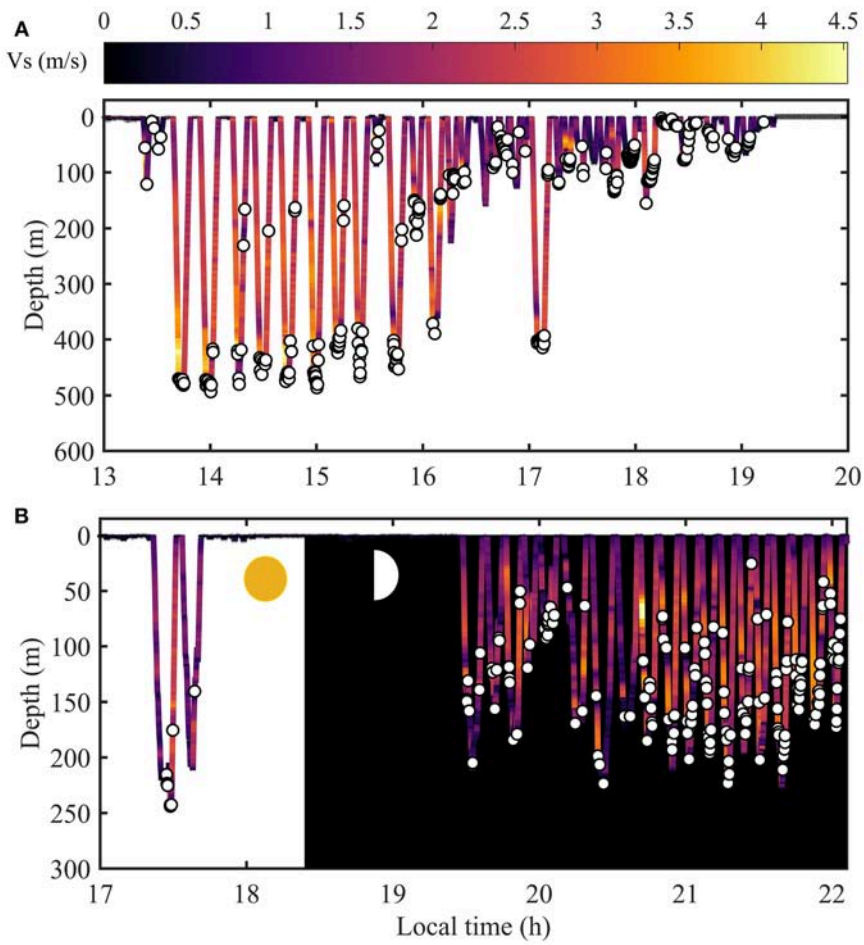

FIGURE 1 | Dive profiles from two Risso's dolphins with **(A)** the longest period of time with consistent deep dives and **(B)** the longest night time foraging period recorded, among 33 tagged individuals. Prey capture attempts are represented by white circles. Dive profile is colored according to vertical swim speed (Vs).

two data points, but it allowed us to estimate the $\dot{V}O_2$ (or field metabolic rate) of the dive based on the overall activity. Regression lines were re-calculated for each dive to account for different tag placements within the same individual (due to potential tag moves) and likely variation of minimum and maximum ODBA values amongst dolphins (**Figure S1** in Data Sheet S1). The resulting intercept and slope of the regression line obtained for a given dive were multiplied either by the average ODBA of the dive+ surface interval, to estimate the average $\dot{V}O_2$ per dive, or by the average ODBA of the dive phase (descent, bottom and ascent) to estimate the average $\dot{V}O_2$ of each phase, as follows:

$$\dot{V}O_2 = [(\dot{V}O_{2\min} - \mathrm{ODBA}_{\min} * \mathrm{slope}) + (\dot{V}O_{2\max} - \dot{V}O_{2\min}) / \mathrm{ODBA}_{\max} - \mathrm{ODBA}_{\min})] * \mathrm{ODBA}_{\mathrm{dive/phase}} \quad (3)$$

Recorded $\mathrm{ODBA}_{\min}$ and $\mathrm{ODBA}_{\max}$ per dive were regressed as a function of duration of the deployment, to rule out correlation between these variables (**Figure S2** in Data Sheet S1). The ratio between the estimated metabolic costs of each dive phase in different dive types was used comparatively, to assess relative differences in dolphin metabolic costs when diving to different depths.

Statistical Modeling

To assess differences in dive parameters by dive type, we used generalized linear mixed-effects models fitted in R, using the package glmmTMB (Brooks et al., 2017). We modeled each dive parameter as a function of habitat and dive type, controlling for effects of age class (via fixed effects) and individual differences and temporal autocorrelation (via a random intercept of tag ID). We used Gaussian models with identity link, except for the following parameters. Inter-buzz interval and buzz duration were modeled using gamma family with log link, to account for right-skew and overdispersion of residuals, and for number of buzzes a negative binomial type I with log link and an offset for dive duration, since data are count data, and to account for right skew and overdispersion of residuals. We used ANOVA to compare models with and without habitat and dive type as predictors, and in the case of a significant result, we used Tukey's method to assess pairwise differences between dive types [using R package emmeans (Lenth, 2018)].

TABLE 2 | Generalized Additive Mixed Model (GAMM) estimates for the effects of mode and type of Controlled Exposure Experiments (CEE) on behavioral criteria of 33 Risso's dolphins.

Parametric coefficients:	Estimate	Std. Error	*t*- value	Pr(>|t|)
Buzz rate	R-sq.(adj) = 0.03 Scale est. = 29.48 *n* = 277			
(Intercept)	0.23	1.46	3.59	0.001
CEE mode	0.73	0.48	1.49	0.14
CEE type	−1.06	0.67	−1.58	0.12
Max Dive depth	R-sq.(adj) = −0.001 Scale est. = 10494 *n* = 300			
(Intercept)	70.93	26.27	2.70	0.007
CEE mode	15.87	8.78	1.81	0.07
CEE type	7.21	12.13	0.59	0.55

The response variables are buzz rate and maximum dive depth with individual dolphin as random effect.

RESULTS

A total of 124 h of acoustic and movement data from 33 Risso's dolphins (20 adults, 5 sub-adults, 1 juvenile, and 7 individuals of unknown age) resulted in 331 dives during 22 deployments as analyzed here. Most tags recorded data during daytime only but two documented 2 h 19 min and 3 h 30 min after local sunset, respectively, resulting in an overall time coverage from 7:25 a.m. to 9:57 p.m. local (UTC−7) (**Table 1**, **Figure 1**). No clear time-of-day dependent pattern of feeding behavior or inshore-offshore movements were detected from plots of the seabed depth at the focal follow positions of the dolphins in relation to time of day. These results are based on a small sample size without full day/night periods from tag records. GAMMs revealed no significant effect of CEEs on the buzz rate per dive nor the maximum dive depth in any of the 18 out of 33 tagged dolphins subject to the experiments (**Table 2**).

Habitat

Hydroacoustic sampling of the biotic structure in the water column throughout the Santa Catalina Basin >560 m seabed depth, i.e., deep-water habitat, revealed prey fields vertically stratified into four prey features comprising three sound-scattering layers. Each prey layer was horizontally identified as follows: *Shallow* [30–90 m], *Midwater* [200–300 m], and *Deep* [350–450 m], and a zone of scattered patches between 100 and 200 m depth named *Intermediate* (see Figure 2 in Arranz et al., 2018). The shallow layer was dominated by larval fish and small crustaceans, the midwater layer by myctophids and krill, and the deep layer primarily by dragonfish, squid, shrimp, and large krill (Benoit-Bird et al., 2017). Scattered patches were not directly sampled to confirm potential composition but echo characteristics were consistent with small schooling fish. Measures of the horizontal patch structure are reported by Benoit-Bird et al. (2017). Prey patch aggregations had similar topological extent, 100 individuals across, irrespective of taxonomic composition, animal size, and depth. Inter-individual spacing increased with relative animal size within each taxonomic group. When *Grampus* were detected by AUV echosounder sampling in the deep-water habitat of the dolphins, they were found mostly within the boundaries of monospecific aggregations with a frequency response corresponding to squid (Benoit-Bird et al., 2017). About half of the dolphins ($N = 17$) stayed within the deep-water habitat during most of the recording time, whereas the other animals ($N = 16$) stayed in shallow-water habitat (**Table 1**). In the deep-water habitat, 39% of the dives performed by the dolphins were

shallow (to a max depth of 30–90 m), 35% intermediate (to a maximum depth of 90–200 m), 15% midwater (to a maximum depth of 200–300 m), and 8% were deep dives (to a maximum depth >350 m).

Foraging Behavior

Dolphins spent 83 (SD 48)% of the time near (<20 m) or at the surface and 17 (SD 35)% of the time diving. The pattern of dive cycles differed among individuals, with variable-duration bouts of foraging dives interspersed with periods at or near the surface (entailing behaviors like resting, traveling, socializing) (**Figure 1**). Tagged dolphins foraged throughout the day, with search clicks recorded in 76% of dives and buzzes recorded in 62% of dives. Foraging dives lasted 5.0 [0.7–10] min on average [range], covering a broad range of depths up to 588 m (**Figure 1**). Duration of dives recorded from adult dolphins ($N = 279$ dives) was 4.3 [1.2–10. 7] min, whereas in non-adults (i.e., juveniles and sub-adults, $N = 25$ dives) dive duration was 3.8 [1.5–5.7] min. Deep-water foraging was only recorded in adult dolphins (average maximum dive depth 137 ± 119 m [mean ± SD]), all recorded dives by non-adult dolphins were shallower than 141 m depth (average maximum dive depth 59 ± 34 m). Deep dives occurred mostly in the afternoon, since before noon most data were recorded within the shallow habitat. Diurnal patterns of inshore-offshore movement or vice versa were absent when visualizing plots of seabed depth in relation to time of day (average Pearson's correlation across tags R= −0.14). Seabed depths from focal follows revealed that dolphins were foraging near the seabed when in shallow-waters, although benthopelagic feeding may also take place in the deep-water habitat (**Figure 2**).

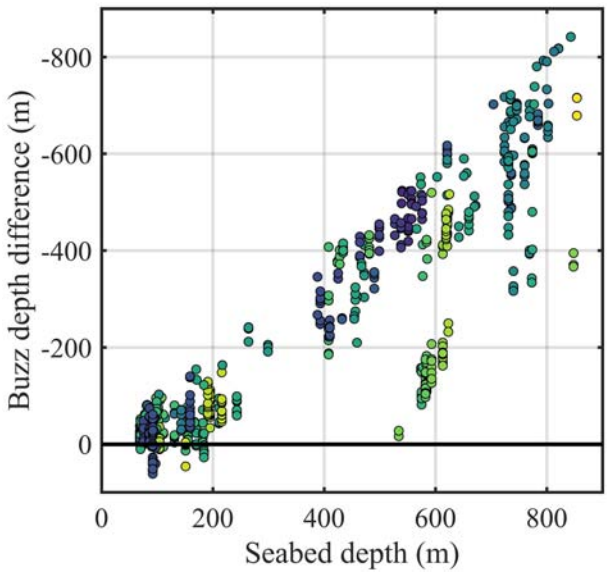

FIGURE 2 | Foraging activity of Risso's dolphins relative to the seabed. Seabed depth from the closest focal follow position gathered within 6 min of the given buzz (x-axis) and difference between buzz depth and seabed depth (y-axis), colored according to individual. Positive differences are the result of the offset between focal follow position from where seabed depth is extrapolated and depth where dolphins are feeding.

Dive Kinematics

Dolphins' descent and ascent rates were up to twice as fast when diving deeper (Spearman's correlation $\rho = 0.59$, p-value < 0.005, and $\rho = 0.65$, p-value < 0.005, respectively). They also tended to adopt higher absolute body pitch angles (Spearman's correlation $\rho = 0.51$, p-value < 0.005) with active stroking on ascent from deeper dives (**Table 3**). The proportion of time spent gliding relative to the duration of the descent phase of each dive increased up to 5 times with maximum depth of the dive (Spearman's correlation $\rho = 0.53$, p-value < 0.005), with an associated dramatic drop in fluke stroking rate (**Figure 4C**). Stroke frequency decreased over the first 30 s of the descent during deep dives, from 15 to < 5 strokes every 20 s, after which they glided for about a minute. After that, they increased stroke frequency again, resulting in high vertical velocities (up to 4.5 m s^{-1}) during the final phase of most descents of deep dives (**Figures 1**, **4E**). Stroking patterns during descents of shallow, intermediate and midwater dives were more variable, with fewer episodes of high vertical swim speed.

Deep dives featured on average twice the number of prey capture attempts in the bottom phase (7 ± 3 buzzes) as shallow dives (3 ± 6 buzzes), whereas in scattered patches and midwater dives dolphins featured 5 ± 4 prey capture attempts, respectively. There was a significant correlation between maximum dive depth and number of buzzes performed at the bottom phase of the dive (Spearman's correlation $\rho = 0.40$, $p < 0.0001$ $N = 307$ dives). Considering only bottom phase foraging rates, estimated as the ratio between the number of prey capture attempts at the bottom of dives and the duration of the bottom phase, these ranged between 79 and 134 prey capture attempts h^{-1} as a function of dive type. Bottom phase foraging rates were on average 79 prey capture attempts h^{-1} in shallow dives [30–90 m], 134 attempts h^{-1} in intermediate dives [100–200 m], 112 attempts h^{-1} in midwater dives [200–300 m], and 102 capture attempts h^{-1} in deep dives [350–450 m].

Feeding during descent and/or ascent of dives increased the number of prey items targeted in shallow dives by 17% (4 ± 7 buzzes), 40% in scattered patches (6 ± 5 buzzes), 60% in midwater dives (8 ± 3 buzzes), and 28% in deep dives (9 ± 3 buzzes). Overall foraging rates, i.e., the cumulative number of buzzes emitted per dive divided by duration of dives, revealed between 28 and 55 prey attempts per hour, depending on the foraging depth. Dolphins pursued on average 32 ± 52 prey items h^{-1} in shallow dives, 36 ± 26 items h^{-1} in intermediate dives, 55 ± 40 items h^{-1} in midwater dives and 28 ± 20 items h^{-1} in deep dives.

GLMMs revealed significant differences in buzz rate for different dive types (chisq = 9.83, p-value = 0.02), although pairwise comparisons indicated significant differences only for shallow vs. intermediate dives (**Data Sheet S2**). Differences in the duration of the bottom-phase of the dive were significant across dive types (chisq = 110.01, p-value = 1.08^{-23}) with differences between intermediate and deep dives, as well as shallow dives and all other dive types. Similarly, mean stroke rate at the bottom phase of the dive differ significantly for all dive types

TABLE 3 | Kinematic data for Risso's dolphins foraging dives, pooling dives from all tagged dolphins by habitat type and depth layer.

		Shallow–water (*N* = 133)		Deep–water habitat (*N* = 168)			
	Units	Shallow (*N* = 95)	Intermediate (*N* = 38)	Shallow (*N* = 71)	Scattered Patches (*N* = 42)	Midwater (*N* = 32)	Deep (*N* = 18)
Depth	m	57[20, 99]	144[100, −266]	54[20, 97]	151[101, 198]	240[200, 309]	460[386, 566]
Duration	min	3.4[1.3, 5.9]	4.8[3.0, 8.0]	2.9[0.2, 6.9]	5.0[3.2, 9.0]	6.5[3.1, 9.4]	8.9[7.4, 10.7]
% feeding	%	52%	94%	53%	92%	90%	89%
Nr buzz	n dive^{-1}	5.7[0, 38]	6.8[0, 22]	2.3[0, 32]	6.5[0, 19]	8[1, 18]	9[3, 16]
Bot duration	min	1.7[0.2, 4.5]	1.9[0.7, 3.9]	1.2[0, 4.7]	2.2[0.6, 4.7]	2.9[0.9, 5.7]	4.1[1.8, 5.9]
Bot stroke r	Hz	0.5[0.1, 1.1]	0.7[0.3, 1.0]	0.5[0.2, 0.9]	0.6[0.1, 1.0]	0.6[0.4, 0.9]	0.7[0.6, 0.8]
Bot buzz r	nmin $^{-1}$	2[0.6, 8]	3[0.6, 9]	1[0.4, 10]	2[0.3, 7]	2[0.2, 5]	2[0.5, 3]
Buzz duration	s	0.8[0.3, 5.7]	1.6[0.3, 4.3]	0.7[0.4, 4.5]	1.2[0.3, 4.0]	1.1[0.3, 2.0]	1.5[0.4, 5.7]
IBI	s	13.3 [7.0, 24.0]	20.0[5.1, 47.5]	7.23[3.7, 14.6]	26[12.4, 49.8]	27[8, 68]	31[6, 85]
Buzz depth	m	34[0, 92]	111[0, 188]	25[0, 80]	109[0, 193]	171[98, 241]	371[210, 488]
Desc stroke r	Hz	0.4[0.05, 0.85]	0.5[0.1, 0.8]	0.5[0, 0.9]	0.5[0.06, 1.2]	0.4[0.2, 1.2]	0.3[0.2, 0.5]
Desc rate	ms^{-1}	0.8[0.2, 1.9]	1.2[0.4, 2.3]	0.8[0.09, 2.6]	1.4[0.2, 2.5]	1.6[0.6, 2.6]	2.4[1.3, 2.9]
Desc pitch	deg	−38.4[−76.7, 49.8]	−39.6[−63.8, −13.6]	−33.9[−75.7, 59.7]	−40.6[−66.1, 11.6]	−42.7[−72.7, −20.6]	−46.9[−69.4, 30.5]
Desc glide	%	8[0, 91]	11[0, 80]	9[0, 73]	21[0, 86]	35[0, 77]	57[0, 79]
Asc rate	ms^{-1}	1[0.1, 2.4]	1.5[0.8, 2.2]	0.9[0.3, 2.1]	1.4[0.7, 2.1]	1.8[0.9, 2.4]	2.2[1.8, 2.9]
Asc pitch	deg	24.2[−23.3, 71.7]	36.9[7.8, 60.9]	28.9[−21.4, 65.5]	44.8[0.2, 69.3]	53.3[30.8, 73.4]	59[25.4, 72.1]
Roll var	deg	26.8[5.3, 46.9]	31.9[8.5, 51.2]	25.3[4.5, 68.4]	26.7[4.6, 47.7]	30.1[13.5, 50.1]	30.9[16.2, 42.9]
Head var	deg	21.6[7.6, 49.6]	23.5[10.6, 36.7]	21.9[5.6, 57.9]	21.2[3.2, 64.8]	25.4[8.2, 59.1]	24.5[12.0, 40.8]
$\dot{V}O_{2desc}$	lO_2min^{-1}	2.8[1.2, 5.7]	2.8[1.4, 5.7]	3.2[2.0, 6.7]	3.1[2.2, 5.0]	2.9[2.3, 4.4]	2.5[2.2, 3.1]
$\dot{V}O_{2bot}$	lO_2min^{-1}	2.9[1.2, 6.1]	3.2 [2.0, 5.4]	3.5 [2.1 9.0]	3.6 [2.4, 6.0]	3.8 [3.0, 5.2]	3.7[3.1, 4.7]
$\dot{V}O_{2asc}$	lO_2min^{-1}	3.1 [1.2, 5.9]	3.4 [2.3, 6.3]	3.5 [2.2 7.3]	3.7 [2.3, 7.1]	3.5 [2.6, 4.5]	3.4 [2.8, 4.9]

Depth: maximum dive depth. Duration: Dive duration. % feeding: Proportion of dives with the buzzes. Nr buzz: Total number of buzzes recorded per dive. Bot duration: Duration of the bottom phase of the dive. Bot stroke r: number of strokes per second averaged in 10 s bins over the duration of the bottom phase of the dive. Bot buzz r: number of buzzes recorded in the bottom phase of the dive divided by bottom time. Buzz duration: time since start to end of the buzz. IBI: Time interval between buzzes; Buzz depth: Average depth of buzzes recorded per dive. Desc stroke r: number of strokes per second averaged in 10 s bins over the duration of the descent phase of the dive. Desc. rate: rate of change in depth recorded during dive descents, in 10 s bin. Desc. pitch: average body pitch angle of the dolphins during the descent phase of dives. Desc. glide: proportion of descent time spent gliding. Asc rate: rate of change in depth recorded during dive ascents, in 10 s bin. Asc pitch: average body pitch angle of the dolphins during the ascent phase of dives. Roll var: variation in roll angle over the 5 s before the buzz. Head var: variation in heading over the 5 s before the buzz. $\dot{V}O_{2desc}$: Estimated field metabolic rate for the descent phase of the dive. $\dot{V}O_{2bot}$: Estimated field metabolic rate for the bottom phase of the dive. $\dot{V}O_{2asc}$: Estimated field metabolic rate for the ascent phase of the dive. $\dot{V}O_2$ estimates calculated using Equation 3.2 in Fahlman et al. (2018). Values are mean [min, max] of all dives of each type.

(chisq = 3, *p*-value = 3.62^{-8}). According to the full model, IBI did not differ by dive type (chisq = 2.69, *p*-value = 0.44), however pairwise comparison for individual dive types reported significant differences between shallow and deep dives. There was also evidence of a difference in roll variance by dive type (chisq = 8.56, *p*-value = 0.03), with shallow dives being different from midwater and deep dives. Buzz duration did not vary among dive types (chisq = 4.28, *p*-value = 0.23). None of the models indicated significant differences in dive response variables when fitted with habitat type as predictor. **Figure 3** shows kernel density of the above modeled parameters separated by age class, habitat and dive type.

Metabolic Costs

GLM results indicated that estimated $\dot{V}O_2$ per dive was similar across dive types and habitats (**Figure S3** in Data Sheet S1) but differed between dive phases (chisq = 120.92, *p*-value = 4.88^{-26}), with descent being different from bottom and ascent estimates (**Figure 5**, **Table 3**). Estimated average $\dot{V}O_2$ per dive was 1.22 ± 0.18 l O_2 min^{-1} for shallow dives, 1.19 ± 0.12 l O_2 min^{-1} for scattered patch dives, 1.18 ± 0.12 l O_2 min^{-1} for midwater dives and 1.11 ± 0.09 l O_2 min^{-1} for deep dives, calculated using Equation 3.2 in Fahlman et al. (2018). The second method used, based on Figure 3B in Fahlman et al. (2018), rendered $\dot{V}O_2$ values that doubled or tripled the previous results but were again consistent across dive types: 1.69 ± 0.25 l O_2 min^{-1} for shallow dives, 1.65 ± 0.17 l O_2 min^{-1} for scattered patches dives, 1.63 ± 0.17 l O_2 min^{-1} for midwater dives and 1.53 ± 0.13 l O_2 min^{-1} for deep dives. Estimates using Kleiber's equation resulted in slightly higher $\dot{V}O_2$ estimates but were also similar among dive types: 3.14 ± 0.46 l O_2 min^{-1} for shallow dives, 3.06 ± 0.32 l O_2 min^{-1} for scattered patch dives, 3.03 ± 0.32 l O_2 min^{-1} for midwater dives and 2.85 ± 0.24 l O_2 min^{-1} for deep dives. Hoppeler's equation yielded an upper bound for $\dot{V}O_{2max}$ of 16.8 l O_2 min^{-1} for a 300 kg dolphin and 26.3 l O_2 min^{-1} for a 500 kg dolphin.

DISCUSSION

The Risso's dolphins in this study appear to employ several mechanisms to maximize foraging efficiency, depending on their feeding depth. The dolphins varied their diving kinematics

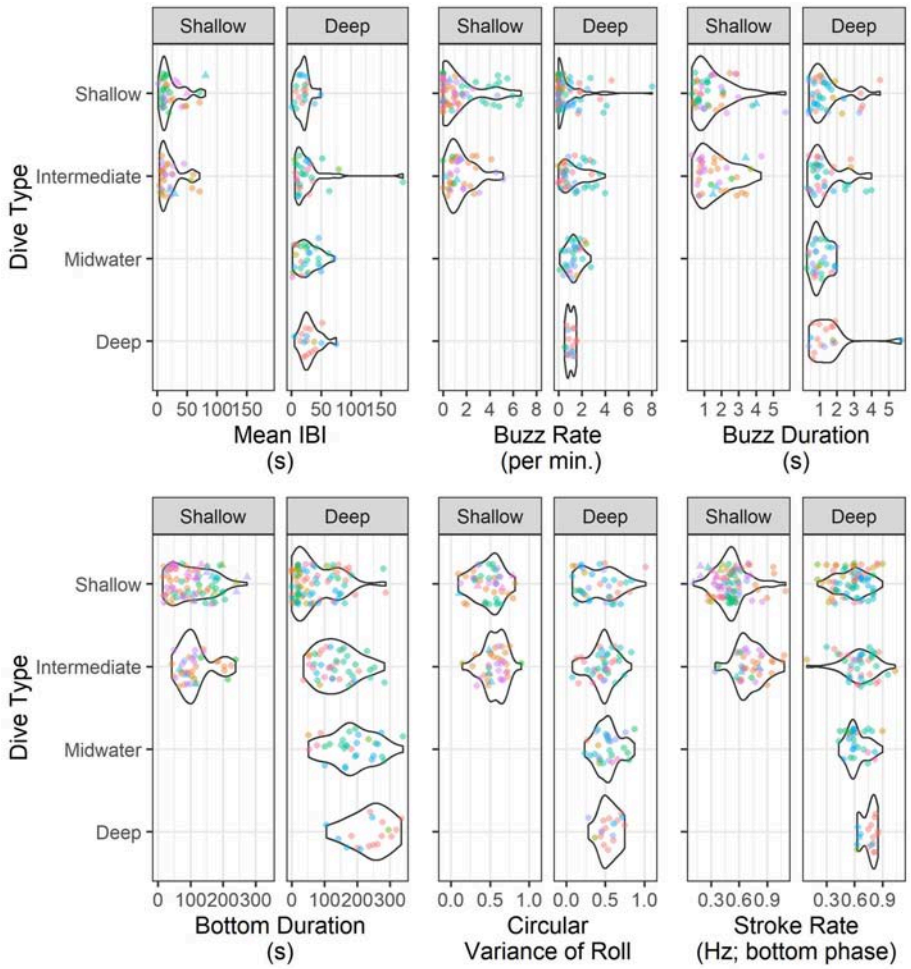

FIGURE 3 | Summary statistics of Risso's dolphins foraging parameters by dive type. Multi-panel violin plot of kernel probability density colored by individual dolphin, different shapes correspond to age class (dots represent adults and triangles non-adults) and separate panels correspond to each habitat. Results of the GLMM (Generalized linear mixed model) fitted for the above parameters with and withouth habitat and dive type as predictors are reported in the text and **Data Sheet S2**.

and prey quantity when foraging in prey layers with different composition. They foraged throughout the day in shallow and deep-water habitats, attempting to capture prey at depths up to 488 m. Foraging dives had maximum dive depths up to 560 m and occurred in bouts representing about 20% of a dolphin's daytime activity, although tag-on durations averaged only a few hours and at most 13.5 h. These foraging dives targeted epipelagic to mesopelagic prey resources and may have also included near-benthic and coastal water foraging. Foraging bouts were interspersed by traveling/resting/socializing periods of variable length at the surface, which may be needed for recovery. Diving patterns were stereotyped when foraging at particular depths irrespective of the habitat type. They altered their activity for different types of dives in response to metabolic demands, indicating that their foraging tactics were influenced by foraging costs and benefits.

When feeding in the shallow-water habitat, buzz depth and seabed depth at focal follow positions point to dolphins targeting benthic organisms during some of these dives. Opportunistic observations report Risso's dolphins feeding on non-gregarious benthic prey, like octopods in very shallow-waters (Ruiz et al., 2011). Stomach contents from stranded specimens from another location reveal that the benthic octopus *Eledone cirrosa* can represent up to 55% of the cephalopod prey consumed by this species (Clarke and Pascoe, 1985; Blanco et al., 2006), which would support the potential benthic feeding strategy inferred from data presented here. Nevertheless, foraging patterns were comparable when diving at similar depths but in different habitats.

Furthermore, dolphins feeding in deep-water exhibited several adaptations to reduce the energy cost of locomotion when searching for food at different depths, such as the use of gliding gaits and higher pitch angles during ascent and descent (**Table 3**). Therefore, despite the longer transit distance to forage for deep-water resources, the dolphins managed to keep their average field metabolic rate similar across dive types (i.e.,

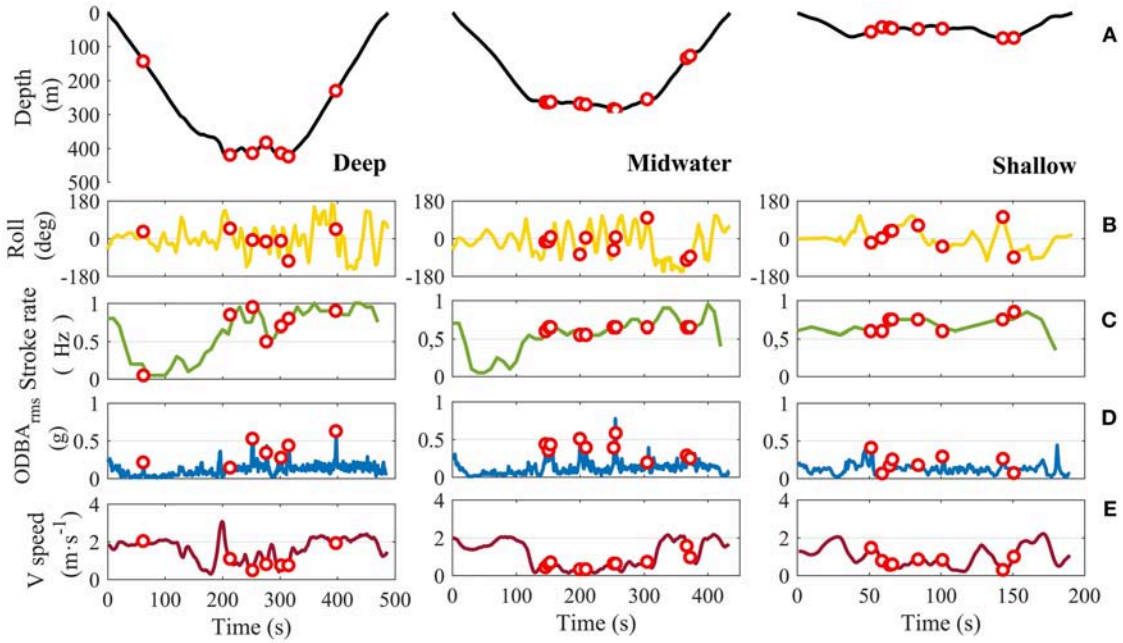

FIGURE 4 | Representative examples of fine-scale kinematics of a Risso's dolphin feeding in a deep-water habitat during deep, midwater, and shallow dives (dolphin with tag id gg13_267a). Dive profiles with buzzes in red **(A)** and associated measurements of body roll **(B)**, fluke stroke rate **(C)**, ODBA$_{rms}$ **(D)** and vertical swim speed **(E)** during the first dive of each type recorded on this tag (15 min after the tag on). Red dots indicate prey capture attempts (buzzes). ODBA$_{rms}$ corresponds to the root-mean-square (rms) of the 2-norm overall dynamic body acceleration (ODBA). Shallow and midwater dives started 5 min before and 12 min after the start of the deep dive, respectively, by the same dolphin and within the same general habitat. Note the gliding periods during the second part of the descent during deep and midwater dives.

shallow, intermediate, midwater, and deep). While our approach to estimate field metabolic rate relies on the assumption that the lowest and highest ODBA for each dive represent resting and maximal metabolic rate. This assumption may not be true for each individual dive, but this analysis allows us to explore the relative metabolic costs within dives, and accounts for possible changes in tag placement on overall ODBA. In addition, the heterogeneity in the regression estimate between ODBA and metabolic rate within an individual between dives was acceptable (C.V. of 32% for slope and of 0.7% for intercept), suggesting that there were not large variation in estimated costs between dives. It has been suggested that glide and stroke behavior helps conserve energy (Williams et al., 2017). Gliding during dive descent may help to reduce the metabolic costs of deep dives up to 40% to balance their need to perform long ascents while fluking actively. Similarly, Steller sea-lions diving to artificial prey patches from 5 to 50 m in experimental studies have been observed to decrease their overall (average) diving metabolic rate and activity level with dive depth (Fahlman et al., 2009, 2013). These adaptations may allow them to extend their time at depth in deeper dives and to make a greater number of prey attempts at the bottom of the dive; although bottom buzz rates remained comparable for shallow vs. deep dives. Foraging during transits from (and to a lesser extent to) foraging depths slightly increases the overall foraging rate during midwater dives compared to intermediate dives, but not in deep dives. This represented about a quarter (25%) of prey caught in deep dives, however if dolphins were still diving deep to forage, it suggests intermediate and midwater prey is of lower quality, with respect to prey energy content and/or prey density per unit volume, compared to deeper prey.

Hydroacoustic sampling within the same general area did not find greater prey density at depth (Benoit-Bird et al., 2017). Active acoustics data revealed that inter-individual distances in schools targeted by Risso's dolphins increased with total body length of prey items (Benoit-Bird et al., 2017). Moreover, the scattering layers were stratified vertically in terms of composition and size. The average length of individuals constituting mono-specific prey patches in the Catalina basin generally increased with depth, while the average density of prey in patches decreased. It therefore seems that the dolphins benefit from deeper foraging trips through accessing prey of varied quality rather than greater prey density. The longer IBI associated with deeper buzzes is consonant with dolphins targeting more widely spaced prey items (i.e., larger distance between individuals) during deep dives or that it requires longer handling times, an interpretation compatible with prey data reported here.

The records of higher $\dot{V}O_2$ in the bottom phase of deep dives is consistent with the registered increase in body roll and stroke rate and suggest a greater effort involved in the pursuit of deep-water prey items. These results support the notion of shift in prey type with increasing foraging depth and could be related to the observed escalation of prey length as

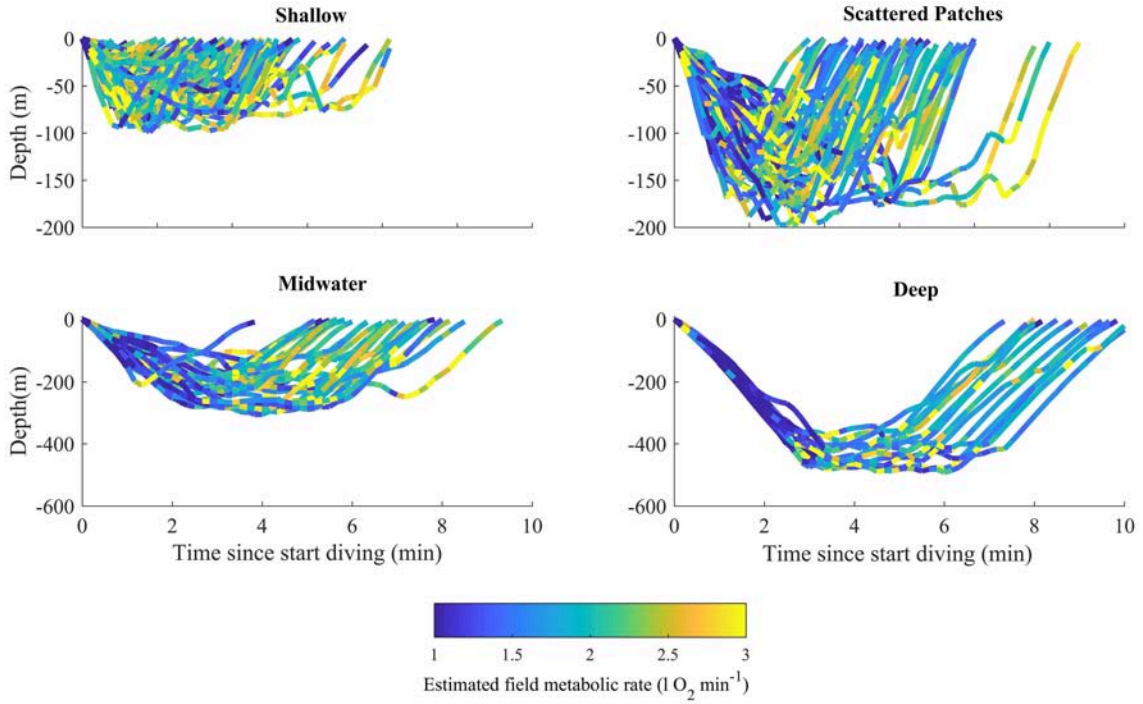

FIGURE 5 | Estimated field metabolic rate of Risso's dolphins in foraging dives performed within the deep-water habitat. Colored lines represent estimates of the field metabolic rate as a function of dive time and depth of the dolphin for each dive type, showing maximum estimated value per every 10 s window.

a function of depth. Stomach contents from stranded Risso's dolphins reveal consumption of large mesopelagic cephalopods, including the family of muscular squid Ommastrephiidae. Examples are the jumbo squid *Dosidicus gigas* (García-Godos and Cardich, 2010; Yates and Palavecino-Sepúlveda, 2011) or the neon flying squid *Ommastrephes bartramii* (Fernández et al., 2017). Such squid, including species from genera Todarodes, have strong locomotor abilities (O'dor and Webber, 1991) and present high energy density per unit of wet weight (3–4.5 kJ g^{-1} wet weight Clarke et al., 1985), constituting a potential high-quality target for Risso's dolphins during deep dives.

Data on swimming speeds of the dolphins while foraging at the bottom could not be estimated reliably in this study (but see Cade et al., 2017), however the relatively high vertical swimming speeds recorded in the bottom phase of deep dives (up to 4.5 m s^{-1}) (**Figure 4**), are coherent with dolphins chasing prey at depth. Deep-water sprints associated with capturing large squid have been described in short-finned pilot whales (*Globicephala macrorhynchus)* (Aguilar de Soto et al., 2008). Similarly, Aoki et al. (2012) reported bursts of speed in sperm whales (*Physeter macrocephalus*), suggesting that they performed these bursts to catch powerful and nutritious deep-water prey (i.e., large and/or muscular). In deep dives, we found no strong evidence of longer buzzes that have been associated with the capture of larger prey items in beaked whales (Johnson et al., 2008), although it may depend on the clicking rate and closing speed at which targets are approached. Nevertheless, the apparently high levels of exercise undertaken by Risso's dolphins during deep-water feeding recorded here are highly significant, together with the measured increase of total body length of prey items in schools targeted by these dolphins as a function of depth. This evidence points to a potential common strategy of some deep-diving toothed whales, in which the capture of larger, more nutritious prey in deep-waters may compensate for the higher metabolic costs of performing longer foraging dives at depth.

Some deep diving species, such as sperm whales and pilot whales, adapt to circadian migrations of prey distribution (Watwood et al., 2006; Aoki et al., 2007; Aguilar de Soto et al., 2008) and exploit deep-water resources when they are available at shallower depths at night. Other species, like Blainville's beaked whales (*Mesoplodon densirostris*) seem to adjust little (Arranz et al., 2011). All prey layers in the deep-water habitat of Risso's dolphins, other than the deepest, have been described to perform diel vertical migrations (Benoit-Bird et al., 2017). It is therefore possible that these dolphins benefit from the availability of deep-water prey in shallower waters at night, so as to reduce the apparently higher energetic costs involved in foraging at depth. Soldevilla et al. (2010) reported higher click detection rates of Risso's dolphins at night within the Catalina basin, suggesting either a higher feeding rate or shallower foraging depths. A few data about night-time foraging behavior of Risso's dolphins presented here are inconclusive, limiting interpretation of whether, and to what extent, this species adapts to circadian changes in prey distribution. Collection of night-time tag data

on foraging dolphins would be needed to better understand the feeding patterns of this species.

A number of methods have been developed to estimate metabolic rate in free-ranging marine mammals. In pinnipeds and smaller cetaceans, indirect measurements have been made using doubly labeled water, or species-specific calibrations of proxies of energy expenditure, such as heart rate and activity (Butler et al., 2004; Maresh et al., 2014). In larger cetaceans, heart rate has seldom been measured *in situ*, nor has the relationship between activity and metabolic cost been validated. However, activity correlates reasonably well with diving metabolic rate in Steller sea-lions (Fahlman et al., 2008, 2013). Recent work has also determined the RMR during restrained near-shore shallow diving or off-shore deep-diving in bottlenose dolphins undergoing capture-release health assessments (Fahlman et al., 2018). Indeed, there is a relative similarity in the deep diving capacity, anatomy, morphology, and body structure of bottlenose dolphins and Risso's dolphins. Despite the fact bottlenose dolphins are within Delphininae and Risso's dolphins within Globicephalinae, groups separated by about 10 million years of evolution, we hypothesize that a comparable relationship exists in Risso's dolphin. While we have made the assumption that the maximal and minimal ODBA represent maximal and resting $\dot{V}O_2$, respectively, we cannot confirm that these are true estimates of these two measures. This is especially true for the resting ODBA, where the variability was higher for tag durations that were < 4 h (**Figures S1, S2**). However, for maximal ODBA and minimal ODBA for tag durations > 4 h and up to 13.5 h there were no systematic trends with tag duration. We therefore argue that if these estimated minimal or maximal values were grossly over- or underestimated, we would have seen at least one outlier for 13 dolphins with an overall tag duration of 92 h. We also used two independent methods, based on Kleiber's equation (Kleiber, 1947) and Fahlman et al. (2018), to estimate the RMR in free-ranging Risso's dolphins. This was to address the caveats associated with the application of respirometry data from restrained bottlenose dolphins in relatively warm water, since temperature differences have a potential impact. Consequently, the estimated absolute metabolic rate is higher in the larger Risso's dolphin, whereas the mass-specific metabolic rate is lower (Lavigne et al., 1986). Although the results of the three methods varied between 1 and 3 l O_2 min^{-1}, they all reveal a consistent overall consumption rate across dive types (**Figure 5**), indicating that Risso's dolphins compensate for energetic costs associated with diving, swimming and feeding at different depths (Davis et al., 2004).

The calculated aerobic dive limit (cADL), the total O_2 stores divided by the diving $\dot{V}O_2$, provides a useful index to indicate whether the animal mainly forages aerobically or possibly uses anaerobic pathways (Butler and Jones, 1997). The majority of diving animals are thought to perform most dives well within their cADL, since this maximizes long-term foraging efficiency (Costa, 2001). Nevertheless, there are some notable examples like fur seals that appear to regularly dive outside their cADL (Costa et al., 2001). In the current study, we used the estimated mass-specific O_2 stores from the bottlenose dolphin [36 ml kg^{-1}, see Table 5 in Ponganis (2011)] and the average diving $\dot{V}O_2$ for each dive type (via Equation 3.2 in Fahlman et al., 2018) to estimate cADL. This resulted in a cADL ranging between 14.8 and 16.2 min and 8.9–9.7 min for adult and non-adult Risso's dolphins, respectively. While our estimated diving $\dot{V}O_2$ entail a number of uncertainties, they provide an initial estimate of energy use and indicate that all dives in the current study are apparently within the estimated cADL.

The Risso's dolphins in this study fed in shallow and deep-water habitats, foraging in different depth layers in deep-waters (occasionally within the same dive) and possibly benthically near the shore when in shallow-waters. In order to balance the energetic needs and costs of foraging at increased distances from the surface, these dolphins altered their dive kinematics to minimize energy consumption during longer transits and extended feeding time with increased depth. They thus allowed for a higher number of prey encounters per dive. Moreover, in spite of the increased overall cost of deep dives, they left longer intervals between prey capture attempts during deep dives. Even faced with the increased need to manage oxygen during deeper and longer dives, prey capture appeared to be more energetic during deep foraging. To maintain energetic returns at increasing distances from the surface, Risso's dolphins appear to choose to feed on larger prey at increasing depth, which points to a potential increased prey size-distance relationship for these predators. This strategy is however difficult to measure in free-ranging diving animals. This adaptive strategy appears to increase their foraging efficiency both within and between foraging bouts, thus enhancing their fitness throughout different habitats. Together with this, these predators show an apparent flexibility in using a variety of resources while maintaining their average metabolic rates per dive similar across foraging depths.

DATA AVAILABILITY

Datasets are available on request. The raw data supporting the conclusions of this manuscript will be made available by the authors, without undue reservation, to any qualified researcher.

AUTHOR CONTRIBUTIONS

ASF, JC, BS, EH, JG, AS, SD, KB-B, and PA carried out the experiments. KB-B, BS, PT, JG, ASF, AF, PA conceived the presented idea. KB-B, EH, ASF, AS, SD, and PA performed the computations. PA wrote the manuscript with support from JG, AF, and PT. The project was supervised and funding provided by KB-B, BS, PT, and JC. All authors discussed the results and contributed to the final manuscript.

FUNDING

Funding for the SOCAL-BRS project was provided by the Chief of Naval Operations Environmental Readiness Division, the US

Navy's Living Marine Resources Program, and the Office of Naval Research Marine Mammal Program. Experiments were performed under the US National Marine Fisheries Service (NMFS) (Permit # 14534-2), Channel Islands National Marine Sanctuary (Permit # 2010-003) (BS principal investigator for both) and IACUC permits issued to the project investigators. The Strategic Environmental Research and Development Program via an Army Corps of Engineers Contract (KB-B and BS) provided funding for data collection and prey analysis. PT acknowledges support from ONR grant N00014-15-1-2553 and from the MASTS pooling initiative (Marine Alliance for Science and Technology for Scotland; supported by the Scottish Funding Council, grant reference HR09011, and contributing institutions).

ACKNOWLEDGMENTS

We would like to thank Selene Fregosi for endless logistical support and effort in processing visual data, the crew of the R/V *Truth* for their help in the field and the two reviewers for their critical review of this manuscript. The authors wish to acknowledge the University of St Andrews Library Open Access Fund for support with Open Access costs.

SUPPLEMENTARY MATERIAL

The Supplementary Material for this article can be found online at: https://www.frontiersin.org/articles/10.3389/fevo.2019.00053/full#supplementary-material

REFERENCES

Acevedo-Gutiérrez, A., Croll, D. A., and Tershy, B. R. (2002). High feeding costs limit dive time in the largest whales. *J. Exp. Biol.* 205, 1747–1753.

Aguilar de Soto, N., Johnson, M., Madsen, P. T., Díaz, F., Domínguez, I., Brito, A., et al. (2008). Cheetahs of the deep sea: deep foraging sprints in short finned pilot whales off tenerife (Canary Islands). *J. Anim. Ecol.* 77, 936–947. doi: 10.1111/j.1365-2656.2008.01393.x

Andersen, K. H., Berge, T., Gonçalves, R. J., Hartvig, M., Heuschele, J., Hylander, S., et al. (2016). Characteristic sizes of life in the oceans, from bacteria to whales. *Ann. Rev. Mar. Sci.* 8, 217–241. doi: 10.1146/annurev-marine-122414-034144

Angel, M. V., and Boxshall, G. A. (1990). Life in the benthic boundary layer: connections to the mid-water and sea floor. *Philo. Transac. R. Soc. Lond. Series A* 331, 15–28. doi: 10.1098/rsta.1990.0053

Aoki, K., Amano, M., Mori, K., Kourogi, A., Kubodera, T., and Miyazaki, N. (2012). Active hunting by deep-diving sperm whales: 3d dive profiles and maneuvers during bursts of speed. *Mar. Ecol. Progr. Ser.* 444, 289–301. doi: 10.3354/meps09371

Aoki, K., Amano, M., Yoshioka, M., Mori, K., Tokuda, D., and Miyazaki, N. (2007). Diel diving behavior of sperm whales off japan. *Mar. Ecol. Progr. Ser.* 349, 277–287. doi: 10.3354/meps07068

Arranz, P., Aguilar de Soto, N., Madsen, P. T., Brito, A., Bordes, F., and Johnson, M. (2011). Following a foraging fish-finder: diel habitat use of blainville's beaked whales revealed by echolocation. *PLoS ONE* 6:E28353. doi: 10.1371/journal.pone.0028353

Arranz, P., Benoit-Bird, K. J., Brandon Southall, L., John, C., Ari, S., Friedlaender, A., et al. (2018). Risso's Dolphins Plan Foraging Dives. *J. Exp. Biol.* 221:jeb165209. doi: 10.1242/jeb.165209

Arranz, P., Deruiter, S. L., Stimpert, A. K., Neves, S., Friedlaender, A. S., Goldbogen, J. A., et al. (2016). Discrimination of fast click series produced by tagged risso's dolphins (*Grampus Griseus*) for echolocation or communication. *J. Exp. Biol.* 219, 2898–2907. doi: 10.1242/jeb.144295

Benoit-Bird, K. J., Moline, M. A., and Southall, B. L. (2017). Prey in oceanic sound scattering layers organize to get a little help from their friends. *Limnol. Oceanogr.* 62, 2788–2798. doi: 10.1002/lno.10606

Blanco, C., Raduán, M. A., and Raga, J. A. (2006). Diet of risso's dolphin (*Grampus Griseus*) in the western mediterranean sea. *Sci. Mar.* 70, 407–411.

Brooks, M. E., Kristensen, K., Van Benthem, K. J., Magnusson, A., Berg, C. W., Nielsen, A., et al. (2017). Glmmtmb balances speed and flexibility among packages for zero-inflated generalized linear mixed modeling. *R J.* 9, 378–400. doi: 10.32614/RJ-2017-066

Butler, P. J., Green, J. A., Boyd, I. L., and Speakman, J. R. (2004). Measuring metabolic rate in the field: the pros and cons of the doubly labelled water and heart rate methods. *Func. Ecol.* 18, 168–183. doi: 10.1111/j.0269-8463.2004.00821.x

Butler, P. J., and Jones, D. R. (1997). Physiology of diving birds and mammals. *Physiol. Rev.* 77 837–899. doi: 10.1152/physrev.1997.77.3.837

Cade, D. E., Barr, K. R., Calambokidis, J., Friedlaender, A. S., and Goldbogen, J. A. (2017). Determining forward speed from accelerometer jiggle in aquatic environments. *J. Exp. Biol.* 221(Pt 2):jeb170449. doi: 10.1242/jeb.170449

Carbone, C., and Houston, A. I. (1996). The optimal allocation of time over the dive cycle: an approach based on aerobic and anaerobic respiration. *Anim. Behav.* 51, 1247–1255. doi: 10.1006/anbe.1996.0129

Clarke, A., Clarke, M. R., Holmes, L. J., and Waters, T. D. (1985). Calorific values and elemental analysis of eleven species of oceanic squids (*Mollusca: Cephalopoda*). *J. Mar. Biol. Assoc. U.K.* 65, 983–986. doi: 10.1017/S0025315400019457

Clarke, M., and Pascoe, P. (1985). The stomach contents of a risso's dolphin (*Grampus Griseus*) stranded at thurleston, south devon. *J. Mar. Biol. Assoc. U.K.* 65, 663–665. doi: 10.1017/S0025315400052504

Clarke, M. R. (1996). Cephalopods as prey. part 3. cetaceans. philosophical transactions of the royal society of london. *Ser. B. Biol. Sci.* 352, 1105–1112.

Costa, D. P. (2001). "*Diving Physiology of Marine* Vertebrates," in *eLS* (Chichester: John Wiley and Sons, Ltd.) doi: 10.1002/9780470015902.a0004230

Costa, D. P., Gales, N. J., and Goebel, M. E. (2001). Aerobic dive limit: how often does it occur in nature? *Compar. Biochem. Physiol.* 129, 771–783. doi: 10.1016/S1095-6433(01)00346-4

Croll, D. A., Acevedo-Gutiérrez, A., Tershy, B. R., and Urbán-Ramírez, J. (2001). The Diving Behavior Of Blue And Fin Whales: Is Dive Duration Shorter Than Expected Based On Oxygen Stores? *Compar. Biochem. Physiol. Part A.* 129, 797–809. doi: 10.1016/S1095-6433(01)00348-8

Daniel, S., Korine, C., and Pinshow, B. (2008). Central-place foraging in nursing, arthropod-gleaning bats. *Can. J. Zool.* 86, 623–626. doi: 10.1139/Z08-041

Davis, R. W., Polasek, L., Watson, R., Fuson, A., Williams, T. M., and Kanatous, S. B. (2004). The diving paradox: new insights into the role of the dive response in air-breathing vertebrates. *Compar. Biochem. Physiol. Part A.* 138, 263–268. doi: 10.1016/j.cbpb.2004.05.003

Deruiter, S. L., Bahr, A., Blanchet, M.-A., Hansen, S. F., Kristensen, J. H., Madsen, P. T., et al. (2009). Acoustic behaviour of echolocating porpoises during prey capture. *J. Exp. Biol.* 212, 3100–3107. doi: 10.1242/jeb.030825

Doniol-Valcroze, T., Lesage, V., Giard, J., and Michaud, R. (2011). Optimal foraging theory predicts diving and feeding strategies of the largest marine predator. *Behav. Ecol.* 22, 880–888. doi: 10.1093/beheco/arr038

Fahlman, A., Brodsky, M., Wells, R., Mchugh, K., Allen, J., Barleycorn, A., et al. (2018). Field energetics and lung function in wild bottlenose dolphins *Tursiops truncatus* in sarasota bay florida. *R. Soc. Open Sci.* 17:171280. doi: 10.1098/rsos.171280

Fahlman, A., Hooker, S. K., Olszowka, A., Bostrom, B. L., and Jones, D. R. (2009). Estimating the effect of lung collapse and pulmonary shunt on gas exchange

during breath-hold diving: the scholander and kooyman legacy. *Res. Physiol. Neurobiol.* 165, 28–39. doi: 10.1016/j.resp.2008.09.013

Fahlman, A., Svärd, C., Rosen, D. A. S., Wilson, R. P., and Trites, A. W. (2013). Activity as a proxy to estimate metabolic rate and to partition the metabolic cost of diving vs. breathing in pre- and post-fasted steller sea lions. *Aquat. Biol.* 18, 175–184. doi: 10.3354/ab00500

Fahlman, A., Wilson, R., Svärd, C., Rosen, D. A. S., and Trites, A. W. (2008). Activity and diving metabolism correlate in steller sea lion *Eumetopias Jubatus*. *Aquat. Biol.* 2, 75–84. doi: 10.3354/ab00039

Fernández, A., Sierra, E., Díaz-Delgado, J., Sacchini, S., Sánchez-Paz, Y., Suárez-Santana, C., et al. (2017). Deadly acute decompression sickness in risso's dolphins. *Sci. Rep.* 7:13621. doi: 10.1038/s41598-017-14038-z

Friedlaender, A. S., Johnston, D. W., Tyson, R. B., Kaltenberg, A., Goldbogen, J., Stimpert, A. K., et al. (2016). Multiple-stage decisions in a marine central-place forager. *R. Soc. Open Sci.* 3:160043. doi: 10.1098/rsos.160043

García-Godos, I., and Cardich, C. (2010). First mass stranding of risso's dolphins (*Grampus griseus*) in peru and its destiny as food and bait. *Mar. Biodiver. Records* 3, 1–4. doi: 10.1017/S1755267209991084

Gibb, H., Andersson, J., and Johansson, T. (2016). Foraging loads of red wood ants: *Formica Aquilonia* (*Hymenoptera*: *Formicidae*) in relation to tree characteristics and stand age. *Peerj* 4:E2049. doi: 10.7717/peerj.2049

Goldbogen, J. A., Calambodkis, J., Croll, D. A., Mckenna, M. F., Oleson, E., Potvin, J., et al. (2012). Scaling of lunge feeding performance in rorqual whales: mass-specific energy expenditure increases with body size and progressively limits diving capacity. *Func. Ecol.* 26, 216–226. doi: 10.1111/j.1365-2435.2011.01905.x

Halsey, L. G. (2017). Relationships grow with time: a note of caution about energy expenditure-proxy correlations, focussing on accelerometry as an example. *Func. Ecol.* 31, 1176–1183. doi: 10.1111/1365-2435.12822

Halsey, L. G., Shepard, E. L. C., and Wilson, R. P. (2011). Assessing the development and application of the accelerometry technique for estimating energy expenditure. *Compar. Biochem. Physiol. Part A* 158, 305–314. doi: 10.1016/j.cbpa.2010.09.002

Hazen, E. L., Friedlaender, A. S., and Goldbogen, J. A. (2015). Blue whales (balaenoptera musculus) optimize foraging efficiency by balancing oxygen use and energy gain as a function of prey density. *Sci. Adv.* 1:e1500469. doi: 10.1126/sciadv.1500469

Houston, A. I., and McNamara, J. M. (1985). A general theory of central-place foraging for single-prey loaders. *Theor. Popul. Biol.* 28, 233–262. doi: 10.1016/0040-5809(85)90029-2

Jefferson, T. A., Webber, M. A., Pitman, R., and Jarrett, B. (2008). *Marine Mammals of the World: a Comprehensive Guide to Their Identification.* London: Academic Press/Elsevier, 573.

Johnson, M., Hickmott, L. S., Aguilar Soto, N., and Madsen, P. T. (2008). Echolocation behaviour adapted to prey in foraging blainville's beaked whale (*Mesoplodon Densirostris*). *Proc. R. Soc. B* 275, 133–139. doi: 10.1098/rspb.2007.1190

Johnson, M., Madsen, P. T., Zimmer, W. M. X., Aguilar Soto, N., and Tyack, P. L. (2004). Beaked whales echolocate on prey. *Biol. Lett.* 271, S383–S386. doi: 10.1098/rsbl.2004.0208

Johnson, M., and Tyack, P. L. (2003). A digital acoustic recording tag for measuring the response of wild marine mammals to sound. *IEEE J. Oceanic Eng.* 28, 3–12. doi: 10.1109/JOE.2002.808212

Kleiber, M. (1947). Body size and metabolic rate. *Physiol. Rev.* 27, 511–541. doi: 10.1152/physrev.1947.27.4.511

Kramer, D. L. (1988). The behavioral ecology of air breathing by aquatic animals. *Can. J. Zool.* 66, 89–94. doi: 10.1139/z88-012

Lavigne, D. M., Innes, S., Worthy, G. A. J., Kovacs, K. M., Schmitz, O. J., and Hickie, J. P. (1986). Metabolic rates of seals and whales. *Can. J. Zool.* 64, 279–284. doi: 10.1139/z86-047

Lenth, R. (2018). *Emmeans: Estimated Marginal Means, Aka Least-Squares Means.* R Package Version 1.3.0. Available online at: https://cran.r-project.org/package=emmeans

Maresh, J. L., Simmons, S. E., Crocker, D. E., Mcdonald, B. I., Williams, T. M., and Costa, D. P. (2014). Free-swimming northern elephant seals have low field metabolic rates that are sensitive to an increased cost of transport. *J. Exp. Biol.* 217, 1485–1495. doi: 10.1242/jeb.094201

Miller, P. J. O., Johnson, M. P., Tyack, P. L., and Terray, E. A. (2004). Swimming gaits, passive drag and buoyancy of diving sperm whales *Physeter macrocephalus*. *J. Exp. Biol.* 207, 1953–1967. doi: 10.1242/jeb.00993

Moline, M. A., Benoit-Bird, K., O'Gorman, D., and Robbins, I. C. (2015). Integration of scientific echo sounders with an adaptable autonomous vehicle to extend our understanding of animals from the surface to the bathypelagic. *J. Atmos. Ocean. Technol.* 32, 2173–2186. doi: 10.1175/JTECH-D-15-0035.1

O'dor, R. K., and Webber, D. M. (1991). Invertebrate athletes: trade-offs between transport efficiency and power density in cephalopod evolution. *J. Exp. Biol.* 160, 93–112.

Orians, G. H., and Pearson, N. E. (1979). "On The Theory Of Central Place Foraging," in *Analysis of Ecological Systems*, eds D. J. Horn, R. D. Mitchell, and G. R.Stairs (Columbus, OH: The Ohio State University Press), 154–177.

Parker, K. L., Gillingham, M. P., Hanley, T. A., and Robbins, C. T. (1996). Foraging efficiency: energy expenditure versus energy gain in free-ranging black-tailed deer. *Can. J. Zool.* 74, 442–450. doi: 10.1139/z96-051

Ponganis, P. J. (2011). Diving mammals. *J. Compar. Physiol. B* 1, 447–465.

Ridgway, S. H., Moore, P. W., Carder, D. A., and Romano, T. A. (2014). Forward shift of feeding buzz components of dolphins and belugas during associative learning reveals a likely connection to reward expectation, pleasure and brain dopamine activation. *J. Exp. Biol.* 217, 2910–2919. doi: 10.1242/jeb.100511

Ruiz, L., Neves, S., Martín, V., Pérez-Gil, M., Tejedor, M., Pérez-Gil, E., et al. Brederlau (2011). *Risso's Dolphin (Grampus Griseus) Population Characteristics Of Canary Islands With An Observation On Octopus Predation*. dissertation, Society For The Study Of Cetaceans In The Canary Archipelago (Secac).

Savage, P. D., Toth, M. J., and Ades, P. A. (2007). A re-examination of the metabolic equivalent concept in individuals with coronary heart disease. *J. Cardiopulm. Rehabil. Preven.* 27, 143–148. doi: 10.1097/01.HCR.0000270693.16882.d9

Sawada, K., and Furusawa, M., and Williamson, M. (1993). Conditions for the precise measurement of fish target strength *in situ*. *Fish. Sci.* 20, 15–21.

Schoener, T. W. (1969). Models of optimal size for solitary predators. *Am. Nat.* 103, 277–313. doi: 10.1086/282602

Schoener, T. W. (1979). Generality of the size-distance relation in models of optimal feeding. *Am. Nat.* 114, 902–914. doi: 10.1086/283537

Soldevilla, M. S., Wiggins, S. M., and Hildebrand, J. A. (2010). Spatial and temporal patterns of risso's dolphin echolocation in the southern california bight. *J. Acoust. Soc. Am.* 127, 120–132. doi: 10.1121/1.3257586

Southall, B., Moretti, D., Abraham, B., Calambokidis, J., Deruiter, S., and Tyack, P. L. (2012). Marine mammal behavioral response studies in southern california: advances in technology and experimental methods. *Mar. Tech. Soc. J.* 46, 48–59. doi: 10.4031/MTSJ.46.4.1

Watanabe, Y. Y., Ito, M., and Takahashi, A. (2014). Testing optimal foraging theory in a penguin–krill system. *Proc. R. Soc. B* 281:20132376. doi: 10.1098/rspb.2013.2376

Watanabe, Y. Y., Sato, K., Watanuki, Y., Takahashi, A., Mitani, Y., Amano, M., et al. (2011). Scaling of swim speed in breath-hold divers. *J. Anim. Ecol.* 80, 57–68. doi: 10.1111/j.1365-2656.2010.01760.x

Watanabe, Y. Y., and Takahashi, A. (2013). Linking animal-borne video to accelerometers reveals prey capture variability. *Proc. Natl. Acad. Sci. U.S.A.* 110, 2199–2204. doi: 10.1073/pnas.1216244110

Watwood, S. L., Miller, P. J. O., Johnson, M. P., Madsen, P. T., and Tyack, P. L. (2006). Deep-diving foraging behavior of sperm whales (Physeter macrocephalus). *J. Anim. Ecol.* 75, 814–825. doi: 10.1111/j.1365-2656.2006.01101.x

Weibel, E. R., and Hoppeler, H. (2005). Exercise-induced maximal metabolic rate scales with muscle aerobic capacity. *J. Exp. Biol.* 208, 1635–1644. doi: 10.1242/jeb.01548

Williams, T. M. (2001). Intermittent swimming by mammals: a strategy for increasing energetic efficiency during diving1. *Am. Zool.* 41, 166–176. doi: 10.1668/0003-1569(2001)041[0166:ISBMAS]2.0.CO;2

Williams, T. M., Davis, R. W., Fuiman, L. A., Francis, J., Le Boeuf, B. J., Horning, M., et al. (2000). Sink or swim: strategies for cost-efficient diving by marine mammals. *Science* 288, 133–136. doi: 10.1126/science.288.5463.133

Williams, T. M., Kendall, T. L., Richter, B. P., Ribeiro-French, C. R., John, J. S., Odell, K. L., et al. (2017). Swimming and diving energetics in dolphins: a stroke-by-stroke analysis for predicting the cost of flight responses in wild odontocetes. *J. Exp. Biol.* 220, 1135–1145. doi: 10.1242/jeb.154245

Wilson, R. P., Mcmahon, C. R., Quintana, F., Frere, E., Scolaro, A., Hays, G. C., et al. (2011). N-Dimensional animal energetic niches clarify behavioural options in a variable marine environment. *J. Exp. Biol.* 214, 646–656. doi: 10.1242/jeb.044859

Wilson, R. P., White, C. R., Quintana, F., Halsey, L. G., Liebsch, N., Martin, G. R., et al. (2006). Moving towards acceleration for estimates of activity-specific metabolic rate in free-living animals: the case of the cormorant. *J. Anim. Ecol.* 75, 1081–1090. doi: 10.1111/j.1365-2656.2006.01127.x

Wood, S. N. (2011). Fast stable restricted maximum likelihood and marginal likelihood estimation of semiparametric generalized linear models. *J. R. Stat. Soc. B* 73, 3–36. doi: 10.1111/j.1467-9868.2010.00749.x

Yates, O., and Palavecino-Sepúlveda, P. (2011). On the stomach contents of a risso's dolphin (*Grampus griseus*) from chile, southeast pacific. *Latin Am. J. Aquat. Mamm.* 9, 171–173. doi: 10.5597/lajam00185

Conflict of Interest Statement: The authors declare that the research was conducted in the absence of any commercial or financial relationships that could be construed as a potential conflict of interest.

The handling editor is currently co-organizing a Research Topic with one of the authors, AF, and confirms the absence of any other collaboration.

Copyright © 2019 Arranz, Benoit-Bird, Friedlaender, Hazen, Goldbogen, Stimpert, DeRuiter, Calambokidis, Southall, Fahlman and Tyack. This is an open-access article distributed under the terms of the Creative Commons Attribution License (CC BY). The use, distribution or reproduction in other forums is permitted, provided the original author(s) and the copyright owner(s) are credited and that the original publication in this journal is cited, in accordance with accepted academic practice. No use, distribution or reproduction is permitted which does not comply with these terms.

frontiers in Ecology and Evolution

ORIGINAL RESEARCH
published: 24 April 2019
doi: 10.3389/fevo.2019.00134

Behavioral and Physiological Responses of Scandinavian Brown Bears (*Ursus arctos*) to Dog Hunts and Human Encounters

Luc Le Grand[1], Neri H. Thorsen[2], Boris Fuchs[3], Alina L. Evans[3], Timothy G. Laske[4], Jon M. Arnemo[3,5], Solve Sæbø[6] and Ole-Gunnar Støen[1,2]*

[1] Faculty of Environmental Sciences and Natural Resource Management, Norwegian University of Life Sciences, Ås, Norway, [2] Norwegian Institute for Nature Research, Trondheim, Norway, [3] Department of Forestry and Wildlife Management, Faculty of Applied Ecology and Agricultural Sciences, Inland Norway University of Applied Sciences, Koppang, Norway, [4] Department of Surgery, University of Minnesota, Minneapolis, MN, United States, [5] Department of Wildlife, Fish and Environmental Studies, Swedish University of Agricultural Sciences, Umeå, Sweden, [6] Faculty of Chemistry, Biotechnology and Food Science, Norwegian University of Life Sciences, Ås, Norway

Innovations in biologging have offered new possibilities to better understand animals in their natural environment. Biologgers can be used by researchers to measure the impact of human disturbances on wildlife and guide conservation decisions. In this study, the behavioral and physiological responses of brown bears (*Ursus arctos*) to hunts using dogs (*Canis lupus familiaris*) and human encounters were assessed to better understand the impact of human outdoor activities on brown bears. In Scandinavia, brown bear hunting and the use of dogs during hunts is increasing in popularity. Nonetheless, not every hunt leads to a killed bear. This means that for each bear that is shot, multiple bears may be chased but not killed. In addition, bears can also be disturbed when encountering non-hunting humans. Heart rates, body temperatures, GPS coordinates and dual-axis activity data were collected from 52 simulated hunts (a simulated hunt using dogs with the bear allowed to flee at the end) and 70 human encounters (humans intentionally approaching the bear) that were carried out on 28 free-ranging female brown bears in two study areas in Sweden. The results showed that: (1) simulated hunts had a greater impact and induced a greater energy cost than human encounters; (2) the amount of time bears rested the day after the simulated hunts increased linearly with the duration of the simulated hunts, implying a lasting behavioral impact relative to the intensity of the disturbance. Although not tested in this study, brown bears that are repeatedly disturbed by dog hunts and human encounters may be unable to compensate the disturbances' energy cost, and their fitness may, therefore, be altered. If it is the case, this effect should be accounted for by managers.

Keywords: activity, body temperature, carnivore, heart rate, human disturbance, hunting dog

OPEN ACCESS

Edited by:
Stan Boutin,
University of Alberta, Canada

Reviewed by:
Carl Soulsbury,
University of Lincoln, United Kingdom
Ximena J. Nelson,
University of Canterbury, New Zealand

****Correspondence:***
Luc Le Grand
luclegrandch@gmail.com

Specialty section:
This article was submitted to Behavioral and Evolutionary Ecology, a section of the journal Frontiers in Ecology and Evolution

Received: *29 November 2018*
Accepted: *03 April 2019*
Published: *24 April 2019*

Citation:
Le Grand L, Thorsen NH, Fuchs B, Evans AL, Laske TG, Arnemo JM, Sæbø S and Støen O-G (2019) Behavioral and Physiological Responses of Scandinavian Brown Bears (Ursus arctos) to Dog Hunts and Human Encounters. Front. Ecol. Evol. 7:134. doi: 10.3389/fevo.2019.00134

INTRODUCTION

Innovations in biologging have increasingly been used in the past few decades to better understand animals in their natural environment (Wilmers et al., 2015). The use of biologgers can also allow researchers to measure human disturbances and guide conservation decisions (Wilson et al., 2015). Hunting practices raise ethical questions and have spurred research on the physiology and

behavior of pursued animals (for example: foxes (*Vulpes vulpes*) (Kreeger et al., 1989), pumas (*Puma concolor*) (Bryce et al., 2017) or red deer (*Cervus elaphus*) (Jarnemo and Wikenros, 2014). Several variables may be used to measure how human outdoor activities disturb wild animals and to determine if the disturbances may incur extra energy costs. Longer traveled distances (Rode et al., 2007), higher heart rates (Kreeger et al., 1989; Ditmer et al., 2015) or higher body temperature (Evans et al., 2016) have, for example, been considered as indicators of disturbances that lead to extra energy costs. In addition, animals may run to flee, with the higher speeds demanding more energy (Pagano et al., 2018). They may also need to recover and rest after a disturbance, preventing their compensation of the lost energy.

Brown bears (*Ursus actos*) have been a game species in Sweden since 1943 (Swenson et al., 2017) with a hunting season starting on August 21st and ending when the quotas set by the county board are filled, or at the latest on October 15th. Family groups (adult females with dependent cubs) are protected but there are no age or sex specifications applied to the hunting quotas (Bischof et al., 2008). In Sweden, legal hunting by humans represents the primary cause of mortality for adult brown bears (Bischof et al., 2017), with the most common hunting method being based on the use of trained hunting dogs (*Canis lupus familiaris*) (Bischof et al., 2008). Dogs are released to pursue the bears with the hunters following and attempting to shoot the bear (hereafter dog hunts). Bear hunting is increasing in popularity with the number of hunters specialized in bear hunting rising (Swenson et al., 2017). There are no statistics known for Sweden, but when hunting black bears (*Ursus americanus*) in a similar way in Virginia (USA), the recorded success is generally low [20%, Vaughan and Inman (2002)]. This means that for each bear that is shot, multiple bears may be chased but not killed.

Hunting is not the only human outdoor activity that affects bears in Sweden. Bears flee when encountered by humans (Moen et al., 2012) and change their movement patterns for at least 2 days following the event (Ordiz et al., 2013b). In areas with higher road densities, bears adopt movement patterns that are more nocturnal and less diurnal, to avoid human activity (Ordiz et al., 2014). Bears avoid denning near roads (Elfström et al., 2008) and select more concealed denning sites near humans (Sahlén et al., 2011). Brown bears have a general anti-predator behavior toward humans. A behavior that is not only affected by hunting activities, but also by the year-round presence of humans. It is therefore important to understand the impacts of both dog hunts and human encounters on brown bears.

To better understand how human outdoor activities influence brown bears in Scandinavia, simulated hunts using dogs with the bear allowed to flee at the end (hereafter simulated hunts) and human encounters (humans intentionally approaching the bear) were conducted on GPS-collared female brown bears. For each experiment, five variables were measured: (1) the distance traveled by the bears, (2) their speed, (3) their heart rate, (4) their body temperature, and (5) their resting behavior. This was done within three different time periods: (1) during a control period (3 days prior to an experiment), (2) during the day of the experiment and (3) during the 2 days following the experiment. The following hypotheses were tested by comparing the five variables at the different time periods: [H1] Dog hunts and human encounters are a source of physiological and behavioral disturbance for brown bears. [H2] The physiological and behavioral impacts of dog hunts on brown bears are greater than the impact of human encounters. [H3] Dog hunts that last longer in time have greater physiological and behavioral impacts on brown bears. [H4] Dog hunts and human encounters have lasting physiological and behavioral effects on brown bears.

MATERIALS AND METHODS

Study Area

In Sweden, brown bears are distributed into three main populations (Norman, 2016). This study was carried out from 2014 to 2016 in two different areas covering the southernmost and northernmost bear subpopulations (61.50°N; 15.06°E & 66.76°N; 21.02°E). In both areas, the landscape is hilly and mostly covered by managed productive forest, mainly composed of Scots pine (*Pinus sylvestris*), Norway spruce (*Picea abies*) and birch (*Betula* spp.).

Data Collection

Human encounters and simulated hunts were conducted on 28 free-ranging female brown bears. The bears were equipped with a VHF transmitter implant (M1255B, Advanced Telemetry Systems, Isanti, USA); a GPS-Plus collar with GSM modems or Iridium modems with an included VHF transmitter and a dual-axis motion sensor (Vectronic Aerospace GmBh, Berlin, Germany); cardiac biologgers (Reveal XT, Medtronic, Minneapolis, USA) implemented with modified software (BearWare, Medtronic, Minneapolis, USA); and temperature biologgers (DST Centi-T, Star-Oddi, Gardabaer, Iceland). The biologgers were surgically implanted in the bears with the cardiac biologgers subcutaneous to the left of the sternum and the temperature biologgers in the abdomen of the bear (Arnemo and Evans, 2017). The cardiac biologgers continuously recorded the bears' inter-beat intervals (R-R, in milli seconds), based on electrocardiogram (ECG) measurements. Every 2 min the mean R-R interval was converted into a heart rate in beats per minute (bpm). The body temperatures of the bears were measured every 4 min with an accuracy of $\pm$ 0.01°C. The activity of the bear was measured as the true acceleration in two orthogonal directions at a frequency of six to eight times per second. The average of the activity values over 5 min for each orthogonal direction was then recorded in the GPS collar with its associated date and time (Friebe et al., 2014).

GPS coordinates of the bears were recorded by default every 30 min or every hour. During the human encounters and the simulated hunts, a GPS location was recorded every minute for 3 or 4 h. During some of the simulated hunts, the dogs were equipped with Ultra High Frequency (UHF) transmitters (Vectronic Aerospace GmbH, Berlin, Germany) that emitted a signal every second, triggering the recording of GPS coordinates every 70 s in the bears' GPS collars at $\leq$ 500 m. The GPS collars on the brown bears scanned for UHF signals for 1.5 s every 8 s, and the recording ended automatically 60 min after the last detection of a dog collar. Humans (hereafter observers) were equipped with

hand-held Garmin GPSMAP 60CSx or Astro 320 and the dogs were equipped with T 5 or DC40 Dog Devices, with all types of equipment being set to record a GPS coordinate every second (Garmin Ltd., Olathe, USA).

For more details on how the bears were captured and immobilized, please refer to Arnemo and Evans (2017). All captures were approved by the Swedish Ethical Committee on Animal Research (application numbers C7/12 and C18/15) and the Swedish Environmental Protection Agency (application numbers NV-00741-18 and NV-01758-14).

Experimental Design

Following the same methods presented by Moen et al. (2012), the human encounters were started between 8:30 and 14:30 local time (GMT+2). The observers walked toward the bear, intending to pass the bear at an approximate distance of 50 m, whilst talking to each other or to themselves if alone, simulating hikers. When the bear had been passed or when the bear ran away, they returned to the car and made sure not to encounter the bear a second time. The 70 human encounters were carried out in 2014 (1st June−7th August; $n = 17$), in 2015 (8th June−28th July; $n = 24$) and in 2016 (2nd June−20th August; $n = 29$). The minimum distance recorded between the observers and the bear was on average 55 ± 27 m (median 51 m, minimum 18 m, maximum 137 m; $n = 70$). In total, 25 female bears were used, with five subadults, 16 adults and four that were used when they were both subadults and adults.

Simulated hunts were started between 8:00 and 17:00. The observers with hunting dogs kept on a leash walked toward the bear until a dog showed interest in the scent of the bear, either in the wind or from its tracks, before the dogs were released and allowed to pursue the bear (**Figure 1**). The simulated hunt was stopped when the dogs came back to the observers or by the observers calling in or intercepting the path of the dogs. The simulated hunts were intended to last about 2 h but ended both earlier and later due to practicalities. During the same simulated hunt, one to six different dogs were used. However, only a maximum of two dogs were let loose simultaneously to hunt the bear. Bears were considered to be disturbed by both types of experiments if the minimum distance recorded between the bear and the observers or dogs at any time was < 200 m.

The 52 simulated hunts were carried out in 2014 (9th August−15th August; $n = 4$), in 2015 (11th June−2nd October; $n = 19$) and in 2016 (18th June−7th October; $n = 29$). The minimum distance recorded between the observers and / or the dogs and the bear was on average 20 ± 34 m (median 5 m, minimum 0 m, maximum 168 m; $n = 52$). The duration of a simulated hunt was defined as the time between when the observers and dogs started heading from the car toward the bear until when they were back at the car. Simulated hunts lasted on average 229 ± 104 min (median 198 min, minimum 67 min, maximum 508 min; $n = 52$). In total, 17 female bears were used, with two subadults, 14 adults and one that was used when it was both a subadult and an adult.

Some bears were used in multiple human encounters and / or simulated hunts during the same year. No research activities that could have affected the bears were carried out for at least 5 days before and 2 days after the experiments.

Data Processing and Statistical Analyses

All the data analyses and data processing were carried out using the statistical programming language and environment, R 3.4.2 (R Core Team, 2017). All data (GPS, activity, heart rate and body temperature) was stored in the WRAM database (Wireless Remote Animal Monitoring, Dettki et al., 2014).

Response Variables

The distance traveled by the bear was measured as the variable TRAVEL, which is the sum of all hourly displacements for each day. In this way, days with GPS coordinates taken with a different frequency were directly comparable. The distances (shortest distance between two points on the WGS84 ellipsoid) between the hourly positions were measured using the distGeo function from the geosphere package, version 1.5-7 (Hijmans, 2017). The maximum speed of the bear was measured as the variable MAXSPEED, which is the highest speed recorded of the day based on all hourly displacements within the 24 h. The heart rate of the bear was measured as the variable HEARTRATE30, which is the highest value measured by a rolling mean ran over all the measured heart rates of the day, with a window of 30 min and a constant forward shift of 2 min. When processing the heart rate data, a constant mismatch between the heart rate and the corresponding time was observed for some bears. The mismatch was corrected through using the correlation between the activity of the bear and its heart rate. Heart rate data was not used in the analysis if the activity data was not available or if the method led to a suggested time shift that was not consistent throughout the data. The body temperature of the bear was measured as the variable T_bAREA, which is the area under the curve of the measured body temperature values and above the median body temperature of the bear over a 24-h period. The median body temperature was based on data from 1st June to 30th September for each bear-year. Days when the bears were involved in research activities (human encounters, simulated hunts or captures) were not included in this data set. The area was calculated using a trapezoidal approximation (all points are connected by a direct line forming multiple trapezoids) using the AUC function from the DescTools package, version 0.99.23 (Signorell, 2017). The resting behavior of the bear was measured as the variable REST, which is the amount of time the bear was resting in minutes during a day. The two values for each orthogonal, measured by the dual-axis motion sensor, were summed resulting in a variable ranging from 0 to 510. A value lower than 23 was considered resting behavior (Gervasi et al., 2006).

Explanatory Variables

Human encounters and simulated hunts were considered as two different treatments in a binary variable, hereafter named TYPE. The variable PERIOD consisted of four unique levels. The 1st level represents the control period defined as the mean values recorded during the 3 days prior to the human encounter day or simulated hunt day. The 2nd level represents the day of the experiment. The 3rd and 4th levels represent the following and

FIGURE 1 | While being hunted, a brown bear can run in order to escape hunting dog(s) and sometimes end up lying on the ground with the dog(s) barking and running around it (baying). When the dog(s) is/are baying the bear, the hunter is typically sneaking in and shooting the bear. **(A)** Plott hound pursuing a bear during a simulated hunt. The dog is equipped with a collar (DC40 Dog Device) used to collect GPS coordinates, as well as a dog harness equipped with a UHF transmitter that triggers the recording of coordinates every 70 s in the GPS-Plus collar fitted on the bear. **(B)** Elkhound baying a bear during a simulated hunt. The same equipment as in **(A)** is illustrated. Scientific Illustration by Juliana D. Spahr, SciVisuals.com (reproduced with permission).

second day after the experiment, respectively. The age of the bears was considered in the binary variable AGE with subadult bears < 4 years old. The duration of the simulated hunts was also used as an explanatory variable.

Model Construction

Linear mixed effect models (LME) were fitted using TRAVEL, MAXSPEED, HEARTRATE30, T_bAREA and REST as response variables, and TYPE, PERIOD, AGE and the interactions as explanatory variables. The experiments' ID nested in the bears' ID were added as random factors. The normality of the residuals was improved by a square root transformation of the response in the TRAVEL, MAXSPEED, HEARTRATE30 and the T_bAREA models. The models were created using the lmer function from the lme4 package, version 1.1-14 (Bates et al., 2014) and fitted using the restricted maximum likelihood (REML) method, as the models were composed of small sample sizes. The final model was obtained by following the backward selection method. The significance of the variables and the interaction were computed using the Anova function from the car package, version 2.1-6 (Fox and Weisberg, 2011), with the type-III method. A pairwise analysis of the estimated marginal means (EMMs) was then performed to interpret the final models using the emmeans package, version 1.1. (Lenth, 2018). This method was used as the models had an unbalanced number of human encounters and simulated hunts (**Table 1**). The EMMs were based on a 0.95 confidence level with the Tukey correction method. Some of the 70 human encounters and 52 simulated hunts did not have data for all the response variables. For this reason, n varied between the different LME models (**Table 1**).

When only considering the simulated hunts data, the variables TRAVEL, MAXSPEED, HEARTRATE30, T_bAREA, and REST were used as response variables in LME models, with the duration of the simulated hunts, the variable AGE and the interaction as explanatory variables. In these models, the variables TRAVEL, MAXSPEED and T_bAREA were square root transformed to improve the normality of the residuals. The models were created following the same method as the method presented for the previous LME models but were created using the lme function from the nlme package, version 3.1-131 (Pinheiro et al., 2017). The model included the ID of the bears as a random factor, as some simulated hunts were carried out on the same bears (**Table 1**).

TABLE 1 | Number of human encounters and simulated hunts with complete data sets.

Variable:	N human encounters (N bears: Subadult, Adult, Both)	N simulated hunts (N bears: Subadult, Adult, Both)
TRAVEL	70 (5, 16, 4)	50 (2, 13, 1)
MAXSPEED	70 (5, 16, 4)	50 (2, 13, 1)
HEARTRATE30	21 (1, 8, 0)	26 (2, 9, 0)
T_bAREA	35 (5, 9, 2)	35 (3, 10, 0)
REST	60 (4, 15, 4)	46 (2, 13, 1)

The number of bears that were used when being subadult, adult or both are also indicated in brackets.

In the models HEARTRATE30 and REST with PERIOD, TYPE, AGE and the interactions as explanatory variables, the variable AGE and the corresponding interactions were not kept in the models after using the backward selection method. However, the interaction between PERIOD and TYPE was significant (all $P < 0.0001$). Both the PERIOD and TYPE variables were thus used in the pairwise analysis of the EMMs. In the models TRAVEL, MAXSPEED, and T_bAREA, the variables AGE, PERIOD and TYPE were kept in the models after using the backward selection method. All three explanatory variables were therefore used in the pairwise analysis of the EMMs.

RESULTS

The distances traveled by both adult and subadult bears were longer during the day of the simulated hunts than during the corresponding control periods (*post hoc* test: estimated difference: both adult and subadult: 755 ± 15 m, $P < 0.0001$, both 10% longer, range measured difference: Adult: −3 to 22 km, Subadult: −1 to 12 km) and longer than during the day of the human encounters (*post hoc* test: estimated difference both adult and subadult: = 527 ± 22 m, $P < 0.0001$, Adult: 3 %, Subadult: 4% longer). Adult and subadult bears did not travel longer distances on the day of the human encounters than during the corresponding control periods (both $P = 0.13$).

Both adult and subadult bears ran faster during the day of the simulated hunts than during the corresponding control periods (*post hoc* test: estimated difference: Adult: 679 ± 61 m h^{-1}, $P < 0.0001$, 31% faster, range measured difference: −280 to 6360 m h^{-1}, Subadult: 455 ± 94 m h^{-1}, $P = 0.0002$, 17% faster, range measured difference:−680 to 3580 m h^{-1}) and ran faster than during the day of the human encounters (*post hoc* test: estimated difference: both: 450 ± 62 m h^{-1}, $P < 0.0001$, Adult 10 % faster, Subadult: 16 % faster). Adult bears also ran faster the day of the human encounters than during the corresponding control periods (*post hoc* test: estimated difference: Adult: 216 ± 53 m h^{-1}, $P = 0.005$, 3% faster, range measured difference: −1470 −8850 m h^{-1}). Subadults, however, did not run faster on the day of the human encounters than during the corresponding control periods ($P > 0.90$).

The maximum heart rates were higher during the day of the simulated hunts than during the corresponding control periods (*post hoc* test: estimated difference = 7 ± 0.06 bpm, $P < 0.0001$, 7% higher, range measured difference: 4–106 bpm) and higher than during the day of the human encounters (*post hoc* test: estimated difference = 3 ± 0.12 bpm, $P < 0.0001$, 3% higher). Bears did not have a different maximum heart rate the day of the human encounters than during the corresponding control periods ($P = 0.18$, maximum measured difference: −50–106 bpm).

The body temperature areas of the adult bears were greater during the day of the simulated hunts than during the corresponding control periods (*post hoc* test: estimated difference = 1553 ± 59 T_bAREA, $P < 0.0001$, 12% greater) but not for subadult bears ($P = 0.15$). The body temperature areas of the bears were not greater during the day of the simulated hunts than during the day of the human encounters (Adult: $P = 0.64$, Subadult: $P = 0.57$). The body temperature areas of both adult and subadult bears were not different on the day of the human encounters compared to during the corresponding control periods (both $P > 0.90$).

The day after the simulated hunts, bears rested more than during the corresponding control periods (*post hoc* test: estimated difference = 68 ± 19 min, $P = 0.008$, 1% more, range measured difference: −4 h 15 min−5 h 15 min) but not more than during the day after the human encounters ($P = 0.62$). The day after the human encounters, bears did not rest more than during the corresponding control periods ($P > 0.90$). The amount of time bears rested the day after the simulated hunts increased linearly with the duration of the simulated hunts (**Figure 2**). Bears did not rest less during the day of the human encounters or the simulated hunts than during the corresponding control periods (both $P > 0.90$). Bears did not rest less during the day of the simulated hunts than the day of the human encounters ($P = 0.18$).

There was no difference between the control periods of the human encounters and the control periods of the simulated hunts (adults or subadults) for the distance traveled, the maximum speed, the maximum heart rate, the body temperature area or how long the bear rested (**Table 2**, all $P > 0.13$). There was no difference between the first and second days following the human encounters or the simulated hunts, compared to the corresponding control periods, for the distance traveled, the maximum speed, the maximum heart rate or the body temperature areas of the bears (all $P > 0.09$). The duration of the simulated hunts had no effect on the distance traveled, maximum speed, maximum heart rate, body temperature area or how long the bear rested the day of the simulated hunt (all $P > 0.15$).

DISCUSSION

During human encounters, adult bears ran faster than during the corresponding control periods, but did not have higher heart rates, higher body temperatures or travel longer distances. There were no significant differences between the day of the human encounters and the corresponding control periods in any of these variables for subadults. These results provide support for the hypothesis that human encounters are a behavioral disturbance

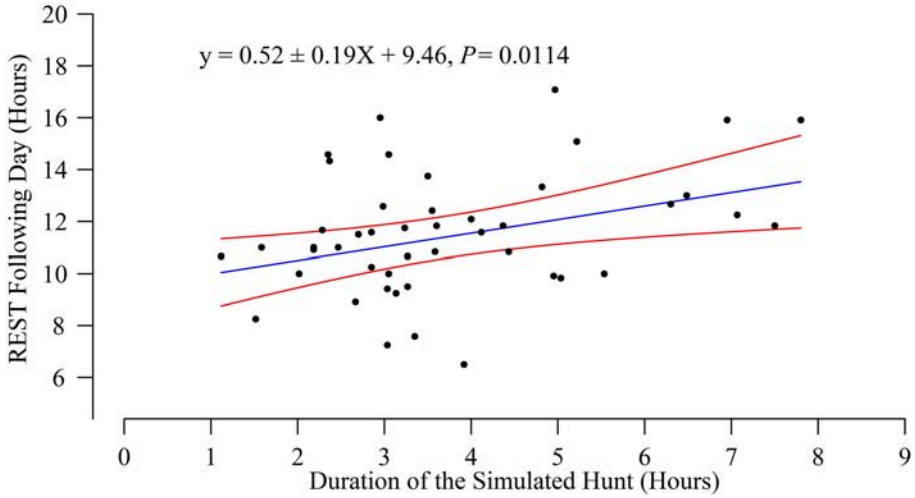

FIGURE 2 | The day after the simulated hunts, female bears rested more if the simulated hunts were longer ($P = 0.0114$). The 46 simulated hunts are represented by the black dots with the regression line, as well as the lower and upper 95% confidence interval. The model REST ∼ Duration of the simulated hunt*AGE was fitted with the Bear ID as a random factor. The variable AGE was not kept after using the backward selection method (Interaction: $P = 0.34$, AGE: $P = 0.29$).

TABLE 2 | Estimated marginal means (EMM) for the control periods of the human encounters and the control periods of the simulated hunts.

Control Period	EMM Human Encounters		EMM Simulated Hunts	
	Subadult	Adult	Subadult	Adult
TRAVEL $_{(m)}$	5836 ± 26	7945 ± 13	5744 ± 33	7838 ± 17
MAXSPEED $_{(mh-1)}$	1115 ± 77	1231 ± 48	1101 ± 85	1217 ± 55
HEARTRATE30 $_{(bpm)}$	109 ± 0.07		104 ± 0.06	
T_bAREA	9165 ± 132	13358 ± 60	8899 ± 167	10271 ± 63
REST $_{(h:min\pm min)}$	10:49 ± 20		10:10 ± 22	

No differences between the control period values were found when carrying out all the possible pairwise comparisons (HumanAdult-HumanSubadult, HumanAdult-HuntAdult, HumanAdult-HuntSubadult, HumanSubadult-HuntSubadult, HuntAdult-HuntSubadult, HuntAdult-HumanSubadult; all P > 0.13).

for brown bears [H1] but do not support the hypothesis that human encounters are a physiological disturbance for brown bears.

Contrary to human encounters, simulated hunts led to a clear disturbance with longer traveled distances, higher speeds and higher heart rates than during the corresponding control periods or the human encounters. Adult female bears also had greater body temperatures compared with the control periods. These results support the hypothesis that dog hunts represent both a behavioral and physiological disturbance [H1]. The results also support the hypothesis that dog hunts have a greater impact on brown bears than human encounters [H2].

During simulated hunts, bears were pursued by dogs and may have been forced to flee in a more dramatic way than when moving away from encountered humans, which is most likely the reason why simulated hunts had a greater impact. Simulated hunts were also characterized by smaller minimum distances as dogs were able to come closer to the bears than observers were during the human encounters. Because running faster can be associated with higher energy costs (Pagano et al., 2018), human encounters and dog hunts can be considered a direct energy cost for adult female brown bears, with dog hunts having the highest impact. Simulated hunts also led to longer traveled distances, higher heart rates and, for adult females, greater body temperature areas, giving further support to the idea that dog hunts represent an important energy cost. The fact that bears use more energy while running than other quadrupedal mammals (Pagano et al., 2018) suggests that human encounters and dog hunts may represent relatively large energy costs in bears.

If an adult female bear is frequently disturbed by human encounters and dog hunts, its body condition may be affected by the energy cost of these disturbances. Females do not always reach their energetic needs, e.g., poor berry seasons affect the reproductive success of lightweight female bears in Sweden (Hertel et al., 2018). Adult females give birth during the denning period and depend on their fat reserves for the gestation and lactation of their cubs (Robbins et al., 2012; Lopez-Alfaro et al., 2013). Even if observed mating, captive adult female brown bears having a body fat content lower than 20% do not give birth (Robbins et al., 2012). Lopez-Alfaro et al. (2013), using an energy consumption model, estimated that with a body fat content below 19%, a female would not be able to reproduce during a hibernation period that lasts over 120 days. In Sweden, adult females spend on average 181 days in winter dens (Friebe et al., 2001). Energy costs due to human encounters and dog hunts may thus affect the body condition of adult female bears and ultimately affect their fitness by altering the reproductive success.

Higgins (1997) compared the body condition of 13 adult female black bears from non-hunted populations with 20 adult female black bears from a hunted population and found an indication that black bears from the hunted population may be lighter and in worse physical condition ($P = 0.09$). However,

Massopust and Anderson (1984) carried out eight dog hunts on five black bears with a maximum of two dog hunts per individual and observed no injuries or abnormal weights on the bears when captured at their den. It is possible that more than two dog hunts are needed to affect the weight of the bears. Tourism (bear viewing), experimentally simulated for one summer in an undisturbed bear area in Alaska, did not lead to losses in weights, nor any changes in body condition (Rode et al., 2007). However, the studied bear population could feed on salmon (*Oncorhynchus kisutch* and *Oncorhynchus nerk*), a more nutrient-rich alimentation than the berries eaten by the Scandinavian brown bears (Welch et al., 1997), giving the bears a better opportunity to maintain their body condition.

Human encounters and dog hunts do not seem to have a profound lasting impact on bears, because there was no difference in distances traveled, maximum speeds, maximum heart rates, and body temperature areas between the control periods and the 2 days after the experiments. This may seem surprising as brown bears change their movement patterns for at least 2 days after human encounters (Ordiz et al., 2013b). Our study was based on hourly displacements and may underestimate the real movement pattern of the bears and thus the behavioral disturbance. The effects found in our study may also have been underestimated, because the bears could have been disturbed during the control periods, making the differences smaller between the experimental days and the control periods. All the human encounters in the project were conducted in the summer and many during the berry picking season, making it likely that the bears also encountered other humans during the control periods. Simulated hunts were not carried out during the bear hunting season, but a few simulated hunts were conducted during the moose hunting season. Dogs used for hunting moose (*Alces alces*) may also chase bears (Bischof et al., 2008).

Bears rested more the day after a simulated hunt compared with the control period and if the simulated hunt was longer. These results support the hypothesis that longer dog hunts may have a greater impact [H3], and that dog hunts may have a lasting behavioral effect on brown bears [H4]. The longer rest after simulated hunts suggests that bears may be fatigued by dog hunts. Longer dog hunts on deer (*Cervus elaphus*) increased the disturbance impact and were associated with a higher concentration in enzymes related to muscle breakdown (Bateson and Bradshaw, 1997). Deer that are shot after a long hunt present physiological signs of extreme exhaustion (Bateson and Bradshaw, 1997). Bears may suffer from similar physiological impacts, and may have to increase their rest to recover from it. Bateson and Bradshaw (1997) concluded that red deer were not well-adapted to fleeing dogs. Bears may be even less adapted to dog hunts than red deer as they are energetically less efficient when running compared to other quadrupedal mammals (Pagano et al., 2018). After prolonged exercise, extra energy consumption can be measured during the recovery time (Børsheim and Bahr, 2003). This may also represent an extra post-disturbance energy cost.

Brown bear hunting in Sweden has known impacts beyond the initial offtake of direct mortality, such as altering life history traits (Bischof et al., 2017; Frank et al., 2017) or inducing an increase in sexually-selected infanticide through an increased male turnover (Swenson et al., 1997). Furthermore, adult bears that would naturally face low mortality rates (Bischof and Zedrosser, 2009; Bischof et al., 2009, 2017) adopt antipredator behaviors in response to human hunting pressure (Ordiz et al., 2013a). For example, when the hunting season starts, bears decrease their foraging activity during the time of the day with the highest risk of being shot, forcing them to forage less efficiently and in areas with poorer berry quality (Hertel et al., 2016). This antipredator behavior, combined with the direct energy costs of human encounters and dog hunts may lead to a lower fitness if it prevents adult females from reaching the required body condition threshold for successful breeding.

CONCLUSION

Dog hunts represent a greater physiological and behavioral source of disturbance for female brown bears than human encounters. Adult female bears were behaviorally disturbed by human encounters but did not travel longer distances or have different heart rates and body temperatures. Simulated hunts had lasting behavioral effects on bears by inducing longer resting periods the day following the actual experiment. Longer resting periods found after longer simulated hunts suggested that the impact of dog hunts increases with their duration. By representing an energy cost, human encounters and dog hunts could lower the fitness of adult female bears if experienced frequently. Further research is needed to assess if bears that are repeatedly disturbed by dog hunts and human encounters are unable to compensate the disturbances' energy cost and if this affects their fitness. Nonetheless, if it is the case, this effect should be accounted for by managers. Human encounters have a lower impact than dog hunts on the bears but are not restricted in time like dog hunts. Thus, they may have a lower impact *per se* but may still have an important impact due to their higher frequency. Distance traveled, speeds, hearts rates, body temperature and resting behavior are universal variables that can be used on other animals to assess the impact of human activities. Looking at behavioral and physiological variables within the same study helps to have a better understanding of the disturbance.

ETHICS STATEMENT

All captures were approved by the Swedish Ethical Committee on Animal Research (application numbers C7/12 and C18/15) and the Swedish Environmental Protection Agency (application numbers NV-00741-18 and NV-01758-14).

AUTHOR CONTRIBUTIONS

LG, JA, and O-GS conceived the ideas and designed the methodology. AE, JA, and O-GS instrumented the bears and recovered devices in the field with input from TL. Pre-database, data-management and submission to WRAM (wireless remote animal monitoring, SLU) was conducted by BF. All authors contributed to the data analyses. LG led the writing of the

manuscript. All authors reviewed the drafts and gave final approval for publication.

FUNDING

This study was funded by the Norwegian Environment Agency and conducted within the Scandinavian Brown Bear Research Project (SBBRP). The SBBRP has primarily been funded by the Swedish Environmental Protection Agency, the Austrian Science Fund, and the Swedish Association for Hunting and Wildlife Management. This is scientific paper 274 from the SBBRP. None of the funders had any role in the conduct of the research and/or preparation of the article.

ACKNOWLEDGMENTS

Veterinarians Martine Angel, Nuria Fandos Esteruelas, and AnneRandi Græsli contributed to device deployment and retrieval. Andrea Friebe,David Ahlqvist, Rasmus Boström and Sven Brunberg deserve a special mentionfor their help in the field as well as all the students and volunteers without whomthe project would not have been possible.

REFERENCES

Arnemo, J. M., and Evans, A. (2017). *Biomedical Protocols for Free-Ranging Brown Bears, Wolves, Wolverines and Lynx*. Inland Norway University of Applied Sciences, Campus Evenstad.

Bates, D., Mächler, M., Bolker, B., and Walker, S. (2014). Fitting linear mixed-effects models using lme4. *J. Stat Soft.* 67, 1–48. doi: 10.18637/jss.v067.i01

Bateson, P., and Bradshaw, E. L. (1997). "Physiological effects of hunting red deer (Cervus elaphus)," in *Proceedings of the Royal Society of London B: Biological Sciences*. (Great Britain: The Royal Society), 1707–1714.

Bischof, R., Bonenfant, C., Rivrud, I. M., Zedrosser, A., Friebe, A., Coulson, T., et al. (2017). Regulated hunting re-shapes the life history of brown bears. *Nat. Ecol. Evol.* 2, 116–123. doi: 10.1038/s41559-017-0400-7

Bischof, R., Fujita, R., Zedrosser, A., Söderberg, A., and Swenson, J. E. (2008). Hunting patterns, ban on baiting, and harvest demographics of brown bears in Sweden. *J. Wildl. Manag.* 72, 79–88. doi: 10.2193/2007-149

Bischof, R., Swenson, J. E., Yoccoz, N. G., Mysterud, A., and Gimenez, O. (2009). The magnitude and selectivity of natural and multiple anthropogenic mortality causes in hunted brown bears. *J. Anim. Ecol.* 78, 656–665. doi: 10.1111/j.1365-2656.2009.01524.x

Bischof, R., and Zedrosser, A. (2009). The educated prey: consequences for exploitation and control. *Behav. Ecol.* 20, 1228–1235. doi: 10.1093/beheco/arp124

Børsheim, E., and Bahr, R. (2003). Effect of exercise intensity, duration and mode on post-exercise oxygen consumption. *Sports Med.* 33, 1037–1060. doi: 10.2165/00007256-200333140-00002

Bryce, C. M., Wilmers, C. C., and Williams, T. M. (2017). Energetics and evasion dynamics of large predators and prey: pumas vs. hounds. *PeerJ.* 5:e3701. doi: 10.7717/peerj.3701

Dettki, H., Brode, M., Giles, T., and Hallgren, J. (2014). "Wireless remote animal monitoring (WRAM)-A new international database e-infrastructure for management and sharing of telemetry sensor data from fish and wildlife," in *7th International Congress on Environmental Modelling and Software*. (San Diego, CA), 122–128.

Ditmer, M. A., Vincent, J. B., Werden, L. K., Tanner, J. C., Laske, T. G., Iaizzo, P. A., et al. (2015). Bears show a physiological but limited behavioral response to unmanned aerial vehicles. *Curr. Biol.* 25, 2278–2283. doi: 10.1016/j.cub.2015.07.024

Elfström, M., Swenson, J. E., and Ball, J. P. (2008). Selection of denning habitats by Scandinavian brown bears Ursus arctos. *Wildl. Biol.* 14, 176–187. doi: 10.2981/0909-6396(2008)14<176:SODHBS>2.0.CO;2

Evans, A. L., Singh, N. J., Fuchs, B., Blanc, S., Friebe, A., Laske, T. G., et al. (2016). Physiological reactions to capture in hibernating brown bears. *Conserv. Physiol.* 4, 1–11. doi: 10.1093/conphys/cow061

Fox, J., and Weisberg, S. (2011). *An R Companion to Applied Regression*. Canada: Sage.

Frank, S. C., Ordiz, A., Gosselin, J., Hertel, A., Kindberg, J., Leclerc, M., et al. (2017). Indirect effects of bear hunting: a review from Scandinavia. *Ursus* 28, 150–164. doi: 10.2192/URSU-D-16-00028.1

Friebe, A., Evans, A. L., Arnemo, J. M., Blanc, S., Brunberg, S., Fleissner, G., et al. (2014). Factors affecting date of implantation, parturition, and den entry estimated from activity and body temperature in free-ranging brown bears. *PLoS ONE* 9:e101410. doi: 10.1371/journal.pone.0101410

Friebe, A., Swenson, J. E., and Sandegren, F. (2001). Denning chronology of female brown bears in central Sweden. *Ursus* 12, 37–45.

Gervasi, V., Brunberg, S., and Swenson, J. E. (2006). An individual-based method to measure animal activity levels: a test on brown bears. *Wildl. Soc. Bull.* 34, 1314–1319. doi: 10.2193/0091-7648(2006)34<1314:AIMTMA>2.0.CO;2

Hertel, A. G., Bischof, R., Langval, O., Mysterud, A., Kindberg, J., Swenson, J. E., et al. (2018). Berry production drives bottom–up effects on body mass and reproductive success in an omnivore. *Oikos* 127, 197–207. doi: 10.1111/oik.04515

Hertel, A. G., Zedrosser, A., Mysterud, A., Støen, O.-G., Steyaert, S. M., and Swenson, J. E. (2016). Temporal effects of hunting on foraging behavior of an apex predator: do bears forego foraging when risk is high? *Oecologia* 182, 1019–1029. doi: 10.1007/s00442-016-3729-8

Higgins, K. (1997). *Hunting Dynamics, Condition Estimates, and Movements of Black Bears Hunted With Hounds in Virginia*. Master thesis, Virginia Polytechnic Institute and State University.

Hijmans, R. J. (2017). *Geosphere: Spherical Trigonometry*. R package Version 1.5—7. Available online at: https://CRAN.R-project.org/package=geosphere

Jarnemo, A., and Wikenros, C. (2014). Movement pattern of red deer during drive hunts in Sweden. *Eur. J. Wildl. Res.* 60, 77–84. doi: 10.1007/s10344-013-0753-4

Kreeger, T. J., Monson, D., Kuechle, V. B., Seal, U. S., and Tester, J. R. (1989). Monitoring heart rate and body temperature in red foxes (Vulpes vulpes). *Can. J. Zool.* 67, 2455–2458.

Lenth, R. (2018). *Emmeans: Estimated Marginal Means, aka Least-Squares Means*. R Package Version 1.1. Available online at: https://CRAN.R-project.org/package=emmeans

Lopez-Alfaro, C., Robbins, C. T., Zedrosser, A., and Nielsen, S. E. (2013). Energetics of hibernation and reproductive trade-offs in brown bears. *Ecol. Model.* 270, 1–10. doi: 10.1016/j.ecolmode1.2013.09.002

Massopust, J. L., and Anderson, R. K. (1984). "The response of black bears to being chased by hunting dogs," in *Proceeding Eastern Workshop Black Bear Management and Research*, 59–65.

Moen, G. K., Stoen, O. G., Sahlen, V., and Swenson, J. E. (2012). Behaviour of solitary adult Scandinavian brown bears (Ursus arctos) when approached by humans on foot. *PLoS ONE* 7:e31699. doi: 10.1371/journal.pone.0031699

Norman, A. J. (2016). *Genomic Studies of Contemporary Processes in Wild Populations*. PhD thesis, Swedish University of Agricultural Sciences.

Ordiz, A., Bischof, R., and Swenson, J. E. (2013a). Saving large carnivores, but losing the apex predator? *Biol. Conserv.* 168, 128–133. doi: 10.1016/j.biocon.2013.09.024

Ordiz, A., Kindberg, J., Sæb,ø, S., Swenson, J. E., and Støen, O.-G. (2014). Brown bear circadian behavior reveals human environmental encroachment. *Biol. Conserv.* 173, 1–9. doi: 10.1016/j.biocon.2014.03.006

Ordiz, A., Støen, O. G., Sæb,ø, S., Sahlen, V., Pedersen, B. E., Kindberg, J., et al. (2013b). Lasting behavioural responses of brown bears to experimental encounters with humans. *J. Appl. Ecol.* 50, 306–314. doi: 10.1111/1365-2664.12047

Pagano, A. M., Carnahan, A. M., Robbins, C. T., Owen, M. A., Batson, T., Wagner, N., et al. (2018). Energetic costs of locomotion in bears: is

plantigrade locomotion energetically economical? *J. Exp. Biol.* 221:jeb175372. doi: 10.1242/jeb.175372

Pinheiro, J., Bates, D., DebRoy, S., Sarkar, D., and and, R, Core Team (2017). *nlme: Linear and Nonlinear Mixed Effects Models*. R Package Version, 3.1-131. Available online at: https://CRAN.R-project.org/package=nlme

R Core Team (2017). *R: A Language and Environment for Statistical Computing*. Vienna: R Foundation for Statistical Computing, Vienna, Austria. R Foundation for Statistical Computing.

Robbins, C. T., Ben-David, M., Fortin, J. K., and Nelson, O. L. (2012). Maternal condition determines birth date and growth of newborn bear cubs. *J. Mammal.* 93, 540–546. doi: 10.1644/11-mamm-a-155.1

Rode, K. D., Farley, S. D., Fortin, J., and Robbins, C. T. (2007). Nutritional consequences of experimentally introduced tourism in brown bears. *J. Wildl. Manag.* 71, 929–939. doi: 10.2193/2006-075.

Sahlén, E., Støen, O.-G., and Swenson, J. E. (2011). Brown bear den site concealment in relation to human activity in Sweden. *Ursus* 22, 152–158. doi: 10.2192/URSUS-D-10-00007.1

Signorell, A. (2017). *DescTools: Tools for Descriptive Statistics*. R Package Version 0.99.23. Available online at: https://cran.r-project.org/package=DescTools

Swenson, J. E., Sandegren, F., Söderberg, A., Bjärvall, A., Franzén, R., and Wabakken, P. (1997). Infanticide caused by hunting of male bears. *Nature* 386, 450.

Swenson, J. E., Schneider, M., Zedrosser, A., Söderberg, A., Franzén, R., and Kindberg, J. (2017). Challenges of managing a European brown bear population; lessons from Sweden, 1943–2013. *Wildl. Biol.* 2017. doi: 10.2981/wlb.00251

Vaughan, M. R., and Inman, K. L. H. (2002). Hunter effort and success rates of hunting bears with hounds in Virginia. *Ursus* 13, 223–230.

Welch, C. A., Keay, J., Kendall, K. C., and Robbins, C. T. (1997). Constraints on frugivory by bears. *Ecology* 78, 1105–1119.

Wilmers, C. C., Nickel, B., Bryce, C. M., Smith, J. A., Wheat, R. E., and Yovovich, V. (2015). The golden age of bio-logging: how animal-borne sensors are advancing the frontiers of ecology. *Ecology* 96, 1741–1753.

Wilson, A. D., Wikelski, M., Wilson, R. P., and Cooke, S. J. (2015). Utility of biological sensor tags in animal conservation. *Conserv. Biol.* 29, 1065–1075. doi: 10.1111/cobi.12486

Conflict of Interest Statement: TL is an employee of Medtronic, Inc. and all cardiac biologgers were donated by Medtronic.

The remaining authors declare that the research was conducted in the absence of any commercial or financial relationships that could be construed as a potential conflict of interest.

Copyright © 2019 Le Grand, Thorsen, Fuchs, Evans, Laske, Arnemo, Sæbø and Støen. This is an open-access article distributed under the terms of the Creative Commons Attribution License (CC BY). The use, distribution or reproduction in other forums is permitted, provided the original author(s) and the copyright owner(s) are credited and that the original publication in this journal is cited, in accordance with accepted academic practice. No use, distribution or reproduction is permitted which does not comply with these terms.

frontiers in Ecology and Evolution

ORIGINAL RESEARCH
published: 08 May 2019
doi: 10.3389/fevo.2019.00154

Use of Acceleration and Acoustics to Classify Behavior, Generate Time Budgets, and Evaluate Responses to Moonlight in Free-Ranging Snowshoe Hares

Emily K. Studd[1], Melanie R. Boudreau[2], Yasmine N. Majchrzak[3], Allyson K. Menzies[1], Michael J. L. Peers[3], Jacob L. Seguin[2], Sophia G. Lavergne[4], Rudy Boonstra[4], Dennis L. Murray[2], Stan Boutin[3] and Murray M. Humphries[1]*

[1] Department of Natural Resource Sciences, Macdonald Campus, McGill University, Sainte-Anne-de-Bellevue, QC, Canada, [2] Department of Biology, Trent University, Peterborough, ON, Canada, [3] Department of Biological Sciences, University of Alberta, Edmonton, AB, Canada, [4] Department of Biological Sciences, Centre for the Neurobiology of Stress, University of Toronto Scarborough, Toronto, ON, Canada

OPEN ACCESS

Edited by:
Frants Havmand Jensen, Woods Hole Oceanographic Institution, United States

Reviewed by:
Ariana Strandburg-Peshkin, Universität Konstanz, Germany
Jack Tatler, University of Adelaide, Australia

***Correspondence:**
Emily K. Studd
emily.studd@mail.mcgill.ca

Specialty section:
This article was submitted to Behavioral and Evolutionary Ecology, a section of the journal Frontiers in Ecology and Evolution

Received: *21 August 2018*
Accepted: *23 April 2019*
Published: *08 May 2019*

Citation:
Studd EK, Boudreau MR, Majchrzak YN, Menzies AK, Peers MJL, Seguin JL, Lavergne SG, Boonstra R, Murray DL, Boutin S and Humphries MM (2019) Use of Acceleration and Acoustics to Classify Behavior, Generate Time Budgets, and Evaluate Responses to Moonlight in Free-Ranging Snowshoe Hares. Front. Ecol. Evol. 7:154. doi: 10.3389/fevo.2019.00154

Technological miniaturization is driving a biologging revolution that is producing detailed and sophisticated techniques of assessing individual behavioral responses to environmental conditions. Among the many advancements this revolution has brought is an ability to record behavioral responses of nocturnal, free-ranging species. Here, we combine captive validations of acceleration signatures with acoustic recordings from free-ranging individuals to classify behavior at two resolutions. Combining these classifications with ∼2 month-long recordings, we describe winter time budgets, and responses of free-ranging snowshoe hares to changing moonlight. We successfully classified snowshoe hare behavior into four categories (not moving, foraging, hopping, and sprinting) using low frequency accelerometry, with an overall model accuracy of 88%, and acoustic recordings to three categories (silence, hopping, and chewing) with an accuracy of 94%. Broad-scale accelerometer-classified categories were composed of multiple fine-scale behavioral states with the composition varying between individuals and across the day. Time budgets revealed that hares spent ∼50% of their time foraging and ∼50% not moving, with most foraging and feeding occurring at night. We found that hares adjusted timing of activity in response to moon phase, with a 6% reduction in foraging and 30% reduction in traveling during the night when the moon was full. Hares compensated for this lost foraging time by extending foraging into the morning hours of the following day. Using two biologging technologies to identify behavior, we demonstrate the possibility of combining multiple devices when documenting behavior of cryptic species.

Keywords: accelerometer, biologging, boreal forest, environmental acoustics, *Lepus americanus*, lunar phases, nocturnal behavior, snowshoe hare

INTRODUCTION

From satellites and drones to biologging devices, new technologies are providing us with the capabilities to answer questions about the natural world, and the species that live within it that could only have been dreamt about a few decades ago. Every year, the number of technologies available to ecologists expands, and the sophistication and capacity of those tools that exist improves (see reviews: Elliott, 2016; Williams et al., 2016). Although initial incorporation of devices on wildlife focused on space use, with a focus on knowing in real time the exact location of an individual, the latest phase of the biologging revolution has, in part, been behaviorally focused, with a desire to know what the individual was doing (Wilmers et al., 2015). One of the most popular devices for behavioral classification is the accelerometer, which measures 3-dimensional acceleration of a species of interest (see **Figure 1**; e.g., Graf et al., 2015) and for which miniaturization has reduced the weight to as little as 0.7 grams (e.g., Axy-4 without battery, Technosmart, Rome, Italy). Taking into account gravity and acceleration profiles of different movement types, these recordings can provide information on posture and orientation, energy expenditure, and activity levels, that should correspond to specific behavioral states (Wilson et al., 2006; Shepard et al., 2008; Gleiss et al., 2011; Brown et al., 2013).

The potential for accelerometers to record behavior over long timeframes, including multi-day, cross-seasonal, and even multi-annual periods, involves a tradeoff between recording duration and the resolution of behavioral classification (Broell et al., 2013; Tatler et al., 2018). Accurate classification of detailed behavioral states requires a sampling rate that is twice the highest frequency present in the signal, referred to as the Nyquist criterion (Beutler, 1966; Chen and Bassett, 2005; Graf et al., 2015). Most classifications target rapid movements like wingbeats or steps (Shepard et al., 2008; Spivey and Bishop, 2013), but the intensive sampling needed to do so tends to limit device longevity below what is necessary for documenting wildlife responses to changes in their environment that occur at seasonal and annual timescales. To increase recording duration, sampling frequency can be lowered at the cost of only capturing behavioral categories with lower Nyquist criterion such as bouts of traveling, foraging, and resting (Campbell et al., 2013; Tatler et al., 2018; Studd et al., 2019). Such information, although less specific, is still highly useful for building activity and energy budgets (Williams et al., 2017; Studd et al., 2019).

To counteract the loss of information from using a lower sampling frequency, it may be necessary to determine the detailed behavioral composition of the broader behavioral categories through different means. In species where direct observations are difficult, this may require combining accelerometers with additional biologging technology such as video or audio recorders (Lynch et al., 2013; Pagano et al., 2018). For large terrestrial species (such as polar bears and caribou), observational data on free-ranging behavior can be obtained with video camera collars (e.g., Thompson et al., 2012; Pagano et al., 2018), while for smaller taxa where weight of monitoring devices becomes limiting, deployment of acoustic recorders may be a potential alternative (Lynch et al., 2013; Couchoux et al., 2015). Acoustic data has been incorporated into many fields within ecology providing new means of quantifying biodiversity (e.g., Depraetere et al., 2012; Gasc et al., 2013), soundscapes (Pijanowski et al., 2011), and animal communication (e.g., Reby and McComb, 2003; Fischer et al., 2004; Thiebault et al., 2016). More recently, a few studies have even revealed the potential of acoustic devices to record non-vocal behavior (e.g., flying, feeding, walking; Ilany et al., 2013; Lynch et al., 2013; Stowell et al., 2017; Wijers et al., 2018).

Here we highlight the potential of using accelerometers and acoustic recorders (attached as collars) to classify the behavior of free-ranging snowshoe hares (*Lepus americanus*), a cryptic small mammal (2 kg). Our primary objective was to determine if we could use low frequency acceleration to identify broad behavioral categories that could be recorded over days to months. In order to do this, we linked accelerometer recordings to observations of captive hares. Additionally, we took advantage of the ability of acoustic recorders to classify non-vocal behavior in order to determine a more detailed composition of accelerometer-based behavioral categories. Our secondary objective was to showcase how these tools, in providing detailed behavioral information over long periods of time, can then be used to investigate daily activity patterns and how aspects of the environment can influence behavior of free-ranging hares. We took a proof of concept approach whereby we explored how light conditions caused by phases of the moon and daylight influenced nocturnal hare behavior.

MATERIALS AND METHODS

The study took place in southwestern Yukon (61°N, 138°W) within the Shakwak trench, an area of boreal forest where snowshoe hares have been the focus of studies for the past 45 years (Krebs et al., 2018). The forest is predominantly white spruce (*Picea glauca*) intermixed with patches of aspen (*Populus tremuloides*) and balsam poplar (*Populus balsamifera*), and an understory of gray willow (*Salix glauca*) and dwarf birch (*Betula pumila var. glandulifera*) (Boonstra et al., 2016). Snowshoe hares exhibit 10-year population cycles, which are, at least in part driven by their primary predators Canada lynx (*Lynx canadensis*), coyote (*Canis latrans*), and great horned owls (*Bubo virginianus;* Rohner and Krebs, 1996; O'Donoghue et al., 1998). During this study, snowshoe hares were in the increase phase of the cycle with densities averaging 1 hare/ha (Krebs et al., 1995).

All snowshoe hares were captured using Tomahawk live-traps (Tomahawk Live Trap Co. Tomahawk, WI, USA) baited with alfalfa and rabbit chow, and set and checked overnight (Keith, 1964). Individuals were fitted with an accelerometer (model Axy3, 4 g, Technosmart, Rome, Italy) and VHF radio transmitter (Model SOM2380, Wildlife Materials Inc., USA, or Model MI-2M, Holohil, Canada, both 27 +/− 1 g) in the form of a collar (31 +/− 1 g, 2.5% of smallest hare mass). Accelerometers rested on the dorsal side of the neck and recorded acceleration on 3 dimensional axes at 1 Hz with a resolution of +/− 8 $g_{-forces}$. To record observations of snowshoe hare behavior, we captured six hares (>1,200 g) in April 2015, attached collars and transferred

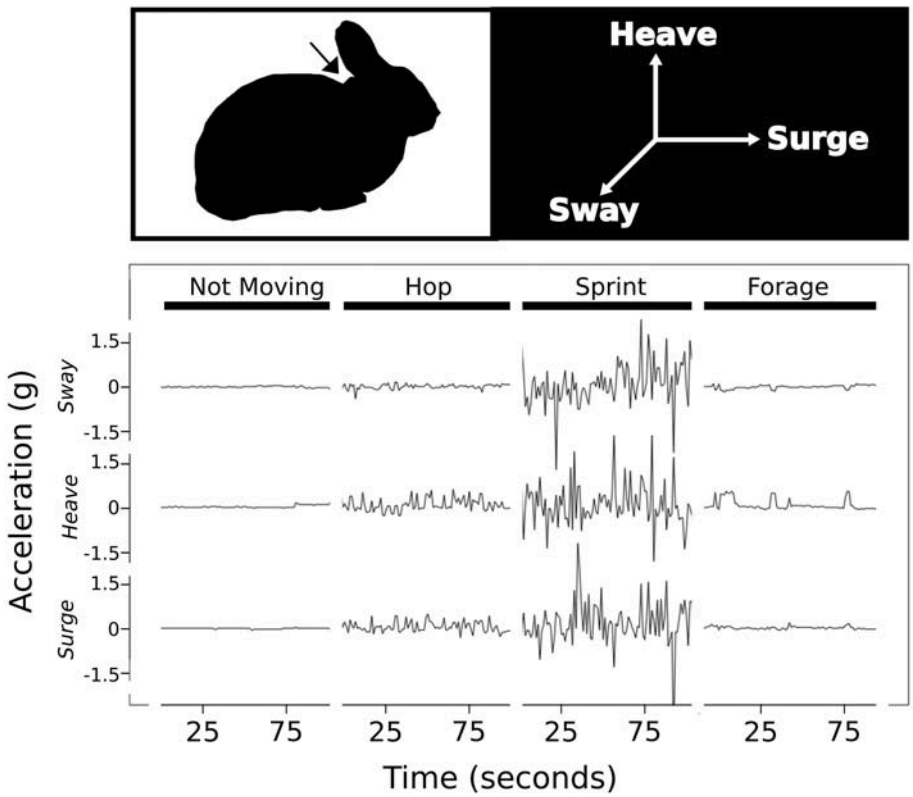

FIGURE 1 | Example of 1 Hz tri-axis accelerometer data and the orientation axis from a collar attached to a captive snowshoe hare. Arrow indicates location where accelerometer rested on the animal.

them to outdoor enclosures (4.5 m by 4.5 m; modified from Sheriff et al., 2009; Lavergne and Boonstra pers comm). Hares were held for three days and supplied with rabbit chow, water, and willow branches collected from the surrounding area. At the completion of observational trials, collars were removed, and hares were released at point of capture. To explore the potential of accelerometers for monitoring behavior over multiple months, we live-trapped and collared 14 free-ranging snowshoe hares between October 2015 and March 2016. Once collared, hares were released at their capture site, and recaptured 1–3 months later (average = 62 days, range: 32–100 days) for collar removal and data download. This research conformed to the guidelines of the American Society of Mammalogists (Sikes et al., 2016) and was approved by the McGill University, University of Alberta, and University of Toronto Animal Care and Use Committees.

Behavioral Observations of Captive and Chased Hare

We used the observations of captive hares to cross-validate behavioral categories based on accelerometer information. For this, 2 h of video (Nikon D90 with 50 mm, Sony Handycam HDR-CX240) were recorded per day for three days capturing morning and dusk activity. During recordings, personnel left the enclosure area to minimize influence of human activity on hare behavior. Hares tended to move rapidly when humans entered the enclosures to provide food and remove droppings, so cameras also recorded during these times. The same time-keeping device was held in frame at the start of each video to sync times for all observations. Videos were watched by two observers who recorded the start and end times of each behavior, which included digging, feeding, grooming, jumping, vigilance (sitting while head moves to look in multiple directions), sprinting, shaking, sitting (motionless), standing, travel with multiple hops, or travel with one hop only. From this we selected the six most common behavioral states that represented 91.8% of all observations and combined them into three broader categories (not moving: sitting and vigilance; foraging: feeding and travel with one hop; traveling: sprinting and travel with multiple hops). This included at least one observation of each behavior per hare per day with the average number of observations of each behavior per hare per day ranging from 8 for feeding to 42 for vigilance (**Table S1**). Since clocks on separate devices did not run at exactly the same rate, we visually identified multiple occasions per day per hare where the animal transitioned from sitting to traveling to calculate the time divergence between each accelerometer and the camera clock to generate a time correction equation for each accelerometer (error = +/− 3 s).

We observed few instances of hares sprinting at maximum speeds in the enclosures. Thus, to capture potential high-speed chase or "fleeing" behavior (an important aspect of predator-prey interactions), we added additional behavioral data from free-ranging snowshoe hares that were chased by a simulated

predator (i.e., a dog, *Canis familiaris*, a model for coyotes; see methods in Boudreau, 2019). For each chase, the time and whether or not the hare sprinted were recorded, and a subset of chases ($n = 47$) where hares were observed sprinting from the dog were used as examples of sprinting behavior.

Accelerometer Classification

Average static acceleration was calculated using a running medians smoothing window of 91 samples (see **Supplementary Materials 1.1** for window size selection method). We removed this long duration static acceleration (general orientation of device) from total acceleration to retain only acceleration generated from the movement of the animal on which all further analyses were based. This remaining acceleration is primarily the measurement of small changes in the posture of the animal that occur during each behavior, and secondarily, measurements of the dynamic acceleration of the movement. To classify acceleration by behavioral categories we constructed a decision tree consisting of three hierarchical divisions (Studd et al., 2019): (1) not moving (no visible motion, i.e., sitting) and moving (any physical movement), (2) all moving into foraging (feeding, travel with one hop) or traveling (travel with multiple hops), and (3) all traveling into hopping (observed in enclosure) and sprinting (observed in simulated chases in the wild). For each division of the tree, observed behavioral data was split between training (70%) and testing (30%), and then subsampled to ensure equal numbers of each behavior. Over each sample window duration, determined by the average duration observed in videos of behavioral states in each division, we calculated the mean, maximum, minimum, range, standard deviation, and sum of acceleration on each of the three axes (surge, heave, and sway), along with the sum of overall acceleration (OA; similar to ODBA in Wilson et al., 2006), and the change in overall acceleration (ΔOA) across all three axes. ΔOA is the change in acceleration (Δa) for each axis from 1 s to the next summed over the time window across all three axes. Threshold values for behavioral categories at each division were determined by a two-step process. First, the percent overlap between the two behavioral categories for each summary statistic was calculated and the statistic with the lowest overlap was selected (**Figure 2A**). Second, the percent error of classification was calculated for every 0.1 increment of the selected statistic between the minimum and maximum values, and the threshold value was set according to the lowest classification error (**Figure 2B**). Using the remaining 30% of the observational data, accuracy for each division of the tree was calculated as proportion of all observations that were correctly classified by the threshold value.

The flexibility of this method allows for different sample duration windows to be used at each division. Sample window size was 12 s for not moving and moving, and 4 s for each of foraging and traveling, and for hopping and sprinting. Different training datasets were used for each division. For the first division we used all not moving and moving events with durations of at least 12 s (91.8% of observed behavior). The second division included all foraging (51% or more feeding with no type of travel) and traveling (51% or more travel with multiple hops) events that lasted at least 4 s (89.4% of observed behavior). The final division included all hopping (low speed travel with multiple hops) and sprinting (simulated predator chases) events with summary statistics calculated over 4 s. Due to low sample size of sprinting events, overall classification accuracy was calculated on the first two divisions only.

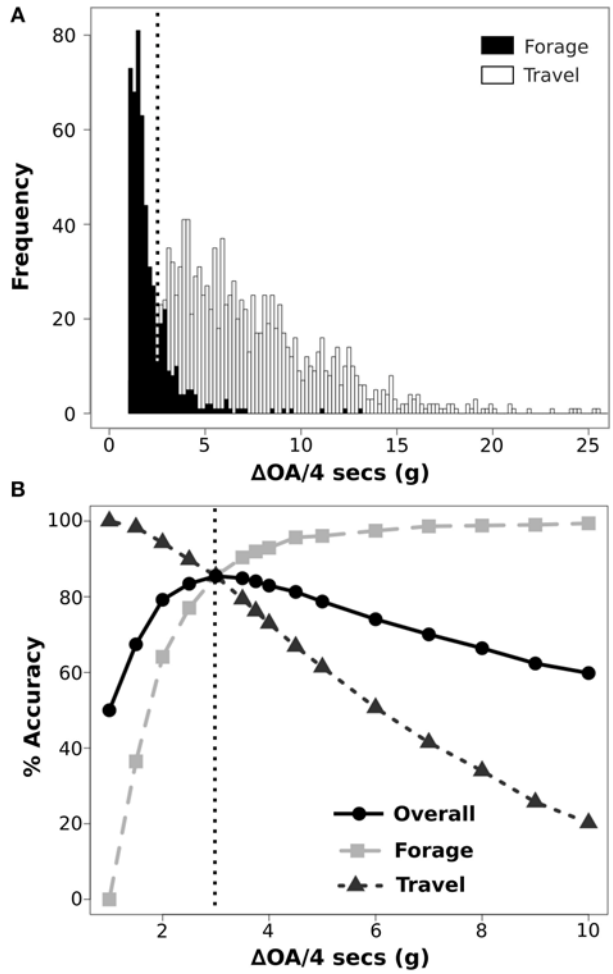

FIGURE 2 | Example illustrating method for determination of threshold values for separation of behavioral states using accelerometer data from collars attached to snowshoe hares. Histograms provide visualization of percent overlap between two behavioral categories using a given summary statistic **(A)**. Optimization is performed by examining the accuracy of the behavioral classification between two behavioral states across a range of values and selecting the value at which the overall accuracy is the highest and where the individual accuracy of each behavior intersects **(B)**. Dotted line represents the selected threshold value for classifying accelerometer data into forage and travel using ΔOA.

Although we used a threshold-based classification approach, much recent accelerometer-based literature uses alternative machine learning methods. These approaches have the advantage of efficient processing for the generation of complex classifications with high accuracies, but the disadvantage of black box, non-transferrable thresholds, and non-hierarchical

trees (Bidder et al., 2014; McClune et al., 2014). Given pros and cons to both approaches, we also explored the accuracy of random forest-based classification, as described more fully in the **Supplementary Materials 1.2**, and briefly describe the outcome of this alternative approach in the results. As the random forest provided similar results, we decided to report the more simple method in the body of the paper.

Using Acoustic Recorders to Refine Accelerometer-Classified Behavior

We used animal-borne acoustic recorders to explore composition of broad behavioral classifications (i.e., not moving, and foraging) generated from our low frequency accelerometer recordings. In January 2018, we captured three male snowshoes hares and fitted them with an accelerometer-VHF combination collar that contained an acoustic recorder (Edic-mini Tiny+ A77, 6.6 g, total collar weight of 41 g, <3% of body mass). Once collared, each individual was released at the capture site and recaptured between 4 and 22 days later. Audio recorded continuously at 16,000 hz with μ-law compression for 3 days following capture. Prior to acoustic analysis, we listened to and recorded the sounds contained within 135–15 s audio clips (45 per recorder) that corresponded to long duration (>15 s) foraging, not moving, and traveling as determined by our accelerometer classification tree. Listeners determined that sounds that suggested chewing (33.4% of audio; see **Audios 1**, **2**, and **3** in Supplementary Materials for example clips), hopping (24.5%), silence (23.6%), and unclassifiable noises (9.3%) could be repeatedly distinguished and were the most common. Although we could not truly validate our sound classification for each behavior, we verified that these sounds could be repeatedly associated with a specific behavior among different observers. Three independent listeners blindly classified a subset of clips into the four categories, and we calculated inter-listener agreement for each type of sound.

We manually extracted 300 s of each sound associated with chewing, hopping, and silence consisting of 20–30 independent clips from each hare. Using 70% of the clips, spectrogram analysis (window = 8,000, overlap = 50) was run on each second using the seewave package in R to determine the acoustic properties (Sueur et al., 2008). A classification algorithm consisting of upper and lower amplitude threshold values at 8 frequencies between 0 and 8 kHz for each sound (chewing, hopping, and silence) was created for each device. Thresholds were the 100% confidence intervals plus or minus 10% for that sound (**Tables S4**, **S5**, **Supplementary Materials 1.3**). However, if thresholds of two sounds overlapped at all frequencies, an optimization was run at the frequency where amplitudes were most distinguishable between sounds, and thresholds were adjusted to the value that generated the lowest misclassification. Any sound that did not meet all specified thresholds for chewing, hopping, or silence was classified as "other." The accuracy of classification, unique to each recorder, was calculated using the remaining 30% of clips.

All audio files were converted to behavioral categories at a 1-s resolution and used to tabulate an acoustic-based behavioral composition of the not moving and foraging categories from accelerometer classification for each hare, and across all hares. To account for drift in the internal clocks of the devices, prior to analysis we aligned the timing between devices by identifying 30 events across the file when both acceleration and acoustic amplitude shifted from a long bout of low values to a long bout of high values (i.e., resting to moving). A linear regression of time divergence over time of recording was calculated and the coefficients were used to readjust acoustic time. However, a ∼20 s error remained post-alignment so behavioral composition was calculated using not moving and foraging accelerometer bouts longer than 90 s, with the first and last 30 s removed.

Daily Time Budgets and Behavioral Responses to Moonlight

From both accelerometer-classified, and acoustic-classified behavior, we determined the daily time budgets of free-ranging individuals. This was calculated as the proportion of 24 h that all hares spent expressing each behavior.

Moonlight illumination levels and daily light phase times (including moon rise and moon set times) for our study site were retrieved with *suncalc* package in R (Agafonkin and Thieurmel, 2017). Moonlight illumination levels were converted into a 3-level categorical variable according to the fraction of the moon that was lit: <0.33 (new), 0.33–0.66, and >0.66 (full). Eight light phases defined by the position of the sun relative to the horizon were used including: day (above horizon minus the first and last hour sunlight; ∼4 h), evening (last hour above horizon; ∼1 h), dusk (0–6° below horizon; ∼1 h), evening twilight (6–18° below horizon; ∼2 h), night (>18° below horizon; ∼12 h), morning twilight (18–6° below horizon; ∼2 h), dawn (6–0° below horizon; ∼1 h), and morning (first hour above horizon; ∼1 h). We removed all times when there was potentially cloud cover using both snowfall measures, which were collected daily from 4 locations throughout the study area, and hourly relative humidity values from the nearest weather station (Haines Junction, 40 km away; Environment Canada). We removed all nights preceding a snowfall measurement >0, and all times when the relative humidity was >85%, since cloud cover is highly correlated with relative humidity (Sandor et al., 2000). Although we did not measure moonlight illumination levels ourselves and do not know the exact values that occurred, moon phase and lunar position are commonly used in studies of the effects of moonlight on wildlife (e.g., Johnson and De León, 2015; Gigliotti and Diefenbach, 2018).

As foraging and not moving were highly correlated (Pearson's correlation coefficient =-0.99), moonlight analysis focused on foraging with the understanding that any major changes seen in foraging times are mirrored by opposite changes in not moving. We quantified accelerometer derived hare behavior in response to moonlight at three temporal scales. At a daily scale, we examined foraging time per 24 h using a generalized linear mixed effects model (GLMM) with moon phase (three level) as a fixed effect (R:lmer; Bates et al., 2015). At a within-day

scale, we examined how foraging time (min/hr) was influenced by moon phase during different times of day using a GLMM with a light phase and moon phase interaction. At this scale we also tested how hopping (min/h) and sprinting (events/h) were influenced by moonlight across light phases. Hopping was examined using the same GLMM as foraging. Sprinting event data was zero-inflated so a hurdle model (Martin et al., 2005; Zuur et al., 2009) was used consisting of a binomial (logit-link) GLMM to test whether individuals sprinted or not during each light phase, and a second GLMM to test whether differences occurred in the number of sprint events during times when hares sprinted at least once. As behavioral states were analyzed separately, a Bonferroni correction (alpha = 0.02) was applied to all analyses at this temporal scale. At an hourly scale, we examined how foraging time (min/h) was influenced by the presence of moon using a GLMM with a moon phase and moon position (set or risen) interaction. This analysis only used hourly foraging values during the darkest light phase (night). All hours when the moon rose, or set were removed to reduce landscape-imposed variation in timing of rising and setting. We included the intermediate moonlight levels in this analysis as it is during this part of each month that the moon rises or sets halfway through the night and the response to moon position relative to the horizon might be most pronounced. All GLMMs included hare ID as a random factor, and for the within-day and hourly scale analysis, date was included as a random factor. Model fit was calculated using conditional R-squared values, and significance of fixed effects were assessed using Wald chi-square (χ^2) tests (Bolker et al., 2009).

RESULTS

Accelerometer Classification

We found that a ΔOA threshold value of 1.15 g-forces distinguished moving from not moving with a 95.8% accuracy using a sample window duration of 12 s. Not moving was correctly classified 94.6% (159/168 events) of the time, while moving had an accuracy of 97.0% (163/168 events; **Figure 3**). A ΔOA threshold of 3.0 g-forces over 4 s further separated any segment classified as moving into foraging (feeding, and short travel) and traveling with an accuracy of 88.1% (traveling = 83.1%, 242/291 events; foraging = 93.1%, 271/291 events; **Figure 3**). Finally, traveling-classified segments were divided into sprinting and hopping (low speed travel) using a OA threshold value of 6.5 g-forces over 4 s with an accuracy of 88.4% (sprinting = 76.9%, 10/13 events; hopping = 100%, 13/13 events; **Figure 3**). The overall accuracy of the classification into three behavioral states (not moving, foraging, and traveling), which accounts for all misclassifications at each level of the tree was 88.0% with slightly lower divisional accuracy than what was calculated when setting the threshold values (**Table 1**). Accuracy varied at the individual level from 80 to 91.7%, with large variation in individual accuracy of classifying traveling and foraging (see **Supplementary Materials** for individual confusion matrices 1.4). Classification using a random forest algorithm generated accuracies ranging from 83.3 to 96.7% depending on the sample window chosen (see **Figure S2**).

Refinement of Accelerometer Behavior Categories Using Acoustic Recorders

Three audio sounds (silence, chewing, and hopping) could consistently be identified by listeners (see **Audios 1, 2**, and **3** in **Supplementary Materials** for example clips; **Table S3**). Inter-rater reliability was 97 and 95% for chewing and silence, respectively. There was 83.3% agreement among all raters for "unclassifiable sounds"; some sound clips were suggested to be hopping or chewing, but there was no consensus across all listeners. Hopping had the lowest among-listener agreement (55.6%) with the most common alternative classification being unclassifiable sound. We are confident in our identification of these four sounds due to (1) the high inter-rater reliability scores, and (2) sounds labeled chewing, hopping, and silence primarily occurred when the hare was foraging, traveling, and not moving according to the accelerometer, respectively. That being said, we have no means to truly validate that these sounds are the behavioral states classified. As such, our acoustic results should be taken with caution as there is a potential for misclassification.

Acoustic spectral analysis of user-classified sounds indicated that silence had no peaks in amplitude at any frequency, chewing had a peak at 250–600 Hz, and hopping had a primary peak at 0–650 Hz and secondary peak at 3,650–4,000 Hz (**Figure 4**), but peak frequencies varied between recorders (**Supplementary Materials 1.3**, **Figure S3**). Automated classification of these three acoustic behavioral states produced an accuracy of 94.1% (**Table 2**) with little variance in accuracy between devices (**Supplementary Materials 1.5**). Only 5.7% of acoustic files did not match the properties of these three behaviors and were classified as other sounds. The majority (∼60%) of these other sounds were short in duration (1 s) and may have consisted of branches or parts of the hare hitting the microphone, or the hare shifting in position. In comparison, only a small amount of the silence (4%), chewing (9.4%), and hopping (22.8%) were short duration (1 s).

Acoustic refinement of accelerometer classification revealed that bouts of foraging were composed of a combination of chewing (42.5%), hopping (35.7%), silence (13.0%), and other sounds (8.8%). The composition of foraging bouts varied among individuals (**Figure 5A**) but, on average, was consistent throughout the day (**Figure 6A**). The behavioral composition of not moving was consistent among individuals and was composed of silence (∼80%) chewing (∼13%), other sounds (∼4%), and hopping (0.3%) (**Figure 5B**). The composition of not moving varied with time of day switching from primarily silence during the day to primarily chewing at night (**Figure 6B**).

Daily Activity

We calculated average daily time budgets of free-ranging snowshoe hares in winter using accelerometer data from all individuals. Hares spent almost all of their time either foraging (∼49%) or not moving (∼49%) with small amounts of traveling (2%; i.e., either long duration hopping or sprinting). Not moving was the predominant behavior during daylight hours, and time spent foraging increased at dusk, remained high throughout

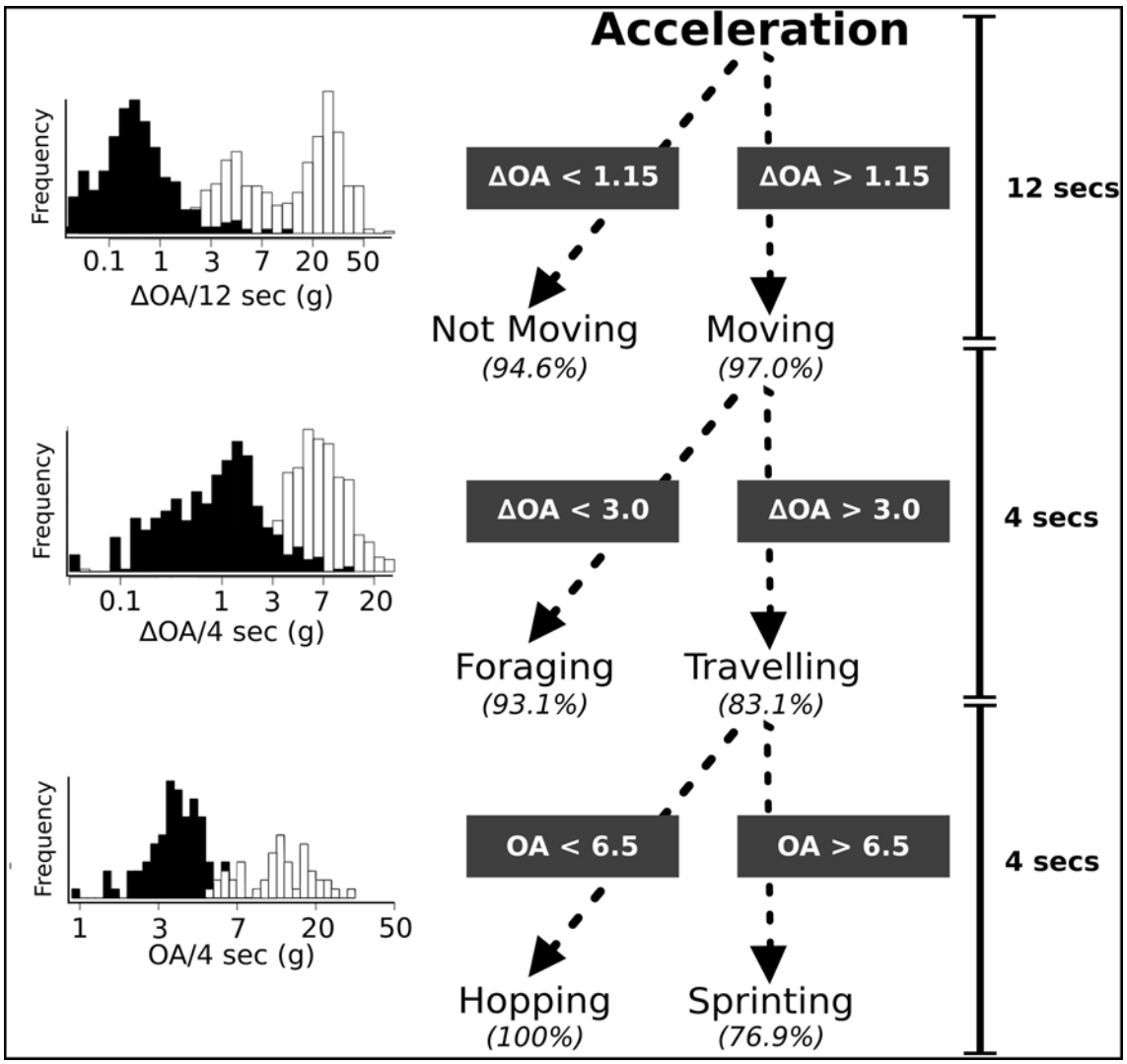

FIGURE 3 | Hierarchal decision tree used to classify snowshoe hare accelerometer data to four behavioral categories. Long duration behavioral states were classified using a 12 s window, while short duration behavior was classified using a 4 s window. The accuracy of each division is the percentage of observed behavior that were classified correctly. Histograms depict the frequency of each behavior occurring at different values of the summary statistic used for the division of the tree. Black represents behavior on left side of the decision tree while white is behavior on right side of decision tree at each split.

the night, and decreased at dawn (**Figures 6B**, **7A**). Acoustic recorders revealed that snowshoe hares split their time between silence (46.3%), chewing (37.5%), and hopping (10.8%) with small amounts of other sounds (5.4%). Hares were mainly silent during daylight, while at night they were chewing and hopping (**Figure 6**).

Moonlight Analysis

Snowshoe hares decreased daily time spent foraging by 40 min per day during a full moon compared to during a new moon ($\chi^2 = 11.6$, df = 2, $P = 0.003$, model $R^2_{(c)} = 0.23$). Time spent foraging, hopping, and the occurrence of sprinting events during each light phase was influenced by the phase of the moon (foraging: $\chi^2 = 230.8$, df = 14, $P < 0.001$, model $R^2_{(c)} = 0.69$; hopping: $\chi^2 = 104.5$, df = 14, $P < 0.001$, model $R^2_{(c)} = 0.37$; sprinting: $\chi^2 = 42.9$, df = 14, $P < 0.001$, model $R^2_{(c)} = 0.67$; **Figure 7**), but the number of sprint events in a light phase was not influenced by the moon ($\chi^2 = 15.2$, df = 14, $P = 0.36$, model $R^2_{(c)} = 0.32$). Hares had the largest decrease in foraging time during the night, with an average decrease of 3 min/h or 51 min between

TABLE 1 | Confusion matrix of accelerometer-based classification of snowshoe hare behavior to three categories: not moving, forage, and travel.

	Not moving	Forage	Travel	Accuracy%
Not moving	68	7	0	90.7
Forage	6	66	3	88.0
Travel	0	11	64	85.3

Overall accuracy is 88.0%.

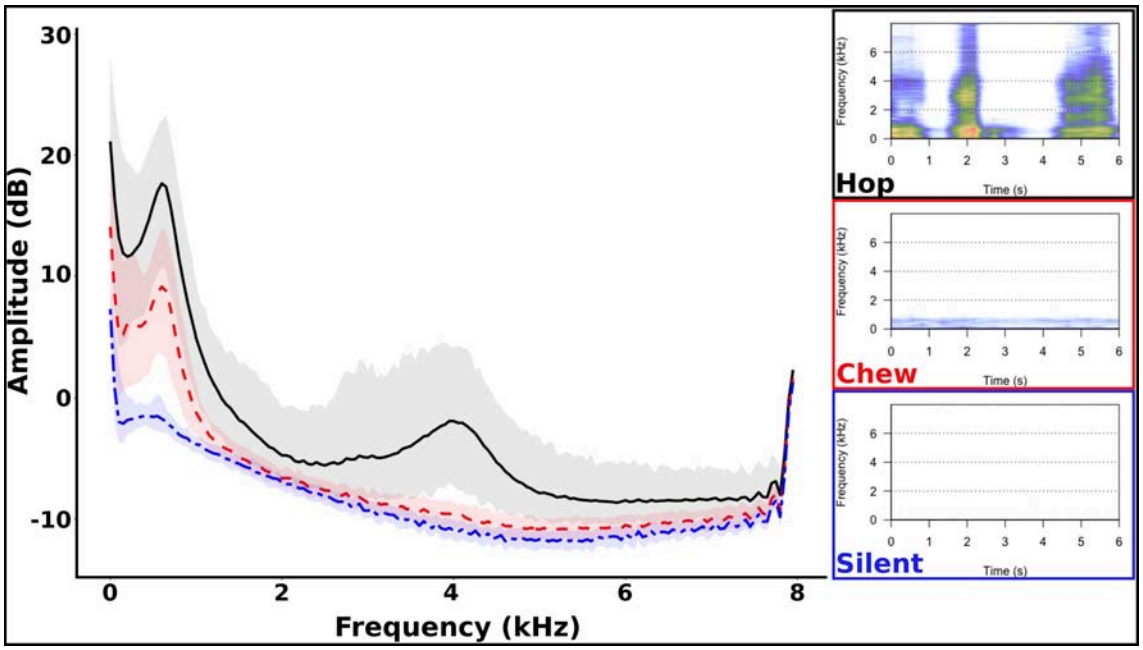

FIGURE 4 | Amplitude frequency spectral properties of hop, chew, and silent sounds from animal-borne acoustic recorders on snowshoe hares **(Right)** and accompanying spectrograms **(Left)**. Shading represents the 95% CI of the amplitude for each behavior.

dusk until dawn during full moons compared to new moons (**Figure 7B**). Hopping, but not sprinting, was also substantially reduced through the darkest phases from twilight until dawn (**Figures 7C,D**). However, this pattern switched during dawn and morning following a full moon when hares spent noticeably more time foraging and hopping and were more likely to sprint than after a new moon (**Figures 7B–D**). Within a single night, snowshoe hare responses to the moon being above or below the horizon depended on the phase of the moon ($\chi^2 = 15.1$, df = 2, $P < 0.001$, model $R^2_{(c)} = 0.30$; **Figure 8**). When the moon was at its brightest (>0.66 fraction is visible), snowshoe hares spent more time foraging per hour during the hours that the moon was below the horizon than when the moon had risen ($t = 2.07$, df = 1,443, $P = 0.039$; **Figure 8**). However, during all other phases of the moon (visible fraction is <0.66), hares decreased time spent foraging when the moon was below the horizon as compared to when it was above the horizon (fraction<0.33: $t = -2.25$, df = 1,436, $P = 0.024$; fraction>0.33: $t = -3.62$, df = 1,444, $P < 0.001$; **Figure 8**).

DISCUSSION

By integrating two biologging technologies (accelerometers and acoustic recorders), we demonstrate the possibility of accurately classifying behavior of a nocturnal, and often difficult to observe, free-ranging mammal over multi-month durations. After achieving high overall accuracy for both accelerometer- and acoustic-based behavioral classification, we were able to explore the composition of broad accelerometer categories revealing inter- and intra-individual differences in behavior. Our demonstration of the potential for accelerometers to assess behavioral responses of hares to moonlight revealed that hares adjust their time spent foraging as light conditions change.

TABLE 2 | Confusion matrix of acoustic-based behavioral classification of snowshoe hare behavior to three categories: silence, chew, and hop.

	Silence	Chew	Hop	Other	Accuracy%
Silence	87	3	0	0	96.7
Chew	0	84	2	4	93.3
Hop	0	5	83	2	92.2

Overall accuracy is 94.1%.

Biologging Behavior

Despite general difficulties in observing cryptic species, we successfully recorded behavior of a nocturnal species for up to 3 months continuously using biologging technology. We found that different technologies were best suited for extracting specific behavioral states and that a combination of technologies may be necessary to understand the complex nature of a species' behavior. For example, although accelerometers could classify foraging behavior, the act of chewing in snowshoe hares did not generate a measurable amount of acceleration. In this particular study, our capacity to detect chewing was limited by low sampling regime but it is also likely that some behavioral acts, like chewing, may be difficult to detect using acceleration at any sampling frequency without adjusting the attachment of the device to a different location (such as to the jaw; Iwata et al., 2012). However, chewing was a behavior that was easily identifiable on the acoustic recorders. Traveling, on the other hand, was more accurately distinguishable with accelerometers

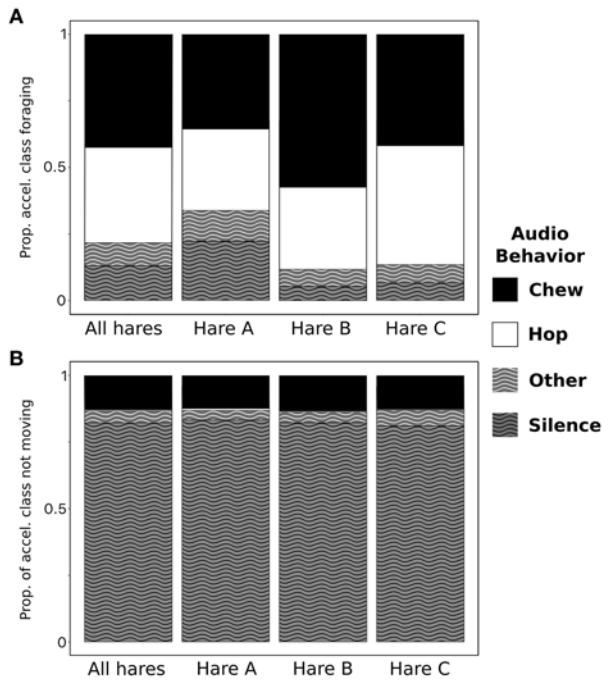

FIGURE 5 | Acoustic determination of time spent chewing (black), hopping (white), silent (black stripe), and other (white stripe) during accelerometer-defined bouts of foraging **(A)** and not moving **(B)**, across all individuals ($n = 3$) and for each individual free-ranging snowshoe hare.

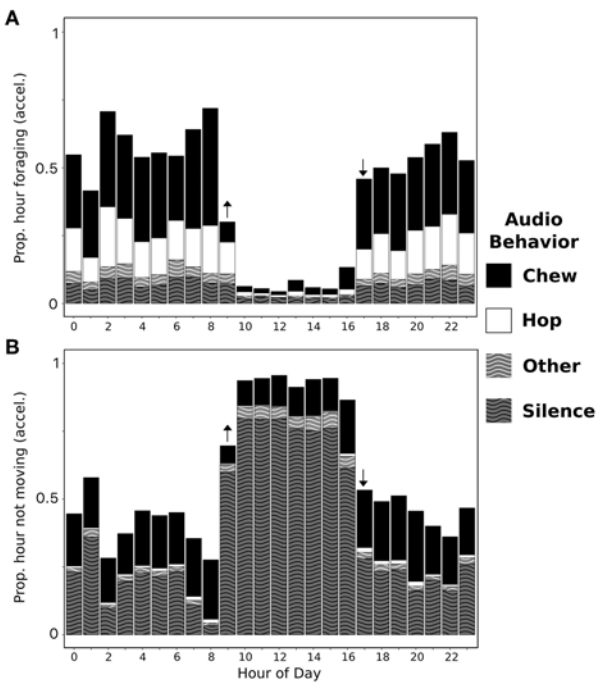

FIGURE 6 | Accelerometer classification of the proportion of each hour of the day spent foraging **(A)** and not moving **(B)** and the acoustic composition (chewing: black, hopping: white, silence: black stripe, or other: white stripe) of those behavioral states. All data was collected over the same 2 days from free-ranging snowshoe hares ($n = 3$) that were outfitted with an accelerometer and an acoustic recorder. Arrows denote sunrise and sunset times.

than through acoustics. Additionally, while we were significantly below the Nyquist criterion for a hare hop (Brown et al., 2013), we show that accurate classification is possible to accuracies (88.0%) comparable to those achieved (75% to 98%) using higher frequencies (3.3 to 40 Hz; Nathan et al., 2012; Bidder et al., 2014; McClune et al., 2014; Hammond et al., 2016). At this lower frequency, the detail of behavioral categories (e.g., foraging instead of feeding and individual hops) is compromised to maintain accuracy. This compromise will not suit researchers interested in describing steps or wingbeats over the span of days, but for researchers interested in behavioral changes over the span of months this will likely be a negligible cost.

Our use of animal-borne acoustic recorders not only provided a means of determining behavioral composition of accelerometer classification, but also demonstrated an alternative technique for collecting continuous behavioral data in circumstances when other methodologies might not be possible. Despite only recording on a few individuals ($n = 3$) for a short duration to test the potential of this technology, we revealed that individual and temporal variation exists in the composition of accelerometer-classified foraging and not moving categories. Although sounds like chewing were easily identifiable, other sounds could not be identified to a particular behavior with any confidence. For this reason, validating acoustic data with behavioral observations would be recommended in order to generate a more detailed classification than what we presented here. Acoustic recorders are rarely used for non-vocal behavior despite their commonality in animal communication research (e.g., Bee and Gerhardt, 2001; Reby and McComb, 2003; Fischer et al., 2004). However, successful applications of acoustics to record behavior all highlight the considerable wealth of information contained in this media form including bodily functions (e.g., heart rate; Couchoux et al., 2015), behavior (e.g., chewing, grooming, wingbeats; Ilany et al., 2013; Stowell et al., 2017; Wijers et al., 2018), and environmental noise (e.g., anthropogenic noise, wind, vocalization of other species; Lynch et al., 2015; Stowell et al., 2017).

Daily Activity

Analyses of both accelerometer and acoustic information revealed that snowshoe hares split their time primarily between not moving and foraging-related behavior with limited time spent traveling. This is a similar pattern as seen in other hare species where vigilance, rest and feeding represented over 95% of the day (Lush et al., 2016). At least in winter, when nights are long and dark, we found that snowshoe hares are characterized by a single daily activity peak centered in the night, with elevated activity extending into dawn and dusk. The limited literature on the behavior of free-ranging snowshoe hares generally classifies the species as exhibiting either crepuscular (Murray, 2003) or nocturnal (Foresman and Pearson, 1999) activity patterns. Using the definition of Anderson and Wiens (2017) and Bartness and Albers (2000), snowshoe hares are likely best classified as a

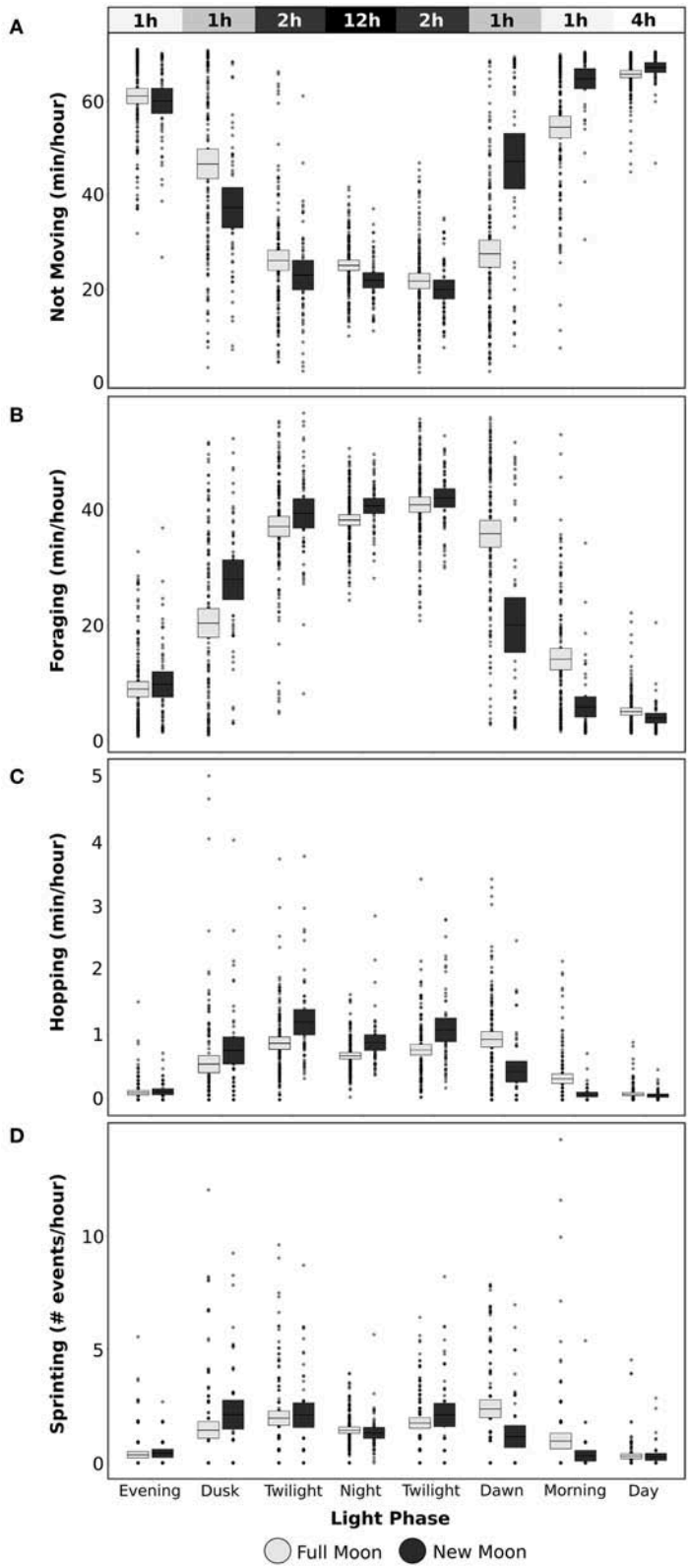

FIGURE 7 | Average time spent by snowshoe hares on each behavior during different light phases of a day and moon phase with light boxes for full moon (lunar illumination > 0.66) and dark boxes for new moon (lunar illumination < 0.33) conditions (mean ± 95% CI). Not moving **(A)**, foraging **(B)**, and hopping **(C)** are presented as time spent (min/h) expressing each behavior, while sprinting **(D)** is depicted as number of events per hour. Bar at top indicates the solar illumination level of each light phase and average number of hours that occur during that phase in a 24-h period.

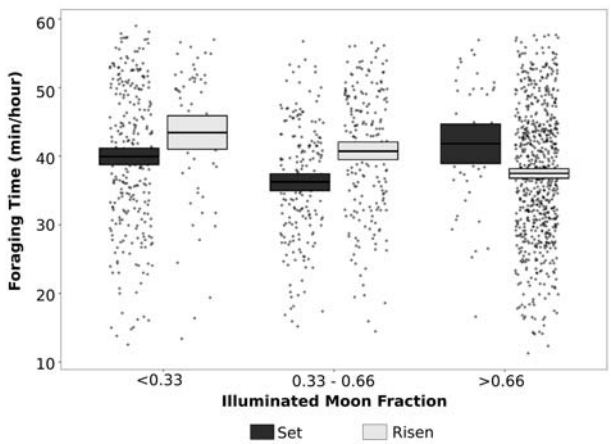

FIGURE 8 | Average foraging time (min/h) of snowshoe hares when moon is above (risen; light gray) or below (set; black) the horizon during different moon illumination fractions (mean ± 95% CI).

nocturnal species, but alternatively as a nocturnal species with activity that extends into the crepuscular period.

Response to Moonlight

For nocturnal animals, moonlight can drastically change the landscape, and impacts the tradeoff between foraging and predation risk (Prugh and Golden, 2014; Gigliotti and Diefenbach, 2018). We found that moonlight conditions caused snowshoe hares to make substantial adjustments in behavior throughout the night, with the magnitude and direction being dependent on the light phase. During the darkest phases of the night (dusk to morning twilight), traveling was reduced by ∼30% and foraging by ∼6% when the moon was full. This reduction in foraging is considerably less than the average reduction found in foraging trials (13.6%) across all species where it has been tested (Prugh and Golden, 2014), but the disproportionate reduction in traveling to foraging suggests that the snowshoe hares were not moving around their environment in the same manner while foraging. These responses to moonlight confirm previous studies in snowshoe hares that have reported decreased activity and adjustments in habitat use under full moon conditions (Gilbert and Boutin, 1991; Griffin et al., 2005; Gigliotti and Diefenbach, 2018). Although we could not directly measure whether moonlight impacts predation risk, increased illumination at night has been linked to increased activity and feeding in various predators including coyotes (Kenaga et al., 2013) and *Lynx* spp. (Rockhill et al., 2013; Heurich et al., 2014). The reduction in activity under full moons suggests that snowshoe hares change their behavior to reduce risk of predation.

Hares appeared to behaviorally compensate for the lost foraging time associated with full moons via an extension of foraging into morning daylight hours. Such compensatory temporal shifts in behavior due to moonlight have also been shown to occur in other species (e.g., *Dipodomys merriami*; Daly et al., 1992). All animals have minimum energy intake requirements that must be achieved through daily foraging (Norberg, 1977) and although some species can reduce this requirement (e.g., through fat storage or use of torpor), snowshoe hares who have limited body fat stores (∼ 4 days resting metabolic support; Whittaker and Thomas, 1983) must forage on a daily basis. This nutritional constraint seems to translate to drastic adjustments in temporally-explicit foraging choices rather than changes in overall foraging time as light conditions change (Gilbert and Boutin, 1991). If choice in timing of foraging is directly related to predation risk, then in hares, moonlight shifts risk of predation from relatively low to relatively high during the night to the extent that it is perceived to be safer to forage in the morning than maintain high foraging rates during the night.

A second compensation that seems to occur is that adjustments in behavior made during the night counteract any increases in predation risk that would be expected. We considered sprinting to be a measure of flightiness, as although some sprints occur from direct predator encounters, the majority are likely responses stemming from wary behavior (Vasquez et al., 2002). If the amount of flightiness is related to the amount of perceived predation risk, as would be expected, then the lack of effect of moonlight on sprinting during the night (**Figure 7D**) suggests that hares reduce their time spent foraging to minimize the level of predation risk, creating a constant level of risk across moonlight conditions. However, the increased sprinting during dawn and morning periods following full moon nights suggests the morning compensational foraging bouts come at a cost. This increased level of perceived predation risk may be due to the morning period being a time when all predators can be active. Predators of hares are characterized as nocturnal/crepuscular (*Lynx canadensis, Canis latrans, Bubo virginianus*), or diurnal/crepuscular *(Accipiter gentilis)*, but many nocturnal species have considerable movement into and throughout the day, especially in winter, making the morning a time when both primarily nocturnal and diurnal predators may be hunting (Ozoga and Harger, 1966; Squires and Reynolds, 1997; Kolbe and Squires, 2007; Arias-Del Razo et al., 2011; Artuso et al., 2013). Despite this increased risk during the compensatory foraging, the strategy of reducing foraging during the night likely results in lower exposure to risk overall.

We additionally found that the extent of moonlight avoidance by snowshoe hares was dependent on the phase of the moon, with diminished foraging times when the moon was above the horizon on full moon nights and below the horizon on partial or new moon nights; a switching of preference that has not been observed previously. Generally in other species, individuals are found to be more active during the darkest hours when the moon is below the horizon regardless of moon phase (Morrison, 1978; Daly et al., 1992). This switching of preference for moonlight would suggest that risk is highest when light conditions are either at their brightest or darkest (Prugh and Golden, 2014). The main predators of snowshoe hares all rely on visual cues for hunting (Wells, 1978; Artuso et al., 2013). As such, a decrease in activity with increasing light may be a response to higher hunting efficiency from their predators through improved vision. Although the darkest conditions may inhibit the predators ability to hunt (Wells, 1978), these conditions will have similar effects on the hares ability to detect predators as they also rely partially on visual senses to detect danger. It may be that the loss of use of one of their senses is enough to cause the hares to select against these conditions for foraging, even if predators are similarly hindered.

Biologgers provide us with the opportunity to investigate detailed behavioral adjustments over long temporal timeframes revealing subtle and short-term responses to environmental change. Every biologging technique has strengths and weaknesses, however, combining biologging technology in complementary ways can allow a circumvention of such issues. Short duration acoustic recorders provided a method of collecting behavioral states of a free ranging nocturnal animal that were not possible with accelerometers and vice versa. This allowed for easier interpretation of the behavioral classification generated from long duration accelerometers. Such multi-faceted approaches will allow us to gain the most detailed insight yet into behavioral responses of species to environmental change.

ETHICS STATEMENT

This research conformed to the guidelines of the American Society of Mammalogists (Sikes et al., 2016) and was approved by the McGill University, University of Alberta, and University of Toronto Animal Care and Use Committees.

AUTHOR CONTRIBUTIONS

ES, AM, MH, MP, YM, and SB conceived the ideas. ES, AM, MP, YM, JS, and MB collected the data. ES analyzed the data and led the writing. All authors contributed critically to the ideas and drafts and gave final approval for publication.

ACKNOWLEDGMENTS

We wish to thank all the field assistants who helped trap hares and Technosmart for troubleshooting devices for us. We thank Agnes MacDonald and her family for long-term access to her trapline, and the Champagne and Aishihik First Nations for supporting our work within their traditional territory. This work was supported by a Natural Sciences and Engineering Council of Canada (NSERC), the Canada Research Chairs program, Northern Studies Training Program, Wildlife Conservation Society, Canada Graduate Scholarship [to ES, MB, YM, and MP.], Vanier Graduate Scholarship [to AM], W. Garfield Weston Award for Northern Research [to ES, AM, and MP], and Ontario Graduate Scholarship [to JS and MB]; NSERC Discovery Grants [to SB, DM, and MH], and Institut Nordique du Quebec (INQ) Chair in Northern Research [to MH].

SUPPLEMENTARY MATERIAL

The Supplementary Material for this article can be found online at: https://www.frontiersin.org/articles/10.3389/fevo.2019.00154/full#supplementary-material

Audio 1 | Example sound clip of chewing from acoustic recorders attached to snowshoe hares.

Audio 2 | Example sound clip of hopping from acoustic recorders attached to snowshoe hares.

Audio 3 | Example sound clip of silence from acoustic recorders attached to snowshoe hares.

REFERENCES

Agafonkin, V., and Thieurmel, B. (2017). *Suncalc: Computer Sun Position, Sunlight Phases, Moon Position and Lunar Phase*. R package version 0.3.

Anderson, S. R., and Wiens, J. J. (2017). Out of the dark: 350 million years of conservatism and evolution in diel activity patterns in vertebrates. *Evolution* 71, 1944–1959. doi: 10.1111/evo.13284

Arias-Del Razo, I., Hernández, L., Laundré, J. W., and Myers, O. (2011). Do predator and prey foraging activity patterns match? A study of coyotes (Canis latrans), and lagomorphs (*Lepus californicus* and *Sylvilagus audobonii*). *J. Arid Environ.* 75, 112–118. doi: 10.1016/j.jaridenv.2010.09.008

Artuso, C., Houston, C. S., Smith, D. G., and Rohner, C. (2013). "Great Horned Owl (Bubo virginianus)," in *The Birds of North America*, ed A. F. Poole (Ithaca, NY: Cornell Lab of Ornithology).

Bartness, T., and Albers, H. (2000). "Activity patterns and the biological clock in mammals," in *Activity Patterns in Small Mammals: An Ecological Approach*, eds S. Halle and N. Stenseth (Berlin: Springer-Verlag), 23–47. doi: 10.1007/978-3-642-18264-8_3

Bates, D., Maechler, M., Bolker, B., and Walker, S. (2015). Fitting linear mixed-effects models using lme4. *J. Stat. Softw.* 67, 1–48. doi: 10.18637/jss.v067.i01

Bee, M. A., and Gerhardt, H. C. (2001). Neighbour-stranger discrimination by territorial male bullfrogs (*Rana catesbeiana*): I. Acoustic basis. *Anim. Behav.* 62, 1129–1140. doi: 10.1006/anbe.2001.1851

Beutler, F. J. (1966). Error-free recovery of signals from irregularly spaced samples. *SIAM Review* 8, 328–335. doi: 10.1137/1008065

Bidder, O. R., Campbell, H. A., Gómez-Laich, A., Urgé, P., Walker, J., Cai, Y., et al. (2014). Love thy neighbour: automatic animal behavioural classification of acceleration data using the K-nearest neighbour algorithm. *PLoS ONE* 9:e88609. doi: 10.1371/journal.pone.0088609

Bolker, B. M., Brooks, M. E., Clark, C. J., Geange, S. W., Poulsen, J. R., Stevens, M. H. H., et al. (2009). Generalized linear mixed models: a practical guide for ecology and evolution. *Trends Ecol. Evol.* 24, 127–135. doi: 10.1016/j.tree.2008.10.008

Boonstra, R., Andreassen, H. P., Boutin, S., Hušek, J., Ims, R. A., Krebs, C. J., et al. (2016). Why do the boreal forest ecosystems of Northwestern Europe differ from those of Western North America? *Bioscience* 66, 722–734. doi: 10.1093/biosci/biw080

Boudreau, M. R. (2019). *The Cascading Effects of Risk in the Wild: How Snowshoe Hares Respond to the Threat of Predation*, Ph.D dissertation. Trent University, 159.

Broell, F., Noda, T., Wright, S., Domenici, P., Steffensen, J. F., Auclair, J. P., et al. (2013). Accelerometer tags: detecting and identifying activities in fish and the effect of sampling frequency. *J. Exp. Biol.* 216, 1255–1264. doi: 10.1242/jeb.077396

Brown, D. D., Kays, R., Wikelski, M., Wilson, R., and Klimley, A. (2013). Observing the unwatchable through acceleration logging of animal behavior. *Anim. Biotelemetr.* 1:20. doi: 10.1186/2050-3385-1-20

Campbell, H. A., Gao, L., Bidder, O. R., Hunter, J., and Franklin, C. E. (2013). Creating a behavioural classification module for acceleration data: using a captive surrogate for difficult to observe species. *J. Exp. Biol.* 216, 4501–4506. doi: 10.1242/jeb.089805

Chen, K. Y., and Bassett, D. R. (2005). The technology of accelerometry-based activity monitors: current and future. *Med. Sci. Sports Exerc.* 37, 490–500. doi: 10.1249/01.mss.0000185571.49104.82

Couchoux, C., Aubert, M., Garant, D., and Réale, D. (2015). Spying on small wildlife sounds using affordable collar-mounted miniature microphones: an innovative method to record individual daylong vocalisations in chipmunks. *Sci. Rep.* 5:10118. doi: 10.1038/srep10118

Daly, M., Behrends, P. R., Wilson, M. I., and Jacobs, L. F. (1992). Behavioural modulation of predation risk: moonlight avoidance and crepuscular compensation in a nocturnal desert rodent, *Dipodomys merriami*. *Anim. Behav.* 44, 1–9. doi: 10.1016/S0003-3472(05)80748-1

Depraetere, M., Pavoine, S., Jiguet, F., Gasc, A., Duvail, S., and Sueur, J. (2012). Monitoring animal diversity using acoustic indices: implementation in a temperate woodland. *Ecol. Indic.* 13, 46–54. doi: 10.1016/j.ecolind.2011.05.006

Elliott, K. H. (2016). Measurement of flying and diving metabolic rate in wild animals: Review and recommendations. *Compar. Biochem. Physiol. Part A* 202, 63–77. doi: 10.1016/j.cbpa.2016.05.025

Fischer, J., Kitchen, D. M., Seyfarth, R. M., and Cheney, D. L. (2004). Baboon loud calls advertise male quality: acoustic features and their relation to rank, age, and exhaustion. *Behav. Ecol. Sociobiol.* 56, 140–148. doi: 10.1007/s00265-003-0739-4

Foresman, K. R., and Pearson, D. E. (1999). Activity patterns of American martens, Martes americana, snowshoe hares, Lepus americanus, and red squirrels, *Tamiasciurus hudsonicus*, in westcentral Montana. *Can. Field Natural.* 113, 386–389.

Gasc, A., Sueur, J., Jiguet, F., Devictor, V., Grandcolas, P., Burrow, C., et al. (2013). Assessing biodiversity with sound: do acoustic diversity indices reflect phylogenetic and functional diversities of bird communities? *Ecol. Indic.* 25, 279–287. doi: 10.1016/j.ecolind.2012.10.009

Gigliotti, L. C., and Diefenbach, D. R. (2018). Risky behavior and its effect on survival: snowshoe hare behavior under varying moonlight conditions. *J. Zool.* 305, 27–34. doi: 10.1111/jzo.12532

Gilbert, B., and Boutin, S. (1991). Effect of moonlight on winter activity of snowshoe hares. *Arctic Alpine Res.* 23, 61–65. doi: 10.2307/1551438

Gleiss, A. C., Wilson, R. P., and Shepard, E. L. C. (2011). Making overall dynamic body acceleration work: on the theory of acceleration as a proxy for energy expenditure. *Methods Ecol. Evol.* 2, 23–33. doi: 10.1111/j.2041-210X.2010.00057.x

Graf, P. M., Wilson, R. P., Qasem, L., Hackländer, K., Rosell, F., and Falcone, E. (2015). The use of acceleration to code for animal behaviours; a case study in free-ranging Eurasian beavers Castor fiber. *PLoS ONE* 10:e0136751. doi: 10.1371/journal.pone.0136751

Griffin, P. C., Griffin, S. C., Waroquiers, C., and Mills, L. S. (2005). Mortality by moonlight: predation risk and the snowshoe hare. *Behav. Ecol.* 16, 938–944. doi: 10.1093/beheco/ari074

Hammond, T. T., Springthorpe, D., Walsh, R. E., and Berg-Kirkpatrick, T. (2016). Using accelerometers to remotely and automatically characterize behavior in small animals. *J. Exp. Biol.* 2, 1618–1624. doi: 10.1242/jeb.136135

Heurich, M., Hilger, A., Küchenhoff, H., Andrén, H., Bufka, L., Krofel, M., et al. (2014). Activity patterns of Eurasian lynx are modulated by light regime and individual traits over a wide latitudinal range. *PLoS ONE* 9:e114143. doi: 10.1371/journal.pone.0114143

Ilany, A., Barocas, A., Kam, M., Ilany, T., and Geffen, E. (2013). The energy cost of singing in wild rock hyrax males: evidence for an index signal. *Anim Behav.* 85, 995–1001. doi: 10.1016/j.anbehav.2013.02.023

Iwata, T., Sakamoto, K. Q., Takahashi, A., Edwards, E. W. J., Staniland, I. J., Trathan, P. N., et al. (2012). Using a mandible accelerometer to study fine-scale foraging behavior of free-ranging Antarctic fur seals. *Mar. Mamm. Sci.* 28, 345–357. doi: 10.1111/j.1748-7692.2011.00482.x

Johnson, M. D., and De León, Y. L. (2015). Effect of an invasive plant and moonlight on rodent foraging behavior in a coastal dune ecosystem. *PLoS ONE* 10:e0117903. doi: 10.1371/journal.pone.0117903

Keith, L. B. (1964). Daily activity pattern of snowshoe hares. *J. Mammal.* 45, 626–627.

Kenaga, B. A., Krebs, R. A., and Clapham, W. B. (2013). Coyote land use inside and outside urban parks. *Am. Midl. Nat.* 170, 298–310. doi: 10.1674/0003-0031-170.2.298

Kolbe, J. A., and Squires, J. R. (2007). Circadian activity patterns of Canada lynx in Western Montana. *J. Wildlife Manage.* 71, 1607–1611. doi: 10.2193/2005-727

Krebs, C. J., Boonstra, R., and Boutin, S. (2018). Using experimentation to understand the 10-year snowshoe hare cycle in the boreal forest of North America. *J. Anim. Ecol.* 87, 87–100. doi: 10.1111/1365-2656.12720

Krebs, C. J., Boutin, S., Boonstra, R., Sinclair, A. R. E., Smith, J. N. M., Dale, M. R. T., et al. (1995). Impact of food and predation on the snowshoe hare cycle. *Science* 269, 1112–1115. doi: 10.1126/science.269.5227.1112

Lush, L., Ellwood, S., Markham, A., Ward, A. I., and Wheeler, P. (2016). Use of tri-axial accelerometers to assess terrestrial mammal behaviour in the wild. *J. Zool.* 298, 257–265. doi: 10.1111/jzo.12308

Lynch, E., Angeloni, L., Fristrup, K., Joyce, D., and Wittemyer, G. (2013). The use of on-animal acoustical recording devices for studying animal behavior. *Ecol. Evol.* 3, 2030–2037. doi: 10.1002/ece3.608

Lynch, E., Northrup, J. M., McKenna, M. F., Anderson, C. R., Angeloni, L., and Wittemyer, G. (2015). Landscape and anthropogenic features influence the use of auditory vigilance by mule deer. *Behav. Ecol.* 26, 75–82. doi: 10.1093/beheco/aru158

Martin, T. G., Wintle, B. A., Rhodes, J. R., Kuhnert, P. M., Field, S. A., Low-Choy, S. J., et al. (2005). Zero tolerance ecology: improving ecological inference by modelling the source of zero observations. *Ecol. Lett.* 8, 1235–1246. doi: 10.1111/j.1461-0248.2005.00826.x

McClune, D. W., Marks, N. J., Wilson, R. P., Houghton, J. D., Montgomery, I. W., McGowan, N. E., et al. (2014). Tri-axial accelerometers quantify behaviour in the Eurasian badger (Meles meles): towards an automated interpretation of field data. *Anim. Biotelemetr.* 2:5. doi: 10.1186/2050-3385-2-5

Morrison, D. W. (1978). Lunar phobia in a neotropical fruit bat, Artibevs jamaicensis (Chiroptera: Phyllostomidae). *Anim. Behav.* 26, 852–855. doi: 10.1016/0003-3472(78)90151-3

Murray, D. (2003). "Snowshoe hares and other hares," in *Wild Mammals of North America: Biology, Management and Conservation*, *2nd Edn*, eds G. Feldhamer, B. Thompson, and J. Chapman (Baltimore, MD: John Hopkins University Press), 147–157.

Nathan, R., Spiegel, O., Fortmann-Roe, S., Harel, R., Wikelski, M., and Getz, W. M. (2012). Using tri-axial acceleration data to identify behavioral modes of free-ranging animals: general concepts and tools illustrated for griffon vultures. *J. Exp. Biologyxperiment. Biol.* 215(Pt 6), 986–996. doi: 10.1242/jeb.058602

Norberg, R. A. (1977). An ecological theory on foraging time and energetics and choice of optimal food-searching method. *J. Anim. Ecol.* 46, 511–529. doi: 10.2307/3827

O'Donoghue, M., Boutin, S., Krebs, C. J., Zuleta, G., Murray, D. L., and Hofer, E. J. (1998). Functional responses of coyotes and lynx to the snowshoe hare cycle. *Ecology* 79, 1193–1208. doi: 10.2307/176736

Ozoga, J. J., and Harger, E. M. (1966). Winter activities and feeding habits of northern michigan coyotes. *J. Wildlife Manage.* 30, 809–818. doi: 10.2307/3798288

Pagano, A. M., Durner, G., Rode, K., Atwood, T., Atkinson, S., Peacock, E., et al. (2018). High-energy, high-fat lifestyle challenges an Arctic apex predator, the polar bear. *Science* 359, 568–572. doi: 10.1126/science.aan8677

Pijanowski, B. C., Villanueva-Rivera, L. J., Dumyahn, S. L., Farina, A., Krause, B. L., Napoletano, B. M., et al. (2011). Soundscape ecology: the science of sound in the landscape. *Bioscience* 61, 203–216. doi: 10.1525/bio.2011.61.3.6

Prugh, L. R., and Golden, C. D. (2014). Does moonlight increase predation risk? Meta-analysis reveals divergent responses of nocturnal mammals to lunar cycles. *J. Anim. Ecol.* 83, 504–514. doi: 10.1111/1365-2656.12148

Reby, D., and McComb, K. (2003). Anatomical constraints generate honesty: acoustic cues to age and weight in the roars of red deer stags. *Anim. Behav.* 65, 519–530. doi: 10.1006/anbe.2003.2078

Rockhill, A. P., DePerno, C. S., Powell, R. A., Baker, L., Warren, R., Diefenbach, D., et al. (2013). The effect of illumination and time of day on movements of bobcats (Lynx rufus). *PLoS ONE* 8:e69213. doi: 10.1371/journal.pone.0069213

Rohner, C., and Krebs, C. J. (1996). Owl predation on snowshoe hares: consequences of antipredator behaviour. *Oecologia* 108, 303–310. doi: 10.1007/BF00334655

Sandor, B. J., Jensen, E. J., Stone, E. M., Read, W. G., Waters, J. W., and Mergenthaler, J. L. (2000). Upper tropospheric humidity and thin cirrus. *Geophys. Res. Lett.* 27, 2645–2648. doi: 10.1029/1999GL011194

Shepard, E., Wilson, R., Quintana, F., Gómez Laich, A., Liebsch, N., Albareda, D., et al. (2008). Identification of animal movement patterns using tri-axial accelerometry. *Endanger. Species Res.* 10, 47–60. doi: 10.3354/esr00084

Sheriff, M. J., Krebs, C. J., and Boonstra, R. (2009). The sensitive hare: sublethal effects of predator stress on reproduction in snowshoe hares. *J. Anim. Ecol.* 78, 1249–1258. doi: 10.1111/j.1365-2656.2009.01552.x

Sikes, R. S., and Mammalogists, A. C., and Animal Care and Use Committee of the American Society of Mammalogists. (2016). Guidelines of the american society of mammalogists for the use of wild mammals in research. *J. Mammal.* 97, 663–688. doi: 10.1093/jmammal/gyw078

Spivey, R. J., and Bishop, C. M. (2013). Interpretation of body-mounted accelerometry in flying animals and estimation of biomechanical power. *J. R. Soc. Interfaces* 10, 20130404–20130404. doi: 10.1098/rsif.2013.0404

Squires, J. R., and Reynolds, R. T. (1997). "Northern Goshawk (Accipiter gentilis)," in *The Birds of North America,* eds A. F. Poole and F. B. Gill (Ithaca, NY: Cornell Lab of Ornithology). doi: 10.2173/bna.298

Stowell, D., Benetos, E., and Gill, L. F. (2017). On-bird sound recordings: automatic acoustic recognition of activities and contexts. *IEEE/ACM Transac. Audio Speech Lang. Proces.* 25, 1193–1206. doi: 10.1109/TASLP.2017.2690565

Studd, E. K., Landry-Cuerrier, M., Menzies, A. K., Boutin, S., Mcadam, A. G., Lane, J. E., et al. (2019). Behavioral classification of low-frequency acceleration and temperature data from a free-ranging small mammal. *Ecol. Evol.* 9, 619–630. doi: 10.1002/ece3.4786

Sueur, J., Aubin, T., and Simonis, C. (2008). Seewave: a free modular tool for sound analysis and sythesis. *Bioacoustics* 18, 213–226. doi: 10.1080/09524622.2008.9753600

Tatler, J., Cassey, P., and Prowse, T. A. A. (2018). High accuracy at low frequency: detailed behavioural classification from accelerometer data. *J. Exp. Biol.* 221:jeb184085. doi: 10.1242/jeb.184085

Thiebault, A., Pistorius, P., Mullers, R., and Tremblay, Y. (2016). Seabird acoustic communication at sea: a new perspective using bio-logging devices. *Sci. Rep.* 6:30972. doi: 10.1038/srep30972

Thompson, I. D., Bakhtiari, M., Rodgers, A. R., Baker, J. A., Fryxell, J. M., and Iwachewski, E. (2012). Application of a high-resolution animal-borne remote video camera with global positioning for wildlife study: observations on the secret lives of woodland caribou. *Wildl. Soc. Bull.* 36, 365–370. doi: 10.1002/wsb.130

Vasquez, R. A., Ebensperger, L. A., and Bozinovic, F. (2002). The influence of habitat on travel speed, intermittent locomotion, and vigilance in a diurnal rodent. *Behav. Ecol.* 13, 182–187. doi: 10.1093/beheco/13.2.182

Wells, M. C. (1978). Coyote senses in predation: environmental influences on their relative use. *Behav. Proc.* 3, 149–158. doi: 10.1016/0376-6357(78)90041-4

Whittaker, M. E., and Thomas, V. G. (1983). Seasonal levels of fat and protein reserves of snowshoe hares in Ontario. *Can. J. Zool.* 61, 1339–1345. doi: 10.1139/z83-180

Wijers, M., Trethowan, P., Markham, A., du Preez, B., Chamaillé-Jammes, S., Loveridge, A., et al. (2018). Listening to lions: animal-borne acoustic sensors improve bio-logger calibration and behaviour classification performance. *Front. Ecol. Evol.* 6:171. doi: 10.3389/fevo.2018.00171

Williams, C. T., Barnes, B. M., and Buck, C. L. (2016). Integrating physiology, behavior, and energetics: Biologging in a free-living arctic hibernator. *Compar. Biochem. Physiol. Part A* 202, 53–62. doi: 10.1016/j.cbpa.2016.04.020

Williams, C. T., Barnes, B. M., Yan, L., and Buck, C. L. (2017). Entraining to the polar day: circadian rhythms in arctic ground squirrels. *J. Exp. Biol.* 220(Pt 17), 3095–3102. doi: 10.1242/jeb.159889

Wilmers, C. C., Nickel, B., Bryce, C. M., Smith, J. A., Wheat, R. E., and Yovovich, V. (2015). The golden age of bio-logging: how animal-borne sensors are advancing the frontiers of ecology. *Ecology* 96, 1741–1753. doi: 10.1890/14-1401.1

Wilson, R. P., White, C. R., Quintana, F., Halsey, L. G., Liebsch, N., Martin, G. R., et al. (2006). Moving towards acceleration for estimates of activity-specific metabolic rate in free-living animals: the case of the cormorant. *J. Anim. Ecol.* 75, 1081–1090. doi: 10.1111/j.1365-2656.2006.01127.x

Zuur, A. F., Ieno, E. N., Walker, N. J., Saveliev, A. A., and Smith, G. M. (eds.). (2009). "Zero-truncated and zero-Inflated models for count data," in *Mixed Effects Models and Extensions in Ecology With R. Statistics for Biology and Health* (New York, NY: Springer), 261–293. doi: 10.1007/978-0-387-87458-6_11

Conflict of Interest Statement: The authors declare that the research was conducted in the absence of any commercial or financial relationships that could be construed as a potential conflict of interest.

The handling editor is currently co-organizing a Research Topic with two of the authors, DM and SB, and confirms the absence of any other collaboration.

Copyright © 2019 Studd, Boudreau, Majchrzak, Menzies, Peers, Seguin, Lavergne, Boonstra, Murray, Boutin and Humphries. This is an open-access article distributed under the terms of the Creative Commons Attribution License (CC BY). The use, distribution or reproduction in other forums is permitted, provided the original author(s) and the copyright owner(s) are credited and that the original publication in this journal is cited, in accordance with accepted academic practice. No use, distribution or reproduction is permitted which does not comply with these terms.

frontiers in Ecology and Evolution

ORIGINAL RESEARCH
published: 29 May 2019
doi: 10.3389/fevo.2019.00179

Individual Daily and Seasonal Activity Patterns in Fox Squirrels (*Sciurus niger*) Quantified by Temperature-Sensitive Data Loggers

***Thomas Wassmer*[1]* *and Roberto Refinetti*[2]**

[1] *Biology Department, Siena Heights University, Adrian, MI, United States,* [2] *Department of Psychological Science, Boise State University, Boise, ID, United States*

Almost all publications on the activity of animals have reported average patterns for the observed group or population and provided little information about the variability of these patterns in individual animals. As natural selection operates mainly on the level of individual animals, detailed data about the everyday life of single individuals and field data of high complexity are needed. This study provides low disturbance continuous recording of the diurnal/circadian activity cycle of individual fox squirrels (*Sciurus niger*) in a natural setting, which allowed us to document the intra-individual and inter-individual pattern variation over the seasons. The daily onsets and offsets of activity were inferred from recordings of skin temperature using iButtons attached to the necks of 14 individual squirrels over almost 4 years resulting in 25 continuous records totalling 1,353 days. All squirrels were clearly diurnal but varied greatly in the number of daily activity bouts showing predominantly unimodal and bimodal patterns. Variations in activity patterns were related mostly to the seasons, followed by the inter-individual variability between squirrels. Fox squirrels spent 66–68% of the day in their nests in spring, summer, and fall, and 77% in winter. In the same season, individual squirrels exited their nests at about the same time every morning. In summer, they left their nests about 3 h earlier in the morning than in winter. The timing of first exits was significantly correlated with the number of daily nest exits and total out-of-nest time (ONT), and both variables were significantly correlated with both photoperiod and daily maximum temperature. Squirrels studied simultaneously showed substantial day-to-day variability in both number of daily exits and total ONT that either matched or exceeded the inter-individual variability. Many squirrels left their nests occasionally during the night, while about half occasionally spent entire nights outside an insulated nest. The timing of nest entries and exits, the modality of the activity pattern, the daily proportion of rest, and the occurrence of activity during the typically inactive time of the activity cycle are all aspects of an animal's activity pattern. They should therefore receive more attention for the characterization of species-specific behavior.

Keywords: activity patterns, seasonality, environmental conditions, personality, chronotype, sciuridae, circadian rhythm, foraging behavior

OPEN ACCESS

Edited by:
Deseada Parejo,
University of Extremadura, Spain

Reviewed by:
Emily K. Studd,
McGill University, Canada
Inger Suzanne Prange,
Appalachian Wildlife Research Institute, United States

****Correspondence:***
Thomas Wassmer
twassmer@sienaheights.edu

Specialty section:
This article was submitted to Behavioral and Evolutionary Ecology, a section of the journal Frontiers in Ecology and Evolution

Received: *26 November 2018*
Accepted: *06 May 2019*
Published: *29 May 2019*

Citation:
Wassmer T and Refinetti R (2019) Individual Daily and Seasonal Activity Patterns in Fox Squirrels (Sciurus niger) Quantified by Temperature-Sensitive Data Loggers. Front. Ecol. Evol. 7:179. doi: 10.3389/fevo.2019.00179

INTRODUCTION

The appropriateness of an animal's activity level and pattern over the cycle of day and night and over the time course of the seasons is essential for its survival (DeCoursey et al., 2000; Larivée et al., 2010; Zhang et al., 2017) and reproductive success (Schmidt et al., 2008; Speakman, 2008; Zhao et al., 2013). The selective pressures to forage efficiently while avoiding injury and death lead to trade-offs in an animal's strategies between starvation and predation (Dall and Boyd, 2002; Higginson et al., 2012; Quinn et al., 2012; McNamara et al., 2016) that will affect both the daily proportions of time to be active and rest and the timing and regularity of rest and activity. Research on both aspects of activity is therefore essential to understand the biology of animal species. Locomotor activity has been shown to follow a reproducible daily pattern in numerous animal species, including tree squirrels (Tester, 1978; Adams, 1984; Koprowski and Corse, 2005; Wassmer and Refinetti, 2016). More than half a century ago, Aschoff (1966) observed that many, if not most, studies of locomotor activity had evinced a bimodal pattern with increased activity at dawn and dusk rather than a consolidated bout during the day or a consolidated bout during the night. Fox squirrels (*Sciurus niger*) are believed to be diurnal with bimodal activity pattern consisting of activity peaks in the early morning and right before sunset (Koprowski, 1994). However, most published data on tree squirrel species have reported average activity patterns for the observed group of animals or population and provided no indications about the variability of these activity patterns in individual animals (Hicks, 1949; Thompson, 1977; Wauters and Dhondt, 1987; Jodice and Humphrey, 1992; Wauters et al., 1992; Bordignon and Monteiro-Filho, 2000; Johnson et al., 2003; Koprowski and Corse, 2005; Ditgen et al., 2007). Only four studies so far have provided data on individual animals in tree squirrels (Zwahlen, 1975; Adams, 1984; Wassmer and Refinetti, 2016; Anders et al., 2017).

It has been suggested that researchers should move away from the "tyranny of the golden mean" (Bennett, 1987) and acknowledge individual behavioral differences as being more than just statistical noise around the group or population mean (Careau et al., 2008; Williams, 2008). This might help to shed light on how selection acts on the inter-individual variation in behavioral and physiological traits as evolution operates at the level of the individual (Roche et al., 2016). In studies on animals' activity cycles and patterns, it is the inter-individual variation in temporal strategies that provides the raw material for natural selection. The "golden mean" is averaging out this variation and obscures our understanding of the fitness impacts of frequency-dependent alternative temporal strategies. Therefore, detailed data about the everyday life of single individuals and field data of high complexity are needed (Halle and Stenseth, 2000).

Although not currently fully included into the concept of animal personalities (Gosling, 2001; Sih et al., 2004; Stamps, 2007; Wolf and Weissing, 2012), an animal's activity cycle and pattern is of essential ecological and evolutionary importance (Hertel et al., 2017) as it influences, e.g., its temporal selection/avoidance of open vs. protective habitats (Boon et al., 2008; Lone et al., 2015), movement rates (Ciuti et al., 2012), and dispersal (Cooper et al., 2017). Individual variation of activity cycles and patterns is also important at the population level because the degree of variation in temporal strategies renders populations to be more or less resilient to changing conditions (Wolf and Weissing, 2012; Dingemanse and Wolf, 2013). A related concept regarding the importance of activity patterns and cycles is the chronotype. Being originally developed as a concept in human psychology, classifying people along a continuum from "morning types" with a preference to develop daily routines during the first half of the day (also called "larks") to "evening types," who prefer daily routines during the second half of the day (also called "owls") (Horne and Ostberg, 1976; Vink et al., 2001), chronotypes are now also used in comparative psychology (Labyak et al., 1997; Masuda and Zhdanova, 2010; Pfeffer et al., 2015; Refinetti et al., 2016). However, in almost all studies, averaged activity patterns are used and only some aspects of the activity pattern such as the activity onset, acrophase, and spread are considered (Refinetti et al., 2016). Despite a current renewal of attempts to combine chronobiology, which is traditionally conducted in laboratories, with field ecology (Helm et al., 2017), the linkage between the related concepts of personality and chronotype is currently underdeveloped. Exceptions are recent studies of human psychology and medicine finding that chronotype, sleep, and personality are linked and appear to have at least partial genetic foundation (Randler et al., 2017) and a study of circadian behavioral variation by the pearly razorfish, *Xyrithchys novacula* (Alós et al., 2017), in which the authors suggested that the observed circadian behavioral variation should be viewed as an independent axis of the fish personality, and that the study of chronotypes and their consequences should be regarded as a novel dimension in understanding within-species fish behavioral diversity.

The current study provides low disturbance continuous recording of several hitherto underrepresented parameters of the diurnal/circadian activity cycle [number of nest exits, in-nest time during daylight, total in-nest time during 24 h, nocturnal out-of-nest time (ONT) of individual fox squirrels (*Sciurus niger*)] in a natural setting. The goal of the present study was to use the recorded patterns of nest entries and exits to study the distribution of unimodal, bimodal, and higher-modal activity patterns and the total ONT during day and night in individual fox squirrels, document the intra-individual (day-to-day) and inter-individual pattern variation over the seasons, and address how the observed variabilities relate to the concepts of animal personalities and chronotype.

MATERIALS AND METHODS

Location

The study was conducted on an 80-ha area encompassing the campus of Siena Heights University and the adjacent Motherhouse campus of the Adrian Dominican Sisters, in rural Adrian, Lenawee County, in southeastern Michigan, USA (41°54′ N, 84°01′ W, 240-m elevation). Long-term climate data for Adrian are shown in **Table 1**. Weather conditions during the study were recorded by the Siena Heights University weather station and uploaded to Weather Underground (https://

TABLE 1 | Long-term climate data for Adrian, MI.

Winter average low temperature	−8°C
Winter average high temperature	0°C
Summer average low temperature	15°C
Summer average high temperature	29°C
Annual average precipitation	863 mm

www.wunderground.com/dashboard/pws/KMIADRIA4). Daily averages as well as high and low temperatures for the correlation matrix (**Table 2**) were retrieved for the Lenawee County Airport (KADG) also via Weather Underground (https://www.wunderground.com/history/airportfrompws/KADG/), while the information on snow fall amounts and snow heights originated from US Climate Data (https://www.usclimatedata.com/climate/adrian/michigan/united-states/usmi0004).

Animals

Fox squirrels were caught with double-door Tomahawk Deluxe Transfer traps (Tomahawk Live Traps, Hazelhurst, WI) permanently attached to the trunk of four tall trees on custom-made platforms (Huggins and Gee, 1995). Squirrels were weighed with Pesola spring scales and ear-tagged with Monel type 5 tags (National Band and Tag Company, Newport, KY). Age was categorized as juvenile, sub-adult, and adult according to weight and fur characteristics and by visual examination of external reproductive organs. Sex of adult and sub-adult squirrels was determined by visual examination of the external reproductive organs (Reighard et al., 2004; Schroeder and Robb, 2005). All work was conducted with approval of the Institutional Animal Care and Use Committee of Siena Heights University and followed appropriate guidelines as outlined by (Schmidt et al., 2008).

Data Collection

Each squirrel was equipped with a data-logger collar containing a temperature-sensitive iButton (DS1922L, Maxim Integrated Products, Inc., San Jose, CA) and released at the site of capture immediately thereafter. Data-logger collars weighed between 8 and 12 g and did not exceed 2% of the animals' body mass. The collar design is described in detail elsewhere (Wassmer, 2017). The monitoring of collar temperature (T_c) is particularly suited to provide an index of location (in-nest vs. out-of-nest), as the temperature of the collar quickly rises to core temperature levels after the animals enter their thermally insulated nests and drops rapidly when the animals leave their nests (Lamb, 1995; Kanda et al., 2005; Lazerte and Kramer, 2011; Murray and Smith, 2012; Wassmer and Refinetti, 2016). These assumptions were confirmed by aligning T_c-records with behavioral logs (Wassmer and Refinetti, 2016) including nest entries. A recent study using a very similar setup with a large population of North American red squirrels (*Tamiasciurus hudsonicus*) confirmed the paradigm with about 700 observations of nest exits and entries (Studd et al., 2016). The iButtons were programmed to record one T_c reading every 5, 10, or 30 min with a thermal accuracy of 0.5 or 0.06°C. The limited memory of the iButton allowed data to be recorded for a minimum of 28 days (at 5-min intervals) to a maximum of 6 months (at 30-min intervals). We obtained data from 25 distinct timeseries from 14 individual squirrels, across the four seasons (**Figure 1**). The corresponding ambient temperatures (T_a) at the times of T_c recordings were obtained by the nearby Siena Heights weather station (<500 m away from the squirrel habitat; see the URL above).

Exact times of entry into and exit from the nest were often easily identified by visual inspection of collar temperature records. To avoid potential subjectivity bias, however, the time series was analyzed by a custom-made computer program developed by one of the authors (RR). The computer algorithm defined a nest entry as the data point when the current temperature was higher than the preceding temperature and also higher than or equal to the mean nightly temperature of the individual squirrel. Similarly, the algorithm defined a nest exit as the data point when the current temperature was lower than the preceding temperature and also lower than the mean nightly temperature of the individual squirrel.

Although this simple algorithm worked well for data sets with a temperature gradient of more than 10–15°C between T_c and T_a, additional specifications had to be included to ensure successful data analysis during warmer periods that resulted in more noisy data sets (e.g., **Figure 9D**). In addition, some collar preparations showed a lower amplitude of T_c fluctuations (e.g., **Figure 10D**), and we recognized that the recording interval (5, 10, and 30 min) has an influence on the selection of meaningful criteria. We therefore re-evaluated the algorithm used in Wassmer and Refinetti (2016) and established several sets of criteria for high/low amplitude, short/long intervals, and clear/noisy patterns (**Table S1**) to include the most recording days possible without compromising the event detection and shifting the detection frame, which would result in incorrect detections for many days after falsely determining an event (nest entry or exit).

The first nest exit on each day was defined as the onset of a squirrel's daily activity, whereas the last nest entry on each day was an indication of the daily activity offset. The number of nest exits each day was used to quantify the modality of the activity pattern for each squirrel. Other dependent variables were diurnal nest time (time a squirrel stayed inside of its nest during daylight hours), total nest time (in-nest time per 24 h), and nocturnal ONT (time spent outside of the nest during the night). For the analyses of seasonality, the meteorological definition of seasons was used: Summer starts June 1, lasting until August 31; fall runs from September 1 until November 30, followed by winter from December 1 through February 28, and finally the spring season lasting from March 1 to May 31.

Data Analysis

Presence of statistically significant 24-h rhythmicity was determined by two methods: chi-square periodogram (Sokolove and Bushell, 1978) and cosinor rhythmometry (Nelson et al., 1979). The daily and seasonal timing of nest exits and entries were analyzed and compared using circular statistics (Batschelet, 1981;

TABLE 2 | Correlation matrix between key climatic factors and dependent variables.

	Means	SD	Day-light	Daily highs	Rain	Snow	Snow depth	Wind avg.	First exits	*N* of exits	ONT totals
Day-light	11.442	2.133	1.000	0.752	0.030	−0.110	−0.189	−0.173	−0.428	0.360	0.275
Daily highs	12.341	10.499		1.000	0.075	−0.216	−0.390	−0.265	−0.449	0.345	0.342
Rain	1.945	5.863			1.000	0.059	−0.034	0.251	−0.010	0.079	−0.024
Snow	0.164	0.983				1.000	0.496	0.188	0.132	−0.080	−0.176
Snow depth	0.647	2.206					1.000	0.103	0.235	−0.146	−0.236
Wind avg.	11.767	6.224						1.000	0.096	−0.045	−0.080
First exits	0.337	0.096							1.000	−0.443	−0.511
N of exits	1.613	0.786								1.000	0.151
ONT totals	7.081	2.924									1.000

Correlations in red are significant at $p < 0.001$.

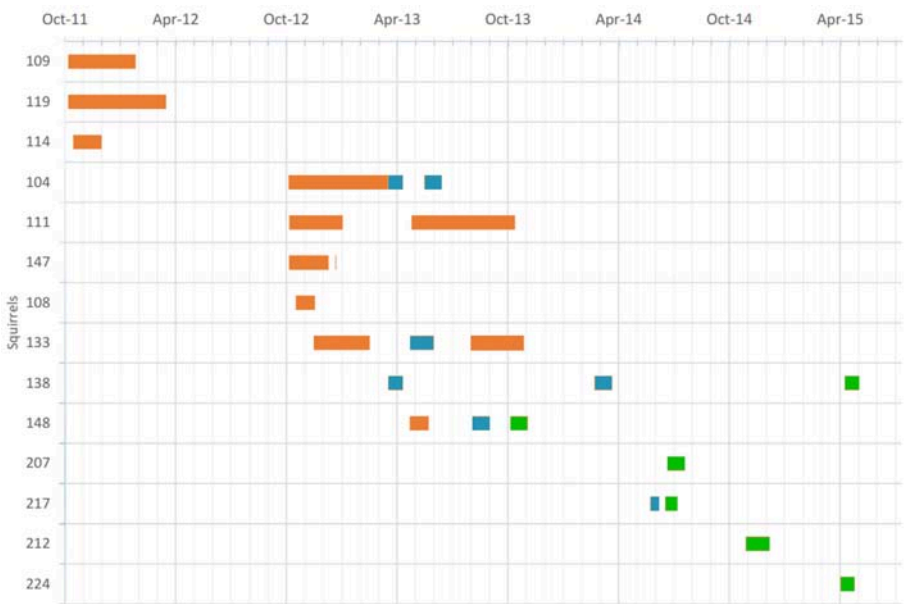

FIGURE 1 | Temporal distribution of 25 individual time series over 14 individual squirrels (y-axis) tagged with thermo-sensitive dataloggers. Orange bars indicate 30-min recording intervals, teal indicates 5-min intervals, and green 10-min intervals.

Fisher, 1993; Mardia and Jupp, 2000). Standard statistical tests were used for comparisons of group means, standard deviations, and standard errors (Siegel and Castellan, 1988; Moore et al., 2013; Zar, 2018). Unless specifically stated, means are presented together with their standard deviation (mean ± SD).

We compared the intra-individual (day-to-day) variation to the inter-individual variation contrasting the standard errors of the means of two data sets of equal length assembled either from consecutive or randomly chosen days.

RESULTS

General Results

In this study, we deployed 27 data-logger collars on 16 individual fox squirrels over almost 4 years. One of the collared animals was never seen again while the data-logger collars of four squirrels that were believed to have been lost were found a year later after the leaf nests of these squirrels deteriorated and the collars fell to the ground. Only the data of one of these collars were lost due to an exhausted iButton battery. In summary, we were able to analyze 25 individual time series of 14 individual animals (**Figure 1**, **Table S2**). All fox squirrels exhibited statistically significant 24-h rhythmicity ($p < 0.0001$) as determined by the chi-square periodogram procedure and by cosinor rhythmometry. Representative records for four fox squirrels are shown in **Figure 2**. For all 14 animals, neck temperature was consistently high (37–38°C) during the night, when the animals remained curled up inside their nests, but oscillated noticeably during the day, when the animals exited the nest one or more times a day. Although T_a oscillated daily, the daily variations in T_c were independent from variations in T_a (**Figures 2**, **9**, **10**). When correlating 2 weeks of recordings of T_c

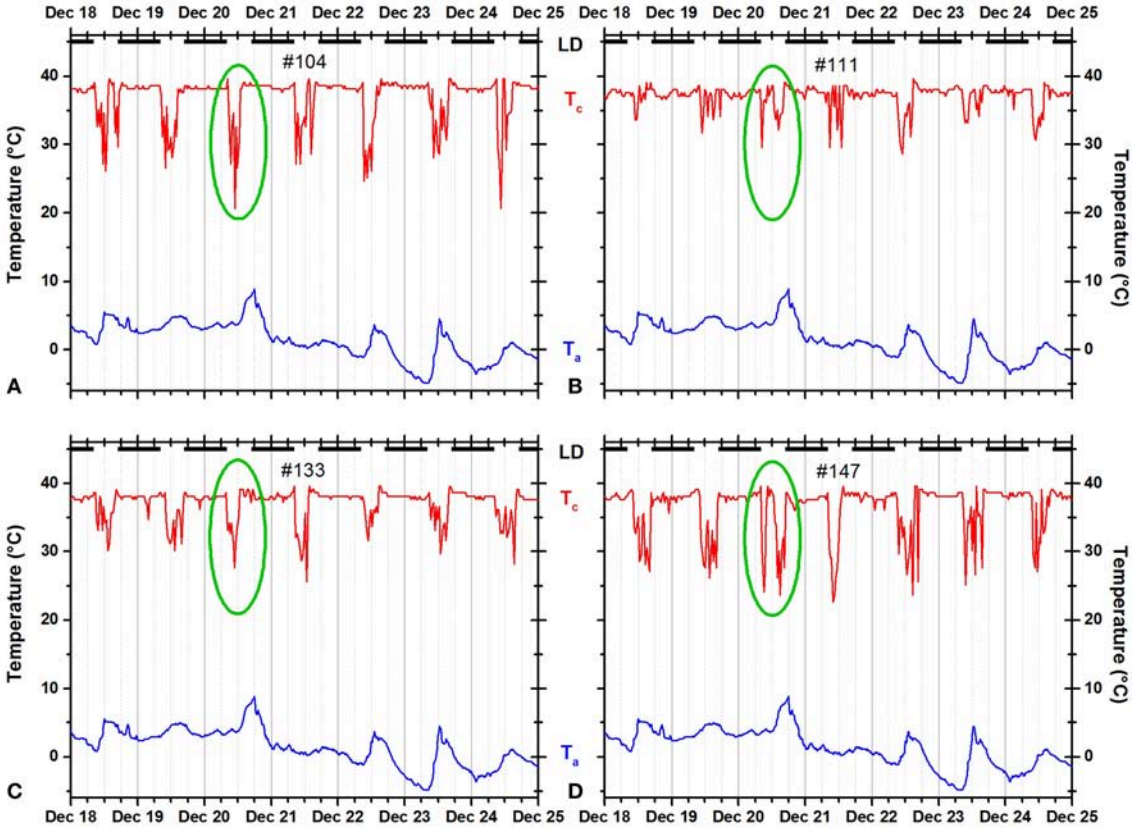

FIGURE 2 | Records of ambient temperature (T_a, blue) and neck skin temperature (T_c, red) for four fox squirrels 104 **(A)**, 111 **(B)**, 133 **(C)**, and 147 **(D)** living outdoors during the winter. The dark horizontal bars at the top of each panel indicate the duration of the dark phase of the natural light–dark cycle. The green ovals mark the time course of body temperature at the same day illustrating individual variability under the same weather conditions. Squirrels 104 and 133 showed a unimodal pattern, whereas squirrels 111 and 147 showed a bimodal pattern.

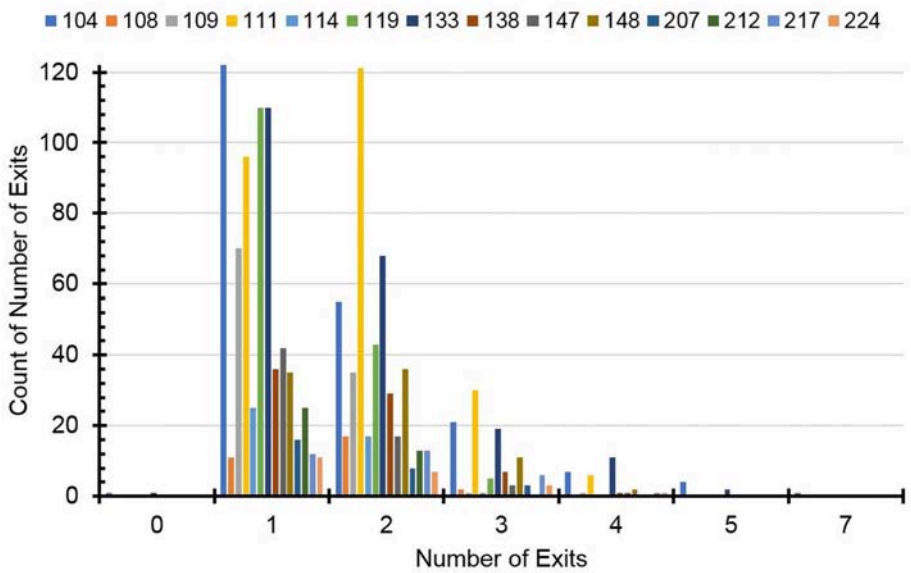

FIGURE 3 | Distribution of the number of exits of individual squirrels.

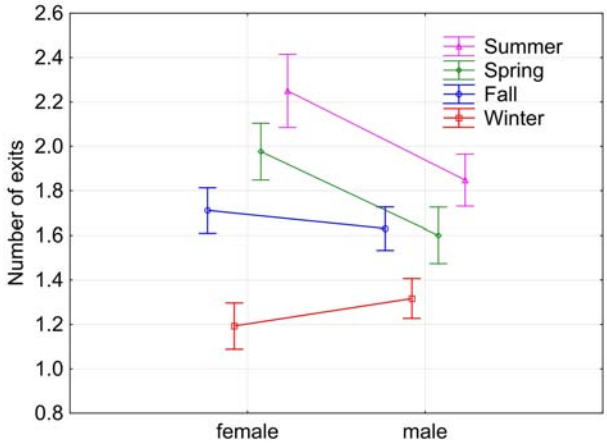

FIGURE 4 | Means (and 95% confidence intervals) of the number of exits by female and male squirrels during the four seasons. Current effect: $F_{(3,1,344)} = 9.2425$, $p < 0.00001$.

at a temporal resolution of 0.5 h (672 data points) to simultaneous recordings of T_a of equal duration and resolution, we found low negative correlations in winter (highest $r = -0.061$, $p > 0.1$) and to some extent higher negative correlations in summer ($r = -0.139$, $p < 0.05$). This indicates that T_c's were slightly higher when T_a's were lower.

In the combined first-order effects on our dependent variables (number of daily nest exits, in-nest time during daylight hours, total daily in-nest time and ONT during night hours), season had the strongest effect [Wilks lambda = 0.287, $F_{(21,3,808)} = 98.9$, $p < 0.0001$] followed by differences between individual squirrels [Wilks lambda = 0.565, $F_{(84,8,129)} = 9.4$, $p < 0.0001$], age [Wilks lambda = 0.846, $F_{(7,1,326)} = 34.629$, $p < 0.0001$], and recording interval [5, 10, or 30 min, Wilks lambda = 0.908, $F_{(14,2,652)} = 9.417$, $p < 0.00001$]. Although a MANOVA revealed no main effect of sex (Wilks lambda = 1.0), it showed an interaction of sex and season [$F_{(3,1,344)} = 9.243$, $p < 0.0005$].

Number of Nest Exits

In the pooled data, the average number of nest exits per day was 1.610 ± 0.788 suggesting a slightly higher proportion of bimodal and higher-modal days with two or more daily activity periods separated by one or more rest period in their nest (e.g., squirrels 111 and 147 in **Figure 2**). However, a histogram of the distribution of unimodal, bimodal, and higher-modal days for all 14 individual squirrels (**Figure 3**) shows that most squirrels had more unimodal than bimodal days, with the exceptions of squirrels 111 and 108. There were much fewer days during which the animals exited three or more times a day indicating fewer trimodal and even less polymodal activity patterns. Individual squirrels differed significantly in the mean number of exits ranging from 1.335 ± 0.537 to 1.875 ± 0.833.

Fox squirrels showed the highest number of nest exits in summer (1.982 ± 0.968) and least in winter (1.263 ± 0.489). All seasons were significantly different from each other except fall and spring (Tukey HSD test, $p < 0.05$). Individual squirrels were predominantly unimodal in winter with average numbers of nest exits between 1.157 and 2.000 and predominantly bimodal in summer with values between 1.519 and 3.115. Some animals showed more exits in fall and/or spring than in summer. Female fox squirrels showed significantly more nest exits in spring and summer (1.976 ± 0.886, 2.250 ± 1.223) than male squirrels [1.600 ± 0.722, 1.848 ± 0.781, $F_{(1,255)} = 13.969$, $p < 0.0005$, **Figure 4**]. On the contrary, there was no sex difference in nest exits in either fall or winter nor during the pooled data for these two seasons [$F_{(1,418)} = 1.166$, $p = 0.281$]. In addition to the seasonal and individual variability, the number of nest exits also showed considerable day-to-day fluctuations in individual squirrels recorded during the same days (**Figure 5A**).

The number of nest exits showed comparable significant correlations to the daily hours of daylight (Pearson's $r = 0.360$, $p < 0.001$) and daily high temperatures ($r = 0.345$, $p < 0.001$). The correlation between the number of exits and snow depth was less pronounced but still significant, while average wind speed, precipitation, and snowfall were not significantly correlated (**Table 2**).

In-nest and Out-of-nest Times

From fall through summer, the animals spent increasingly longer periods inside of their nests during daytime, starting at 3.318 ± 2.485 h in fall to 7.430 ± 2.943 h in summer (**Figure 6A**). All seasons were significantly different from each other regarding time spent in the nest during light hours (Tukey HSD test, $p < 0.05$). Total daily time spent in the nest was highest in winter (18.466 ± 2.129 h) and lowest in spring (15.936 ± 3.060 h); however, only winter was significantly different from every other season (Tukey HSD test, $p < 0.05$, **Figure 6B**). The daily proportion of ONT during civil daylight hours ranged from 0% (observed only once) to 96% with an average of 43 ± 23%. Total nest time allows a rough estimate of the proportion of rest per 24 h. In the pooled data, squirrels spend about 66–68% of 24 h in their nests in spring, summer, and fall, and 77% in winter. This difference was significant (one-way ANOVA and Tukey post-test, $p < 0.00001$).

There were also significant differences between individual squirrels in nest time during daylight hours ranging from 1.698 ± 1.213 to 9.05 ± 2.981 h, total nest time ranging from 12.523 ± 1.899 to 18.488 ± 2.581 h, and nocturnal out of nest time ranging from 0.0285 ± 0.181 to 1.106 ± 2.035 h (Tukey HSD tests, $p < 0.05$). As nest exits, total ONT showed considerable day-to-day fluctuations in individual squirrels recorded during the same days (**Figure 5B**).

Total ONT was best correlated with the daily high temperatures (Pearson's $r = 0.342$) and less to the hours of daylight ($r = 0.275$). In addition, snow depth ($r = -0.236$) and snowfall ($r = -0.176$) were also significantly but less strongly correlated (all probabilities, $p < 0.001$), whereas average wind speed and precipitation did not seem to influence total ONT (**Table 2**).

Timing of First Exits

In all seasons, individual squirrels showed highly significant mean vectors for the timing of their first exits with mean vector

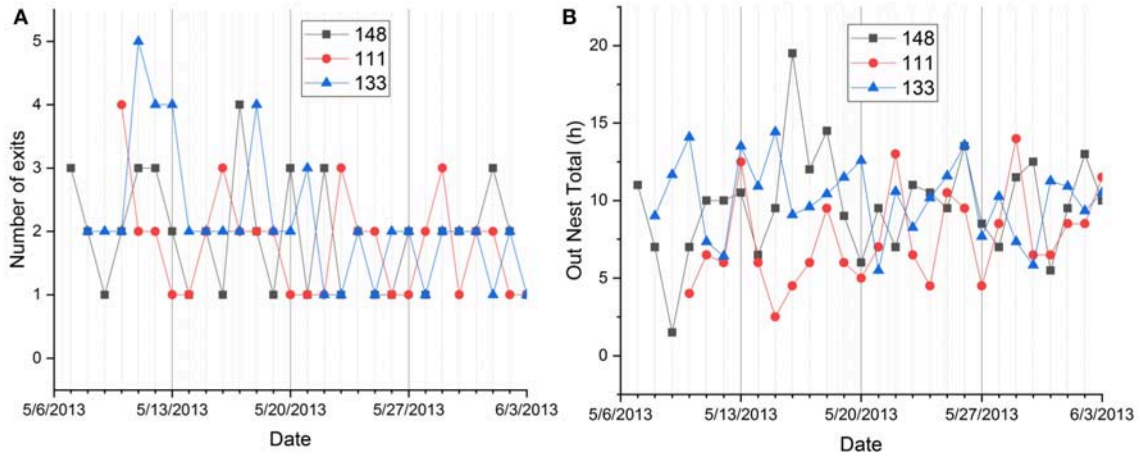

FIGURE 5 | Day-to-day fluctuation of nest exits **(A)** and total out-of-nest time **(B)** in individual squirrels recorded during the same 28 days in spring and summer.

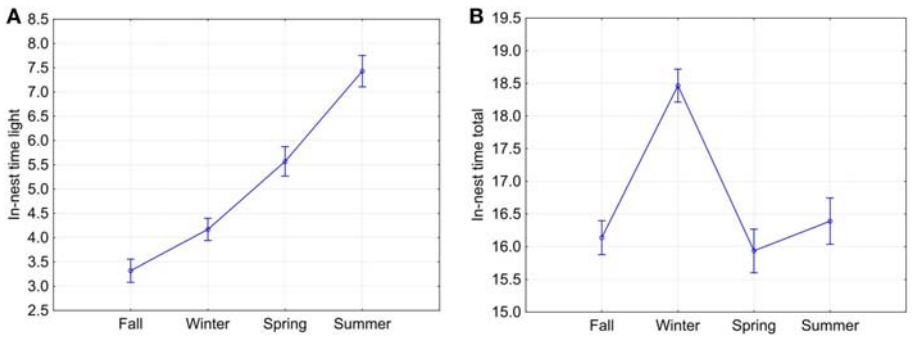

FIGURE 6 | Means (and 95% confidence intervals) of the seasonal in-nest time during daylight **(A)** and in-nest time during the entire 24-h cycle of day and night **(B)**. Current effect: Wilks lambda = 0.30196, $F_{(6,2,694)} = 368.09$, $p = 0.0000$.

lengths (r) between 0.76 and 0.99. Individual squirrels differed significantly in the timing of their first exits (**Figure 7**, **Table 3**). None of the animals was consistently an early or late riser throughout all seasons. In summer, fox squirrels left their nests 3 h earlier in the morning than in winter (Mardia–Watson–Wheeler test on the pooled data of all 14 animals, $p < 0.05$). The range between early and late risers was highest in summer (4.8 h) and lowest in winter (1.83 h). In summer, first exits of individual squirrels were, on average, 1.72 h apart from each other—in winter, the average spacing was only 37 min. Three individual fox squirrels (#104, 111, 133) were recorded throughout all seasons and could be compared to the pooled data. While #104 and #111 showed similar results to the pooled data with first exits in summer occurring about 4:37 and 3:42 h earlier than in winter, respectively, #133 showed different results with first exits earliest in fall (6:48 EST) and spring (7:36 EST) and late exits in summer (9:57 EST) and winter (10:11 EST) only about 0:14 h apart.

In the pooled data for all seasons, the timing of first exits was inversely correlated with the number of daily exits (Pearson's $r = -0.708$, $p = 0.005$) and total time outside nests (Pearson's $r = -0.685$, $p = 0.007$), meaning that squirrels that exited the nest earlier also exited the nest more times each day and spent longer times outside the nest (**Table 4**, **Figure 8**). In addition to the results for the pooled seasons, total time spent outside the nest in fall was also significantly inversely correlated to the timing of first exits in fall.

Continuous Nest Occupancy for More Than 24 h and Nocturnal Out-of-nest Time

Some squirrels occasionally remained in the nest for more than 24 h and/or occasionally failed to return to the nest at night (**Figures 9, 10**). The green oval in **Figure 9B** documents that squirrel #104 did not leave the insulated nest for more than 36 h. In **Figure 10B**, the green oval marks a 35-h time period during which the animal was not resting in an insulated shelter.

Nocturnal ONT occurred occasionally in many fox squirrels. Seven of 14 squirrels spent at least one entire night outside their insulated nests—mostly during warm nights but exceptionally also during winter (for example, **Figure 10B**). The pooled data showed little evidence for seasonality of nocturnal ONT. Only fall (0.556 ± 1.306 h) and winter (0.171 ± 0.761 h) were significantly different from each other (Tukey HSD test, $p < 0.00001$). In

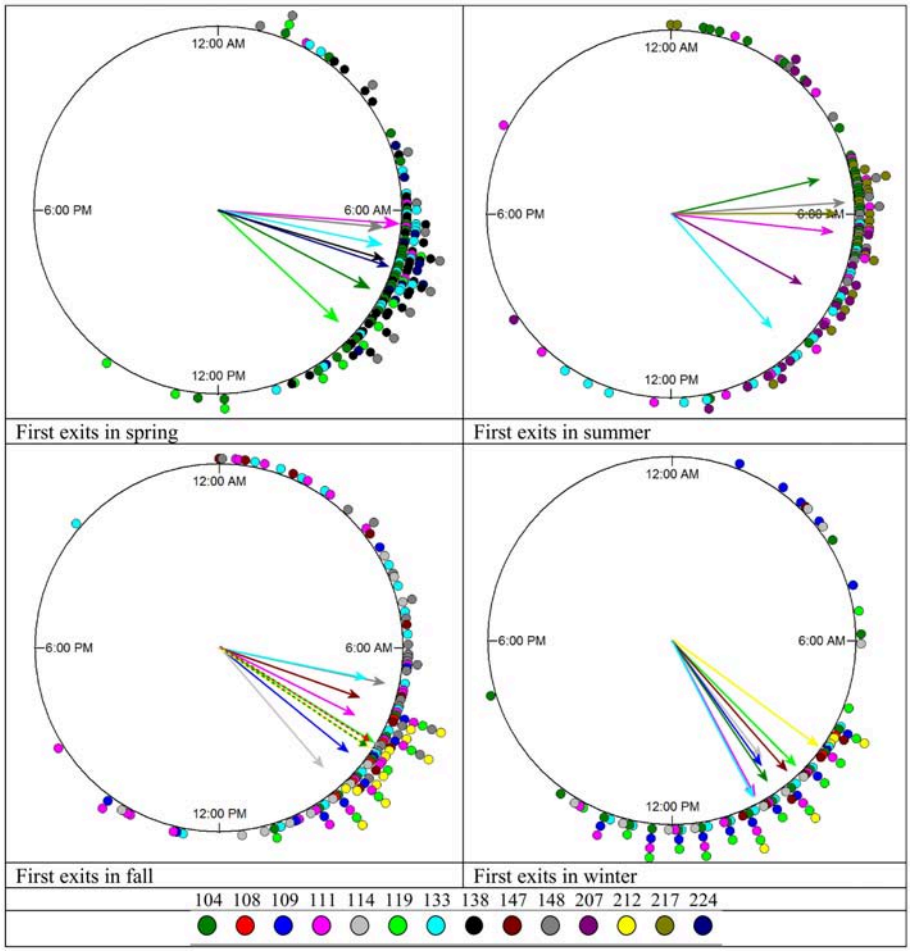

FIGURE 7 | Timing of first exits in individual squirrels during each season. The mean vectors point at the average timing of first entries for each squirrel and are in the same color as the data points plotted on the periphery of the circle (see the color key on the bottom). The length of the mean vector indicates how concentrated or spread the first exits are around this mean time. The exact values can be found in **Table 3**.

contrary to the pooled data for all animals, two of the only three individual animals recorded over all seasons showed significant seasonality in the duration of nocturnal ONT. Squirrel 104 spent the least amount outside of its nest in winter (0.072 ± 0.296 h) and the most amount in summer (0.526 ± 1.002 h). A Tukey HSD test reached significance ($p < 0.05$) for the differences between fall and summer and winter and summer. Squirrel 133 spent also the least amount of nocturnal ONT in winter (0.225 ± 1.105 h) and the most in fall (1.612 ± 2.017 h). Fall vs. winter and fall vs. spring as well as winter vs. summer were significantly different (Tukey HSD, $p < 0.05$). Contrary to the frequent occurrence of ONT during night, the example of continuous in-nest time for more than 24 h shown in **Figure 9B** was the only occurrence of this type in our dataset.

Comparison Between the Intra- and Inter-individual Data Variability

Indices of intra- and inter-individual variabilities were calculated by analysis of consecutive data segments of individual animals and simultaneous (or randomized) segments of different individuals. Inter-individual and intra-individual variabilities were generally comparable to each other regarding time of first exit from the nest, number of exits per day, and time spent outside the nest per day in all four seasons (**Table 5**). For the four seasons combined, inter-individual variability exceeded intra-individual variability for total time outside the nest, and this difference was caused by a difference in the spring (**Table 5**).

DISCUSSION

General Results

Individual squirrels differed significantly in the number of exits (and by this in the number of activity periods), diurnal nest time, total nest time, and nocturnal ONT. All recorded variables also showed significant seasonal variation. To a much lesser degree, age and recording interval contributed to the variance in the data, while the sex of squirrels only showed a significant effect in the interaction of sex and season (**Figure 4**). We also detected

TABLE 3 | Circular statistics of the seasonal timing of first exits in individual squirrels.

First exits in spring

Squirrel	104	111	119	133	138	148	224
N	55	22	35	25	73	25	22
Mean vector (EST)	07:48	06:17	08:51	06:48	07:05	06:23	07:13
Mean vector length (r)	0.902	0.962	0.879	0.892	0.936	0.888	0.967
CSD (h)	01:43	01:03	01:56	01:49	01:23	01:51	00:59
Rayleigh test (Z)	44.787	20.351	27.046	19.899	63.976	19.695	20.567
Rayleigh test (p)	<0.001	<0.001	<0.001	<0.001	<0.001	<0.001	<0.001
MWW test:	104	111	119	133	138	148	224
104	—	<0.001	0.103	<0.001	0.055	0.054	0.006
111	22.528	—	<0.001	<0.001	0.034	0.237	0.003
119	4.551	38.979	—	<0.001	<0.001	<0.001	<0.001
133	15.807	17.432	15.213	—	0.002	0.04	<0.001
138	5.814	6.749	18.774	12.739	—	0.316	0.033
148	5.82	2.877	15.303	6.431	2.304	—	0.007
224	10.187	11.787	19.426	18.372	6.811	9.79	—

First exits in summer

Squirrel	104	111	133	148	207	217
N	26	92	45	20	27	32
Mean vector (EST)	05:06	06:25	09:56	05:44	07:52	06:00
Mean vector length (r)	0.823	0.883	0.846	0.947	0.806	0.901
CSD (h)	02:23	01:54	02:12	01:15	02:30	01:44
Rayleigh test (Z)	17.615	71.709	32.213	17.953	17.556	25.961
Rayleigh test (p)	<0.001	<0.001	<0.001	<0.001	<0.001	<0.001
MWW test	104	111	119	133	138	148
104	—	0.015	<0.001	0.029	<0.001	0.055
111	8.417	—	<0.001	0.513	<0.001	0.594
133	32.017	45.973	—	<0.001	0.008	<0.001
148	7.106	1.333	32.164	—	<0.001	0.326
207	19.022	25.976	9.747	23.097	—	<0.001
217	5.82	2.877	15.303	6.431	2.304	—

First exits in fall

Squirrel	104	108	109	111	114	119	133	147	148	212
N	40	28	32	92	24	32	82	39	39	27
MV (EST)	08:13	08:06	08:34	07:46	09:16	08:04	07:36	07:17	06:49	08:13
MVL (r)	0.981	0.988	0.902	0.82	0.858	0.981	0.76	0.812	0.916	0.988
CSD (h)	00:44	00:35	01:43	02:24	02:06	00:44	02:49	02:27	01:35	00:35
Rayl. (Z)	38.509	27.321	26.055	61.935	17.68	30.819	47.399	25.73	32.747	26.375
Rayl. (p)	<0.001	<0.001	<0.001	<0.001	<0.001	<0.001	<0.001	<0.001	<0.001	<0.001
MWW	104	108	109	111	114	119	133	147	148	212
104	—	0.256	0.007	<0.001	<0.001	0.066	<0.001	0.057	0.004	0.785
108	2.725	—	0.003	<0.001	<0.001	0.581	<0.001	0.006	0.038	0.934
109	9.892	11.752	—	0.06	0.032	<0.001	<0.001	0.574	0.003	0.01
111	26.316	18.023	5.633	—	<0.001	<0.001	0.005	0.079	0.16	<0.001
114	28.633	28.357	6.877	30.032	–	<0.001	<0.001	<0.001	<0.001	0.001
119	5.444	1.085	14.471	28.609	28.735	—	<0.001	0.001	0.003	0.546
133	57.441	45.861	29.37	10.663	22.345	50.189	—	<0.001	0.848	<0.001
147	5.719	10.355	1.111	5.084	27.145	13.385	14.05	—	0.002	0.428
148	11.042	6.537	11.637	3.662	39.979	11.611	0.329	12.833	—	<0.001
212	0.484	0.137	9.263	14.68	13.368	1.21	43.207	1.696	16.002	—

(Continued)

TABLE 3 | Continued

	First exits in winter							
Squirrel	104	109	111	114	119	133	147	212
N	89	75	47	19	91	88	24	11
MV (EST)	09:43	09:36	10:07	09:30	09:01	10:11	09:15	08:21
MVL (r)	0.92	0.837	0.949	0.793	0.947	0.958	0.937	0.98
CSD (h)	01:33	02:16	01:13	02:36	01:15	01:07	01:22	00:45
Rayl. (Z)	75.336	52.583	42.365	11.941	81.541	80.789	21.086	10.57
Rayl. (p)	<0.001	<0.001	<0.001	<0.001	<0.001	<0.001	<0.001	<0.001
MWW	104	109	111	114	119	133	147	212
104	—	0.389	0.022	0.809	0.001	0.018	0.661	0.004
109	1.891	—	0.443	0.317	<0.001	0.658	0.516	0.002
111	7.655	1.626	—	0.328	<0.001	0.957	0.532	0.002
114	0.425	2.295	2.231	—	<0.001	0.025	0.686	0.003
119	13.181	28.846	30.276	15.23	—	<0.001	0.042	0.006
133	7.988	0.836	0.088	7.397	36.37	—	0.134	0.002
147	0.827	1.322	1.262	0.753	6.357	4.019	—	0.002
212	11.035	12.691	12.259	11.894	10.331	12.343	12.416	—

The upper unshaded part describes the circular distribution of first exits for each squirrel, whereas the shaded lower area shows the results of pairwise Mardia–Watson–Wheeler tests (MWW). The upper part provides the significance levels—the lower values are the W scores of the tests. EST, Eastern Standard Time; CSD, circular standard deviation.

TABLE 4 | Linear correlations between the timing of first exits and modality (number of nest exits per day) and timing of first exits and total time spent outside of the nest per 24 h (total ONT).

Season	Variable pairs	*N*	Pearson's *r*	*P*-value
Spring	First Exit–Modality	7	−0.622	0.136
	First Exit–Total ONT	7	−0.419	0.349
Summer	First Exit–Modality	6	−0.650	0.163
	First Exit–Total ONT	6	−0.336	0.515
Fall	First Exit–Modality	10	−0.481	0.159
	First Exit–Total ONT	10	−0.777	0.008
Winter	First Exit–Modality	9	−0.550	0.125
	First Exit–Total ONT	9	−0.509	0.162
All seasons	First Exit–Modality	14	−0.708	0.005
	First Exit–Total ONT	14	−0.685	0.007

Correlations in red are significant.

substantial day-to-day variations in the dependent variables of individual squirrels (**Figure 5**) that were partially correlated to weather events (**Table 2**).

T_c was barely and insignificantly negatively correlated with T_a in winter, and only slightly higher but significantly inversely correlated in summer. The inverse nature of these correlations shows that T_c was not merely following fluctuations of T_a in any season. Compared to significant correlations between T_a and other environmental factors such as snow fall (**Table 2**), the T_c-T_a correlations were smaller and, in the majority, insignificant. We are therefore confident that T_c is a reliable proxy to infer nest entries and exits.

Number of Nest Exits

Individual squirrels showed slightly more unimodal than bimodal days and only rarely exited more frequently than twice per day (**Figure 3**). The number of daily exits showed a distinct seasonality with significantly more exits in summer than in winter. In addition, the number of exits was significantly correlated with the hours of daylight and weather parameters, especially the daily maximum temperature (**Table 2**). These seasonal trends agree with the results of most studies on fox squirrels (Hicks, 1949; Adams, 1984; Koprowski and Corse, 2005) and other tree squirrels (Thompson, 1977; Wauters et al., 1992), which reported bimodal patterns in summers, and unimodal patterns in winter. However, in the current study, we found gradual and erratic rather than categorical and continuous changes in the seasonal distribution of activity patterns in individual squirrels with the occurrence of bimodal days in winter (**Figure 2**) and unimodal days in summer (**Figure 10**), substantial day-to-day fluctuations (**Figure 5A**), and more nest exits occurring in fall/winter than summer in some squirrels suggest that the seasonal variability in the activity patterns is driven not only by changes in the photoperiod and temperature (Halle and Stenseth, 2000) but also by (stochastic) environmental factors such as unfavorable weather (**Table 2** and Williams et al., 2014; Studd et al., 2016), predation (Eriksen et al., 2011; Connolly and Orrock, 2017), social interactions (Schmidt et al., 2008; Agostini et al., 2012), and/or intrinsic individual characteristics such as personality (Boon et al., 2008; Careau et al., 2008) and chronotype (Refinetti et al., 2016; Alós et al., 2017). As in the case shown in **Figure 2**, on the same day, December 20, 2012, two of four animals (#111 and #147) showed a bimodal pattern, while the other two animals showed a unimodal pattern. It is unlikely that weather conditions influenced the activity patterns of these animals in different ways, but we cannot exclude other possible extrinsic factor such as predation or social interactions, or intrinsic differences between the animals. There are only two studies known to us comparing individual activity

patterns in tree squirrels over the seasons of the year (Studd et al., 2016; Anders et al., 2017). Anders et al. (2017) found unimodal, bimodal, and even trimodal patterns in the Eurasian red squirrel (*Sciurus vulgaris*) in Japan during the months of July to October. We also found trimodal and even polymodal patterns in some seasons of the current study. However, these patterns often occurred during the warmer months when the gradient between T_c and T_a was reaching levels below 10°C and the detection of entries and exits was not always satisfactory (**Figures 9, 10**). Nevertheless, as Anders et al. (2017) used a data logger capable of recording collar temperature and light intensity simultaneously, their detection of trimodal patterns supports that some of the trimodal or polymodal patterns we detected might not be artifacts. Studd et al. (2016) used an almost identical design to the current study to investigate the activity patterns of lactating female North American red squirrels (*Tamiasciurus hudsonicus*) in southwestern Yukon, Canada, between February and June. The authors found an overall pattern of transition from unimodal daily activity centered at the end of the day on cold days to bimodal daily activity at intermediate temperatures and unimodal daily activity centered at the beginning of the day on warm days. Studd et al. (2016) confirmed the influence of weather conditions previously reported by Williams et al. (2014) also in lactating females from the same population of red squirrels using light sensors. Both studies found trimodal patterns in lactating females. We also found trimodal patterns in the current study (e.g., several days in **Figure 10C**). The animal shown (#133) is a female and the month of May falls within the predominant lactation period for fox squirrels (Koprowski, 1994); thus, it is possible that this squirrel was lactating and needed to forage more food to cover the higher energy demand (Havera, 1979) while having to return in regular intervals to nurse her offspring leading to a trimodal pattern (Williams et al., 2014; Studd et al., 2016).

In-nest and Out-of-nest Times

From fall through summer, fox squirrels spent increasingly longer periods inside of their nests during daytime while total time spent in the nest during the full 24-h cycle of day and night was highest in winter (**Figure 6**). Nocturnal out-of-nest activity was highest in fall and lowest in winter.

There were also significant differences between individual squirrels in nest time during daylight hours, total nest time and nocturnal ONT. While longer in-nest times during the long daylight hours of summer can simply be a consequence of longer days, long in-nest times in winter can be caused by the long nights and colder temperatures of this season. The surprising and seemingly contradictory difference between in-nest time during daylight and during the entire 24-h activity cycle is based on significantly shorter in-nest time during the daylight hours in fall as compared to any other month (**Figure 6A**). We speculate that this difference makes sense in the light of the fox squirrel's natural history, with fall being the food caching season and with the approaching reproductive season in winter (Koprowski 1994). Nocturnal ONT, which was always short (on average below 37 min in the pooled data) but was more than four times longer in fall than in winter can also not be simply related to the changes in photoperiod. Here we suspect again a joint influence of the still mild night temperatures in fall, the end of the food-caching season, and the approaching major mating season causing significantly longer nocturnal ONT in fall compared to winter. These assumptions are supported by our findings that both photoperiod and certain weather conditions especially daily maximum temperatures were significantly correlated to total ONT (**Table 2**).

In the study by Studd et al. (2016) that we cited above in the discussion of the number of nest exits, temperature also highly affected the proportion of time spent out of the nest during morning hours (from 10% at −30°C to approximately 100% at temperatures of 0°C). As temperatures increased from −20°C to 15°C, time spent out during afternoon declined from 75% to 10%, and time spent out during the evening declined from 100% to almost 0%. Anders et al. (2017) found that the daily activity time of red squirrels generally increased with increasing temperature and decreased with increased precipitation and average wind speed across both years. We can confirm this trend for temperature but not for precipitation and wind speed (**Table 2**). Studd et al. (2016) confirmed the influence of weather conditions previously reported by Williams et al. (2014) also in lactating females from the same population of red squirrels using light sensors.

Total nest time allows a rough estimate of the proportion of rest per 24 h. In the pooled data, squirrels spend about 66–68% of 24 h in their nests in spring, summer, and fall, and 77% in winter. As visual focal animal observations (Altmann, 1974) of six squirrels during various hours of the day when the animals were outside of their nests indicated that the animals were sitting or lying quietly, apparently resting, during 45–67% of the time observed (Wassmer and Refinetti, 2016), the total rest time might be considerably longer, probably in the realm of 80–85%. Studd et al. (2016) described nest attendance patterns of lactating red squirrels (*Tamiasciurus hudsonicus*) as highly variable as the daily proportion of time spent out of the nest during civil daylight hours ranged from 5% to 85% with an average of 45%. Diurnal in-nest time of fox squirrels (*Sciurus niger*) in this study was very similar ranging from 0 to 96% with an average of 43%.

Timing of First Exits

In all seasons, first exits of individual squirrels were significantly concentrated around a narrow window of time in the early to late morning (**Figure 7**) and were in many cases significantly different from each other (**Table 3**). However, none of the individual squirrels recorded during multiple seasons was clearly and consistently an early or late riser. In summer, first exits of individual squirrels were more spread out, whereas in winter, individual squirrels exited their nest much closer to each other, which is expected as winter days are substantially shorter than summer days. Interestingly this mimics the distribution of activity onsets in the nocturnal Ord's kangaroo rat (*Dipodomys ordii*) (White and Geluso, 2007), which also shows a wider range of individual activity onsets in summer and a much narrower range in winter. Enright (1966) showed that in house finches kept under controlled conditions in a laboratory, cooler temperature at a constant photoperiod and shorter photoperiods at the same ambient temperature caused delayed activity onsets. Our results

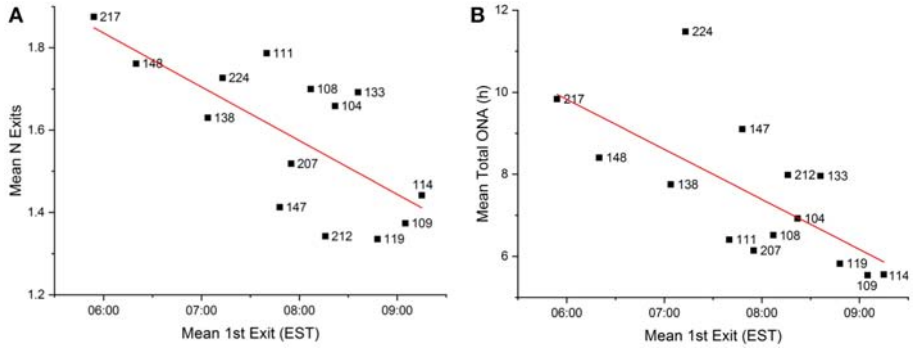

FIGURE 8 | (A) Correlation between the mean timing of first exits and the mean number of exits (modality) of all recorded fox squirrel (numbers) in all seasons (Pearson's $r = -0.708$, $p = 0.005$). **(B)** Correlation between the mean timing of first exits and the mean total time spent outside the nest per 24 h of all recorded squirrels in all seasons of the year (Pearson's $r = -0.685$, $p = 0.007$).

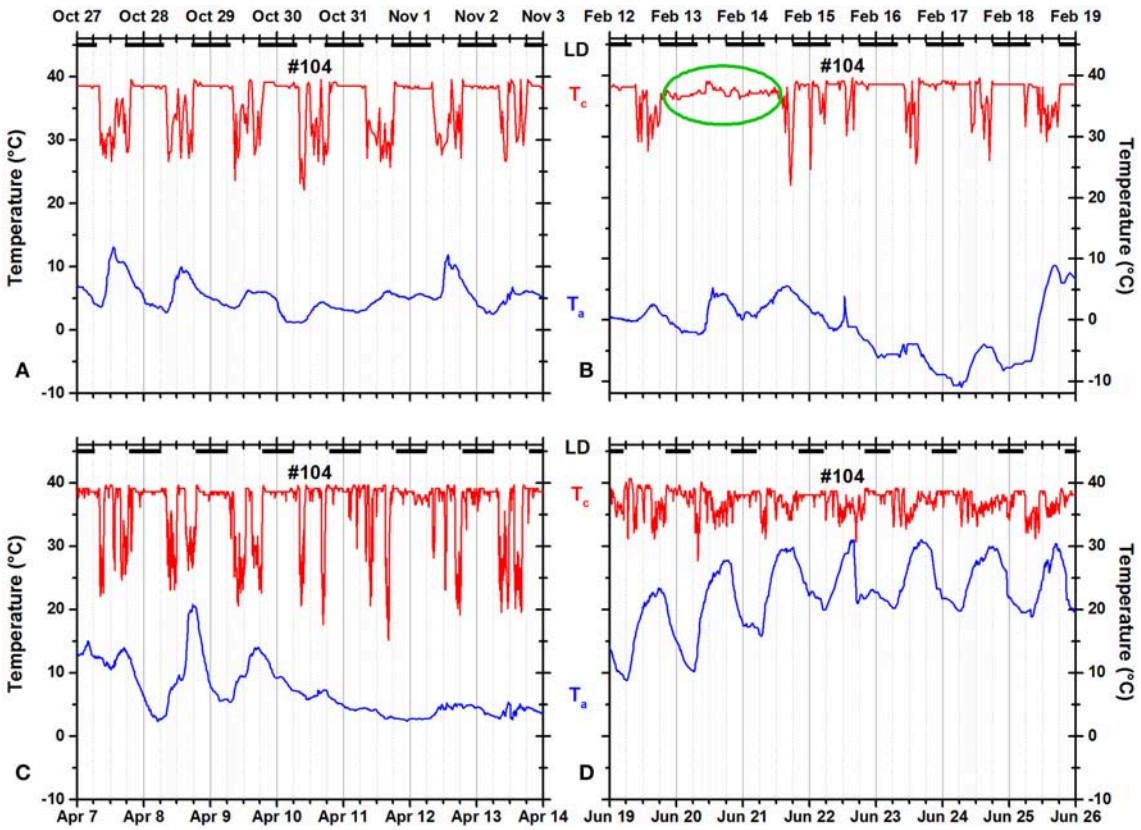

FIGURE 9 | Records of ambient temperature (T_a, blue) and neck skin temperature (T_c, red) for fox squirrel #104 in **(A)** fall, **(B)** winter, **(C)** spring, and **(D)** summer. The dark horizontal bars at the top of each panel indicate the duration of the dark phase of the natural light–dark cycle. The green oval in **(B)** marks a day when the squirrel did not leave its insulated nest.

indicate that both daylength and temperature had simultaneously the same effects on fox squirrels in the wild. As first exits constitute activity onsets, these results are complementary to the (seasonal) changes of the unimodal–polymodal gradient and the total in-nest/out-of-nest time (proportion of activity/rest) and are therefore aspects of the overall activity pattern of fox squirrels.

The number of nest exits was significantly inversely correlated with the timing of the first daily exits in the pooled data for all seasons. This means that the early riser chronotype showed significantly more nest exits than the late riser chronotype (**Table 4**). The larger number of exits might reflect a behavioral trait of early risers or simply the availability of a longer daily

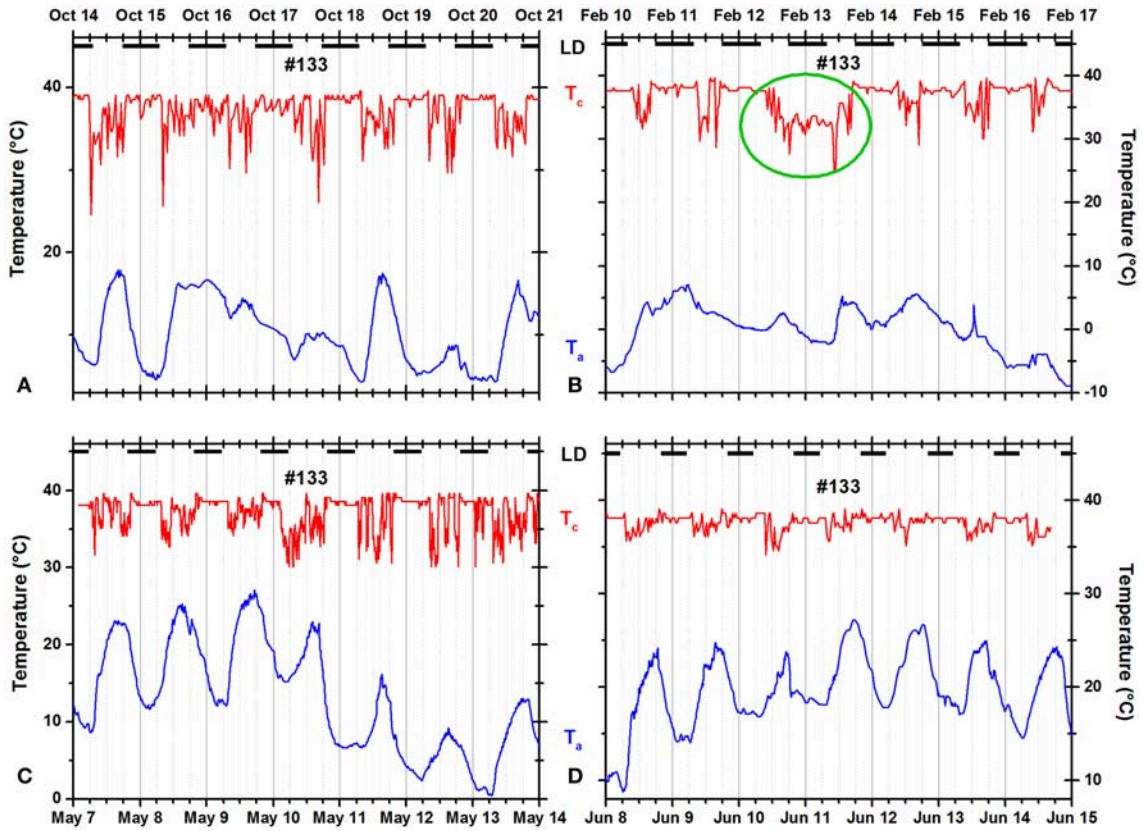

FIGURE 10 | Records of ambient temperature (T_a, blue) and neck skin temperature (T_c, red) for fox squirrel #133 in **(A)** fall, **(B)** winter, **(C)** spring, and **(D)** summer. The dark horizontal bars at the top of each panel indicate the duration of the dark phase of the natural light–dark cycle. The green oval in **(B)** marks a day when the squirrel did not visit its insulated nest for more than 30 h.

activity time. Under controlled laboratory conditions, early-rising antelope ground squirrels were found to have significantly longer daily activity times (Refinetti et al., 2016), and this association may occur also in the fox squirrel, which would contribute to the higher number of nest exits.

Continuous Nest Occupancy for More Than 24 h and Nocturnal Out-of-nest Time

Nocturnal ONT occurred occasionally in many fox squirrels—mostly during warm nights but exceptionally also during winter (for example, **Figure 10B**). While most nocturnal ONT occurred only for brief periods, some events took the entire night. In the pooled data and in two out of three animals recorded in all seasons, nocturnal ONT was shortest in winter (0.1–0.2 h) and longest in fall or summer (0.5–1.6 h). Except for a recent publication (Anders et al., 2017) using continuously logged temperature data as well, nocturnal ONT was not known to occur in tree squirrels so far. This clearly demonstrates a key advantage of data loggers to discover previously hidden details of animal behavior and natural history. We can only speculate why fox squirrels spent time outside of their nests during some nights. Temperatures outside of the nests might be more comfortable in summer than the insulated nests or invite for short trips for urination and defecation. In colder nights, such as the documented example in **Figure 10B**, it might be that the squirrel's nest was destroyed or not available.

While nocturnal ONT was detected repeatedly, continued nest occupancy for more than 24 h was only found once in the entire data set (**Figure 9B**). Squirrel 104 is a female, but the middle of February would be relatively late for parturition to happen. However, the date falls well into the lactation period while weather conditions were not specifically unfavorable (no precipitation or snow, relatively warm with highs around 3.5°C and lows at −6°C).

Nocturnal ONT (or more general, activity during the typically inactive time of the activity cycle) and days with unusual patterns are two more dimensions that should be considered to describe the bandwidth of activity patterns more inclusively.

Comparison Between the Intra- and Inter-individual Data Variability

The inter-individual variabilities of total ONT and the number of exits were either higher than the intra-individual variabilities or comparable to them (**Table 5**). These results underline the importance of studying the activity patterns of individual tree squirrels to complement and contrast pooled data for entire

TABLE 5 | Comparison between the intra-individual and inter-individual variation in three variables.

Season	Variable	*N*	Mean SE intra-individual	Mean SE inter-individual	*t*	*p*-value (one-tail)
Spring	First exit (h)	7	0.531	0.547	−0.133	0.448
	Number of exits	7	0.271	0.273	−0.021	0.492
	Total ONT (h)	7	0.894	1.4	−2.503	0.015
Summer	First exit	6	0.745	0.998	−1.176	0.135
	Number of exits	6	0.382	0.305	0.691	0.258
	Total ONT	6	0.972	1.285	−1.450	0.091
Fall	First exit	8	0.184	0.188	−0.122	0.452
	Number of exits	8	0.188	0.184	0.122	0.452
	Total ONT	8	0.87	0.67	1.654	0.060
Winter	First exit	8	0.359	0.45	−0.828	0.212
	Number of exits	8	0.173	0.176	−0.210	0.419
	Total ONT	8	0.616	0.753	−1.708	0.055
All seasons	First exit	14	0.477	0.554	−1.013	0.161
	Number of exits	14	0.186	0.185	0.077	0.470
	Total ONT	14	0.654	0.841	−2.607	0.008

Intra-individual variation was calculated as the standard error (SE) for each fox squirrel recorded during a certain season and during an equal amount of consecutive or random days (N). Inter-individual variation was calculated using N consecutive (or random) days during which all squirrels recorded during this season (N) were recorded. ONT, Out-of-nest time. Red denotes significant correlations.

groups and populations but also hint at the astonishing day-to-day variabilities within the same squirrels (**Figure 5**). Very few researchers have compared intra- and inter-individual variabilities of circadian rhythms. We are aware of only four studies that conducted such comparison for the rhythms of body temperature (Refinetti and Piccione, 2005; Romeijn and Van Someren, 2011), melatonin secretion (Barassin et al., 1999), and cortisol secretion (Selmaoui and Touitou, 2003). In one of these studies (Refinetti and Piccione, 2005), four different species were used: the laboratory rat, the 13-lined ground squirrel, the domestic dog, and the horse. Intra- and inter-individual variabilities were computed for the mean level, range of oscillation, acrophase, and robustness of the rhythm. The variabilities differed in different parameters of the rhythm and in different species but, whenever there was a difference between inter-individual variability and intra-individual variability, the latter was always smaller than the former. That is, the day-to-day variability of an individual's rhythm never exceeded the variability between the rhythms of different individuals, which is the same as we found in this study on fox squirrels.

CONCLUSIONS

The results of our study illustrate the importance and advantages of collecting activity-related data from individual animals. Such data allow the estimation of how much individual fox squirrels differ from each other and how much they can fluctuate from day to day. We found that the magnitude of inter-individual variability of a number of behavioral variables was similar to the magnitude of intra-individual (day-to-day) variability. Although on most days the squirrels spent the night in their nests and exited the nest one or more times during the day, there was considerable variation (10–20% of the mean) from one squirrel to another and from day to day for the same animal.

We were working with a relatively small sample size and, due to the storage limitations of iButtons, with brief bouts of data. The idiosyncratic behaviors of individual fox squirrels that we documented might therefore not be entirely representative of a larger population of fox squirrels. However, some of the patterns and behaviors described here were not known before and illustrate the value of using data loggers to discover hidden details of the lives of even common species living in close proximity to humans in a suburban to urban setting.

There are possible methodological shortcomings in the use of collar temperature as a proxy of activity. In late spring/summer when higher ambient temperatures occur, the overnight patterns of T_c of several animals indicated that they did not spend the night in insulated nests (e.g., **Figures 9D**, **10C**). On such days it is much more difficult—and sometimes impossible—to detect and distinguish in-nest time from ONT using our method. We therefore plan to supplement and extend the current study by using combined temperature and light sensors (Anders et al., 2017). We also plan to look at the patterns recorded for female fox squirrels during their expected gestation and lactation periods and compare these results to Studd et al. (2016) and Williams et al. (2014).

ETHICS STATEMENT

All work was conducted with approval of the Institutional Animal Care and Use Committee of Siena Heights University and followed appropriate guidelines as outlined by Sikes et al. (2012).

AUTHOR CONTRIBUTIONS

TW conceived, designed, and performed the data collection. TW and RR analyzed the data and wrote/edited the paper. RR designed the custom software used in the data analysis.

FUNDING

This research was funded by the Biology Department of Siena Heights University and a Siena Heights University Faculty Development Grant.

ACKNOWLEDGMENTS

We would like to thank the Siena Heights University Biology Department and Faculty Development Grant for supporting this research, Cindy Canale, Institute of Evolutionary Biology and Environmental Studies, University of Zurich, for the initial design of the collar, Siena Heights students Ryan Gumbleton and Crystal Wilcoxen for assistance in animal trapping and the preparation of collars, and John L. Koprowski, University of Arizona, Robert McCleery, University of Florida, and Murray M. Humphries, McGill University, for advice. We would also like to thank the Boise State University Psychology Department for supporting this research.

SUPPLEMENTARY MATERIAL

The Supplementary Material for this article can be found online at: https://www.frontiersin.org/articles/10.3389/fevo.2019.00179/full#supplementary-material

REFERENCES

Adams, C. E. (1984). Diversity in fox squirrel spatial relationships and activity rhythms. *Tex. J. Sci.* 36, 197–203.

Agostini, I., Holzmann, I., and Di Bitetti, M. S. (2012). Influence of seasonality, group size, and presence of a congener on activity patterns of howler monkeys. *J. Mammal.* 93, 645–657. doi: 10.1644/11-MAMM-A-070.1

Alós, J., Martorell-Barcel,ó, M., and Campos-Candela, A. (2017). Repeatability of circadian behavioural variation revealed in free-ranging marine fish. *R. Soc. Open Sci.* 4:160791. doi: 10.1098/rsos.160791

Altmann, J. (1974). Observational study of behavior: sampling methods. *Behaviour* 49, 227–267. doi: 10.1163/156853974x00534

Anders, J. L., Uchida, K., Watanabe, M., Tanio, I., Shimamoto, T., Hamada, M., et al. (2017). Usefulness and limitation of a tiny light-temperature logger to monitor daily activity levels of arboreal squirrels in temperate areas. *Mamm. Res.* 62, 397–404. doi: 10.1007/s13364-017-0326-0

Aschoff, J. (1966). Circadian activity pattern with 2 peaks. *Ecology* 47, 657–662. doi: 10.2307/1933949

Barassin, S., Saboureau, M., Kalsbeek, A., Bothorel, B., Vivien-Roels, B., and Malan, A., et al, and (1999). Interindividual differences in the pattern of melatonin secretion of the Wistar rat. *J. Pineal Res.* 27, 193–201.

Batschelet, E. (1981). *Circular Statistics in Biology*. New York, NY: Academic Press.

Bennett, A. F. (1987). "Interindividual variability: an underutilized resource," in *New directions in ecological physiology*, eds M. E. Feder, A. F. Bennett, W. W. Burggren, and R. B. Huey (New York, NY: Cambridge University Press), 147–69.

Boon, A. K., Réale, D., and Boutin, S. (2008). Personality, habitat use, and their consequences for survival in North American red squirrels Tamiasciurus hudsonicus. *Oikos* 117, 1321–1328. doi: 10.1111/j.0030-1299.2008.16567.x

Bordignon, M., and Monteiro-Filho, E. L. A. (2000). Behaviour and daily activity of the squirrel Sciurus ingrami in a secondary araucaria forest in southern Brazil. *Can. J. Zool.* 78, 1732–1739. doi: 10.1139/cjz-78-10-1732

Careau, V., Thomas, D., Humphries, M. M., and Reale, D. (2008). Energy metabolism and animal personality. *Oikos* 117, 641–653. doi: 10.1111/j.0030-1299.2008.16513.x

Ciuti, S., Muhly, T. B., Paton, D. G., McDevitt, A. D., Musiani, M., and Boyce, M. S. (2012). Human selection of elk behavioural traits in a landscape of fear. *Proc. R. Soc. Lond. B Biol. Sci.* 279:4407. doi: 10.1098/rspb.2012.1483

Connolly, B. M., and Orrock, J. L. (2017). Habitat-specific capture timing of deer mice (*Peromyscus maniculatus*) suggests that predators structure temporal activity of prey. *Ethology* 124, 105–112. doi: 10.1111/eth.12708

Cooper, E. B., Taylor, R. W., Kelley, A. D., Martinig, A. R., Boutin, S., Humphries, M. M., et al. (2017). Personality is correlated with natal dispersal in North American red squirrels (*Tamiasciurus hudsonicus*). *Behaviour* 154, 939–961. doi: 10.1163/1568539X-00003450

Dall, S. R. X., and Boyd, I. L. (2002). Provisioning under the risk of starvation. *Evol. Ecol. Res.* 4, 883–896.

DeCoursey, P. J., Walker, J. K., and Smith, S. A. (2000). A circadian pacemaker in free-living chipmunks: essential for survival? *J. Comp. Physiol. A Neuroethol. Sens. Neural. Behav. Physiol.* 186, 169–180. doi: 10.1007/s003590050017

Dingemanse, N. J., and Wolf, M. (2013). Between-individual differences in behavioural plasticity within populations: causes and consequences. *Anim. Behav.* 85, 1031–1039. doi: 10.1016/j.anbehav.2012.12.032

Ditgen, R. S., Shepherd, J. D., and Humphrey, S. R. (2007). Big cypress fox squirrel (*Sciurus niger avicennia*) diet, activity and habitat use on a golf course in southwest Florida. *Am. Midl. Nat.* 158, 403–414. doi: 10.1674/0003-0031(2007)158[403:Bcfssn]2.0.Co;2

Enright, J. T. (1966). Influences of seasonal factors on the activity onset of the house finch. *Ecology* 47, 662–666. doi: 10.2307/1933950

Eriksen, A., Wabakken, P., Zimmermann, B., Andreassen, H. P., Arnemo, J. M., Gundersen, H., et al. (2011). Activity patterns of predator and prey: a simultaneous study of GPS-collared wolves and moose. *Anim. Behav.* 81, 423–431. doi: 10.1016/j.anbehav.2010.11.011

Fisher, N. I. (1993). *Statistical Analysis of Circular Data*. New York, NY: Cambridge University Press.

Gosling, S. D. (2001). From mice to men: what can we learn about personality from animal research? *Psychol. Bull.* 127, 45–86. doi: 10.1037/0033-2909.127.1.45

Halle, S., and Stenseth, N. C. (2000). *Activity Patterns in Small Mammals: An Ecological Approach*. New York, NY: Springer.

Havera, S. P. (1979). Energy and nutrient cost of lactation in fox squirrels. *J. Wildl. Manage* 43, 958–965. doi: 10.2307/3808281

Helm, B., Visser, M. E., Schwartz, W., Kronfeld-Schor, N., Gerkema, M., Piersma, T., et al. (2017). Two sides of a coin: ecological and chronobiological perspectives of timing in the wild. *Philos. Trans. R. Soc. Lond. B Biol. Sci.* 372:246. doi: 10.1098/rstb.2016.0246

Hertel, A. G., Swenson, J. E., and Bischof, R. (2017). A case for considering individual variation in diel activity patterns. *Behav. Ecol.* 28, 1524–1531. doi: 10.1093/beheco/arx122

Hicks, E. A. (1949). Ecological factors affecting the activity of the western fox squirrel, *Sciurus niger rufiventer* (Geoffroy). *Ecol. Monogr.* 19, 287–302. doi: 10.2307/1943272

Higginson, A. D., McNamara, J. M., and Houston, A. I. (2012). The starvation–predation trade-off predicts trends in body size, muscularity, and adiposity between and within taxa. *Am. Nat.* 179, 338–350. doi: 10.1086/664457

Horne, J. A., and Ostberg, O. (1976). A self-assessment questionnaire to determine morningness–eveningness in human circadian rhythms. *Int. J. Chronobiol.* 4, 97–110.

Huggins, J. G., and Gee, K. L. (1995). Efficiency and selectivity of cage trap sets for gray and fox squirrels. *Wildl. Soc. Bull.* 23, 204–207. doi: 10.2307/3782791

Jodice, P. G. R., and Humphrey, S. R. (1992). Activity and diet of an urban-population of big cypress fox squirrels. *J. Wildl. Manage* 56, 685–692. doi: 10.2307/3809461

Johnson, C. H., Elliott, J. A., and Foster, R. (2003). Entrainment of circadian programs. *Chronobiol. Int.* 20, 741–774. doi: 10.1081/CBI-120024211

Kanda, L. L., Fuller, T. K., and Friedland, K. D. (2005). Temperature sensor evaluation of opossum winter activity. *Wildl. Soc. Bull.* 33, 1425–1431. doi: 10.2193/0091-7648(2005)33[1425:tseoow]2.0.co;2

Koprowski, J. L. (1994). Sciurus niger. *Mamm. Species* 479, 1–9. doi: 10.2307/3504263

Koprowski, J. L., and Corse, M. C. (2005). Time budgets, activity periods, and behavior of Mexican fox squirrels. *J. Mammal.* 86, 947–952. doi: 10.1644/1545-1542(2005)86[947:Tbapab]2.0.Co;2

Labyak, S. E., Lee, T. M., and Goel, N. (1997). Rhythm chronotypes in a diurnal rodent, *Octodon degus*. *Am. J. Physiol. Regul. Integr. Comp. Physiol.* 273 (3 Pt 2), R1058–R1066. doi: 10.1152/ajpregu.1997.273.3.R1058

Lamb, T. D. (1995). Photoreceptor spectral sensitivities: common shape in the long-wavelength region. *Vis. Res.* 35, 3083–3091. doi: 10.1016/0042-6989(95)00114-F

Larivée, M. L., Boutin, S., Speakman, J. R., McAdam, A. G., and Humphries, M. M. (2010). Associations between over-winter survival and resting metabolic rate in juvenile North American red squirrels. *Funct. Ecol.* 24, 597–607. doi: 10.1111/j.1365-2435.2009.01680.x

Lazerte, S. E., and Kramer, D. L. (2011). Using thermosensitive radiotelemetry to document rest and activity in a semifossorial rodent. *Wildl. Soc. Bull.* 35, 481–488. doi: 10.1002/wsb.74

Lone, K., Loe, L. E., Meisingset, E. L., Stamnes, I., and Mysterud, A. (2015). An adaptive behavioural response to hunting: surviving male red deer shift habitat at the onset of the hunting season. *Anim. Behav.* 102, 127–138. doi: 10.1016/j.anbehav.2015.01.012

Mardia, K. V., and Jupp, P. E. (2000). *Directional Statistics*. New York, NY: J. Wiley.

Masuda, K., and Zhdanova, I. V. (2010). Intrinsic activity rhythms in *Macaca mulatta*: their entrainment to light and melatonin. *J. Biol. Rhythms* 25, 361–371. doi: 10.1177/0748730410379382

McNamara, J. M., Higginson, A. D., and Verhulst, S. (2016). The influence of the starvation–predation trade-off on the relationship between ambient temperature and body size among endotherms. *J. Biogeogr.* 43, 809–819. doi: 10.1111/jbi.12695

Moore, D. S., Notz, W., and Fligner, M. A. (2013). *The Basic Practice of Statistics*. New York, NY: W.H. Freeman.

Murray, I. W., and Smith, F. A. (2012). Estimating the influence of the thermal environment on activity patterns of the desert woodrat (*Neotoma lepida*) using temperature chronologies. *Can. J. Zool.* 90, 1171–1180. doi: 10.1139/z2012-084

Nelson, W., Tong, Y. L., Lee, J. K., and Halberg, F. (1979). Methods for cosinor-rhythmometry. *Chronobiologia* 6, 305–323.

Pfeffer, M., Wicht, H., von Gall, C., and Korf, H.-W. (2015). Owls and larks in mice. *Front. Neurol.* 6:101. doi: 10.3389/fneur.2015.00101

Quinn, J. L., Cole, E. F., Bates, J., Payne, R. W., and Cresswell, W. (2012). Personality predicts individual responsiveness to the risks of starvation and predation. *Proc. R. Soc. B* 279, 1919. doi: 10.1098/rspb.2011.2227

Randler, C., Schredl, M., and Göritz, A. S. (2017). Chronotype, sleep behavior, and the big five personality factors. *SAGE Open* 7:2158244017728321. doi: 10.1177/2158244017728321

Refinetti, R., and Piccione, G. (2005). Intra- and inter-individual variability in the circadian rhythm of body temperature of rats, squirrels, dogs, and horses. *J. Therm. Biol.* 30, 139–146. doi: 10.1016/j.jtherbio.2004.09.003

Refinetti, R., Wassmer, T., Basu, P., Cherukalady, R., Pandey, V. K., Singaravel, M., et al. (2016). Variability of behavioral chronotypes of 16 mammalian species under controlled conditions. *Physiol. Behav.* 161, 53–59. doi: 10.1016/j.physbeh.2016.04.019

Reighard, S. L., Bucholz, A. D., Haahr, J. A., and Jenks, J. A. (2004). Fox squirrel weight and age structure in mast and non-mast forests. *Proc. Soc. Dak. Acad. Sci.* 83, 47–54.

Roche, D. G., Careau, V., and Binning, S. A. (2016). Demystifying animal 'personality' (or not): why individual variation matters to experimental biologists. *J. Exp. Biol.* 219, 3832. doi: 10.1242/jeb.146712

Romeijn, N., and Van Someren, E. J. W. (2011). Correlated fluctuations of daytime skin temperature and vigilance. *J. Biol. Rhythms* 26, 68–77. doi: 10.1177/0748730410391894

Schmidt, K., Nakanishi, N., Izawa, M., Okamura, M., Watanabe, S., Tanaka, S., et al. (2008). The reproductive tactics and activity patterns of solitary carnivores: the Iriomote cat. *J. Ethol.* 27:165. doi: 10.1007/s10164-008-0101-4

Schroeder, M. A., and Robb, L. A. (2005). "Criteria for gender and age," in *Techniques for Wildlife Investigations and Management*. Ed C. E. Braun (Bethesda, MD: The Wildlife Society), 303–38.

Selmaoui, B., and Touitou, Y. (2003). Reproducibility of the circadian rhythms of serum cortisol and melatonin in healthy subjects: a study of three different 24-h cycles over six weeks. *Life Sci.* 73, 3339–3349. doi: 10.1016/j.lfs.2003.05.007

Siegel, S., and Castellan, N. J. (1988). *Nonparametric Statistics for the Behavioral Sciences*. New York, NY: McGraw-Hill.

Sih, A., Bell, A. M., Johnson, J. C., and Ziemba, R. E. (2004). Behavioral syndromes: an integrative overview. *Q. Rev. Biol.* 79, 241–277. doi: 10.1086/422893

Sikes, R. S., Paul, E., and Beaupre, S. J. (2012). Standards for wildlife research: taxon-specific guidelines versus US Public Health Service Policy. *Bioscience* 62, 830–834. doi: 10.1525/bio.2012.62.9.9

Sokolove, P. G., and Bushell, W. N. (1978). Chi square periodogram—its utility for analysis of circadian-rhythms. *J. Theor. Biol.* 72, 131–160. doi: 10.1016/0022-5193(78)90022-X

Speakman, J. R. (2008). The physiological costs of reproduction in small mammals. *Philos. Trans. R. Soc. Lond. B Biol. Sci.* 363, 375–398. doi: 10.1098/rstb.2007.2145

Stamps, J. A. (2007). Growth-mortality tradeoffs and 'personality traits' in animals. *Ecol. Lett.* 10, 355–363. doi: 10.1111/j.1461-0248.2007.01034.x

Studd, E. K., Boutin, S., McAdam, A. G., and Humphries, M. M. (2016). Nest attendance of lactating red squirrels (*Tamiasciurus hudsonicus*): influences of biological and environmental correlates. *J. Mammal.* 97, 806–814. doi: 10.1093/jmammal/gyw010

Tester, J. R. (1978). "Analysis of circadian rhythms of free-ranging mammals," in Fourth *International Symposium on Biotelemetry*, eds H. J. Klewe and H. P. Kimmich (Braunschweig: International Symposium on Biotelemetry), 167–70.

Thompson, D. C. (1977). Diurnal and seasonal activity of the grey squirrel (*Sciurus carolinensis*). *Can. J. Zool.* 55, 1185–1189. doi: 10.1139/z77-153

Vink, J. M., Groot, A. S., Kerkhof, G. A., and Boomsma, D. I. (2001). Genetic analysis of morningness and eveningness. *Chronobiol. Int.* 18, 809–822. doi: 10.1081/CBI-100107516

Wassmer, T. (2017). Detailed illustrated description of iButton collars for small mammals. *Figshare Digital Repository*. doi: 10.6084/m9.figshare.5149834.v1

Wassmer, T., and Refinetti, R. (2016). Daily activity and nest occupation patterns of fox squirrels (*Sciurus niger*) throughout the year. *PLoS ONE* 11:e0151249. doi: 10.1371/journal.pone.0151249

Wauters, L., Swinnen, C., and Dhondt, A. A. (1992). Activity budget and foraging behavior of red squirrels (*Sciurus vulgaris*) in coniferous and deciduous habitats. *J. Zool.* 227, 71–86.

Wauters, L. A., and Dhondt, A. A. (1987). Activity budget and foraging behaviour of the red squirrel (*Sciurus vulgaris* Linnaeus, 1758) in a coniferous habitat. *Z. Säuget. Mamm. Biol.* 52, 341–353.

White, J. A., and Geluso, K. (2007). Seasonal differences in onset of surface activity of Ord's kangaroo rat *(Dipodomys ordii). J. Mammal.* 88, 234–240. doi: 10.1644/05-Mamm-a-312r3.1

Williams, C. T., Wilsterman, K., Kelley, A. D., Breton, A. R., Stark, H., Humphries, M. M., et al. (2014). Light loggers reveal weather-driven changes in the daily activity patterns of arboreal and semifossorial rodents. *J. Mammal.* 95, 1230–1239. doi: 10.1644/14-MAMM-A-062

Williams, T. D. (2008). Individual variation in endocrine systems: moving beyond the 'tyranny of the Golden Mean'. *Philos. Trans. R. Soc. Lond. B Biol. Sci.* 363:3. doi: 10.1098/rstb.2007.0003

Wolf, M., and Weissing, F. J. (2012). Animal personalities: consequences for ecology and evolution. *Trends Ecol. Evol.* 27, 452–461. doi: 10.1016/j.tree.2012.05.001

Zar, J. H. (2018). *Biostatistical Analysis*. Upper Saddle River, NJ: Pearson Education, Inc.

Zhang, J., Hull, V., Ouyang, Z., He, L., Connor, T., Yang, H., et al. (2017). Modeling activity patterns of wildlife using time-series analysis. *Ecol. Evol.* 7, 2575–2584. doi: 10.1002/ece3.2873

Zhao, Z. J., Song, D. G., Su, Z. C., Wei, W. B., Liu, X. B., and Speakman, J. R. (2013). Limits to sustained energy intake. XVIII. Energy intake and reproductive output during lactation in Swiss mice raising small litters. *J. Exp. Biol.* 216, 2349–2358. doi: 10.1242/Jeb.078436

Zwahlen, R. (1975). Locomotor activity of squirrels (*Sciurus vulgaris*). *Oecologia* 22, 79–98. doi: 10.1007/bf00345260

Conflict of Interest Statement: The authors declare that the research was conducted in the absence of any commercial or financial relationships that could be construed as a potential conflict of interest.

Copyright © 2019 Wassmer and Refinetti. This is an open-access article distributed under the terms of the Creative Commons Attribution License (CC BY). The use, distribution or reproduction in other forums is permitted, provided the original author(s) and the copyright owner(s) are credited and that the original publication in this journal is cited, in accordance with accepted academic practice. No use, distribution or reproduction is permitted which does not comply with these terms.

frontiers in Ecology and Evolution

ORIGINAL RESEARCH
published: 31 May 2019
doi: 10.3389/fevo.2019.00200

Overall Dynamic Body Acceleration in Straw-Colored Fruit Bats Increases in Headwinds but Not With Airspeed

M. Teague O'Mara[1,2,3], Anne K. Scharf[1,2,3], Jakob Fahr[1,4], Michael Abedi-Lartey[1,3], Martin Wikelski[1,2,3], Dina K. N. Dechmann[1,2,3] and Kamran Safi[1,2,3]*

[1] Department of Migration, Max Planck Institute of Animal Behavior, Radolfzell, Germany, [2] Centre for the Advanced Study of Collective Behaviour, University of Konstanz, Konstanz, Germany, [3] Department of Biology, University of Konstanz, Konstanz, Germany, [4] Braunschweig University of Technology, Zoological Institute, Braunschweig, Germany

Atmospheric conditions impact how animals use the aerosphere, and birds and bats should modify their flight to minimize energetic expenditure relative to changing wind conditions. To investigate how free-ranging straw-colored fruit bats (*Eidolon helvum*) fly with changing wind support, we use data collected from bats fit with GPS loggers and an integrated triaxial accelerometer and measure flight speeds, wingbeat frequency, and overall dynamic body acceleration (ODBA) as an estimate for energetic expenditure. We predicted that if ODBA reflects energetic expenditure, then we should find a curvilinear relationship between ODBA and airspeed consistent with aerodynamic theory. We expected that bats would lower their airspeed with tailwind support and that ODBA will decrease with increasing tailwinds and increase with wingbeat frequency. We found that wingbeat frequency has the strongest positive relationship with ODBA. There was a small, but negative, relationship between airspeed and ODBA, and bats decreased ODBA with increasing tailwind. Bats flew at ground speeds of 9.6 ± 2.4 ms^{-1} (Mean $\pm$ SD, range: 4.3–23.9 ms^{-1}) and airspeeds of 10.2 ± 2.5 ms^{-1}, and did not modify their wingbeat frequency with speed. Free-ranging straw-colored fruit bats therefore exerted more total ODBA in headwinds but not when they changed their airspeed. It is possible that the flexibility in wingbeat kinematics may make flight of free-ranging bats less costly than currently predicted or alternatively that the combination of ODBA and airspeed at our scales of measurement does not reflect this relationship in straw-colored fruit bats. Further work is needed to understand the full potential of free-ranging bat flight and how well bio-logging techniques reflect the costs of bat flight.

Keywords: ***Eidolon helvum*, flight, energy landscape, energy expenditure, bio-logging, ODBA**

OPEN ACCESS

Edited by:
Frants Havmand Jensen, Woods Hole Oceanographic Institution, United States

Reviewed by:
Andy TD Bennett, Deakin University, Australia
Judy Shamoun-Baranes, University of Amsterdam, Netherlands

****Correspondence:***
M. Teague O'Mara
tomara@orn.mpg.de

Specialty section:
This article was submitted to Behavioral and Evolutionary Ecology, a section of the journal Frontiers in Ecology and Evolution

Received: *10 October 2018*
Accepted: *15 May 2019*
Published: *31 May 2019*

Citation:
O'Mara MT, Scharf AK, Fahr J, Abedi-Lartey M, Wikelski M, Dechmann DKN and Safi K (2019) Overall Dynamic Body Acceleration in Straw-Colored Fruit Bats Increases in Headwinds but Not With Airspeed. Front. Ecol. Evol. 7:200. doi: 10.3389/fevo.2019.00200

INTRODUCTION

Vertebrate flapping flight is an energetically costly, but economical form of locomotion. Many birds and bats modulate their airspeed, the speed at which they fly relative to the moving air column, in relation to the amount of wind support they receive (Hedenström, 2003; Pennycuick, 2008; Safi et al., 2013; Sapir et al., 2014). They generally increase airspeed with headwind and crosswind (Hedenström et al., 2002; Pennycuick, 2008; Kogure et al., 2016), but decrease airspeed with tailwind to lower overall energetic expenditure. However, measuring instantaneous energetic expenditure is difficult in the wild (Butler et al., 2004; Green et al., 2009), and instead of direct

measurement, theoretical relationships built from first principles and wind-tunnel experiments are largely applied to predict the energy requirements of free-flying animals (Pennycuick, 1978; Norberg, 1990; Rayner, 1999; Tobalske et al., 2003b). These relationships are based on the size and shape of a bird, its airspeed, and the resulting power requirements for that flight (Rayner, 1999; Pennycuick, 2008). However, predictions from these models do not always match field-based measures, such as the extreme flight speeds of Brazilian free-tailed bats that are far outside the maximum predicted power these small bats should be capable of (McCracken et al., 2016). Body-mounted accelerometers are a way to show how total power requirements change throughout flight in free-ranging animals, as well as shed light on limited aspects of their wingbeat mechanics (Gleiss et al., 2011; Elliott et al., 2013; Bishop et al., 2015; Elliott, 2016; Hicks et al., 2017). By applying accelerometer-derived motion estimates for both behavior and energy expenditure we should be able to better understand the ways that bats and birds respond to their environment.

The use of tri-axial accelerometry (ACC) combined with GPS data provides a window into the energetic strategies used by animals at fine spatial and temporal scales. ACC data can be interpreted as a measure of the amount of effort used to fly, assuming that the costs of movement constitute the bulk of an animal's energy expenditure (Karasov, 1992; Gleiss et al., 2011; Halsey et al., 2011; Hernandez-Pliego et al., 2017). The relative cost of movement has been estimated from ACC using dynamic body acceleration (DBA) and the full sum of all three axes, Overall Dynamic Body Acceleration (ODBA). For birds, ODBA and other DBA measures have been calibrated against energy consumption during running and walking (Wilson et al., 2006), and inferred in free-flying birds through correlations between heart rate and ACC (Duriez et al., 2014; Bishop et al., 2015; Hicks et al., 2017). Furthermore, models of flapping flight estimate biomechanical power from acceleration data (Spivey and Bishop, 2013). While mechanical power output does not have a direct linear relationship with metabolic power input (Biewener, 2006; Gleiss et al., 2011; Spivey and Bishop, 2013), DBA measures can explain a substantial proportion of total daily energetic expenditure (DEE) or energy expenditure during specific activities in vertebrates in general (Gleiss et al., 2011; Elliott et al., 2013; Duriez et al., 2014; Bishop et al., 2015; Elliott, 2016; Stothart et al., 2016; Hicks et al., 2017). This daily, integrative summary of DEE from DBA is even more effective when the portion of high-energy locomotion (e.g., flapping flight) is modeled separately from other behaviors (Green et al., 2009; Elliott et al., 2013; Duriez et al., 2014; Bishop et al., 2015; Stothart et al., 2016). Changes in acceleration can also be used to identify the behavioral context and activity of flight (e.g., flapping vs. gliding) (Elliott et al., 2013; Williams et al., 2015; Abedi-Lartey et al., 2016; Leos-Barajas et al., 2017) as well as stroke frequency and wingbeat strength (Sato et al., 2008; Kogure et al., 2016). These fundamental components have been used to infer foraging success and mass gain via increases in wingbeat frequency (Sato et al., 2008; O'Mara et al., 2019) as well as the costs of movement trajectories (Nathan et al., 2012; Amelineau et al., 2014; Duriez et al., 2014) with wind across various scales (Kogure et al., 2016; Scacco et al., 2019). There is therefore a strong time-integrated relationship between total ODBA and DEE, but it is unknown how ODBA reflects energy expenditure at finer time scales of individual behaviors, or if ODBA reflects the general non-linear relationship of power output across a range of known flight speeds (Spivey and Bishop, 2013).

Experimental work in wind tunnels has yielded the best insight into how birds and bats adjust their flight behavior and energy expenditure to increasing airspeeds. In general, birds fly faster by increasing wingbeat amplitude and/or wingbeat frequency. However, the interaction between these two adjustments can be species- and speed-dependent (Tobalske et al., 2003a; Tobalske, 2007; Altshuler et al., 2015), and be combined with an elongation of the downstroke ratio and rotation of the wings into a more vertical orientation. While birds and bats fly in similar ways at a broad level, flight behavior in these groups can differ dramatically. Bat wing motions tend to have similar, but greater overall amplitude than birds (Taylor et al., 2003), and bat wings are both relatively massive and have that mass distributed more distally than birds (Thollesson and Norberg, 1991). Like birds, bats modulate their wingbeat amplitude with speed, but to a lesser degree and tend to show either a negative or no relationship between airspeed and wingbeat frequency (Riskin et al., 2010; Hubel et al., 2016). To increase airspeed, bats reduce wingbeat frequency and wingbeat amplitude, but place their wings in a more vertical orientation (Bullen and McKenzie, 2002; Riskin et al., 2010; Iriarte-Diaz et al., 2012; Swartz et al., 2012; Hubel et al., 2016). Furthermore, large fruit bats decrease wingbeat frequency, extend their wings less fully across the entire wingbeat and increase the duration of their wingbeat downstroke to fly faster across a speed range of 3–6 ms^{-1} (Riskin et al., 2010). For many species, however, the airspeeds that typify free-ranging flight have yet to be achieved in wind tunnels making it difficult to extrapolate from captive conditions to those in the wild where animals may both choose faster speeds and must compensate for changing aerial environments.

The African straw-colored fruit bat (*Eidolon helvum*) is an ideal species to test how individual measures of flight behavior and energetics from accelerometry relate to environmental conditions. Fruit bats use constant flapping flight and rarely glide or soar (Harris et al., 1990; Lindhe Norberg and Norberg, 2012). During their commuting flights of up to 90 km from a central roost (Sapir et al., 2014; Fahr et al., 2015; Abedi-Lartey et al., 2016; van Toor et al., 2019), they decrease airspeed with wind support, and increase airspeed with crosswinds (Sapir et al., 2014). We hypothesize that if ODBA reflects relative energetic expenditure or power output in bats, then we will find a curvilinear relationship between ODBA and airspeed similar to the theoretical total power requirements of flight (Usherwood et al., 2011; Spivey and Bishop, 2013). Furthermore, if these bats follow aerodynamic theory, they should reduce airspeed with wind support. We then predict a negative relationship between ODBA and tailwind support, and that ODBA will be strongly and positively associated with wingbeat frequency. Lastly, we expect that as in wind tunnel studies, wingbeat frequency will decrease with airspeed and increase with wind support.

METHODS

Capture and Handling

We collected data from 36 *Eidolon helvum* that wore collar-mounted (O'Mara et al., 2014) GPS and triaxial accelerometry (ACC) loggers (e-obs, GmbH, Munich, Germany). The loggers recorded position every 2.5 min and acceleration every minute for a duration of 13–14 s at a sampling frequency of 18.74–20 Hz (**Table 1**). These data were taken from a larger data set with a mix of logger positions and sampling rates. The full data set of all animals is available at the Movebank Data Repository doi: 10.5441/001/1.k8n02jn8 (Scharf et al., 2019). Data were collected in Ouagadougou (12.397° N, 1.488° W), Burkina Faso; in Kibi (6.165° N, 0.555° W), Ghana, and in Kasanka National Park (12.586° S, 30.243° E), Zambia where all animals were locally foraging from a central roost during tracking. *Eidolon helvum* were captured early in the morning with canopy mist nets as they returned from foraging which ensured that the animals had fed before handling (Fahr et al., 2015). We weighed all bats with Pesola spring balances (±0.5 g) and selected individuals with sufficient body mass (278.4 ± 20.5 g) to carry GPS + ACC loggers. Mean total logger mass was 20.95 ± 0.90 g which was 7.56 ± 0.59% of body mass.

Accelerometry Analysis

We extracted wingbeat frequency and ODBA from the ACC data. As indicated by the manufacturer we first transformed the raw acceleration data into ms^{-2}. ACC data were collected in bursts on three axes (X—sway, Y—surge, Z—heave, **Figure 1**) for a duration of 13–14 s every 1 min at 18.74–20 Hz (**Table 1**). As the tags were attached on a collar and could move freely around the neck of the animal, the Z and X axis orientation may not be consistent. However, measurement along Y remains in the same orientation regardless of the position on the collar. We applied an ordination to rotate the acceleration data in uncorrelated and orthogonal principal components per burst on all three axes. We extracted the first PC representing the axis containing most of the variance (PC1 mean per individual: 82 ± 6% of variance, range: 70–92%). We extracted the oscillation owed to the movement using a Fast Fourier Transformation (FFT) on the PC1 of each burst. The FFT provided the spectrogram and thus the dominant frequency of each burst corresponding to the wingbeat frequency, if present. We also calculated the average ODBA value for each burst (j) along the three axes (x, y, z) as:

$$ODBA_j = \frac{\sum_{i=1}^{n} |x_i - \overline{x}| + |y_i - \overline{y}| + |z_i - \overline{z}\,|}{n}$$

x_i represents the ith component and $\overline{x}$ the mean of all n samples of the x-axis of burst j, and likewise for y and z. Based on the variance in the amplitude of the dominant frequency extracted from the FFT and the ODBA extracted from the acceleration data, each burst could be assigned to either flapping or non-flapping. High variance in the dominant frequency was a reliable indicator of the presence of a regular oscillation in the acceleration data. If no regular oscillation was recorded, the FFT resulted in a weak and shallow dominant frequency with little difference in amplitude. Clear outliers in respect to wingbeat frequency (<2 or >8 bps, representing about 1% of all bursts classified as flapping) were removed from further analysis. The *moveACC* R library used to do this can be found at: https://gitlab.com/anneks/moveACC.git.

Airspeed Calculation

To calculate airspeed, we first annotated the GPS tracks with the wind conditions at every location using the Env-DATA tool in Movebank (Dodge et al., 2013). We used the U and V component of wind from the "ECMWF Interim Full Daily SFC Wind" 10 m above ground data set (Dee et al., 2011). The U component refers to the velocity of the East-West (zonal) component of wind where positive values indicate west to east flow, and the V component refers to the velocity of the North-South (meridional) component of wind where positive values indicate south to north flow. The ECMWF reanalysis provides estimates of weather conditions at a resolution of 0.75 degrees (ca. 83.4 km), every 6 h at 10 m above ground. This wind information gives broad insight into how bats compensate for environmental conditions, and while this may not be wholly reflective of the instantaneous conditions experienced by the bat, these prevailing wind speed data combined with GPS at similar resolution to our data set have allowed detailed inference into the flight behavior of bats and birds (Safi et al., 2013; Sapir et al., 2014; Flack et al., 2016; Van Doren et al., 2016). We then calculated the ground speed for each segment between consecutive GPS points and calculated airspeed, crosswind and wind support (Safi et al., 2013) using the associated wind conditions. Wind support was calculated as the length of the wind vector in the direction of the bat's flight where positive values represent tailwind and negative values headwind and are given as total support in ms^{-1}. Crosswind was calculated as the value of the speed of the wind vector perpendicular to the travel direction (Safi et al., 2013). The absolute value of crosswind, regardless of the side from which it came, was then used in analysis.

Segment Behavioral Classification

To identify periods of continuous flight we joined the GPS and ACC data sorted by timestamps per individual. Based on the time of the data recorded we assigned the ACC data to each corresponding segment between two consecutive GPS locations. We identified segments that contained missed fixes based on their corresponding GPS schedule and excluded them from further analysis. For each of the remaining segments we calculated the percentage of ACC bursts identified with flapping behavior. We only included segments where 100% of the bursts were classified as flapping in our analysis to further restrict the data to segments with continuous flight. We calculated the mean value of the wingbeat frequency and ODBA for each segment.

Analysis

We used a series of generalized linear mixed effects models in R 3.3.2 (R Core Team, 2016) in *MASS::glmmPQL* (Venables and Ripley, 2002; Pinheiro et al., 2018) to test how wind conditions affect different aspects of flight. The dataset used in these models (**Table S1**) contained only those segments assigned with flapping without missed GPS fixes. This resulted

TABLE 1 | Deployment information for GPS+ACC loggers on *E. helvum*.

Study Site	Year	Attachment	GPS schedule	GPS run time	ACC burst duration (s)	ACC sampling rate (Hz)	Number of bats tagged	Median # nights tracked	Range # nights tracked
Ouagadougou, Burkina Faso	2013	Collar	2.5 min/30 min (ACC informed)	16–6 h	14.088	18.74	5	5.310	3.01–17.04
Ouagadougou, Burkina Faso	2014	Collar	2.5 min/30 min (ACC informed)	16–6 h	14.088	18.74	7	4.330	0.24–5.47
Kibi, Ghana	2012	Collar	2.5 min/30 min (ACC informed)	16–6 h	14.088	18.74	4	4.220	1.24–5.25
Kibi, Ghana	2013	Collar	2.5 min/30 min (ACC informed)	16–6 h	14.088	18.74	5	3.230	2.25–4.95
Kasanka NP, Zambia	2013	Collar	2.5 min/30 min (ACC informed)	16–6 h	14.088	18.74	5	4.480	0.47–5.49
Kasanka NP, Zambia	2014	Collar	2.5 min/30 min (ACC informed)	16–6 h	13.2	20.00	15	6.050	0.37–7.36

After data processing and cleaning to limit analysis to only those segments without missed GPS fixes and where bats were constantly flapping their wings, our final sample size was a total of 3,391 locations from 36 bats over 138 nights (3.8 ± 2.4 nights per bats, range: 1–8 nights).

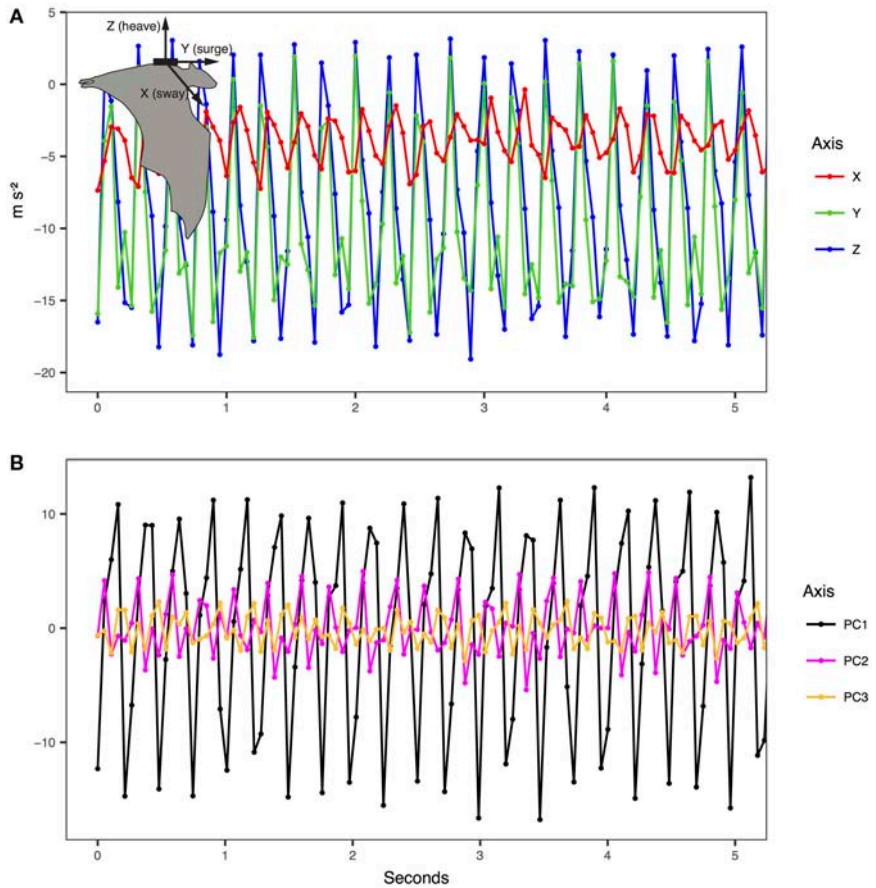

FIGURE 1 | Example of tri-axial accelerometry measurements and principal component conversion for *E. helvum* (inset). **(A)** The raw data were transformed according to manufacturer instructions into ms^{-2}. **(B)** The principal components reflect the standardized major wave forms for the three axes for each burst of acceleration.

in a total of 3,391 locations from 36 bats over 138 nights (3.8 ± 2.4 nights per bats, range: 1–8 nights). As the wind conditions could only be calculated for GPS positions, we assigned the mean wingbeat frequency and ODBA values of the segment to the last point of each segment. We constructed models for each of the response variables: ground speed of

the segment, airspeed, ODBA, and wingbeat frequency. Each model included fixed effects of wind support and the absolute value of crosswind as a cofactor. Additionally, we constructed a single model that included ODBA as the response variable, with wind support, absolute value of crosswind, wingbeat frequency, and airspeed as fixed effects. Finally, we also tested in two separate models how wingbeat frequency relates to airspeed and to ground speed of the segment. All models accounted for individual difference by including individual identity as random effect nested within tag manufacturing generation as each generation of tag had its own acceleration transformation procedure. We found no evidence of a temporal autocorrelation structure in our data. We used a Box-Cox transformation of the response variables to meet conditions for Gaussian linear models using the function *MASS::boxcox* (Venables and Ripley, 2002) and report the power transformation exponent (**Table 2**). The predictions were back-transformed accordingly. We calculated *p*-values for fixed effects through Wald approximation in *nlme* (Pinheiro et al., 2018), and because of our large sample size and nested random effects we consider $p = 0.001$ as our significance threshold.

Data Availability Statement

All raw GPS and ACC data are available from the Movebank Data Repository doi: 10.5441/001/1.k8n02jn8. The final annotated dataset used in our analyses can be found in **Supplementary Dataset 1**.

RESULTS

Data from 36 straw-colored fruit bats allowed us to calculate ODBA and wingbeat frequency from the tri-axial accelerometer (**Figure 1**), and ground speed from GPS. Using regional wind models we then derived airspeed, wind support, and crosswinds for each segment between successive GPS points. In all of our models, there was substantial individual variation as well as effects of the GPS tag generation, with individual identity showing a larger standard deviation in all models. The combined random effects of tag generation and individual identity accounted for a moderate, but inconsistent, amount of variation within each model (**Table 2**). The addition of the random effects always substantially increased the fit of the model (R^2 conditional, **Table 2**) when compared to the fixed effects alone (R^2 marginal, **Table 2**).

Straw-colored fruit bats flew at ground speeds of 4.3–23.9 ms^{-1} (Mean ± SD: 9.6 ± 2.4, **Figure 2A**), which resulted in a mean airspeed of 10.2 ± 2.5 ms^{-1} (range: 0.4–22.7 ms^{-1}, **Figure 2B**). To do so, they used a relatively narrow range of wingbeat frequencies (4.12 ± 0.21 bps, range: 3.19–5.04 bps, **Figure 2C**), and ODBA (12.76 ± 1.54 ms^{-2}, range: 8.78–19.81 ms^{-2}, **Figure 2D**). Bats modulated their flight behavior in response to the direction of wind support (**Figure 2**). Ground speed increased with tailwind (**Figure 2B**, **Table 2**), and bats decreased airspeed with increasing tailwind support (**Figure 2B**, **Table 2**). Wingbeat frequency increased slightly with wind support (**Figure 2C**) and ODBA decreased with wind support (**Figure 2D**). Crosswinds had a slightly negative effect on ground speed (**Figure S1A**), but no effect on total airspeed, wingbeat frequency, or ODBA (**Table 2**, **Figures S1B–D**).

When we tested the effects of wind support, crosswinds, wingbeat frequency, and airspeed on the ODBA generated by bats in a single model (**Figure 3**, **Table 2**), we again found that ODBA decreased with wind support (**Figure 3A**) and that there was no effect of crosswinds (**Figure 3B**). ODBA was strongly and positively associated with wingbeat frequency (**Figure 3C**) and decreased with airspeed. Wingbeat frequency was not associated with either airspeed (**Figure 4A**, **Table 2**) or ground speed (**Figure 4B**). Bats therefore generated less total ODBA as they received increasing tailwind support and did not increase wingbeat frequency to fly faster at lower ODBA values.

DISCUSSION

By integrating GPS and ACC data collected from free flying *E. helvum* with regional wind models, we show that straw-colored fruit bats increase wingbeat frequency with wind support (**Figure 2C**), and that flying into headwind increases fruit bat ODBA, while increasing airspeed slightly decreases ODBA (**Figures 3A,D**, **Table 2**). As in previous work (Sapir et al., 2014), bats reduced their airspeed with increasing wind support (**Figure 2B**) likely to reduce costs of flight, or to maintain ground speed to aid in visual navigation (Chapman et al., 2011; Hedenström and Åkesson, 2017). However, these airspeed changes were not achieved by changing wingbeat frequency or increasing ODBA accumulation.

ODBA had a strongly positive relationship with wingbeat frequency, which is expected from work on free-ranging birds (Elliott et al., 2014; Bishop et al., 2015). Beyond this first generalization, relationships between ODBA and wingbeat frequency with airspeed or wind support do not follow consistent patterns among species. While several studies show that free-ranging animals adjust their flight speeds in response to wind support and cross winds, there are few examples of how the mechanics of flight behavior respond to changing wind conditions. In general, free-flying birds flap their wings faster to increase airspeed (Usherwood et al., 2011; Elliott et al., 2014), and some increase wingbeat amplitude or DBA (Usherwood et al., 2011; Elliott et al., 2014), while others do not (Kogure et al., 2016). Free-flying European shags do not change their wingbeat frequency relative to head or tailwind, but show a general curvilinear relationship between wind support and wingbeat strength (Kogure et al., 2016). It could be expected that if the frequency and strength of a wingbeat comprise the bulk of ODBA, then either no relationship or a negative relationship (Kogure et al., 2016) with wind support would appear, such as the relationship we find in *E. helvum*. However, kittiwakes and murres decrease wingbeat frequency with wind support, and increase DBA with increasing wind support (Elliott et al., 2014). With these few studies, the instantaneous relationships between DBA measures and wind support seem to be complex and species-specific, but could also be related to the resolution of the data measured. Leveraging the existing wealth of GPS+ACC tracking, especially when combined with higher resolution wind

TABLE 2 | GLMM results for the effect of wind support on bat ground speed, airspeed, wingbeat frequency, and ODBA.

Model	Estimate	Value ± standard error	*p*-value	DF	t	R^2 marginal	R^2 conditional	Box-Cox exponent	Random effects	Standard deviation
Ground speed ~ Wind support + abs(CrossWind)	(Intercept)	0.770 ± 0.00197	<0.001	3353	391.42	0.152	0.324	−0.116	Tag generation	0.00163
	Wind support	−0.005 ± 0.000177	<0.001		−26.79				Bat ID	0.00901
	abs(Crosswind)	0.001 ± 0.0004	<0.001		3.73				Residual	0.0181
Airspeed ~ Wind support + abs(CrossWind)	(Intercept)	13 ± 0.284	<0.001	3,353	45.86	0.079	0.226	1.117	Tag generation	0.0794
	Wind support	−0.596 ± 0.0326	<0.001		−18.26				Bat ID	1.46
	abs(Crosswind)	0.001 ± 0.0737	0.99		0.02				Residual	3.35
Wingbeat Frequency ~ Wind support + abs(CrossWind)	(Intercept)	15.5 ± 0.193	<0.001	3,353	80.13	0.009	0.471	1.926	Tag generation	0.0935
	Wind support	0.084 ± 0.0111	<0.001		7.54				Bat ID	1.06
	abs(Crosswind)	−0.000354 ± 0.0253	0.99		−0.01				Residual	1.14
ODBA ~ Wind support + abs(CrossWind)	(Intercept)	0.353 ± 0.00212	<0.001	3,353	165.80	0.017	0.463	−0.412	Tag generation	9.14e−13
	Wind support	0.001 ± 0.000131	<0.001		9.93				Bat ID	0.000150
	abs(Crosswind)	0.000563 ± 0.000298	0.06		1.89				Residual	0.000181
ODBA ~ Wind support + abs(CrossWind) + Wingbeat frequency + Airspeed	(Intercept)	0.465 ± 0.00574	<0.001	3,351	80.93	0.192	0.628	−0.460	Tag generation	0.00000119
	Wind support	0.0193 ± 0.000122	<0.001		15.90				Bat ID	0.0127
	abs(Crosswind)	0.00532 ± 0.000261	0.04		2.04				Residual	0.0118
	Wingbeat frequency	−0.0379 ± 0.00127	<0.001		−29.90					
	Airspeed	0.000491 ± 0.0000883	<0.001		5.56					
Airspeed ~ Wingbeat frequency	(Intercept)	15.906 ± 1.76	<0.001	3,354	9.04	0.000294	0.158	1.157	Tag generation	0.0997
	Wingbeat frequency	−0.348 ± 4.18	0.41		−0.83				Bat ID	1.72
Ground speed ~ Wingbeat frequency	(Intercept)	0.587 ± 0.0142	<0.001	3,354	41.08	0.000443	0.181	−0.252	Tag generation	2.96
	Wingbeat frequency	−0.00348 ± 0.00338	0.30		−1.03				Bat ID	15.83

Intercept, slope, and adjusted R^2 are given for the full model including the absolute value of crosswind as a covariate and the Box-Cox transformation exponent used for each model.

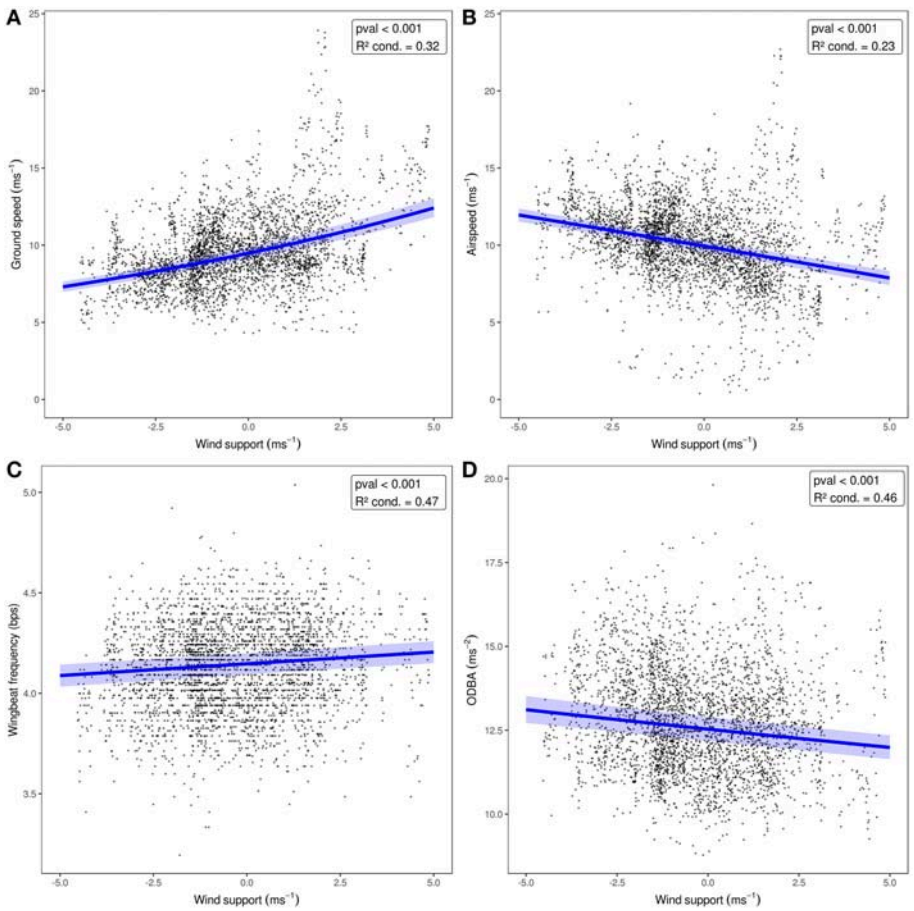

FIGURE 2 | The effect of wind support (headwind to tailwind) on *E. helvum* flight behavior when crosswinds are held at zero. GLMM results are shown in blue for **(A)** ground speed, **(B)** airspeed, **(C)** wingbeat frequency, and **(D)** ODBA. The 95% confidence interval for each model, including random effects, is shown as the shaded area around the line.

data, would help to clarify these patterns across a broader range of conditions.

The relationship between airspeed and power (Rayner, 1999; Pennycuick, 2008) predicts that if DBA is a true measure of energy expenditure or effort (Usherwood et al., 2011; Spivey and Bishop, 2013), then we should observe some curvilinear relationship between ODBA and airspeed in the bats we sampled. ODBA had a more strongly negative relationship with wind support than airspeed, illustrating that bats required more effort to make forward progress when faced with headwind, regardless of their airspeed. This is reasonable as bats increased their airspeed when facing headwinds, and that low speeds should be the most energetically costly for birds and bats (Tobalske et al., 2003b; Hedenstrom and Johansson, 2015; Hubel et al., 2016). However, there are several non-mutually exclusive explanations for why ODBA did not have a strong relationship with airspeed, especially at the high end of speed. First, the wind data used in this study were collected at a relatively large spatial (83 km) and temporal (6 h) scale. While many of our measures directly related to wind perform as expected (e.g., reduction of airspeed and reduced ODBA with wind support), it is possible that wind sampled at this scale cannot give a high enough resolution insight into accelerometry-derived measures of energetic expenditure relative to speed. Additionally, the true speed-power curve predicted for *E. helvum* may be very flat at moderate to high speeds (Dial et al., 1997; Tobalske et al., 2003b; von Busse et al., 2013) further complicating this relationship. Second, in all of our models, the inclusion of random effects of tag generation and individual identity greatly improved the conditional R^2 of the models over the marginal R^2, sometimes by as much as 0.46. This suggests that the movement patterns among individuals can be highly variable, and that bats likely employ a diversity of solutions to compensate for wind support to generate air speeds and ground speeds (Sapir et al., 2014). Since bats make many adjustments in the shape of their wings and the angle of attack of their wingbeat to fly faster (Riskin et al., 2008; Iriarte-Diaz et al., 2011; Hubel et al., 2012, 2016), these adjustments are unlikely to be captured by ODBA (Spivey and Bishop, 2013).

It is possible that due to bat flight kinematics, accelerometers do not accurately capture bat flight effort, despite their effectiveness on birds. Acceleration measures have the greatest reproducibility and comparability across individuals and taxa

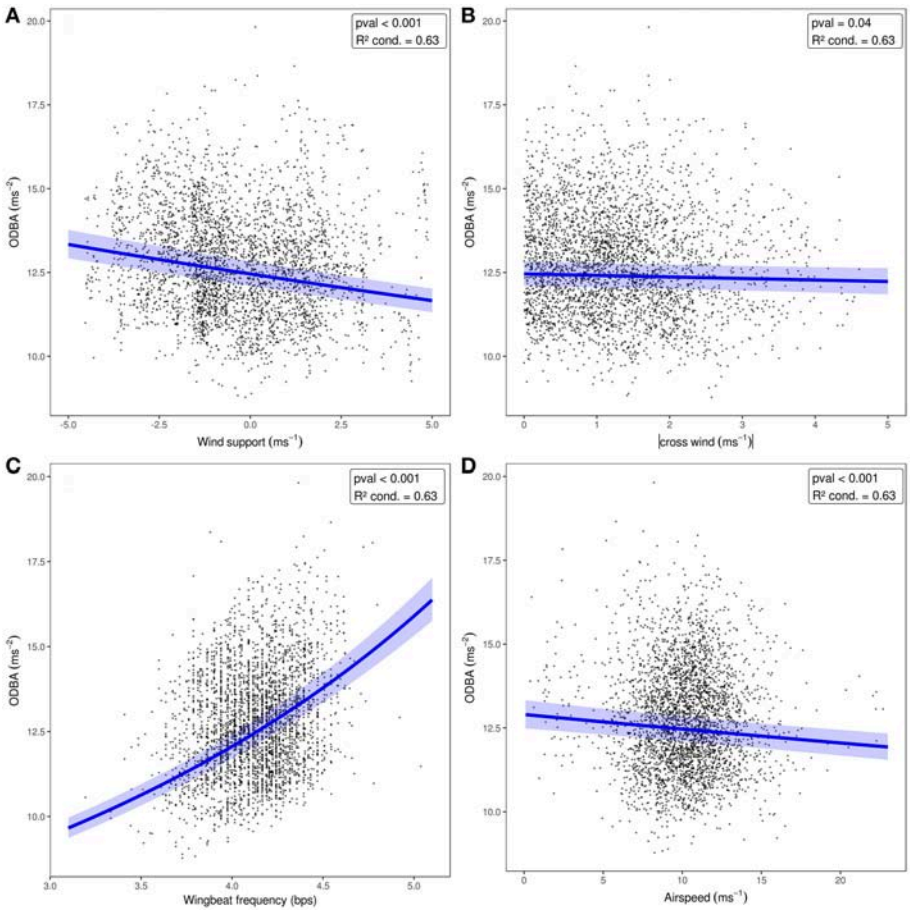

FIGURE 3 | ODBA relative to wind support **(A)**, crosswind **(B)**, wingbeat frequency **(C)**, and airspeed **(D)** included together in one model. The blue lines show predicted ODBA for each fixed effect where wingbeat frequency and airspeed were set to their means [4.2, 10.2, respectively for **A,B**], and the effect of wind support and crosswind were set to 0 **(C,D)**. The 95% confidence interval for each model, including random effects, is shown as the shaded area around the line.

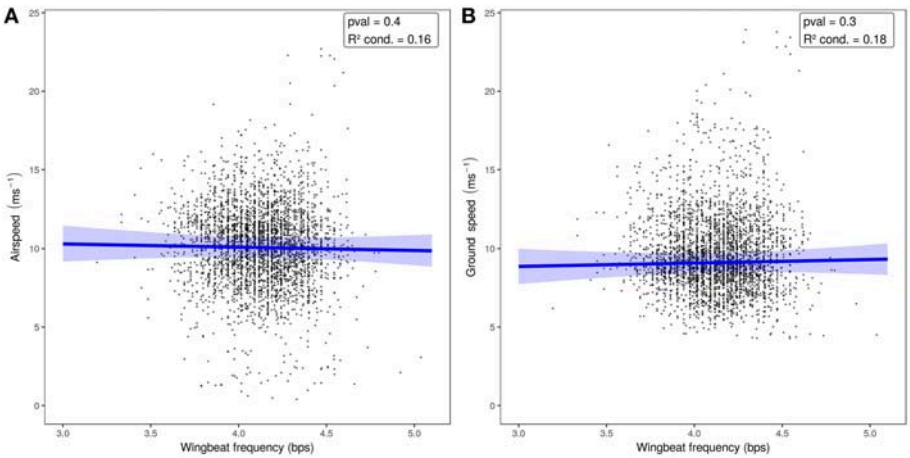

FIGURE 4 | Airspeed **(A)** and ground speed **(B)** relative to wingbeat frequency. The predictive models and 95%CI (in blue) show no relationship between wingbeat frequency and either measure of speed.

when placed close to the center of mass (Halsey et al., 2011; Spivey and Bishop, 2013) to avoid the increased acceleration experienced as one moves away from this point. The center of mass of a bat, however, changes across a wingbeat cycle (Iriarte-Diaz et al., 2011). The tag placement on the collar, when on the back of the neck, would have been cranial (ahead) to the center of mass on the bats upstroke and directly dorsal (above) to the center of mass on the downstroke (Iriarte-Diaz et al., 2011). As bats fly faster, the largest differences in acceleration are found in surge (or Y in this study, **Figure 1**), while the vertical acceleration of the center of mass largely tracks speed (Iriarte-Diaz et al., 2011). Furthermore, as bat wings are both relatively more massive and have that mass distributed more distally than birds (Thollesson and Norberg, 1991), even accelerometers mounted directly above the center of mass may not fully capture aspects of wingbeat kinematics such as amplitude. Wingbeat frequencies and relative measures such as ODBA should still reflect the animal's movement, but changes in the distribution of lift and thrust may not be tractable with a single three-dimensional accelerometer. Calibration of accelerometers on bats flying at known speeds in a wind tunnel would delineate these relationships.

It is also possible that instead of an instantaneous measure of power output, ODBA may reflect the costs of movement across longer periods of time (Elliott et al., 2013; Halsey and Goldbogen, 2017). Calibrations of ODBA against metabolic rate are typically conducted with walking or running animals, and generally show positive relationships (Halsey et al., 2011). This includes birds, for which there is currently no direct calibration between in-flight DBA and metabolic rate, though heart rate and DBA generally show positive relationships (Duriez et al., 2014; Bishop et al., 2015; Hicks et al., 2017), and DBA measures are positively correlated with First-Principals estimates for climbing power in Harris's hawks (Van Walsum et al., 2019). Despite this, the sum of DBA does explain a substantial (>70%) amount of daily energetic expenditure in many flying birds (Gleiss et al., 2011; Elliott et al., 2013; Duriez et al., 2014; Bishop et al., 2015; Elliott, 2016; Stothart et al., 2016; Hicks et al., 2017). As an integrative measure, DBA can explain 81% of DEE (Elliott et al., 2013); however, models using only the time away from the nest, without acceleration, also explain 72% of DEE (Elliott et al., 2013; Stothart et al., 2016), which is within the 18% range of error for doubly-labeled water studies (Speakman, 1997; Butler et al., 2004). Direct calibration of accelerometry with both energetic measures and kinematics across a range of known speeds will clarify how current bio-logging techniques capture the energetics of bat flight.

We found no relationship between wingbeat frequency and airspeed, and ODBA decreased slightly with faster airspeeds. To fly faster in wind tunnels bats generally do not change wingbeat frequency, but rely on amplitude and kinematic adjustments (Hedenstrom et al., 2007; Hubel et al., 2010, 2012, 2016; Riskin et al., 2010, 2012; Iriarte-Diaz et al., 2011, 2012; Hedenstrom and Johansson, 2015; Hedenström and Lindström, 2017). *Eidolon helvum* in a wind tunnel fly with wingbeat frequencies of 4.5–5.7 bps (Carpenter, 1986), and video of free-flying *E. helvum* emerging from their roosts showed bats flew at 4.4 ± 0.43 bps (Lindhe Norberg and Norberg, 2012). Both of these short estimates are higher than our mean observations (4.07 ± 0.28 bps, maximum: 5.96), but still are within the range of frequencies measured. The free-flying bats we sampled traveled with airspeeds substantially higher than the speeds at which many bats will willingly fly in wind tunnel studies (von Busse et al., 2013), and flew with lower wingbeat frequencies that appear to be consistent. This may be facilitated by the large variation in *E. helvum* wing camber and Strouhal number (ratio of stroke frequency and amplitude by speed) when compared to other pteropodid bats (Riskin et al., 2010). The many joints and anisotropic, compliant wing membrane of bat wings (Swartz et al., 1996; Cheney et al., 2015; Czenze et al., 2017) allow fine kinematic control by *E. helvum*, which could mean that their true speed-power curve is very flat (Tobalske et al., 2003b), and there is a broad range of airspeeds over which they fly at the same efficiency. *Eidolon helvum* appear to choose a wingbeat frequency and then rely on the strength of their wingbeats and kinematic adjustments to the shape and attack angle of their wingbeats (Riskin et al., 2010; Iriarte-Diaz et al., 2011, 2012) to modify their flight in response to changing wind conditions.

In general, the combination of GPS and accelerometry gives unparalleled access to the flight behavior of free-ranging individuals over extended time and space, especially when combined when high-resolution wind models. However, the relationships derived from birds may not directly translate to bats without additional calibration. Future work that delineates the relationship between on-board accelerometry and DBA measures with metabolic and mechanical power and flight kinematics across a range of airspeeds will help clarify what we may infer from data derived from bio-logging techniques. This will yield greater insight into the energy landscapes that animals face and the decisions they take in relationship to their environments in the wild.

ETHICS STATEMENT

All work was in accordance to local customs and the guidelines of the American Society of Mammalogists for the use of wild animals in research (Sikes and Gannon, 2011) and was carried out under approval from local authorities. Work in Ghana was approved by the Wildlife Division of the Forestry Commission (FCWD/GH-01 24/08/09, 02/02/11), and by Colonel Samuel Bel-Nono, Director of the Veterinary Services, Ghana Armed Forces Medical Directorate. Work in Zambia was approved by the Zambia Wildlife Authority (ZAWA 421902, 29/11/13, ZAWA 547649, 26/11/14). Work in Burkina Faso was conducted under approval from Mr. Moustapha Sarr, Director of the Parc Urbain Bangr-Weoogo, Ouagadougou.

AUTHOR CONTRIBUTIONS

MTO, AS, DD, MW, JF, and KS designed the study. DD, MW, JF, and MA-L collected the data. AS, KS, and MTO analyzed the data. MTO, AS, and KS wrote the manuscript. All authors commented on and approved the manuscript.

FUNDING

This study was supported by the Max Planck Institute for Ornithology, the Max Planck Society, and field work in Zambia 2014 was supported through funds obtained by the Institute of Novel and Emerging Infectious Diseases (Prof. Dr. Martin H. Groschup, Friedrich-Loeffler-Institute, Greifswald, Germany) from the Federal Foreign Office of Germany (ref # ZMVI6-FKZ2513AA0374).

ACKNOWLEDGMENTS

We thank Richard Suu-Ire for help with logistics and permits in Ghana, Lackson Chama for help with permits in Zambia, and Sebastian Stockmaier, Roland Kays, Natalie Weber and Frank Willems for help in the field in Zambia. We would also like to thank Sarah Davidson and the Movebank team for their help with data curation. We also thank Sharon Swartz for comments on a previous draft of this manuscript that greatly improved this work, as well as comments from the reviewers (AB and JS-B) and the editor, Frants Jensen.

SUPPLEMENTARY MATERIAL

The Supplementary Material for this article can be found online at: https://www.frontiersin.org/articles/10.3389/fevo.2019.00200/full#supplementary-material

REFERENCES

Abedi-Lartey, M., Dechmann, D. K. N., Wikelski, M., Scharf, A. K., and Fahr, J. (2016). Long-distance seed dispersal by straw-coloured fruit bats varies by season and landscape. *Glob. Ecol. Conserv.* 7, 12–24. doi: 10.1016/j.gecco.2016.03.005

Altshuler, D. L., Bahlman, J. W., Dakin, R., Gaede, A. H., Goller, B., Lentink, D., et al. (2015). The biophysics of bird flight: functional relationships integrate aerodynamics, morphology, kinematics, muscles, and sensors. *Can. J. Zool.* 93, 961–975. doi: 10.1139/cjz-2015-0103

Amelineau, F., Peron, C., Lescroel, A., Authier, M., Provost, P., and Gremillet, D. (2014). Windscape and tortuosity shape the flight costs of northern gannets. *J. Exp. Biol.* 217 (Pt 6), 876–885. doi: 10.1242/jeb.097915

Biewener, A. A. (2006). Patterns of mechanical energy change in tetrapod gait: pendula, springs and work. *J. Exp. Zool. A Comp. Exp. Biol.* 305, 899–911. doi: 10.1002/jez.a.334

Bishop, C. M., Spivey, R. J., Hawkes, L. A., Batbayar, N., Chua, B., Frappell, P. B., et al. (2015). The roller coaster flight strategy of bar-headed geese conserves energy during Himalayan migrations. *Science* 347, 250–254. doi: 10.1126/science.1258732

Bullen, R. D., and McKenzie, N. L. (2002). Scaling bat wingbeat frequency and amplitude. *J. Exp. Biol.* 205, 2615–2626.

Butler, P. J., Green, J. A., Boyd, I., and Speakman, J. (2004). Measuring metabolic rate in the field: the pros and cons of the doubly labelled water and heart rate methods. *Funct. Ecol.* 18, 168–183. doi: 10.1111/j.0269-8463.2004.00821.x

Carpenter, R. E. (1986). Flight physiology of intermediate-sized fruit bats (Pteropodidae). *J. Exp. Biol.* 120, 79–103.

Chapman, J. W., Klaassen, R. H., Drake, V. A., Fossette, S., Hays, G. C., Metcalfe, J. D., et al. (2011). Animal orientation strategies for movement in flows. *Curr. Biol.* 21, R861–870. doi: 10.1016/j.cub.2011.08.014

Cheney, J. A., Konow, N., Bearnot, A., and Swartz, S. M. (2015). A wrinkle in flight: the role of elastin fibres in the mechanical behaviour of bat wing membranes. *J. R. Soc. Interface* 12:20141286. doi: 10.1098/rsif.2014.1286

Czenze, Z. J., Brigham, R. M., Hickey, A. J. R., and Parsons, S. (2017). Stressful summers? Torpor expression differs between high- and low-latitude populations of bats. *J. Mammal.* 98, 1249–1255. doi: 10.1093/jmammal/gyx071

Dee, D. P., Uppala, S. M., Simmons, A. J., Berrisford, P., Poli, P., Kobayashi, S., et al. (2011). The ERA-Interim reanalysis: configuration and performance of the data assimilation system. *Q. J. R. Meteorol. Soc.* 137, 553–597. doi: 10.1002/qj.828

Dial, K. P., Biewener, A. A., Tobalske, B. W., and Warrick, D. R. (1997). Mechanical power output of bird flight. *Nature* 390, 67–70. doi: 10.1038/36330

Dodge, S., Bohrer, G., Weinzierl, R., Davidson, S. C., Kays, R., Douglas, D., et al. (2013). The environmental-data automated track annotation (Env-DATA) system: linking animal tracks with environmental data. *Mov. Ecol.* 1:3. doi: 10.1186/2051-3933-1-3

Duriez, O., Kato, A., Tromp, C., Dell'Omo, G., Vyssotski, A. L., Sarrazin, F., et al. (2014). How cheap is soaring flight in raptors? A preliminary investigation in freely-flying vultures. *PLoS ONE* 9:e84887. doi: 10.1371/journal.pone.0084887

Elliott, K. H. (2016). Measurement of flying and diving metabolic rate in wild animals: review and recommendations. *Comp. Biochem. Physiol. A Mol. Integr. Physiol.* 202, 63–77. doi: 10.1016/j.cbpa.2016.05.025

Elliott, K. H., Chivers, L. S., Bessey, L., Gaston, A. J., Hatch, S. A., Kato, A., et al. (2014). Windscapes shape seabird instantaneous energy costs but adult behavior buffers impact on offspring. *Mov. Ecol.* 2:17. doi: 10.1186/s40462-014-0017-2

Elliott, K. H., Le Vaillant, M., Kato, A., Speakman, J. R., and Ropert-Coudert, Y. (2013). Accelerometry predicts daily energy expenditure in a bird with high activity levels. *Bio. Lett.* 9:20120919. doi: 10.1098/rsbl.2012.0919

Fahr, J., Abedi-Lartey, M., Esch, T., Machwitz, M., Suu-Ire, R., Wikelski, M., et al. (2015). Pronounced seasonal changes in the movement ecology of a highly gregarious central-place forager, the African straw-coloured fruit bat (*Eidolon helvum*). *PLoS ONE* 10:e0138985. doi: 10.1371/journal.pone.0138985

Flack, A., Fiedler, W., Blas, J., Pokrovsky, I., Kaatz, M., Mitropolsky, M., et al. (2016). Costs of migratory decisions: a comparison across eight white stork populations. *Sci. Adv.* 2:e1500931. doi: 10.1126/sciadv.1500931

Gleiss, A. C., Wilson, R. P., and Shepard, E. L. C. (2011). Making overall dynamic body acceleration work: on the theory of acceleration as a proxy for energy expenditure. *Methods Ecol. Evol.* 2, 23–33. doi: 10.1111/j.2041-210X.2010.00057.x

Green, J. A., Halsey, L. G., Wilson, R. P., and Frappell, P. B. (2009). Estimating energy expenditure of animals using the accelerometry technique: activity, inactivity and comparison with the heart-rate technique. *J. Exp. Biol.* 212 (Pt 4), 471–482. doi: 10.1242/jeb.026377

Halsey, L. G., and Goldbogen, J. (2017). Relationships grow with time: a note of caution about energy expenditure-proxy correlations, focussing on accelerometry as an example. *Funct. Ecol.* 31, 1176–1183. doi: 10.1111/1365-2435.12822

Halsey, L. G., Shepard, E. L., and Wilson, R. P. (2011). Assessing the development and application of the accelerometry technique for estimating energy expenditure. *Comp. Biochem. Physiol. A Mol. Integr. Physiol.* 158, 305–314. doi: 10.1016/j.cbpa.2010.09.002

Harris, S., Cresswell, W. J., Forde, P. G., Trewhella, W. J., Woollard, T., and Wray, S. (1990). Home-range analysis using radio-tracking data—a review of problems and techniques particularly as applied to the study of mammals. *Mamm. Rev.* 20, 97–123.

Hedenström, A. (2003). "Twenty-Three Testable Predictions About Bird Flight," in *Avian Migration*, eds P. Berthold, E. Gwinner, and E. Sonnenschein (Berlin: Springer), 563–582.

Hedenström, A., and Åkesson, S. (2017). Adaptive airspeed adjustment and compensation for wind drift in the common swift: differences between day and night. *Anim. Behav.* 127, 117–123. doi: 10.1016/j.anbehav.2017.03.010

Hedenström, A., Alerstam, T., Green, M., and Gudmundsson, G. (2002). Adaptive variation of airspeed in relation to wind, altitude and climb rate by migrating birds in the Arctic. *Behav. Ecol. Sociobiol.* 52, 308–317. doi: 10.1007/s00265-002-0504-0

Hedenstrom, A., and Johansson, L. C. (2015). Bat flight: aerodynamics, kinematics and flight morphology. *J. Exp. Biol.* 218 (Pt 5), 653–663. doi: 10.1242/jeb.031203

Hedenstrom, A., Johansson, L. C., Wolf, M., von Busse, R., Winter, Y., and Spedding, G. R. (2007). Bat flight generates complex aerodynamic tracks. *Science* 316, 894–897. doi: 10.1126/science.1142281

Hedenström, A., and Lindström, Å. (2017). Wind tunnel as a tool in bird migration research. *J. Avian Biol.* 48, 37–48. doi: 10.1111/jav.01363

Hernandez-Pliego, J., Rodriguez, C., Dell'Omo, G., and Bustamante, J. (2017). Combined use of tri-axial accelerometers and GPS reveals the flexible foraging strategy of a bird in relation to weather conditions. *PLoS ONE* 12:e0177892. doi: 10.1371/journal.pone.0177892

Hicks, O., Burthe, S., Daunt, F., Butler, A., Bishop, C., and Green, J. A. (2017). Validating accelerometry estimates of energy expenditure across behaviours using heart rate data in a free-living seabird. *J. Exp. Biol.* 220 (Pt 10), 1875–1881. doi: 10.1242/jeb.152710

Hubel, T. Y., Hristov, N. I., Swartz, S. M., and Breuer, K. S. (2012). Changes in kinematics and aerodynamics over a range of speeds in *Tadarida brasiliensis*, the Brazilian free-tailed bat. *J. R. Soc. Interface* 9, 1120–1130. doi: 10.1098/rsif.2011.0838

Hubel, T. Y., Hristov, N. I., Swartz, S. M., and Breuer, K. S. (2016). Wake structure and kinematics in two insectivorous bats. *Philos. Trans. R. Soc. B* 371:20150385. doi: 10.1098/rstb.2015.0385

Hubel, T. Y., Riskin, D. K., Swartz, S. M., and Breuer, K. S. (2010). Wake structure and wing kinematics: the flight of the lesser dog-faced fruit bat, *Cynopterus brachyotis*. *J. Exp. Biol.* 213 (Pt 20), 3427–3440. doi: 10.1242/jeb.043257

Iriarte-Diaz, J., Riskin, D. K., Breuer, K. S., and Swartz, S. M. (2012). Kinematic plasticity during flight in fruit bats: individual variability in response to loading. *PLoS ONE* 7:e36665. doi: 10.1371/journal.pone.0036665

Iriarte-Diaz, J., Riskin, D. K., Willis, D. J., Breuer, K. S., and Swartz, S. M. (2011). Whole-body kinematics of a fruit bat reveal the influence of wing inertia on body accelerations. *J. Exp. Biol.* 214 (Pt 9), 1546–1553. doi: 10.1242/jeb.037804

Karasov, W. H. (1992). Daily energy expenditure and the cost of activity in mammals. *Am. Zool.* 32, 238–248. doi: 10.1093/icb/32.2.238

Kogure, Y., Sato, K., Watanuki, Y., Wanless, S., and Daunt, F. (2016). European shags optimize their flight behavior according to wind conditions. *J. Exp. Biol.* 219 (Pt 3), 311–318. doi: 10.1242/jeb.131441

Leos-Barajas, V., Photopoulou, T., Langrock, R., Patterson, T. A., Watanabe, Y. Y., Murgatroyd, M., et al. (2017). Analysis of animal accelerometer data using hidden Markov models. *Methods Ecol. Evol.* 8, 161–173. doi: 10.1111/2041-210x.12657

Lindhe Norberg, U. M., and Norberg, R. A. (2012). Scaling of wingbeat frequency with body mass in bats and limits to maximum bat size. *J. Exp. Biol.* 215 (Pt 5), 711–722. doi: 10.1242/jeb.059865

McCracken, G. F., Safi, K., Kunz, T. H., Dechmann, D. K. N., Swartz, S. M., and Wikelski, M. (2016). Airplane tracking documents the fastest flight speeds recorded for bats. *R. Soc. Open Sci.* 3:160398. doi: 10.1098/rsos.160398

Nathan, R., Spiegel, O., Fortmann-Roe, S., Harel, R., Wikelski, M., and Getz, W. M. (2012). Using tri-axial acceleration data to identify behavioral modes of free-ranging animals: general concepts and tools illustrated for griffon vultures. *J. Exp. Biol.* 215, 986–996. doi: 10.1242/jeb.058602

Norberg, U. M. (1990). *Vertebrate Flight: Mechanics, Physiology, Morphology, Ecology and Evolution*. Berlin: Springer-Verlag.

O'Mara, M. T., Wikelski, M., and Dechmann, D. K. N. (2014). 50 years of bat tracking: device attachment and future directions. *Methods Ecol. Evol.* 5, 311–319. doi: 10.1111/2041-210x.12172

O'Mara, M. T., Wikelski, M., Kranstauber, B., and Dechmann, D. K. N. (2019). Common noctules exploit low levels of the aerosphere. *R. Soc. Open Sci.* 6:181942. doi: 10.1098/rsos.181942

Pennycuick, C. J. (1978). Fifteen testable predictions about bird flight. *Oikos* 30, 165–176. doi: 10.2307/3543476

Pennycuick, C. J. (2008). *Modelling the Flying Bird*. London: Academic Press.

Pinheiro, J., Bates, D., DebRoy, S., Sarkar, D., and Team, R. C. (2018). *nlme: Linear and Nonlinear Mixed Effects Models*. Available online at: https://CRAN.R-project.org/package=nlme

R Core Team (2016). *R: A Language and Environment for Statistical Computing*. Vienna: R Foundation for Statistical Computing.

Rayner, J. M. (1999). Estimating power curves of flying vertebrates. *J. Exp. Biol.* 202 (Pt 23), 3449–3461.

Riskin, D. K., Bergou, A., Breuer, K. S., and Swartz, S. M. (2012). Upstroke wing flexion and the inertial cost of bat flight. *Proc. R. Soc. B* 279, 2945–2950. doi: 10.1098/rspb.2012.0346

Riskin, D. K., Iriarte-Diaz, J., Middleton, K. M., Breuer, K. S., and Swartz, S. M. (2010). The effect of body size on the wing movements of pteropodid bats, with insights into thrust and lift production. *J. Exp. Biol.* 213 (Pt 23), 4110–4122. doi: 10.1242/jeb.043091

Riskin, D. K., Willis, D. J., Iriarte-Diaz, J., Hedrick, T. L., Kostandov, M., Chen, J., et al. (2008). Quantifying the complexity of bat wing kinematics. *J. Theoret. Biol.* 254, 604–615. doi: 10.1016/j.jtbi.2008.06.011

Safi, K., Kranstauber, B., Weinzierl, R., Griffin, L., Rees, E. C., Cabot, D., et al. (2013). Flying with the wind: scale dependency of speed and direction measurements in modelling wind support in avian flight. *Mov. Ecol.* 1:4. doi: 10.1186/2051-3933-1-4

Sapir, N., Horvitz, N., Dechmann, D., Fahr, J., and Wikelski, M. (2014). Commuting fruit bats beneficially modulate their flight in relation to wind. *Proc. R. Soc. B* 281:20140018. doi: 10.1098/rspb.2014.0018

Sato, K., Daunt, F., Watanuki, Y., Takahashi, A., and Wanless, S. (2008). A new method to quantify prey acquisition in diving seabirds using wing stroke frequency. *J. Exp. Biol.* 211 (Pt 1), 58–65. doi: 10.1242/jeb.009811

Scacco, M., Flack, A., Duriez, O., Wikelski, M., and Safi, K. (2019). Static landscape features predict uplift locations for soaring birds across Europe. *R. Soc. Open Sci.* 6:181440. doi: 10.1098/rsos.181440

Scharf, A. K., Fahr, J., Abedi-Lartey, M., Safi, K., Dechmann, D. K. N., Wikelski, M., et al. (2019). Data from: overall dynamic body acceleration in straw-colored fruit bats increases in headwinds but not with airspeed. *Movebank Data Reposit.* doi: 10.5441/001/1.k8n02jn8

Sikes, R. S., and Gannon, W. L. (2011). Guidelines of the American Society of Mammalogists for the use of wild mammals in research. *J. Mammal.* 92, 235–253. doi: 10.1644/10-mamm-f-355.1

Speakman, J. R. (1997). *Doubly Labelled Water: Theory and Practice*. London: Chapman & Hall.

Spivey, R. J., and Bishop, C. M. (2013). Interpretation of body-mounted accelerometry in flying animals and estimation of biomechanical power. *J. R. Soc. Interface* 10:20130404. doi: 10.1098/rsif.2013.0404

Stothart, M. R., Elliott, K. H., Wood, T., Hatch, S. A., and Speakman, J. R. (2016). Counting calories in cormorants: dynamic body acceleration predicts daily energy expenditure measured in pelagic cormorants. *J. Exp. Biol.* 219 (Pt 14), 2192–2200. doi: 10.1242/jeb.130526

Swartz, S. M., Groves, M. S., Kim, H. D., and Walsh, W. R. (1996). Mechanical properties of bat wing membrane skin. *J. Zool.* 239, 357–378.

Swartz, S. M., Iriarte-Diaz, J., Riskin, D. K., and Breuer, K. S. (2012). "A bird? A plane? No, it's a bat: an introduction to the biomechanics of bat flight," in *Evolutionary History of Bats: Fossils, Molecules and Morphology*, eds G. F. Gunnell and N. B. Simmons (Cambridge: Cambridge University Press), 317–352.

Taylor, G. K., Nudds, R. L., and Thomas, A. L. (2003). Flying and swimming animals cruise at a Strouhal number tuned for high power efficiency. *Nature* 425, 707–711. doi: 10.1038/nature02000

Thollesson, M., and Norberg, U. M. (1991). Moments of intertia of bat wings and body. *J. Exp. Biol.* 158, 19–35.

Tobalske, B. W. (2007). Biomechanics of bird flight. *J. Exp. Biol.* 210, 3135–3146. doi: 10.1242/jeb.000273

Tobalske, B. W., Hedrick, T. L., and Biewener, A. A. (2003a). Wing kinematics of avian flight across speeds. *J. Avian Biol.* 34, 177–184. doi: 10.1034/j.1600-048X.2003.03006.x

Tobalske, B. W., Hedrick, T. L., Dial, K. P., and Biewener, A. A. (2003b). Comparative power curves in bird flight. *Nature* 421, 363–366. doi: 10.1038/nature01284

Usherwood, J. R., Stavrou, M., Lowe, J. C., Roskilly, K., and Wilson, A. M. (2011). Flying in a flock comes at a cost in pigeons. *Nature* 474, 494–497. doi: 10.1038/nature10164

Van Doren, B. M., Horton, K. G., Stepanian, P. M., Mizrahi, D. S., and Farnsworth, A. (2016). Wind drift explains the reoriented morning flights of songbirds. *Behav. Ecol.* 27, 1122–1131. doi: 10.1093/beheco/arw021

van Toor, M. L., O'Mara, M. T., Abedi-Lartey, M., Wikelski, M., Fahr, J., and Dechmann, D. K. N. (2019). Linking colony size with quantitative estimates

of ecosystem services of African fruit bats. *Curr. Biol.* 29, R237–R238. doi: 10.1016/j.cub.2019.02.033

Van Walsum, T. A., Perna, A., Bishop, C. M., Murn, C. P., Collins, P. M., Wilson, R. P., et al. (2019). Exploring the relationship between flapping behaviour and accelerometer signal during ascending flight, and a new approach to calibration. *Ibis*. doi: 10.1111/ibi.12710

Venables, W. N., and Ripley, B. D. (2002). *Modern Applied Statistics with S*. (New York, NY:Springer-Verlag), 498. doi: 10.1007/978-0-387-21706-2

von Busse, R., Swartz, S. M., and Voigt, C. C. (2013). Flight metabolism in relation to speed in Chiroptera: testing the U-shape paradigm in the short-tailed fruit bat *Carollia perspicillata*. *J. Exp. Biol.* 216 (Pt 11), 2073–2080. doi: 10.1242/jeb.081760

Williams, H. J., Shepard, E. L. C., Duriez, O., and Lambertucci, S. A. (2015). Can accelerometry be used to distinguish between flight types in soaring birds? *Anim. Biotelem.* 3:45. doi: 10.1186/s40317-015-0077-0

Wilson, R. P., White, C. R., Quintana, F., Halsey, L. G., Liebsch, N., Martin, G. R., et al. (2006). Moving towards acceleration for estimates of activity-specific metabolic rate in free-living animals: the case of the cormorant. *J. Anim. Ecol.* 75, 1081–1090. doi: 10.1111/j.1365-2656.2006.01127.x

Conflict of Interest Statement: The authors declare that the research was conducted in the absence of any commercial or financial relationships that could be construed as a potential conflict of interest.

Copyright © 2019 O'Mara, Scharf, Fahr, Abedi-Lartey, Wikelski, Dechmann and Safi. This is an open-access article distributed under the terms of the Creative Commons Attribution License (CC BY). The use, distribution or reproduction in other forums is permitted, provided the original author(s) and the copyright owner(s) are credited and that the original publication in this journal is cited, in accordance with accepted academic practice. No use, distribution or reproduction is permitted which does not comply with these terms.

frontiers in Ecology and Evolution

METHODS
published: 09 July 2019
doi: 10.3389/fevo.2019.00257

An Arduino-Based RFID Platform for Animal Research

Eli S. Bridge[1], Jay Wilhelm[2], Meelyn M. Pandit[3], Alexander Moreno[4], Claire M. Curry[5], Tyler D. Pearson[5], Darren S. Proppe[6], Charles Holwerda[7], John M. Eadie[8], Tez F. Stair[8], Ami C. Olson[8,9], Bruce E. Lyon[10], Carrie L. Branch[11†], Angela M. Pitera[11], Dovid Kozlovsky[11†], Benjamin R. Sonnenberg[11], Vladimir V. Pravosudov[11] and Jessica E. Ruyle[4]*

[1] Oklahoma Biological Survey, University of Oklahoma, Norman, OK, United States, [2] Department of Mechanical Engineering, Ohio University, Athens, OH, United States, [3] Department of Biology, University of Oklahoma, Norman, OK, United States, [4] School of Electrical and Computer Engineering, University of Oklahoma, Norman, OK, United States, [5] University of Oklahoma Libraries, University of Oklahoma, Norman, OK, United States, [6] Department of Biology, Calvin College, Grand Rapids, MI, United States, [7] Department of Engineering, Calvin College, Grand Rapids, MI, United States, [8] Department of Wildlife, Fish, and Conservation Biology, University of California, Davis, Davis, CA, United States, [9] California Department of Fish and Wildlife, Sacramento, CA, United States, [10] Department of Ecology and Evolutionary Biology, University of California, Santa Cruz, Santa Cruz, CA, United States, [11] Department of Biology, University of Nevada, Reno, NV, United States

OPEN ACCESS

Edited by:
Frants Havmand Jensen,
Woods Hole Oceanographic Institution, United States

Reviewed by:
Friederike Hillemann,
University of Oxford, United Kingdom
Arne Iserbyt,
University of Antwerp, Belgium
Kenneth C. Welch,
University of Toronto Scarborough, Canada

***Correspondence:**
Eli S. Bridge
ebridge@ou.edu

†Present Address:
Carrie L. Branch,
Cornell Lab of Ornithology, Cornell University, Ithaca, NY, United States
Dovid Kozlovsky,
Department of Biology, University of Ottawa, Ottawa, ON, Canada

Specialty section:
This article was submitted to Behavioral and Evolutionary Ecology, a section of the journal Frontiers in Ecology and Evolution

Received: 08 March 2019
Accepted: 18 June 2019
Published: 09 July 2019

Citation:
Bridge ES, Wilhelm J, Pandit MM, Moreno A, Curry CM, Pearson TD, Proppe DS, Holwerda C, Eadie JM, Stair TF, Olson AC, Lyon BE, Branch CL, Pitera AM, Kozlovsky D, Sonnenberg BR, Pravosudov VV and Ruyle JE (2019) An Arduino-Based RFID Platform for Animal Research. Front. Ecol. Evol. 7:257. doi: 10.3389/fevo.2019.00257

Radio Frequency Identification (RFID) technology has been broadly applied in the biological sciences to yield new insights into behavior, cognition, population biology, and distributions. RFID systems entail wireless communication between small tags that, when stimulated by an appropriate radio frequency transmission, emit a weak, short-range wireless signal that conveys a unique ID number. These tags, which often operate without a battery, can be attached to animals such that their presence at a particular location can be detected by an RFID reader. This paper describes an RFID data-logging system that can serve as the core for a wide variety of field and laboratory applications for monitoring the activities of individual animals. The core electronics are modeled on an Arduino circuit board, which is a hobbyist electronics system. Users can customize the hardware and software to accommodate their needs. We demonstrate the utility of the system with cursory descriptions of three real-world research applications. The first is a large-scale deployment that was used to examine individual breeding behaviors across four local populations of Wood Ducks. The second application employed an array of RFID-enabled bird feeders that allowed for tests of spatial cognition. Third, we describe a nest-box monitoring system that both records visits from breeding birds and administers experimental treatments, such as increasing temperature or playing audio recordings, in accordance to the presence/absence of individual birds. With these examples we do not attempt to relate details with regard to research findings; rather our intent is to demonstrate some of the possibilities enabled by our low-cost RFID system. Detailed descriptions, design files, and code are made available by means of the Open Science Framework.

Keywords: biologging, feeder, nestbox, behavior, cognition, data logging, PIT tag, bioinformatics

INTRODUCTION

The term "biologging" typically evokes a research endeavor that involves tracking the locations of animals as they move throughout a home range or embark on a migration. However, biologging can also be employed to reveal intimate details about the behavioral patterns of individual animals. Radio Frequency Identification (RFID) technology has emerged as a useful biologging tool for monitoring animal activities at specific locations, such as feeding stations, nests, and burrows (Bonter and Bridge, 2011; Dogan et al., 2016; Bandivadekar et al., 2018; Iserbyt et al., 2018). RFID is a form of short-distance communication between a reading unit and one or more transponder tags (often called Passive Integrated Transponders or PIT tags). PIT tags use energy emitted by the reader unit to emit a weak signal (either with radio waves or magnetic coupling) that contains a unique identification code. PIT tags typically do not need a battery, which allows them to function forever (in theory), and they can be sized down for use on some very small species, including insects (Sumner et al., 2007; Russell et al., 2017; Barlow et al., 2019).

RFID typically entails only short-range communication, with tag-reading ranges from over 50 cm in high power systems to a few millimeters. Hence, a fundamental limitation to the system is that tags and readers must come close to an antenna for tag reading to occur. RFID is widely used as a marking method wherein tagged animals are captured and scanned manually in a manner similar to the "microchips" used in veterinary care of pets and livestock (Thorstad et al., 2013; Anu and Canessane, 2017). However, RFID can also be effectively employed in automated, remote sensing systems, with stationary readers that record specific animal activities, such as accessing a food source or nest (e.g., Zuckerberg et al., 2009; Bonter and Bridge, 2011; Catarinucci et al., 2014b; Ibarra et al., 2015; Zenzal and Moore, 2016). More advanced systems have implemented cognitive tests in lab and field settings with experimental routines customized for individual animals (Croston et al., 2016; Morand-Ferron et al., 2016)

Although RFID systems are relatively inexpensive compared to other forms of biologging, cost can still be a barrier to the use of RFID in research, especially if large numbers of reading units are required. Another barrier is customization. Many commercial RFID systems are configured for door-entry security or applications in commerce and these systems are not likely to benefit researchers who wish to track animals. To address these issues, we have developed a low-cost, short-range RFID reader that is compatible with a popular amateur electronics platform called Arduino (Arduino LLC, Scarmagno, Italy). The device is essentially an Arduino circuit board with two RFID-reader circuits and basic data-logging infrastructure (i.e., a real time clock and memory) built into it. Like all Arduinos the microprocessor on the circuit board can be programed using the open-source Arduino programming language and the free Arduino IDE (Integrated Development Environment) software. The device is also compatible with a wide array of accessories, such as environmental sensors, motor controllers, LCD screens, and wireless communications modules, that have been designed to work with the Arduino platform.

This paper provides both a brief description of this RFID system and accounts of its implementation in three different research capacities. The first account describes a simple data logging system that was deployed on a very large scale. Second, we describe a more sophisticated system that has been used to evaluate memory and cognition in free living animals. Finally, we describe a nest box that can carry out experimental protocols based on individual birds entering and leaving. We hope that these examples inspire new uses for our RFID system. To help new users get started we have made all of our designs, and code open source, and they are freely available via the Open Science Framework (OSF) at https://osf.io/9j7ax/. This OSF project page contains files available for download as well as links to Github repositories where current firmware versions are maintained.

MATERIALS AND EQUIPMENT

In designing the RFID reader, we took an open-source design for the Arduino M0, and added two RFID circuits, a real time clock, an SD card socket, and a flash memory module for data backup (**Figure 1**). We also simplified the voltage regulation circuit and reassigned some of the inputs and outputs to accommodate the tag-reading, time-keeping, and memory functions. The RFID reader retained the high-performance Atmel SAMD microcontroller that is featured on the Arduino M0. The RFID reader can be programmed in the same manner as the Arduino M0, using the Arduino IDE; however, we had to provide a customized board definition for the IDE because of the changes made to some of the input/output pins. A board definition is a collection of code that allows for a seamless interface between a particular piece of hardware and the Arduino IDE. This board definition as well as all design files for the RFID reader are accessible via our OSF project page.

This RFID reader design follows a previous version described in Bridge and Bonter (2011). However, the new design has several key features that were not previously available. Foremost is the ability to implement custom programming using open source tools—the previous version was programmed using a proprietary language. In addition, dual RFID circuits, a superior microprocessor, increased memory capacity, more input/output pins, and the Arduino compatible hardware, set the new design apart from its predecessor.

The RFID reader has two RFID circuits or modules built in. Users can alternate between the two modules or use just one of them. Each RFID module requires an external antenna, which usually consists of a thin coil of magnet wire. In our system, a functional antenna coil generally has to be <15 cm in diameter, but beyond that antennas can vary greatly in size and shape. Users of our system can either make their own antennas or purchase them from third-party providers (e.g., Q-kits, Kingston, Ontario, store.qkits.com). Antennas can be hand wound, such that users can customize antenna size and shape to match their application. The reader is designed to work with antennas with an inductance of 1.25–1.3 mH. Hence, the process of making antennas requires

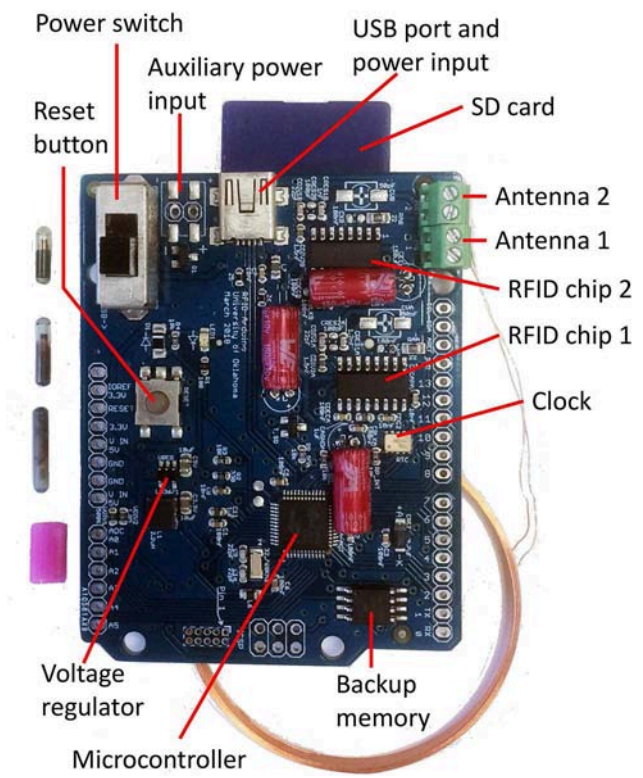

FIGURE 1 | The RFID reader circuit board with key components labeled. The dimensions of the board are those of a standard Arduino: 68.58 × 53.34 mm. Four PIT tags are shown to the left of the circuit board. The bottom tag is an RFID leg band.

inductance measurements with an LCR meter. We provide some guidelines for making antennas in our OSF project page, and users can follow our examples or use them as a starting point for their own designs. Either way, it will likely require some trial and error to find the correct number of turns for a given antenna size and shape. We plan to improve the process of antenna design with an online tool for simulating and testing RFID antennas, but this tool is still in development.

A typical deployment of an RFID reader involves polling for tags at regular intervals. In this context, "polling" means emitting a radio-frequency carrier wave at or around 125 kHz, while "listening" for a return signal from a tag. Emitting this carrier wave requires about 90 mA with a 5 V power supply, which is costly in terms of power requirements, so our firmware offers a power saving algorithm wherein a brief polling period of about 30 ms is used to determine if a tag is present. If no tag is detected, the reader can enter a "sleep" mode that uses about 100 μA for a specified period of time before polling again. If a tag is detected, then the reader will extend the duration of the polling effort to read the tag ID. The frequency and duration of reading attempts can be set by the user in a manner that balances power usage and the prospect of missing tags that enter the read range. In addition, the RFID reader can alternate polling efforts between its two RFID modules to attempt to detect tags with two different antennas.

An onboard SD-card socket is available for primary data storage. Data are typically stored in the form of a comma-delineated text file. Hence, the SD card can be removed from the circuit board and inserted into a computer or mobile device to transfer and examine data. There is also a flash memory unit (AT45DB321E) permanently attached to the circuit board, which can serve as back-up storage in case there is a problem with the SD card. This built-in memory unit has a capacity of 32 Mbits or 4,000,000 bytes, which is sufficient for recording over 200,000 data reads, assuming only a tag ID and timestamp are stored.

The circuit board can be produced in small quantities at a cost of about $30 (USD) per unit. The most expensive components are the microcontroller (~$4), the real-time clock (~$2), the SD card socket (~$2), backup memory (~$2), and the RFID front-end integrated circuit (EM4095; ~$2). Prices can vary considerably depending on electronics components markets, and quantities purchased. The $30 production cost includes $3 for the circuit board and $10 for assembly. Full details and sources for components and assembly are available on the OSF project page.

The reader is configured to operate at 5 V. This voltage makes them compatible with a wide variety of power supplies designed for charging or maintaining cellular telephones. The circuit board may also be powered via a USB connection or a USB AC/DC converter/charger. It is possible to use higher or lower voltages, but that requires an additional power adaptor to establish a 5 V power supply for the circuit board. Solar-powered systems have been employed for some field applications, negating the need for large batteries and frequent battery changes. The OSF project page provides several suggestions for power supplies and photovoltaic systems.

As described above, the RFID reader alternates between polling for tags and "sleeping" in low-power mode. Based on measures of power usage for these two modes it is possible to calculate how long a given battery will last. For example, If there is a 1-s sleep interval between polling attempts and there is a minimal 30 ms poll time, average power use would be 2.7 mA and a 10 amp-h battery would last over 3,600 h. However, if tags are polled 5 times per second with a 30 ms polling period, then the same 10 amp-h battery would last about 730 h. These are very simplistic calculations. Another factor to consider is the power requirement of tag reads. Also, it is possible to implement a prolonged sleep period (i.e., nighttime sleep mode) to conserve power when animals are not likely to be detected. A spreadsheet calculator is provided on our OSF project page. This spreadsheet provides estimates of battery life based on RFID-polling settings, expected numbers of tag reads, implementation of prolonged sleep periods, and battery parameters.

The reader is configured to work at a frequency of 125 kHz, and it is compatible with tags that adhere to the EM41XX protocol, which includes EM4100 and EM4112. Other commonly used RFID communication protocols include the ISO11784/5 and Trovan standards. These protocols differ with regard to data encoding, the size and structure of the identification number, and the associated error checking algorithms as well as the bit rate and (in some cases) the radio frequency. Communication via these other protocols is possible with the ETAG reader but would require, at minimum, different tag reading functions in

the firmware. It may also be necessary to implement hardware changes to be able to read other types of tags, especially if they work at frequencies other than 125 kHz. In addition, some forms of RFID involve active tags that often increase the read range by amplifying the transmitted signal. Thus far, our testing has only involved passive RFID tags (i.e., tags with no battery). Fortunately, compatible (EM41XX) tags are available in a wide variety of configurations including implantable glass ampoules and plastic leg bands. Tag are available through a variety of vendors. In particular, Cyntag (Cynthiana, Kentucky, USA) is a good source for glass ampoule tags, and Eccel technology LTD (Groby, Leicester, UK) is the primary supplier of small RFID leg bands. See our OSF website for more details and a list of compatible tags.

Because the RFID reader is based on the Arduino electronics format, a wide range of customization is possible both in terms of hardware and software. The reader is configured to mimic an Arduino M0. Hence it has 22 input/output pins that can serve as integration points for sensors, LCD arrays, lights, data interfaces, and motor controllers. The reader can be programmed using free, open-source Arduino IDE software. The Arduino programming language is a set of C/C++ functions, and the developers provide full documentation for programming with C in the Arduino IDE. There are also hundreds of libraries written for the Arduino IDE that provide accessibility to various hardware components (e.g., sensors, motor controllers, and LCD screens), with minimal programming requirements. The code we have developed for the RFID reader has custom routines associated with tag reading and power conservation, but it also makes use of existing Arduino libraries.

We have provided a core Arduino sketch (i.e., program) that runs the RFID reader as a simple data logger. This code can readily be configured to allow for a variety of different RFID polling strategies and sleep schedules. This code can also serve as a starting point for new sketches that incorporate new functionality. For example, some RFID tags can be programmed to store and later transmit data. Although we have not dealved into these methods, it should be possible to configure the RFID reader to program tags. This code as well as sketches for the projects described below are available through our OSF project webpage.

To demonstrate what is possible through the combination of low-cost and versatility made available by our RFID reader, we briefly describe three actual field applications that have broken new ground through the use of RFID-based biologging. These projects have employed a variety of different RFID hardware and software configurations and are not necessarily the same as the current system documented on the OSF project page. Nevertheless, the systems employed in these projects are very similar to the most current hardware version, and the current systems are equally capable of supporting these research applications. Note that it is not our intent for the descriptions below to serve as a final record of the ecological and behavioral research that was enabled by RFID technology. Rather we present these examples to illustrate a variety of scenarios where RFID is useful or even critical for addressing research questions.

METHODS

Implementation 1: Large-Scale Monitoring of Wood Duck Populations

Our first example of the utility of our RFID system is an effort to quantify brood parasitism and other breeding behaviors in Wood Ducks (*Aix sponsa*). Wood Ducks are facultative conspecific brood parasites, which means that females will sometimes lay eggs in the nest of another Wood Duck female (Bellrose et al., 1994). Researchers at the University of California (JME, TFS, ACO, BEL) deployed RFID data loggers on more than 200 Wood Duck nest boxes in the vicinity of Davis, California, with the aim of determining patterns of conspecific brood parasitism. Ultimately, this project sought to investigate life-history trade-offs and kin selection as explanations for the evolution of conspecific brood parasitism in a species with precocial offspring and a complex life history.

Each nest box in the study was equipped with a single-antenna RFID reader configured as a simple data logger. The antenna on each box encircled the entrance hole, such that a duck's tag ID would be recorded and stored each time it passed through the antenna upon entering and leaving (**Figure 2A**). The battery and circuit board were housed in a sealable plastic box affixed on the side of each nest box. This configuration allowed easy access for battery changes and data offloads. Each animal involved in the study had a pit tag implanted under the skin in the region of the back between the scapula. The research team tagged every female that used a nest box and all nestlings that hatched in the study area. Although the configuration of the RFID equipment was not remarkable, the scale of the effort was. The ongoing project has entailed monitoring hundreds of nests over the course of five field seasons, with as many as 197 systems active at once. Over three field seasons, this effort employed a total of 74 student volunteers engaged in changing batteries, offloading data, and troubleshooting. In the most recent field season, the research team designed and deployed a solar-charging system that would allow a reader to operate uninterrupted for an entire season (see **Figure 2A** and the OSF project page), greatly reducing personnel time and nest disturbance.

In total, the study followed 1,873 nest attempts by 454 breeding females (with 506 females registered at least once at a nest box). Some of these females were among the 4,128 ducklings that were tagged as part of the study. As a result of this intensive effort, up to 60% of breeding females had been tagged as ducklings in some populations, providing a unique opportunity to follow individuals of known origin, genotype, maternity, phenotype (size, physiological traits including hormones), and kinship to other females in the population throughout their entire lives. Because PIT loss rates were $<1\%$, and battery power was not a limitation, the tags provided information for as long as there were active RFID readers and tagged birds present. During the study (now extending into its sixth year), over 1 million RFID detections have been recorded at nest boxes.

The RFID network revealed complex patterns of nest use among females (Eadie et al., in preparation). The distribution of the number of nests in which females visited and laid eggs was

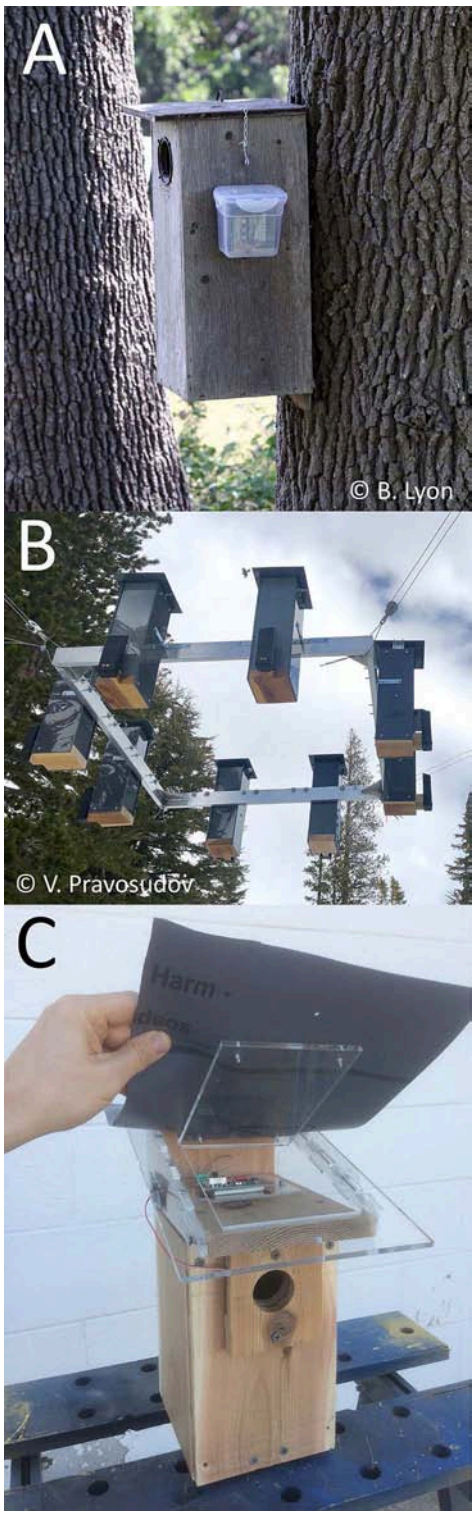

FIGURE 2 | (A) RFID-equipped Wood Duck nest box deployed near Davis California. RFID reader and battery are housed in a water-tight plastic box attached to the side of the box (painted in camouflage at other installations). The hand-wrapped and tuned antenna was coated in plasti-dip and secured around the nest entrance hole with zip ties. The antenna leads connect to the

(Continued)

FIGURE 2 | RFID reader in the plastic box. In more recent implementations, only the RFID reader is mounted on the box in a smaller plastic case and the battery is moved to an external box on the ground and attached to a solar panel. This reduced weight and size of the box on the nest, insured constant charging of the battery via solar panel, and easier monitoring of the battery status. Also, field crews could check and download SD cards from the RFID reader without having to remove or work around the battery. **(B)** An array of eight RFID-enabled birdfeeders that can selective administer food to carry out spatial memory and cognitive tests. The array can be raised and lowered on cables such that the feeders were protected from non-avian foragers and suspended well above snow cover. Electronics and rechargeable lithium batteries are housed entirely inside the feeder. Antennas are imbedded into a wooden perch that is coated with waterproof epoxy. **(C)** A bluebird nest box capable of issuing experimental treatments (noise and temperature) in accordance with the bird or birds present in the box. The box employs two RFID reading circuits with separate antennas to better determine which birds are present. Electronics are housed in the "attic" above the nesting cavity, and they are accessed by lifting the flexible roof cover as shown. Batteries can also go in the attic or may be mounted externally.

highly non-random—some females ranged widely and visited numerous boxes (>25) while other females were faithful to only one or two boxes. There was also considerable variation in nest-box "attractiveness"—some boxes were visited by as many as 19 different females during a single breeding season, whereas other identical nest boxes nearby were never visited. Nest quality/attractiveness may be a key determinant of why multiple females lay eggs in the same nest. Preliminary social network analyses suggest that groups of females share similar nest site preferences and visit the same subset of nest boxes. Females in the same nest-visiting groups appear to be more likely to be related and from the same cohort (Stair et al., in preparation).

The results also suggest that conspecific brood parasitism is a flexible life history strategy that allows females to adjust reproductive effort to match investment with the probability of success (Lyon and Eadie, 2008, 2018). By integrating both a life-history perspective (what are females doing and why) and kinship (how does relatedness shape these tradeoffs), RFID technology coupled with population-wide genotyping has allowed for a more comprehensive understanding of the evolution and ecology of conspecific brood parasitism and its relation to other breeding systems. RFID monitoring at every nest site along with PIT-tagging all breeding females and nestlings provides a rare opportunity to follow individual females through their entire lifetime and probe more deeply into the ecological, physiological, and genetic factors that influence their intriguing breeding behavior.

Implementation 2: A Feeder Array for Assessing Spatial Memory and Cognition

A second example of the RFID system allows for tests of spatial cognition (spatial learning and memory) in Mountain Chickadees (*Poecile gambeli*) in the Sierra Nevada Mountains. These birds live year-round in mountainous habitat that can receive up to six meters of snow depth in the winter. To survive these conditions the birds must store or cache food (usually pine seeds) and then recover them days or weeks later when other food sources are unavailable in winter. Hence, a large

capacity for spatial cognitive ability is key to the survival of these birds, and individual variation in spatial learning and memory ability is of great interest in understanding the ecology and evolution of these animals as well as food-caching species in general.

Researchers at the University of Nevada (VP, CB, DK, AP, and BS) have devised and implemented a means of evaluating spatial learning and memory in a population of Mountain Chickadees using arrays of RFID-enabled bird feeders that can selectively feed specific individuals. The feeders are equipped with a motorized door, controlled by the RFID circuit board, that can be lowered or raised to allow or deny access to food. An antenna is embedded in a perch positioned in front of the door such that the feeder can recognize individuals on the perch and operate the door accordingly to provide or withhold food. Movement of the door is accomplished with a rack-and-pinon gear mechanism powered by a small gear motor. A limit switch is used in conjunction with the door to indicate to the circuit board when the door had reached a fully open or fully closed position. The motor is controlled by a customized accessory circuit board that features a TB6612FNG motor controller (details on OSF project page).

The learning and memory tests employed arrays of eight RFID-enabled bird feeders that were mounted together on a square frame with two feeders on each side facing outward (see **Figure 2B** and Pitera et al., 2018). One or two of these arrays (depending on the study) were situated at high and low elevations sites. The arrays were suspended on cables stretched between trees so the feeders could be raised above the reach of bears and rodents. Prior to testing, the feeders were all configured in the open position. That is, the doors were all open such that all birds have access to clearly visible food (sunflower seeds). RFID data logging was enabled at this time such that the researchers could determine which tagged birds were visiting the feeders, but the RFID reads did not affect access to food.

After this initial acclimation period of about a week, the feeders were switched to "feed-all mode," wherein the door remained closed until any bird with a tag is detected on the perch. In "feed-all" mode, any bird with a tag will cause the feeder door to open. This training mode allowed birds to become accustomed to the movement of the door.

After another initialization period in feed-all mode, the feeders were reconfigured into "target mode" such that each bird will have access to food at only one of the eight feeders. Spatial learning and memory were assessed based on how many non-rewarding feeders a bird visited prior to visiting the assigned, rewarding feeder during each trial. A trial starts when a bird visits any feeder in the array and ends with the visit to the rewarding feeder. Birds that quickly learn and remember the location of the rewarding feeder (as evinced by progressively fewer visits to non-rewarding feeders) are deemed as having superior spatial learning and memory ability. In addition to testing spatial cognition, the system can test reversal spatial learning and memory performance by switching the rewarding feeder for each bird after the completion of the spatial learning and memory task (which usually took 4 days). The number of errors (e.g., number of non-rewarding feeders visited prior to visiting the rewarding feeder) during a 4-days reversal trial provides a measure of spatial learning and memory flexibility as a bird needs to stop visiting the feeder that provided food in the previous spatial learning and memory task and learn the location of a new rewarding feeder.

This system was applied to Mountain Chickadees living at two different elevations. The birds at high elevation (∼2,400 m) face more severe and longer winter conditions and rely more heavily on caching and recovering food for overwinter survival than do birds at lower elevation (∼1,900 m). The RFID system provided a means of testing several key hypotheses relating spatial cognitive ability to environmental conditions and fitness. First, the spatial cognitive tests revealed that the high elevation birds had better spatial learning and memory ability than did the low elevation birds (Croston et al., 2016). Second, the system revealed that individual variation in spatial learning and memory performance is associated with differences in survival in first-year, juvenile birds during their first winter, showing that spatial cognition is affected by natural selection at high elevations (Sonnenberg et al., 2019). Moreover, a series of spatial learning and memory reversal tests suggested a potential tradeoff between cognitive flexibility and spatial learning/memory (Croston et al., 2017; Tello-Ramos et al., 2018). RFID data collected in this system were also used to show that daily foraging routines in chickadees differ between elevations and among seasons. Moreover, it was apparent that spatial learning and memory performance was associated with daily foraging routines. In particular, chickadees with better spatial cognition had daily foraging routines that resembled those in milder environment and seasons, likely due to greater predictability of foraging success for these individuals (Pitera et al., 2018). Most recently the system has revealed that females allocate more reproductive effort when mated with males with better spatial learning and memory performance (Branch et al., 2019). Finally, ongoing work in this system involves analyzing chickadee social networks using RFID data to address the associations between social and cognitive phenotypes as well as the potential role of cognitive phenotype in structuring these social networks.

Implementation 3: A Nest Box Platform for Experimental Manipulation

Several studies have already employed RFID to generate a detailed activity log for birds that use artificial nest boxes (e.g., Johnson et al., 2013; Stanton et al., 2016; Zarybnicka et al., 2016; Schuett et al., 2017; Chien and Chen, 2018; Firth et al., 2018). With this third application example we describe a project that takes the next logical step forward—using RFID to orchestrate experimental treatments that can be applied individually to breeding adults and offspring. This project involved a nest box designed for Eastern Bluebirds (*Sialia sialis*) that could manipulate environmental noise and/or nestbox temperature in accordance with which birds were inside the box (**Figure 2C**). The project has progressed through several versions of the RFID-enabled nestbox, but not all features have been tested in the field (notably the temperature manipulation). Hence, the functions described here should be regarded as features that are available for a technology-driven nestbox study.

To help ensure that treatments are applied accurately to the targeted individuals, the nestbox was configured to make use of

two antennas. One antenna was mounted to encircle the entrance to the nest box, and it would capture birds as they entered or exited. The second antenna was positioned inside the nest box, and it could verify the presence of a bird therein. The tag-polling strategy was conceived such that the entrance antenna was used for most of the monitoring, and polling by the internal antenna was only done periodically or when the entrance antenna had received a tag. This arrangement was necessary because birds will often rest on the nestbox entrance but not go in. Or they may fly up to the entrance but quickly fly away. The dual antenna system provided assurance that a bird had entered the nestbox.

Following the general example of Lendvai et al. (2015b), artificial noise was incorporated into the system by means of a generic serial MP3 music player module and a 1 W speaker (catalex.taobao.com). These items were purchased as a single kit for about $4. The MP3 player accesses and plays audio tracks from a mini-SD card. The microcontroller on the RFID circuit board communicated with the MP3 player via a simple serial interface. Hence, the RFID reader could control the timing, duration, and volume of playbacks. We used a transistor to control the power supply to the MP3 player, such that it could be powered down when it was not being used (see OSF project page for details). Similarly, we have configured the RFID circuit board to control the power supply to an electronic heating pad (WireKinetics Co, Ltd, Taipei, Taiwan). As with the speaker system we used a simple transistor circuit to provide current to the heating pad directly from the power supply (i.e., battery).

As part of a pilot study, a single noise emitting system was deployed on an active bluebird nest in Kent County Michigan. The system was programmed to emit noise from 05:30 to 11:00 each day when both parents were absent from the nest box. The system was successful in administering an effective treatment throughout the majority of a nesting effort. The sample size is, of course, too small to reach any conclusions, and based on this initial effort, we plan to continue this experiment in future breeding seasons. The heating pad has not yet been tested, but we plan to do so in the spring of 2019, and the results will be posted to our OSF project page.

DISCUSSION

The example studies described above do not by any means exhaust the possibilities offered by our low-cost RFID system. Given the wide array of hardware and software tools available as part of the Arduino electronics platform there are many other applications with respect to data logging and experimental manipulations that could be brought to bear in the context of RFID-based biologging. A few potential and/or recently executed applications are as follows:

- Interfacing the RFID reader with a WiFi network to get wireless RFID data transferred in real time to a data collection hub (Ramudzuli et al., 2017; Rosval, personal communication).
- Using visits to a feeding station to generate association data for use in a network model (Psorakis et al., 2015; Zonana et al., 2019).
- Evaluating and quantifying social behavior in free living animals (Aplin et al., 2013, 2014, 2015b; Zeus et al., 2017; Sabol et al., 2018).
- Administration of manipulation-based cognitive tests (Aplin et al., 2015a; Morand-Ferron et al., 2015).
- Monitoring use of food or other resources (Crates et al., 2016).
- Selective food supplementation experiments (Small et al., 2013).
- Targeted delivery of nutrients or drugs to specific animals (Schoech and Bowman, 2003).
- Environmental data logging to match conditions with behavior.
- Nest visitation patterns in colonial species (Leighton and Echeverri, 2016).
- Quantifying movement and exploratory behavior (Catarinucci et al., 2014a; Ousterhout and Semlitsch, 2014).
- Monitoring health and behavior in captive animal populations (Whitham and Miller, 2016).
- Quantifying stopover duration and behavior in migrating species (Zenzal and Moore, 2016).
- Automated Collection of body-mass and other morphometric data (Hou et al., 2015; Small, unpublished).

As new applications come online, we intend to incorporate them as modules into our OSF project page.

There is a clear taxonomic bias in the examples described in this paper; they are all applied to avian study systems. However, this bias is due to the common interests of the research teams and not limitations in the applicability of RFID systems to other taxa. PIT tags have been used in a wide variety of vertebrates and even on a few insects (Sumner et al., 2007; Bonter and Bridge, 2011; Dogan et al., 2016; Whitham and Miller, 2016). Nevertheless, their applicability to bird research should not be surprising majority of bird species require small (<1 g) tracking devices.

A major advantage to automated systems like the ones described here is the potential for continuous data recording. Traditional monitoring methods often involve sampling the activity schedules of animals—for example, a researcher may visually monitor a burrow entrance for 3 h every other day, or one may video record activity at a feeding station for 5 h every day. Although these methods may be adequate for finding averages associated with events that happen regularly, they may be inadequate for detecting rare or even infrequent events (like brood parasitism or fledging). Automated systems obviate the need for sampling such that you can capture the entirety of a breeding attempt or activity period (see Lendvai et al., 2015a).

As is the case with all research efforts that involve attaching devices to animals, researchers must make every effort to minimize the adverse effects of equipping animals with PIT tags. There are numerous studies of the effects of PIT tags on survival and behavior, with most of this research focused on fish (Keck, 1994; Low et al., 2005; Nicolaus et al., 2008; Burdick, 2011; Thorstad et al., 2013; Guimaraes et al., 2014; Ratnayake et al., 2014; Moser et al., 2017; Schlicht and Kempenaers, 2018). The vast majority of these studies conclude that the effect of implanted PIT tags is negligible. The Wood Duck research described above entailed injecting tags in both females and

ducklings intrascapularly using a PIT-tag syringe, and in 6 years, no deleterious effects have been detected on females or ducklings in the wild. Related projects have involved tagging >500 ducklings in captivity and raising >200 to the fledging stage with no adverse effects on survival or health observed in the course of regular monitoring by staff veterinarians. Tag loss has been <1% (Eadie et al., in preparation).

We do not know of a systematic study that has investigated the effects of externally mounted PIT tags. In particular, external mounting would largely apply to bird species, wherein PIT tags are incorporated into leg bands (see **Figure 1**). Our own experience has indicated no problems other than those typically associated with leg bands. More specifically, the studies of Mountain Chickadees described above have involved tagging over 1,000 individuals with RFID leg bands. Thus far, there has been one instance where the leg band appeared to cause an injury. However, there are unpublished reports of apparent injuries and mortality in association with RFID leg bands (Curry, unpublished data; Morand-Ferron et al., personal communication). We advocate the use of compact RFID leg bands like those supplied by Eccel technology, which minimize the size of the tag (see **Figure 1**), and we recommend caution in selecting the appropriate band size for the species (or individual) being tagged.

It is important to note that our device is not the only RFID reader available for field biologists. Among the alternatives for low-frequency (120–150 MHz) readers, the lowest-cost options include several RFID reader modules that can simply read tag data and communicate with a computer or microcontroller. Examples include the ID-12 and ID-20 readers (ID Innovations, Canning Vale, WA, Australia), the Paralax RFID module (Parallax, Inc, Rocklin, CA, USA), the MIKROE-262 and MIKROE-1434 modules (Mikroelektronika D.O.O., Belgrade, Serbia), and the RFIDREAD-RW Module (Priority 1 Design, Melbourne, Australia). These sorts of modules range in cost from about $10–50 (USD). There are a few commercially available RFID readers that can log data in a manner similar to our ETAG reader. For example, Priority 1 Design offers the RFIDLOG circuitboard for ∼$50 (USD). A more robust, fully enclosed RFID reader/datalogger is available from Eccel Technology, Ltd (Leicester, UK), for ∼$400 (USD). For applications that require read ranges >2–3 cm, there are high power RFID readers capable of read distances of 50 cm or more. Unfortunately, readers that offer this increased read range will typically cost considerably more than the low power systems. Examples of high-power systems include Biomark readers, such as the IS1001, which costs ∼$1,500 (USD), and systems from Oregon RFID (Portland, OR, USA) with a minimum cost of just over $2,000 (USD). Although there are many RFID readers available, there are few if any standalone systems that can be programmed by the user to carry out complex protocols. Our ETAG reader offers this key feature.

To facilitate widespread collaboration and sharing of information, we have established a project within the Open Science Framework at https://osf.io/9j7ax/. This information repository contains technical information relating to the RFID system and the research applications described in this paper, and it is open to the public to view and download materials. It also allows for ongoing updates and expansion such that we can continue to add new applications and contributors into the foreseeable future. New developments on the horizon include wireless networks for real-time data delivery, and online software tools for designing antennas that will culminate in an online simulator for testing virtual antennas prior to making a physical prototype. We are also developing web-based data portal and archive for uploading, storing and managing RFID data. We hope that our RFID system and the forthcoming tools will prove to be useful resources for the biologging community, and we invite our readers to take part in our efforts to expand the utility of RFID technology for animal tracking and monitoring.

ETHICS STATEMENT

All animal research was conducted according to accepted ethical standards and with approval from the authors' respective Institutional Animal Care and Use Committees (IACUC). Specifically, the research described in this manuscript followed IACUC-approved protocols R16-010, 00603, and 20971 for the University of Oklahoma, the University of Nevada Reno, and the University of California Davis, respectively. All field efforts sought to minimize negative impacts on birds by working with animals only during favorable conditions and by following best practices for animal handling and tagging.

AUTHOR CONTRIBUTIONS

EB participated in designing and implementing the RFID systems and drafted the main text of the article. JW and AM helped design the RFID circuit board, wrote key elements of the firmware, and served as a grant PI. MP and DP designed and implemented the experimental bluebird nestbox and contributed to writing this section of the text. CH designed and implemented the solar charging system used on the bluebird boxes. CC served as a grant PI and along with TP has built data infrastructure for the RFID system and managed the OSF project page. JE, TS, AO, and BL carried out the field study of Wood Ducks, and JE and BL helped draft this section of text. CB, AP, DK, BS, and VP conceived and executed the spatial memory testing. VP and AP helped to draft this section of the text. JR served as the overall project manager and grant PI for the project, and she provided editorial assistance on the manuscript.

FUNDING

Funding for the technology development came from the National Science Foundation: NSF IDBR 1556313 to JR and EB; NSF IDBR 1556316 to JW; NSF ABI 1458402 to CC, JR, and EB. The NSF also provided funding for two of the featured RFID implementations: IOS 1351295 and NSF IOS 1856181 to VP; NSF IOS 1355208 to JE and BL. Development and testing of the bluebird nestbox was supported by a George Miksch Suttton Scholarship, a grant from the North American Bluebird Society, and an OU Biological Station Award to MP.

ACKNOWLEDGMENTS

We wish to thank all of our colleagues who tested prototypes and provided feedback. We also thank the many field assistants and student volunteers who were involved in the field research described in this paper. Finally, thanks also to Elena Bridge for assembling hundreds of RFID circuit boards.

REFERENCES

Anu, V. M., and Canessane, R. A. (2017). Livestock monitoring using RFID with R^+ tree indexing. *Biomed. Res. India* 28, 2407–2410.

Aplin, L. M., Farine, D. R., Mann, R. P., and Sheldon, B. C. (2014). Individual-level personality influences social foraging and collective behaviour in wild birds. *Proc. R. Soc. Biol. Sci.* 281:20141016. doi: 10.1098/rspb.2014.1016

Aplin, L. M., Farine, D. R., Morand-Ferron, J., Cockburn, A., Thornton, A., and Sheldon, B. C. (2015a). Experimentally induced innovations lead to persistent culture via conformity in wild birds. *Nature* 518, 538–541. doi: 10.1038/nature13998

Aplin, L. M., Farine, D. R., Morand-Ferron, J., Cole, E. F., Cockburn, A., and Sheldon, B. C. (2013). Individual personalities predict social behaviour in wild networks of great tits (*Parus major*). *Ecol. Lett.* 16, 1365–1372. doi: 10.1111/ele.12181

Aplin, L. M., Firth, J. A., Farine, D. R., Voelkl, B., Crates, R. A., Culina, A., et al. (2015b). Consistent individual differences in the social phenotypes of wild great tits, *Parus major*. *Anim. Behav.* 108, 117–127. doi: 10.1016/j.anbehav.2015.07.016

Bandivadekar, R. R., Pandit, P. S., Sollmann, R., Thomas, M. J., Logan, S. M., Brown, J. C., et al. (2018). Use of RFID technology to characterize feeder visitations and contact network of hummingbirds in urban habitats. *PLoS ONE* 13:e208057. doi: 10.1371/journal.pone.0208057

Barlow, S. E., O'Neill, M. A., and Pavlik, B. M. (2019). A prototype RFID tag for detecting bumblebee visitations within fragmented landscapes. *J. Biol. Eng.* 13:13. doi: 10.1186/s13036-019-0143-x

Bellrose, F. C., Holm, D. J., Wildlife Management Institute, and Illinois Natural History Survey. (1994). *Ecology and Management of the Wood Duck.* Mechanicsburg, PA: Stackpole Books.

Bonter, D. N., and Bridge, E. S. (2011). Applications of radio frequency identification (RFID) in ornithological research: a review. *J. Field Ornithol.* 82, 1–10. doi: 10.1111/j.1557-9263.2010.00302.x

Branch, C. L., Pitera, A. M., Kozlovsky, D. Y., Bridge, E. S., and Pravosudov, V. V. (2019). Smart is the new sexy: Female mountain chickadees increase reproductive investment when mated to males with better spatial cognition. *Ecol. Lett.* 22, 897–903. doi: 10.1111/ele.13249

Bridge, E. S., and Bonter, D. N. (2011). A low-cost radio frequency identification device for ornithological research. *J. Field Ornithol.* 82, 52–59. doi: 10.1111/J.1557-9263.2010.00307.X

Burdick, S. M. (2011). Tag loss and short-term mortality associated with passive integrated transponder tagging of Juvenile Lost River Suckers. *N. Am. J. Fish. Manage.* 31, 1088–1092. doi: 10.1080/02755947.2011.641067

Catarinucci, L., Colella, R., Mainetti, L., Patrono, L., Pieretti, S., Secco, A., et al. (2014a). An animal tracking system for behavior analysis using radio frequency identification. *Lab Anim.* 43, 323–329. doi: 10.1038/laban.547

Catarinucci, L., Colella, R., Mainetti, L., Patrono, L., Pieretti, S., Sergi, I., et al. (2014b). Smart RFID antenna system for indoor tracking and behavior analysis of small animals in colony cages. *IEEE Sens. J.* 14, 1198–1206. doi: 10.1109/JSEN.2013.2293594

Chien, Y. R., and Chen, Y. X. (2018). An RFID-based smart nest box: an experimental study of laying performance and behavior of individual hens. *Sensors* 18:E859. doi: 10.3390/s18030859

Crates, R. A., Firth, J. A., Farine, D. R., Garroway, C. J., Kidd, L. R., Aplin, L. M., et al. (2016). Individual variation in winter supplementary food consumption and its consequences for reproduction in wild birds. *J. Avian Biol.* 47, 678–689. doi: 10.1111/jav.00936

Croston, R., Branch, C. L., Pitera, A. M., Kozlovsky, D. Y., Bridge, E. S., Parchman, T. L., et al. (2017). Predictably harsh environment is associated with reduced cognitive flexibility in wild food-caching mountain chickadees. *Anim. Behav.* 123, 139–149. doi: 10.1016/j.anbehav.2016.10.004

Croston, R., Kozlovsky, D. Y., Branch, C. L., Parchman, T. L., Bridge, E. S., and Pravosudov, V. V. (2016). Individual variation in spatial memory performance in wild mountain chickadees from different elevations. *Anim. Behav.* 111, 225–234. doi: 10.1016/j.anbehav.2015.10.015

Dogan, H., Çaglar, M. F., Yavuz, M., and Gözel, M. A. (2016). Use of radio frequency identification systems on animal monitoring. *SDU Int. J. Technol. Sci.* 8, 38–53.

Firth, J. A., Verhelst, B. L., Crates, R. A., Garroway, C. J., and Sheldon, B. C. (2018). Spatial, temporal and individual-based differences in nest-site visits and subsequent reproductive success in wild great tits. *J. Avian Biol.* 49:e01740. doi: 10.1111/jav.01740

Guimaraes, M., Correa, D. T., Filho, S. S., Oliveira, T. A. L., Doherty, P. F., and Sawaya, R. J. (2014). One step forward: contrasting the effects of Toe clipping and PIT tagging on frog survival and recapture probability. *Ecol. Evol.* 4, 1480–1490. doi: 10.1002/ece3.1047

Hou, L. L., Verdirame, M., and Welch, K. C. (2015). Automated tracking of wild hummingbird mass and energetics over multiple time scales using radio frequency identification (RFID) technology. *J. Avian Biol.* 46, 1–8. doi: 10.1111/jav.00478

Ibarra, V., Araya-Salas, M., Tang, Y. P., Park, C., Hyde, A., Wright, T. F., et al. (2015). An RFID Based Smart Feeder for Hummingbirds. *Sensors* 15, 31751–31761. doi: 10.3390/s151229886

Iserbyt, A., Griffioen, M., Borremans, B., Eens, M., and Muller, W. (2018). How to quantify animal activity from radio-frequency identification (RFID) recordings. *Ecol. Evol.* 8, 10166–10174. doi: 10.1002/ece3.4491

Johnson, L. S., Hebert, R. M., Napolillo, F. M., and Allen, A. (2013). The process of fledging in the Mountain Bluebird. *J. Field Ornithol.* 84, 367–376. doi: 10.1111/jofo.12036

Keck, M. B. (1994). Test for detrimental effects of pit tags in neonatal snakes. *Copeia* 1, 226–228. doi: 10.2307/1446690

Leighton, G. M., and Echeverri, S. (2016). Population genomics of sociable weavers *Philetairus socius* reveals considerable admixture among colonies. *J. Ornithol.* 157, 483–492. doi: 10.1007/s10336-015-1307-1

Lendvai, A. Z., Akcay, C., Ouyang, J. Q., Dakin, R., Domalik, A. D., St. John, P. S., et al. (2015a). Analysis of the optimal duration of behavioral observations based on an automated continuous monitoring system in tree swallows (*Tachycineta bicolor*): is one hour good enough? *PLoS ONE* 10:e141194. doi: 10.1371/journal.pone.0141194

Lendvai, A. Z., Akcay, C., Weiss, T., Haussmann, M. F., Moore, I. T., and Bonier, F. (2015b). Low cost audiovisual playback and recording triggered by radio frequency identification using Raspberry Pi. *Peerj* 4:e742v1. doi: 10.7287/peerj.preprints.742v1

Low, M., Eason, D., and McInnes, K. (2005). Evaluation of passive integrated transponders for identification of Kakapo, Strigops habroptilus. *Emu-Austr. Ornithol.* 105, 33–38. doi: 10.1071/MU04060

Lyon, B. E., and Eadie, J. M. (2008). Conspecific brood parasitism in birds: a life-history perspective. *Annu. Rev. Ecol. Evol. Syst.* 39, 343–363. doi: 10.1146/annurev.ecolsys.39.110707.173354

Lyon, B. E., and Eadie, J. M. (2018). "Why do birds lay eggs in the nests of conspecifics?" in *Avian Brood Parasitism: Behaviour, Ecology, Evolution and Coevolution, 1st Edn.*, ed M. Soler (New York, NY: Springer Berlin Heidelberg), 105–123.

Morand-Ferron, J., Cole, E. F., and Quinn, J. L. (2016). Studying the evolutionary ecology of cognition in the wild: a review of practical and conceptual challenges. *Biol. Rev.* 91, 367–389. doi: 10.1111/brv.12174

Morand-Ferron, J., Hamblin, S., Cole, E. F., Aplin, L. M., and Quinn, J. L. (2015). Taking the operant paradigm into the field: associative learning in wild great tits. *PLoS ONE* 10:e133821. doi: 10.1371/journal.pone.0133821

Moser, M. L., Jackson, A. D., Mueller, R. P., Maine, A. N., and Davisson, M. (2017). Effects of passive integrated transponder (PIT) implantation on Pacific lamprey ammocoetes. *Anim. Biotel.* 5:1. doi: 10.1186/s40317-016-0118-3

Nicolaus, M., Bouwman, K. M., and Dingemanse, N. J. (2008). Effect of PIT tags on the survival and recruitment of great tits *Parus major*. *Ardea* 96, 286–292. doi: 10.5253/078.096.0215

Ousterhout, B. H., and Semlitsch, R. D. (2014). Measuring terrestrial movement behavior using passive integrated transponder (PIT) tags: effects of tag size on detection, movement, survival, and growth. *Behav. Ecol. Sociobiol.* 68, 343–350. doi: 10.1007/s00265-013-1656-9

Pitera, A. M., Branch, C. L., Bridge, E. S., and Pravosudov, V. V. (2018). Daily foraging routines in food-caching mountain chickadees are associated with variation in environmental harshness. *Anim. Behav.* 143, 93–104. doi: 10.1016/j.anbehav.2018.07.011

Psorakis, I., Voelkl, B., Garroway, C. J., Radersma, R., Aplin, L. M., Crates, R. A., et al. (2015). Inferring social structure from temporal data. *Behav. Ecol. Sociobiol.* 69, 857–866. doi: 10.1007/s00265-015-1906-0

Ramudzuli, Z.R., Malekian, R., and Ye, N. (2017). Design of a RFID system for real-time tracking of laboratory animals. *Wireless Per. Commun.* 95, 3883–3903. doi: 10.1007/s11277-017-4030-9

Ratnayake, C. P., Morosinotto, C., Ruuskanen, S., Villers, A., and Thomson, R. L. (2014). Passive integrated transponders (PIT) on a small migratory passerine bird: absence of deleterious short and long-term effects. *Ornis Fennica* 91, 244–255.

Russell, A. L., Morrison, S. J., Moschonas, E. H., and Papaj, D. R. (2017). Patterns of pollen and nectar foraging specialization by bumblebees over multiple timescales using RFID. *Sci. Rep.* 7:42448. doi: 10.1038/srep42448

Sabol, A. C., Solomon, N. G., and Dantzer, B. (2018). How to study socially monogamous behavior in secretive animals? Using social network analyses and automated tracking systems to study the social behavior of prairie voles. *Front. Ecol. Evol.* 6:178. doi: 10.3389/fevo.2018.00178

Schlicht, E., and Kempenaers, B. (2018). The immediate impact of ringing, blood sampling and PIT-tag implanting on the behaviour of blue tits *Cyanistes caeruleus*. *Ardea* 106, 39–98. doi: 10.5253/arde.v106i1.a8

Schoech, S. J., and Bowman, R. (2003). Does differential access to protein influence differences in timing of breeding of Florida Scrub-Jays (*Aphelocoma coerulescens*) in suburban and wildland habitats? *Auk* 120, 1114–1127. doi: 10.2307/4090282

Schuett, W., Jarvisto, P. E., Calhim, S., Velmala, W., and Laaksonen, T. (2017). Nosy neighbours: large broods attract more visitors. A field experiment in the pied flycatcher, *Ficedula hypoleuca. Oecologia* 184, 115–126. doi: 10.1007/s00442-017-3849-9

Small, T. W., Bridge, E. S., and Schoech, S. J. (2013). "Short-term effects and long-term consequences of supplemental food on a free-living threatened species, the Florida Scrub-Jay," in *Annual Meeting of the American Ornithologists' Union and the Cooper Ornithological Society, 14–17 August 2013* (Chicago, IL).

Sonnenberg, B. R., Branch, C. L., Pitera, A. M., Bridge, E., and Pravosudov, V. V. (2019). Natural selection and spatial cognition in wild food-caching mountain chickadees. *Curr. Biol.* 29, 670–676.e3. doi: 10.1016/j.cub.2019.01.006

Stanton, R. L., Morrissey, C. A., and Clark, R. G. (2016). Tree swallow (*Tachycineta bicolor*) foraging responses to agricultural land use and abundance of insect prey. *Can. J. Zool.* 94, 637–642. doi: 10.1139/cjz-2015-0238

Sumner, S., Lucas, E., Barker, J., and Isaac, N. (2007). Radio-tagging technology reveals extreme nest-drifting behavior in a eusocial insect. *Curr. Biol.* 17, 140–145. doi: 10.1016/j.cub.2006.11.064

Tello-Ramos, M. C., Branch, C. L., Pitera, A. M., Kozlovsky, D. Y., Bridge, E. S., and Pravosudov, V. V. (2018). Memory in wild mountain chickadees from different elevations: comparing first-year birds with older survivors. *Anim. Behav.* 137, 149–160. doi: 10.1016/j.anbehav.2017.12.019

Thorstad, E. B., Rikardsen, A. H., Alp, A., and Okland, F. (2013). The use of electronic tags in fish research–an overview of fish telemetry methods. *Turkish J. Fish. Aquat. Sci.* 13, 881–896. doi: 10.4194/1303-2712-v13_5_13

Whitham, J. C., and Miller, L. J. (2016). Using technology to monitor and improve zoo animal welfare. *Anim. Welfare* 25, 395–409. doi: 10.7120/09627286.25.4.395

Zarybnicka, M., Kubiznak, P., Sindelar, J., and Hlavac, V. (2016). Smart nest box: a tool and methodology for monitoring of cavity-dwelling animals. *Methods Ecol. Evol.* 7, 483–492. doi: 10.1111/2041-210X.12509

Zenzal, T. J., and Moore, F. R. (2016). Stopover biology of ruby-throated hummingbirds (*Archilochus colubris*) during autumn migration. *Auk* 133, 237–250. doi: 10.1642/AUK-15-160.1

Zeus, V. M., Puechmaille, S. J., and Kerth, G. (2017). Conspecific and heterospecific social groups affect each other's resource use: a study on roost sharing among bat colonies. *Anim. Behav.* 123, 329–338. doi: 10.1016/j.anbehav.2016.11.015

Zonana, D. M., Gee, J. M., Bridge, E. S., Breed, M. D., and Doak, D. F. (2019). Assortative behavior structures social networks in a quail hybrid zone. *Am. Nat.* 193, 852–865. doi: 10.1086/703158

Zuckerberg, B., Woods, A. M., and Porter, W. F. (2009). Poleward shifts in breeding bird distributions in New York State. *Glob. Chang. Biol.* 15, 1866–1883. doi: 10.1111/j.1365-2486.2009.01878.x

Conflict of Interest Statement: The authors declare that the research was conducted in the absence of any commercial or financial relationships that could be construed as a potential conflict of interest.

Copyright © 2019 Bridge, Wilhelm, Pandit, Moreno, Curry, Pearson, Proppe, Holwerda, Eadie, Stair, Olson, Lyon, Branch, Pitera, Kozlovsky, Sonnenberg, Pravosudov and Ruyle. This is an open-access article distributed under the terms of the Creative Commons Attribution License (CC BY). The use, distribution or reproduction in other forums is permitted, provided the original author(s) and the copyright owner(s) are credited and that the original publication in this journal is cited, in accordance with accepted academic practice. No use, distribution or reproduction is permitted which does not comply with these terms.

frontiers in Ecology and Evolution

ORIGINAL RESEARCH
published: 27 August 2019
doi: 10.3389/fevo.2019.00317

Dynamic-Parameter Movement Models Reveal Drivers of Migratory Pace in a Soaring Bird

Joseph M. Eisaguirre[1,2], Marie Auger-Méthé[3,4], Christopher P. Barger[5], Stephen B. Lewis[6], Travis L. Booms[5] and Greg A. Breed[1,7]*

[1] Department of Biology and Wildlife, University of Alaska Fairbanks, Fairbanks, AK, United States, [2] Department of Mathematics and Statistics, University of Alaska Fairbanks, Fairbanks, AK, United States, [3] Department of Statistics, University of British Columbia, Vancouver, BC, Canada, [4] Institute for the Oceans and Fisheries, University of British Columbia, Vancouver, BC, Canada, [5] Alaska Department of Fish and Game, Fairbanks, AK, United States, [6] United States Fish and Wildlife Service, Juneau, AK, United States, [7] Institute of Arctic Biology, University of Alaska Fairbanks, Fairbanks, AK, United States

OPEN ACCESS

Edited by:
Frants Havmand Jensen,
Woods Hole Oceanographic Institution, United States

Reviewed by:
Anne K. Scharf,
Max Planck Institute of Ornithology, Germany
Peter E. Smouse,
Rutgers University, The State University of New Jersey, United States

***Correspondence:**
Joseph M. Eisaguirre
jmeisaguirre@alaska.edu

Specialty section:
This article was submitted to Behavioral and Evolutionary Ecology, a section of the journal Frontiers in Ecology and Evolution

Received: 11 March 2019
Accepted: 07 August 2019
Published: 27 August 2019

Citation:
Eisaguirre JM, Auger-Méthé M, Barger CP, Lewis SB, Booms TL and Breed GA (2019) Dynamic-Parameter Movement Models Reveal Drivers of Migratory Pace in a Soaring Bird. Front. Ecol. Evol. 7:317. doi: 10.3389/fevo.2019.00317

Long distance migration can increase lifetime fitness, but can be costly, incurring increased energetic expenses and higher mortality risks. Stopover and other en route behaviors allow animals to rest and replenish energy stores and avoid or mitigate other hazards during migration. Some animals, such as soaring birds, can subsidize the energetic costs of migration by extracting energy from flowing air. However, it is unclear how these energy sources affect or interact with behavioral processes and stopover in long-distance soaring migrants. To understand these behaviors and the effects of processes that might enhance use of flight subsidies, we developed a flexible mechanistic model to predict how flight subsidies drive migrant behavior and movement processes. The novel modeling framework incorporated time-varying parameters informed by environmental covariates to characterize a continuous range of behaviors during migration. This model framework was fit to GPS satellite telemetry data collected from a large soaring and opportunist foraging bird, the golden eagle (*Aquila chrysaetos*), during migration in western North America. Fitted dynamic model parameters revealed a clear circadian rhythm in eagle movement and behavior, which was directly related to thermal uplift. Behavioral budgets were complex, however, with evidence for a joint migrating/foraging behavior, resembling a slower paced fly-and-forage migration, which could facilitate efficient refueling while still ensuring migration progress. In previous work, ecological and foraging conditions are usually considered to be the key aspects of stopover location quality, but taxa, such as the golden eagle, that can tap energy sources from moving fluids to drive migratory locomotion may pace migration based on both foraging opportunities and available flight subsidies.

Keywords: Bayesian, correlated random walk, golden eagle, movement ecology, soaring flight

INTRODUCTION

Long-distance migration can relax competition and permit use of seasonally available resources, helping many animals maximize lifetime fitness (Newton, 2008; Avgar et al., 2014). Those benefits, however, come at substantial costs, including greater vulnerability to predators, uncertain conditions, mechanical wear, elevated energy expenditure, and time (Alerstam and Hedenström, 1998; Clark and Butler, 1999; Hedenström, 2008; Newton, 2008; Avgar et al., 2014). As many migrant species cannot store sufficient energy for nonstop, long-distance migration, stopover evolved as a behavior for strategically resting and refueling en route (Gill, 2007).

Migrant species are adapted for utilizing either soaring or flapping flight, and the different flight modes translate into stopover strategy (Hedenström, 1993; Gill, 2007). Generally, soaring flight is favorable for larger birds and flapping flight for smaller birds, though the partitioning of time for each flight mode during migration is dependent on the tradeoff between time and energy (Hedenström, 1993; Duerr et al., 2015; Katzner et al., 2015; Miller et al., 2016). In theory, a time-minimizing migrator would be expected to fly with greater directional persistence and stronger directional bias than would an energy-expenditure minimizer. Such net energy maximizers would be expected to take advantage of en route foraging opportunities and may divert or delay to replenish energy reserves. (Note that "energy minimization" has been used to describe this strategy e.g., Alerstam, 2011; Miller et al., 2016, but we use "net energy maximization" for clarity.) If time is less important, a net energy maximizer is less restricted and can spend additional time seeking an energetically superior path; the emergent path would then be more tortuous with less directional bias toward the final destination at any given point along the route. Time minimization and net energy maximization strategies are not mutually exclusive, however, and the emergent strategy and behaviors in any given migrating individual lies along a continuum (Alerstam, 2011; Miller et al., 2016).

Obligate soaring migrants must also consider routes based on their energy landscape (Shamoun-Baranes et al., 2010), the energetic constraints of movement over space (Shepard et al., 2013), which also contributes to a migrant's location along the behavioral continuum. While soaring migrants can stopover, their energy landscape is more complex. Meteorological conditions are at least as important as foraging resources for soaring migrants, which can be extremely dynamic and subsidize the energetic cost of flight directly via uplift (Pennycuick, 1971; Alerstam, 1979; Spaar and Bruderer, 1997; Gill, 2007; Duerr et al., 2012; Murgatroyd et al., 2018).

The flight performance of soaring migrants relative to subsidies provided by meteorological conditions has been well documented (Pennycuick, 1971; Alerstam, 1979; Spaar and Bruderer, 1997), establishing a clear link between diurnal migrant behavior and development of the atmospheric boundary layer. Two primary forms of uplift arise by (1) wind interacting with topography to form upslope wind or mountain waves (air currents forming standing waves established on the lee side of mountains; hereafter orographic uplift) and (2) solar heating of the earth's surface to generate thermal uplift. Other forms arise from turbulent eddies over small landscape features and ocean waves modifying the air. The dynamic nature of atmospherically-driven flight subsidies requires detailed movement data as well as carefully designed analytical techniques to investigate certain mechanisms hidden in those data.

Our understanding of migratory processes has advanced enormously in the past 30 years, as animal tracking technology developed from a novelty of coarse observation to a core method for observing animal behavior and movement in incredible detail (Luschi et al., 1998; Sawyer et al., 2005; Bridge et al., 2011; Katzner et al., 2015; Hooten et al., 2017). Global Positioning System (GPS) telemetry, in particular, allows remote observation of animal relocations across a broad spatiotemporal scale. GPS transmitters are now light and reliable enough to study the complete migrations of many large soaring migrants, including golden eagles *Aquila chrysaetos*, which often rely on flight subsidies during migration (Katzner et al., 2015). Golden eagles and other large soaring birds have been used as model systems for phenomenologically evaluating questions about migratory flight performance and migration strategies (*sensu* Duerr et al., 2012; Lanzone et al., 2012; Katzner et al., 2015; Vansteelant et al., 2015; Miller et al., 2016; Shamoun-Baranes et al., 2016; Rus et al., 2017). For example, Lanzone et al. (2012) and Katzner et al. (2015) found that golden eagles use both thermal and orographic uplift to subsidize migratory flight, although thermal soaring was often more efficient in long distance, directed flight (Duerr et al., 2012). While these studies have contributed to our understanding of soaring migration and have laid a foundation for more detailed approaches, they relate meteorology to derived movement metrics, rather than incorporate them into process-based models that mechanistically predict movement, and ignore the temporal dependence between serially observed locations (i.e., autocorrelation). Not accounting for such autocorrelation imparts bias on certain estimated parameters (e.g., variances) thereby affecting inference through, for example, underestimating uncertainty. Consequently, the links between resources distributed over the landscape, such as flight subsidies, and behavioral budgets, including stopover behavior, during migrations of soaring birds remain unclear.

Unlike previous approaches, process-based, mechanistic movement models allow explicit inference of the underlying mechanisms driving movement (e.g., changes in behavior) that may not be available from conventional phenomenological analytical approaches (Turchin, 1998; Nathan et al., 2008; Hooten et al., 2017). While it is impossible to understand fully the intricacies in animal movement, we can pose mathematical models (e.g., correlated random walks) to approximate the movement process (Kareiva and Shigesada, 1983; Turchin, 1998). We can then fit these models statistically to observed data to estimate parameters describing behavior and its relationship with dynamic environmental features that moving animals experience (Blackwell, 1997, 2003; Morales et al., 2004; Breed et al., 2017; Hooten et al., 2017). Many of the recently developed mechanistic movement models are built in a discrete state-switching framework, where animals switch between discrete behavioral states (see Hooten et al., 2017, and references

cited therein). Choosing both the biologically relevant and quantitatively supported number of states, as well as interpreting the identified states in a biological context, remains challenging (Patterson et al., 2017; Pohle et al., 2017). Often, this challenge leads researchers to artificially limit the number of states and/or collapse two or more states into one biologically interpretable state. For example Pirotta et al. (2018), presented a model with five discrete kinds of avian flight, but the complexity of the model made interpreting those states difficult and poorly matched classifications manually identified by an expert.

In many cases, a more natural approach to modeling an animal's movement process is along a dynamic continuum, rather than as switching between discrete behavioral states (Breed et al., 2012; Auger-Méthé et al., 2017; Jonsen et al., 2019). Modeling along a continuum may be an especially useful approach for understanding movement behavior in soaring birds, considering the dynamic nature of atmospheric processes that influence movements. Here, we developed and applied a flexible mechanistic movement model based on a correlated random walk with time-varying parameters. This novel model was fit to movement data collected via GPS telemetry to understand how individuals in a population of long-distance soaring migrants use flight subsidies and budget stopover and migration behavior. Specifically, we were interested in identifying which flight subsidies influence stopover and migratory behavior and how the effect of key subsides and behaviors varied between spring and fall migrations. Our approach resembled continuous-time correlated random walks (Johnson et al., 2008; Blackwell et al., 2015; Gurarie et al., 2017; Michelot and Blackwell, 2019), but was easily implemented and yielded a relatively small number of dynamic parameters that could be directly interpreted biologically. A set of candidate models could be ranked, with model selection approaches, providing inference on how behavioral budgets and meteorological variables interacted to give rise to the observed migration paths. Modeling the effects of dynamic wind and uplift variables as time-varying movement behaviors of migratory golden eagles further allowed new details to emerge without imposing artificially discrete states.

METHODS

Model System

The golden eagle is a large, soaring raptor, distributed across the Holarctic (Watson, 2010). Golden eagles are predatory and opportunistic, utilizing many taxa for food resources, ranging from small mammals and birds to ungulates, often scavenging carrion (Kochert et al., 2002; Watson, 2010). While many populations are classified as partial migrants, most individuals that summer and breed above approximately 55°N in North America are considered true long-distance migrants (Kochert et al., 2002; Watson, 2010). The population we observed in this study migrates over the mountainous regions of western North America between a breeding range primarily in southcentral Alaska, USA and a broad overwintering range in western North America that ranges from the southwestern US to central British Columbia and Alberta, Canada (Bedrosian et al., 2018).

Data Collection

We captured golden eagles with a remote-fired net launcher, placed over carrion bait near Gunsight Mountain, Alaska (61.67°N 147.35°W). Captures occurred between mid-March and mid-April 2014-2016. Fifty-three adult and sub-adult eagles were equipped with 45-*g* back pack solar-powered Argos/GPS platform transmitter terminals (PTTs; Microwave Telemetry, Inc., Columbia, MD, USA). Eagles were sexed molecularly and aged by plumage.

PTTs were programmed to record GPS locations on duty cycles, ranging from 8 to 14 fixes per day during migration, depending on year of deployment. PTTs deployed in 2014 were set to record 13 locations at 1-h intervals centered around solar noon plus a location at midnight local time. PTTs deployed in 2015 were programmed to record 8 locations with 1-h intervals centered around solar noon, and PTTs deployed in 2016 took eight fixes daily at regular 3-h time intervals. Note that the PTTs deployed in 2015 did not record locations overnight. Poor battery voltage from September to March often resulted in PTTs failing to take all programmed fixes, so the resulting GPS tracks had missing observations during these periods. Tags lasted multiple seasons, and in fact many are still deployed and transmitting at this writing. We chose to limit this analysis to the migrations that occurred in 2016. The spring and fall migratory pathways of the 2016 migration from 26 tags were available and suitable for analysis in that year: 11 deployed in 2014, 7 deployed 2015, and 8 deployed 2016. Tracks were suitable for analysis based on having few missing data, with no more than a few days of consecutive missing locations.

Movement data were managed in the online repository Movebank (https://www.movebank.org/), and we used the Track Annotation Service (Dodge et al., 2013) to extract flight subsidy (wind and uplift) data, specific to each PTT location and time of recording that location, along eagle tracks. The Track Annotation Service derives uplift variables from elevation models and weather and atmospheric reanalyses (Bohrer et al., 2012). We followed the Movebank recommendations for interpolation methods; details are below.

Movement Model

We developed a correlated random walk (CRW) movement model to reveal how changes in behavior give rise to the movement paths of migrating eagles. We chose to use a dynamic, time-varying correlation parameter, which represents behavior as a continuum rather than discrete categories, to capture complex behavioral patterns that could occur on multiple temporal and spatial scales (Breed et al., 2012; Auger-Méthé et al., 2017; Jonsen et al., 2019). We believe this approach can offer substantial flexibility, as a continuous range of behaviors is more realistic and, as we show, more naturally allows modeling behavior as a function of covariates.

The basic form of the model was a first-difference CRW presented by Auger-Méthé et al. (2017), which can take the form:

$$\mathbf{x}_i|\mathbf{x}_{i-1},\mathbf{x}_{i-2} \sim \mathcal{N}_2\left(\mathbf{x}_{i-1} + \gamma_i \frac{\Delta t_i}{\Delta t_{i-1}}(\mathbf{x}_{i-1} - \mathbf{x}_{i-2}),\ \mathbf{\Sigma}_i\right), \quad (1)$$

where

$$\mathbf{\Sigma}_i = \begin{bmatrix} \Delta t_i^2 \sigma_x^2 & 0 \\ 0 & \Delta t_i^2 \sigma_y^2 \end{bmatrix}, \quad \sigma_x, \sigma_y > 0. \tag{2}$$

Here, $\Delta t_i = t_i - t_{i-1}$ represents the time interval between Cartesian coordinate vectors $\mathbf{x}_i$ and $\mathbf{x}_{i-1}$ for the observed locations of the animal at times t_i and t_{i-1}. Incorporating autocorrelation in behavior, γ_i constitutes a random walk, such that

$$\gamma_i | \gamma_{i-1} \sim \mathcal{N}\left(\gamma_{i-1},\ \Delta t_i^2 \sigma_\nu^2\right), \quad \sigma_\nu > 0. \tag{3}$$

γ_i correlates displacements (or "steps") and can be interpreted to understand the type of movement, and thus behavior, of migrating individuals: estimates of γ_i closer to one indicate directionally-persistent, larger-scale migratory movement, while estimates of γ_i closer to zero indicate more-tortuous, smaller-scale stopover movement (Breed et al., 2012; Auger-Méthé et al., 2017). Scaling γ_i by $\frac{\Delta t_i}{\Delta t_{i-1}}$ and the variance components by Δt_i^2 allows us to accommodate unequal time intervals (Auger-Méthé et al., 2017), which can arise from a PTT's pre-programmed duty cycles and/or missed location attempts. This assumes that over longer time intervals an animal is likely to move greater distances and that the previous step will have less influence on the current step. Notably, in introducing Δt_i, this CRW essentially becomes a correlated velocity model presented in terms of displacement vectors $(\mathbf{x}_{i-1} - \mathbf{x}_{i-2})$ (Johnson et al., 2008; Blackwell et al., 2015; Gurarie et al., 2017), most closely resembling the autocorrelated velocity model presented by Gurarie et al. (2017). Because location error of GPS data is negligible compared to the movement of most large vertebrates (Hooten et al., 2017), we did not incorporate an observation equation to handle location error. While a covariance parameter could be added to the model, we chose to fix covariance to zero (equation 2), which assumes that movement in the x and y dimensions are independent. This assumption has been suggested to be potentially problematic (Dunn and Gipson, 1977; Blackwell, 1997); however, it is common and has been shown to draw reasonable inference from real data, as well as recover known parameters from simulated data (Breed et al., 2012, 2017; Auger-Méthé et al., 2017; Jonsen et al., 2019). To support this, we compared results from the model assuming zero covariance to one fit assuming equal variance in x and y—like estimating covariance, this ensures invariance under linear transformation of the coordinate system—to illustrate that inference remains unaffected by this assumption (**Appendix 1**).

Extending this CRW to introduce environmental covariates, we first made the assumption that an individual's behavior can be adequately explained by the previous behavior plus some effects of environmental conditions and random noise. This modeling approach and philosophy aligns with the movement ecology paradigm presented by Nathan et al. (2008): An animal's movement path is influenced by its internal state and the environmental conditions it experiences. We modified the behavioral (or internal state) process—previously described above as a pure random walk in one dimension (Equation 3)—similar to a linear model with a *logit* link function. The *logit* link constrains $\gamma_i \in [0, 1]$ and allowed us to model it as a linear combination of continuously-distributed random variables (Jonsen et al., 2019). These variables were different meteorological conditions affecting flight subsidies. Now,

$$\gamma_i' = \log\left(\frac{\gamma_i}{1 - \gamma_i}\right), \tag{4}$$

where

$$\gamma_i' = \gamma_{i-1}' + \mathbf{Z}_i^{\mathrm{T}} \boldsymbol{\beta} + \epsilon_i, \tag{5}$$

$$\epsilon_i \sim \mathcal{N}\left(0,\ \Delta t_i^2 \sigma_\nu^2\right), \tag{6}$$

and $\mathbf{Z}_i^{\mathrm{T}}$ is the row vector of environmental covariates associated with $\mathbf{x}_i$. Each element of the vector $\boldsymbol{\beta}$ is an estimated parameter representing the magnitude and direction of the effect of its respective covariate on the correlation parameter γ_i in addition to the effect of γ_{i-1}. Note that including γ_{i-1} here preserves explicit serial correlation in the behavioral process so that any additional environmental effect is not overestimated. γ_i' is only used to estimate γ_i; any behavioral interpretations are made in terms of γ_i.

Model Fitting

Subsetting Tracks

Of the 26 eagles producing suitable data in 2016, we fit the model to 15 spring and 16 fall adult golden eagle migration tracks recorded by 18 adult males and 8 adult females in 2016. This included both spring and fall migrations for five individuals. In reporting the results, we assumed any individual random effects of including both migrations for these few individuals to be negligible, which seems reasonable given fitted parameters presented in **Table S1** in Appendix. The model was fit only to the migratory periods, plus two fixes prior to departure to ensure valid parameter estimates at the onset of migration. Data were constrained to migratory periods under the following rules: The first migration step was identified as the first directed movement away from what was judged to be an individual's summer (or winter) range with no subsequent return to that range, and the final migration step was defined as the step terminating in the apparent winter (or summer) range. This assignment was usually straightforward; however, in some cases there were apparent pre-migration staging areas. These were not considered part of migration and excluded from the analysis here; movement data from these individuals collected during the breeding and overwintering periods are neither presented nor analyzed here.

Environmental Covariates

Golden eagles can switch between using thermal and orographic uplift as flight subsidies (Lanzone et al., 2012; Katzner et al., 2015), so we included both variables as covariates affecting the correlation parameter in the behavioral process of the CRW (equation 5). Thermal uplift $\mathbf{z}_{tu}$ and orographic uplift $\mathbf{z}_{ou}$ are measured in m/s with $\mathbf{z}_{tu}, \mathbf{z}_{ou} \in [0, \infty)$. Thermal uplift was bilinearly interpolated from European Center for Medium-Range Weather Forecasts (ECMWF) reanalyses, and orographic uplift from the nearest neighbor (grid cell) by pairing National Center for Environmental Predictions (NCEP) North

American Regional Reanalysis (NARR) data with the Advanced Spaceborne Thermal Emission Reflection Radiometer (ASTER) Global Digital Elevation Model (GDEM; Brandes and Ombalski, 2004; Bohrer et al., 2012). We also introduced wind as a covariate in the behavioral process, as it can influence eagle flight as well as the flight and energy landscape of many birds during migration (Shamoun-Baranes et al., 2017). Wind data were bilinearly interpolated from the NCEP NARR u (easterly/zonal) and v (northerly/meridional) components of wind predicted 30 m above ground in m/s, from which we calculated the wind support $\mathbf{z}_{tw}$, such that $\mathbf{z}_{tw} \in (-\infty, \infty)$ (Safi et al., 2013), where positive values correspond to tailwind and negative values headwind. The bearings used to calculate each $z_{tw,i}$ were the compass bearings required to arrive at $\mathbf{x}_{i+1}$ from $\mathbf{x}_i$.

We included a time of day interaction in the model because of clear diurnal effects. This also helped reduce zero inflation, particularly for thermal uplift, which often decays to zero after sunset due to heat flux and atmospheric boundary layer dynamics. To introduce the interaction, we used a dummy variable $\mathbf{z}_0$, such that $z_{0,i} = 0$ when t_i fell after sunset but before sunrise and $z_{0,i} = 1$ when t_i fell after sunrise but before sunset. This assumed behavior was not dependent on the covariates at night—the combination of covariates becomes zero when $z_{0,i} = 0$—which is sensible given observed diurnal behavioral cycles. Sunrise and sunset times local to each GPS point were calculated in R with the "sunriset" function in the package "maptools" (Bivand and Lewin-Koh, 2016; R Core Team, 2016). Writing out the matrix operation in Equation (5), the final overall formulation of the behavioral process for the full model was:

$$\gamma_i' = \gamma_{i-1}' + \left[\beta_0 + \beta_{ou}(z_{ou,i} \times z_{0,i}) + \beta_{tu}(z_{tu,i} \times z_{0,i}) + \beta_{tw}(z_{tw,i} \times z_{0,i})\right] + \epsilon_i, \quad (7)$$

Prior to fitting the model, we followed Gelman et al. (2008) and *log*-transformed the uplift covariates and standardized variance to 0.25. We used a shifted *log*-transformation (Fox and Weisberg, 2019); adding one to the covariates prior to the *log*-transformation preserved zeros (i.e., zeros mapped to zero under the transformation). The distribution of raw wind support data appeared Gaussian, so it was only centered and standardized.

Parameter Estimation and Model Selection

We fit our correlated random walk (CRW) in a Bayesian framework. Because the model has explicit serially correlated parameters, we used Hamiltonian Monte Carlo (HMC) over more conventional Markov-chain Monte Carlo (MCMC; e.g., Metropolis steps) to sample efficiently from a posterior with such correlation.

Gelman et al. (2008) suggested Cauchy priors for logistic regression parameters; however, Ghosh et al. (2015) found that sampling from the posterior can be inefficient due to the fat tails of the Cauchy distribution. We thus chose Student-t priors centered on zero ($\mu = 0$ and $\sigma = 2.5$) with five degrees of freedom as weakly informative priors for the covariate parameters. Weakly informative normal priors were placed on the variance parameters of the model.

We implemented HMC with R and Stan through the package "rstan" (R Core Team, 2016; Stan Development Team, 2016). Working R and Stan code, including details on prior choice, and example data are provided as **Supplementary Material**, as well as supplementary tables and figures (**Appendices 1–3**). The model was fit to each track independently with five chains of 300,000 HMC iterations, including a 200,000 iteration warm-up phase, and retaining every tenth sample. Convergence to the posterior distribution was checked with trace plots, effective sample sizes, posterior plots of parameters, and Gelman diagnostics ($\hat{R}$) for each model fit.

We compared candidate models with leave-one-out cross-validation approximated by Pareto-smoothed importance sampling (PSIS-LOO) in R with the package "loo" (Vehtari et al., 2016, 2017). The candidate models included possible combinations of environmental covariates plus a null CRW model without covariates. To limit model complexity and because we were interested in competing hypotheses about key predictors of behavior, we chose not to include interactions beyond time-of-day. We ranked the models by the expected *log* pointwise predictive density (elpd; i.e., out-of-sample predictive accuracy) transformed onto the deviance scale (looic; Vehtari et al., 2017), which created a measure on the same scale as common information criterion (e.g., AIC) and allowed applying the rules of more traditional information-theoretic model selection (e.g., Burnham and Anderson, 2004). The model with the lowest looic was considered the best fit to the data, but if other models were within two looic of the top model, each, including the top model, were considered equally supported by the data.

To understand how the predictive ability of the full model varied among tracks, we also computed a pointwise average of the elpd for each track (Vehtari et al., 2017). Normalizing by the sample size allowed comparing the out of sample predictive ability of the full model across individual migration tracks (**Table S1** in Appendix). The elpd (and looic), being sums, are otherwise dependent on the sample size for each model fit.

RESULTS

Model Performance and Diagnostics

We fit eight candidate formulations of our CRW model to 31 migration tracks, equating to 248 total model fits. Chain mixing, Gelman diagnostics ($\hat{R}$) close to one, and large effective sample sizes for all parameters indicated convergence to the posterior for most model fits. Posteriors of parameters appeared symmetric, also indicating the model was well behaved (**Figure S1** in Appendix). Across all migration tracks, the full model showed strong evidence of convergence, but for five tracks, we did not consider the null model converged to the posterior (e.g., $\hat{R} > 1.01$). The five migrations for which the null model did not converge were not included from formal model selection.

Behavior During Migration

Median (interquartile range) departure and arrival dates were 5 March (4.5 d) and 27 March (6.4 d) in the spring and 29 September (11.7 d) and 16 November (15.5 d) in the fall. On

TABLE 1 | Summary statistics of flight subsidies encountered by migrating golden eagles that summer in Alaska.

Season	Orographic uplift	Thermal uplift	Wind support
	mean[a] (*s.d.*)	*mean* (*s.d.*)	*mean* (*s.d.*)
Spring	0.41 (0.71)	0.61 (0.48)	2.09 (3.06)
Fall	0.43 (0.71)	0.39 (0.34)	1.37 (3.45)

Variables were interpolated in space and time from weather reanalyses to eagle locations recorded by GPS telemetry. Units for all variables are m/s.
[a]*grand mean across discrete GPS locations with individual migration tracks pooled.*

average, eagles encountered similar orographic uplift in spring and fall but more intense thermal uplift and tailwind in the spring (**Table 1**).

The model revealed that eagles changed their behavior on multiple scales. First, there were very strong daily rhythms in behavior during migration, with birds migrating or moving more slowly and tortuously during the day and stopping at night (**Figures 1**, **2**). Explicitly including a time-of-day interaction could cause a daily rhythm to emerge as an artifact of model specification. However, accounting for serial correlation in behavior (Equation 5) limited that possibility. Additionally, prolonged periods of movement without an apparent daily rhythm suggest that, where daily rhythms are observed they are not a product of model specification (**Figure 2**). Second, there was some evidence of stopover-like behavior, but with individuals continually moving along the migration route while exhibiting less directional persistence in movement (**Figure 3**). The continuation along the migration route while in a stopover-like state is highlighted by track segments extended over space associated with low and intermediate estimates of γ_i (blue/purple in **Figure 3**).

There was also a clear effect of season on movement patterns and behavior. Spring was characterized by straighter, more direct trajectories and punctuated by slower, more tortuous, stopover-like movement; whereas, fall movements were much more tortuous overall and regular patterns in changes in movement rate and/or tortuosity less clear (**Figures 1**–**3**). The distributions of estimated γ values also clearly indicate that daytime movements were most frequently directed migratory moves in the spring; whereas, in the fall, the bimodal distribution indicates more equivalent partitioning between directed migratory moves and slower stopover type movement, with significant time spent exhibiting behaviors associated with intermediate tortuosity and movement rate (**Figure 3**).

Environmental Covariates

While there were differences in some environmental covariates between spring and fall (**Table 1**), parameter estimates from the full model (all covariates) indicate that there was little to no difference in effect of flight subsidies (i.e., wind and uplift) on behavior between spring and fall (**Figure 4**, **Table S1** in Appendix). Including environmental covariates in the behavioral process, though, improved model fit for almost all fitted migrations (**Table 2**). Positive coefficients on the thermal uplift covariate indicate that increasing thermal uplift resulted in more highly-correlated displacements, or migratory movements. Despite that, there were some migration bouts not associated with great thermal uplift (**Figures 1**, **2**). Coefficients close to zero for orographic uplift and wind support indicate that, in general, they were not strong drivers of directionally-persistent movements.

Based on the model selection, the best-fitting formulation of the environmental drivers of the behavioral process was variable across individuals. However, in almost all cases, some form of flight subsidy was used and there was little difference between the spring and fall seasons in the pattern of subsidy use (**Table 2**). The high variability across individuals (**Table S1** in Appendix) was likely due to differing weather patterns and thus subsidy sources encountered and/or used by each eagle as migrations were not synchronous (in time or space) across individuals. In addition, inter-individual variation was much larger than any difference attributable to demographic variables; we found no evidence that difference in sex or age explained patterns of flight subsidy use during migration. Note, though, that all eagles included in this analysis were in adult plumage, so strong age effects would not necessarily be expected.

Comparing the pointwise elpd across tracks revealed that the out of sample predictive ability of the full model varied among individuals (**Table S1** in Appendix). It also showed that predictive ability was greater for fall migrations than spring.

DISCUSSION

Here, we develop and demonstrate how dynamic parameter CRW models fit to GPS data reveal the effects of variable flight subsides available along migration routes. Use of these subsidies gives rise to diverse patterns in the movement of a long-distance soaring migrant. Behavioral changes occur continuously as available subsidies shift over time and space. These key driving mechanisms underlie emergent movement paths, yet such processes are often hidden in the discrete satellite observations available. Our mechanistic modeling approach allowed linking of dynamic meteorology to changes in behavior, and those changes in behavior to the observed movement paths, revealing time series of behaviors more complex than individuals simply apportioning time between migration and stopover.

Model Performance

Incorporating time-varying parameters into movement models has been a relatively infrequently utilized approach (Breed et al., 2012; Auger-Méthé et al., 2017; Jonsen et al., 2019). Here we provide a case study for its utility and developed the approach for achieving practical biological inference about movement processes. Modeling the serial correlation in movement as a function of environmental covariates (equation 4), allowed simultaneous inference of behavior and the effect of environmental covariates on behavior from animal trajectories with regular and irregular duty cycles and containing missing observations. While other methods exist to handle missing data, the behavioral patterns we found would be more difficult to reveal with a state-switching movement model (e.g., hidden Markov models (HMMs); Michelot et al., 2016) because each

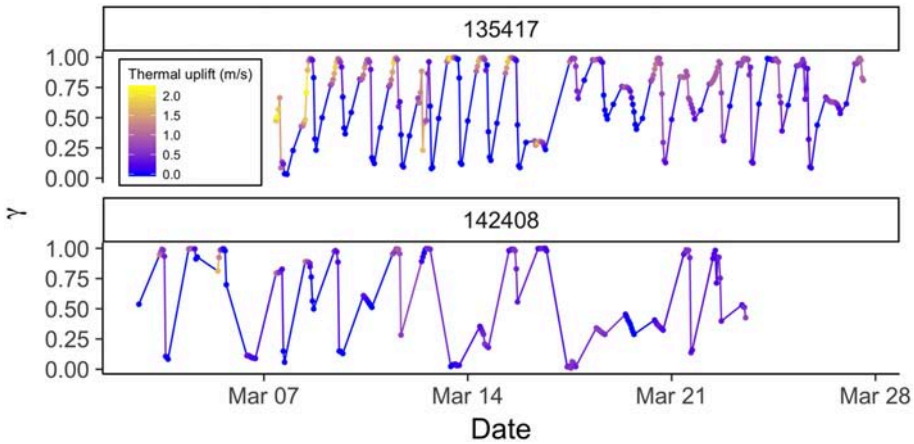

FIGURE 1 | Time series of behavior parameter γ from correlated random walk model with full behavioral process (orographic uplift, thermal uplift, and wind support as predictors) for two golden eagles during spring migration with PTTs reporting on different duty cycles. Upper panel is 13 hourly centered on solar noon plus one at midnight, and the lower panel is 8 hourly centered on solar noon. γ close to one reflect movements associated with migratory behavior, and γ close to zero stopover behavior. Points are times of observations, and lines are linear interpolations between points. Hue indicates intensity of thermal uplift, with yellow indicating greater and blue lower. Note the daily rhythm in behavior associated with intense thermal uplift, stopover periods of one or more days, and the intermediate periods suggesting fly-and-forage.

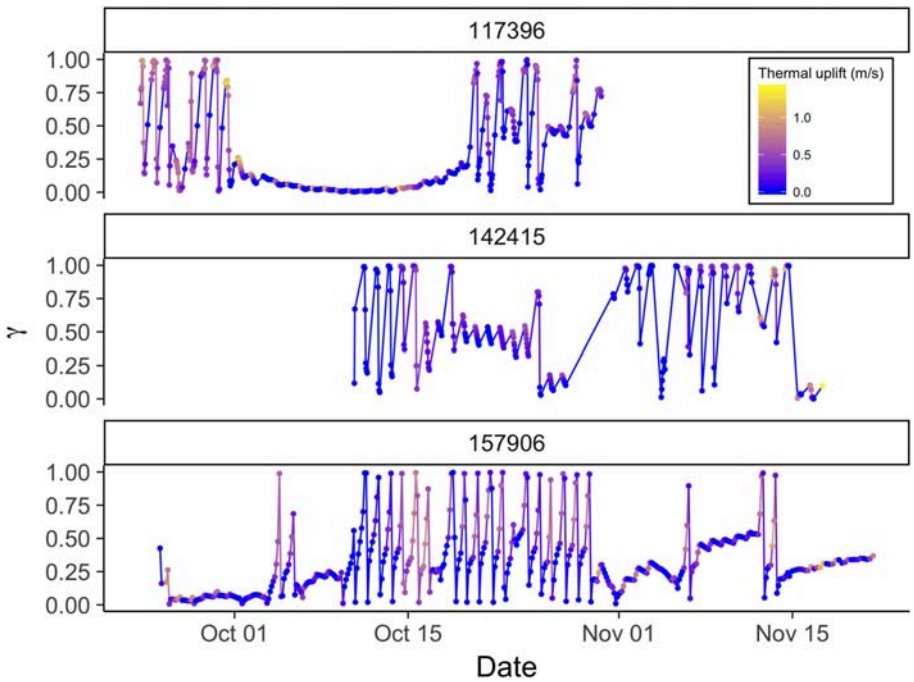

FIGURE 2 | Time series of behavior parameter γ from correlated random walk model with full behavioral process (orographic uplift, thermal uplift, and wind support as predictors) for three golden eagles during fall migration with PTTs reporting on different duty cycles. Upper panel is 13 hourly centered on solar noon plus one at midnight, middle panel is 8 hourly centered on solar noon, and lower panel is fixed 3-h interval. γ close to one reflect movements associated with migratory behavior, and γ close to zero stopover behavior. Points are times of observations, and lines are linear interpolations between points. Hue indicates intensity of thermal uplift, with yellow indicating greater thermal uplift and blue lower. Note the daily rhythm in behavior and extended stopovers as well as periods intermediate values suggesting fly-and-forage.

step would be forced into a discrete behavioral state from a set of usually 2–3 discrete states. Moreover, although hidden-state models have been introduced that have more than five discrete states (e.g., McClintock et al., 2012), these states can require ancillary data streams (e.g., accelerometry) to discriminate and remain extremely difficult to employ and interpret in practice

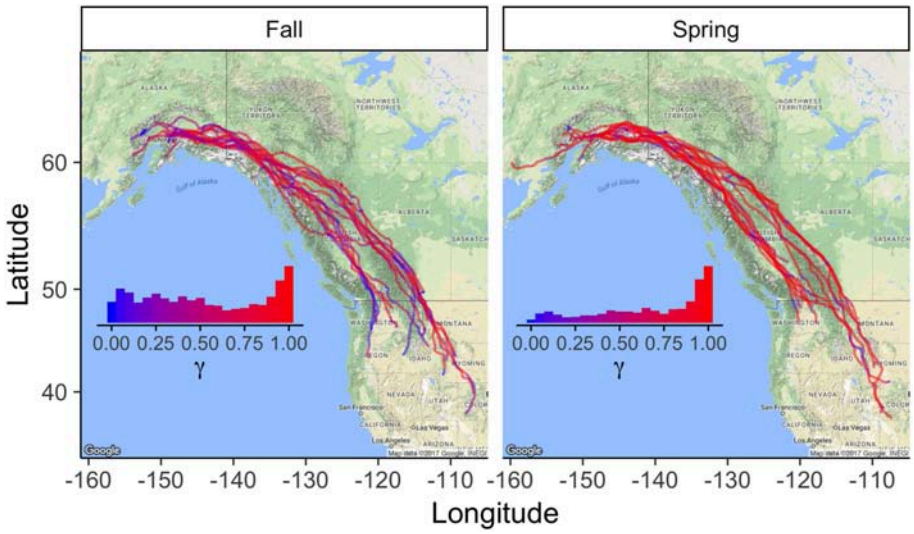

FIGURE 3 | Golden eagle migration trajectories ($N = 15$ spring and $N = 16$ fall). Hue indicates value of behavioral parameter γ estimated with the correlated random walk model with full behavioral process, including orographic uplift, thermal uplift, and wind support as predictors. Insets show the relative frequencies of estimates of γ assigned to the displacements between observed daytime GPS locations. γ close to one reflect movements associated with migratory behavior, and γ close to zero stopover behavior. Daily rhythms, revealed in **Figures 1**, **2**, are not apparent here because the birds moved so little at night.

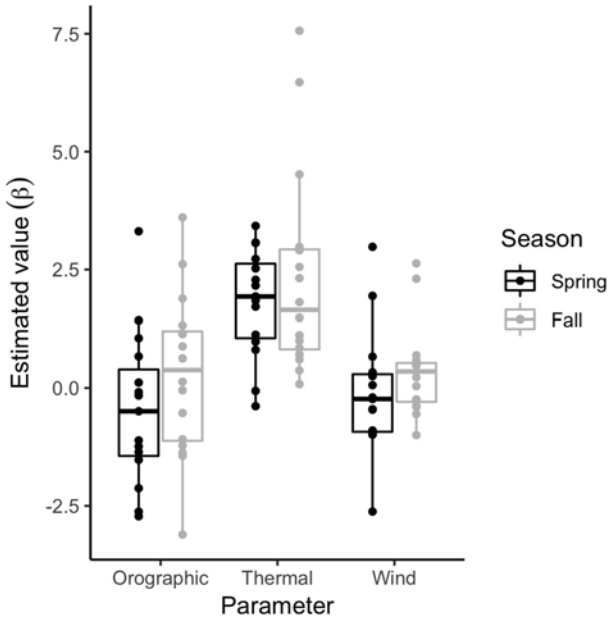

FIGURE 4 | Point estimates of environmental covariate effect parameters (β_{ou}, β_{tu}, β_{tw}) on golden eagle behavior and movements during migration ($N = 15$ spring and $N = 16$ fall). Estimates are from the correlated random walk model with full behavioral process, including orographic uplift, thermal uplift, and wind support as predictors.

TABLE 2 | Number of golden eagle migration tracks recorded by GPS transmitters that each candidate formulation of the behavioral process in the correlated random walk model fit the best, according to approximate leave-one-out cross-validation (**Table S1**).

Model	looic tally[a]		
	Spring	Fall	Total
Full[b]	4	3	7
Therm + twind	2	4	6
Oro + therm	3	3	6
Oro	3	3	6
Therm	2	3	5
Oro + twind	2	2	4
Twind	0	3	3
Null	1	1	2

"therm" corresponds to thermal uplift, "oro" to orographic uplift, and "twind" to wind support.
[a] *tally given to model with lowest information criterion (looic; Vehtari et al., 2016); if one or more models were within two looic of the top model, each was given a tally.*
[b] *oro + therm + twind.*

(Patterson et al., 2017; Pohle et al., 2017). Finally, as HMMs include greater numbers of potential states, they tend to fit better than models with fewer states as judged by classical model selection approaches, such as AIC, even when additional states are neither biologically meaningful nor sensible (Pohle et al., 2017). Implementing models with dynamic parameters that can be interpreted along a behavioral continuum seems a more natural approach for many animal movement questions.

Effects of Tag Programming

While our CRW model revealed the same trends across duty cycles and was generally robust to the different duty cycles (**Figures 1**, **2**), the most detail in daily behavioral rhythms was revealed in tracks with a fixed 3-hr time interval (lower panel in **Figure 2**), as it provided data throughout the 24-h day at regular intervals. The other duty cycles were initially chosen to minimize

the risk of battery depletion overnight. Although generally robust, duty cycles did affect model fitting. HMC permitted Bayesian inference rather efficiently for our model, considering elevated correlation in the posterior of parameters due to the model formulation. Model fits typically took no more than a few hours, though tracks with much more than several hundred locations sometimes took longer. Preliminary fitting of our model with Stan and Template Model Builder (TMB; following Auger-Méthé et al., 2017) suggested that Maximum Likelihood estimation (when fit with TMB) tends to fail frequently when tag programming results in uneven temporal coverage of each day (e.g., our 2015 duty cycle), while Bayesian inference still provided sensible parameter estimates in most cases. Although the model presented herein and the model presented by Auger-Méthé et al. (2017) can make up for irregular time intervals between observations, they do have limitations. Breed et al. (2011) offer an in-depth discussion of tag programming and its effects on model fitting and inference.

Flight Subsidies as Drivers Migration of Behavior

Thermal uplift is a flight subsidy dependent on daily atmospheric boundary layer dynamics, and it was clearly an important driver of the daily rhythm in eagle movement (**Figure 4**, **Table S1** in Appendix). Intense thermal uplift was often associated with the peaks in daily migration bouts (**Figure 1**). The larger magnitude of the thermal uplift effect, relative to orographic uplift, was somewhat surprising, as many individuals in our sample followed the Rocky Mountains, a large potential source of orographic uplift. Golden eagles are known to use orographic uplift as a flight subsidy while migrating through the Appalachian Mountains in eastern North America (Katzner et al., 2015). Much of the Appalachians, however, is characterized by long, unbroken, linearly-oriented ridges. Wind blowing over these ridges produces long stretches of predictable orographic uplift (Rus et al., 2017). The Rocky Mountains, by contrast, are far more rugged and nonuniform, and conditions that might produce suitable upslope winds and mountain waves, as well as strong tailwinds, likely also generate violent turbulence and could impede efficient migratory flight. Soaring raptors have been shown to use small-scale turbulence to achieve subsidized flight (Allen et al., 1996; Mallon et al., 2016); however, unpredictable, nonstationary violent turbulence, which can occur in large, high-elevation mountain ranges (Ralph et al., 1997), could produce unfavorable migratory conditions. The large effect of thermal uplift, thus, could indicate that the Rocky Mountains, a spine that spans almost the entire migration corridor for this population, as well as some areas further west (Bedrosian et al., 2018), serves as a network of thermal streets for migrating eagles (Pennycuick, 1998). More explicitly, intense sun on south facing slopes would be expected to generate linear series of thermals that birds could glide between during both spring and fall migration. It is important to keep in mind that the migrants could capitalize on fine-scale, localized features of certain flight subsidies, like orographic uplift and tailwind, that may not have been captured by the interpolated meteorological data used in our analyses. However, model selection for models including those variables did indicate they explained some variance in eagle movement, which we discuss further below.

Despite meteorological conditions along migration paths that differed between spring and fall and a stark difference between behavioral budgets, our results showed no clear difference in the use of flight subsidies between the spring and fall seasons (**Figure 4**). This finding contrasts with season-specific effects of flight subsidies on golden eagle migration shown phenomenologically in eastern North America, where thermal uplift was shown to be the key subsidy in migratory performance during spring, while wind with some additional support from thermal uplift is most important in the fall (Duerr et al., 2015; Rus et al., 2017). Although our results indicate that eagles use similar flight subsidizing strategies in both seasons, consistent with the differences from the eastern population, the actual behaviors performed during spring and fall migrations differed considerably. In spring, eagles used subsidies to drive a migration that allows timely arrival on the breeding grounds, consistent with a time minimization strategy. In the fall, flight was subsidized to minimize net energy use, which emerged as a much more diverse behavioral repertoire during a slower fall migration (**Figure 3**; Miller et al., 2016). The more rapid and direct flight punctuated by bouts of tortuous, stopover-like movement in the spring (**Figure 3**), suggest eagles pause, refuel, and/or perhaps wait for better migration conditions. This suggests eagles may employ, at least in part, a net energy maximization strategy (Hedenström, 1993; Miller et al., 2016), despite the need for timely arrival on the breeding grounds to avoid fitness costs (Both and Visser, 2001).

The behavioral time series of spring migrations showed some evidence of individuals responding less to thermal uplift as latitude increased (**Figure 1**). This likely corresponded to a general decay in thermal uplift as individuals migrated northward (**Supplementary Material**, **Figure S2** in Appendix). Reduced thermal uplift availability would be expected at higher latitudes due to the larger amounts of remaining spring snowpack and lower solar angles. Thus, golden eagles, and likely other soaring birds, migrating to high latitudes may need to budget behaviors carefully between time minimization and net energy maximization during spring migration to best take advantage of the reduced flight subsidy from thermal uplift and mitigate the greater energy demands of flight at higher latitudes.

While our results show that thermal uplift is the most important flight subsidy for the majority of migrating eagles sampled, the model selection indicated orographic uplift and wind support improved out of sample predictive accuracy and explained some variance in eagle movement. Additionally, variability in top models across individuals (**Table 2**, **Table S1** in Appendix) suggests among-individual variance in flight-subsidizing strategy. Although some of this variability can be attributed to real individual differences in behavioral strategy, it is at least as likely that individuals encountered different subsidies en route and used the subsidies they had available, as migrations across our sample were not synchronous. Given that orographic uplift and wind support parameter estimates were negative or close to zero for many individuals (**Figure 4**, **Table S1**

in Appendix), those covariates likely predicted the periods of slower, more tortuous movements (i.e., γ_i closer to zero). Wind support occurred in top models for more individuals in the fall (**Table 2**, **Table S1** in Appendix), which is consistent with findings from others (McIntyre et al., 2008; Rus et al., 2017) and suggests it may be important during southbound migrations. Additionally, although there was variance among the types and combinations of subsidies used, the null model (without flight subsidies) was the best fitting model for very few tracks (**Table 2**, **Table S1** in Appendix), evidence that weather and flight subsidies are of importance to migrating golden eagles, and likely also to the migrations of similar soaring species. Lastly, we found that the full model had, on average, better predictive ability in fall than spring (**Table S1** in Appendix), suggesting that the weather variables explained more of the variance within movement paths in fall compared to spring; during spring migration, other internal state variables associated with greater time limitation that were not explicitly accounted for in the models were likely responsible for this seasonal difference.

Daily Rhythm and Migratory Pace

The full movement model revealed two clear, nested behavioral patterns in the long-distance migrations of golden eagles. First, there was a daily rhythm where inferred directed migratory movements (i.e., γ_i close to one) occurred most frequently around midday or early afternoon (**Figures 1**, **2**). Mechanistic models of animal movement have revealed diel behavioral rhythms in other taxa (Jonsen et al., 2006). The basic aspects of daily rhythms in vertebrate behavior have hormone controls (Cassone, 1990), but the benefits can include balancing migration progress and foraging bouts (Newton, 2008). Soaring migrants also benefit by synchronizing diel movement patterns with diel atmospheric cycles. That is, consistent with our results, diurnal soaring migrants express a general circadian behavioral rhythm, where flight performance and behavior is strongly tied to thermal development of the planetary boundary layer to take best advantage of atmospherically generated flight subsides (Kerlinger et al., 1985; Leshem and Yom-Tov, 1989; Spaar and Bruderer, 1996, 1997; Mateos-Rodríguez and Liechti, 2012).

The second behavioral pattern revealed was a general stopover pattern, whereby eagles changed behavior for one to several days while en route (**Figures 1–3**). These changes were consistent with searching movements (i.e., γ intermediate or close to zero), possibly representing foraging behavior. In terms of soaring raptors, however, very few reports of movement patterns and behavior during stopovers have been published. Stopover segments have been previously identified by speed or some other metric calculated from tracks, then excluded from subsequent analyses (e.g., Katzner et al., 2015; Vansteelant et al., 2015); occasionally, authors noted apparent enhanced tortuosity but explored it no further (e.g., Vansteelant et al., 2017). On occasions where stopover behavior was considered, classifications based on stay duration and travel distance or speed with hard, often arbitrarily chosen cutoffs between migrating and stopover segments were used (Chevallier et al., 2011; Katzner et al., 2012; Duerr et al., 2015; Miller et al., 2016). In contrast, our modeling framework aligned with the movement ecology paradigm (Nathan et al., 2008); it used the observed data—GPS locations, rather than a derived metric—and a theoretical movement process to infer behavior from movement patterns along tracks on a spectrum ranging from stopped to rapid, directionally-persistent movement.

Our analyses, however, showed that eagles still tended to continue along their migration route during periods of movement most resembling stopover, but with reduced movement rate and directional persistence (**Figures 1–3**). This pattern suggests a joint migration/opportunistic foraging behavior that resembles fly-and-forage migration (Strandberg and Alerstam, 2007; Åkesson et al., 2012; Klaassen et al., 2017), which is consistent with observations of en route hunting behavior of golden eagles by Dekker (1985). Such behavior could be used to maintain balance between time expenses and energy intake, as it allows simultaneous migration progress and foraging.

This pattern does not fall very well within the "stopover" paradigm (Gill, 2007; Newton, 2008), however, as true stops during the migrations we observed were rare, except for expected nightly stops. Rather, migrants seemed to change their *pace*—either by slowing down, moving more tortuously, or both—but still generally moved toward their migratory destination (**Figures 1–3**). Thus, instead of a discrete behavioral framework, whereby migrants switch between two migratory phases (migration and stopover) with very different movement and behavioral properties, we propose that, for certain taxa, a continuous alternative framework "migratory pacing" may be more appropriate and a natural way to interpret en route migratory behavior and movement dynamics. Such taxa would include some and perhaps many soaring migrants, as well some migrating species in other fluid environments such as fishes and marine mammals. Soaring birds, even when energy reserves are relatively depleted, likely can still make steady progress toward a migratory goal when flight subsidies are available. Flapping migrants, on the other hand, would not be able to achieve this as readily, due in part to the greater energy demands for sustained flight, and would require more regular refueling stopovers where migration progress is temporarily completely arrested. Both opportunism in foraging and use of energetic subsidies are likely key characters of fly-and-forage behavior and the ability to change pace of migration without actually stopping, as they relax the need for individuals to stopover in specific, food-rich habitats, which are required by most migrants with less flexibility in food and that lack the morphological specialization to maximally exploit the energetic subsidies available in moving fluids (Gill, 2007; Piersma, 2007).

Our model results revealed seasonal variability in migratory pacing by golden eagles. The tendency for eagles to exhibit movements matching fly-and-forage behavior, and pace their migrations more slowly was most apparent during fall migration. In contrast, spring migration was usually composed of much more punctuated events of slower-paced movements but these were still extended over space (**Figure 3**), indicating the eagles pace their migration and employ a mixed behavioral strategy to some extent in spring as well. During spring, hibernating mammalian prey would be minimally available, leaving carrion, along with a few non-migratory and -hibernating species (e.g.,

ptarmigan *Lagopus* spp. and hare *Lepus* spp.), as major food sources, which could help explain the more punctuated bouts of slower-pacing. Alternatively, individuals could have been slowed by poor weather conditions (Rus et al., 2017). Scavenging large ungulate carcasses would be extremely rewarding in terms of energy accumulation. Much of the carrion we used successfully to capture eagles was large ungulate (e.g., moose *Alces alces*), strongly suggesting that the population we sampled uses carcasses during migration. The bimodal distribution for the behavioral parameter γ in fall shows that eagles tended to budget daytime behaviors approximately equally between rapid, directed and slower-paced movements (**Figure 3**); the high frequency and range of intermediate values are, again, evidence for the more complex fly-and-forage and pacing dynamic, rather than eagles simply switching between stopover and migration. This behavioral complexity might be biologically important, allowing eagles to arrive on winter home ranges in better condition compared to migration strategies that do not incorporate en route foraging opportunity. In contrast to fall, daytime movements in the spring were typically faster-paced (i.e., larger-scale and directionally-persistent; **Figure 3**), consistent with a time minimization strategy, where eagles need to partition time more in favor of migration progress to ensure timely arrival on breeding grounds (Hedenström, 1993; Alerstam, 2011; Miller et al., 2016). We thus see in eagles, and propose more generally, that such pacing varies between and within seasons along the continuum between time minimization and net energy maximization strategies (Alerstam, 2011; Miller et al., 2016). A migrant's pace would be expected to depend upon their energetic demands, energetic subsidies available from the environment, and the importance of arriving at the migration terminus in a timely fashion (Nathan et al., 2008).

Implications and Conclusions

We developed and applied a movement model with time-varying parameters to help reveal the mechanisms underlying the migration of a long-distance soaring migrant that relies on incredibly dynamic flight subsidies. We found that variation in flight subsidies gives rise to changes in migrant behavior with thermal uplift seemingly most important. While these findings might be expected given previous phenomenological analyses (e.g., Duerr et al., 2012; Lanzone et al., 2012; Katzner et al., 2015; Vansteelant et al., 2015; Miller et al., 2016; Shamoun-Baranes et al., 2016; Rus et al., 2017), we were able to show how meteorology is a mechanism influencing changes in movement patterns and thus behavior.

In the behavioral budgets of migrating golden eagles, we identified an expected daily rhythm, as well as evidence for behavioral dynamics that would allow nearly simultaneous foraging and migration, which is greater complexity than the traditional stopover paradigm allows. Migratory pacing, facilitated by fly-and-forage behavior, expands the traditional notion of stopover, whereby a bird migrates until resting and refueling is required, at which point it stops for a brief period in specific habitat suitable for efficient foraging (Gill, 2007; Newton, 2008). This advance was enabled by incorporating time-varying parameters into the movement model, which revealed new behavioral patterns during migration of long-distance soaring migrants. While time-varying, dynamic parameters have been infrequently employed in movement modeling (Breed et al., 2012; Jonsen et al., 2013; Auger-Méthé et al., 2017), we have shown it is a promising approach that can overcome certain limitations in discrete state-switching models and help provide novel insight into animal behavior.

This approach also has potential for further development and for revealing additional new patterns in soaring bird movement; it has already been shown to help provide new insight for other taxa as well (Jonsen et al., 2019). Although we demonstrated the approach for several individual eagles, applying our methods across a larger sample and across more years will increase the inferential strength of our results. For example, previous work found effects of wind support and orographic uplift (e.g., Katzner et al., 2015; Vansteelant et al., 2015), where we, in accounting for an eagles' underlying movement process and the inherent autocorrelation in that process, found that those meteorological variables may be of less importance, at least compared to thermal uplift. It remains unclear though, whether these are system-specific findings or a more general result. Additionally, the model we present has potential to help assess effects of habitat on the movement decisions of soaring birds and other species. One potential avenue for such would be incorporating the model into a resource selection framework (e.g., step selection function). Furthermore, given the movement process is parameterized in terms of coordinate vectors, the position likelihood could be straightforwardly extended to include the z axis to investigate questions regarding flight height of soaring birds or dive depth of marine species, assuming data of acceptable temporal resolution and location error are, or become, available.

DATA AVAILABILITY

All movement data used for this manuscript are managed in the online repository Movebank (https://www.movebank.org/; IDs 17680093 and 19389828). The data contain information considered sensitive by the State of Alaska, but they could be made available at the discretion of the Alaska Department of Fish & Game and U.S. Fish & Wildlife Service. Code to fit the movement model to data and example data are provided as **Supplementary Material**.

ETHICS STATEMENT

Field procedures were conducted following the ADF&G Animal Care & Use Committee protocol #2013-036 and University of Alaska Fairbanks Institutional Animal Care & Use Committee protocol #859448.

AUTHOR CONTRIBUTIONS

JE and GB conceived the ideas of the research presented herein. JE, MA-M, and GB designed analytical methods. TB, CB, and SL designed the field methodology. TB, CB, SL, and JE collected the data. JE analyzed the data, and led the manuscript. All authors

contributed to drafts and editing of the manuscript and provided final approval for publication.

ACKNOWLEDGMENTS

We thank M. Kohan, B. Robinson, T. & D. Hawkins and many others for support in the field and J. Liguori and N. Paprocki for help aging eagles. We also thank T. Avgar, P. Doak, T. Katzner, K. Kielland, C. McIntyre, A. Scharf, and P. Smouse for helpful comments on drafts of the manuscript. Funding was provided by the Alaska Department of Fish & Game (ADF&G) through the federal State Wildlife Grant Program, and the U.S. Fish & Wildlife Service (USFWS) provided PTTs and data. JE was supported by the Calvin J. Lensink Fund during part of the project. MA-M acknowledges the support of the Natural Sciences and Engineering Research Council of Canada. The findings and conclusions of this paper are those of the authors and do not necessarily represent the views of the USFWS. This manuscript has been released as a pre-print at Eisaguirre et al. (2019).

SUPPLEMENTARY MATERIAL

The Supplementary Material for this article can be found online at: https://www.frontiersin.org/articles/10.3389/fevo.2019.00317/full#supplementary-material

REFERENCES

Åkesson, S., Klaassen, R., Holmgren, J., Fox, J. W., and Hedenström, A. (2012). Migration routes and strategies in a highly aerial migrant, the common swift Apus apus, revealed by light-level geolocators. *PLoS ONE* 7:e41195. doi: 10.1371/journal.pone.0041195

Alerstam, T. (1979). Optimal use of wind by migrating birds: combined drift and overcompensation. *J. Theor. Biol.* 79, 341–353. doi: 10.1016/0022-5193(79)90351-5

Alerstam, T. (2011). Optimal bird migration revisited. *J. Ornithol.* 152, 5–23. doi: 10.1007/s10336-011-0694-1

Alerstam, T., and Hedenström, A. (1998). The development of bird migration theory. *J. Avian Biol.* 29, 343–369. doi: 10.2307/3677155

Allen, P. E., Goodrich, L. J., and Bildstein, K. L. (1996). Within- and among-year effects of cold fronts on migrating raptors at Hawk Mountain, Pennsylvania, 1934-1991. *Auk* 113, 329–338. doi: 10.2307/4088899

Auger-Méthé, M., Albertsen, C. M., Jonsen, I. D., Derocher, A. E., Lidgard, D. C., Studholme, K. R., et al. (2017). Spatiotemporal modelling of marine movement data using Template Model Builder (TMB). *Mar. Ecol. Prog. Ser.* 565, 237–249. doi: 10.3354/meps12019

Avgar, T., Street, G., and Fryxell, J. M. (2014). On the adaptive benefits of mammal migration. *Can. J. Zool.* 92, 481–490. doi: 10.1139/cjz-2013-0076

Bedrosian, B. E., Domenech, R., Shreading, A., Hayes, M. M., Booms, T. L., and Barger, C. R. (2018). Migration corridors of adult Golden Eagles originating in northwestern North America. *PLoS ONE* 13:e0205204. doi: 10.1371/journal.pone.0205204

Bivand, R., and Lewin-Koh, N. (2016). *maptools: Tools for Reading and Handling Spatial Objects, Version 0.8-39*.

Blackwell, P. G. (1997). Random diffusion models for animal movement. *Ecol. Model.* 100, 87–102. doi: 10.1016/S0304-3800(97)00153-1

Blackwell, P. G. (2003). Bayesian inference for Markov processes with diffusion and discrete components. *Biometrika* 90, 613–627. doi: 10.1093/biomet/90.3.613

Blackwell, P. G., Niu, M., Lambert, M. S., and Lapoint, S. D. (2015). Exact Bayesian inference for animal movement in continuous time. *Methods Ecol. Evol.* 7, 184–195. doi: 10.1111/2041-210X.12460

Bohrer, G., Brandes, D., Mandel, J. T., Bildstein, K. L., Miller, T. A., Lanzone, M., et al. (2012). Estimating updraft velocity components over large spatial scales: contrasting migration strategies of golden eagles and turkey vultures. *Ecol. Lett.* 15, 96–103. doi: 10.1111/j.1461-0248.2011.01713.x

Both, C., and Visser, M. E. (2001). Adjustment to climate change is constrained by arrival date in a long-distance migrant bird. *Nature* 411, 296–298. doi: 10.1038/35077063

Brandes, D., and Ombalski, D. W. (2004). Modeling raptor migration pathways using a fluid-flow analogy. *J. Rapt. Res.* 38, 195–207.

Breed, G. A., Costa, D. P., Goebel, M. E., and Robinson, P. W. (2011). Electronic tracking tag programming is critical to data collection for behavioral time-series analysis. *Ecosphere* 2:10. doi: 10.1890/ES10-00021.1

Breed, G. A., Costa, D. P., Jonsen, I. D., Robinson, P. W., and Mills-Flemming, J. (2012). State-space methods for more completely capturing behavioral dynamics from animal tracks. *Ecol. Model.* 235–236, 49–58. doi: 10.1016/j.ecolmodel.2012.03.021

Breed, G. A., Golson, E. A., and Tinker, M. T. (2017). Predicting animal home-range structure and transitions using a multistate Ornstein-Uhlenbeck biased random walk. *Ecology* 98, 32–47. doi: 10.1002/ecy.1615

Bridge, E. S., Thorup, K., Bowlin, M. S., Chilson, P. B., Diehl, R. H., Fléron, R. W., et al. (2011). Technology on the Move: recent and Forthcoming Innovations for Tracking Migratory Birds. *BioScience* 61, 689–698. doi: 10.1525/bio.2011.61.9.7

Burnham, K. P., and Anderson, R. (2004). Multimodel inference: understanding AIC and BIC in model selection. *Sociol. Methods Res.* 33, 261–304. doi: 10.1177/0049124104268644

Cassone, V. M. (1990). Effects of melatonin on vertebrate circadian systems. *Trends Neurosci.* 13, 457–464. doi: 10.1016/0166-2236(90)90099-V

Chevallier, D., Le Maho, Y., Brossault, P., Baillon, F., and Massemin, S. (2011). The use of stopover sites by Black Storks (*Ciconia nigra*) migrating between West Europe and West Africa as revealed by satellite telemetry. *J. Ornithol.* 152, 1–13. doi: 10.1007/s10336-010-0536-6

Clark, C. W., and Butler, R. W. (1999). Fitness components of avian migration: a dynamic model of Western Sandpiper migration. *Evol. Ecol. Res.* 1, 443–453.

Dekker, D. (1985). Hunting behavior of golden eagles, Aquila chrysaetos, migrating in southwestern Alberta. *Can. Field-Natur.* 99, 383–385.

Dodge, S., Bohrer, G., Weinzierl, R., Davidson, S. C., Kays, R., Douglas, D., et al. (2013). The environmental-data automated track annotation (Env-DATA) system: linking animal tracks with environmental data. *Movem. Ecol.* 1:3. doi: 10.1186/2051-3933-1-3

Duerr, A. E., Miller, T. A., Lanzone, M., Brandes, D., Cooper, J., O'Malley, K., et al. (2012). Testing an emerging paradigm in migration ecology shows surprising differences in efficiency between flight modes. *PLoS ONE* 7:e35548. doi: 10.1371/journal.pone.0035548

Duerr, A. E., Miller, T. A., Lanzone, M., Brandes, D., Cooper, J., O'Malley, K., et al. (2015). Flight response of slope-soaring birds to seasonal variation in thermal generation. *Funct. Ecol.* 29, 779–790. doi: 10.1111/1365-2435.12381

Dunn, J. E., and Gipson, P. S. (1977). Analysis of radio telemetry data in studies of home range. *Biometrics* 33, 85–101. doi: 10.2307/2529305

Eisaguirre, J. M., Auger-Méthé, M., Barger, C. P., Lewis, S. B., Booms, T. L., and Breed, G. A. (2019). Environmentally-driven dynamic parameters in mechanistic movement models reveal complex migratory pacing in a soaring bird. *bioRxiv [Preprint]*. doi: 10.1101/465427

Fox, J., and Weisberg, S. (2019). *An R Companion to Applied Regression, 3rd Edn*. Thousand Oaks, CA: SAGE Publications Inc.

Gelman, A., Jakulin, A., Pittau, M. G., and Su, Y. S. (2008). A weakly informative default prior distribution for logistic and other regression models. *Ann. Appl. Stat.* 2, 1360–1383. doi: 10.1214/08-AOAS191

Ghosh, J., Li, Y., and Mitra, R. (2015). On the use of Cauchy prior distributions for Bayesian logistic regression. *ArXiv* 1507.07170.

Gill, F. B. (2007). *Ornithology, 3rd Edn*. New York, NY: W. H. Freeman and Company.

Gurarie, E., Fleming, C. H., Fagan, W. F., Laidre, K. L., Hernández-Pliego, J., and Ovaskainen, O. (2017). Correlated velocity models as a fundamental

unit of animal movement: synthesis and applications. *Movem. Ecol.* 5, 1–18. doi: 10.1186/s40462-017-0103-3

Hedenström, A. (1993). Migration by soaring or flapping flight in birds: the relative importance of energy cost and speed. *Philos. Trans. R. Soc. B Biol. Sci.* 342, 353–361. doi: 10.1098/rstb.1993.0164

Hedenström, A. (2008). Adaptations to migration in birds: behavioural strategies, morphology and scaling effects. *Philos. Trans. R. Soc. B* 363, 287–299. doi: 10.1098/rstb.2007.2140

Hooten, M. B., Johnson, D. S., McClintock, B. T., and Morales, J. M. (2017). *Animal Movement: Statistical Models for Telemetry Data*. New York, NY: CRC Press.

Johnson, D. S., London, J. M., Lea, M.-A., and Durban, J. W. (2008). Continuous-time correlated random walk model for animal telemetry data. *Ecology* 89, 1208–1215. doi: 10.1890/07-1032.1

Jonsen, I. D., Basson, M., Bestley, S., Bravington, M. V., Patterson, T. A., Pedersen, M. W., et al. (2013). State-space models for bio-loggers: a methodological road map. *Deep-Sea Res. II Top. Stud. Oceanogr.* 88–89, 34–46. doi: 10.1016/j.dsr2.2012.07.008

Jonsen, I. D., McMahon, C. R., Patterson, T. A., Auger-Méthé, M., Harcourt, R., Hindell, M. A., et al. (2019). Movement responses to environment: fast inference of variation among southern elephant seals with a mixed effects model. *Ecology* 100, 1–8. doi: 10.1002/ecy.2566

Jonsen, I. D., Myers, R. A., and James, M. C. (2006). Robust hierarchical state-space models reveal diel variation in travel rates of migrating leatherback turtles. *J. Anim. Ecol.* 75, 1046–1057. doi: 10.1111/j.1365-2656.2006.01129.x

Kareiva, P. M., and Shigesada, N. (1983). Analyzing insect movement as a correlated random walk. *Oecologia* 56, 234–238. doi: 10.1007/BF00379695

Katzner, T. E., Brandes, D., Miller, T., Lanzone, M., Maisonneuve, C., Tremblay, J. A., et al. (2012). Topography drives migratory flight altitude of golden eagles: implications for on-shore wind energy development. *J. Appl. Ecol.* 49, 1178–1186. doi: 10.1111/j.1365-2664.2012.02185.x

Katzner, T. E., Turk, P. J., Duerr, A. E., Miller, T. A., Lanzone, M. J., Cooper, J. L., et al. (2015). Use of multiple modes of flight subsidy by a soaring terrestrial bird, the golden eagle Aquila chrysaetos, when on migration. *J. R. Soc. Interface* 12:20150530. doi: 10.1098/rsif.2015.0530

Kerlinger, P., Bingman, V., and Able, K. P. (1985). Comparative flight behavior of migrating hawks studied with tracking radar during autumn in Central New York. *Can. J. Zool.* 63, 755–761. doi: 10.1139/z85-110

Klaassen, R. H., Schlaich, A. E., Bouten, W., and Koks, B. J. (2017). Migrating Montagu's harriers frequently interrupt daily flights in both Europe and Africa. *J. Avian Biol.* 48, 180–190. doi: 10.1111/jav.01362

Kochert, M. N., Steenhof, K., McIntyre, C. L., and Craig, E. H. (2002). "Golden Eagle (Aquila chrysaetos)," in *The Birds of North America*, ed A. Poole (Ithaca, NY: Cornell Lab of Ornithology). Available online at: https://birdsna.org/Species-Account/bna/species/684/articles/introduction

Lanzone, M. J., Miller, T. A., Turk, P., Brandes, D., Halverson, C., Maisonneuve, C., et al. (2012). Flight responses by a migratory soaring raptor to changing meteorological conditions. *Biol. Lett.* 8, 710–713. doi: 10.1098/rsbl.2012.0359

Leshem, Y., and Yom-Tov, Y. (1989). The use of thermals by soaring migrants. *Ibis* 183, 667–674. doi: 10.1111/j.1474-919X.1996.tb04768.x

Luschi, P., Hays, G. C., Del Seppia, C., Marsh, R., and Papi, F. (1998). The navigational feats of green sea turtles migrating from Ascension Island investigated by satellite telemetry. *Proc. R. Soc. Lond. Ser. B Biol. Sci.* 265, 2279–2284. doi: 10.1098/rspb.1998.0571

Mallon, J. M., Bildstein, K. L., and Katzner, T. E. (2016). In-flight turbulence benefits soaring birds. *Auk* 133, 79–85. doi: 10.1642/AUK-15-114.1

Mateos-Rodríguez, M., and Liechti, F. (2012). How do diurnal long-distance migrants select flight altitude in relation to wind? *Behav. Ecol.* 23, 403–409. doi: 10.1093/beheco/arr204

McClintock, B. T., King, R., Thomas, L., Matthiopoulos, J., McConnell, B. J., and Morales, J. M. (2012). A general discrete-time modeling framework for animal movement using multistate random walks. *Ecol. Monogr.* 82, 335–349. doi: 10.1890/11-0326.1

McIntyre, C. L., Douglas, D. C., and Collopy, M. W. (2008). Movements of Golden Eagles (*Aquila chrysaetos*) from interior Alaska during their first year of independence. *Auk* 125, 214–224. doi: 10.1525/auk.2008.125.1.214

Michelot, T., and Blackwell, P. G. (2019). State-switching continious-time correlated random walks. *Methods Ecol. Evol.* 10, 637–649. doi: 10.1111/2041-210X.13154

Michelot, T., Langrock, R., and Patterson, T. A. (2016). moveHMM: an R package for the statistical modelling of animal movement data using hidden Markov models. *Methods Ecol. Evol.* 7, 1308–1315. doi: 10.1111/2041-210X.12578

Miller, T. A., Brooks, R. P., Lanzone, M. J., Brandes, D., Cooper, J., Tremblay, J. A., et al. (2016). Limitations and mechanisms influencing the migratory performance of soaring birds. *Ibis* 158, 116–134. doi: 10.1111/ibi.12331

Morales, J. M., Haydon, D. T., Frair, J., Holsinger, K. E., and Fryxell, J. M. (2004). Extracting more out of relocation data: building movement models as mixtures of random walks. *Ecology* 85, 2436–2445. doi: 10.1890/03-0269

Murgatroyd, M., Photopoulou, T., Underhill, L. G., Bouten, W., and Amar, A. (2018). Where eagles soar: fine-resolution tracking reveals the spatiotemporal use of differential soaring modes in a large raptor. *Ecol. Evol.* 8, 6788–6799. doi: 10.1002/ece3.4189

Nathan, R., Getz, W. M., Revilla, E., Holyoak, M., Kadmon, R., Saltz, D., et al. (2008). A movement ecology paradigm for unifying organismal movement research. *Proc. Natl. Acad. Sci. U.S.A.* 105, 19052–19059. doi: 10.1073/pnas.0800375105

Newton, I. (2008). *The Migration Ecology of Birds*. London: Academic Press.

Patterson, T. A., Parton, A., Langrock, R., Blackwell, P. G., Thomas, L., and King, R. (2017). Statistical modelling of individual animal movement: an overview of key methods and a discussion of practical challenges. *AStA Adv. Stat. Anal.* 101, 399–438. doi: 10.1007/s10182-017-0302-7

Pennycuick, C. (1998). Field observations of thermals and thermal streets, and the theory of cross-country soaring flight. *J. Avian Biol.* 29, 33–43. doi: 10.2307/3677338

Pennycuick, C. J. (1971). Soaring behavior and performance of some East African birds, observed from a motor-glider. *Ibis* 114, 178–218. doi: 10.1111/j.1474-919X.1972.tb02603.x

Piersma, T. (2007). Using the power of comparison to explain habitat use and migration strategies of shorebirds worldwide. *J. Ornithol.* 148(Suppl. 1):S45–S59. doi: 10.1007/s10336-007-0240-3

Pirotta, E., Katzner, T., Miller, T. A., Duerr, A. E., Braham, M. A., and New, L. (2018). State-space modelling of the flight behaviour of a soaring bird provides new insights to migratory strategies. *Funct. Ecol.* 32, 2205–2215. doi: 10.1111/1365-2435.13180

Pohle, J., Langrock, R., van Beest, F. M., and Schmidt, N. M. (2017). Selecting the number of states in hidden Markov models: pragmatic solutions illustrated using animal movement. *J. Agricult. Biol. Environ. Stat.* 22, 270–293. doi: 10.1007/s13253-017-0283-8

R Core Team (2016). *R: A Language and Environment for Statistical Computing*. R Core Team.

Ralph, F. M., Neiman, P. J., and Levinson, D. (1997). Lidar observations of a breaking mountain wave associated with extreme turbulence. *Geophys. Res. Lett.* 24, 663–666. doi: 10.1029/97GL00349

Rus, A. I., Duerr, A. E., Miller, T. A., Belthoff, J. R., and Katzner, T. E. (2017). Counterintuitive roles of experience and weather on migratory performance. *Auk* 134, 485–497. doi: 10.1642/AUK-16-147.1

Safi, K., Kranstauber, B., Weinzierl, R., Griffin, L., Rees, E. C., Cabot, D., et al. (2013). Flying with the wind: scale dependency of speed and direction measurements in modelling wind support in avian flight. *Movem. Ecol.* 1:4. doi: 10.1186/2051-3933-1-4

Sawyer, H., Lindzey, F., and McWhirter, D. (2005). Mule deer and pronghorn migration in western Wyoming. *Wildl. Soc. Bull.* 33, 1266–1273. doi: 10.2193/0091-7648(2005)33[1266:MDAPMI]2.0.CO;2

Shamoun-Baranes, J., Bouten, W., Loon, E. E. V., Meijer, C., Camphuysen, C. J., and Shamoun-baranes, J. (2016). Flap or soar? How a flight generalist responds to its aerial environment. *Philos. Trans. R. Soc. B* 371:20150395. doi: 10.1098/rstb.2015.0395

Shamoun-Baranes, J., Bouten, W., and Van Loon, E. E. (2010). Integrating meteorology into research on migration. *Integr. Compar. Biol.* 50, 280–292. doi: 10.1093/icb/icq011

Shamoun-Baranes, J., Liechti, F., and Vansteelant, W. M. (2017). Atmospheric conditions create freeways, detours and tailbacks for migrating birds. *J. Compar. Physiol. A* 203, 509–529. doi: 10.1007/s00359-017-1181-9

Shepard, E. L. C., Wilson, R. P., Rees, W. G., Grundy, E., Lambertucci, S. A., and Vosper, S. B. (2013). Energy landscapes shape animal movement ecology. *Am. Nat.* 182, 298–312. doi: 10.1086/671257

Spaar, R., and Bruderer, B. (1996). Soaring migration of Steppe Eagles Aquila nipalensis in Southern Israel: flight behaviour under various wind and thermal conditions. *J. Avian Biol.* 27, 289–301. doi: 10.2307/3677260

Spaar, R., and Bruderer, B. (1997). Optimal flight behavior of soaring migrants: a case study of migrating steppe buzzards, Buteo buteo vulpinus. *Behav. Ecol.* 8, 288–297. doi: 10.1093/beheco/8.3.288

Stan Development Team (2016). *RStan: The R Interface to Stan, Version 2.10.1*. Stan Development Team.

Strandberg, R., and Alerstam, T. (2007). The strategy of fly-and-forage migration, illustrated for the osprey (Pandion haliaetus). *Behav. Ecol. Sociobiol.* 61, 1865–1875. doi: 10.1007/s00265-007-0426-y

Turchin, P. (1998). *Quantitative Analysis of Movement: Measuring and Modeling Population Redistribution in Animals and Plants*. Sunderland, MA: Sinauer Associates.

Vansteelant, W. M. G., Bouten, W., Klaassen, R. H. G., Koks, B. J., Schlaich, A. E., Diermen, J. V., et al. (2015). Regional and seasonal flight speeds of soaring migrants and the role of weather conditions at hourly and daily scales. *J. Avian Biol.* 46, 25–39. doi: 10.1111/jav.00457

Vansteelant, W. M. G., Shamoun-Baranes, J., McLaren, J., van Diermen, J., and Bouten, W. (2017). Soaring across continents: decision-making of a soaring migrant under changing atmospheric conditions along an entire flyway. *J. Avian Biol.* 48, 887–896. doi: 10.1111/jav.01298

Vehtari, A., Gelman, A., and Gabry, J. (2016). loo: efficient leave-one-out cross-validation and WAIC for Bayesian models. R package version 1.0.0.

Vehtari, A., Gelman, A., and Gabry, J. (2017). Practical Bayesian model evaluation using leave-one-out cross-validation and WAIC. *Stat. Comput.* 27, 1413–1432. doi: 10.1007/s11222-016-9696-4

Watson, J. (2010). *The Golden Eagle, 2nd Edn*. New Haven, CT: Yale University Press.

Conflict of Interest Statement: The authors declare that the research was conducted in the absence of any commercial or financial relationships that could be construed as a potential conflict of interest.

Copyright © 2019 Eisaguirre, Auger-Méthé, Barger, Lewis, Booms and Breed. This is an open-access article distributed under the terms of the Creative Commons Attribution License (CC BY). The use, distribution or reproduction in other forums is permitted, provided the original author(s) and the copyright owner(s) are credited and that the original publication in this journal is cited, in accordance with accepted academic practice. No use, distribution or reproduction is permitted which does not comply with these terms.

frontiers in Ecology and Evolution

ORIGINAL RESEARCH
published: 10 September 2019
doi: 10.3389/fevo.2019.00338

Scales of Blue and Fin Whale Feeding Behavior off California, USA, With Implications for Prey Patchiness

Ladd M. Irvine, Daniel M. Palacios, Barbara A. Lagerquist and Bruce R. Mate*

Department of Fisheries and Wildlife, Marine Mammal Institute, Oregon State University, Newport, OR, United States

Intermediate-duration archival tags were attached to eight blue whales (*Balaenoptera musculus*; four females, three males, one of unknown sex), and five fin whales (*B. physalus*; two females, one male, two of unknown sex) off southern California, USA, in summer 2014 and 2015. Tags logged 1-Hz data from tri-axial accelerometers, magnetometers, and a depth sensor, while acquiring Fastloc GPS locations. Tag attachment duration ranged from 18.3 to 28.9 d for blue whales and 4.9–16.0 d for fin whales, recording 1,030–4,603 dives and 95–3,338 GPS locations per whale across both species. Feeding lunges (identified from accelerometer data) were used to characterize "feeding bouts" (i.e., sequences of feeding dives with <60 min of consecutive non-feeding dives), within-bout behavior, and to examine the spatial distribution of feeding effort. Whales fed near the tagging locations (Point Mugu and San Miguel Island) for up to 7 d before dispersing as far south as Ensenada, Mexico, and north to Cape Mendocino, California. Dispersal within southern California waters differed by sex in both species with males undertaking offshore, circuitous excursions, while females remained more coastal, suggesting that movement patterns on the feeding grounds may not be exclusively related to energy gain. Feeding bout characteristics were similar for both species, with the median bout having 24 dives and lasting 3.3 h for blue whales ($n = 242$), and 19 dives while lasting 2.7 h for fin whales ($n = 59$). Bout duration was positively correlated with the number of feeding lunges per dive within a bout for both species, suggesting whales left poor-quality prey patches quickly but fed intensively for up to 34.9 h when prey was abundant. Feeding bouts occurred further apart as the distance from shore increased, but there was no corresponding difference in the number of feeding lunges per dive, suggesting the whales were feeding at the same rate throughout their range, but that prey was more dispersed in offshore waters. This may be evidence of two feeding strategies, with spatially aggregated foraging around highly localized, topographically forced upwelling centers nearshore, and more dispersed foraging in larger areas of elevated, but patchy, productivity offshore.

Keywords: data loggers, accelerometers, GPS tracking, blue whale, fin whale, feeding behavior, sexual segregation

OPEN ACCESS

Edited by:
Stan Boutin,
University of Alberta, Canada

Reviewed by:
Inger Suzanne Prange,
Appalachian Wildlife Research Institute (United States), United States
Kimberly Goetz,
National Institute of Water and Atmospheric Research (NIWA), New Zealand

****Correspondence:***
Ladd M. Irvine
ladd.irvine@oregonstate.edu

Specialty section:
This article was submitted to Behavioral and Evolutionary Ecology, a section of the journal Frontiers in Ecology and Evolution

Received: *02 February 2019*
Accepted: *23 August 2019*
Published: *10 September 2019*

Citation:
Irvine LM, Palacios DM, Lagerquist BA and Mate BR (2019) Scales of Blue and Fin Whale Feeding Behavior off California, USA, With Implications for Prey Patchiness. Front. Ecol. Evol. 7:338. doi: 10.3389/fevo.2019.00338

INTRODUCTION

Blue (*Balaenoptera musculus*) and fin (*B. physalus*) whales are the two largest species of cetaceans and both occur off the west coast of the United States (USA). Blue whales arrive seasonally beginning in the late spring-early summer and feed on aggregations of krill (*Thysanoessa spinifera and Euphausia pacifica*; Fiedler et al., 1998; Croll et al., 2005; Nickels et al., 2018) until the late fall-early winter when they migrate south to breeding areas off Baja California, Mexico, in the Gulf of California, and near an offshore oceanographic feature called the Costa Rica Dome (Mate et al., 1999; Bailey et al., 2010; Irvine et al., 2014). Although the seasonal movements of fin whales are less well-understood, they occur year-round off southern California (Stafford et al., 2009; Sirovic et al., 2015; Scales et al., 2017) suggesting they do not follow the typical baleen whale pattern of migrating to lower latitudes during the winter to breed and calve (see also Edwards et al., 2015; Geijer et al., 2016; Jiménez López et al., 2019). Fin whales primarily feed on the same species of krill as blue whales, but can also feed on small fish and squid (Pauly et al., 1998). Both species are listed in the USA as "Endangered" under the Endangered Species Act and consequently are labeled as "Depleted" and "Strategic" stocks under the Marine Mammal Protection Act. Additionally, blue whales are considered "Endangered" and fin whales "Vulnerable" according to the IUCN Red List of Threatened Species (Cooke, 2018a,b).

As with other rorquals, blue and fin whales feed by engulfing large volumes of water and schooling prey, then expelling the water through fibrous baleen plates to retain the prey (Goldbogen et al., 2017). This engulfment, termed "lunge feeding," occurs during a rapid acceleration through/into a school of prey and can happen multiple times per dive. The evolution of this feeding behavior is closely tied with the animal's large size, as it allows them to efficiently exploit highly concentrated prey patches (Goldbogen et al., 2011, 2012; Goldbogen and Madsen, 2018). In blue whales this feeding behavior has been shown to vary based on local prey concentrations, indicating they are able to adapt foraging strategies to maximize prey capture (Goldbogen et al., 2015) and energetic efficiency (Hazen et al., 2015).

While sexual differences in distribution and behavior are well-documented in toothed whales (Bigg et al., 1990; Whitehead, 2003; Parsons et al., 2009), such dynamics are less well-understood for rorqual whales, which are largely non-sexually dimorphic, but are known to occur (e.g., Laidre et al., 2009). Sex-based differences in acoustic behavior have been documented for both blue and fin whales, with most of the more complex vocal repertoire of each species being produced exclusively by males and believed to be related to reproduction, while singular calls are produced by both sexes in the context of foraging (Croll et al., 2002; Oleson et al., 2007; Stimpert et al., 2015; Lewis et al., 2018). Further, spatial variability in the type and rate of calling has been documented in blue whales off southern California, suggesting there may be spatial separation of behavioral activities (Lewis and Sirovic, 2018), although a lack of direct observation makes the underlying process unclear, as both feeding and reproductive calls are recorded throughout the feeding season in southern California (Lewis and Sirovic, 2018). Considering that animals in southern California waters are exposed to a variety of regional stressors like ship strikes (Berman-Kowalewski et al., 2010; Redfern et al., 2013) and anthropogenic sound (Goldbogen et al., 2013; DeRuiter et al., 2017), a potential spatial segregation arising from behavioral differences between sexes could lead to disproportionate impacts (Sprogis et al., 2016) over short temporal scales (Pirotta et al., 2018) or on long-term population fitness (Pirotta et al., 2019).

To understand broad-scale ecological patterns arising from observed species distributions, including interactions among sympatric species, it is often relevant to understand how fine-scale behavior influences the larger trend (Evans, 2012). The movements and distribution of blue and fin whales at the scale of the eastern North Pacific Ocean have been described using satellite telemetry (Bailey et al., 2010; Irvine et al., 2014; Scales et al., 2017), ship based surveys (Redfern et al., 2013), and acoustic data (Burtenshaw et al., 2004; Sirovic et al., 2015). However, there is little data to explain how the broad-scale distributions of these animals are influenced by variations in behavior at more local scales. Here we used intermediate-duration data-logging tags to examine the fine-scale movements and diving behavior of blue and fin whales off southern and central California over periods of multiple weeks. Our primary goal was to characterize how feeding behavior varies across this region, including potential differences between the sexes and between the two species, which occur in sympatry in this region. Our results indicate a strong spatial and temporal heterogeneity in blue and fin whale foraging behavior, with implications for prey patchiness and quality. As such, this study provides new insights into the underlying drivers of broad-scale movement and occurrence during the feeding season for two of earth's largest predators.

MATERIALS AND METHODS

Tag Configuration and Deployment

This study used Advanced Dive Behavior (ADB) tags, a configuration of the Wildlife Computers (Seattle, WA, USA) MK-10 time-depth recorder platform, which can record depth, temperature, and tri-axial accelerometer, and magnetometer data at 1-Hz resolution for multiple weeks before releasing from the whale for recovery (Mate et al., 2017). A Fastloc® GPS receiver and patch antenna were included in each tag to acquire GPS-quality locations (Bryant, 2007), along with an Argos Platform Terminal Transmitter for sending GPS location and summarized dive data messages via the satellite-based Argos Data Collection and Location System. Complete details of ADB tag construction and design configuration are provided in Mate et al. (2017).

Tags were deployed on blue and fin whales in southern California waters during August 2014 and July 2015. Field work was supported by the 25.6-m research vessel R/V *Pacific Storm*. Tags were mounted in a semi-implantable stainless steel housing and deployed at close range (2–4 m) from a 6.7-m rigid-hulled inflatable boat using the Air Rocket Transmitter System, a modified compressed-air line-throwing gun (Heide-Jorgensen et al., 2001; Mate et al., 2007). Tags were deployed 1–4.5 m

forward of the dorsal fin of the whale and no more than 20 cm down from the mid-line, following the protocol described in Mate et al. (2007). Tags were programmed to release from their housing for recovery 21 d after the start of field operations or if the tag recorded no change in depth for 24 h, indicating the housing had been shed from the whale and sunk to the bottom with the tag still attached. Following release, tags were located and recovered using an uplink receiver that was capable of acquiring, decoding, and solving Argos-transmitted Fastloc GPS location messages sent by the tags in real time, along with information on the tag's general location and the rate and direction of drift. A discussion of factors affecting attachment duration and tag recovery is presented in Mate et al. (2017).

Whenever possible, skin and blubber samples were collected simultaneously to tagging (on the same surfacing) using a crossbow. Crossbow bolts were fitted with circular cutting tips 4 cm in length and 8 mm in diameter, which removed a plug of skin and blubber from the whale. Sex determination was made from skin samples by amplification of regions on the X and Y chromosomes (Aasen and Medrano, 1990; Gilson et al., 1998).

Data Collection and Transmission

Tags were programmed to collect data from the various sensors (depth, accelerometer, magnetometer, and temperature) at 1 Hz for the duration of the deployment. While deployed, acquisition of a Fastloc GPS location was attempted every 7 min or the next time the whale surfaced after this time had elapsed. All data were stored in an onboard archive for download after tag recovery. The dive summary data from the Argos transmissions were not used in this study, although locations estimated from Argos transmissions (Argos, 2016) were used to examine movements of whales whose tags were not recovered. Further details about ADB tag dive summary messages are described in Mate et al. (2017).

Data Analysis

Maps were made using ArcGIS® software ArcMap™ 10.3 by Esri and the ArcGIS Online Ocean Basemap. Data manipulation and analysis for this study was conducted using Matlab (The Mathworks Inc, 2015) and R (R Core Team, 2018). The same suite of analyses were used for both blue and fin whales, except as noted for cases when data for one species were too limited for complete analyses. To detect feeding lunges, the change in the acceleration vector ("Jerk") was calculated from the accelerometer data as the norm of the difference between consecutive acceleration values (Simon et al., 2012; Allen et al., 2016). The Jerk is thus a measure of rapid changes in acceleration and orientation of the tagged whale. Lunge-feeding events in rorquals are characterized by a peak in Jerk with a coincident increase in the roll angle for multiple seconds, as the whale typically accelerates and rolls when opening its mouth to engulf prey (Goldbogen et al., 2006; Simon et al., 2012; Allen et al., 2016). A subsequent minimum in the Jerk value, as the whale ceases most movement to expel the water and filter out prey, signals the end of the lunge. Together, these three criteria (Jerk maximum, increase in roll, and subsequent Jerk minimum) were used to identify feeding lunges in the data records based on the lunge detection methodology described by Allen et al. (2016), but modified to use a more conservative Jerk peak threshold and without the use of acoustic data. The large number of dives recorded by tags during their deployment periods precluded direct confirmation of each feeding lunge identified by the lunge detection algorithm for the entire data record. Instead, we implemented a validation protocol by randomly selecting 10% of dives from each track and visually reviewing them to estimate the percentage of correctly detected lunges (true positives), falsely detected lunges (false positives), and correctly identified feeding dives (dives with at least one true positive). Validation statistics were summarized for each tag and are presented briefly in the Results section, with a more detailed description in the **Supplementary Material**.

Dive summaries were generated for each track by isolating any submergence >10 m in depth (hereafter a "dive") from the tag's depth record and calculating maximum dive depth, dive duration, and the number of lunges that occurred during the dive. The dive end times were then matched to the nearest GPS location recorded by the tag, as locations were generally collected as the whale surfaced from a dive. If there was not a location within 10 min of a dive, a location was estimated by linear interpolation between the temporally closest GPS locations before and after the dive using the dive time to determine where on the line the location should fall. For tracks with less frequent GPS locations this resulted in linear segments of interpolated dive locations that do not represent the exact movement of the whale.

In order to distinguish between series of related feeding dives, a log-survivorship analysis (Holford, 1980; Gentry and Kooyman, 1986) was conducted on the time between feeding dives (i.e., dives with at least one detected lunge) for each tag record. In this case, the log-survivorship analysis graphically showed the number of feeding dive sequences (on a log scale) as a function of the time between them, and the goal was to identify a point along the curve where the number of feeding dive sequences stabilized as time between feeding dives continued to increase, suggesting a natural break in the data. Sequences of dives defined by this criterion were isolated and labeled "feeding bouts." To assess the horizontal extent of each feeding bout and the overall spatial scale of foraging effort, minimum convex polygons were created using the corresponding dive locations for bouts with at least three GPS locations (i.e., not including bouts with interpolated dive locations; see **Supplementary Figure 1**). We report feeding bout summary statistics including bout duration, time, and distance between consecutive bouts, and distance to the closest bout from the entire track. We also report summaries of dives within each feeding bout, including number of dives per bout, mean maximum dive depth and duration, mean number of lunges per dive, and the number of dives without a lunge. The univariate distributions of feeding bout metrics were assessed graphically using probability density plots, while inter-species comparisons of the distributions were made using Bhattacharyya's similarity coefficient (Bhattacharyya, 1943; Guillerme and Cooper, 2016). When Bhattacharyya's similarity coefficient between two distributions is <0.05, the distributions are significantly different, and when the coefficient is >0.95, the distributions are significantly similar. Values between these two thresholds can be used to indicate the probability of overlap between the distributions but cannot be

used to determine if they are significantly different or similar (Guillerme and Cooper, 2016).

Trends among these metrics were formally assessed using generalized linear mixed models (GLMMs), with the tag number as a random-effect grouping variable to account for differences between individuals, a fixed-effect "species" indicator variable, and an interaction term between the predictor of interest and the species indicator variable when inter-species comparisons were desired (Bolker et al., 2009; Harrison et al., 2018). Variables were log-transformed as needed based on graphical assessment of the data. Models were implemented in R using the lme4 package (Bates et al., 2015) or GLMMadaptive (Rizopoulos, 2019) using a two part/hurdle model if it was necessary to account for zero inflated data (GLMMzi). *P*-values were derived using the lmerTest package (Kuznetsova et al., 2017). We report and discuss *p*-values from these GLMMs in the context of levels of support for the outcome (rather than as a binary threshold of significance), with *p*-values <0.01 offering strong support, *p*-values between 0.01 and 0.1 offering suggestive, but inconclusive support, and *p*-values >0.1 offering no support (Gerrodette, 2011; Greenland et al., 2016; Wasserstein and Lazar, 2016).

To further examine fine-scale differences in feeding behavior between individuals, we isolated sections of tracks where two whales were in proximity to each other. Whales were considered to be in proximity when locations from one track were no more than 1 km away from another whale within 30 min from the time of the location. We present a representative map of these track sections and also report dive summary statistics for each section of track in close proximity to another whale for comparison between individuals.

RESULTS

During this study, eight blue whales were tracked for a median of 22.4 d (range = 18.3–28.9 d; **Table 1**) and five fin whales were tracked for a median of 14.2 d (range = 4.9–16.0 d; **Table 1**). Tags were deployed near Point Mugu in 2014 and off the west end of San Miguel Island in 2015 with the exception of blue Whale # 2015_838, which was deployed near Point Mugu in 2015 (**Figure 1**). All eight blue whale tags and three of five fin whale tags were recovered. In two cases the tags were found on the shore several years after having been thought to be lost.

Tagged animals of both species dispersed as far north as Cape Mendocino in northern California, and as far south as Ensenada, Baja California, Mexico, during their tracking periods (**Figures 2**, **3** and **Supplementary Figure 4**). However, most of the tracks, and the majority of feeding dives (89%) occurred within southern California waters. Two blue whales (Whale # 2014_5650 and Whale # 2015_4177) and one fin whale (Whale # 2014_5685) made a clockwise loop across a large portion of southern California waters. All three of these whales were male, while females remained closer to shore until leaving southern California waters (**Figures 2**, **3**).

The eight blue whale ADB tags recorded a median of 126 dives > 10 m in depth per day (range = 73–207 dives/d; **Table 1**), whereas the three recovered fin whale tags recorded a median of 106 dives/d (range = 84–210 dives/d; **Table 1**). The number of Fastloc GPS locations recorded by the tags varied widely, with recovered blue whale tags recording a median of 72 locations per day (range = 10–139; **Table 1**) and recovered fin whale tags recording a median of 46.5 locations per day (range = 1–99; **Table 1**). Some variability in the number of locations was likely due to different hardware configurations within the tags, as all tags using newer Fastloc v. 3 technology recorded at least 54 locations per day while only one tag using Fastloc v. 1 recorded more than 47 locations per day (**Table 1**; see also Mate et al., 2017).

Validation of the feeding lunge detection algorithm indicated a mean true positive rate of 70.5% (sd = 20.1%) and a mean false positive rate of 13.6% (sd = 10.0%). The mean percentage of correctly identified feeding dives (dives with at least one lunge) was 85.3% (sd = 16.8%), suggesting mis-classified lunges (both false positive or false negative) often occurred during dives with other correctly identified lunges. Additional details of the validation methodology and results are presented in the **Supplementary Materials**.

Tagged whales of both species generally made deeper dives during the daytime than at night (**Supplementary Figures 2, 3** and **Supplementary Table 1**), although there was high variability within and between individuals, and daytime surface feeding was recorded on multiple occasions both visually while in the field and in the data record. Daytime dive depths were deepest near San Miguel Island where maximum dive depths reached 362 m for blue whales and 365 m for fin whales. Dive durations were as long as 30.7 min for blue whales and 23.1 min for fin whales (**Supplementary Figures 2, 3** and **Supplementary Table 1**). Almost no feeding lunges were recorded during dives >20 min in duration for either species. Feeding activity (as measured by lunge-feeding events) generally took place during daylight hours, although nighttime lunges were recorded on some occasions for both species (**Supplementary Figures 2, 3** and **Supplementary Table 1**). Most blue whale feeding effort was concentrated near the tagging areas, with additional areas of elevated feeding effort southwest of San Miguel Island and offshore of central California (**Figure 2** and **Supplementary Figure 4**). Whales tagged near Point Mugu also heavily used the nearshore waters extending south to San Diego. Tagged fin whales showed a similar trend (**Figure 3** and **Supplementary Figure 4**).

Log-survivorship curves for all tags stabilized at 60 min or less (**Supplementary Figure 5**), so a criterion of at least 60 min with no feeding dives was used to differentiate between feeding bouts. A total of 242 blue whale feeding bouts and 59 fin whale feeding bouts were identified in the tag records (**Tables 2**, **3**). For blue whales, the median number of feeding bouts made per whale was higher in 2014 (median = 35, range = 22–38, 4 tags) compared to 2015 (median = 23, range = 17–45, 4 tags), despite tags remaining attached for a median of over 7 d longer in 2015 (**Table 1**). The number of fin whale feeding bouts was more similar across years (range = 13–25 bouts, 3 tags), although the more limited number and duration of tracks was too small for inter-annual comparisons. Across both years, feeding bouts were separated by a median of 5.7 h (range = 1–231.9 h) for

TABLE 1 | Deployment summary for ADB tags attached to eight blue and five fin whales in southern California waters during August 2014 and July 2015.

Species	Year	Tag ID	Sex	Tag generation	Recovered?	Duration (d)	# Dives	# GPS locations	Dives/d	GPS Locs/d	Total Distance (km)
Blue	2014	2014_5644	Female	G3	Yes	19	1,392	185	73	10	1,454
Blue	2014	2014_5650	Male	G4	Yes	20	3,004	2,297	150	115	1,708
Blue	2014	2014_5655	Female	G3	Yes	19.8	4,089	799	207	40	1,563
Blue	2014	2014_5803	Female	G4	Yes	18.3	2,789	2,539	152	139	2,033
Blue	2015	2015_838	Female	G4	Yes	25.9	4,603	3,338	178	129	2,137
Blue	2015	2015_840	Unknown	G3	Yes	24.8	2,252	1,558	91	63	1,610
Blue	2015	2015_4177	Male	G4	Yes	27.5	2,824	1,480	103	54	2,545
Blue	2015	2015_5650	Male	G4	Yes	28.9	2,298	2,337	80	81	2,509
					Median	22.4	2,807	1,928	126	72	1,871
Fin	2014	2014_5685	Male	G3	Yes	14.2	1,188	95	72	6	1,037
Fin	2014	2014_5790	Female	G3	No*	13.3	279	14	21	1	426
Fin	2014	2014_5838	Female	G3	Yes	4.9	1,030	228	210	47	133
Fin	2015	2015_5644	Unknown	G4	No*	15.4	406	12	26	1	1,517
Fin	2015	2015_5654	Unknown	G4	Yes	16	1,695	1,591	106	99	1,370
					Median	14.4	1,030	95	72	6	1,037
					Median (recovered tags)	10.5	1,188	228	106	47	1,037

Data were transmitted through Service Argos, Inc.

Some tags were not recovered due to poor weather and the tag's distance to shore after release (>160 km in some cases) limiting recovery opportunities. See Mate et al. (2017) for additional details.

blue whales and a median of 3.1 h (range = 1–227.6 h) for fin whales, and were generally small in area (median = 5.6 km^2, range = 0.003–546.5 km^2 for blue whales; and median = 7.6 km^2, range = 0.001–317.1 km^2 for fin whales). The median blue whale feeding bout contained 23.5 feeding dives over 3.3 h (range = 4–360 feeding dives and 0.2–34.9 h, respectively), while the median fin whale feeding bout contained 19 feeding dives and lasted 2.7 h (range = 4–142 feeding dives and 0.3–19.6 h, respectively; **Tables 2**, **3**).

Median bout duration for the four female blue whale tags (3.9 h) was twice that of males (1.8 h) although median bout duration of Whale # 2014_5644 (a female) was = 1.9 h. Female feeding bouts had a lower proportion of non-feeding dives than those of males (0.26 vs. 0.38; **Table 2**). The distribution of feeding bout duration was similar for both blue and fin whales (Bhattacharyya's similarity coefficient = 0.934), with a strong peak near 2 h and a secondary peak at 14–15 h (**Figure 4**). Mean feeding lunges per dive within bouts varied substantially for both blue and fin whales, but feeding bout duration increased with increasing mean lunges per dive (GLMM, p-value <0.001), with no significant difference between blue and fin whales (GLMM, interaction p-value = 0.84; **Figure 5**). The median bout duration for one blue whale (Whale # 2015_840, of unknown sex) was 12.2 h, suggesting it fed almost continuously during daylight hours on many days. Another blue whale (# 2015_838) fed continuously for almost 1.5 days (**Table 2** and **Figure 2**).

Comparison of the distributions for closest feeding bout and for the distance to shore of a feeding bout between blue and fin whales (**Figure 4**) using Bhattacharyya's similarity coefficient was inconclusive in terms of providing support for similarity or difference between them, although the probability of overlap was relatively high in both cases (Bhattacharyya's similarity coefficient = 0.840 and 0.833, respectively). Investigation of the distance between closest feeding bouts required accounting for zero-inflated data, as 44% of bouts overlapped spatially with at least one other bout from the same track, resulting in many zero distances. As the distance to shore of a feeding bout increased, the distance between closest feeding bouts also increased (GLMMzi, p-value <0.005), indicating that feeding bouts were more dispersed further offshore (**Figure 5**). However, there was no significant difference in the average number of lunges per dive made within bouts as a function of the distance from shore (GLMM, p-value = 0.77), suggesting the whales were feeding at the same rate throughout the study area. There was suggestive but inconclusive evidence that bouts were more dispersed for fin whales compared to blue whales after accounting for the distance to shore (GLMMzi p-value = 0.093), but there were no inter-species differences in the effect of distance to shore on both the distance to the closest bout (GLMMzi interaction p-value = 0.80) or the number of lunges per dive (GLMM interaction p-value = 0.96).

In two cases, a tagged whale passed through an area without stopping, where another tagged whale of the same species was feeding. Blue Whale # 2015_4177 (a male) passed through an area 1 day after Whale # 2015_840 (of unknown sex) had fed nearly continuously during daylight hours in the same location and more broadly for 12 d (**Supplementary Figure 6**). Similarly, fin

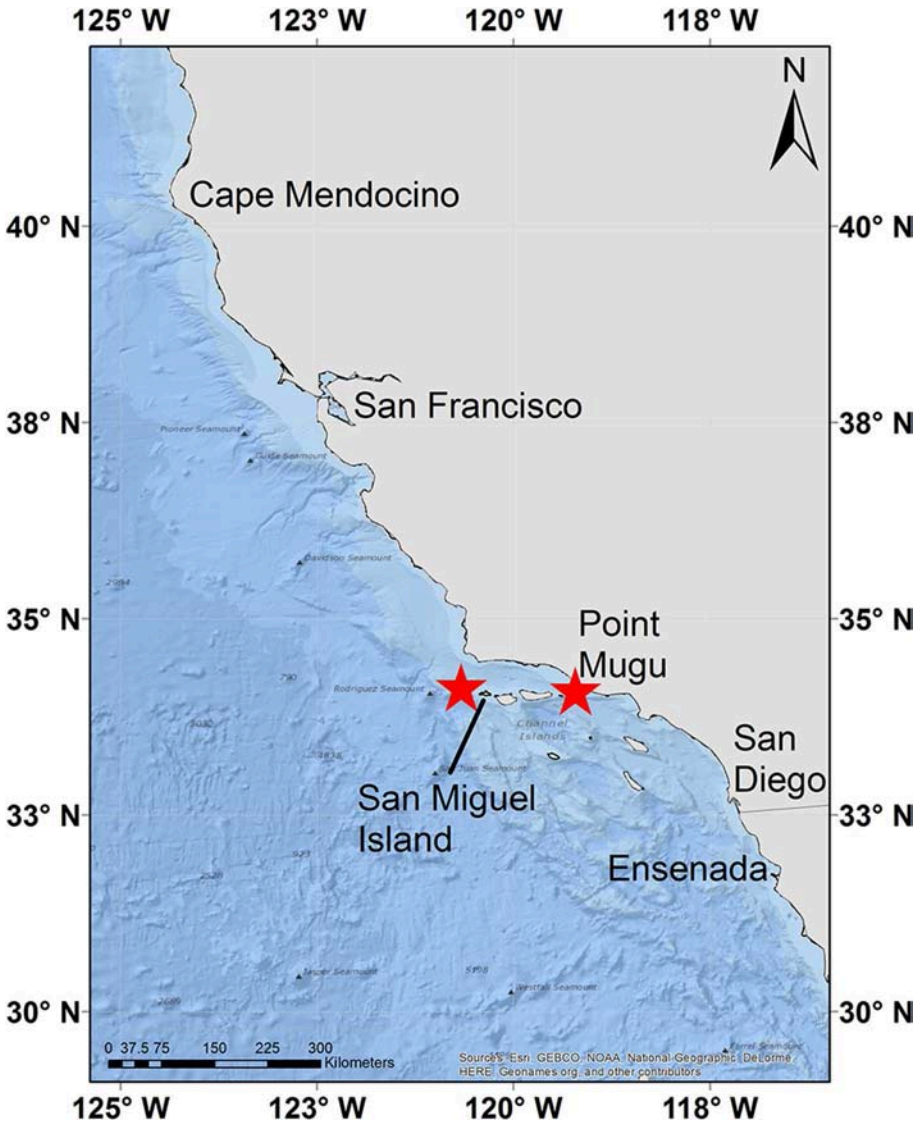

FIGURE 1 | A map of the study area with ADB tag deployment locations marked by red stars.

Whale # 2014_5685 (a male) passed through a different area <1 day before Whale # 2014_5838 (a female) spent 4 d feeding there (not shown). Both whales passing through were male and their movements were part of a larger circuit of southern California waters (**Figures 2**, **3**). The males' dive records were visually reviewed to ensure no feeding lunges had been missed by the lunge detection algorithm during this period of time.

One pair of blue whales each from 2014 to 2015 were recorded feeding in the same geographic space, in one case showing strong differences in dive behavior and in the other showing strong similarities. Whale # 2014_5650 (a male) and Whale # 2014_5803 (a female), tagged off Point Mugu, were in close proximity 13 times across an 8-d period, including times with both feeding and non-feeding behavior (**Supplementary Table 2**). While the characteristics of close-proximity periods were highly variable, Whale # 2014_5803 generally dove more deeply and recorded more feeding lunges than Whale # 2014_5650. On two occasions it dove to over twice the depth as Whale # 2014_5650, and in one instance, was foraging when Whale # 2014_5650 was not (**Supplementary Table 2**). During one of the longer periods of close proximity, both whales appeared to have been behaving similarly after passing closer than 0.5 km from each other (**Supplementary Figures 7, 8**), with both whales making foraging dives to a similar depth. An hour later, Whale # 2014_5803 was feeding at almost twice the depth as Whale # 2014_5650 (**Supplementary Figures 7, 8**) while in the same geographic space. In contrast, in 2015, Whale # 2015_4177 (a male) and Whale # 2015_5650 (also a male), tagged off San Miguel Island, fed in close proximity for 4.5 h on 8 July (the day they were tagged). These whales fed at approximately

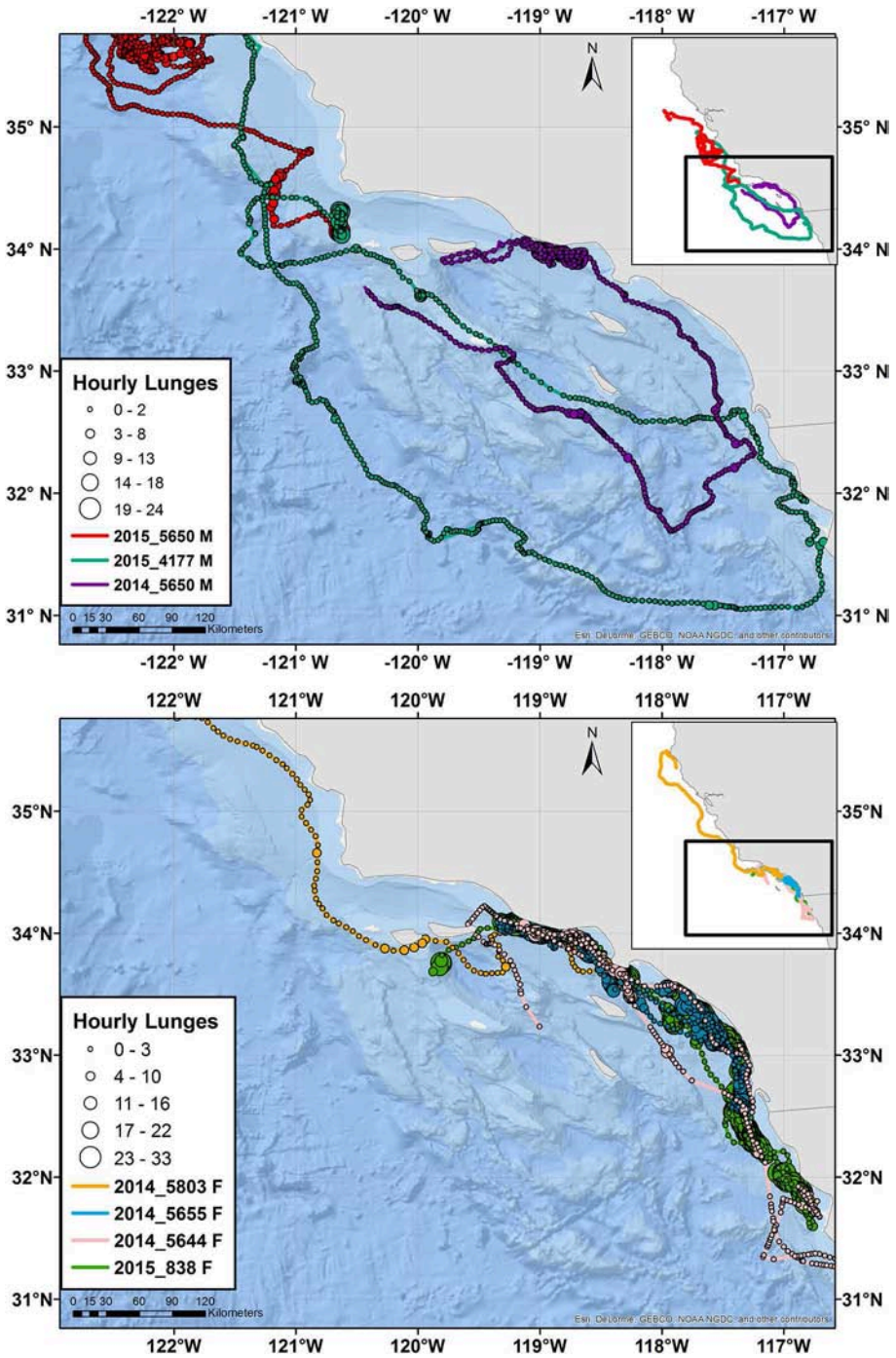

FIGURE 2 | Tracks of male (top) and female (bottom) blue whales instrumented with ADB tags in August 2014 and July 2015. Main maps zoom in on southern California, while the inset maps show the full extent of the tracks with the zoomed region identified by a black square. Circles indicate hourly average locations, with circle size scaling to number of feeding lunges per hour and circle color indicating a different individual, per the tag number shown in the key. The track for one additional blue whale of unknown sex is presented in **Supplementary Figure 4**.

the same depth (mean maximum dive depth = 273 and 212 m, respectively; **Supplementary Figure 9**) and shifted their feeding depth shallower during and after sunset with remarkable synchrony. Three other close-proximity events were recorded in 2015 but all were very limited in duration and number of dives recorded, so will not be presented. Other tagged whales from 2014 may have been in close proximity but the smaller number of Fastloc GPS locations collected by those tags did not

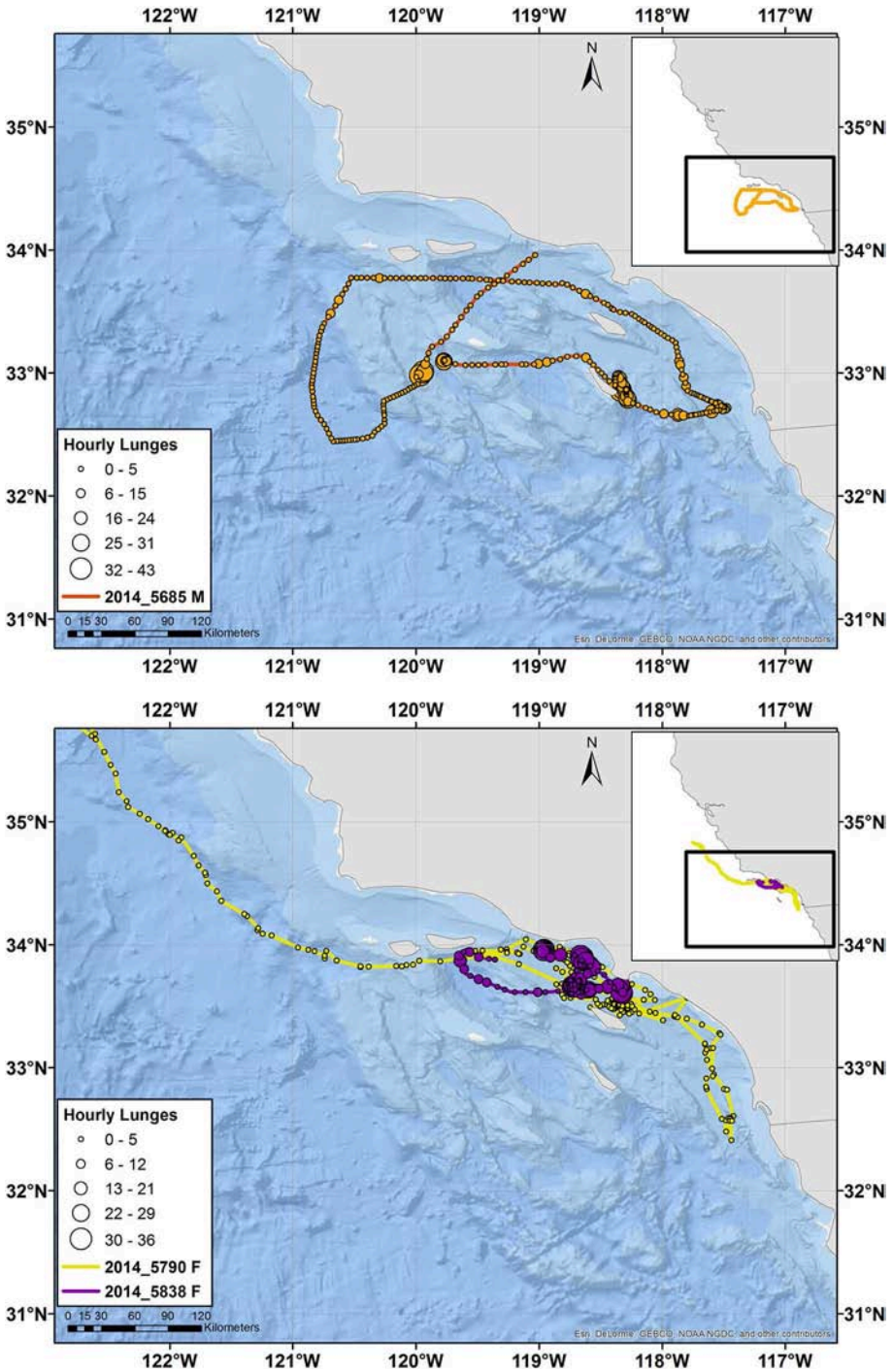

FIGURE 3 | Tracks of male (top) and female (bottom) fin whales instrumented with ADB tags off southern California in August 2014. Main maps zoom in on southern California, while the inset maps show the full extent of the tracks with the zoomed region identified by a black square. Circles indicate hourly average locations, with circle size scaling to number of feeding lunges per hour and circle color indicating a different individual, per the tag number shown in the key. Note that the tag for Whale # 2014_5790 was not recovered and therefore no feeding data are available, but locations received through Argos are shown. The tracks for two additional fin whales of unknown sex are presented in **Supplementary Figure 4**.

allow for fine-scale resolution of their movements. In contrast to blue whales, there were no instances of close proximity between tagged fin whales, or between blue and fin whales, despite both being tagged in the same areas; in one case on the same day (e.g., blue Whale # 2014_5655 and fin Whale # 2014_5685), and in two cases of fin whales (Whale #s 2014_5790 and 2014_5838) being

TABLE 2 | Summary of dives occurring during feeding bouts made by eight blue whales instrumented with ADB tags off southern California in August 2014 and July 2015.

Whale ID	Sex		# Dives/Bout	Mean max dive depth (m)	Mean dive duration (min)	Mean lunges per dive	Dives with no lunges	Bout duration (h)	Area of bout (km^2)	Time to next bout (h)	Dist. to next bout (km)
2014_5644 # bouts = 22	Female	Median	13	83.1	9.4	1	4.5	1.9	2.00E – 02	12.1	11.8
		Min	4	14.7	1.4	0.3	0	0.7	2.60E – 04	1.1	0
		Max	57	206.6	15.7	3.1	27	9.1	4.09E + 01	139.9	214.3
2014_5650 # bouts = 39	Male	Median	14	51.3	6.9	0.7	6	1.5	1.20E + 00	2.5	3.9
		Min	4	15	2.4	0.2	0	0.3	7.00E – 03	1.1	0
		Max	138	253.5	13.1	3.5	85	13.4	5.61E + 01	78.4	184.3
2014_5655 # bouts = 38	Female	Median	36.5	98.3	6.1	1.5	6	4.3	4.20E + 00	3.7	6.4
		Min	5	16.2	2.1	0.2	0	0.5	1.00E – 06	1.1	0
		Max	182	210	11.1	3.3	46	16.2	2.17E + 02	17.5	95
2014_5803 # bouts = 35	Female	Median	28	78.4	6.2	0.8	7	4.0	1.08E + 01	6.6	10.9
		Min	4	33.7	1.7	0.2	0	0.6	1.00E – 01	1.1	0
		Max	191	215.6	11.3	2.9	69	15.3	5.47E + 02	22.3	113.5
2015_838 # bouts = 45	Female	Median	59	108.0	6.2	1.8	14	6.7	1.71E + 01	3.5	6.1
		Min	4	14.9	1.5	0.2	0	0.7	8.75E – 04	1.0	0
		Max	360	170.9	11.2	3.6	95	35.0	1.74E + 02	14.9	85.0
2015_840 # bouts = 19	Unknown	Median	56	134.9	10.1	2.1	9	12.2	2.69E + 01	9	4.5
		Min	5	13	2.9	0.8	0	0.2	3.20E – 04	1.7	0
		Max	100	229.2	13.6	3.5	31	17.4	9.70E + 01	231.9	173.7
2015_4177 # bouts = 17	Male	Median	10	72	11.7	0.8	4	1.9	2.00E + 00	13.5	33.4
		Min	5	23.8	3.9	0.4	1	0.7	1.00E – 04	1.1	0
		Max	74	187.7	17.4	2.2	19	13.5	2.52E + 01	227.6	484
2015_5650 # bouts = 27	Male	Median	7	90.3	11.4	1	3	1.8	1.50E + 00	9.9	8
		Min	4	18.2	2	0.4	0	0.3	3.10E – 04	1.1	0
		Max	81	192.5	14.7	3	22	16.1	2.35E + 02	80.3	205.6

Total bouts = 242.

Feeding bouts are sequences of dives with no more than 60 min between dives with recorded feeding lunges. Unknown sex whales are cases where no biopsy sample was collected. Note that scientific notation is used for the area of bout column, as values spanned several orders of magnitude.

tagged on a day when a tagged blue whale (Whale # 2014_5655) was re-sighted nearby.

DISCUSSION

The data presented here constitute the longest continuous dive behavior records collected to date for blue and fin whales, which allowed us to examine fine-scale behavior over timescales that previously have not been possible. Both species were observed and tagged concurrently during this study and subsequently occupied generally similar areas during their tracking periods, allowing for a comparative analysis between these two species, which occur in sympatry off California. Our focus was on characterizing feeding effort and its scales of variability over periods of multiple weeks. Short- to intermediate-duration (<6 h) feeding bouts were most numerous for both species and there was a positive correlation between bout duration and the number of feeding lunges made per dive within a bout. Blue whales have been shown to adjust their behavior and number of lunges made per dive based on the density of prey in the area (Goldbogen et al., 2015; Hazen et al., 2015), so the correlation between bout duration and number of lunges per dive suggests that the whales tracked in this study left lower-density prey patches quickly, while staying longer, and foraging more intensely, in higher-density patches. Some of the observed short-duration bouts may also represent the whales exhausting a highly localized abundance of prey. These results suggest the whales were following the marginal value theorem (Charnov, 1976), a foundational model of ecological theory that postulates that animals feeding in a patchy environment make decisions about when to depart a patch based on their assessment of its value, with the main prediction being that animals should spend more time in patches of higher quality (Mcnair, 1982).

Feeding bouts were more dispersed further offshore, although the whales were able to feed at the same rate throughout southern California waters, as the number of lunges per dive within a feeding bout did not change as a function of distance to shore. While there was evidence of inter-species differences in relation to distance from shore, they may have been the result of the more extensive use of offshore waters or more limited sample size of fin whales. The greater distance between bouts offshore suggests there may be two feeding strategies, with whales concentrating on highly localized, physically forced upwelling centers nearshore, such as off San Miguel Island (Fiedler et al., 1998), and more dispersed areas of elevated productivity offshore,

TABLE 3 | Summary of dives occurring during feeding bouts made by three fin whales instrumented with ADB tags off southern California in August 2014 and July 2015.

Tag #	Sex		# Dives/Bout	Mean Max Dive Depth (m)	Mean Dive Duration (min)	Mean Lunges per Dive	Dives With No Lunges	Bout Duration (h)	Area Of Bout (km^2)	Time To Next Bout (h)	Dist. To Next Bout (km)
2014_5685	Male	Median	12	63.0	9.2	0.9	5.0	2.5	1.95E + 00	3.0	12.1
# bouts = 25		Min	4	18.8	2.7	0.4	0.0	0.8	1.30E − 05	0.0	0.0
		Max	88	174.7	15.9	3.0	16.0	14.6	1.94E + 02	61.2	81.1
2014_5838	Female	Median	10	72.0	11.7	0.8	4.0	1.9	1.96E + 00	10.0	33.4
# bouts = 13		Min	5	23.8	3.9	0.4	1.0	0.7	1.02E − 04	0.0	0.0
		Max	74	187.7	17.4	2.2	19.0	13.5	2.52E + 01	227.6	484.0
2015_5654	Unknown	Median	22	98.7	8.6	3.3	2.0	3.4	7.64E + 00	6.7	9.4
# bouts = 21		Min	4	28.4	1.7	0.4	0.0	0.7	2.24E − 01	0.0	0.0
		Max	119	247.5	11.7	5.2	55.0	15.7	1.32E + 02	47.8	111.4

Total bouts = 59.

Feeding bouts are sequences of dives with no more than 60 min between dives with feeding lunges. Unknown sex whales are cases where no biopsy sample was collected. Note that scientific notation is used for the area of bout column, as values spanned several orders of magnitude.

likely driven by nearshore productivity that has been advected offshore, or by open-ocean Ekman pumping (Rykaczewski and Checkley, 2008). This has a range of implications for both habitat modeling and abundance estimation, as well as for managers trying to mitigate anthropogenic interactions, as the multiple scales of behavior and occurrence should be accounted for.

The spatial scale of feeding bouts was highly variable within and between individuals. The size of the feeding bout areas was likely an overestimate, as convex hulls are sensitive to irregular, concave shapes of the underlying points (Burgman and Fox, 2003; **Supplementary Figure 1**) and GPS locations were somewhat sparse in some cases, such that the number of locations may have been insufficient to define the true extent of the area being used for feeding. Despite this, median feeding bout size for fin and blue whales (5.6 and 7.6 km^2, respectively) appeared to correspond with the spatial scale of krill patches described off central California (1.8–7.4 km; Santora et al., 2011a). While some of the feeding bouts were significantly larger than the median values (>200 km^2), krill patches up to 18 km in extent have been recorded in some years (Santora et al., 2011a), suggesting the larger feeding bouts may have been indicative of broad-scale areas of elevated krill abundance.

Logistics and expense limit direct study of key prey resources such as krill to fine-scales, from which broader-scale predictions are made and sometimes compared to the distribution of predatory species for validation (Santora et al., 2011a,b, 2014, 2017). Modeled krill distributions have also been used to better understand spatial and temporal aspects of their patchiness (Dorman et al., 2015; Messie and Chavez, 2017). The feeding data for tagged blue and fin whales presented here can offer further insight into the distribution and scale of prey patches across southern and central California waters, similar to how seabird foraging tracks have been used to infer prey availability and patch quality in other areas (Chimienti et al., 2017). Since direct observations of prey abundance were not available for this study, linking blue and fin whale feeding bouts to modeled krill distribution could be an additional step to both validate krill models and tie the overserved whale behavior more directly to prey abundance.

Tagged whale feeding behavior characteristics (like maximum dive depth or lunges per dive) fit into broadly similar ranges across individuals, although there was also evidence of fine-scale variability among individuals within those ranges, exemplified by the instances where two tagged blue whales (Whale # 2014_5803 and Whale # 2014_5650) were feeding in close proximity to one another but at different depths. Without knowing the structure of the prey field, it is difficult to be sure if these differences were related to the individual or the composition of prey being exploited. The observed differences may be a reflection of different individuals having different energetic requirements, allowing some whales to forage less intensively on lower prey concentrations (e.g., less dense prey at shallower depths), different age classes, or different prey species. However, across their entire tracks, Whale # 2014_5803 fed at deeper depths than Whale # 2014_5650, and this trend continued when the two occupied the same geographic space, suggesting the observed variability in dive behavior between individuals was likely due to different foraging strategies. It is not unusual for individuals to use a subset of their population's ecological niche due to variations of intrinsic traits or trade-offs that restrict an individual's ability to generalize (Bolnick et al., 2003). Further work is needed to better understand individual differences in rorqual behavior.

Previous work has found evidence of broad-scale spatial segregation between blue and fin whales off southern California (Fiedler et al., 1998; Irvine et al., 2014; Sirovic et al., 2015; Scales et al., 2017). However, our results showed that feeding behavior of tagged blue and fin whales was similar over a broad scale, with feeding occurring in relatively localized areas (median bout duration = 3.3 and 2.7 h, respectively; median bout area = 5.6 and 7.6 km^2, respectively) and with similar non-feeding periods in between (median time between bouts = 5.7 and 3.1 h, respectively). At finer scales, the characteristics of individual feeding bouts were also similar between the two species, with the

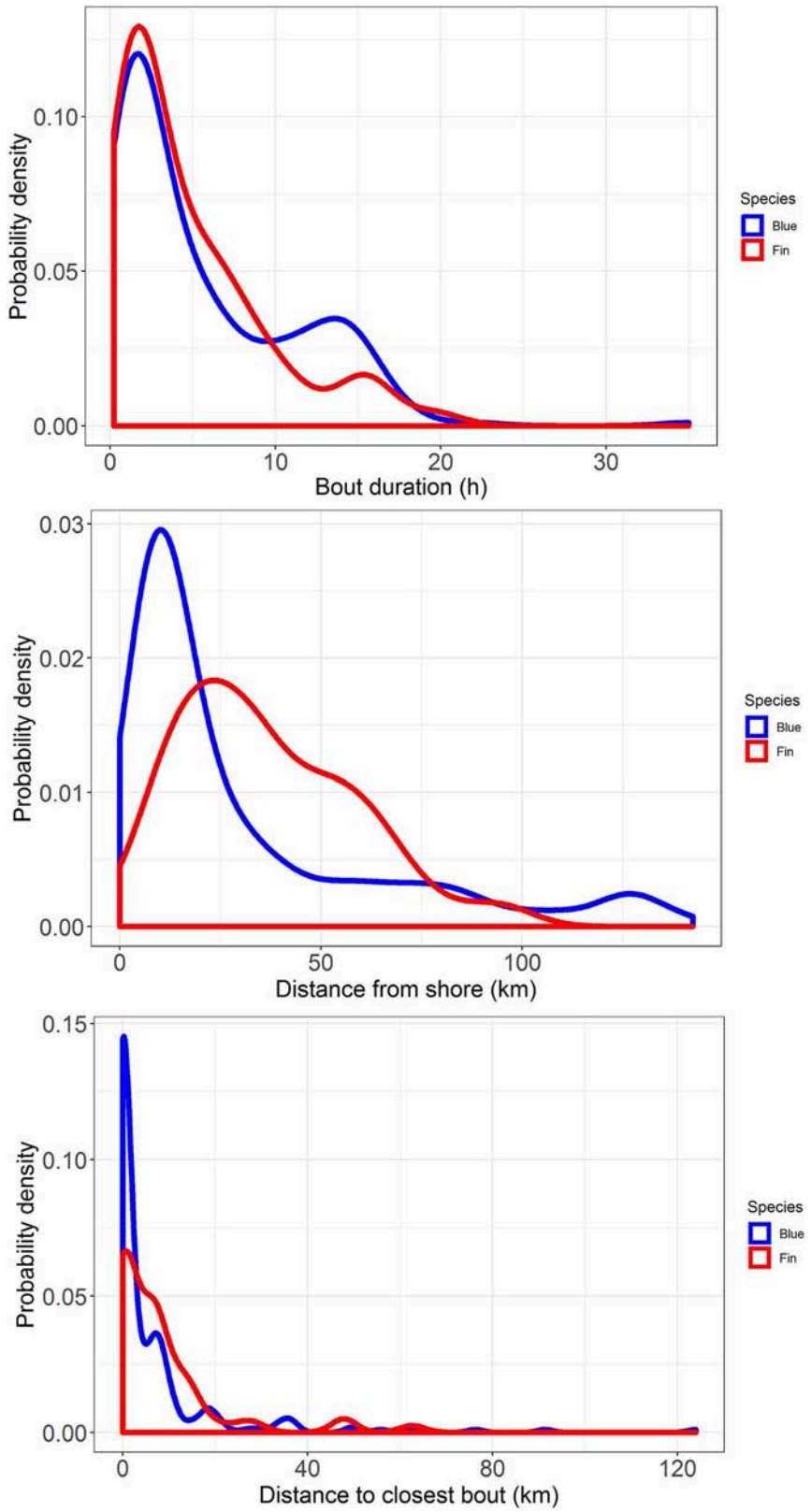

FIGURE 4 | Probability density plots of feeding bout duration **(top)**, distance from shore (middle), and distance to the closest bout **(bottom)** for blue whales (blue lines), and fin whales (red lines) tracked off southern California with ADB tags in August 2014 and July 2015.

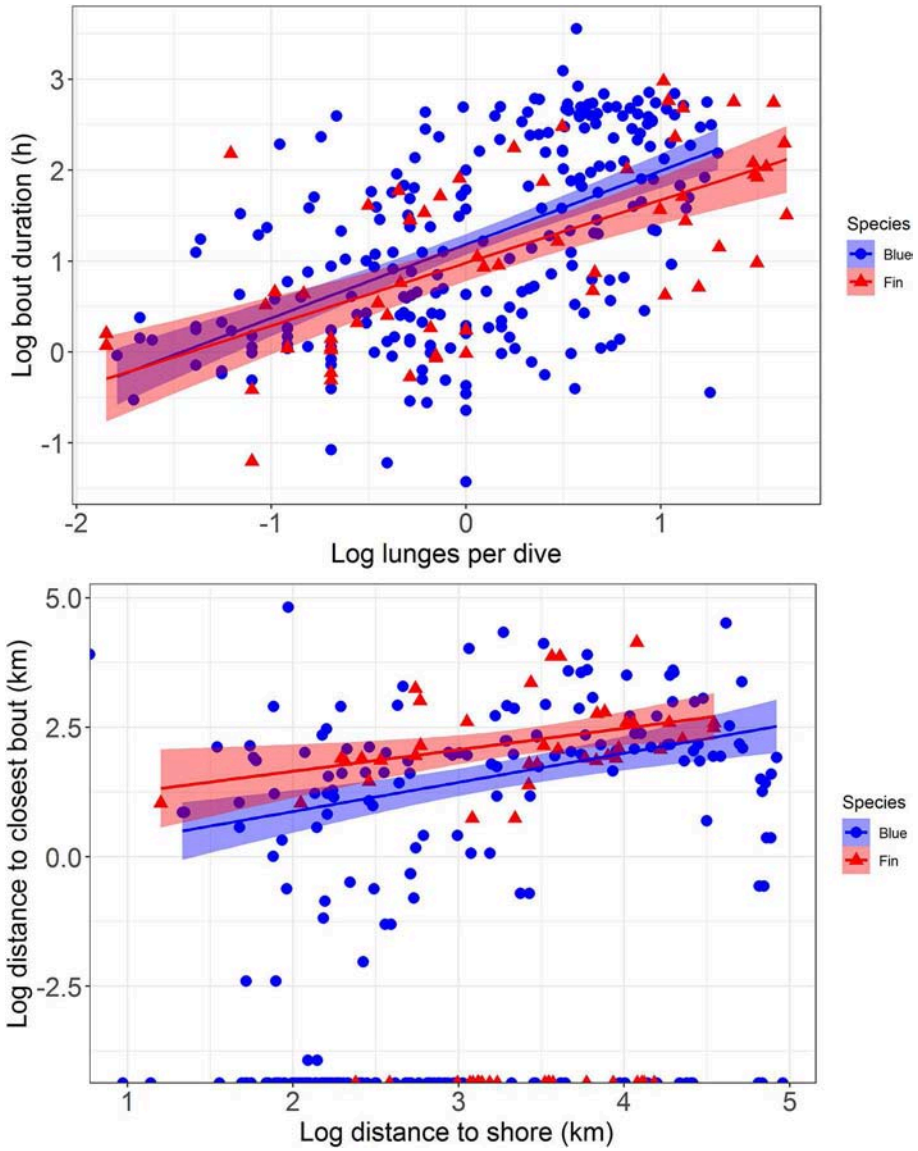

FIGURE 5 | The relationship between average number of feeding lunges per dive within a feeding bout and the duration of that bout **(top)** and the distance to shore of a feeding bout compared to the distance to the next closest bout **(bottom)**, with regression lines and 95% confidence intervals fitted to the data. Data are from blue whales (blue circles and lines) and fin whales (red triangles and lines) tracked with ADB tags off southern California in August 2014 and July 2015.

exception that fin whales recorded a higher maximum number of lunges per dive than blue whales (5.2 vs. 3.6, on average), consistent with previously observed species-specific differences in feeding rates (Friedlaender et al., 2015).

The observed similarities in feeding behaviors between the two species are likely a result of the highly specialized nature of lunge-feeding behavior (Goldbogen et al., 2006, 2011, 2017; Cade et al., 2016) and suggests the whales were feeding on krill given their highly stereotyped behavior (Cade et al., 2016). This further suggests the two species may potentially compete for a similar prey resource. Variations in the target prey species (Fossette et al., 2017), and even life stage of the same krill species (Santora et al., 2010), have also been shown to affect the spatial distribution of sympatric whale species. There was suggestive evidence that fin whale feeding bouts were more dispersed compared to blue whales, so it is possible that fine scale differences in the timing or location of feeding between the two species may be the underlying driver of the previously observed broad-scale differences in spatial distribution (Fiedler et al., 1998; Irvine et al., 2014; Sirovic et al., 2015; Scales et al., 2017). However, without an understanding of the underlying distribution and demographics of the local prey resources, it is difficult to attribute a reason to any inter-species differences in the spatial distribution of fine-scale feeding we observed.

Three tagged whales (two blue and one fin; all males) made clockwise circuits of southern California waters with only limited

feeding effort, despite passing through areas where other tagged whales were feeding. Blue whales have been shown to adjust their dive behavior based on the density of prey in the area (Goldbogen et al., 2015; Hazen et al., 2015), so it is possible they encountered prey in insufficient concentrations for them to feed upon. More broadly, males and females of central-place foragers are known to have different sex-based foraging strategies arising from different energetic requirements during reproduction and resulting in differential exploitation of the offshore and coastal environment (Breed et al., 2006; Austin et al., 2019). A similar process could be driving the observed differences between male blue and fin whales. Alternatively, blue whales are known to engage in social behavior while in southern California (Lomac-MacNair and Smultea, 2016). Visual inspection of the tag records revealed that many dives made by individuals of both species during the circuits of offshore waters had the characteristics of dives made while whales are vocalizing (shallow, flat-bottomed, minimal acceleration; see Calambokidis et al., 2007; Oleson et al., 2007; Stimpert et al., 2015). Additionally, it has been suggested that the better acoustic propagation properties of offshore waters (Sirovic et al., 2015) make them advantageous for reproductive calls (Lewis and Sirovic, 2018). Thus, we speculate these circuits in southern California waters by males of both species were related to reproduction, although we caution that this is based on a rather small number of individuals. Little is known about blue and fin whale breeding behavior, but our interpretation implies that courtship, or at least advertising and searching for a potential mate, may begin while on the feeding grounds.

The potential difference in movement and areas occupied by males and females has the added implication of possible sex-based differences in exposure to regional stressors like anthropogenic sound (Goldbogen et al., 2013; DeRuiter et al., 2017) or ship strikes (Berman-Kowalewski et al., 2010; Redfern et al., 2013), which are of particular concern in the Southern California Bight. Differing levels of exposure to anthropogenic stressors arising from sexual segregation is a common situation for wildlife (Sprogis et al., 2016), and is especially problematic if it occurs to a species where one sex may be more susceptible to such impacts (Symons et al., 2014; Baird et al., 2015). If further studies confirm our observations about sex–specific differences in habitat use (at least within southern California), managers may need to consider mitigation strategies that explicitly address differential impacts based on sex.

The movements of whales on the feeding grounds are generally assumed to be driven by the search for prey, such that fine-scale behavior can be directly linked to broad-scale ecological patterns like distribution. The results presented here support this idea, showing whales of both species quickly left presumably poor-quality prey patches, with the implication that variable prey density drives local whale movements, while the existence of multiple, persistent hotspots of krill aggregation along the west coast of the USA drive the broad-scale seasonal movement pattern (Abrahms et al., 2019; Palacios et al., 2019). However, sex also appeared to influence movement patterns and habitat use, at least within southern California waters. While this result is based on a relatively limited number of individuals, it constitutes a substantial refinement to our understanding of blue and fin whale behavior on the feeding grounds. Continuing to link fine-scale behavior to broader-scale movement is an important area of research, which was aided by the comparatively long data records generated by the tags used in this study. Developing a better understanding of the underlying mechanisms driving broad-scale behavior is critical to better assist the recovery of these endangered whales.

DATA AVAILABILITY

The data used in this study are published as a Movebank Data Repository under a Creative Commons Zero license (Irvine et al., 2019).

ETHICS STATEMENT

Tagging was conducted under the authorization of National Marine Fisheries Service Marine Mammal Protection Act/Endangered Species Act Research/Enhancement Permit No. 14856 and Oregon State University Institutional Animal Care and Use Committee Permit No. 4495.

AUTHOR CONTRIBUTIONS

LI conceived the study, led field work, conducted the data analysis, and drafted the manuscript. DP helped secure funding for the project, helped conceive the study, participated in the field work, consulted on analysis methodologies, and critically reviewed the manuscript. BL participated in the field work, assisted with data analysis, and critically reviewed the manuscript. BM secured funding for the project and critically reviewed the manuscript.

FUNDING

Funding for this study was provided by the Department of the Navy, Commander, U.S. Pacific Fleet under the Marine Species Monitoring Program via subcontract with HDR, Inc. (Contract No. N62470-15-D-8006). We thank Jessica Bredvik (Naval Facilities Engineering Command, Southwest) for technical and contract support, and Kristen Ampela (HDR, Inc.) for project management.

ACKNOWLEDGMENTS

We thank the people who assisted with tagging, including Tomas Follett, Craig Hayslip, Theresa Kirchner, and Natalie Mastick, as well as the crew of the R/V *Pacific Storm*. We thank C. Scott Baker and Debbie Steel of the Cetacean Conservation and Genomics Laboratory at Oregon State University for genetic sex determination of biopsy samples of tagged whales. The Argos Data Collection and Location System was used for this project (http://www.argos-system.org/). The system is operated by CLS. Argos is an international program that relies on instruments

provided by the French Space Agency (CNES) flown on polar-orbiting satellites operated by NOAA, EUMETSAT, and the Indian Space Research Organization (ISRO). We also thank two reviewers and the Topic Editor San Boutin for helpful comments that significantly improved earlier drafts of this manuscript.

SUPPLEMENTARY MATERIAL

The Supplementary Material for this article can be found online at: https://www.frontiersin.org/articles/10.3389/fevo.2019.00338/full#supplementary-material

REFERENCES

Aasen, E., and Medrano, J. F. (1990). Amplification of the ZFY and ZFX genes for sex identification in humans, cattle, sheep and goats. *Bio Technol.* 8, 1279–1281. doi: 10.1038/nbt1290-1279

Abrahms, B., Hazen, E. L., Aikens, E. O., Savoca, M. S., Goldbogen, J. A., Bograd, S. J., et al. (2019). Memory and resource tracking drive blue whale migrations. *Proc. Natl. Acad. Sci. U.S.A.* 116, 5582–5587. doi: 10.1073/pnas.1819031116

Allen, A. N., Goldbogen, J. A., Friedlaender, A. S., and Calambokidis, J. (2016). Development of an automated method of detecting stereotyped feeding events in multisensor data from tagged rorqual whales. *Ecol. Evol.* 6, 7522–7535. doi: 10.1002/ece3.2386

Argos (2016). *Argos User's Manual 2007–2016*. Collecte Localisation Satellites. Available online at: http://www.argos-system.org/manual/

Austin, R. E., De Pascalis, F., Arnould, J. P. Y., Haakonsson, J., Votier, S. C., Ebanks-Petrie, G., et al. (2019). A sex-influenced flexible foraging strategy in a tropical seabird, the magnificent frigatebird. *Mar. Ecol. Prog. Ser.* 611, 203–214. doi: 10.3354/meps12859

Bailey, H., Mate, B. R., Palacios, D. M., Irvine, L., Bograd, S. J., and Costa, D. P. (2010). Behavioural estimation of blue whale movements in the northeast pacific from state-space model analysis of satellite tracks. *Endanger. Species. Res.* 10, 93–106. doi: 10.3354/esr00239

Baird, R. W., Mahaffy, S. D., Gorgone, A. M., Cullins, T., McSweeney, D. J., Oleson, E. M., et al. (2015). False killer whales and fisheries interactions in Hawaiian waters: evidence for sex bias and variation among populations and social groups. *Mar. Mamm. Sci.* 31, 579–590. doi: 10.1111/mms.12177

Bates, D. M., Mächler, M., Bolker, B., Walker, S. (2015). Fitting linear mixed-effects models using lme4. *J. Statist. Softw.* 67, 1–48. doi: 10.18637/jss.v067.i01

Berman-Kowalewski, M., Gulland, F. M. D., Wilkin, S., Calambokidis, J., Mate, B., Cordaro, J., et al. (2010). Association between blue whale (*Balaenoptera musculus*) mortality and ship strikes along the California coast. *Aquat. Mamm.* 36, 59–66. doi: 10.1578/AM.36.1.2010.59

Bhattacharyya, A. K. (1943). On a measure of divergence between two statistical populations defined by their probability distributions. *Bull. Calcutta Math. Soc.* 35, 99–109.

Bigg, M. A., Olesiuk, P. F., Ellis, G. M., Ford, K. B., and Balcomb, K. C III. (1990). Social organization and genealogy of resident killer whales (orcinus orca) in the coastal waters of British Columbia and Washington State. *Rep Int Whal Comm.* 12, 383–405.

Bolker, B. M., Brooks, M. E., Clark, C. J., Geange, S. W., Poulsen, J. R., Stevens, M. H., et al. (2009). Generalized linear mixed models: a practical guide for ecology and evolution. *Trends Ecol. Evol.* 24, 127–135. doi: 10.1016/j.tree.2008.10.008

Bolnick, D. I., Svanbäck, R., Fordyce, J. A., Yang, L. H., Davis, J. M., Hulsey, C. D., et al. (2003). The ecology of individuals: incidence and implications of individual specialization. *Am. Nat.* 161, 1–28. doi: 10.1086/343878

Breed, G. A., Bowen, W. D., McMillan, J. I., and Leonard, M. L. (2006). Sexual segregation of seasonal foraging habitats in a non-migratory marine mammal. *Proc. R. Soc. B-Biol. Sci.* 273, 2319–2326. doi: 10.1098/rspb.2006.3581

Bryant, E. (2007). *2D Location Accuracy Statistics for Fastloc Cores Running Firmware Versions 2.2 & 2.3.* Wildtrack Telemetry Systems Ltd., 6.

Burgman, M. A., and Fox, J. C. (2003). Bias in species range estimates from minimum convex polygons: implications for conservation and options for improved planning. *Anim. Conserv.* 6, 19–28. doi: 10.1017/S1367943003003044

Burtenshaw, J. C., Oleson, E. M., Hildebrand, J. A., McDonald, M. A., Andrew, R. K., Howe, B. M., et al. (2004). Acoustic and satellite remote sensing of blue whale seasonality and habitat in the Northeast Pacific. *Deep Sea Res.* 51, 967–986. doi: 10.1016/j.dsr2.2004.06.020

Cade, D. E., Friedlaender, A. S., Calambokidis, J., and Goldbogen, J. A. (2016). Kinematic diversity in rorqual whale feeding mechanisms. *Curr. Biol.* 26, 2617–2624. doi: 10.1016/j.cub.2016.07.037

Calambokidis, J., Schorr, G. S., Steiger, G. H., Francis, J., Bakhtiari, M., Marshall, G., et al. (2007). Insights into the underwater diving, feeding, and calling behavior of blue whales from a suction-cup-attached video-imaging tag (Crittercam). *Mar. Technol. Soc. J.* 41, 19–29. doi: 10.4031/002533207787441980

Charnov, E. L. (1976). Optimal foraging, the marginal value theorem. *Theor. Popul. Biol.* 9, 129–136. doi: 10.1016/0040-5809(76)90040-X

Chimienti, M., Cornulier, T., Owen, E., Bolton, M., Davies, I. M., Travis, J. M. J., et al. (2017). Taking movement data to new depths: inferring prey availability and patch profitability from seabird foraging behavior. *Ecol. Evol.* 7, 10252–10265. doi: 10.1002/ece3.3551

Cooke, J. G. (2018a). *Balaenoptera musculus. IUCN Red List Threat. Species* 2018:e.T2477A50226195. doi: 10.2305/IUCN.UK.2018-2.RLTS.T2477A50226195.en

Cooke, J. G. (2018b). *Balaenoptera physalus. IUCN Red List Threat. Species* 2018: e.T2478A50349982. doi: 10.2305/IUCN.UK.2018-2.RLTS.T2478A50349982.en

Croll, D. A., Clark, C. W., Acevedo, A., Tershy, B., Flores, S., Gedamke, J., et al. (2002). Only male fin whales sing loud songs. *Nature* 417:809. doi: 10.1038/417809a

Croll, D. A., Marinovic, B., Benson, S., Chavez, F. P., Black, N., Ternullo, R., et al. (2005). From wind to whales: trophic links in a coastal upwelling system. *Mar. Ecol. Prog. Ser.* 289, 117–130. doi: 10.3354/meps289117

DeRuiter, S. L., Langrock, R., Skirbutas, T., Goldbogen, J. A., Calambokidis, J., Friedlaender, A. S., et al. (2017). A multivariate mixed hidden Markov model for blue whale behaviour and responses to sound exposure. *Ann. Appl. Stat.* 11, 362–392. doi: 10.1214/16-AOAS1008

Dorman, J. G., Sydeman, W. J., Garcia-Reyes, M., Zeno, R. A., and Santora, J. A. (2015). Modeling krill aggregations in the central-northern California Current. *Mar. Ecol. Prog. Ser.* 528, 87–99. doi: 10.3354/meps11253

Edwards, E. F., Hall, C., Moore, T. J., Sheredy, C., and Redfern, J. V. (2015). Global distribution of fin whales balaenoptera physalus in the post-whaling era (1980-2012). *Mamm. Rev.* 45, 197–214. doi: 10.1111/mam.12048

Evans, M. R. (2012). Modelling ecological systems in a changing world. *Philos. Trans. R. Soc. Lond. B Biol. Sci.* 367, 181–190. doi: 10.1098/rstb.2011.0172

Fiedler, P. C., Reilly, S. B., Hewitt, R. P., Demer, D., Philbrick, V. A., Smith, S., et al. (1998). Blue whale habitat and prey in the California Channel Islands. *Deep Sea Res.* 45, 1781–1801. doi: 10.1016/S0967-0645(98)80017-9

Fossette, S., Abrahms, B., Hazen, E. L., Bograd, S. J., Zilliacus, K. M., Calambokidis, J., et al. (2017). Resource partitioning facilitates coexistence in sympatric cetaceans in the California Current. *Ecol. Evol.* 7, 9085–9097. doi: 10.1002/ece3.3409

Friedlaender, A. S., Goldbogen, J. A., Hazen, E. L., Calambokidis, J., and Southall, B. L. (2015). Feeding performance by sympatric blue and fin whales exploiting a common prey resource. *Mar. Mamm. Sci.* 31, 345–354. doi: 10.1111/mms.12134

Geijer, C. K. A., Notarbartolo di Sciara, G., and Panigada, S. (2016). Mysticete migration revisited: are mediterranean fin whales an anomaly? *Mamm. Rev.* 46, 284–296. doi: 10.1111/mam.12069

Gentry, R. L., and Kooyman, G. C. (1986). *Furs Seals: Maternal Strategies on Land and at Sea. Furs Seals: Maternal Strategies on Land and at Sea*. Princeton, NJ: Princeton University Press.

Gerrodette, T. (2011). Inference without significance: measuring support for hypotheses rather than rejecting them. *Mar. Ecol.* 32, 404–418. doi: 10.1111/j.1439-0485.2011.00466.x

Gilson, A., Syvanen, M., Levine, K., and Banks, J. (1998). Deer gender determination by polymerase chain reaction: validation study and application to tissues, bloodstains, and hair forensic samples from california. *Med. Microbiol. Immunol.* 84, 159–169.

Goldbogen, J. A., Cade, D. E., Calambokidis, J., Friedlaender, A. S., Potvin, J., Segre, P. S., et al. (2017). How baleen whales feed: the biomechanics of engulfment and filtration. *Ann. Rev. Mar. Sci.* 9, 367–386. doi: 10.1146/annurev-marine-122414-033905

Goldbogen, J. A., Calambokidis, J., Croll, D. A., McKennaet, M. F., Oleson, E., Potvin, J., et al. (2012). Scaling of lunge-feeding performance in rorqual whales: mass-specific energy expenditure increases with body size and progressively limits diving capacity. *Funct. Ecol.* 26, 216–226. doi: 10.1111/j.1365-2435.2011.01905.x

Goldbogen, J. A., Calambokidis, J., Oleson, E., Potvin, J., Pyenson, N. D., Schorr, G., et al. (2011). Mechanics, hydrodynamics and energetics of blue whale lunge feeding: efficiency dependence on krill density. *J. Exp. Biol.* 214, 698–699. doi: 10.1242/jeb.054726

Goldbogen, J. A., Calambokidis, J., Shadwick, R. E., Oleson, E. M., McDonald, M. A., and Hildebrand, J. A. (2006). Kinematics of foraging dives and lunge-feeding in fin whales. *J. Exp. Biol.* 209 (Pt 7):1231–1244. doi: 10.1242/jeb.02135

Goldbogen, J. A., Hazen, E. L., Friedlaender, A. S., Calambokidis, J., DeRuiter, S. L., Stimpert, A. K., et al. (2015). Prey density and distribution drive the three-dimensional foraging strategies of the largest filter feeder. *Funct. Ecol.* 29, 951–961. doi: 10.1111/1365-2435.12395

Goldbogen, J. A., and Madsen, P. T. (2018). The evolution of foraging capacity and gigantism in cetaceans. *J. Exp. Biol.* 221 (Pt 11):jeb166033. doi: 10.1242/jeb.166033

Goldbogen, J. A., Southall, B. L., DeRuiter, S. L., Calambokidis, J., Friedlaender, A. S., Hazen, E. L., et al. (2013). Blue whales respond to simulated mid-frequency military sonar. *Proc. Biol. Sci.* 280:20130657. doi: 10.1098/rspb.2013.0657

Greenland, S., Senn, S. J., Rothman, K. J., Carlin, J. B., Poole, C., Goodman, S. N., et al. (2016). Statistical tests, P values, confidence intervals, and power: a guide to misinterpretations. *Eur. J. Epidemiol.* 31, 337–350. doi: 10.1007/s10654-016-0149-3

Guillerme, T., and Cooper, N. (2016). Effects of missing data on topological inference using a total evidence approach. *Mol. Phylogenet. Evol.* 94(Pt A), 146–158. doi: 10.1016/j.ympev.2015.08.023

Harrison, X. A., Donaldson, L., Correa-Cano, M. E., Evans, J., Fisher, D. N., Goodwin, C. E. D., et al. (2018). A brief introduction to mixed effects modelling and multi-model inference in ecology. *PeerJ.* 6:e4794. doi: 10.7287/peerj.preprints.3113

Hazen, E. L., Friedlaender, A. S., and Goldbogen, J. A. (2015). Blue whales (*Balaenoptera musculus*) optimize foraging efficiency by balancing oxygen use and energy gain as a function of prey density. *Sci. Adv.* 1:e1500469. doi: 10.1126/sciadv.1500469

Heide-Jorgensen, M. P., Kleivane, L., Oien, N., Laidre, K. L., and Jensen, M. V. (2001). A new technique for deploying satellite transmitters on baleen whales: tracking a blue whale (*Balaenoptera musculus*) in the north atlantic. *Mar. Mamm. Sci.* 17, 949–954. doi: 10.1111/j.1748-7692.2001.tb01309.x

Holford, T. R. (1980). The analysis of rates and of survivorship using log-linear models. *Biometrics* 36, 299–305. doi: 10.2307/2529982

Irvine, L. M., Mate, B. R., Winsor, M. H., Palacios, D. M., Bograd, S. J., Costa, D. P., et al. (2014). Spatial and temporal occurrence of blue whales off the U.S. West coast, with implications for management. *PLoS ONE* 9:e102959. doi: 10.1371/journal.pone.0102959

Irvine, L. M., Palacios, D. M., Lagerquist, B. A., Mate, B. R., and Follett, T. M. (2019). Data from: scales of blue and fin whale feeding behavior off California, USA, with implications for prey patchiness. *Movebank Data Repos.* doi: 10.5441/001/1.47h576f2

Kuznetsova, A., Brockhoff, P. B., and Christensen, R. H. B. (2017). Lmertest package: tests in linear mixed effects models. *J. Stat. Softw.* 82, 1–26. doi: 10.18637/jss.v082.i13

Laidre, K. L., Heagerty, P. J., Heide-Jorgensen, M. P., Witting, L., and Simon, M. (2009). Sexual segregation of common minke whales (*Balaenoptera acutorostrata*) in greenland, and the influence of sea temperature on the sex ratio of catches. *ICES J. Mar. Sci.* 66, 2253–2266. doi: 10.1093/icesjms/fsp191

Lewis, L. A., Calambokidis, J., Stimpert, A. K., Fahlbusch, J., Friedlaender, A. S., McKenna, M. F., et al. (2018). Context-dependent variability in blue whale acoustic behaviour. *R. Soc. Open Sci.* 5:180241. doi: 10.1098/rsos.180241

Lewis, L. A., and Sirovic, A. (2018). Variability in blue whale acoustic behavior off southern california. *Mar. Mamm. Sci.* 34, 311–329. doi: 10.1111/mms.12458

Lomac-MacNair, K., and Smultea, M. (2016). Blue whale (*Balaenoptera musculus*) behavior and group dynamics as observed from an aircraft off southern California. *Anim. Behav. Cogn.* 3, 1–21 doi: 10.12966/abc.02.01.2016

López, J. M. E., Palacios, D. M., Jaramillo Legorreta, A., Urbán R, J., and Mate, B. R. (2019). Fin whale movements in the Gulf of California, Mexico, from satellite telemetry. *PLoS ONE* 14:e0209324. doi: 10.1371/journal.pone.0209324

Mate, B., Mesecar, R., and Lagerquist, B. (2007). The evolution of satellite-monitored radio tags for large whales: one laboratory's experience. *Deep-Sea Res. II* 54, 224–247. doi: 10.1016/j.dsr2.2006.11.021

Mate, B. R., Irvine, L. M., and Palacios, D. M. (2017). The development of an intermediate-duration tag to characterize the diving behavior of large whales. *Ecol. Evol.* 7, 585–595. doi: 10.1002/ece3.2649

Mate, B. R., Lagerquist, B. A., and Calambokidis, J. (1999). Movements of North Pacific blue whales during the feeding season off southern California and their southern fall migration. *Mar. Mamm. Sci.* 15, 1246–1257. doi: 10.1111/j.1748-7692.1999.tb00888.x

The Mathworks Inc. (2015). *Matlab 2015b [Software].* Natick, MA: The Mathworks Inc.

Mcnair, J. N. (1982). Optimal giving-up times and the marginal value theorem. *Am. Nat.* 119, 511–529. doi: 10.1086/283929

Messie, M., and Chavez, F. P. (2017). Nutrient supply, surface currents, and plankton dynamics predict zooplankton hotspots in coastal upwelling systems. *Geophys. Res. Lett.* 44, 8979–8986. doi: 10.1002/2017GL074322

Nickels, C. F., Sala, L. M., and Ohman, M. D. (2018). The morphology of euphausiid mandibles used to assess selective predation by blue whales in the southern sector of the California Current system. *J. Crust. Biol.* 38, 563–573. doi: 10.1093/jcbiol/ruy062

Oleson, E. M., Calambokidis, J., Burgess, W. C., McDonald, M. A., LeDuc, C. A., and Hildebrand, J. A. (2007). Behavioral context of call production by eastern north pacific blue whales. *Mar. Ecol. Prog. Ser.* 330, 269–284. doi: 10.3354/meps330269

Palacios, D. M., Bailey, H., Becker, E. A., Bograd, S. J., DeAngelis, M. L., Forney, K. A., et al. (2019). Ecological correlates of blue whale movement behavior and its predictability in the California Current ecosystem during the summer-fall feeding season. *Mov. Ecol.* 7:26. doi: 10.1186/s40462-019-0164-6

Parsons, K. M., Balcomb, K. C., Ford, J. K. B., and Durban, J. W. (2009). The social dynamics of southern resident killer whales and conservation implications for this endangered population. *Anim. Behav.* 77, 963–971. doi: 10.1016/j.anbehav.2009.01.018

Pauly, D., Trites, A. W., Capuli, E., Christensen, V. (1998). Diet composition and trophic levels of marine mammals. *ICES J. Mar. Sci.* 55, 467–481. doi: 10.1006/jmsc.1997.0280

Pirotta, E., Mangel, M., Costa, D. P., Goldbogen, J., Harwood, J., Hin, V., et al. (2019). Anthropogenic disturbance in a changing environment: modelling lifetime reproductive success to predict the consequences of multiple stressors on a migratory population. *Oikos*. 128, 1340–1357. doi: 10.1111/oik.06146

Pirotta, E., Mangel, M., Costa, D. P., Mate, B., Goldbogen, J. A., Palacios, D. M., et al. (2018). A dynamic state model of migratory behavior and physiology to assess the consequences of environmental variation and anthropogenic disturbance on marine vertebrates. *Am. Nat.* 191, E40–E56. doi: 10.1086/695135

R Core Team (2018). *R: A Language and Environment for Statistical Computing*. Vienna: R Foundation for Statistical Computing.

Redfern, J. V., McKenna, M. F., Moore, T. J., Calambokidis, J., Deangelis, M. L., Becker, E. A., et al. (2013). Assessing the risk of ships striking large whales in marine spatial planning. *Conserv. Biol.* 27, 292–302. doi: 10.1111/cobi.12029

Rizopoulos, D. (2019). *Glmmadaptive: Generalized Linear Mixed Models Using Adaptive Gaussian Quadrature*. R package version 0.6-0. Available online at: https://cran.R-project.Org/package=glmmadaptive (accessed May 14, 2019).

Rykaczewski, R. R., and Checkley, D. M. (2008). Influence of ocean winds on the pelagic ecosystem in upwelling regions. *Proc. Natl. Acad. Sci. U.S.A.* 105, 1965–1970. doi: 10.1073/pnas.0711777105

Santora, J. A., Dorman, J. G., and Sydeman, W. J. (2017). Modeling spatiotemporal dynamics of krill aggregations: size, intensity, persistence, and coherence with seabirds. *Ecography* 40, 1300–1314. doi: 10.1111/ecog.02250

Santora, J. A., Ralston, S., and Sydeman, W. J. (2011a). Spatial organization of krill and seabirds in the central california current. *ICES J. Mar. Sci.* 68, 1391–1402. doi: 10.1093/icesjms/fsr046

Santora, J. A., Reiss, C. S., Loeb, V. J., and Veit, R. R. (2010). Spatial association between hotspots of baleen whales and demographic patterns of antarctic krill euphausia superba suggests size-dependent predation. *Mar. Ecol. Prog. Ser.* 405, 255–269. doi: 10.3354/meps08513

Santora, J. A., Schroeder, I. D., and Loeb, V. J. (2014). Spatial assessment of fin whale hotspots and their association with krill within an important antarctic feeding and fishing ground. *Mar. Biol.* 161, 2293–2305. doi: 10.1007/s00227-014-2506-7

Santora, J. A., Sydeman, W. J., Schroeder, I. D., Wells, B. K., and Field, J. C. (2011b). Mesoscale structure and oceanographic determinants of krill hotspots in the california current: implications for trophic transfer and conservation. *Prog. Oceanograph.* 91, 397–409. doi: 10.1016/j.pocean.2011.04.002

Scales, K. L., Schorr, G. S., Hazen, E. L., Bograd, S. J., Miller, P. I., Andrews, R. D., et al. (2017). Should I stay or should I go? *Modelling year-round habitat suitability and drivers of residency for* fin whales in the california current. *Diver. Distrib.* 23, 1204–1215. doi: 10.1111/ddi.12611

Simon, M., Johnson, M., and Madsen, P. T. (2012). Keeping momentum with a mouthful of water: behavior and kinematics of humpback whale lunge feeding. *J. Exp. Biol.* 215, 3785–3798. doi: 10.1242/jeb.071092

Sirovic, A., Rice, A., Chou, E., Hildebrand, J. A., Wiggins, S. M., Roch, M. A., et al. (2015). Seven years of blue and fin whale call abundance in the Southern California Bight. *Endang. Species Res.* 28, 61–76. doi: 10.3354/esr00676

Sprogis, K. R., Raudino, H. C., Rankin, R., MacLeod, C. D., and Bejde, L. (2016). Home range size of adult indo-pacific bottlenose dolphins (*tursiops aduncus*) in a coastal and estuarine system is habitat and sex-specific. *Mar. Mamm. Sci.* 32, 287–308. doi: 10.1111/mms.12260

Stafford, K. M., Citta, J. J., Moore, S. E., Daher, M. A., and George, J. E. (2009). Environmental correlates of blue and fin whale call detections in the north pacific ocean from 1997–2002. *Mar. Ecol. Prog. Ser.* 395, 37–53. doi: 10.3354/meps08362

Stimpert, A. K., DeRuiter, S. L., Falcone, E. A., Joseph, J., Douglas, A. B., Moretti, D. J., et al. (2015). Sound production and associated behavior of tagged fin whales (*balaenoptera physalus*) in the southern california bight. *Anim. Biotel.* 3:23. doi: 10.1186/s40317-015-0058-3

Symons, J., Pirotta, E., and Lusseau, D. (2014). Sex differences in risk perception in deep-diving bottlenose dolphins leads to decreased foraging efficiency when exposed to human disturbance. *J. Appl. Ecol.* 51, 1584–1592. doi: 10.1111/1365-2664.12337

Wasserstein, R. L., and Lazar, N. A. (2016). The asa statement on *p*-values: context, process, and purpose. *Am. Stat.* 70, 129–133. doi: 10.1080/00031305.2016.1154108

Whitehead, H. (2003). *Sperm Whale Societies: Social Evolution in the Ocean. Sperm Whale Societies: Social Evolution in the Ocean.* Chicago: University of Chicago Press.

Conflict of Interest Statement: The authors declare that the research was conducted in the absence of any commercial or financial relationships that could be construed as a potential conflict of interest.

Copyright © 2019 Irvine, Palacios, Lagerquist and Mate. This is an open-access article distributed under the terms of the Creative Commons Attribution License (CC BY). The use, distribution or reproduction in other forums is permitted, provided the original author(s) and the copyright owner(s) are credited and that the original publication in this journal is cited, in accordance with accepted academic practice. No use, distribution or reproduction is permitted which does not comply with these terms.

frontiers in Ecology and Evolution

ORIGINAL RESEARCH
published: 24 September 2019
doi: 10.3389/fevo.2019.00333

Matches and Mismatches Between Seabird Distributions Estimated From At-Sea Surveys and Concurrent Individual-Level Tracking

Matthew J. Carroll[1], Ewan D. Wakefield[1,2], Emily S. Scragg[1], Ellie Owen[1], Simon Pinder[1], Mark Bolton[1], James J. Waggitt[3] and Peter G. H. Evans[3,4]*

[1] Royal Society for the Protection of Birds Centre for Conservation Science, The Lodge, Sandy, United Kingdom, [2] Institute of Biodiversity Animal Health and Comparative Medicine, College of Medical, Veterinary and Life Sciences, University of Glasgow, Glasgow, United Kingdom, [3] School of Ocean Sciences, Bangor University, Bangor, United Kingdom, [4] Sea Watch Foundation, Amlwch, United Kingdom

Mapping the distribution of seabirds at sea is fundamental to understanding their ecology and making informed decisions on their conservation. Until recently, estimates of at-sea distributions were generally derived from boat-based visual surveys. Increasingly however, seabird tracking is seen as an alternative but each has potential biases. To compare distributions from the two methods, we carried out simultaneous boat-based surveys and GPS tracking in the Minch, western Scotland, in June 2015. Over 8 days, boat transect surveys covered 950 km, within a study area of ~6,700 km^2 centered on the Shiant Islands, one of the main breeding centers of razorbills, and guillemots in the UK. Simultaneously, we GPS-tracked chick-rearing guillemots ($n = 17$) and razorbills ($n = 31$) from the Shiants. We modeled counts per unit area from boat surveys as smooth functions of latitude and longitude, mapping estimated densities. We then used kernel density estimation to map the utilization distributions of the GPS tracked birds. These two distribution estimates corresponded well for razorbills but were lower for guillemots. Both methods revealed areas of high use around the focal colony, but over the wider region, differences emerged that were likely attributable to the influences of neighboring colonies and the presence of non-breeding birds. The magnitude of differences was linked to the relative sizes of these populations, being larger in guillemots. Whilst boat surveys were necessarily restricted to the hours of daylight, GPS data were obtained equally during day and night. For guillemots, there was little effect of calculating separate night and day distributions from GPS records, but for razorbills the daytime distribution matched boat-based distributions better. When GPS-based distribution estimates were restricted to the exact times when boat surveys were carried out, similarity with boat survey distributions decreased, probably due to reduced sample sizes. Our results support the use of tracking data for defining seabird distributions around tracked birds' home colonies, but only when nearby colonies are neither large nor numerous. Distributions of animals around isolated colonies can be determined using GPS loggers but that of animals around aggregated colonies is best suited to at-sea surveys or multi-colony tracking.

Keywords: distribution mapping, guillemot, razorbill, GPS tags, tracking, at-sea surveys, Hebrides

OPEN ACCESS

Edited by:
Thomas Wassmer, Siena Heights University, United States

Reviewed by:
Vitor H. Paiva, University of Coimbra, Portugal
Anthony Gaston, Environment and Climate Change Canada, Canada

****Correspondence:***
Mark Bolton
mark.bolton@rspb.org.uk

Specialty section:
This article was submitted to Behavioral and Evolutionary Ecology, a section of the journal Frontiers in Ecology and Evolution

Received: *12 March 2019*
Accepted: *21 August 2019*
Published: *24 September 2019*

Citation:
Carroll MJ, Wakefield ED, Scragg ES, Owen E, Pinder S, Bolton M, Waggitt JJ and Evans PGH (2019) Matches and Mismatches Between Seabird Distributions Estimated From At-Sea Surveys and Concurrent Individual-Level Tracking. Front. Ecol. Evol. 7:333. doi: 10.3389/fevo.2019.00333

INTRODUCTION

Since the 1990s, new technology has allowed researchers to track the movements of seabirds using bird-borne devices that are sufficiently small and cost-effective to provide statistically robust sample sizes for a range of species (Burger and Shaffer, 2008). Tags deployed on breeding birds most frequently use the Global Positioning System (GPS) to obtain high frequency, high precision records of locations. In the UK, several seabird species have been tracked, with data now collected on hundreds of individuals from tens of colonies (e.g., Harris et al., 2012; Chivers et al., 2013; Robertson et al., 2014; Dean et al., 2015; Soanes et al., 2016).

GPS tracking has a number of attractive features: The cost per tag is relatively low; data are recorded in all light and weather conditions; and, increasingly, automatic data retrieval is possible, making recapture unnecessary. As birds are usually caught on land, tracking data are obtained from birds known to have been attending specific colonies, and thus can be used to identify important areas for focal colonies (e.g., Chivers et al., 2013; Redfern and Bevan, 2014). Moreover, the distributions of birds of known sex, age or breeding status can be estimated separately (e.g., Phillips et al., 2004; Cleasby et al., 2015; Grecian et al., 2018). However, usually only a small number of birds can be tracked from each colony, and constraints on battery life or the opportunities to re-catch birds, mean that tags are often only deployed for days or weeks. As such, the resulting data may not represent overall colony-level distributions well (Soanes et al., 2013). Further, because it is most practicable to catch and recapture birds on the nest, the birds tracked are usually breeding individuals, so non-breeding individuals are generally poorly represented or entirely absent in tracking samples. Finally, tracking indicates presence in an area, but not absence, potentially limiting interpretation of distribution estimates derived using this method.

Prior to the advent of tracking, the most widely used method for determining distributions of seabirds at sea was through visual surveys, conducted either from boats (Tasker et al., 1984; Stone et al., 1995; Camphuysen et al., 2004; Gjerdrum et al., 2012) or aircraft (Wildfowl and Wetlands Trust Consulting, 2009). These surveys generally use a combination of distance and plot sampling techniques conducted from linear transects (Ronconi and Burger, 2009; Thomas et al., 2010; Miller et al., 2013). Latterly, digital still and video cameras have also been deployed on aircraft to capture survey data (Buckland et al., 2012). At-sea surveys have several potential advantages over tracking: They establish not only the presence but also absence of birds; sample sizes (number of individuals) are much larger; all birds, regardless of species, size, breeding status or colony of origin can be recorded. However, at-sea surveys typically cover relatively small areas, or if larger areas are covered, there may be considerable time lags between coverage of different sub areas. Hence, fine-scale variation in distribution may be poorly resolved. It is largely impractical to link birds seen at sea to their breeding colony of origin, and in many species, it may be impossible to determine the sex, breeding status or age of birds. Finally, at-sea surveys cannot be conducted at night and may be impractical in high winds and sea states.

Due to the differing strengths and weaknesses of the two methods, distributions derived from both have sometimes been combined to inform seabird conservation management (e.g., Louzao et al., 2009). However, as yet, there has been no direct comparison of the distribution estimates produced by the contemporaneous use of the two methods. Assessment of the comparability of the two approaches is critical to the interpretation of differences in seabird distribution over time, or in different areas, when data have been collected using different methods. Such an examination is considered important given the increasing need to understand the distributions of seabirds at sea, and the growth of satellite tracking. Here, we report the findings of such a comparison. We undertook boat-based surveys of common guillemots *Uria aalge* (hereafter, guillemots) and razorbills *Alca torda* in the Minch, western Scotland, in June 2015. At the same time, we GPS-tracked breeding individuals of these species from one of their principal colonies in the area, the Shiant Islands (hereafter, the Shiants). These species are appropriate models for our study because they are abundant in the study area, of high conservation concern and large enough to track using low cost GPS tags. Using density surface modeling (at-sea data) and kernel density analysis (tracking data) we then estimated the distribution of birds and addressed the following questions: (i) How similar are the distributions estimated using the two methods? (ii) How does this vary if tracking-based distributions are restricted to night or daytime data, or data from periods of weather too poor for boat survey? (iii) What are the potential causes of discrepancies between distributions derived from the two methods?

METHODS

Study Area

The waters of the North Minch in West Scotland host seabird breeding colonies of national importance (Mitchell et al., 2004) (**Figure 1**). The last national census (known as "Seabird 2000"), where attempts were made to count all colonies, was in 1998–2002 (Mitchell et al., 2004). However, the two main colonies in the region have been counted more recently (and more frequently). These are the Shiants (57.90°N, 6.36°W), situated in the south west of the area, holding an estimated 9,100 guillemot individuals and 8,000 razorbill individuals in 2015, and Handa Island (58.38°N, 5.19°W), in the north east of the Minch, holding ∼54,700 guillemots and 5,000 razorbills in 2014 (http://archive.jncc.gov.uk/smp/searchCounts.aspx). Small numbers of guillemots and razorbills breed elsewhere in the North Minch, mainly along the north-west coast of Skye, the largest being at Rubha Hunish (57.42°N, 6.21°W) close to the northern tip of the Trotternish Peninsula (http://jncc.defra.gov.uk/page-4460) where 5,100 guillemots and 350 razorbills were counted in 1998–2002 (http://jncc.defra.gov.uk/page-4460).

Data Collection

Tracking Data

Razorbills and guillemots breeding on the Shiants were tracked using an adapted version of the open-source Mataki tag platform (http://mataki.org/) manufactured by debug innovations, Cambridge, with additional programming and construction

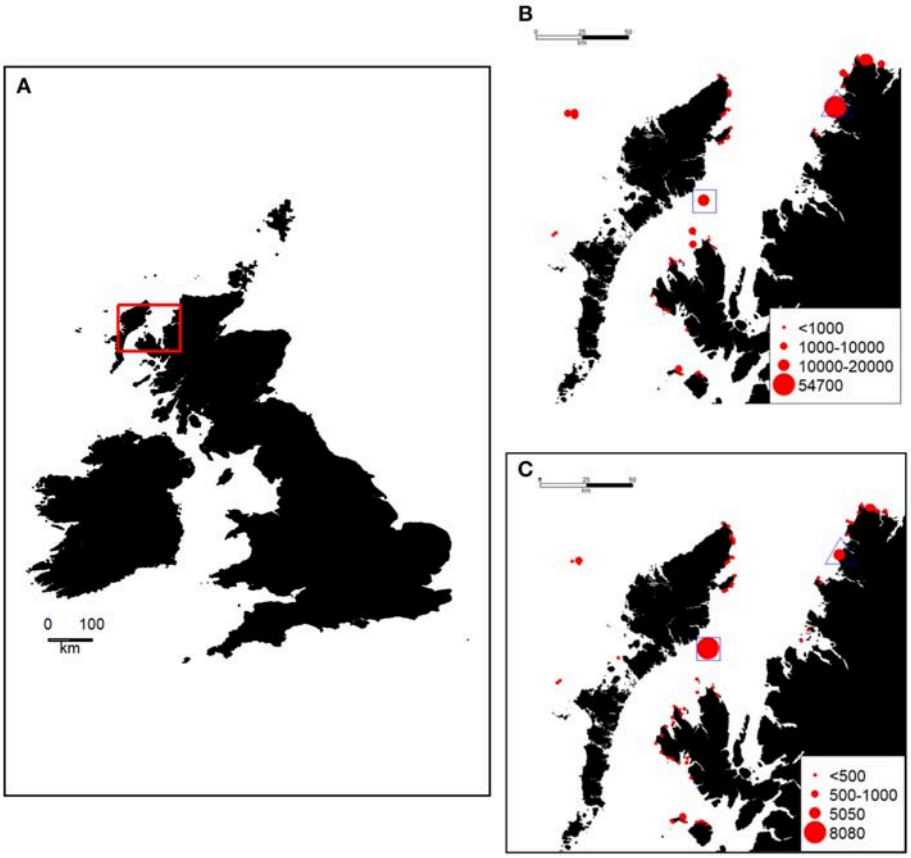

FIGURE 1 | (A) Location of the study area (red box) in the British Isles, size of Guillemot **(B)** and Razorbill **(C)** colonies in and around the study area [estimated number of individuals, from the Seabird Monitoring Programme Database www.jncc.gov.uk/smp (Mitchell et al., 2004). During the study, these species were GPS-tracked from a colony on the Shiants (blue square). At the same time, a boat-based survey was undertaken throughout the study area as shown in **Figure 3**. The location of Handa Island is indicated by a blue triangle.

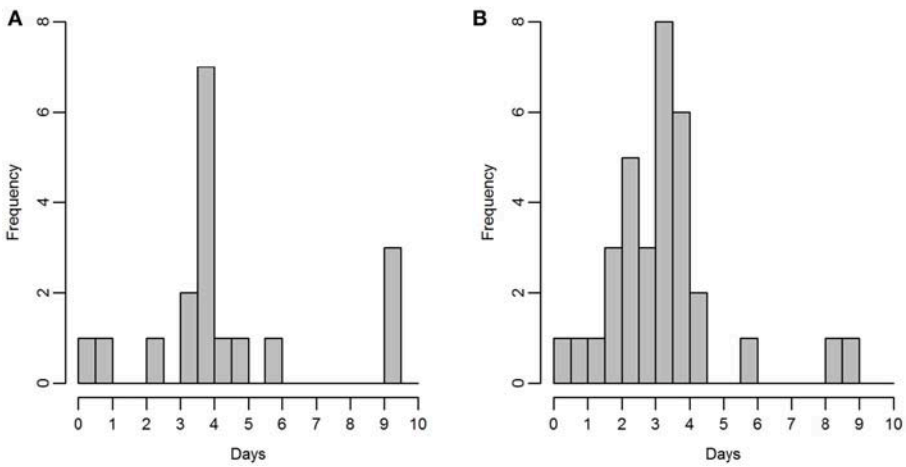

FIGURE 2 | Duration of time for which tags were active, for **(A)** guillemot and **(B)** razorbill; bins represent half days.

also required. Unlike archival GPS tags, they do not need to be recovered to retrieve data, which is wirelessly transmitted periodically to base stations. Birds tending eggs or small chicks were caught on the nest using a wire noose or by hand, and tags were attached to back feathers using waterproof Tesa® tape. Tag mass was 19 g, equivalent to <3.2% body weight of razorbills

and <2.3% body weight of guillemots. Between the 7th and 23rd of June (**Figure 2**), tags were deployed on 20 guillemots and 39 razorbills. Prior to deployment, the battery performance on the Mataki tag was not well-known. Hence, three different temporal tracking resolutions were used in the field: One fix every 100 s (analyses based upon 2 guillemots, 7 razorbills), 200 s (10 guillemots, 18 razorbills), or 600 s (6 guillemots, 8 razorbills).

At-Sea Survey Data

Boat-based surveys using the standard European Seabirds At Sea (ESAS) methodology (Camphuysen et al., 2004) were carried out throughout the Minch (an area of c. 6,700 km^2) on 8 days between 9 and 24 June 2015. In brief, the survey was carried out by experienced, ESAS-qualified, seabird surveyors (EW, DS, and SP). The observer searched for all birds flying or sitting on the water within 300 m of one side of the transect line, while a second person recorded sightings. One surveyor generally observed for an entire transect, except on very long transects, resulting in a median shift of 56 min (range 12–177 min). The side of the transect line surveyed was chosen on a transect-by-transect basis to cater for environmental effects (glare, etc.) on detectability. Birds were recorded in 1-min bins, corresponding to a mean distance of 250 m (±21 m SD) traveled. Birds first detected on the water were recorded in one of four distance bands running parallel to the boat's track: A 0–50 m, B 50–100 m, C 100–200 m, and D 200–300 m from the track line. Birds in flight were not recorded in distance bands as their detectability varies little within the 300 m transect. However, a "snapshot" method was used to account for the flux of birds through the transect (Tasker et al., 1984). Birds in flight were recorded as being in the transect if they were within a 300 × 300 m box at a given time interval, with an audible countdown timer being used to prepare the observer to undertake the snapshot instantaneously to reduce bias associated with a protracted snapshot (Gaston et al., 1987). The interval was set according to the boat's speed such that it occurred with every 300 m of transect covered. Transects were primarily aligned north-south and east-west (**Figure 3**). In addition, sea state, wind direction and strength, precipitation, and visibility were recorded at regular intervals. Surveys were only undertaken in sea states ≤ 4.

Data Analysis

Tracking Data

To achieve a common temporal resolution across birds, all tracks were first rediscretised to a 600-second interval using linear interpolation in the "adehabitatLT" R package (Calenge, 2006). Locations were projected in Lambert azimuthal equal area projection. Locations within 500 m of each bird's nest and all location records falling on land were removed. Kernel density estimation (Worton, 1989), implemented in the "adehabitatHR" R package (Calenge, 2006) with a bivariate Gaussian kernel was then used to determine the utilization distributions (UDs) of the tracked birds. Grid resolution was set to 2 × 2 km and the smoothing parameter *h* was selected using the *ad hoc* method (least-squares cross-validation was trialed but failed to converge). The degree to which the sample of birds tracked represented the wider colony was tested using the procedures of Lascelles et al. (2016). Razorbills were better represented than were guillemots, but both datasets were sufficiently representative.

In order to examine whether potential discrepancies between distributions were due to boat surveys being restricted to hours of daylight and calm sea states, UDs were produced using subsets

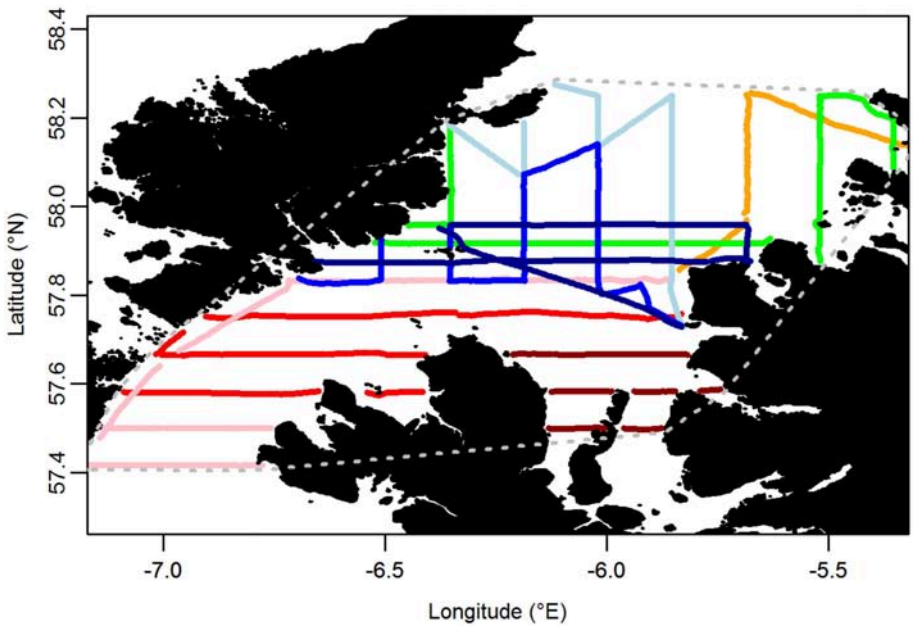

FIGURE 3 | Transects carried out on at-sea surveys. Each color represents a different day of the survey. Gray dotted line encompasses the area over which indices of similarity between at-sea and tracking based distributions were calculated.

of tracking data. These comprised (1) *all* data, (2) *daytime* data, (3) *night-time* data, and (4) tracking data recorded at the same time as the boat survey was being conducted (i.e., in daylight and weather conditions suitable for visual survey—hereafter *contemporary* data).

At-Sea Survey Data

Transects were divided into segments of length corresponding to 1 min of survey time. Density (counts/unit area in each segment) was then modeled as a function of a 2-dimensional spatial spline. Methods followed Bradbury et al. (2014), with the exception that distance correction and density surface modeling were carried out in two separate steps as described by Miller et al. (2013). The detectability of birds on the water decreases with distance so the first stage was to apply a factor to correct for the proportion of birds not detected in the 300 m transect. Following Kober et al. (2010), the corrected abundance x was calculated for each species using Equation 1:

$$x = \frac{(nA + nB) \times 3}{(nA + nB + nC + nD)}, \quad (1)$$

where nA, nB, nC, and nD are the total counts in each distance band. The numerator is multiplied by 3 (the ratio of total area of bands A+B+C+D to total area of bands A+B) (Pollock et al., 2000). This assumes that detection within 100 m of the boat is perfect. As in Kober et al. (2010), correction factors were calculated separately for sea states 0 (very calm) and 1–3 (ripples to wavelets, small whitecaps); unlike in Kober et al. (2010), no calculations were made for sea states 4–5, as very little survey effort was carried out above sea state 3. Correction factors are presented in **Table 1**. Abundances of birds on the water were multiplied by the appropriate correction factor, and then added to counts of birds in flight (assumed to have perfect detection) to give a total abundance in each transect segment (**Figure 4**).

In the second step, spatial variations in distance-corrected abundances were modeled using generalized additive mixed models (GAMMs) fitted in the "mgcv" R package (Wood, 2003, 2011, 2017). A negative binomial error structure and log link function were specified. "Transect" and "hour-within-transect" were treated as random effects in an attempt to model spatial and temporal clustering of observations (Zuur et al., 2014). An offset of log(segment length) was also included to account for slight variation in the distances traveled each minute (Miller et al., 2013). The fixed effect in each GAMM. The fixed effect in each GAMM were coordinates (eastings and northings), which were combined into a 2-dimensional and continuous variable. The maximum basis dimension (k) for the spline was selected by fitting a range of k values and examining resulting models' Akaike Information Criterion (AIC) values; the final value selected was 150, which represented the point at which adding further complexity provided no further AIC improvements. After model fitting, density was predicted on the same 2 km grid used for UD estimation. Grid cells containing land were excluded from predictions. Hereafter, we assume that the mean proportion of time that birds use a location within the study area is approximately proportional to density predicted from the at-sea survey data. Hereafter, we therefore refer these grids, normalized to sum to one, as UDs. Although there are potential theoretical objections to this interpretation, we assume it here pragmatically, as it allows similarity between the density estimates made using the two methods to be calculated using well-established metrics (Sansom et al., 2018).

Spatial autocorrelation was present in model residuals for both species. However, when an exponential spatial correlation structure was added (using the "gamm" function, and penalized quasi likelihood), for guillemots there was no significant difference in predicted densities. For razorbills, the model did not converge. It was therefore considered impractical to further reduce residual spatial autocorrelation.

TABLE 1 | Correction factors applied to counts of seabirds detected on the water within a 300 m wide transect during the at-sea survey.

	Guillemot	Razorbill
Sea state 0	1.646	2.017
Sea state 1-3	1.991	2.132

Comparing Estimated Distributions

To compare the distribution of birds estimated using tracking data and at-sea survey data, density grids were clipped to a focal area. First, this was defined by the minimum convex polygon (MCP) encompassing the at-sea surveys (**Figure 3**). The most north-easterly transects occurred within 20 km of the major guillemot and razorbill colony on Handa Island (**Figure 1**), which could strongly influence seabird distributions in the region. Therefore, a second focal area was considered, defined by a circle centered on the Shiants with a 50 km radius, approximately representing 1.1 x the maximum foraging range of each species observed in our study. Results using the 50 km radius area were nearly identical to those using the MCP area and are not therefore discussed further.

Densities outside the focal area were set to NA and density values within the focal area were then normalized to sum to unity once more. The similarity and overlap of different UDs (nominally, UD_1 and UD_2 in the descriptions below) were then calculated using indices described by Fieberg and Kochanny (2005). First, the 95 and 50% core areas (CAs) were calculated, i.e., the areas in which 95 and 50% usage is expected to occur, and plotted where these overlapped between UD_1 and UD_2. The area of overlap between core areas of UD_1 and UD_2 was then expressed both as a percentage of the area of UD_1, and as a percentage of the area of UD_2. Secondly, the Spearman correlation coefficient (ρ) between the ranks of probability densities in UD_1 and UD_2 was calculated (White and Garrott, 1990). Equal values within UDs were assigned the mean of the rank of those values. Whilst this measure may be limited in identifying overlap of UDs (Fieberg and Kochanny, 2005), it is a simple and widely understood measure of similarity. Positive correlation coefficients indicate that UDs are similar, whilst negative correlation coefficients indicate that higher densities in one UD are matched by lower densities in the other. ρ was calculated across the entire focal area.

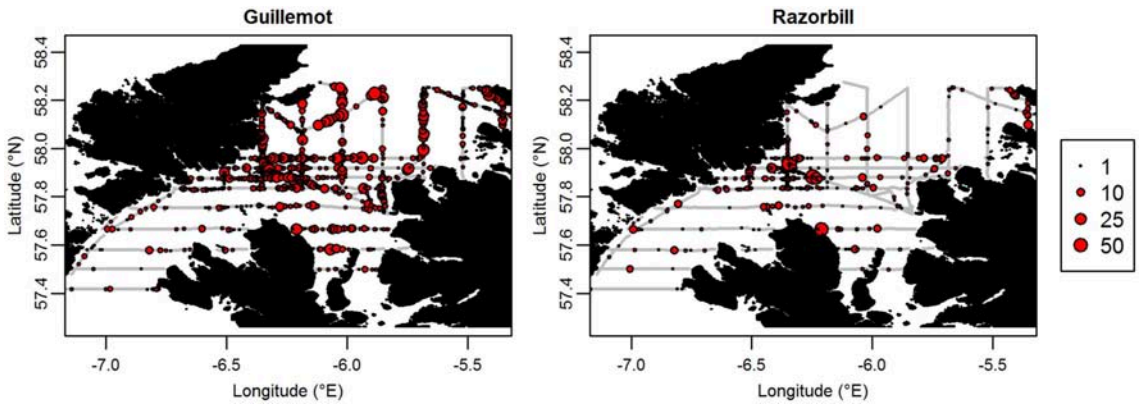

FIGURE 4 | Raw abundances from at-sea surveys, after distance correction.

Finally, two metrics were calculated, which it has been demonstrated give more reliable estimates of UD overlap (Fieberg and Kochanny, 2005). The utilization distribution overlap index (UDOI) is calculated following Equation 2:

$$UDOI = A_{1,2} \int_{-\infty}^{\infty} \int_{-\infty}^{\infty} UD_1\left(x,y\right) \times UD_2\left(x,y\right)\, dx\, dy \quad (2)$$

where, $A_{1,2}$ indicates the area of overlap between UD_1 and UD_2, whilst $UD_1(x,y)$ indicates the value of UD_1 at location (x,y). This index shows the amount of overlap relative to two UDs that use the same space and are uniformly distributed: UDs with perfect overlap and uniform probability distributions have UDOI = 1, whereas completely non-overlapping UDs have UDOI = 0. Overlapping UDs with non-uniform yet coincident probability distributions have UDOI > 1. This metric therefore indicates when two UDs show a high concentration of probability in the same area.

The second overlap metric used was Bhattacharyya's Affinity (BA), which is calculated following Equation 3 (Fieberg and Kochanny, 2005):

$$BA = \int_{-\infty}^{\infty} \int_{-\infty}^{\infty} \sqrt{UD_1\left(x,y\right)} \times \sqrt{UD_2\left(x,y\right)}\, dx\, dy \quad (3)$$

BA is 0 for two non-overlapping UDs, and 1 for identical UDs. This metric indicates overall similarity of UDs. Both UDOI and BA were calculated for the entire focal area.

RESULTS

Tracking Data

Two guillemot tags and six razorbill tags returned no data so were excluded from further analyses, leaving sample sizes of 18 guillemots and 33 razorbills. Tags recorded data for between 6 h and 9.25 days (**Figure 2**). Mean duration was 105 h (SD ± 61 h) for guillemots and 78 h (SD ± 42 h) for razorbills. The last data were collected for both species on the 27th of June. Rediscretisation and data trimming resulted in 5,246 and 5,769 locations for guillemots and razorbills, respectively. Daytime UDs were estimated using tracking data from 17 guillemots and 31 razorbills (3,229 and 3,500 locations, respectively); night-time UDs from 16 guillemots and 30 razorbills (2,017 and 2,269 locations, respectively); and contemporaneous UDs from 15 guillemots and 24 razorbills (734 and 1,090 locations, respectively). The smoothing parameter h was 2.2 km for guillemots and 2.7 km for razorbills. The raw tracks for both species are shown in **Figure 5**.

At-Sea Survey Data

The sea state during boat-based surveys was generally low (0 for 9% of the survey, 1 for 23%, 2 for 39%, 3 for 23%, and 4 for 6%) and 950 km of transect was surveyed. In total, 2,338 guillemots (859 in flight, 1,479 on water) and 776 razorbills (453 in flight, 323 on water) were detected (1 and 5% of guillemots/razorbills in flight and on the water respectively, could not be assigned to species and were excluded from the analysis).

Tracking Distributions vs. At-Sea Survey Distributions

Guillemot

Tracking data indicated that the highest guillemot density occurred immediately to the north of the Shiants; lower guillemot densities were spread relatively evenly around the islands (**Figure 6A**). Guillemot density estimated from boat surveys was spread more evenly and over a larger area, with the highest densities around and to the north of the Shiants, to the north and north-east extremes of the survey area, and off the north-east coast of Skye (**Figure 6B**).

The more even density surfaces from the boat survey meant that core areas (CAs) were much larger, leading to high overlap as a proportion of tracking CAs, but low overlap as a proportion of boat survey CAs (**Table 2**). Both survey methods found the south-west corner of the survey area to be outside the 95% CA, and the south-west and east regions of the survey area to be outside the 50% CA (**Figure 7A**). However, whilst tracking CAs were mostly contained within the larger boat survey CAs, tracking CAs were confined to the areas around the Shiants; more distant areas included in boat survey CAs were not included in the tracking CAs (**Figure 7A**). Similarity indices indicated moderate similarity between UDs estimated from the two data sources (**Table 2**). Correlation coefficients and BA indicated that boat surveys and GPS produced moderately similar distributions,

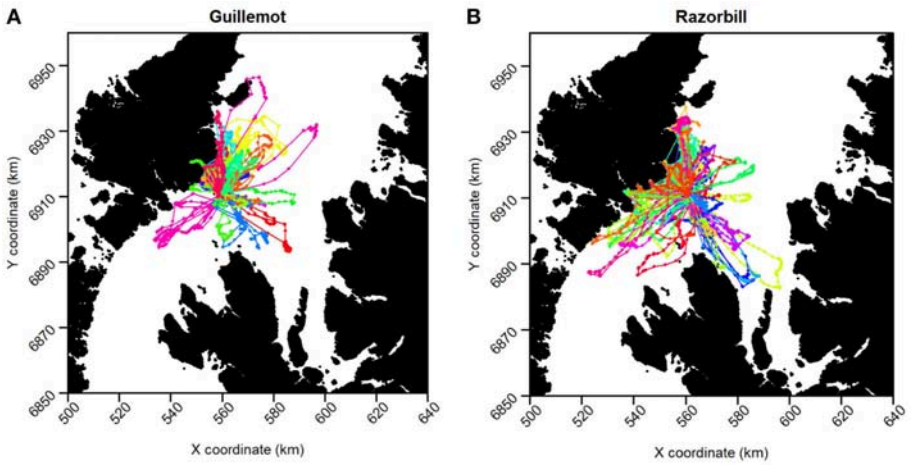

FIGURE 5 | GPS tracks of **(A)** Guillemot and **(B)** Razorbill individuals. Each color represents a different individual.

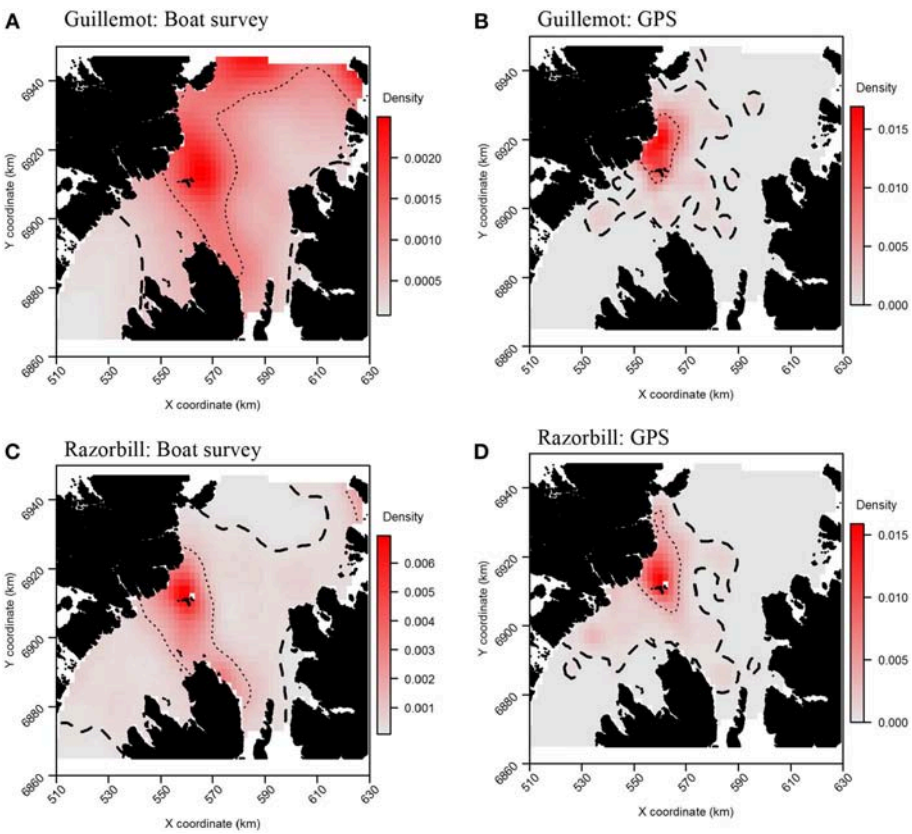

FIGURE 6 | Guillemot **(A,B)** and Razorbill **(C,D)** utilization distributions from boat surveys compared with concurrent GPS tracks. Darker reds indicate higher probability densities. Thick, dashed line indicates extent of 95% home range; thin, dotted line indicates extent of 50% home range.

and UDOI was >1, indicating reasonably good concordance in probability densities.

Razorbill

For razorbills, the highest densities also occurred primarily to the north of the Shiants (**Figures 6C,D**). GPS and boat survey distributions indicated an approximate north-west to south-east spread of high density, with this most pronounced in boat survey data, where the 50% CA extended as far as Skye. The pronounced high abundances in the north observed in guillemot distributions were less evident in razorbills, although a likely effect of the colony on Handa in the north-east was again observed. Both

TABLE 2 | Overlap and similarity between seabird utilization distributions (UDs) estimated using data from at-sea surveys and GPS tracking.

Species	Data used to estimate:		% overlap[a] between:		ρ	UDOI	BA
	UD_1	UD_2	95% CAs	50% CAs			
Guillemot	At-sea	GPS, all	30, 96	14, 100	0.59	1.22	0.66
	At-sea	GPS, day	25, 98	11, 100	0.59	1.26	0.62
	At-sea	GPS, night	31, 94	16, 100	0.57	1.10	0.66
	GPS, day	GPS, night	85, 66	58, 42	0.96	4.40	0.88
	At-sea	GPS, contemp[b]	12, 100	8, 100	0.58	0.62	0.49
	GPS, all	GPS, contemp.	38, 100	57, 93	0.71	2.95	0.87
Razorbill	At-sea	GPS, all	41, 100	32, 87	0.65	2.43	0.82
	At-sea	GPS, day	35, 100	22, 100	0.67	3.02	0.80
	At-sea	GPS, night	42, 98	23, 42	0.61	1.49	0.76
	GPS, day	GPS, night	88, 71	66, 27	0.95	3.10	0.86
	At-sea	GPS, contemp.	18, 99	19, 100	0.65	2.14	0.73
	GPS, all	GPS, contemp.	43, 97	53, 100	0.84	3.78	0.88

[a]The percentage of the core area (CA) of UD_1 that overlaps with the core area of UD_2 and vice versa. [b]Tracking data collected contemporaneously with bouts of at-sea survey (i.e., in daylight and low sea states). ρ, Spearman rank correlation coefficient; UDOI, the Utilization Distribution Overlap Index; BA, the Bhattacharyya Affinity.

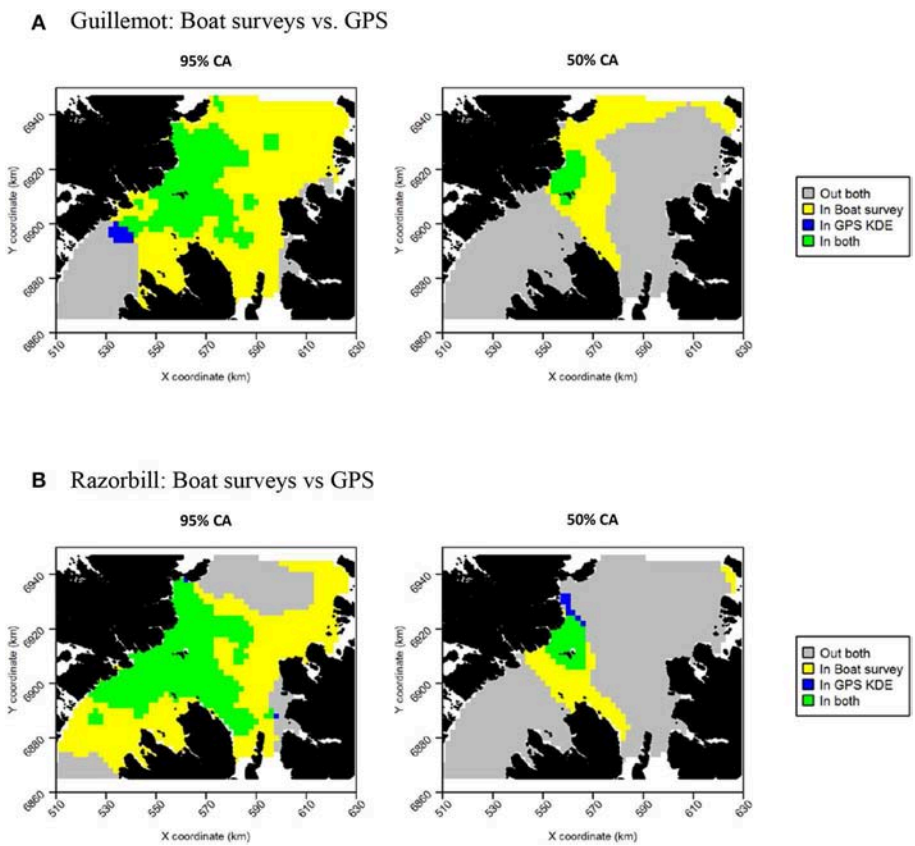

FIGURE 7 | Overlap between guillemot **(A)** and razorbill **(B)** core areas (CAs) derived from boat surveys compared with GPS tracking. In both maps, gray indicates areas outside of the CA in both data sources, and green indicates areas inside the CA in both data sources; blue and yellow indicate areas in the CA in one data source but not the other.

GPS and boat survey distributions indicated a low-density area immediately east of the Shiants and low densities in the north.

Core area comparisons were again influenced by the more even, larger distributions derived from boat survey data, with GPS CAs mostly contained within boat survey CAs. However, although boat survey CAs were larger, there was higher spatial concordance with tracking CAs (**Table 2**), and there appeared to be better concordance visually (**Figure 7B**). The 95% CAs

extended in all directions away from the Shiants, but the tracking derived CA did not extend as far as that derived from the at-sea survey (**Figure 7B**). The 50% CAs matched well around the Shiants, but the tracking CA did not extend to Skye. Overlap metrics indicated better concordance between the distribution estimates made using tracking and at-sea survey datasets than for guillemots (**Table 2**). Correlations were again only moderate, but BA > 0.8 and UDOI > 2.4 indicated high similarity between the UDs. The high UDOI statistics are likely to reflect the good matching of high densities found to the north of the Shiants.

Effects of Day/Night on Distribution Similarity

Guillemot

Daytime and night-time distributions were generally similar for guillemots (**Figures 8A,B**). Both distributions showed the greatest density to occur to the north of the Shiants, but this was more pronounced at night, whilst in daytime the high-density area extended slightly south of the islands. The 95% core area extended over a larger area at night, but both time periods showed the CA to extend in all directions from the islands. Both daytime and night-time core areas were substantially smaller than those derived from at-sea surveys. Consequently, the tracking derived CAs were almost completely contained within the at-sea survey CAs. However, higher proportional overlap was seen with the night-time GPS data (**Table 2**). The daytime and night-time CAs were very similar, with high overlap and similar spatial distributions (**Figure 9**). Congruence between at-sea survey and tracking derived UDs was similar, regardless of whether daytime or night-time data were used to derive the latter. All overlap and similarity indices were broadly similar for daytime and night-time data, with neither proving better across all metrics.

Razorbill

Razorbills showed slightly greater differences between daytime and night-time distributions than guillemots (**Figures 8C,D**, **Table 2**). In daytime, the distribution was centered on the Shiants, whilst at night-time, the distribution extended much further to the north. Although the 95% tracking CA extended to Skye at daytime, it extended further in all directions at night-time. Further, the 50% tracking CA extended to a second center at night-time, to the south-west of the Shiants. Tracking vs. at sea survey core area overlap was slightly greater at night-time (**Table 2**; **Figure 10**). However, the extension of the 50% tracking CA at night-time to the north-east and south-west of the Shiants was not reflected in the at-sea survey CA. This was the only instance of the tracking data identifying a core area outside that detected indicated by the at-sea data. Perhaps due to the better matching of the 50% CAs derived from at-sea and tracking data, overlap metrics were typically higher when the daytime tracking data were used (**Table 2**). In particular, UDOI was substantially higher in daytime, suggesting that areas of high density matched well with those identified in boat surveys. BA and correlation values were broadly similar, however, suggesting that both daytime and night-time showed broadly the same patterns overall.

Effects of Temporal Matching on Distribution Similarity

For both species, the tracking UDs derived from data recorded only during bouts of at-sea survey were much smaller than their equivalents derived from the entire tracking data set, presumably due to the smaller number of locations in the former (**Figure 11**). For guillemots, the highest density was again to the north of the Shiants, but the 95% CA extended north and south of the islands, and was unlike that derived from any other data source. For razorbills, higher densities were centered around the Shiants, with less of the northward bias seen when using the full dataset. For both species, the smaller CAs identified from the subset of tracking data meant that overlap was smaller than when the whole dataset was used (**Table 2**; **Figures 12**, **13**) and similarity between the tracking and at-sea survey derived UDs was generally lower than when the full tracking data set was used to estimate distributions, although some metrics produced similar values to those seen with the full dataset (**Table 2**).

DISCUSSION

Similarity Between Different Data Sources

The degree of similarity between seabird distributions derived from boat surveys and GPS tracking differed between the two species: it was moderate for guillemots but somewhat stronger for razorbills. For both species, similarity was greatest close to the Shiants, with boat surveys and GPS tracking both indicating higher densities just to the north of the islands. This was evident for razorbills in particular, for which the two methods showed remarkably good concordance in the location of the 50% core area. However, GPS tracking did not identify areas of high density further away from the islands which were indicated by the boat surveys, particularly in the north of the survey area. For razorbills, moderately high densities near to Skye were suggested from GPS tracking, whereas the boat survey showed this pattern more strongly. However, both data sources agreed well as to locations of low densities, with guillemots in particular present at low densities in the south-west of the survey area and, to a lesser extent, in the east.

When GPS data were sub-sampled to produce daytime and night-time distributions separately, the effect differed slightly between the two species. For guillemots, there was high similarity between day and night, and therefore with the overall GPS distribution. However, for razorbills, day and night distributions differed slightly, with the daytime distribution generally showing a better match to the boat survey distribution.

Boat surveys can only be carried out in daylight and when weather conditions permit, whereas GPS tags record locations in all light and weather conditions. It was anticipated that restricting GPS records to contemporary periods in which boat surveys had been carried out would improve the match to boat survey data. However, the sub-sampled GPS dataset was substantially smaller than when the full dataset was used, so although some similarity metrics indicated similar performance to the full dataset, there appeared to be a somewhat poorer match in general. Indeed, due

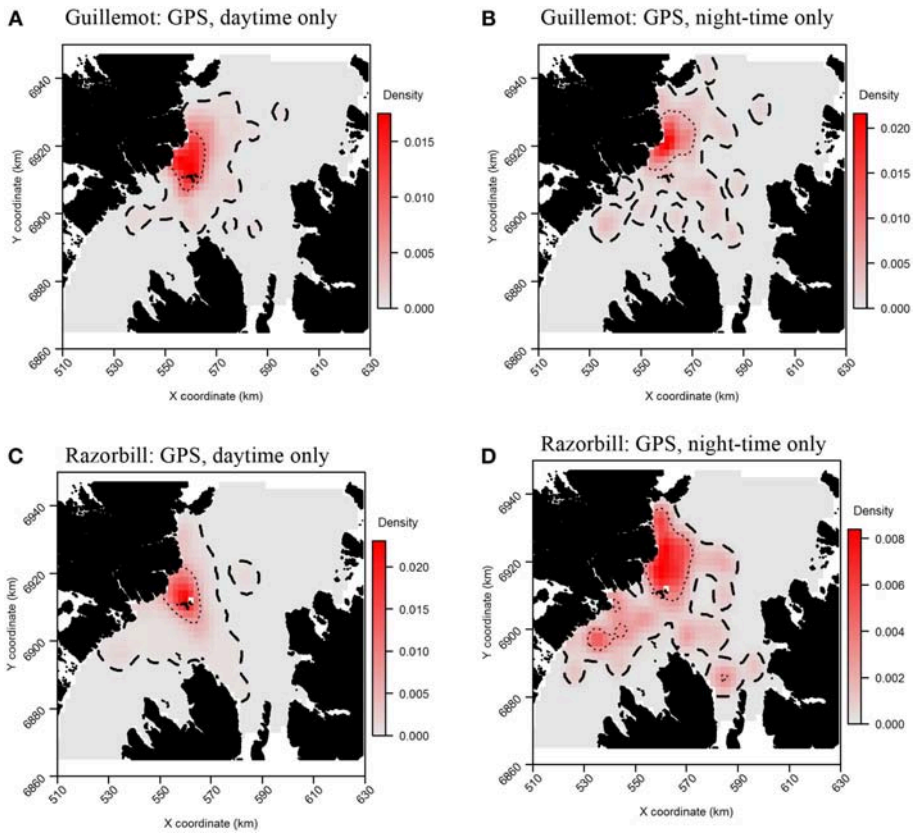

FIGURE 8 | Guillemot **(A,B)** and Razorbill **(C,D)** utilization distributions from daytime and night-time subsets of GPS data. Darker reds indicate higher probability densities. Thick, dashed line indicates extent of 95% home range; thin, dotted line indicates extent of 50% home range.

to the reduced dataset, sample size effects could account for the poorer match.

Potential Reasons for Differences

Limitations of Single-Colony Tracking

One of the most likely causes of differences in distribution from the two data sources was that birds were only tracked from the Shiants, whereas birds observed on boat surveys could originate from other colonies within the study area. Handa Island, lying to the north-east of the study area, supports the largest colonies of guillemots and razorbills in the UK (Mitchell et al., 2004), and is likely to account for the high densities observed in the north of the boat survey area. Indeed, Poisson-kriged distributions from data collected over several decades presented by Kober et al. (2010) also show high densities to occur in the areas identified by boat surveys, suggesting that they are not artifacts of our sampling or analysis. Thus, one major difference in the datasets is that tracking birds from the Shiants cannot indicate the distribution of birds originating from Handa Island. This will likely have been a greater issue for guillemots since Handa supports six times more guillemots than razorbills. This may explain the greater correspondence between GPS tracks and boat survey results for razorbill. The wider distribution of birds, particularly guillemots, closer to Skye detected during boat surveys probably reflected the colonies around Rubha Hunish off the northern tip of Skye. In order to accurately identify wider distributions in a region using GPS tracking, it would be necessary to track birds from multiple major colonies, to produce a predictive model to estimate likely distribution of birds from all colonies in the region (e.g., Wakefield et al., 2017).

Data Resolution and Sampling Effort

Boat survey methodology could also have contributed to differences. The temporal and spatial resolution of survey transects can influence the resolution of the resulting distributions (Camphuysen et al., 2004). Coarser resolutions might allow larger areas to be surveyed, but will limit the ability to identify fine-scale distribution patterns. Conversely, the high accuracy, frequent records obtained from GPS tracking enable finely-resolved distributions to be estimated. Some of the differences found here may result from the difference in resolution of the input data; for example, this could be responsible for differences in the shape of 95% CAs to the north of the Shiants. Further, boat survey findings are highly sensitive to temporal variation in abundances within days and seasons (Camphuysen et al., 2004). This is perhaps most strongly illustrated by the presence of a flock on a transect, which would cause a very high abundance to be recorded, but which may not be present if the transect were repeated, even a short time later. Repeat sampling of transects (Camphuysen et al., 2004) or use

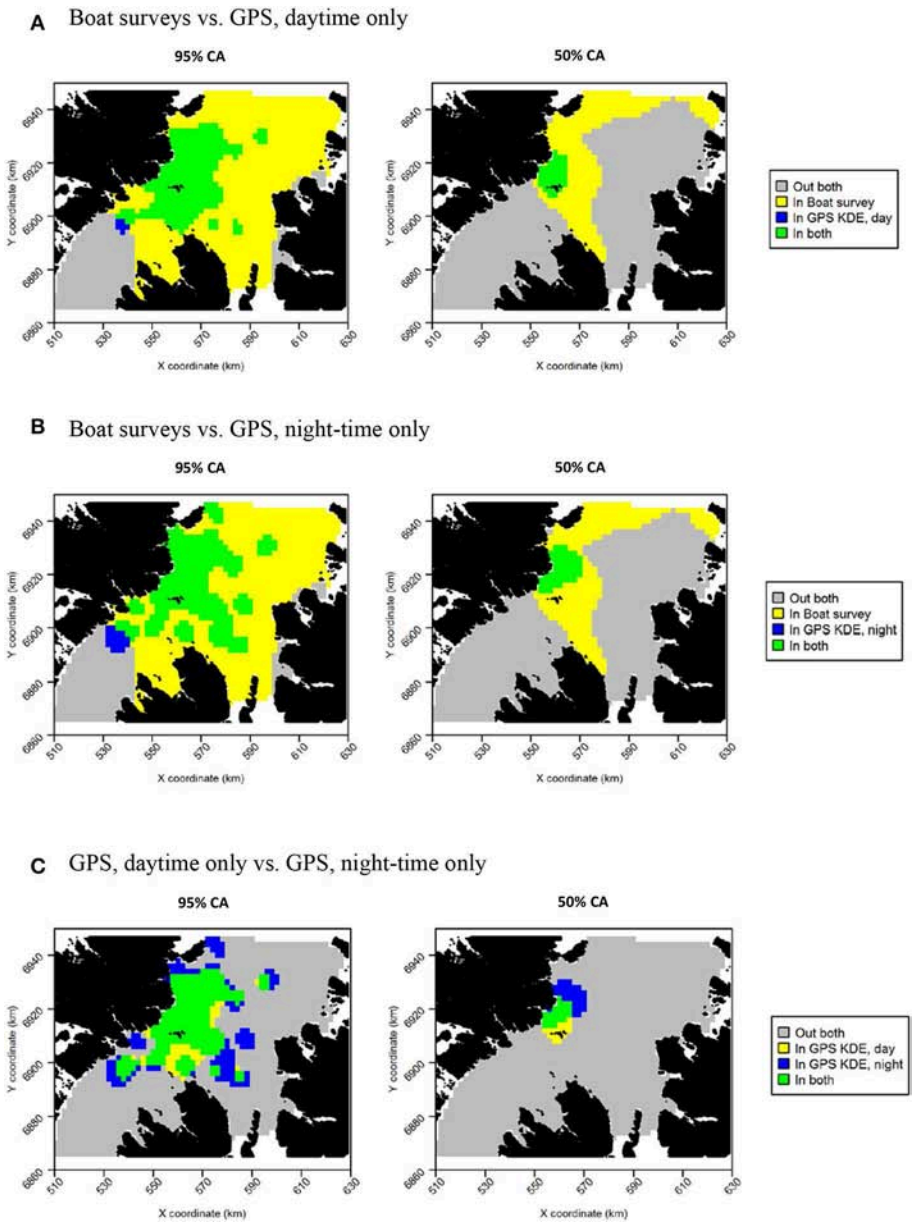

FIGURE 9 | Overlap between guillemot core areas (CAs) derived from boat surveys, GPS tracking in daytime and GPS tracking at night-time. In all maps, gray indicates areas outside of the CA in both data sources, and green indicates areas inside the CA in both data sources; blue and yellow indicate areas in the CA in one data source but not the other. **(A)** Boat surveys vs. GPS, daytime only. **(B)** Boat surveys vs. GPS, night-time only. **(C)** GPS, daytime only vs. GPS, night-time only.

of data from multiple surveys (e.g., Kober et al., 2010; Bradbury et al., 2014) would reduce the influence of short term temporal fluctuations in abundance, but with inevitable increase in survey costs per unit area.

A further consideration of sampling effort is the colony-level representativeness of the sample of birds tracked. The 31 razorbills and 17 guillemots included in kernel density estimates represent a tiny fraction of their respective populations on the Shiants (c. 0.4% of razorbills and 0.1% of guillemots). It may therefore also be the case that for guillemots, where the proportion and absolute number of birds tracked was smaller, resulting distributions were less representative of the colony as a whole. Indeed, the number of birds, and the number of trips carried out by each bird, influences resulting home range estimates (Soanes et al., 2013), so sample size effects may contribute to the differences in distributions between data sources (see sensitivity analysis in Carroll et al., 2017).

Sampling Constraints

Differences in the time of day and sea states when sampling is conducted is also an important consideration. GPS tracking typically occurs continuously once the tag is attached, thus sampling locations in all light and weather conditions. Conversely, boat surveys can only take place in the daytime

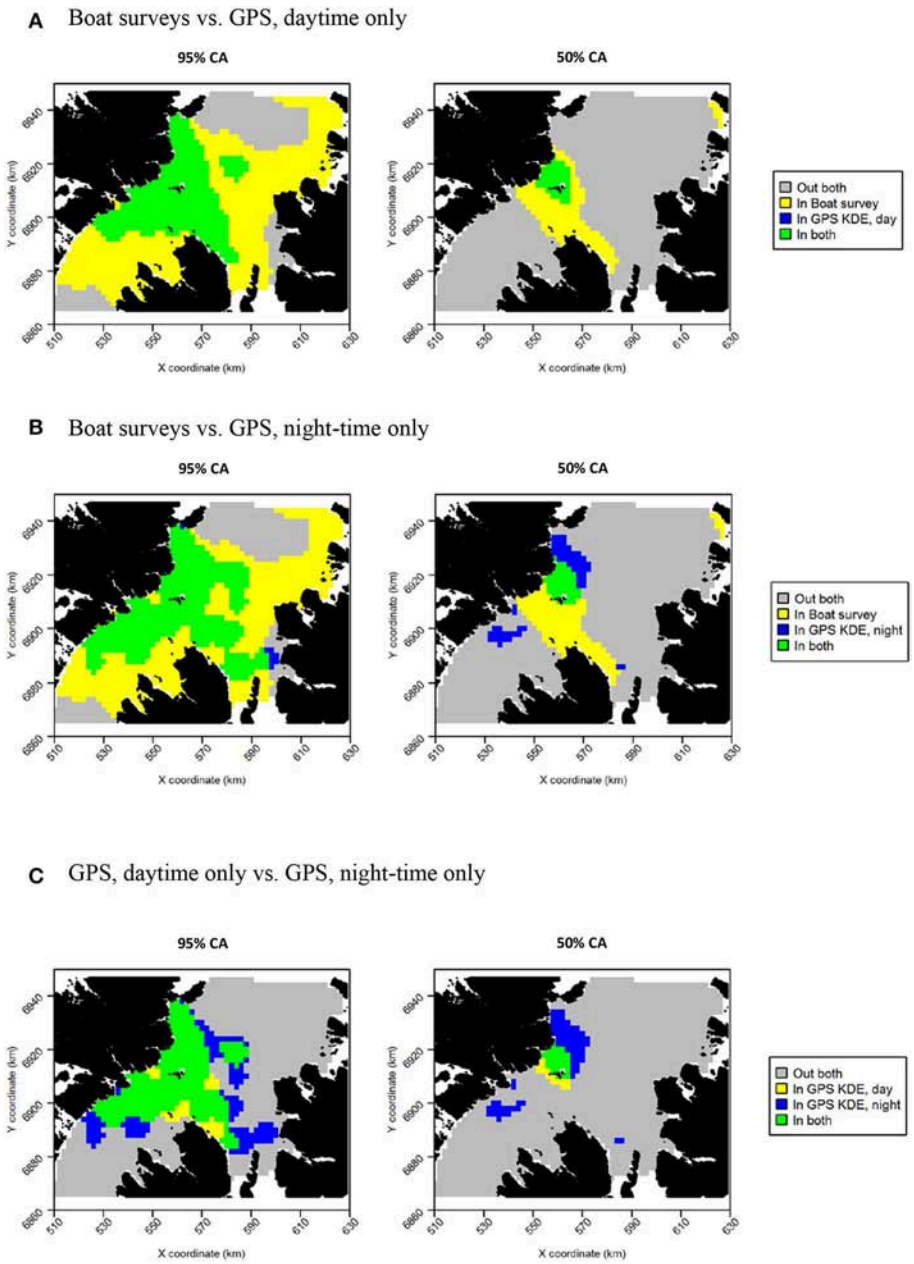

FIGURE 10 | Overlap between razorbill core areas (CAs) derived from boat surveys, GPS tracking in daytime and GPS tracking at night-time. In all maps, gray indicates areas outside of the CA in both data sources, and green indicates areas inside the CA in both data sources; blue and yellow indicate areas in the CA in one data source but not the other. **(A)** Boat surveys vs. GPS, daytime only. **(B)** Boat surveys vs. GPS, night-time only. **(C)** GPS, daytime only vs. GPS, night-time only.

and in good weather and consequently represent distributions during these conditions. However, in this study sub-setting GPS datasets to be contemporary with boat survey data did not consistently result in greater similarity of distributions. The potential improvement in similarity may be offset to some degree by the counteracting effect of reduction in the sample size of GPS records, leading to sparser distributions and a poorer representation of the colony distribution. For guillemots, there was little difference between night and day GPS distributions, and sub-setting to contemporary locations did not improve the similarity to boat surveys. The similarity between day and night GPS distributions, and the similar match of both to boat survey data suggests that there may therefore be little bias associated with conducting boat surveys during daylight on estimated guillemot distributions. On the other hand, for razorbills, night-time and daytime GPS distributions showed greater differences, and the daytime GPS distribution showed greater similarity (measured by UDOI) with boat surveys, as expected. Further sub-setting of GPS data to contemporary locations decreased the similarity with boat survey data, likely to due to reduced sample size.

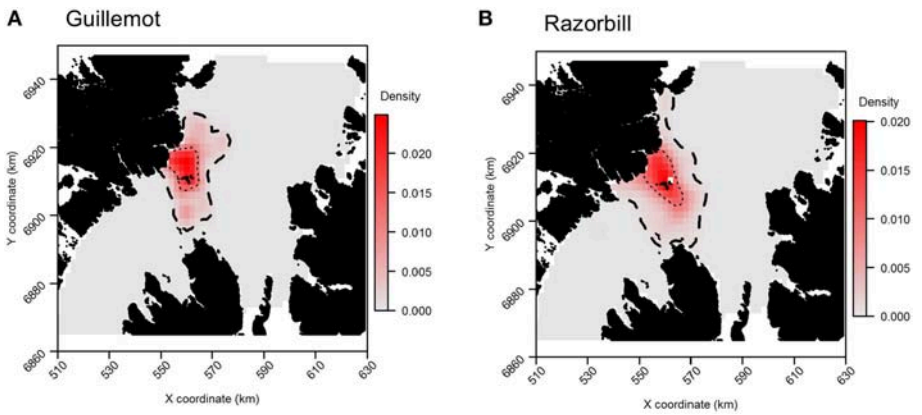

FIGURE 11 | Guillemot **(A)** and Razorbill **(B)** utilization distributions from GPS data collected only during times when boat surveys were being carried out. Darker reds indicate higher probability densities. Thick, dashed line indicates extent of 95% home range; thin, dotted line indicates extent of 50% home range.

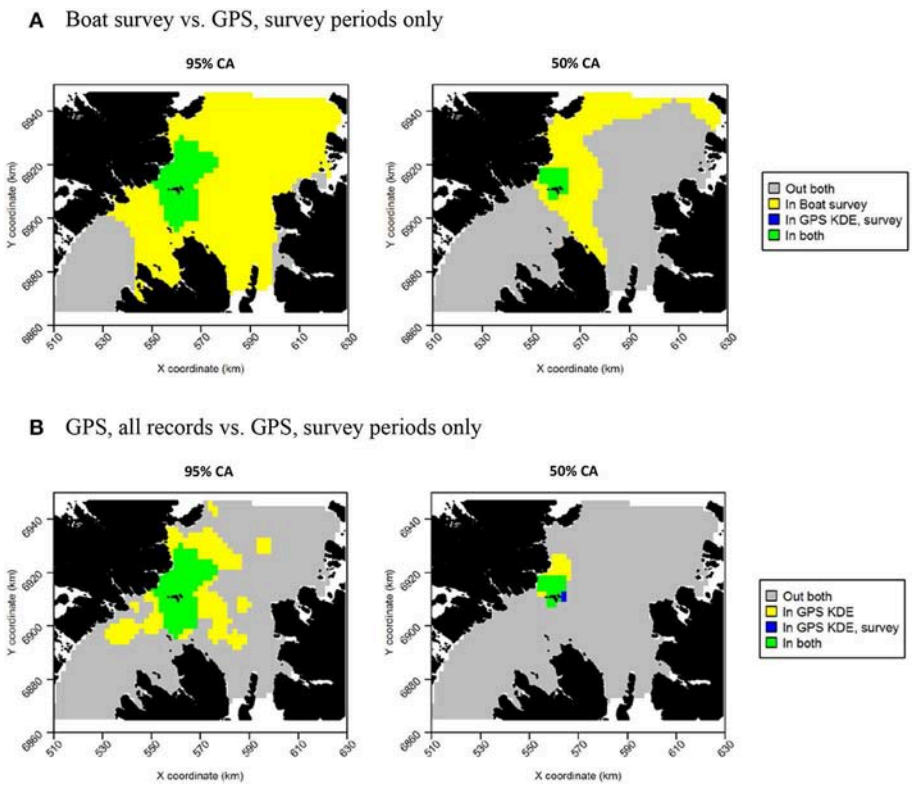

FIGURE 12 | Overlap between guillemot core areas (CAs) derived from boat surveys, GPS tracking during boat survey periods only and all GPS tracking data. In all maps, gray indicates areas outside of the CA in both data sources, and green indicates areas inside the CA in both data sources; blue and yellow indicate areas in the CA in one data source but not the other. **(A)** Boat survey vs. GPS, survey periods only. **(B)** GPS, all records vs. GPS, survey periods only.

Biases in at Sea Survey Data

Surveying birds from boats can result in multiple sources of error in density estimates (Gaston et al., 1987; Hyrenbach, 2001; Ronconi and Burger, 2009). Due to the study design and the conditions under which the data were collected, the errors should have been uniformly distributed throughout the study area and therefore should not have introduced systematic bias in the boat-based UD estimates. For example, while the ability to detect birds may have differed among observers and weather conditions, observer effort was spread evenly throughout the survey area and weather conditions were good throughout the survey. Hence, we think it unlikely that systematic biases in at-sea data collection could have accounted for the observed differences in the at-sea and tracking based UDs.

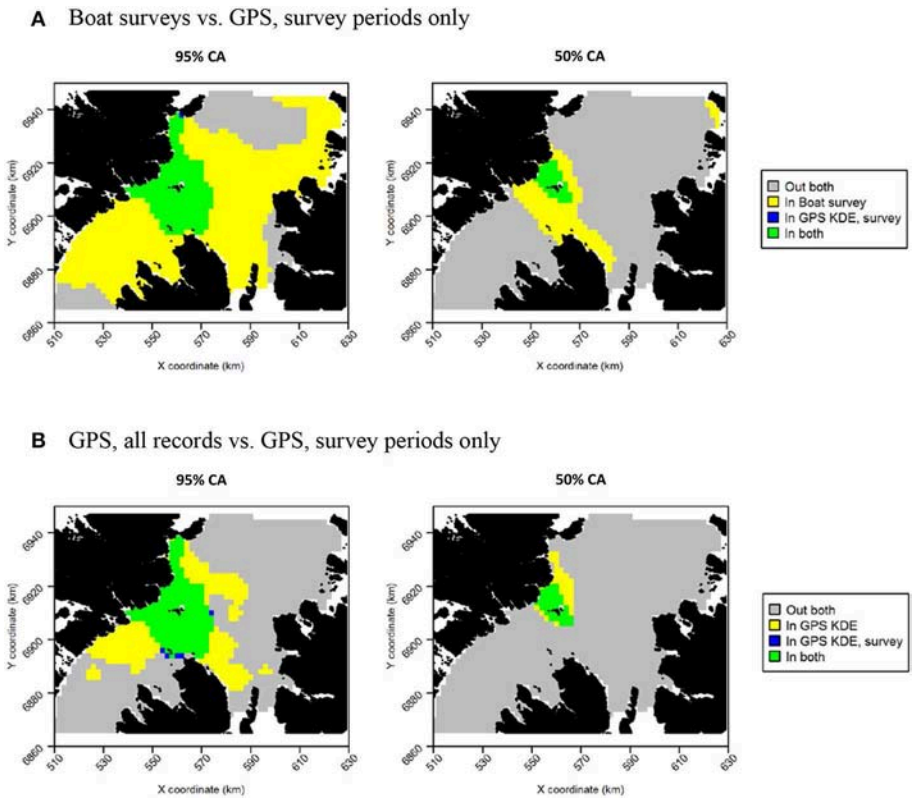

FIGURE 13 | Overlap between razorbill core areas (CAs) derived from boat surveys, GPS tracking during boat survey periods only and all GPS tracking data. In all maps, gray indicates areas outside of the CA in both data sources, and green indicates areas inside the CA in both data sources; blue and yellow indicate areas in the CA in one data source but not the other. **(A)** Boat surveys vs. GPS, survey periods only. **(B)** GPS, all records vs. GPS, survey periods only.

Breeding and Behavioral Status of Sampled Individuals

It is also important to consider the breeding status, and hence time budget and central place foraging constraints, of the individuals sampled. Due to practical limitations in approaching and capturing birds, GPS tracking is most frequently carried out on breeding individuals. Conversely, boat surveys sample all birds at sea, regardless of breeding status. If breeders, non-breeders and failed breeders share the same habitat preferences, there may be little impact of sampling bias in breeding status on resulting distributions. However, there may be important differences in the distributions of breeding and non-breeding individuals. Notably, non-breeders do not need to return to the colony to fulfill nest-attendance functions so can travel further (e.g., Votier et al., 2011). Breeding adults and immatures may also have dietary differences (Campioni et al., 2016) leading to them foraging in different areas (e.g., Fayet et al., 2015). The overall impact of this on estimated distributions depends on the proportion of the total population comprising non-breeders: fewer non-breeders would make distributions from boat surveys and GPS tracking appear more similar. It has been estimated that there are around 0.74-0.75 non-breeding immatures per adult at guillemot and razorbill breeding colonies (Furness, 2015). However, breeding age adults may skip breeding in some years: on the Isle of May, 5-10% of guillemots around the colony each year did not breed (Harris and Wanless, 1995), and the rate of skipping breeding can vary (e.g., Reed et al., 2015). Therefore, the presence of immatures and non-breeding adults in the at-sea population sampled by boat surveys could lead to differences with GPS-derived distributions; developing our understanding of the distributions on non-breeders at sea will be an important step in addressing this issue.

Breeding stage can also influence the distribution of seabirds at sea, due to difference in the constraints on nest attendance operating during incubation, brood-guard and post-guard periods (e.g., Wakefield et al., 2011; Dean et al., 2015). When selecting individuals for tag deployment, no attempt was made to target birds at a particular breeding stage and it is likely that the breeding stage of the tracked individuals reflected that of the colony as a whole. Hence the breeding stage of the birds observed from contemporaneous boat surveys is likely to be similar to that of the tracked sample.

In our study, we did not attempt to discriminate differences in the distribution of birds in different behavioral states. Whilst away from the colony on foraging trips, guillemots and razorbills rearing small chicks tracked in the North Sea spent 28.8 ± 9.5 and 17.5 ± 10.6% (mean ± sd) of their time, respectively underwater (Thaxter et al., 2010). Dive times average 46.4 ± 27.4 and 50.4

± 7.4 s for guillemots during long and short dives, respectively and 23.1 ± 14.9 s for razorbills, which made only short dives. The average boat speed in our survey was 14 ± 3 km/h, so guillemots and razorbills would have been out of sight during dives for on average the time it took to traverse ∼190 and 90 m of transect, respectively. This effect could have been further exacerbated if auks dived to escape the approaching survey vessel, although it is our experience that common guillemots and razorbills only respond in this way when the vessel is very close and they are likely to have already been detected. Nonetheless, it is likely that up to around 29% of guillemots and 18% of razorbills would not have been detected during the boat survey, leading to a concomitant underestimate of density (Buckland et al., 2015). This would have biased the boat based UDs lower in foraging areas, causing a systematic bias if foraging behavior was distributed non-uniformly. Although GPS loggers do not record locations while birds are diving, the interpolation scheme we used to fill gaps in the GPS data would have greatly reduced any similar bias in the tracking-based UDs. Hence, the spatial bias in the boat-based but not tracking-based UDs could partially explain why the latter suggested higher bird densities close to the Shiants than the former (**Figure 4**), i.e., breeding birds could have been diving intensively in an annulus around the colony Ashmole's halo (Gaston et al., 2007) and therefore missed more frequently than for example, non-breeders foraging less intensively at a greater distance.

Data Types and Analytical Approaches

Tracking individuals over time, and counting the abundance of birds along transects at sea, represent two very different types of data. The analytical processes required to estimate densities from such data are extremely different, and rely on different assumptions. Differences in the distributions resulting from the two methods may therefore be due, in part, to differences in the data types and the differences in the ways in which they are processed. Furthermore, there is no standard approach to converting raw survey data into a continuous density surface. Accordingly, various methods have been used, and the differences between these methods could contribute to perceived differences in resulting distributions. Such effects were noted by Bradbury et al. (2014) "The Poisson kriging method used by Kober et al. gave more scattered discreet [*sic* areas of higher density whereas the DSM of this study generally gave wider smooths over areas." Analytical differences could be particularly acute in the present study, where GPS distributions reflect the raw data, whereas boat survey distributions were modeled. One consequence of this is that zero values occur rarely in modeled boat survey distributions, whereas they occur across large areas in GPS distributions; this alone may influence overlap metric scores. Had it been possible to replicate the Poisson kriging method of Kober et al. (2010), the patchier densities may have matched GPS distributions better. Other analytical considerations will also have influenced resulting distributions. The form of spatial smooth used in GAMMs can affect outputs; a large maximum basis dimension was selected based on AIC, thus allowing a relatively complex distribution to be modeled, but similar studies have used simpler splines (e.g., Winiarski et al., 2013) or different forms of splines (e.g., Bradbury et al., 2014). In GPS distributions, the smoothing parameter used in kernel density estimation influences the size and shape of resulting core areas, with the rule-of-thumb method producing larger, smoother kernels than least-squares cross-validation or the plug-in method (Walter et al., 2011).

There are a number of analytic approaches that could further help in a comparison of distributions generated from tracking with those from boat surveys in this region. It would be beneficial to explicitly examine the sensitivity of KDEs derived from GPS data. The first step would be to restrict the number of birds and data points included, to explicitly consider sample size effects. This would be used to examine two questions: first, whether the larger sample of birds is likely to be responsible for the better matching of razorbill than guillemot distributions, and second, whether reduced sample sizes caused poorer matching in the comparisons with contemporary GPS and boat survey data. The second step would be to examine the methods used for producing KDEs, trialing plug-in estimators for the smoothing parameter and trialing Brownian bridge movement models. Although these different methods should not produce substantially different results, understanding the degree to which these assumptions affect distributions would be informative.

After understanding KDE sensitivity, it would be beneficial to model GPS data rather than simply estimating kernel densities from the raw data. Since boat survey data were modeled as a function of spatial location, using a similar approach for GPS data would allow closer matching of methods. However, this is not straightforward: different modeling approaches are available, with Wakefield et al. (2017) using a Poisson point-process method using only presence data, and other analyses (Wakefield et al., 2012; Wilson et al., 2014; Cleasby et al., 2015) using a "case-control" approach whereby observed presences are matched by "pseudo-absences." Each method brings with it complexities and assumptions, so could introduce further analytical reasons for observed differences. However, modeling GPS data, which would likely provide smoother core area estimates, would allow examination of the degree to which differences are driven by analytical method.

Once a predictive model structure for GPS data has been established, it would be possible to introduce habitat predictor variables to both GPS and boat survey models. Distributions may be better modeled by considering the habitat variables that determine which areas the birds use (see Wakefield et al., 2017). This approach should also allow predictions to be made beyond the Shiants for GPS data. On the other hand, inclusion of habitat variables could also introduce artifacts as distributions become related to spatially-variable predictors.

CONCLUSIONS

Similarities in core-areas of animals from the focal colony were obtained, but suspected influences of neighboring colonies and non-breeders are apparent in differences between methods. The magnitude of differences is linked to the relative sizes of these populations—being larger in common guillemots where neighboring colonies were considerably larger than the focal colonies. These results support the use of GPS loggers for

defining distributions of species in certain regions, but only when neighboring colonies are neither large nor widespread. Therefore, these results support the use of a flexible approach tailored to the needs of the study. Distributions of animals around isolated colonies could be achieved using GPS loggers but that of animals around aggregated colonies is best suited to at-sea surveys or multi-colony tracking.

DATA AVAILABILITY

The datasets for this manuscript are not publicly available as yet because they are being used for an upcoming publication comparing seabird and cetacean distributions in the study. Requests to access the datasets should be directed to MB at mark.bolton@rspb.org.uk. The tracking dataset will subsequently be available from http://www.seabirdtracking.org/.

ETHICS STATEMENT

This study was carried out in accordance with the principles of the UK Animals (Scientific Procedures) Act 1986. Capture, handling and tagging of birds was carried out under all appropriate licenses, issued by the British Trust for Ornithology, on behalf of the UK Government Home Office.

AUTHOR CONTRIBUTIONS

PE and MB initiated this collaboration, conceived the project, and obtained the funding. EO developed the tags and organized the tracking of birds on the Shiants, which was undertaken by ES. PE organized and led the boat surveys in which JW participated and EW and SP undertook field observations. MC conducted the analyses, prepared the figures and tables, and wrote an initial draft of the paper. All authors provided critical feedback on the manuscript. PE prepared the final manuscript and handled the submission.

FUNDING

The study was funded by the UK Government Department of Energy and Climate Change (DECC, now the Department for Business, Energy and Industrial Strategy) under the Offshore Energy Strategic Environmental Assessment programme (OESEA-15-54), the Sea Watch Foundation, and RSPB. EW is funded by the Natural Environment Research Council (Independent Research Fellowship NE/M017990/1).

ACKNOWLEDGMENTS

We thank John Hartley (Hartley Anderson Ltd.) for project management on behalf of DECC; Pia Anderwald, Jerry Gillham, Kathy James, Ali MacLennan, David Shackleton, Tom Stringell, Gemma Veneruso, and Caroline Weir for assistance with the vessel surveys; the Shiants Auk Ringing Group for field assistance on the Shiants; Andrew Asque and Nigel Butcher for development of the tags, David Lambie for boat charter and assistance; and Tom and Adam Nicolson for permission to work on the Shiants. Fieldwork was conducted under license from Scottish Natural Heritage and the British Trust for Ornithology.

REFERENCES

Bradbury, G., Trinder, M., Furness, B., Banks, A. N., Caldow, R. W., and Hume, D. (2014). Mapping seabird sensitivity to offshore wind farms. *PLoS ONE* 9:e106366. doi: 10.1371/journal.pone.0106366

Buckland, S. T., Burt, M. L., Rexstad, E. A., Mellor, M., Williams, A., and Woodward, R. (2012) Aerial surveys of seabirds: the advent of digital methods. *J. Appl. Ecol.* 49, 960–967. doi: 10.1111/j.1365-2664.2012.02150.x

Buckland, S. T., Rexstad, E. A., Marques, T. A., and Oedekoven, C. S. (2015). *Distance Sampling: Methods and Applications*. Cham: Springer International Publishing.

Burger, A. E., and Shaffer, S. A. (2008). Application of tracking and data-logging technology in research and conservation of seabirds. *Auk* 125, 253–264. doi: 10.1525/auk.2008.1408

Calenge, C. (2006). The package adehabitat for the R software: a tool for the analysis of space and habitat use by animals. *Ecol. Modell.* 197, 516–519. doi: 10.1016/j.ecolmodel.2006.03.017

Camphuysen, C. J., Fox, A. D., Leopold, M. F., and Petersen, I. K. (2004). *Towards Standardised Seabirds at Sea Census Techniques in Connection With Environmental Impact Assessments for Offshore Wind Farms in the UK: A Comparison of Ship and Aerial Sampling Methods for Marine Birds and Their Applicability to Offshore Wind Farm Assessments*. Texel: Royal Netherlands Institute for Sea Research.

Campioni, L., Granadeiro, J. P., and Catry, P. (2016). Niche segregation between immature and adult seabirds: does progressive maturation play a role? *Behav. Ecol.* 27, 426–433. doi: 10.1093/beheco/arv167

Carroll, M. J., Wakefield, E. W., Scragg, E. S., Pinder, S., Shackleton, D., Owen, E., et al. (2017). *Supplement 1: Representativeness Testing of GPS Tracking Data*. Sandy: Royal Society for the Protection of Birds.

Chivers, L. S., Lundy, M. G., Colhoun, K., Newton, S. F., Houghton, J. D. R., Reid, N. (2013). Identifying optimal feeding habitat and proposed Marine Protected Areas (pMPAs) for the black-legged kittiwake (*Rissa tridactyla*) suggests a need for complementary management approaches. *Biol. Conserv.* 164, 73–81. doi: 10.1016/j.biocon.2013.04.022

Cleasby, I. R., Wakefield, E. D., Bodey, T. W., Davies, R., Patrick, S. C., Newton, J., et al. (2015). Sexual segregation in a wide-ranging marine predator is a consequence of habitat selection. *Mar. Ecol. Prog. Ser.* 518, 1–12. doi: 10.3354/meps11112

Dean, B., Kirk, H., Fayet, A., Shoji, A., Freeman, R., Leonard, K., et al. (2015). Simultaneous multi-colony tracking of a pelagic seabird reveals cross-colony utilization of a shared foraging area. *Mar. Ecol. Prog. Ser.* 538, 239–248. doi: 10.3354/meps11443

Fayet, A. L., Freeman, R., Shoji, A., Padget, O., Perrins, C. M., Guilford, T. (2015). Lower foraging efficiency in immatures drives spatial segregation with breeding adults in a long-lived pelagic seabird. *Anim. Behav.* 110, 79–89. doi: 10.1016/j.anbehav.2015.09.008

Fieberg, J., and Kochanny, C. O. (2005). Quantifying home-range overlap: the importance of the utilization distribution. *J. Wildl. Manag.* 69, 1346–1359. doi: 10.2193/0022-541X(2005)69[1346:QHOTIO]2.0.CO;2

Furness, B. (2015). *Non-breeding Season Populations of Seabirds in UK Waters: Population Sizes for Biologically Defined Minimum Population Scales (BDMPS)*. Natural England Commissioned Report number 164. Natural England, Peterborough.

Gaston, A. J., Collins, B. L., and Diamond, A. W. (1987). The "snapshot" count for Estimating densities of flying seabirds during boat transects: a cautionary comment. *Auk Ornithol. Adv.* 104, 336–338.

Gaston, A. J., Ydenberg, R. C., and Smith, G. E. J. (2007). Ashmole's halo and population regulation in seabirds. *Mar. Ornithol.* 35, 119–126.

Gjerdrum, C., Fifield, D. A., and Wilhelm, S. I. (2012). *Eastern Canada Seabirds at Sea (ECSAS) Standardized Protocol for Pelagic Seabird Surveys From Moving and Stationary Platforms*. Tech. Rep. 515, 37 pp., Can. Wildlife Serv., Atl. Reg., Dartmouth, Nova Scotia. Available online at: http://www.cnlopb.nl.ca/pdfs/hmdcjdb/ecseabird.pdf.

Grecian, W. J., Lane, J. V., Michelot, T., Wade, H. M., and Hamer, K. C. (2018) Understanding the ontogeny of foraging behaviour: insights from combining marine predator bio-logging with satellite-derived oceanography in hidden Markov models. *J. R. Soc.* Interface 15:20180084. doi: 10.1098/rsif.2018.0084

Harris, M. P., Bogdanova, M. I., Daunt, F., and Wanless, S. (2012). Using GPS technology to assess feeding areas of Atlantic Puffins *Fratercula arctica*. *Ringing Migr.* 27, 43–49. doi: 10.1080/03078698.2012.691247

Harris, M. P., and Wanless, S. (1995). Survival and non-breeding of adult common guillemots Uria aalge. *Ibis* 137, 192–197. doi: 10.1111/j.1474-919X.1995.tb03239.x

Hyrenbach, K. D. (2001). Albatross response to survey vessels: implications for studies of the distribution, abundance, and prey consumption of seabird populations. *Mar. Ecol. Prog. Ser.* 212, 283–295. doi: 10.3354/meps212283

Kober, K., Webb, A., Win, I., Lewis, M., O'Brien, S., Wilson, L., et al. (2010). An Analysis of the Numbers and Distribution of Seabirds Within the British Fishery Limit Aimed at Identifying Areas That Qualify as Possible Marine SPAs. JNCC Report 431, JNCC, Peterborough, UK.

Lascelles, B. G., Taylor, P. R., Miller, M. G. R., Dias, M., Oppel, S., Torres, L., et al. (2016). Applying global criteria to tracking data to define important areas for marine conservation. *Divers. Distrib.* 22, 422–431. doi: 10.1111/ddi.12411

Louzao, M., Bécares, J., Rodríguez, B., Hyrenbach, K. D., Ruiz, A., and Arcos, J. M. (2009). Combining vessel-based surveys and tracking data to identify key marine areas for seabirds. *Mar. Ecol. Prog. Ser.* 391, 183–197. doi: 10.3354/meps08124

Miller, D. L., Burt, M. L., Rexstad, E. A., and Thomas L. (2013). Spatial models for distance sampling data: recent developments and future directions. *Methods Ecol. Evol.* 4, 1001–1010. doi: 10.1111/2041-210X.12105

Mitchell, P. I., Newton, S. F., Ratcliffe, N., and Dunn, T. E. (2004). *Seabird Populations of Britain and Ireland*. London: T & AD Poyser.

Phillips, R. A., Silk, J. R. D., Phalan, B., Catry, P., and Croxall, J. P. (2004) Seasonal sexual segregation in two Thalassarche albatross species: competitive exclusion, reproductive role specialization or foraging niche divergence? *Proc. R. Soc. Lond.* B 271, 1283–1291. doi: 10.1098/rspb.2004.2718

Pollock, C. M., Mavor, R., Weir, C. R., Reid, A., White, R., Tasker, M. L., et al. (2000). *The Distribution of Seabirds and Marine Mammals in the Atlantic Frontier, North and West of Scotland*. 1861075057, Peterborough: JNCC.

Redfern, C. P. F., and Bevan, R. M. (2014). A comparison of foraging behaviour in the North Sea by Black-legged Kittiwakes *Rissa tridactyla* from an inland and a maritime colony. *Bird Study* 61, 17–28. doi: 10.1080/00063657.2013.874977

Reed, T., Harris, M., and Wanless, S. (2015). Skipped breeding in common guillemots in a changing climate: restraint or constraint? *Front. Ecol. Evol.* 3:1. doi: 10.3389/fevo.2015.00001

Robertson, G. S., Bolton, M., Grecian, W. J., and Monaghan, P. (2014). Inter- and intra-year variation in foraging areas of breeding kittiwakes (Rissa tridactyla). *Mar. Biol.* 161, 1973–1986. doi: 10.1007/s00227-014-2477-8

Ronconi, R. A., and Burger, A. E. (2009). Estimating seabird densities from vessel transects: distance sampling and implications for strip transects. *Aquat. Biol.* 4, 297–309. doi: 10.3354/ab00112

Sansom, A., Wilson, L. J., Caldow, R. W. G., and Bolton, M. (2018) Comparing marine distribution maps for seabirds during the breeding season derived from different survey and analysis methods. *PLoS ONE* 13:e0201797. doi: 10.1371/journal.pone.020179

Soanes, L. M., Arnould, J. P. Y., Dodd, S. G., Sumner, M., and Green, J. A. (2013). How many seabirds do we need to track to define home-range area? *J. Appl. Ecol.* 50, 671–679. doi: 10.1111/1365-2664.12069

Soanes, L. M., Bright, J. A., Angel, L. P., Arnould, J. P., Bolton, M., Berlincourt, M., et al. (2016). Defining marine important bird areas: testing the foraging radius approach. *Biol. Conserv.* 196, 69–79. doi: 10.1016/j.biocon.2016.02.007

Stone, R. E., Webb, A., Barton, C., Ratcliffe, N., Reed, T. C., Tasker, M. L., et al. (1995). *An Atlas of Seabird Distribution in North-West European Waters*. Peterborough: Joint Nature Conservation Committee.

Tasker, M. L., Jones, P. H., Dixon, T., and Blake, B. F. (1984). Counting seabirds at sea from ships - a review of methods employed and a suggestion for a standardized approach. *Auk* 101, 567–577.

Thaxter, C. B., Wanless, S., Daunt, F., Harris, M. P., Benvenuti, S., Watanuki, Y., et al. (2010). Influence of wing loading on the trade-off between pursuit-diving and flight in common guillemots and razorbills. *J. Exp. Biol.* 213, 1018–1025. doi: 10.1242/jeb.037390

Thomas, L., Buckland, S. T., Rexstad, E. A., Laake, J. L., Strindberg, S., Hedley, S. L., et al. (2010). Distance software: design and analysis of distance sampling surveys for estimating population size. *J. Appl. Ecol.* 47, 5–14. doi: 10.1111/j.1365-2664.2009.01737.x

Votier, S. C., Grecian, W. J., Patrick, S., and Newton, J. (2011). Inter-colony movements, at-sea behaviour and foraging in an immature seabird: results from GPS-PPT tracking, radio-tracking and stable isotope analysis. *Mar. Biol.* 158, 355–362. doi: 10.1007/s00227-010-1563-9

Wakefield, E. D., Owen, E., Baer, J., Daunt, F., Dodd, S. G., Green, J. A., et al. (2017). Breeding density, fine-scale tracking and large-scale modelling reveal the regional distribution of four seabird species. *Ecol. Appl.* 27, 2074–2091 doi: 10.1002/eap.1591

Wakefield, E. D., Phillips, R. A., and Belchier, M. (2012). Foraging black-browed albatrosses target waters overlaying moraine banks - a consequence of upward benthic-pelagic coupling? *Antarct. Sci.* 24, 269–280. doi: 10.1017/S0954102012000132

Wakefield, E. D., Phillips, R. A., Trathan, P., Arata, J., Gales, R., Huin, N., et al. (2011). Accessibility, habitat preference and conspecific competition limit the global distribution of breeding albatrosses. *Ecol. Monogr.* 81, 141–167. doi: 10.1890/09-0763.1

Walter, W. D., Fischer, J. W., Baruch-Mordo, S., and VerCauteren, K. C. (2011). "What is the proper method to delineate home range of an animal using today's advanced GPS telemetry systems: the initial step," in *Modern Telemetry*, ed O. Krejcar (InTech Open Access Publisher), 249–268. http://www.intechopen.com/books/show/title/modern-telemetry.

White, G. C., and Garrott, R. A. (1990). *Analysis of Wildlife Radio-Tracking Data*. San Diego, CA: Academic Press.

Wildfowl and Wetlands Trust Consulting (2009). *Aerial Surveys of Waterbirds in the UK: 2007/08*. WWT Report to UK Department of Energy and Climate Change, 297.

Wilson, L. J., Black, J., Brewer, M. J., Potts, J. M., et al. (2014). *Quantifying Usage of the Marine Environment by Terns Sterna sp. Around Their Breeding Colony SPAS*. JNCC Report No. 500., JNCC, Peterborough, UK.

Winiarski, K. J., Miller, D. L., Paton, P. W. C., and McWilliams, S. R. (2013). Spatially explicit model of wintering common loons: conservation implications. *Mar. Ecol. Prog. Ser.* 492, 273–283. doi: 10.3354/meps10492

Wood, S. N. (2003). Thin-plate regression splines. *J. R. Stat. Soc. B* 65, 95–114. doi: 10.1111/1467-9868.00374

Wood, S. N. (2011). Fast stable restricted maximum likelihood and marginal likelihood estimation of semiparametric generalized linear models. *J. R. Stat. Soc. B* 73, 3–36. doi: 10.1111/j.1467-9868.2010.00749.x

Wood, S. N. (2017). *Generalized Additive Models: An Introduction With R. 2nd Edn*. Boca Raton, FL: Chapman and Hall/CRC Press.

Worton, B. J. (1989). Kernel methods for estimating the utilization distribution in home-range studies. *Ecology* 70, 164–168.

Zuur, A. F., Saveliev, A. A., and Ieno, E. N. (2014). *A Beginner's Guide to Generalised Additive Mixed Models With R*. Newburgh: Highland Statistics Limited.

Conflict of Interest Statement: The authors declare that the research was conducted in the absence of any commercial or financial relationships that could be construed as a potential conflict of interest.

Copyright © 2019 Carroll, Wakefield, Scragg, Owen, Pinder, Bolton, Waggitt and Evans. This is an open-access article distributed under the terms of the Creative Commons Attribution License (CC BY). The use, distribution or reproduction in other forums is permitted, provided the original author(s) and the copyright owner(s) are credited and that the original publication in this journal is cited, in accordance with accepted academic practice. No use, distribution or reproduction is permitted which does not comply with these terms.

frontiers in Ecology and Evolution

ORIGINAL RESEARCH
published: 21 January 2020
doi: 10.3389/fevo.2019.00504

Behavioral Biomarkers for Animal Health: A Case Study Using Animal-Attached Technology on Loggerhead Turtles

Alexandra C. Arkwright[1,2], Emma Archibald[1], Andreas Fahlman[2], Mark D. Holton[1], Jose Luis Crespo-Picazo[2], Vicente M. Cabedo[2], Carlos M. Duarte[3], Rebecca Scott[4], Sophie Webb[1], Richard M. Gunner[1] and Rory P. Wilson[1]*

[1] Swansea Lab for Animal Movement, Biosciences, College of Science, Swansea University, Swansea, United Kingdom, [2] Fundación Oceanogràfic de la Comunitat Valenciana, Valencia, Spain, [3] Red Sea Research Centre and Computational Biology Research Centre, King Abdullah University of Science and Technology, Thuwal, Saudi Arabia, [4] Future Ocean Cluster of Excellence, GEOMAR Helmholtz Centre for Ocean Research, Kiel, Germany

Vertebrates are recognized as sentient beings. Consequently, urgent priority is now being given to understanding the needs and maximizing the welfare of animals under human care. The general health of animals is most commonly determined by physiological indices e.g., blood sampling, but may also be assessed by documenting behavior. Physiological health assessments, although powerful, may be stressful for animals, time-consuming and costly, while assessments of behavior can also be time-consuming, subject to bias and suffer from a poorly defined link between behavior and health. However, behavior is recognized as having the potential to code for stress and well-being and could, therefore, be used as an indicator of health, particularly if the process of quantifying behavior could be objective, formalized and streamlined to be time efficient. This study used Daily Diaries (DDs) (motion-sensitive tags containing tri-axial accelerometers and magnetometers), to examine aspects of the behavior of bycaught loggerhead turtles, *Caretta caretta* in various states of health. Although sample size limited statistical analysis, significant behavioral differences (in terms of activity level and turn rate) were found between "healthy" turtles and those with external injuries to the flippers and carapace. Furthermore, data visualization (spherical plots) clearly showed atypical orientation behavior in individuals suffering gas emboli and intestinal gas, without complex data analysis. Consequently, we propose that the use of motion-sensitive tags could aid diagnosis and inform follow-up treatment, thus facilitating the rehabilitation process. This is particularly relevant given the numerous rehabilitation programs for bycatch sea turtles in operation. In time, tag-derived behavioral biomarkers, TDBBs for health could be established for other species with more complex behavioral repertoires such as cetaceans and pinnipeds which also require rehabilitation and release. Furthermore, motion-sensitive data from animals under human care and wild conspecifics could be compared in order to define a set of objective behavioral states (including activity levels) for numerous species housed in zoos and aquaria and/or wild species to help maximize their welfare.

Keywords: animal behavior, animal health assessment, archival tag, accelerometer, magnetometer, bycatch, rehabilitation, sea turtle

OPEN ACCESS

Edited by:
Dennis Murray,
Trent University, Canada

Reviewed by:
Jacob Brownscombe,
Dalhousie University, Canada
Adrian C. Gleiss,
Murdoch University, Australia

****Correspondence:***
Alexandra C. Arkwright
a.arkwright@hotmail.co.uk

Specialty section:
This article was submitted to Behavioral and Evolutionary Ecology, a section of the journal Frontiers in Ecology and Evolution

Received: *16 November 2018*
Accepted: *11 December 2019*
Published: *21 January 2020*

Citation:
Arkwright AC, Archibald E, Fahlman A, Holton MD, Crespo-Picazo JL, Cabedo VM, Duarte CM, Scott R, Webb S, Gunner RM and Wilson RP (2020) Behavioral Biomarkers for Animal Health: A Case Study Using Animal-Attached Technology on Loggerhead Turtles. Front. Ecol. Evol. 7:504. doi: 10.3389/fevo.2019.00504

INTRODUCTION

Animals are recognized as cognizant beings, with high priority now given to understanding behavioral requirements and maximizing animal welfare under human care (Hawkins, 2004; Boissy et al., 2007; Shorter et al., 2017). Generally, animal well-being is evaluated through physiological health assessments e.g., periodic blood sampling, which can cause animals distress and pain (Abou-Ismail et al., 2007; Burman et al., 2007; Scollo et al., 2014) whilst also being expensive and time consuming (Hawkins, 2004). However, animal health can also be assessed through behavior, requiring an understanding of differing behavioral states that result from factors like elevated stress, infirmity, and injury (Broom and Johnson, 1993; Rushen, 2003; Lawrence, 2008). At present, assessments of behavior can be time-consuming, subject to bias and suffer from a poorly defined link between behavior and well-being in general (Broom and Johnson, 1993; Rushen, 2003; Lawrence, 2008). Animal-attached technology may thus provide a solution to many of these issues, enabling the process of quantifying behavior to be formalized and streamlined to be time-efficient and objective (see Cooke et al., 2004; Ropert-Coudert and Wilson, 2005; Ellwood et al., 2007; Cooke, 2008; Guesgen and Bench, 2017).

The attachment of tags to animals, which started decades ago [as early as the 1960s in marine vertebrates (Kooyman, 2004)], has transformed our understanding of animal behavior and eco-physiology (Naito, 2004) and catalyzed the development of whole new disciplines such as movement ecology (Nathan et al., 2008). In particular, archival-, rather than transmission-tag technology [aka bio-logging, where multiple parameters are recorded (Ropert-Coudert and Wilson, 2005)], has demonstrated its use in helping transform our understanding of animal physiology (Block, 2005; Sherub et al., 2017), behavior (Brown et al., 2013), and ecology (Wilmers et al., 2015). Biologging also has huge potential in areas relating to animal well-being *via* studies on farmed animals, particularly cattle (Turner et al., 2000; Shirai and Yokoyama, 2014; Thorup et al., 2015), but also aquaculture (Andrewartha et al., 2015) and with respect to conservation (Cooke, 2008; Ropert-Coudert et al., 2009; Bograd et al., 2010; Wilson et al., 2015). Accelerometer biologgers have also proved valuable for tracking behavioral changes and the survival of various fish species (including blacktip sharks, *Carcharhinus limbatus* (Whitney et al., 2016); arapaima, *Arapaima cf. arapaima* (Lennox et al., 2018), and bonefish, *Albula spp.* (Brownscombe et al., 2013) post-release, following fishery-related and recreational capture. For farmers, tagging has a wide range of applications from locating animals that have escaped their paddocks and tracking resource consumption (Sikka et al., 2006), to detecting lameness (Thorup et al., 2015); activities which would usually require manpower and time. Recently biotelemetry has also gained popularity within pet caring practices with dog owners tracking their pets to know their whereabouts (Mancini et al., 2012).

Somewhat surprisingly, given the clear potential of biologging to monitor animal health, the tagging community has done relatively little work in zoos and aquaria (with the exception of some studies that have used animals under human care to help identify behaviors with a view to using loggers on wild animals (Shepard et al., 2008; Ismail et al., 2012). One notable study that does, however, report on the potential of logging technology to study the well-being of animals under human care, is that by Shorter et al. (2017), which examined the activity of a total of ca. 57 h of data derived from 5 bottlenose dolphins, *Tursiops truncatus*, using motion-sensing animal-attached tags (DTAGS, see Johnson and Tyack, 2003). Another study, on Koalas at a conservation center, used accelerometers in combination with electrocardiogram recorders to assess heart rate during periods of inactivity whilst animals where in the presence and absence of tourists (Ropert-Coudert et al., 2009). Otherwise the lack of tags on animals maintained in a controlled environment *per se* is particularly curious since tags are unlikely to be lost (Bidder et al., 2014), animals are easy to catch compared to their wild counterparts and can even be trained to participate voluntarily (Ward and Melfi, 2015; Shorter et al., 2017). Moreover, the issue of animal welfare is repeatedly raised within the context of zoos and aquaria (Hill and Broom, 2009). Indeed, many of the major issues discussed relating to animal welfare, such as the incidence of stereotypic behaviors (Mason and Rushen, 2008), stress (Wiepkema and Koolhaas, 1993), and assessing the extent to which behaviors exhibited by animals under human care conform to those of their wild conspecifics (Veasey et al., 1996), could potentially be well quantified by logger technology (Wilson et al., 2014; Pagano et al., 2017).

A decade ago, a multi-sensor archival tag, the "Daily Diary," DD (which records tri-axial acceleration and tri-axial magnetometry, temperature and pressure), was conceived to quantify the behavior and ecology of threatened megafauna (Wilson et al., 2008). However, this tool has not been used, until now, to elucidate the link between animal behavior and health (Broom and Johnson, 1993; Rushen, 2003; Lawrence, 2008). Since behavioral state should relate to biomarkers of stress and well-being, the DD has the potential to be used to derive metrics which act as "behavioral biomarkers" of health (Broom, 1991; Lawrence, 2008) and form part of a less invasive diagnosis process (requiring no physiological samples).

The present study used DD loggers to examine aspects of the behavior of bycaught loggerhead turtles, *Caretta caretta*, housed in the "Arca del Mar" rehabilitation center at the Oceanogràfic aquarium, Valencia, Spain. Sea turtles being rehabilitated at the center commonly suffer bycatch-related external and/or internal injuries, including gas emboli (i.e., the formation of gas bubbles within the blood stream and tissues) and decompression sickness (Portugues et al., 2018). No animal was caught for the purpose of this study. The aim of this study was to investigate whether tag-derived "behavioral biomarkers" (TDBBs) for health could be established by monitoring changes in movement behaviors determined by multi-sensor tags and validated through conventional health assessments during sea turtle rehabilitation. We hypothesized that specific behavioral aspects would vary in accordance with a particular illness/injury, thus enabling the creation of TDBBs that could then be used to track recovery and potentially serve as diagnostic tools. This article also discusses how data from motion- and orientation-sensitive animal-attached tags might be used to derive useful metrics (such

as activity level and turning rate) for assessing animal health and welfare in human controlled environments.

METHOD

Animals

All of the loggerhead turtles used in this study were accidentally captured (bycaught) in gillnet and trawling fisheries off the coast of eastern Spain except potentially: three that were found floating at the surface, two that were transferred from other aquariums and one that was found stranded (see **Table 1**). Sea turtles were brought to the facility by staff from the local strandings network; the duration from the point of accidental capture to arriving at the center was not known. All bycaught turtles from participating fishing boats were brought to the clinic even if the animal did not exhibit visible signs of disease or trauma. Sea turtles were typically brought to the center with a variety of bycatch-related external and/or internal injuries including gas emboli and decompression sickness (Garcia-Parraga et al., 2014; Portugues et al., 2018).

Veterinary Care

Clinical examination was carried out at the rehabilitation center, "Arca del Mar" which is managed by the Fundación Oceanogràfic in Valencia, Spain. The facility has a permit from the Valencian Regional Government for sea turtle rehabilitation (both bycaught and stranded) and post-mortem examination. Upon arrival, all turtles underwent a health assessment including a complete physical examination, blood sample collection and diagnostic imaging (radiographs and ultrasound). Vets used turtle entry number (a running count of the number of turtles admitted year on year) to identify individuals; for ease the same identification numbers were used in this manuscript. Turtle numbers were preceded by a T to help differentiate them from other numbers within the text. Sea turtles at the facility were housed in circular tanks, ranging from 2 to 6 m in diameter and with a water depth of 0.95 m. Two different filtration systems operated maintaining "A" and "B" tanks at temperatures of ∼20°C and ∼24°C, respectively, in order to acclimatize sea turtles to lower temperatures before they were released. All animals admitted were maintained at the rehabilitation center until they were deemed fit for release.

Gas Embolism and Decompression Sickness

It has recently been found that some bycaught loggerheads exhibit gas emboli within the blood stream and tissues and suffer symptoms of decompression sickness; afflicted animals have also been found to display anomalous behaviors ranging from being comatose to being hyperactive (Garcia-Parraga et al., 2014). Embolisms can lead to organ injury, impairment, and even animal mortality, especially in individuals with moderate to severe gas emboli that do not receive hyperbaric O_2 treatment (Garcia-Parraga et al., 2014).

The presence and severity of gas emboli were determined by radiographs and ultrasound examination and scored on a 5-point scale: no intravascular gas detected, very mild, mild, moderate and severe (for further details see Garcia-Parraga et al., 2014; Fahlman et al., 2017). Animals with observable gas emboli received recompression therapy using pure O_2 from a pressurized medical O_2 cylinder. This hyperbaric oxygen treatment was administered via a custom-built hyperbaric chamber (41 × 77 cm, internal height and diameter). After recompression treatment (which was often administered overnight due to turtles arriving in the afternoon/evening), another health assessment was conducted to evaluate the resolution of gas emboli. Individuals were only placed in holding tanks once no gas emboli were detected in the blood (usually the morning after recompression treatment) and were considered to be in a state of recovery (convalescent) from that moment on. Turtles remained under daily supervision until their blood values and their feeding, swimming and diving behaviors were normal.

Tagging

Sea turtle behavior was studied by equipping animals with acceleration- and magnetic-field-measuring data-loggers ["Daily Diaries," DD, housing dimensions 54 × 29 × 22 mm, mass 22 g, although there was some variation in size (Wilson et al., 2008)] recording at 20 Hz per channel. Devices measured both acceleration [logged with respect to gravity (∼1 g), range; ± 16 g] and magnetic field intensity [recorded in Gauss (G) at 0.73 mG resolution, range; ± 0.88 G] in three orthogonal axes: heave (dorso-ventral), sway (lateral) and surge (anterior-posterior). In addition to describing behavior *via* body posture, body "vibrancy" (Halsey et al., 2011b) and body rotation (Williams et al., 2017), tags quantified proxies for energy expenditure (Dynamic Body Acceleration—DBA, specifically VeDBA (Halsey et al., 2011b), and the physical characteristics of the animal's environment, i.e., temperature and pressure (Wilson et al., 2008).

In order to attach the DDs, bycaught turtles were lifted out of their holding tank and placed onto a foam mat and/or into a plastic box. Tags were attached to the second central scute of the carapace with a two-part epoxy (Veneziani Subcoat S), pre-mixed in water. Animals were tagged opportunistically for deployment periods lasting just over a day, up to six consecutive days during April-May and November-May 2017–2018. When possible, turtles were tagged as soon as they were released into one of the holding tanks at the rehabilitation center. This varied according to condition; for healthy turtles and those with minor injuries, individuals could be admitted to a tank following a veterinary health assessment, whereas for turtles with gas emboli (which typically received hyperbaric treatment overnight), this was usually the day following recompression treatment. All protocols were approved by the Oceanogràfic Animal Care & Welfare Committee (OCE-16-18) and the Swansea University Animal Welfare Ethical Review Body (STU_BIOL_82015_011117151527_1). No medical procedures were conducted solely for research purposes.

Data Analysis

The data were analyzed using custom designed software "Daily Diary Multi Trace" (DDMT, http://wildbytetechnologies.com/software.html), R-Studio (version 3.6.0, R Foundation for Statistical Computing, Vienna, Austria, http://www.R-project.org/), the R packages "nlme," [version 3.1–141 (Pinheiro and

TABLE 1 | Summary of tagged turtle data including: turtle identification number, entry to and release dates from the rehabilitation center, bycatch origin, weight (kg), cause of injury/disease (when known), and the animals' state of health upon entry, and on the date of tagging (as deduced via veterinary examination).

Turtle ID	Entry	Release	Origin	Weight (kg)	Cause of injury/disease	State of health upon entry	Tagging date	State of health when tagged
T297	03/01/17	22/08/17	Cullera	5.4	Trawl/bottom fishing	Severe GE, died and was resuscitated	17/04/17	Healthy
T308	16/02/17	30/06/17	Calpe	10	Trawl/bottom fishing	Moderate GE	18/04/17	Healthy
T318	15/03/17	20/04/17	Cullera	3.5	Trawl/bottom fishing	Moderate GE	18/04/17	Healthy
T320	17/03/17	21/04/17	Peniscola	9.47	Trawl/bottom fishing	Mild-Moderate GE	18/04/17	Healthy
T322	23/03/17	21/04/17	Peniscola	5.55	Trammel net	Drowned, died and was resuscitated	18/04/17	Healthy
T324	31/03/17	13/05/17	Valencia	17	Trawl/bottom fishing	Healthy	29/04/17	Healthy
T325	03/04/17	29/04/17	Valencia	11.54	Trawl/bottom fishing	Healthy	22/04/17	Healthy
T326	04/04/17	11/06/17	Gandia	15.5	Trammel net	Drowned, died and was resuscitated	25/04/17	Convalescent
T330	12/04/17	06/05/17	Oropesa	5.6	Unknown (found floating at surface)	Healthy	22/04/17	Healthy
T331	18/04/17	08/06/17	Gandia	3.07	Trammel net	Intestinal gas, floatability issues	22/04/17	Floatability issues
T332	26/04/17	DIED	San Sebastian	18.9	Unknown (transferred from another aquarium)	Multi-organ failure	29/04/17	Multi-organ failure
T339	22/07/17	10/04/18	Benidorm	4.2	Stranded with gillnet associated injuries	Severely damaged and infected right front flipper	29/11/17	Damaged and infected right front flipper
T342	11/10/17	TBC*	Vinaroz	15.8	Trawl/bottom fishing	Severe carapace trauma and damage to spinal cord	15/12/17	Severe carapace trauma and damage to spinal cord
T343	23/10/17	20/06/18	San Sebastian	11.19	Unknown (transferred from another aquarium)	Floatability issues	15/12/17	Floatability issues
T344	26/09/17	18/12/17	Vinaroz	12.1	Trammel net	Healthy	29/11/17	Healthy
T345	02/11/17	20/12/17	Vinaroz	17.1	Trammel net	Healthy	29/11/17	Healthy
T347	03/11/17	TBC*	Murcia	4.52	Unknown, found stranded (transferred from another aquarium)	Carapace trauma, partial front flipper amputation	24/05/18	Carapace trauma, partial front flipper amputation
T350	28/11/17	27/12/17	Peniscola	15	Trawl/bottom fishing	Moderate GE	29/11/17	Convalescent
T352	05/12/17	06/06/18	Cullera	4.45	Trawl/bottom fishing	Severe GE, died and was resuscitated	07/12/17	Bites and skin infection
T359	02/01/18	04/03/18	Benicarlo	20.8	Trawl/bottom fishing	Moderate GE	03/01/18	Convalescent
T362	16/01/18	06/03/18	Cullera	13	Trawl/bottom fishing	Moderate GE	09/02/18	Healthy
T380	05/03/18	10/04/18	Calpe	8.4	Trawl/bottom fishing	Moderate GE	12/03/18	Convalescent
T383	14/03/18	14/04/18	Cullera	11.6	Trawl/bottom fishing	Moderate GE	15/03/18	Convalescent
T384	15/03/18	06/04/18	El Saler	15.2	Trawl/bottom fishing	Mild GE	16/03/18	Convalescent
T385	18/03/18	20/07/18	Valencia	8.6	Trawl/bottom fishing	Healthy	15/06/18	Healthy
T393	28/03/18	04/05/18	El Saler	28.71	Trawl/bottom fishing	Moderate GE	18/04/18	Convalescent
T396	28/03/18	05/07/18	Vinaroz	22	Trawl/bottom fishing	Healthy	08/05/18	Healthy
T397	05/04/18	03/06/18	Gandia	7.3	Trammel net	Drowned and was resuscitated	08/05/18	Convalescent
T399	06/04/18	08/06/18	Cullera	5.7	Trammel net	Healthy	06/06/18	Healthy
T402	16/04/18	09/06/18	Burriana	5.7	Trawl/bottom fishing	Healthy	29/05/18	Healthy
T403	06/05/18	29/06/18	El Perello	7.24	Unknown (found floating at surface)	Healthy	11/06/18	Healthy
T404	07/05/18	06/07/18	Almenara	3.24	Unknown (found floating at surface)	Wounded neck	13/06/18	Wounded neck
T405	01/06/18	12/07/18	Peniscola	34.24	Trawl/bottom fishing	Very mild GE	26/06/18	Healthy

NB: gas emboli (GE) was categorized as mild, moderate or severe; turtles that entered with GE were considered "convalescent" when tagged within a couple of days of admission as they were only released into holding tanks following hyperbaric chamber treatment and once there was no sign of GE in the blood.
**TBC to be confirmed.*

Bates, 2000; Pinheiro et al., 2015)] and "MuMIn," [version 1.43.6 (Barton, 2019)] and Microsoft Excel (version 365). Data visualization with DDMT displayed sensor lines (tri-axial acceleration, tri-axial magnetic field intensity, pressure, temperature and derivatives—see below) on the y-axis against time on the x-axis as well as multi-dimensional plots that were used to reveal patterns in the data (Walker et al., 2016; Wilson et al., 2016; Williams et al., 2017). These took the form of spherical (tri-axial) plots where two axes (the horizontal axes) displayed two different parameters, such as time and animal body pitch, while the third, vertical, axis displayed a frequency count. This enabled the incidence of particular conditions to be examined easily. Certain parameters, such as pitch and roll, have values that describe a sphere, resulting in frequency histograms forming on the surface of a sphere.

Derivatives used for describing behaviors included the dynamic body acceleration (*DBA*), specifically the Vectorial Dynamic Body Acceleration (VeDBA), using methods described in Qasem et al. (2012), because *DBA* is a proxy for both energy expenditure in vertebrates in general (Halsey et al., 2011b) and loggerhead turtles in particular (Halsey et al., 2011a, cf. Enstipp et al., 2011), as well as being a useful general measure for activity (Gleiss et al., 2011). Another useful derivative when examining animal behavior is that of compass heading (i.e., orientation about the yaw axis or turning) (Bidder et al., 2015; Walker et al., 2015b; Williams et al., 2017). DDMT software uses calibration data to correct for iron distortions and tilt offsets prior to calculating heading on a scale of 0–360°. Any tilt of the DD causes a distortion in the compass heading values, which are corrected through the use of the static component of acceleration (due to gravity; 9.81 m/s^{-2}), the animal's pitch and roll values, in relation to the output of the tri-axial magnetometers (Walker et al., 2016); also known as a tilt-compensated compass. For information regarding the stages and equations involved in the computation of pitch, roll and compass heading see Bidder et al. (2015) and Walker et al. (2015b). Subsequent analyses including mean VeDBA per hour and heading (specifically the number of turns per hour surpassing a threshold of 45°) were calculated using data undersampled from 20 Hz to 4 Hz; VeDBA and heading data was also smoothed over 2 s to reduce noise. VeDBA and heading were used in statistical analysis after data visualizations indicated differences in animal movement (pitch, roll and directionality) for turtles in various states of health and because the two parameters combined provided a straight-forward (and therefore easily applicable) but also reasonably comprehensive way of investigating potential differences in movement behavior.

A linear mixed-effects model (LMEM) was performed to see if turtle condition (included as a predictor) affected the relationship between the number of turns per hour (surpassing a threshold of 45°) and mean VeDBA per hour. A log transform was performed on both the dependent (VeDBA) and independent (turn rate) variables to normalize the data and turtle ID was incorporated into the model as a random effect to account for inter-individual differences (for example, turtle size and sex). Tank size was also included in the model to account for any confounding effects it might have; consequently, the model included all turtles ($n = 22$) tagged post July 2017 for which tank size (i.e., the available water mass) was known (see **Table 1**).

In order to perform the analysis, turtle condition was grouped into three categories: healthy ($n = 9$; used as baseline reference), external injury ($n = 5$; e.g., skin lesions and flipper and carapace damage) and internal injury ($n = 8$; e.g., intestinal gas and gas emboli). To account for diurnal changes in behavior the model contained 24 h of data per turtle with the analysis starting 1 h after each turtle had been released into a tank to allow for acclimatization post handling. The model was run using the "lme" function in R, from the "nlme" package (Pinheiro and Bates, 2000; Pinheiro et al., 2015); to allow for heterogeneity of variance between individuals (indicated by model diagnostic plots) the model was updated to include the "varIdent" function (Gałecki and Burzykowski, 2013). Akaike Information Criterion (AIC) values along with forwards stepwise selection were used to find the best fitting model and p-values were obtained via the "anova" summary. Marginal and conditional R^2 values for model goodness-of-fit were calculated using the "r.squaredGLMM" function in the "MuMIn" package (Barton, 2019), (the marginal R^2 indicated the variance explained by fixed factors, and conditional R^2 indicated the variance explained by both fixed and random factors) (Nakagawa and Schielzeth, 2013). The magnitude of dependence in scores attributable to differences between turtles (turtle ID) was quantified via the intraclass correlation coefficient (ICC). This was estimated as proportion of variance in the dependent variable (VeDBA) resulting from turtle ID, to total variance; where σ_τ^2 was the estimated turtle variance and σ_ε^2 was the estimated residual variance (Kenny and Hoyt, 2009).

$$ICC = \frac{\sigma_\tau^2}{\sigma_\tau^2 + \sigma_\varepsilon^2}$$

RESULTS

Thirty-three turtles were tagged during this study; upon the date of tagging, 17 were considered healthy (based on veterinarian assessments), eight were recovering from various degrees of gas emboli (convalescent), four had external injuries (on the neck, flipper, and/or carapace), two had floatability issues and one suffered multi-organ failure of unknown causes (see **Table 1** for details). Despite the relatively large sample size, the variation in condition and small number of comparable individuals for condition (especially with respect to correcting for e.g., size and sex) meant that we had little capacity to verify our results statistically; as such we were unable to link specific pathologies with movement data.

Nonetheless, statistical analysis did indicate that turtle condition [grouped into healthy ($n = 9$), external injury ($n = 5$) and internal injury ($n = 8$)] affected behavior, specifically the relationship between mean VeDBA and the number of 45° turns performed per hour (**Table 2**; **Figure 1**). Forwards stepwise selection and AIC values showed that the full model incorporating all covariates (turn rate, turtle condition, turtle ID and tank size) yielded the best goodness-of-fit (marginal $R^2 = 0.81$; conditional $R^2 = 0.96$). The number of turns per hour

TABLE 2 | Linear mixed-effects model (LMEM) estimates of fixed effects, *p*-values and 95% confidence intervals for log-transformed VeDBA.

Variable	Est.	S.E.	*t*-value	d.f.	95% CI	*p*-value
Intercept	−5.06	0.12	−47.04	505	[−5.270, −4.850]	0.00
Log turns/hour (45°)	0.33	0.02	17.04	505	[0.292, 0.367]	0.00
External injury	0.18	0.06	3.01	15	[0.052, 0.301]	0.01
Internal injury	0.07	0.04	1.52	15	[−0.025, 0.157]	0.15
Tank size (3,074 kg)	−0.05	0.07	−0.69	15	[−0.188, 0.095]	0.50
Tank size (3,458 kg)	0.01	0.06	0.16	15	[−0.120, 0.140]	0.87
Tank size (6,148 kg)	−0.14	0.06	−2.09	15	[−0.273, 0.001]	0.05
Tank size (19,212 kg)	−0.19	0.07	−2.87	15	[−0.335, −0.051]	0.01

The analysis was performed to see if turtle condition (healthy, external injury or internal injury) affected the relationship between the number of turns per hour (surpassing a threshold of 45°) and mean VeDBA per hour during the first 24 h of tag attachment.

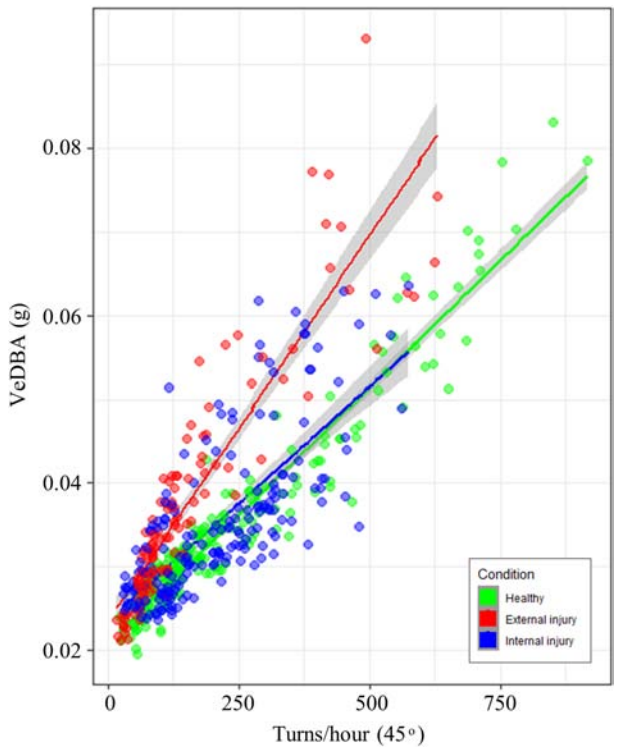

FIGURE 1 | Relationship between the number of turns per hour that surpassed a 45° threshold and mean VeDBA (g) per hour. Data points and regression lines are colored according to turtle condition (healthy = green, external injury = red and internal injury = blue); 95% confidence intervals are indicated by the gray shading either side of regression lines. Line gradients indicate that the relationship between turning rate and VeDBA differed little between healthy turtles and those with internal injuries; turtles with external injuries however, had substantially higher VeDBA values per number of turns.

(that surpassed 45°) significantly affected VeDBA (LMEM: $\chi^2_{(2)} = 143.28$, $p < 0.001$); for every 10% increase in turn rate, VeDBA increased by just over 3% [Est. = 0.33 ± 0.02 (S.E), $t = 17.04$, 95% CI [0.292, 0.367], $p < 0.001$]. The largest tank size (containing a water mass of 19,212 kg) had a significant negative effect on this relationship. External injuries had a significant positive effect on turtle activity; per 10% increase in turn rate, VeDBA increased by almost 2% [Est. = 0.18 ± 0.06 (S.E), $t = 3.01$, 95% CI [0.052, 0.301], $p = 0.01$]. Internal injuries, however, did not significantly affect the relationship between turn rate and activity [Est. = 0.07 ± 0.054 (S.E.), $t = 1.52$, 95% CI [−0.025, 0.157], $p = 0.15$]. The intraclass correlation coefficient (ICC) was high (0.98), indicating high similarity between values from the same group ($n = 22$).

Movement Patterns for Various Conditions

Raw acceleration data showing movement patterns for turtles in varying states of health indicated differences at the individual level and in relation to condition (**Figures 2**, **3**) although more data are needed to be able to have the statistical power to determine this. A period of initial heightened activity was apparent in all example turtles (except T332) and ranged from half an hour to 3 h (see **Figure 2**, individuals T402 and T384, respectively) or more (see **Figure 3**, individuals T350 and T359). Acceleration data together with depth (pressure) data showed that turtles generally exhibited alternating active and rest periods (with rest periods at the bottom of the tank typically lasting 10–15 min). This behavior was most clearly defined in healthy turtles. Rest periods in turtles recovering from gas emboli (T383 and T384) were less distinguishable (as the acceleration traces were not as smooth) and more erratic. Magnetometry data (indicating animal orientation), changed closely in accordance with acceleration movement in healthy example turtles and individuals recovering from gas emboli (**Figure 3**). The trace that differed most from the others was that of T332 with multi-organ failure (**Figure 2**) that died soon after tagging. The turtle remained at the surface and moved little (as indicated by the elevated depth trace remaining constant and the small spikes in the VeDBA trace compared to the other turtles, respectively; **Figure 2**).

Activity Over Time

As observed previously, VeDBA (activity) in all healthy and unhealthy turtles (except T332 with multi-organ failure) was markedly raised for the first 3 to 4 h (**Figure 4**), particularly in animals with gas emboli (**Figure 4B**). After this initial period, VeDBA values tended to remain low and constant (<0.05 *g*) although some infirm individuals exhibited erratic periods of higher and lower VeDBAs (see **Figure 4**, individuals T331 and T384 in particular and **Figure 5**). The mean VeDBA for healthy turtles and standard deviation (**Figure 4**) were calculated using the seven turtles considered free of both disease and injury upon admission (despite 17 being considered healthy on the date of tagging) due to the subtle or undetectable long-term damage that gas emboli (particularly severe cases) can cause. During the first 24 h of tagging the VeDBA values of most afflicted turtles were within one standard deviation of healthy ones. However, the two rehabilitating turtles that deviated most frequently (T342 and T347) had both suffered severe carapace traumas (the latter also had a damaged fore flipper). Consistently low VeDBA values were recorded for T342, whereas for T347 they were within the healthy turtle range for the first 12 h and then rose markedly above but in

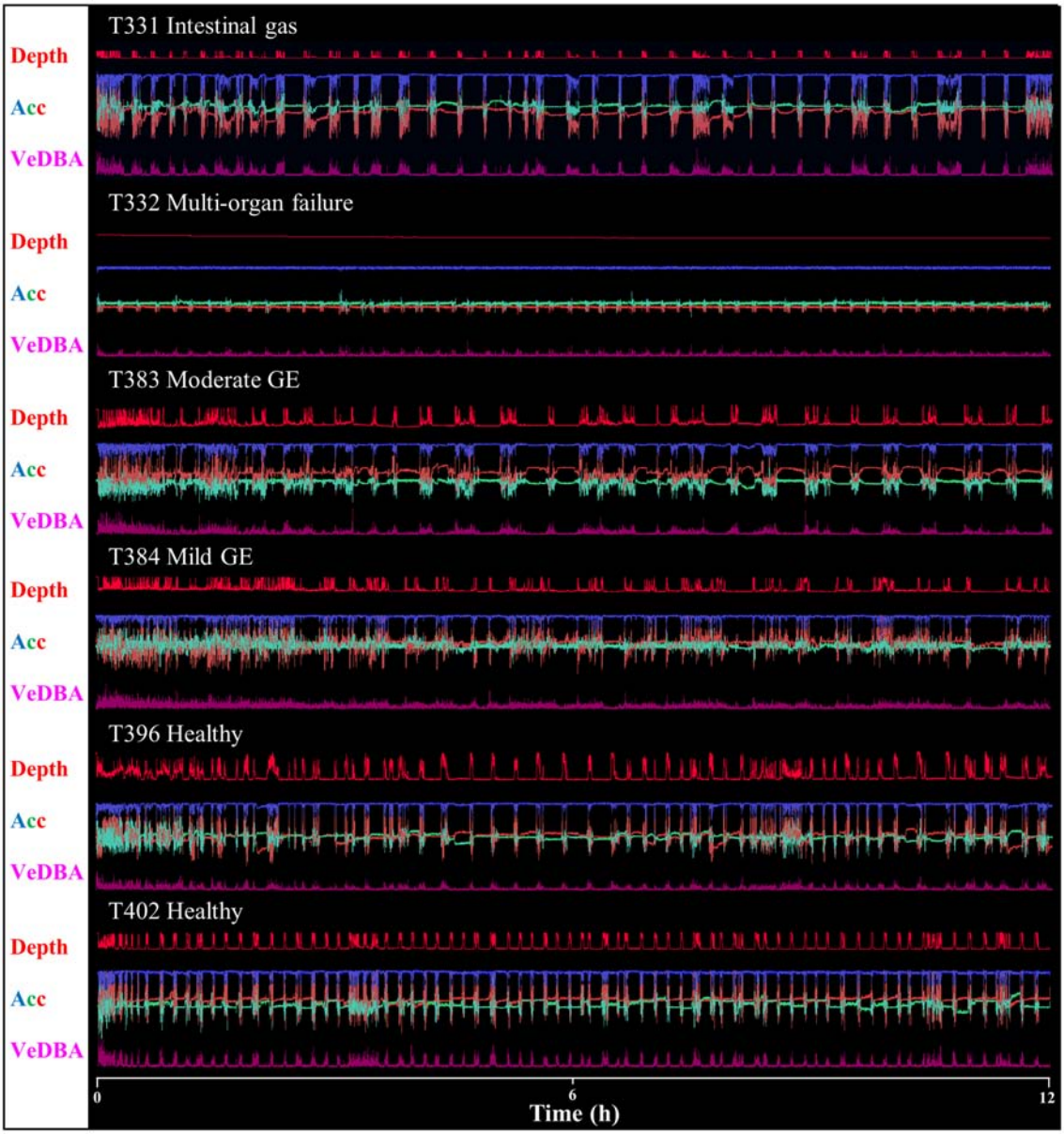

FIGURE 2 | Daily Diary recordings for five different individuals in various conditions showing depth (dives are readily apparent), the three orthogonal acceleration channels (Acc) and a general activity metric (VeDBA – for definition see text). Scale is omitted to declutter graph, but acceleration limits are −1 – 1 *g*, and the depth limit is *ca*. 1 m). Data show 12 h from the first time a turtle was tagged. Note how traces vary with animal condition, in particular individual T332 with multi-organ failure that, unlike the other individuals, did not exhibit regular, alternating rest and dive periods. Most animals displayed increased activity at first, that decreased with time; this was most evident in animals with gas emboli (GE) where an initial period of 2–3 h of high activity was visible (cf. **Figure 2**).

parallel with a small hump in VeDBA observed in healthy turtles some 20 h post-tagging.

Pitch, Roll, and Directionality

G-sphere visualizations of body pitch and roll [derived from the acceleration data, which showed the time allocated to different pitch and roll values [body attitude] (Wilson et al., 2016)] indicated slight differences between healthy and unhealthy rehabilitating turtles (**Figure 6**). Animals with serious illnesses and reduced activity generally occupied a smaller area of the g-sphere relative to healthy turtles; however, individuals recovering from gas emboli tended to occupy a slightly greater area. Magnetometry plots (m-plots, see Williams et al., 2017) showed clearer differences in movement behavior; unhealthy animals generally displayed greater variability in directionality than healthy ones (**Figure 7**). Variability in orientation was also observed in a turtle that underwent MRI, with rose plots indicating directionality becoming more concentrated with time post-scan (**Figure 8**).

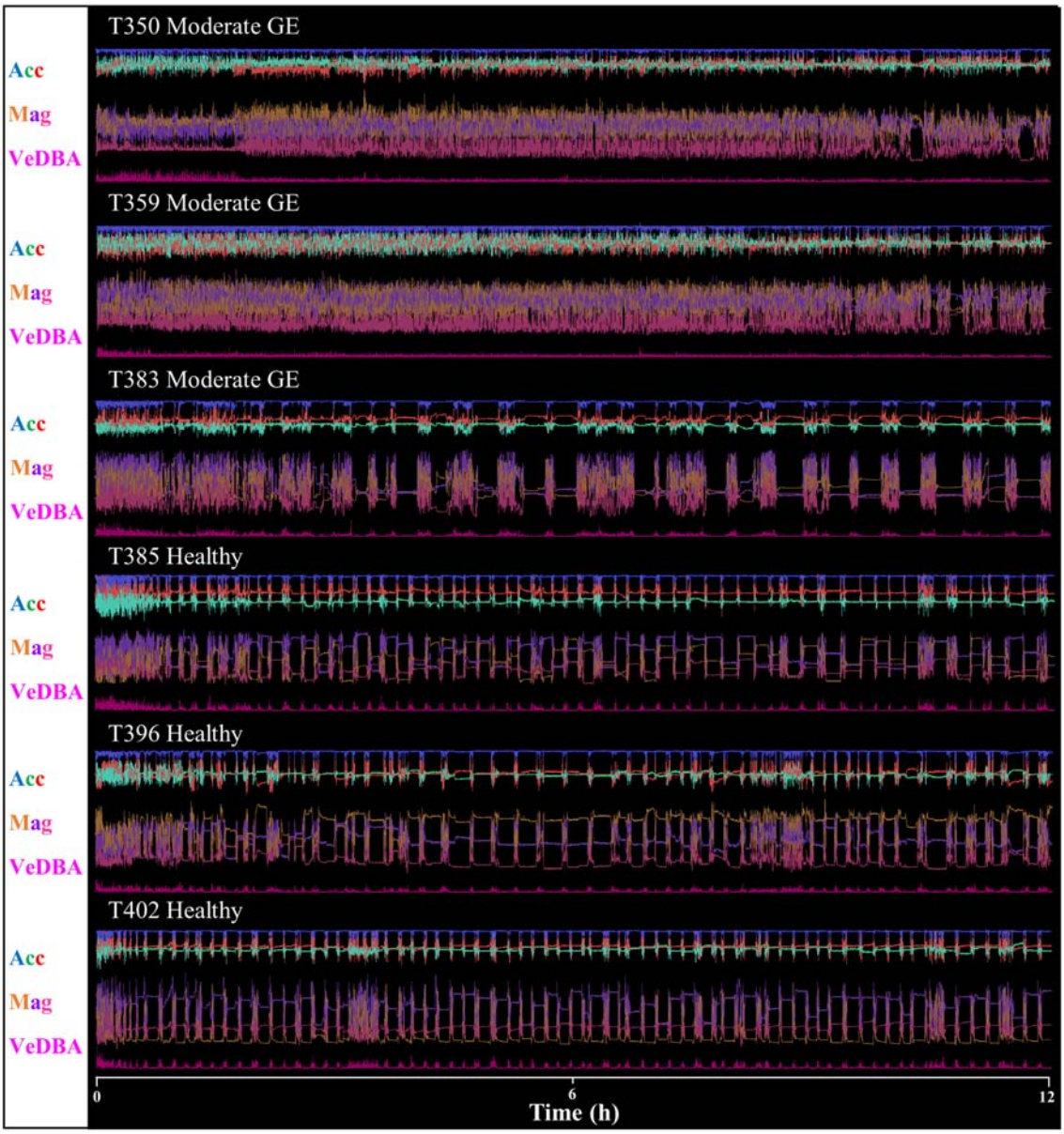

FIGURE 3 | Daily Diary recordings for five different individuals in various conditions showing the three orthogonal acceleration channels (Acc), three magnetometry channels (Mag) and a general activity metric (VeDBA—for definition see text). Scale is omitted to declutter graph; acceleration limits are −1–1 *g*, magnetometry limits 0.2−0.8 G). Data show 12 h from the first time a turtle was tagged. Note how traces vary between individuals that are healthy and those with gas emboli (GE); the former tended to display regular, alternating rest and dive periods, exhibited by the magnetic field data, and the latter exhibited increased activity lasting 3 h or more.

DISCUSSION

The purpose of this study was to investigate the effectiveness of animal-attached loggers to elucidate behavior in order to assess animal health in sea turtles undergoing rehabilitation. Behavior is recognized as having the potential to serve as an indicator of health (Abou-Ismail et al., 2007; Burman et al., 2007; Scollo et al., 2014; Guesgen and Bench, 2017), so movement-sensitive tags, such as the DDs used in this study, could be used to provide an objective and time-efficient way of quantifying behavior *via* the creation of TDBBs for health. Our statistical analysis, although with limited power, indicated that behavior (specifically the relationship between mean VeDBA and the number of 45° turns per hour) differed significantly between healthy individuals and those with external injuries (e.g., flipper damage, carapace trauma and skin lesions). Although this study focused on loggerhead turtles undergoing rehabilitation following fisheries interaction, the approach could potentially be adopted for a suite of aquatic (cf. Shorter et al., 2017), terrestrial (Mason and Rushen, 2008) or aerial species (Shepard et al., 2008). Our limited access to animals

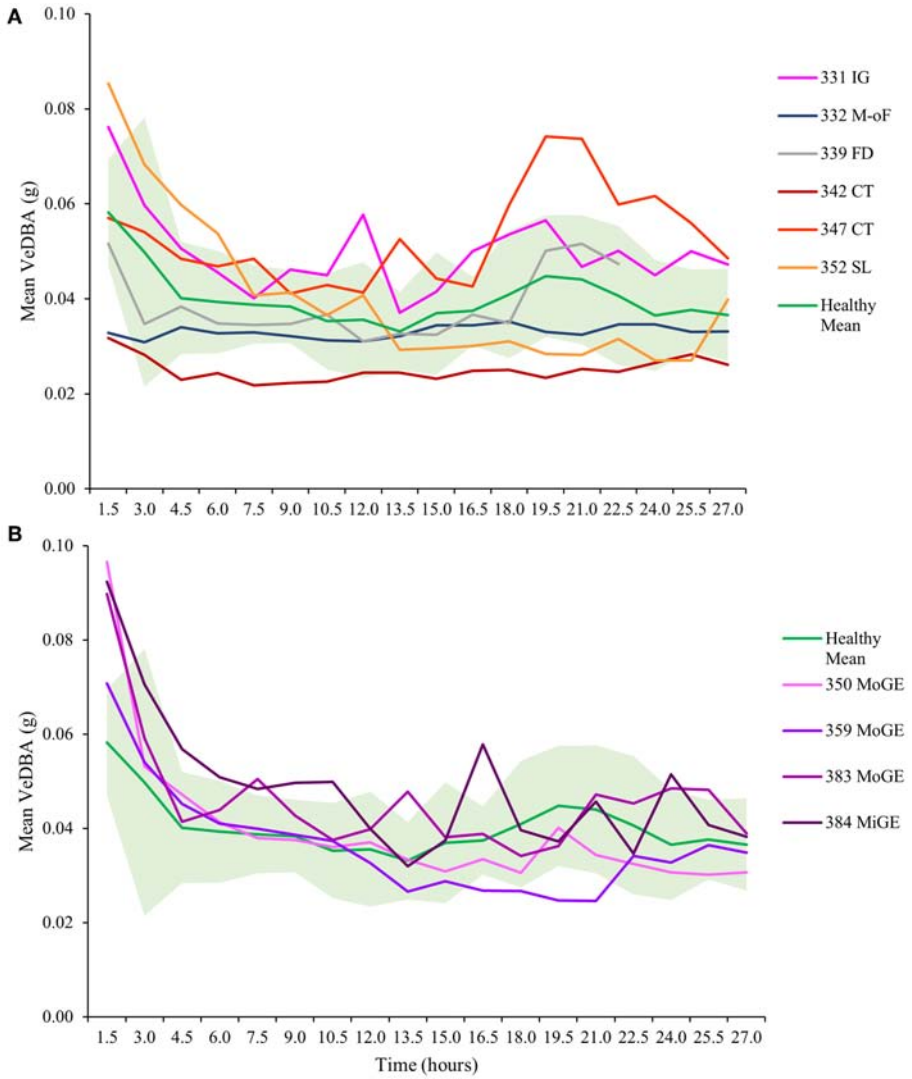

FIGURE 4 | Mean VeDBA (calculated over hourly intervals) in turtles with **(A)** various diseases and injuries and **(B)** turtles with gas emboli (GE), from the first moment they were tagged (cf. **Figures 2**, **3**). Turtles are identified by number (see **Table 1**). IG, intestinal gas; M-oF, multi-organ failure; FD, flipper damage; CT, carapace trauma; SL, skin lesions; MoGE, moderate gas emboli; MiGE, mild gas emboli. The mean VeDBA of turtles that were considered healthy upon entry (individuals T324, T325, T330, T344, T345, T385, and T396) is shown in green; the shaded light green area represents one standard deviation. Note the initially high values observed in most turtles for the first three to four hours (particularly in animals with GE).

precluded us from presenting exhaustive data analyses from a suite of turtles of defined size, unknown sex and in various states of health, so by in large we present sample data as examples of the features that can be resolved using this technology and speculate how these relate to health status.

Behavior and Condition

After being released into a holding tank, bycatch turtles generally exhibited a period of elevated activity ranging from half an hour to several hours (when examined over a 24 h period). In part this was probably due to tagging occurring during the day when activity levels were higher and there was more disturbance (caused by feeding and tank cleaning). In healthy turtles, this initial increase in activity typically lasted <2 h whereas in individuals with gas emboli this was always 3 h or more. This disparity could reflect the condition of the turtle, especially given that individuals with gas emboli have been known to display abnormal behavior, ranging from hyperactive to catatonic (Garcia-Parraga et al., 2014). However, disparities may also arise from a variety of other factors: side-effects of hyperbaric treatment, stress induced by handling (Grandin, 1997; Moberg, 2000; Carere and van Oers, 2004; Waiblinger et al., 2004; Gourkow and Fraser, 2006; Hemsworth et al., 2011), tag attachment (Bridger and Booth, 2003; Geertsen et al., 2004; Vandenabeele et al., 2011; Walker et al., 2011; Thomson and Heithaus, 2014), re-entering the water after many hours

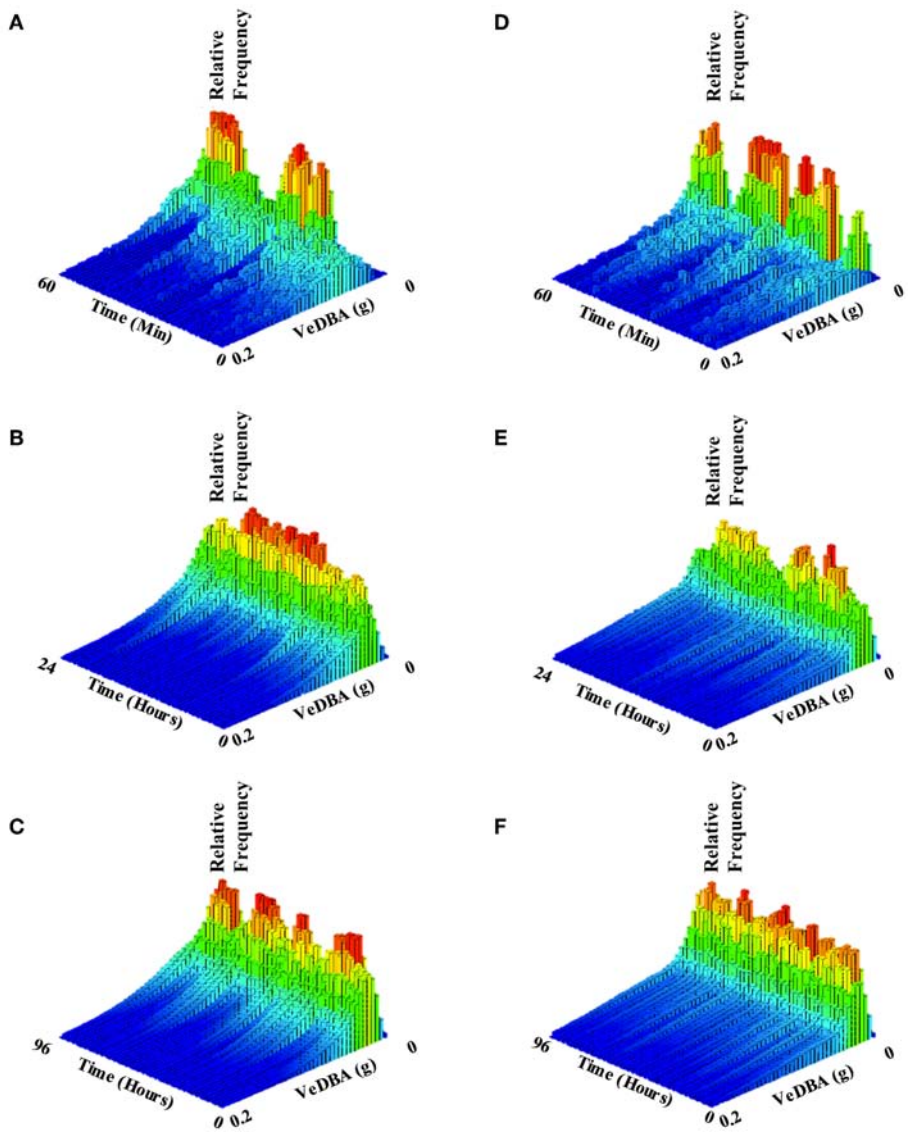

FIGURE 5 | Histograms showing allocation of activity (VeDBA) over varying time intervals, of two example turtles: T324, which was considered healthy (figures on the left; **A–C**) and T331 which had intestinal gas and associated floatability issues (figures on the right; **C,D,F**). Histograms cover time periods of one hour **(A,D)**, 24 h **(B,E)** and four days **(C,F)**. Bar color and height indicate the relative number of observations within the time interval. Note how, in both example turtles, lower VeDBA values occurred most frequently (red bars) but that the individual with intestinal gas exhibited erratic periods of high VeDBA, showing high effort in bursts interspaced by a high frequency of rests (cf. **A,D**) compared to the healthy individual. As the time period over which the animals are examined increases, the healthy individual spends more time overall exhibiting greater activity (manifest by the higher VeDBA - nominally from swimming) than the unhealthy animal (cf. **B,C** with **E,F**).

on land and being released into an unknown environment (Teixeira et al., 2007; Roe et al., 2010). These factors make it difficult to know what truly "healthy" turtle behavior in a rehabilitation center looks like using tag data. Nonetheless, significant behavioral differences in relation to activity and turn rate were found between "healthy" turtles and those with external injuries (see section Metrics That Might Indicate Changing State and Behavioral Breadth). Our statistical analysis also indicated that within group values had a high similarity, thus indicating that once healthy, turtles in rehabilitation exhibited similar behavior.

Interestingly, the relationship between activity level and turning for turtles with internal injuries did not differ significantly from healthy animals. However, the internal injuries included in analysis were unlikely to affect energy expenditure and movement to the same degree as missing part of a flipper or sustaining severe carapace trauma. Most of the turtles (six out of eight) that suffered internal injuries were admitted with gas emboli and as such were only released into a tank once they had no gas bubbles left in their blood (as per the standard veterinary procedure). By this time these individuals may have recovered sufficiently to exhibit activity levels and turning rates

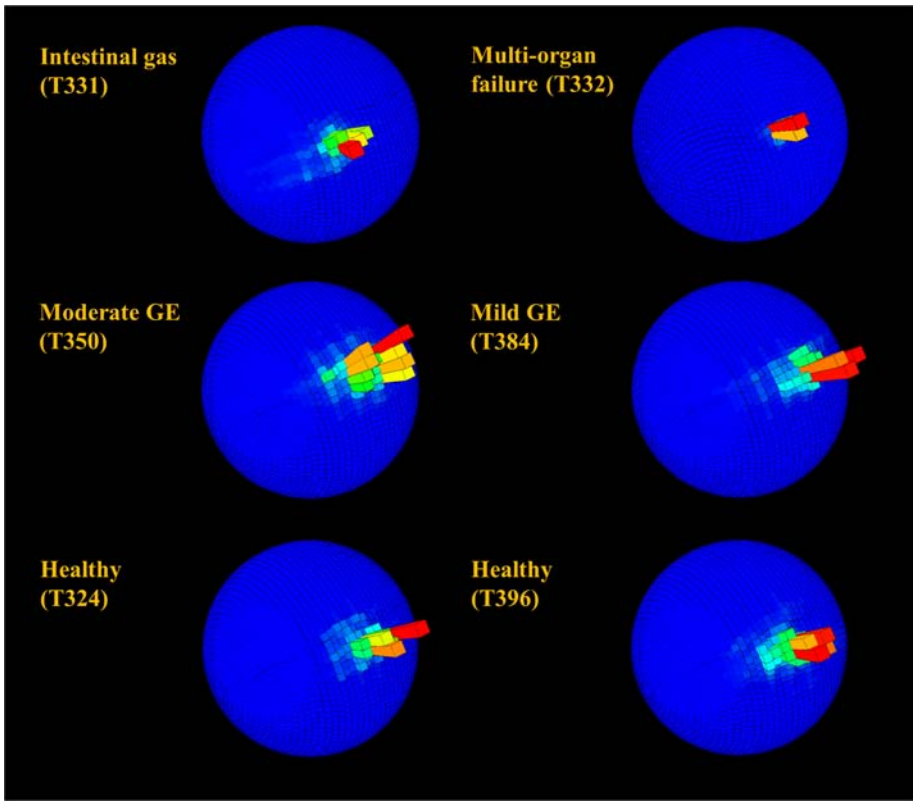

FIGURE 6 | Spherical histograms showing relative time (bar height and color; the mode is shown in red) over 24 h allocated to body pitch and roll (see Wilson et al., 2016 for more detail) in rehabilitating turtles. Individuals in rehabilitation are identified by number (see **Table 1**) and suffered from various diseases including gas emboli (GE). Despite the superficial semblance of plots, very infirm individuals (in particular T332) with reduced activity generally occupied a small area of the sphere relative to healthy turtles, whereas individuals with mild to moderate GE generally occupied a slightly greater area.

akin to those of "healthy" turtles. Potential differences between healthy animals and those with internal damage may have also been more apparent if two turtles with severe internal complications (T331 and T332) could have been included in statistical analysis. They were excluded from the analysis because the available water mass in which they had to move was unknown and our analysis suggested that tank size significantly affected behavior.

Further behavioral comparisons of healthy turtles and individuals recovering from internal injuries such as gas emboli and intestinal gas indicated other potential differences relating to condition. Rest and active periods (typically composed of active ascents and descents interspaced with resting on the tank floor) were often less defined in convalescent turtles; not only did rest intervals appear more sporadically, but acceleration traces were noisier, probably indicating impaired movement control during recovery and/or post hyperbaric treatment. Magnetometer plots also indicated a difference between healthy rehabilitating turtles and those with gas emboli, the latter tending to display less directionality, potentially indicating impaired stability or movement control. Differences between healthy and infirm individuals with intestinal gas (T331) and multi-organ failure (T332) were even more apparent, with deviations covering almost half, or more, of the m-sphere, respectively. Indeed, the trace that differed most from the others was that of turtle T332; the animal remained at the surface and was relatively inactive for the duration of tagging (4 days). As with many animals, maintaining a very low energy state and fatigue can be indicative of serious illness and a precursor of death (Drake et al., 2003; Gailliot et al., 2006). With a sufficient sample size, a range of expected energy levels (including the duration of "rest" and "active" periods as well as changes in VeDBA over time) for a given condition could be calculated, although these would also have to take into account turtle age, size, sex, and surroundings i.e., enclosure size, enrichment and water temperature, if found to be relevant.

Metrics That Might Indicate General Activity Patterns

We suggest that it should be possible to assess health status using VeDBA as a metric of general activity, for example, the comparison of animals with gas emboli vs. healthy individuals, aside from showing different postural changes, also demonstrated different VeDBA signatures. The paddling behavior in diseased animals was more intense and prolonged than in healthy

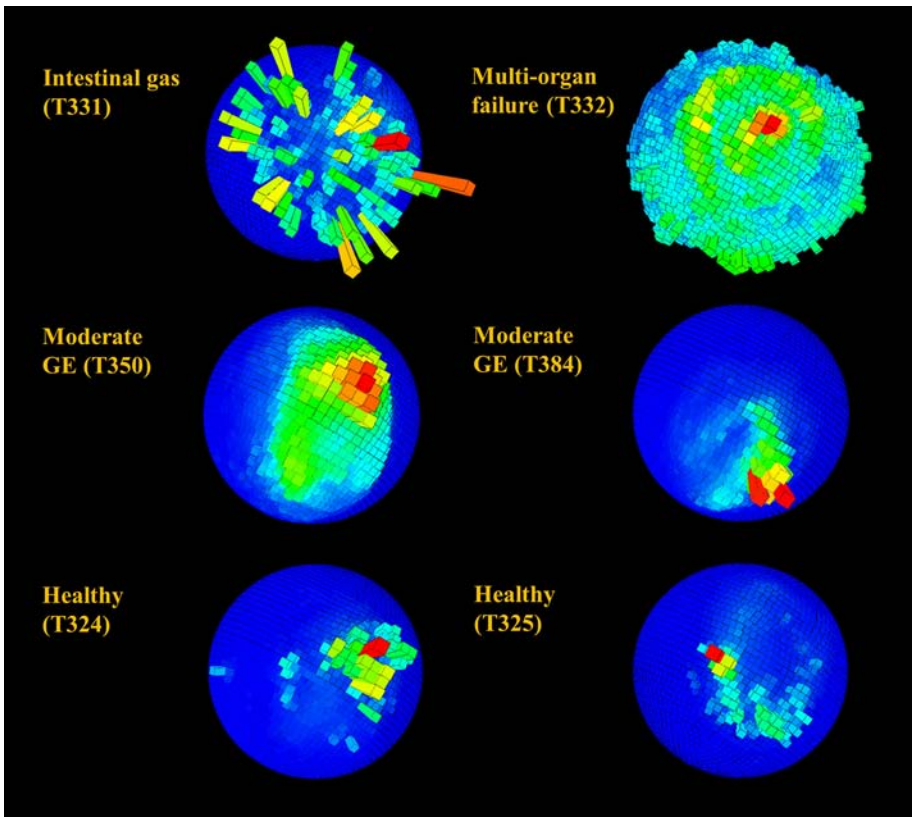

FIGURE 7 | Spherical magnetometer histogram plot (m-plot see Williams et al., 2017) showing relative time allocation (bar height and color; the mode is shown in red) to direction in rehabilitating turtles during a 24 h period. Individuals are identified by number (see **Table 1**) and suffered from various diseases including gas emboli (GE). Note the generally higher directionality observed in healthy individuals and the clear lack of directionally in animals T331 and T332.

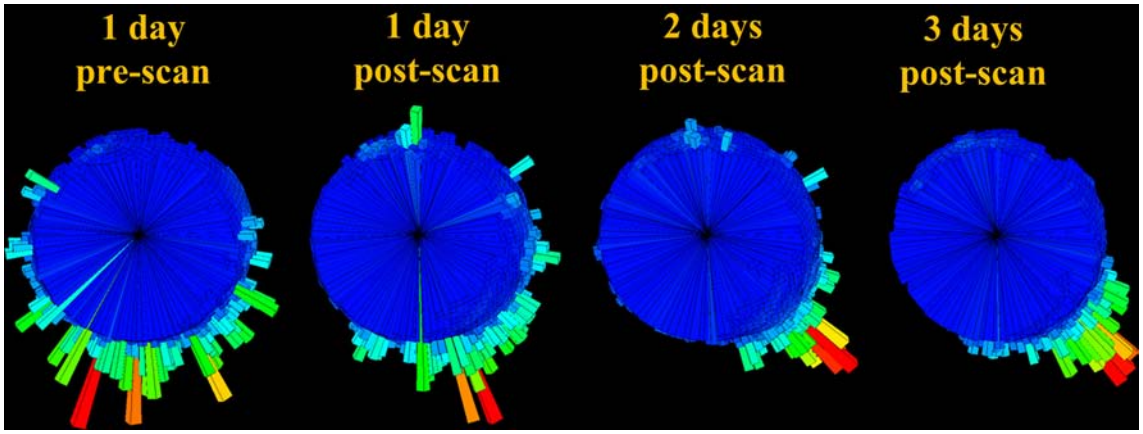

FIGURE 8 | Body orientation histogram (rose plot) over 24 h time-periods for T383 prior to undergoing an MRI scan and for the 3 days following this. Bar length denotes length of time allocated to each direction (the mode is shown in red). Note how the appreciable variability pre-MRI scan appears to diminish with time after the scan.

individuals. This could have been a side effect of being out of the water for a number of hours and/or hyperbaric treatment, which is thought to increase activity (Vicente Marco *pers. comm.*). Increased activity was also observed in the individual with intestinal gas. The link between VeDBA and physical condition was clearer in this case because the extra gas within the body caused greater buoyancy, making it more difficult to dive and requiring more vigor (Minamikawa et al., 2000). Thus, while

attempting to dive underwater in order to rest on the tank floor, as is normal, individuals with overall body densities less than that of seawater must spend additional energy paddling to overcome the added buoyancy, resulting in elevated VeDBA during descent (cf. Wilson and McMahon, 2006).

A very different VeDBA signature was observed for the individual that died of multi-organ failure; our study animal never reached the bottom of the tank to rest (cf. Minamikawa et al., 2000). Instead, periods of attempted descent were interspaced with periods of rest at the surface. This pattern became clear when comparing the VeDBA trace (which was consistently low) with that of depth.

Metrics That Might Indicate Disease/Injury

We suggest that diagnostics of health could be based on multiple parameters in a disease/injury identification key that could be combined to form specific TDBBs. Thus, an indication that a turtle has problems with buoyancy could be provided by having: (i) a higher incidence of body pitched-down, (ii) a greater incidence of high VeDBA and (iii) greater amplitude in VeDBA cycles stemming from exhaustion (recovery time at the surface due to greater oxygen use while underwater). This, for example, was observed in an individual with intestinal gas which had higher buoyancy than controls and was unable to descend the water column and reach the bottom of the tank without excessive paddling. A clear signal that this was the case was given by body pitch angle since the animal spent a large proportion of the time swimming down (with the body pitched forward) against buoyancy, whereas control animals only had the body pitched forward for the short periods they spent moving from the water surface to their preferred depths.

In fact, the body attitude of the individual with intestinal gas not only differed with respect to that of the healthy animal with regard to pitch, for which a mechanistic basis can be proposed (see above), it also differed with respect to roll (as observed in magnetometer plots—cf. Williams et al., 2017), indicating apparent instability which was not the case in healthy animals. This apparent lack of control was also observed in example individuals recovering from gas emboli and with multi-organ failure. We suggest that consideration of body posture, particularly in sea turtles (and potentially other aquatic species), and derivatives of this, such as rate of change of body posture, would be a useful way of documenting deviations in health status from the "norm."

Additionally, assessing changes in body posture before and after treatment could help to track animals through recovery and elucidate potential negative side effects of certain procedures, in particular, MRI scans, which expose animals to high magnetic fields in order to generate high quality diagnostic images (superior to those of radiographs and ultrasound) (Rübel et al., 1994; Walzer et al., 2003; Jandial et al., 2005; Thornton et al., 2005). Despite evidence that sea turtles rely on geomagnetic cues to navigate and reach specific nesting and feeding sites (Lohmann et al., 2004; Putman et al., 2011), MRIs have been widely used in anatomical examinations of the ear (Ketten and Bartol, 2005), head (Arencibia et al., 2012) and coelomic structures (Valente et al., 2006), as well as to investigate internal injuries caused by the ingestion of debris (Gasau and Ninou, 2000) and internal tumors in turtles with fibropapillomatosis (Croft et al., 2004). To date, no study has considered whether exposing turtles to intense magnetic fields could impair navigational abilities post-release. In this study, we presented information of the directionality in a single turtle (that had been admitted with gas emboli) pre- and post-MRI, which indicated increased directionality in the days following the scan. The implications of this possibly transient effect and whether this behavioral change should be attributed to recovering from gas emboli or magnetic field exposure or another factor is unknown and requires further study.

Monitoring Periods

After initial release into rescue tanks, VeDBA values from afflicted turtles during day 1 of tagging were typically within one standard deviation of healthy turtles. However, the probability of values from infirm turtles falling outside of this range would be likely to increase as a function of time and treatment; for example, sedatives would reduce activity whereas hyperbaric treatment and physiotherapy may increase it. Certain afflictions were more likely to alter behavior only in the short-term. For example, most turtles with gas emboli often did not exhibit defined active and rest periods (as observed in healthy turtles) for a few hours after release into a rescue tank. Nevertheless, veterinary diagnostics indicate that after hyperbaric treatment, turtles show full gas reabsorption. It is worth noting that in cases with severe gas emboli, bubble formation may have caused permanent damage. Observations also indicated that turtles were more active during daylight hours and therefore diel patterns should be taken into account when considering how long animals should be monitored. For many turtles, a second peak in VeDBA was observed some 20 h post-tagging, between 8:00 a.m. and 12:00 p.m. (noon), which was consistent with increasing light levels (the start of a new day) and tank cleaning and feeding (which takes place most mornings).

The infirm turtles that differed most from the general "healthy turtle" trend were T342 and T347; both had suffered traumas to the carapace and the latter also had a partially amputated flipper. The two turtles were first tagged some months after arriving at the center (T342 was tagged 2 months after arriving and T347 almost 7 months) due to treatment and/or injuries making the standard tag deployment procedure not feasible. The VeDBA values exhibited by T342 were consistently below the mean of healthy turtles whereas for T347 they were within the healthy turtles' range for the first 12 hours and then rose markedly above them. This rise, which peaked between 10:00 a.m. and 12:00 p.m., coincided with tank cleaning (which may cause animals some disturbance) and feeding. For T347, all swimming, but in particular descending to the bottom of the tank in order to eat, required exertion that was clearly greater than the norm, thus illustrating the potential for injury-specific feeding signatures as part of TDBBs relating to physical condition. The data from T342 and T347 also demonstrate that certain injuries, especially those involving flippers or carapace trauma, have long-lasting or even permanent effects on behavior. Consequently, monitoring the activity of such individuals at regular intervals over the long-term could provide a valuable tool when assessing recovery, especially

if specific TDBBs defining expected improvements existed and could be used in comparison.

In future, baseline data on expected VeDBA values for a variety of conditions through time could be determined by attaching DDs to turtles in rehabilitation centers and aquaria around the world. Such collaboration would be needed to build a behavioral repository of certified healthy animals, taking into account turtle size, sex, season, water temperature, enrichment, and enclosure size/available water mass. Although we found no significant relationship between available water mass and VeDBA, our analysis included turtles in various states of health and was only based on data from the first 24 h of tagging (whilst this should encompass diel changes, it would not take into account more longitudinal trends). The collection of such baseline data is of primary importance when defining suitable lengths of time to monitor rehabilitating animals.

Metrics That Might Indicate Changing State and Behavioral Breadth

This work begins the examination of the health of managed care animals by comparing the behavior of rehabilitating turtles with various diseases and injuries. The small sample size makes this necessarily speculative at the moment, but the results provided should encourage researchers to develop a common data base, or at least to share data, in order to gain the statistical power to differentiate conditions using tag-derived metrics confidently. In addition to increasing the sample size for turtles, it would benefit zoological institutions to expand the work to other taxa (cf. Ropert-Coudert et al., 2009 and Shorter et al., 2017). It is also important for workers using DD-type tags (cf. Johnson and Tyack, 2003) incorporating *inter alia* sophisticated and powerful sensors such as accelerometers and magnetometers, to recognize the large number of potentially important variables that can be gleaned from such devices to aid in the discrimination of differing behavioral states. These include, but are not limited to, animal heading (Williams et al., 2017), saccadic movement (Wilson et al., 2015) and rates of change of a suite of parameters (e.g., depth, pitch, roll, yaw) over different time intervals (Wilson et al., 2018) and there is an increasing number of analytical systems available to help in this (e.g., Walker et al., 2015a; Wilson et al., 2018).

There are, however, some metrics that will be more universal than others, and an example of this is VeDBA—a powerful metric that codes for overall body activity and acts as a proxy for metabolic rate (Qasem et al., 2012). Normally, we would expect the healthiest animals to be the most active, although the particular cases of intestinal gas and gas emboli show that this is not always true. Another less frequently used but extremely useful derivative is that of animal heading (turning) (Bidder et al., 2015; Walker et al., 2015b; Williams et al., 2017). Unlike VeDBA, which is derived from acceleration data and as such is affected by currents in air and water that can distort the signal-to-noise ratio (Halsey et al., 2011b), compass heading is not. VeDBA is also of limited use when examining the behavior of slow moving, relatively inactive or gliding animals that maintain a steady velocity for extended periods, for example turtles (Wyneken, 1997; Eckert, 2002) and soaring birds (Williams et al., 2015). In such cases, using magnetometers and examining movement patterns about the yaw axis may elucidate behaviors that are not evident in acceleration data alone (Williams et al., 2017). We found that VeDBA and heading in unison showed a promising way of differentiating between healthy and infirm turtles with external injuries. This was not surprising as severe flipper damage and carapace trauma affecting the spinal cord (as observed in individuals T342 and T347) had a clearly visible impact on the swimming and maneuverability of individuals. Critically though, it is specifically the combination of parameters (here dynamic acceleration and turning rates) that demonstrates that mixed sensor outputs can be particularly useful in TDBBs for state and our work is a first step in this direction. Although tagging animals with obvious external injuries would be unnecessary for diagnostic purposes, examining their behavior over time could be beneficial in order to track recovery and determine when behavior has returned to "normal" relative to healthy individuals. In some cases, behavioral biomarkers may indicate that an animal will never be fit for re-release into the wild.

Implications for Other Species

Given the ever-growing welfare concerns for animals maintained in zoos and aquaria (Johnson and Tyack, 2003; Shepard et al., 2008; Ismail et al., 2012) and the myriad research opportunities that these venues provide, it is surprising that little quantitative information (which is readily available via biologging) exists in relation to the activity and health of most species (Flint and Bonde, 2017; Shorter et al., 2017). This is especially pertinent to managed marine vertebrates (particularly cetaceans and other pinnipeds), whose presence in aquaria is regularly scrutinized (Rose et al., 2017). As such, current health and welfare assessments and monitoring practices, which generally rely on qualitative observations (including what individuals eat and social interactions) could be greatly aided by the collection of behavior in a quantifiable manner (Shorter et al., 2017). Studies using tags on farmed animals show how advantageous this could be; for example, improved lameness detection via leg-mounted accelerometers on dairy cows (Thorup et al., 2015).

In contrast to observational monitoring, which takes time and has a large degree of subjectivity (Broom and Johnson, 1993; Rushen, 2003; Lawrence, 2008; Rose et al., 2017), biologging enables the collection of quantitative data in a fast (often at several Hertz) and unbiased manner (Block, 2005; Sherub et al., 2017). Furthermore, information is recorded in sufficient detail to; (i) develop species-specific guidelines to standardize captive assessments, (ii) determine if adequate welfare requirements are being fulfilled, i.e., by defining what constitutes "typical" or "healthy" behavior and (iii) provide guidance on whether an animal is suitable for release after rehabilitation (Rose et al., 2017). This has particularly important implications for a wide range of species (including fish, sea turtles, birds, pinnipeds and cetaceans) that are frequently injured in fishery related interactions or by marine debris (Raum-Suryan et al., 2009; Adimey et al., 2014; Gall and Thompson, 2015; Jambeck et al., 2015; Nelms et al., 2015; Stelfox et al., 2016).

Unlike the animals in human care, logging devices have been widely used with their wild counterparts (Eckert, 2002; Shorter

et al., 2017). The information derived from these applications is highly valuable as understanding natural behavior and ecology is key to informing appropriate welfare standards for animals in captivity (Eckert, 2002; Shorter et al., 2017) and the wild (Rose et al., 2017). It also informs critical decisions such as whether to conserve natural habitats or recreate them artificially-these decisions usually involve vulnerable animals (for example dugongs and manatees) and can have major consequences (Rose et al., 2017).

Limitations and Perspectives

This dataset provides a small first step in demonstrating the usefulness of tags for collecting information on animals in human care. However, studies with a greater sample size and covering longer tag attachment durations are necessary to give proper statistical credibility to these initial findings. Nonetheless, significant behavioral differences (related to VeDBA verses the number of turns per hour) were found between healthy controls and turtles with external injuries to the flippers and carapace, suggesting that even with limited data, the utility of this tool is justifiable. Furthermore, comparisons between healthy individuals and those with gas emboli, intestinal gas and multi-organ failure, in the form of spherical plots revealed appreciable differences in orientation during a 24 h time window.

Although our categorization of turtle health status relied on veterinary diagnostic techniques (including blood sampling, radiographs and ultrasounds), the goal of creating illness specific TDBBs would be to limit the use of these potentially invasive and stress inducing procedures. In addition, the use of tags that transmit data would enable remote data collection in real time (Laske et al., 2014; Wilmers et al., 2015), both reducing animal handling and speeding up diagnosis/ our ability to track an animal's recovery. This would make our approach suitable to a variety of different applications in captive animal monitoring.

The financial and societal value of many species in managed care means that even limited data such as ours are appreciably better than nothing if it helps to enhance animal health and well-being. Indeed, within the zoo veterinary field, approaches are developed by slowly increasing findings from individual animals to larger numbers (Swaisgood and Shepherdson, 2005; Kuhar, 2006). Reaching the appropriate sample size required to obtain biologically or statistically significant results is a notable difficulty, often because few (if any) individuals are maintained in zoos/aquaria. Furthermore, in this circumstance, animals were tagged opportunistically as they entered the rehabilitation center with a variety of different injuries and diseases, which reduced suitable comparisons.

CONCLUSION

This manuscript showcases how data collected from motion- and orientation-sensitive animal-attached technology can be used to derive metrics which may aid animal health assessments and that could in time be combined to form an injury/disease identification guide. For example, data visualization showed behavioral differences between "healthy" sea turtles and individuals suffering gas emboli and intestinal gas, with the latter apparently paddling more frequently and spending more time with the body pitched downwards (presumably in order to compensate for increased buoyancy). Appropriate visualization showed such diagnostic patterns immediately without complex data analysis. We also found that VeDBA and compass heading in unison showed a promising way of differentiating between healthy and infirm turtles with external injuries to the flippers and carapace. Given this, we propose that the use of motion-sensitive tags could aid diagnosis and inform therapy, in particular cases follow-up, monitoring improvement and response to treatment. This is particularly relevant to turtles, given the numerous rehabilitation programs for bycatch sea turtles in operation. We suggest that establishing tag-derived behavioral biomarkers (TDBBs) for health in these animals based on the visualizations and metrics discussed in this paper is therefore timely and should both facilitate and improve the rehabilitation process.

Future Directions

Obvious further developments on the work presented here would be to equip more individuals with tags in order to augment sample size and validity and test the various metrics highlighted in this paper. After establishing TDBBs in loggerheads, the next step would be to trial them on other sea turtle species to gauge whether they were transferable or easily adaptable. Another line of work would be to ascertain whether TDBBs could be made specific to not just different diseases and injuries but also animal states (i.e., positive: happy or negative: sad, fearful, aggressive etc.) in order to use behavior as a measure of welfare (Benn et al., 2019). If successful, TDBBs could be adapted to fit other bycaught species in the same way that farm animal welfare assessments have been modified for zoos (Fraser, 2009; Hill and Broom, 2009) and aquaria [for example the "C-Well" welfare assessment index for dolphins in managed care (Clegg et al., 2015)]. In other words, TDBBs could be established for other species undergoing rehabilitation and release with more complex behavioral repertoires such as cetaceans and pinnipeds. Furthermore, motion-sensitive data from animals in human care and wild conspecifics could be compared in order to define a set of expected behavioral states and/or activity levels for numerous species housed in zoos/aquaria to help ensure their welfare. Finally, animal health is an increasing concern for wild populations, and appropriate validation of objective TDBBs in managed care populations could be of relevance when studying health and welfare in free-ranging animals.

DATA AVAILABILITY STATEMENT

The datasets generated for this study are available on request to the corresponding author.

ETHICS STATEMENT

This study was carried out in accordance with the recommendations of the Animal Care and Welfare Committee

of the Oceanogràfic Foundation (OCE-17-16 and amendment OCE-29-18). The protocol was approved by the Oceanogràfic Animal Care and Welfare Committee (OCE-16-18).

This study was also carried out in accordance with the recommendations of the Animal (Scientific Procedures) Act 1986 (Amended 2012) and the associated Code of Practice for accommodation and care of animals, Swansea University, Animal Welfare Ethical Review Body. The protocol was approved by the Swansea University, Animal Welfare Ethical Review Body (STU_BIOL_82015_011117151527_1).

AUTHOR CONTRIBUTIONS

AA, EA, AF, CD, and RW: experimental conception and design. AA, EA, AF, VC, and JC-P: data collection. AA, EA, AF, MH, RG, and RW: data analysis. AA, EA, AF, RG, and RW: manuscript preparation. All authors contributed to manuscript revision, read and approved the submitted version.

FUNDING

This research contributes to the CAASE project funded by King Abdullah University of Science and Technology (KAUST) under the KAUST Sensor Initiative. The Fundación Oceanogràfic provided a student bursary for AA and paid the costs to run the rehabilitation facility ARCA were all the work was done.

ACKNOWLEDGMENTS

We are grateful to Phil Hopkins for help with the tag housings. We would like to thank all the professionals at the Oceanogràfic, especially at the rehabilitation center (ARCA) taking care of the animals, for their efforts and dedication to provide excellent animal care. We are very grateful to all the fishermen contributing to the project as well as to the Valencian Government, especially to the Servicio de Vida Silvestre de la Conselleria d'Agricultura, Medi Ambient, Canvi Climàtic i Desenvolupament Rural de la Generalitat Valenciana.

REFERENCES

Abou-Ismail, U., Burman, O., Nicol, C., and Mendl, M. (2007). Can sleep behaviour be used as an indicator of stress in group-housed rats (*Rattus norvegicus*)? *Anim. Welf.* 16, 185–188.

Adimey, N. M., Hudak, C. A., Powell, J. R., Bassos-Hull, K., Foley, A., Farmer, N. A., et al. (2014). Fishery gear interactions from stranded bottlenose dolphins, Florida manatees and sea turtles in Florida, USA. *Mar. Pollut. Bull.* 81, 103–115. doi: 10.1016/j.marpolbul.2014.02.008

Andrewartha, S., Elliott, N., McCulloch, J., and Frappell, P. (2015). Aquaculture sentinels: smart-farming with biosensor equipped stock. *J. Aquac. Res. Dev.* 7, 1–4. doi: 10.4172/2155-9546.1000393

Arencibia, A., Hidalgo, M. R., Vázquez, J. M., Contreras, S., Ramírez, G., and Orós, J. (2012). Sectional anatomic and magnetic resonance imaging features of the head of juvenile loggerhead sea turtles (*Caretta caretta*). *Am. J. Vet. Res.* 73, 1119–1127. doi: 10.2460/ajvr.73.8.1119

Barton, K. (2019). *Package 'MuMIn'*. R package version, 1.43.6. Available online at: https://CRAN.R-project.org/package=MuMIn

Benn, A. L., McLelland, D. J., and Whittaker, A. L. (2019). A review of welfare assessment methods in reptiles, and preliminary application of the welfare quality® protocol to the pygmy blue-tongue skink, *Tiliqua adelaidensis*, using animal-based measures. *Animals* 9:27. doi: 10.3390/ani9010027

Bidder, O., Arandjelović, O., Almutairi, F., Shepard, E., Lambertucci, S. A., Qasem, L., et al. (2014). A risky business or a safe BET? A Fuzzy Set Event Tree for estimating hazard in biotelemetry studies. *Anim. Behav.* 93, 143–150. doi: 10.1016/j.anbehav.2014.04.025

Bidder, O., Walker, J., Jones, M., Holton, M., Urge, P., Scantlebury, D., et al. (2015). Step by step: reconstruction of terrestrial animal movement paths by dead-reckoning. *Mov. Ecol.* 3:23. doi: 10.1186/s40462-015-0055-4

Block, B. A. (2005). Physiological ecology in the 21st century: advancements in biologging science. *Integr. Comp. Biol.* 45, 305–320. doi: 10.1093/icb/45.2.305

Bograd, S. J., Block, B. A., Costa, D. P., and Godley, B. J. (2010). Biologging technologies: new tools for conservation. Introduction. *Endang. Species Res.* 10, 1–7. doi: 10.3354/esr00269

Boissy, A., Manteuffel, G., Jensen, M. B., Moe, R. O., Spruijt, B., Keeling, L. J., et al. (2007). Assessment of positive emotions in animals to improve their welfare. *Physiol. Behav.* 92, 375–397. doi: 10.1016/j.physbeh.2007.02.003

Bridger, C. J., and Booth, R. K. (2003). The effects of biotelemetry transmitter presence and attachment procedures on fish physiology and behavior. *Rev. Fish. Sci.* 11, 13–34. doi: 10.1080/16226510390856510

Broom, D. M. (1991). Animal welfare: concepts and measurement. *J. Anim. Sci.* 69, 4167–4175. doi: 10.2527/1991.69104167x

Broom, D. M., and Johnson, K. G. (1993). *Stress and Animal Welfare*. Springer Science & Business Media. doi: 10.1007/978-94-024-0980-2

Brown, D. D., Kays, R., Wikelski, M., Wilson, R., and Klimley, A. P. (2013). Observing the unwatchable through acceleration logging of animal behavior. *Anim. Biotelem.* 1:20. doi: 10.1186/2050-3385-1-20

Brownscombe, J. W., Thiem, J. D., Hatry, C., Cull, F., Haak, C. R., Danylchuk, A. J., et al. (2013). Recovery bags reduce post-release impairments in locomotory activity and behavior of bonefish (*Albula spp.*) following exposure to angling-related stressors. *J. Exp. Mar. Biol. Ecol.* 440, 207–215. doi: 10.1016/j.jembe.2012.12.004

Burman, O. H., Ilyat, A., Jones, G., and Mendl, M. (2007). Ultrasonic vocalizations as indicators of welfare for laboratory rats (*Rattus norvegicus*). *Appl. Anim. Behav. Sci.* 104, 116–129. doi: 10.1016/j.applanim.2006.04.028

Carere, C., and van Oers, K. (2004). Shy and bold great tits (*Parus major*): body temperature and breath rate in response to handling stress. *Physiol. Behav.* 82, 905–912. doi: 10.1016/S0031-9384(04)00312-9

Clegg, I., Borger-Turner, J., and Eskelinen, H. (2015). C-well: the development of a welfare assessment index for captive bottlenose dolphins (*Tursiops truncatus*). *Anim. Welf.* 24, 267–282. doi: 10.7120/09627286.24.3.267

Cooke, S. J. (2008). Biotelemetry and biologging in endangered species research and animal conservation: relevance to regional, national, and IUCN Red List threat assessments. *Endang. Species Res.* 4, 165–185. doi: 10.3354/esr00063

Cooke, S. J., Hinch, S. G., Wikelski, M., Andrews, R. D., Kuchel, L. J., Wolcott, T. G., et al. (2004). Biotelemetry: a mechanistic approach to ecology. *Trends Ecol. Evol.* 19, 334–343. doi: 10.1016/j.tree.2004.04.003

Croft, L. A., Graham, J. P., Schaf, S. A., and Jacobson, E. R. (2004). Evaluation of magnetic resonance imaging for detection of internal tumors in green turtles with cutaneous fibropapillomatosis. *J. Am. Vet. Med. Assoc.* 225, 1428–1435. doi: 10.2460/javma.2004.225.1428

Drake, R., Frost, J., and Collins, J. J. (2003). The symptoms of dying children. *J. Pain Symp. Manage.* 26, 594–603. doi: 10.1016/S0885-3924(03)00202-1

Eckert, S. A. (2002). Swim speed and movement patterns of gravid leatherback sea turtles (*Dermochelys coriacea*) at St Croix, US Virgin Islands. *J. Exp. Biol.* 205, 3689–3697.

Ellwood, S. A., Wilson, R. P., and Addison, A. C. (2007). "Technology in conservation: a boon but with small print," in *Key Topics in Conservation Biology*, eds D. Macdonald and K. Service (Oxford: Blackwell Publishing), 105–119

Enstipp, M. R., Ciccione, S., Gineste, B., Milbergue, M., Ballorain, K., Ropert-Coudert, Y., et al. (2011). Energy expenditure of freely swimming adult green

turtles (*Chelonia mydas*) and its link with body acceleration. *J. Exp. Biol.* 214, 4010–4020. doi: 10.1242/jeb.062943

Fahlman, A., Crespo-Picazo, J. L., Sterba-Boatwright, B., Stacy, B. A., and, Garcia-Parraga, D. (2017). Defining risk variables causing gas embolism in loggerhead sea turtles (*Caretta caretta*) caught in trawls and gillnets. *Sci. Rep.* 7:2739. doi: 10.1038/s41598-017-02819-5

Flint, M., and Bonde, R. K. (2017). "Assessing welfare of individual sirenians in the wild and in captivity," in *Marine Mammal Welfare. Animal Welfare, Vol. 17,* ed. A. Butterworth (Cham: Springer), 381–393. doi: 10.1007/978-3-319-46994-2_21

Fraser, D. (2009). Assessing animal welfare: different philosophies, different scientific approaches. *Zoo Biol.* 28, 507–518. doi: 10.1002/zoo.20253

Gailliot, M. T., Schmeichel, B. J., and Baumeister, R. F. (2006). Self-regulatory processes defend against the threat of death: Effects of self-control depletion and trait self-control on thoughts and fears of dying. *J. Personal. Soc. Psychol.* 91:49. doi: 10.1037/0022-3514.91.1.49

Gałecki, A., and Burzykowski, T. (eds.). (2013). "Fitting linear models with heterogeneous variance: the gls () function," in *Linear Mixed-Effects Models Using R* (New York, NY: Springer), 149–158. doi: 10.1007/978-1-4614-3900-4_8

Gall, S. C., and Thompson, R. C. (2015). The impact of debris on marine life. *Mar. Pollut. Bull.* 92, 170–179. doi: 10.1016/j.marpolbul.2014.12.041

Garcia-Parraga, D., Crespo-Picazo, J., Bernaldo de Quiros, Y., Cervera, V., Martí-Bonmati, L., Díaz-Delgado, J., et al. (2014). Decompression sickness ('the bends') in sea turtles. *Dis. Aquat. Organ.* 111, 191–205. doi: 10.3354/dao02790

Gasau, S. P., and Ninou, F. A. (2000). Work of the foundation for the conservation and recovery of marine life. *Mar. Turtle Newsl.* 87, 5–7.

Geertsen, B. M., Teilmann, J., Kastelein, R., Vlemmix, H., and Miller, L. A. (2004). Behaviour and physiological effects of transmitter attachments on a captive harbour porpoise (*Phocoena phocoena*). *J. Cetacean Res. Manage.* 6, 139–146.

Gleiss, A. C., Wilson, R. P., and Shepard, E. L. (2011). Making overall dynamic body acceleration work: on the theory of acceleration as a proxy for energy expenditure. *Methods Ecol. Evol.* 2, 23–33. doi: 10.1111/j.2041-210X.2010.00057.x

Gourkow, N., and Fraser, D. (2006). The effect of housing and handling practices on the welfare, behaviour and selection of domestic cats (*Felis sylvestris catus*) by adopters in an animal shelter. *Anim. Welfare* 15, 371–377.

Grandin, T. (1997). Assessment of stress during handling and transport. *J. Anim. Sci.* 75, 249–257. doi: 10.2527/1997.751249x

Guesgen, M., and Bench, C. (2017). What can kinematics tell us about the affective states of animals? *Anim. Welf.* 26, 383–397. doi: 10.7120/09627286.26.4.383

Halsey, L. G., Jones, T. T., Jones, D. R., Liebsch, N., and Booth, D. T. (2011a). Measuring energy expenditure in sub-adult and hatchling sea turtles via accelerometry. *PLoS ONE.* 6:e22311. doi: 10.1371/journal.pone.0022311

Halsey, L. G., Shepard, E. L., and Wilson, R. P. (2011b). Assessing the development and application of the accelerometry technique for estimating energy expenditure. *Comp. Biochem. Physiol. Part A* 158, 305–314. doi: 10.1016/j.cbpa.2010.09.002

Hawkins, P. (2004). Bio-logging and animal welfare: practical refinements. *Mem. Natl. Inst. Polar Res.* 58, 58–68.

Hemsworth, P. H., Rice, M., Karlen, M. G., Calleja, L., Barnett, J. L., Nash, J., et al. (2011). Human–animal interactions at abattoirs: Relationships between handling and animal stress in sheep and cattle. *Appl. Anim. Behav. Sci.* 135, 24–33. doi: 10.1016/j.applanim.2011.09.007

Hill, S. P., and Broom, D. M. (2009). Measuring zoo animal welfare: theory and practice. *Zoo Biol.* 28, 531–544. doi: 10.1002/zoo.20276

Ismail, A., Rahman, F., Miyazaki, N., and Naito, Y. (2012). Initial application of bio-logging techniques on captive Milky Stork (*Mycteria cinerea*) in Malaysia. *Trop. Ecol.* 53, 177–181.

Jambeck, J. R., Geyer, R., Wilcox, C., Siegler, T. R., Perryman, M., Andrady, A., et al. (2015). Plastic waste inputs from land into the ocean. *Science* 347, 768–771. doi: 10.1126/science.1260352

Jandial, R., Greenberg, M., Aryan, H., Taylor, W., Sutherland-Smith, M., Kearns, K., et al. (2005). Lumbar diskectomy in a human-habituated western lowland gorilla. *Internet J. Neurosur.* 1, 1–11. doi: 10.5580/17c3

Johnson, M. P., and Tyack, P. L. (2003). A digital acoustic recording tag for measuring the response of wild marine mammals to sound. *IEEE J. Ocean. Eng.* 28, 3–12. doi: 10.1109/JOE.2002.808212

Kenny, D. A., and Hoyt, W. T. (2009). Multiple levels of analysis in psychotherapy research. *Psychother. Res.* 19, 462–468. doi: 10.1080/10503300902806681

Ketten, D. R., and Bartol, S. M. (2005). *Functional Measures of Sea Turtle Hearing.* Woods Hole, MA: Woods Hole Oceanographic Institution. doi: 10.21236/ADA446809

Kooyman, G. L. (2004). Genesis and evolution of bio-logging devices: 1963-2002. *Mem. Natl. Inst. Polar Res.* 58, 15–22.

Kuhar, C. W. (2006). In the deep end: pooling data and other statistical challenges of zoo and aquarium research. *Zoo Biol.* 25, 339–352. doi: 10.1002/zoo.20089

Laske, T. G., Garshelis, D. L., and Iaizzo, P. A. (2014). Big data in wildlife research: remote web-based monitoring of hibernating black bears. *BMC Physiol.* 14:13. doi: 10.1186/s12899-014-0013-1

Lawrence, A. B. (2008). Applied animal behaviour science: past, present and future prospects. *Appl. Anim. Behav. Sci.* 115, 1–24. doi: 10.1016/j.applanim.2008.06.003

Lennox, R. J., Brownscombe, J. W., Cooke, S. J., and Danylchuk, A. J. (2018). Post-release behaviour and survival of recreationally-angled arapaima (*Arapaima cf. arapaima*) assessed with accelerometer biologgers. *Fisheries Res.* 207, 197–203. doi: 10.1016/j.fishres.2018.05.007

Lohmann, K. J., Lohmann, C. M., Ehrhart, L. M., Bagley, D. A., and Swing, T. (2004). Animal behaviour: geomagnetic map used in sea-turtle navigation. *Nature* 428, 909–910. doi: 10.1038/428909a

Mancini, C. J., Van Der Linden, Bryan, J., and Stuart, A. (2012). "Exploring interspecies sensemaking: dog tracking semiotics and multispecies ethnography," in *Proceedings of the 2012 ACM Conference on Ubiquitous Computing* (Pittsburgh, PA), 143–152. doi: 10.1145/2370216.2370239

Mason, G., and Rushen, J. (2008). *Stereotypic Animal Behaviour: Fundamentals and Applications to Welfare*. Wallingford: CAB International.

Minamikawa, S., Naito, Y., Sato, K., Matsuzawa, Y., Bando, T., and Sakamoto, W. (2000). Maintenance of neutral buoyancy by depth selection in the loggerhead turtle *Caretta caretta*. *J. Exp. Biol.* 203, 2967–2975.

Moberg, G. P. (2000). "Biological response to stress: implications for animal welfare," in *The Biology of Animal Stress: Basic Principles and Implications for Animal Welfare*, eds G. P. Moberg and J. A. Mnech (London: CABI Publishing), 1–21. doi: 10.1079/9780851993591.0001

Naito, Y. (2004). New steps in bio-logging science. *Mem. Natl. Inst. Polar Res.* 58, 50–57.

Nakagawa, S., and Schielzeth, H. (2013). A general and simple method for obtaining R^2 from generalized linear mixed-effects models. *Methods Ecol. Evol.* 4, 133–142. doi: 10.1111/j.2041-210x.2012.00261.x

Nathan, R., Getz, W. M., Revilla, E., Holyoak, M., Kadmon, R., Saltz, D., et al. (2008). A movement ecology paradigm for unifying organismal movement research. *Proc. Natl. Acad. Sci. U.S.A.* 105, 19052–19059. doi: 10.1073/pnas.0800375105

Nelms, S. E., Duncan, E. M., Broderick, A. C., Galloway, T. S., Godfrey, M. H., Hamann, M., et al. (2015). Plastic and marine turtles: a review and call for research. *ICES J. Mar. Sci.* 73, 165–181. doi: 10.1093/icesjms/fsv165

Pagano, A. M., Rode, K. D., Cutting, A., Owen, M., Jensen, S., Ware, J., et al. (2017). Using tri-axial accelerometers to identify wild polar bear behaviors. *Endang. Species Res.* 32, 19–33. doi: 10.3354/esr00779

Pinheiro, J., Bates, D., DebRoy, S., and Sarkar, D. (2015). *R Core Team: nlme: Linear and Nonlinear Mixed Effects Models*. R package version 3.1-122. Available online at: http://CRAN.R-project.org/package=nlme

Pinheiro, J. C., and Bates, D. M. (2000). *Mixed Effects Models in S and S-Plus*. New York, NY: Springer-Verlag. doi: 10.1007/B98882

Portugues, C., Crespo-Picazo, J. L., García-Párraga, D., Altimiras, J., Lorenzo, T., Borque-Espinosa, A., et al. (2018). Impact of gas emboli and hyperbaric treatment on respiratory function of loggerhead sea turtles (*Caretta caretta*). *Conserv. Physiol.* 6:cox074. doi: 10.1093/conphys/cox074

Putman, N. F., Endres, C. S., Lohmann, C. M., and Lohmann, K. J. (2011). Longitude perception and bicoordinate magnetic maps in sea turtles. *Curr. Biol.* 21, 463–466. doi: 10.1016/j.cub.2011.01.057

Qasem, L., Cardew, A., Wilson, A., Griffiths, I., Halsey, L. G., Shepard, E. L., et al. (2012). Tri-axial dynamic acceleration as a proxy for animal energy expenditure; should we be summing values or calculating the vector? *PLoS ONE* 7:e31187. doi: 10.1371/journal.pone.0031187

Raum-Suryan, K. L., Jemison, L. A., and Pitcher, K. W. (2009). Entanglement of Steller sea lions (*Eumetopias jubatus*) in marine debris: Identifying

causes and finding solutions. *Mar. Pollut. Bull.* 58, 1487–1495. doi: 10.1016/j.marpolbul.2009.06.004

Roe, J. H., Frank, M. R., Gibson, S. E., Attum, O., and Kingsbury, B. A. (2010). No place like home: an experimental comparison of reintroduction strategies using snakes. *J. Appl. Ecol.* 47, 1253–1261. doi: 10.1111/j.1365-2664.2010.01886.x

Ropert-Coudert, Y., Brooks, L., Yamamoto, M., and Kato, A. (2009). ECG response of koalas to tourists proximity: a preliminary study. *PLoS ONE* 4:e7378. doi: 10.1371/journal.pone.0007378

Ropert-Coudert, Y., and Wilson, R. P. (2005). Trends and perspectives in animal-attached remote sensing. *Front. Ecol. Environ.* 3, 437–444. doi: 10.1890/1540-9295(2005)003[0437:TAPIAR]2.0.CO;2

Rose, N. A., Hancock Snusz, G., Brown, D. M., and Parsons, E. (2017). Improving captive marine mammal welfare in the United States: science-based recommendations for improved regulatory requirements for captive marine mammal care. *J. Int. Wildlife Law Policy* 20, 38–72. doi: 10.1080/13880292.2017.1309858

Rübel, A., Kuoni, W., and Augustiny, N. (1994). Emerging techniques: CT scan and MRI in reptile medicine. *Semin. Avian Exotic Pet Med.* 3, 156–160.

Rushen, J. (2003). Changing concepts of farm animal welfare: bridging the gap between applied and basic research. *Appl. Anim. Behav. Sci.* 81, 199–214. doi: 10.1016/S0168-1591(02)00281-2

Scollo, A., Gottardo, F., Contiero, B., and Edwards, S. A. (2014). Does stocking density modify affective state in pigs as assessed by cognitive bias, behavioural and physiological parameters? *Appl. Anim. Behav. Sci.* 153, 26–35. doi: 10.1016/j.applanim.2014.01.006

Shepard, E. L. C., Wilson, R. P., Quintana, F., Gómez Laich, A., Liebsch, N., Albareda, D. A., et al. (2008). Identification of animal movement patterns using tri-axial accelerometry. *Endang. Species Res.* 10, 47–60. doi: 10.3354/esr00084

Sherub, S., Fiedler, W., Duriez, O., and Wikelski, M. (2017). Bio-logging, new technologies to study conservation physiology on the move: a case study on annual survival of Himalayan vultures. *J. Comp. Physiol. A* 203, 531–542. doi: 10.1007/s00359-017-1180-x

Shirai, M., and Yokoyama, S. (2014). "Grazing behavior and local management of cattle and buffaloes in rural laos," in *Integrated Studies of Social and Natural Environmental Transition in Laos,* eds S. Yokoyama, K. Okamoto, C. Takenaka, and I. Hirota (Tokyo: Springer), 63–84. doi: 10.1007/978-4-431-54956-7_4

Shorter, A. K., Shao, Y., Ojeda, L., Barton, K., Rocho-Levine, J., Hoop, J., et al. (2017). A day in the life of a dolphin: using bio-logging tags for improved animal health and well-being. *Mar. Mamm. Sci.* 33, 785–802. doi: 10.1111/mms.12408

Sikka, P., Corke, P., Valencia, P., Crossman, C., Swain, D., and Bishop-Hurley G. (2006). "Wireless adhoc sensor and actuator networks on the farm," in *Proceedings of the 5th ACM/IEEE International Conference on Information Processing in Sensor Networks (IPSN)* (New York, NY: ACM), 492–499. doi: 10.1145/1127777.1127852

Stelfox, M., Hudgins, J., and Sweet, M. (2016). A review of ghost gear entanglement amongst marine mammals, reptiles and elasmobranchs. *Mar. Pollut. Bull.* 111, 6–17. doi: 10.1016/j.marpolbul.2016.06.034

Swaisgood, R. R., and Shepherdson, D. J. (2005). Scientific approaches to enrichment and stereotypies in zoo animals: what's been done and where should we go next? *Zoo Biol.* 24, 499–518. doi: 10.1002/zoo.20066

Teixeira, C. P., De Azevedo, C. S., Mendl, M., Cipreste, C. F., and Young, R. J. (2007). Revisiting translocation and reintroduction programmes: the importance of considering stress. *Anim. Behav.* 73, 1–13. doi: 10.1016/j.anbehav.2006.06.002

Thomson, J. A., and Heithaus, M. R. (2014). Animal-borne video reveals seasonal activity patterns of green sea turtles and the importance of accounting for capture stress in short-term biologging. *J. Exp. Mar. Biol. Ecol.* 450, 15–20. doi: 10.1016/j.jembe.2013.10.020

Thornton, S. J., Hochachka, P. W., Crocker, D. E., Costa, D. P., LeBoeuf, B. J., Spielman, D. M., et al. (2005). Stroke volume and cardiac output in juvenile elephant seals during forced dives. *J. Exp. Biol.* 208, 3637–3643. doi: 10.1242/jeb.01789

Thorup, V. M., Munksgaard, L., Robert, P.-E., Erhard, H., Thomsen, P., and Friggens, N. (2015). Lameness detection via leg-mounted accelerometers on dairy cows on four commercial farms. *Animal* 9, 1704–1712. doi: 10.1017/S1751731115000890

Turner, L., Udal, M., Larson, B., and Shearer, S. (2000). Monitoring cattle behavior and pasture use with GPS and GIS. *Can. J. Anim. Sci.* 80, 405–413. doi: 10.4141/A99-093

Valente, A. L. S., Cuenca, R., Zamora, M. A., Parga, M. L., Lavin, S., Alegre, F., et al. (2006). Sectional anatomic and magnetic resonance imaging features of coelomic structures of loggerhead sea turtles. *Am. J. Vet. Res.* 67, 1347–1353. doi: 10.2460/ajvr.67.8.1347

Vandenabeele, S., Wilson, R., and Grogan, A. (2011). Tags on seabirds: how seriously are instrument-induced behaviours considered? *Anim. Welfare UFAW J.* 20:559–571.

Veasey, J., Waran, N., and Young, R. (1996). On comparing the behaviour of zoo housed animals with wild conspecifics as a welfare indicator. *Anim. Welf.* 5, 13–24.

Waiblinger, S., Menke, C., Korff, J., and Bucher, A. (2004). Previous handling and gentle interactions affect behaviour and heart rate of dairy cows during a veterinary procedure. *Appl. Anim. Behav. Sci.* 85, 31–42. doi: 10.1016/j.applanim.2003.07.002

Walker, J., Borgo, R., and Jones, M. W. (2016). TimeNotes: a study on effective chart visualization and interaction techniques for time-series data. *IEEE Trans. Visual. Comput. Graph.* 22, 549–558. doi: 10.1109/TVCG.2015.2467751

Walker, J. S., Jones, M. W., Laramee, R. S., Bidder, O. R., Williams, H. J., Scott, R. et al. (2015a). TimeClassifier: a visual analytic system for the classification of multi-dimensional time series data. *Vis. Comp.* 31, 1067–1078. doi: 10.1007/s00371-015-1112-0

Walker, J. S., Jones, M. W., Laramee, R. S., Holton, M. D., Shepard, E. L., Williams, H. J., et al. (2015b). Prying into the intimate secrets of animal lives; software beyond hardware for comprehensive annotation in 'Daily Diary' tags. *Mov. Ecol.* 3:29. doi: 10.1186/s40462-015-0056-3

Walker, K. A., Trites, A. W., Haulena, M., and Weary, D. M. (2011). A review of the effects of different marking and tagging techniques on marine mammals. *Wildlife Res.* 39, 15–30. doi: 10.1071/WR10177

Walzer, C., Url, A., Robert, N., Kübber-Heiss, A., Nowotny, N., and Schmidt, P. (2003). Idiopathic acute onset myelopathy in cheetah (*Acinonyx jubatus*) cubs. *J. Zoo Wildlife Med.* 34, 36–46. doi: 10.1638/1042-7260(2003)34[0036:IAOMIC]2.0.CO;2

Ward, S. J., and Melfi, V. (2015). Keeper-animal interactions: differences between the behaviour of zoo animals affect stockmanship. *PLoS ONE* 10:e0140237. doi: 10.1371/journal.pone.0140237

Whitney, N. M., White, C. F., Gleiss, A. C., Schwieterman, G. D., Anderson, P., Hueter, R. E., et al. (2016). A novel method for determining post-release mortality, behavior, and recovery period using acceleration data loggers. *Fisheries Res.* 183, 210–221. doi: 10.1016/j.fishres.2016.06.003

Wiepkema, P., and Koolhaas, J. (1993). Stress and animal welfare. *Anim. Welf.* 2, 195–218.

Williams, H., Shepard, E., Duriez, O., and Lambertucci, S. A. (2015). Can accelerometry be used to distinguish between flight types in soaring birds? *Anim. Biotelem.* 3:45. doi: 10.1186/s40317-015-0077-0

Williams, H. J., Holton, M. D., Shepard, E. L., Largey, N., Norman, B., Ryan, P. G., et al. (2017). Identification of animal movement patterns using tri-axial magnetometry. *Mov. Ecol.* 5:6. doi: 10.1186/s40462-017-0097-x

Wilmers, C. C., Nickel, B., Bryce, C. M., Smith, J. A., Wheat, R. E., and Yovovich, V. (2015). The golden age of bio-logging: how animal-borne sensors are advancing the frontiers of ecology. *Ecology* 96, 1741–1753. doi: 10.1890/14-1401.1

Wilson, A. D., Wikelski, M., Wilson, R. P., and Cooke, S. J. (2015). Utility of biological sensor tags in animal conservation. *Conserv. Biol.* 29, 1065–1075. doi: 10.1111/cobi.12486

Wilson, R. P., Grundy, E., Massy, R., Soltis, J., Tysse, B., Holton, M., et al. (2014). Wild state secrets: ultra-sensitive measurement of micro-movement

can reveal internal processes in animals. *Front. Ecol. Environ*. 12, 582–587. doi: 10.1890/140068

Wilson, R. P., Holton, M. D., di Virgilio, A., Williams, H., Shepard, E. L., Lambertucci, S. et al. (2018). Give the machine a hand: a Boolean time-based decision-tree template for rapidly finding animal behaviours in multisensor data. *Methods Ecol. Evol*. 9, 2206–2215. doi: 10.1111/2041-210X.13069

Wilson, R. P., Holton, M. D., Walker, J. S., Shepard, E. L., Scantlebury, D. M., Wilson, V. L., et al. (2016). A spherical-plot solution to linking acceleration metrics with animal performance, state, behaviour and lifestyle. *Mov. Ecol.* 4:22. doi: 10.1186/s40462-016-0088-3

Wilson, R. P., and McMahon, C. R. (2006). Measuring devices on wild animals: what constitutes acceptable practice? *Front. Ecol. Environ*. 4, 147–154. doi: 10.1890/1540-9295(2006)004[0147:MDOWAW]2.0.CO;2

Wilson, R. P., Shepard, E. L. C., and Liebsch, N. (2008). Prying into the intimate details of animal lives: use of a daily diary on animals. *Endang. Species Res.* 4, 123–137. doi: 10.3354/esr00064

Wyneken, J. (1997). *Sea Turtle Locomotion. The Biology of Sea Turtles*. Boca Raton, FL: CRC Press.

Conflict of Interest: The authors declare that the research was conducted in the absence of any commercial or financial relationships that could be construed as a potential conflict of interest.

The handling editor is currently co-organizing a Research Topic with one of the authors, AF, and confirms the absence of any other collaboration.

Copyright © 2020 Arkwright, Archibald, Fahlman, Holton, Crespo-Picazo, Cabedo, Duarte, Scott, Webb, Gunner and Wilson. This is an open-access article distributed under the terms of the Creative Commons Attribution License (CC BY). The use, distribution or reproduction in other forums is permitted, provided the original author(s) and the copyright owner(s) are credited and that the original publication in this journal is cited, in accordance with accepted academic practice. No use, distribution or reproduction is permitted which does not comply with these terms.

Advantages of publishing in Frontiers

OPEN ACCESS
Articles are free to read for greatest visibility and readership

FAST PUBLICATION
Around 90 days from submission to decision

HIGH QUALITY PEER-REVIEW
Rigorous, collaborative, and constructive peer-review

TRANSPARENT PEER-REVIEW
Editors and reviewers acknowledged by name on published articles

Frontiers
Avenue du Tribunal-Fédéral 34
1005 Lausanne | Switzerland

Visit us: www.frontiersin.org
Contact us: info@frontiersin.org | +41 21 510 17 00

REPRODUCIBILITY OF RESEARCH
Support open data and methods to enhance research reproducibility

DIGITAL PUBLISHING
Articles designed for optimal readership across devices

FOLLOW US
@frontiersin

IMPACT METRICS
Advanced article metrics track visibility across digital media

EXTENSIVE PROMOTION
Marketing and promotion of impactful research

LOOP RESEARCH NETWORK
Our network increases your article's readership